



HAL
open science

Fight or flight ? : oxygen tolerance mechanisms and spore morphogenesis in the enteropathogen *Clostridium difficile*

Carolina Feliciano

► **To cite this version:**

Carolina Feliciano. Fight or flight ? : oxygen tolerance mechanisms and spore morphogenesis in the enteropathogen *Clostridium difficile*. Molecular biology. Université Sorbonne Paris Cité, 2019. English. NNT : 2019USPCC086 . tel-03855175

HAL Id: tel-03855175

<https://theses.hal.science/tel-03855175v1>

Submitted on 16 Nov 2022

HAL is a multi-disciplinary open access archive for the deposit and dissemination of scientific research documents, whether they are published or not. The documents may come from teaching and research institutions in France or abroad, or from public or private research centers.

L'archive ouverte pluridisciplinaire **HAL**, est destinée au dépôt et à la diffusion de documents scientifiques de niveau recherche, publiés ou non, émanant des établissements d'enseignement et de recherche français ou étrangers, des laboratoires publics ou privés.

Thèse de doctorat
de l'Université Sorbonne Paris Cité
Préparée à l'Université Paris Diderot
Ecole doctorale Bio Sorbonne Paris Cité (Bio SPC) ED562
Laboratoire Pathogénèse des Bactéries Anaérobies

Fight or flight?

Oxygen tolerance mechanisms and spore morphogenesis
in the enteropathogen *Clostridium difficile*

Par Carolina ALVES FELICIANO

Thèse de doctorat de Microbiologie

Dirigée par le Docteur Bruno Dupuy

Présentée et soutenue publiquement à Institut Pasteur le 1 Février 2019

Président du jury : M. le Professeur Olivier DUSSURGET, Université Paris Diderot

Rapporteurs : M^{me} le Docteur Aimee SHEN, Tufts University

Rapporteur : M^{me} le Docteur Véronique BROUSSOLLE, INRA Avignon

Examineur : M. le Professeur Frédéric BARBUT, Université Paris Descartes

Examineur : M. le Docteur Philippe GAUDU, INRA Micalis

Examineur : M^{me} le Professeur Isabelle MARTIN-VERSTRAETE, Université Paris Diderot

Directeur de thèse : M. le Docteur Bruno DUPUY, Institut Pasteur

Résumé:

Clostridium difficile qui est une bactérie anaérobie stricte et sporulante, est la principale cause des diarrhées associées à la prise d'antibiotiques. Les spores jouent un rôle central dans le cycle infectieux de *C. difficile* : résistance en dehors de l'hôte, persistance des bactéries et transmission de l'infection. Lorsqu'elles sont ingérées par l'hôte, les spores de *C. difficile* germent dans le côlon en présence de certains sels biliaires pour former des cellules végétatives qui vont produire des toxines responsables des symptômes.

Les cellules végétatives sont exposées à différents stress incluant les espèces réactives de l'oxygène et de l'azote (ROS/RNS) produites par le système immunitaire de l'hôte lors de l'inflammation. De plus, bien que le tractus intestinal soit considéré comme anoxique, une faible teneur en oxygène (O₂) est présente dans l'intestin et elle va augmenter après un traitement antibiotique. Pour survivre dans cet environnement oxydant hostile, *C. difficile* a développé des mécanismes de protection, des voies de détoxification et des systèmes de réparation. Le facteur sigma alternatif de la réponse générale au stress, σ^B , joue un rôle important dans la protection de *C. difficile* face aux stress rencontrés dans l'hôte incluant l'O₂ et les ROS. Parmi les gènes contrôlés positivement par σ^B , nous avons identifié des gènes codant pour des protéines probablement impliquées dans la tolérance à l'O₂ et la détoxification des ROS, comme les deux réverses rubrerythines (revRbrs), CD1524 et CD1474, et les protéines de type flavodiiron (FDPs), CD1157 et CD1623. Nous avons montré que les gènes codant les deux revRbrs et *CD1623* sont exprimés sous le contrôle de σ^B et de manière hétérogène dans la population bactérienne. Le gène *CD1157* est lui exprimé à partir de deux promoteurs dépendants l'un de σ^A et l'autre de σ^B . Nous avons ensuite montré que *CD1157* a une activité O₂-réductase alors que les deux revRbrs ont une activité H₂O₂- et O₂-réductase, l'H₂O₂ étant le substrat préféré. De plus, nous avons montré qu'un double mutant $\Delta CD1474\text{-}\Delta CD1524$ et un mutant *CD1157* sont moins tolérants à une faible tension en O₂ et que le mutant $\Delta CD1623$ est plus sensible à l'exposition à l'air. Ces résultats démontrent le rôle clé de ces protéines dans la tolérance à l'O₂ et la réponse au stress oxydant chez *C. difficile*.

Au cours du cycle infectieux, dans le côlon, certaines cellules végétatives sporulent. Les couches de surface des spores, le manteau et l'exosporium, permettent aux spores de résister aux stress physiques et chimiques. Cependant, peu de choses sont connues sur leurs mécanismes d'assemblage. Dans ce travail, nous avons caractérisé une nouvelle protéine, CotL, qui est nécessaire pour l'assemblage des couches externes de la spore. Nous avons montré que le gène *cotL* est exprimé dans la cellule mère sous le double contrôle des facteurs sigma de sporulation, σ^E et σ^K . La protéine CotL est localisée dans le manteau de la spore, et les spores du mutant *cotL* ont un défaut morphologique majeur au niveau des couches du manteau et de l'exosporium. De plus, les spores du mutant contiennent une quantité réduite de plusieurs protéines du manteau et de l'exosporium et présentent un défaut dans leur localisation dans des cellules en cours de sporulation. Enfin, les spores du mutant *cotL* sont plus sensibles au lysozyme et présentent un défaut de germination, un phénotype vraisemblablement associé à la modification de la structure des couches externes de la spore. Ces résultats suggèrent fortement que CotL est une protéine morphogénétique essentielle à l'assemblage des couches externes de la spore chez *C. difficile*.

Mots clefs: *Clostridium difficile*, Manteau de la spore, Morphogénèse, CotL, Oxygène, ERO, détoxification, Rubrerythines, protéine Flavodiiron.

"Like people, cells usually deliberate very carefully before committing to dramatic changes in their lifestyle."

Stephens 1998

Acknowledgments

First of all, I would like to thank all the members of the jury who agreed to evaluate my thesis work.

I would like to thank the boss and my supervisor Bruno Dupuy, for the opportunity to work in his lab and for his help and support throughout this journey. Thank you for the rich scientific environment as well as excellent working conditions. Thank you for your positive attitude.

Thank you to my supervisor Isabelle Martin-Verstraete. Thank you for believing in me and chose me for this PhD position. Thank you for always find time for me, my questions and my most stressful moments. Thank you for all I learned from you, for all the discussions and for sharing with me your passion for science.

Elodie, my partner in crime. Thank you for the support during these last 3 years. Traveling together, Christmas cookies and crepes at home are key moments that I won't forget. Continue singing, no matter the place you will be!

Nicolas, thank you for all the moments, for everything you taught me me during these 3 years and the helpful discussions. It was so great to work with you! Wish you a “trevo de 4 folhas”.

Johann, thank you for the scientific exchanges, sense of humor and for always be positive.

Thanks also to all the present and former colleagues of the LPBA, Anna, Audrey, Claire, Julian, Marc, Olga, Ritsuko, Transito and Yannick for their help, exchanges and work atmosphere.

I would like to thank Miguel Teixeira, Filipe Folgosa and Maria Martins, from ITQB, Portugal. I loved the 2 months I spent with you in your lab. Thank you for teaching me so much while I have been there. Thank you for the coffee breaks eating “pasteis de nata” and “bolo de arroz”.

Thank you to Laura and Candice that were always there to help me with the microscope.

Thank you all the members of the kitchen that were always willing to help.

Um grande Obrigado to the Portuguese crew, Flávia, Marisa, Sofia, Marta, Alexa, Francisco, Jorge Pereira, Jorge, Filipe, Alicia, André, Pedro, Monica, Carolina Cassona, Carla, Araújo, Freire, Teixeira for your friendship, support, and relaxing moments. You know we are a big family. Espero encontrar-vos algures no mundo.

Finalmente, um grande obrigado aos meus pais e à minha irmã pelo apoio incondicional, não só durante estes 3 anos, mas sempre. Obrigado por estarem sempre comigo, seja por skype, messenger, ou quando faço visitas surpresa. Obrigado aos meus avós e à minha tia Xana por me apoiarem sempre e acreditarem em mim. Tenho a melhor família que poderia desejar.

List of abbreviations

ATP	adenosine triphosphate
bp	base pairs
BCAA	branched-chain amino-acids
Ca	calcium
CA	cholate
CAMPs	cationic antimicrobial peptides
CCCP	cyanide <i>m</i> -chlorophenylhydrazone
CDCA	chenodeoxycholate
CDI	<i>Clostridium difficile</i> infection
Dfx	desulfoferrodoxin
DNA	deoxyribonucleic acid
DPA	dipicolinic acid
FAD	flavin adenine dinucleotide
FDP	flavodiiron protein
FMN	flavin mononucleotide
FMT	faecal microbiota transplantation
FS	forespore
GRs	germinant receptors
GTP	guanosine-5'-triphosphate
H ₂ O ₂	hydrogen peroxide
Fe	iron
kb	kilobase
kDa	kiloDalton
MAMPs	microbial associated molecular patterns
MTG	mitotracker Green
MC	mother cell
MCD	mother cell distal
MCP	mother cell proximal
NADH-OR	NADH oxidoreductase
NO	nitric oxide
NROR	NADH rubredoxin oxidoreductase
O ₂	oxygen
ONOO ⁻	peroxynitrite
PG	peptidoglycan
Rbr	rubrerythrin
Rd	rubredoxin
revRbr	reverse rubrerythrin
RNA	ribonucleic acid
RNS	reactive nitrogen species
ROS	reactive oxygen species
SASPs	small acid soluble proteins
SCFAs	short chain fatty acids
SM	sporulation medium

SNP	sodium nitroprusside
SOD	superoxide dismutase
SOR	superoxide reductase
TA	taurocholate
Trx	Thioredoxin
TSS	transcriptional start site
TEM	Transmission electron microscopy
UV	ultraviolet

Table of Contents

Table of Contents	7
Introduction	11
Chapter 1: The enteric pathogen <i>Clostridium difficile</i>	12
I. <i>Clostridium difficile</i>	12
I.1. <i>C. difficile</i> infection cycle	13
I.2. CDI risk factors and colonization resistance against <i>C. difficile</i>	14
I.3. Epidemiology	17
I.4. Treatments of CDI	18
I.4.a. Conventional treatments.....	18
I.4.b. Faecal microbiota transplantation	19
I.4.c. Immunotherapy	19
II. Virulence factors and colonization in <i>C. difficile</i>	20
II.1. The TcdA and TcdB toxins	20
II.1.a. Mechanism of action of TcdA and TcdB.....	20
II.1.b. Regulation of <i>tcdA</i> and <i>tcdB</i> expression.....	21
II.2. The binary toxin CDT.....	23
II.3. Other virulence factors: the colonization factors.....	24
Chapter 2: The stress response and the role of σ^B	25
I. Stresses encountered during gut infection	25
II. σ^B , the alternative sigma factor of general stress response.....	25
II.1 σ^B in <i>B. subtilis</i>	25
II.1.a The role of σ^B and the mechanism of its activation.....	25
II.1.b. The signal transduction pathway responsible for the activation of σ^B	26
II.2. Diversity of the mechanism of σ^B activation in other Firmicutes	27
II.3. The σ^B regulon.....	28
II.4. The role of σ^B in <i>C. difficile</i>	30
II.4.a. Characterization of the σ^B signaling pathway in <i>C. difficile</i>	32
Conservation of the partner switching mechanism	32
Players and signals in the activation of σ^B	33
Chapter 3: Oxygen and Reactive Oxygen Species detoxification	34
I. Cell defense mechanisms against these compounds present in bacteria.....	34
I.1. Catalases and superoxide dismutases.....	34
I.2. Alternative detoxification systems: NADH-dependent reductases.....	34
I.2.a. Rubrerythrins (Rbrs)	35
I.2.b. Flavodiiron proteins (FDPs)	36
II. O ₂ and ROS detoxification in <i>C. difficile</i>	37
II.1. The exposure of <i>C. difficile</i> to O ₂ , ROS and NO during infection.....	37
II.2. The response of <i>C. difficile</i> to O ₂ and oxidative stress.....	38
Chapter 4: Sporulation and Germination	41
I. General stress response and sporulation: two survival mechanisms in <i>C. difficile</i>	41
II. The sporulation process	41
II.1. Regulation of sporulation in <i>B. subtilis</i>	42
II.1.a Initiation of sporulation	43
II.1.b. The forespore line of gene expression: σ^F and σ^G	44
II.1.c. The mother cell line of gene expression: σ^E and σ^K	46

II.2. Regulation of sporulation in clostridia	47
II.2.a. Sporulation in <i>C. difficile</i>	48
Initiation of sporulation	48
Sigma factors and transcriptional regulators	49
The forespore regulatory network: σ^F and σ^G	50
The mother cell regulatory network: σ^E and σ^K	51
The skin ^{Cd} element	52
III. Germination	53
III.1. Germination in <i>B. subtilis</i>	53
III.2. Germination in <i>C. difficile</i>	54
Chapter 5: The spore	56
I. Structure of the spore	56
II. Spore resistance	56
II.1. Functions of the spore coat	57
III. Spore surface layers of bacilli and clostridia	58
III.1. Conservation of proteins	58
III.2. Spore coat organization in <i>B. subtilis</i>	59
III.2.a. Coat morphogenetic proteins	59
III.2.b. Coat assembly	62
III.2.c. Coat morphogenesis in real time	62
III.3. Spore coat of <i>B. cereus</i> group	64
III.4. The Exosporium layer	64
III.5. Spore surface layers of <i>C. difficile</i>	66
III.5.a. Morphogenesis of the <i>C. difficile</i> spore coat	67
III.5.b. Spore coat and exosporium proteins	68
III.5.c. Morphogenetic proteins of <i>C. difficile</i> exosporium	70
III.5.d. Representative model of the proteins at the spore surface layers	71
<u>Objectives of the thesis</u>	72
<u>Results</u>	73
Spore coat morphogenesis	74
I. Article: CotL, a new morphogenetic spore coat protein of	74
<i>Clostridium difficile</i>	74
II. Complementary results on Spore coat morphogenesis	105
II.1. Investigation of potential CotL partners	105
II.1.a. Identification of proteins interacting with CotL by BACTH	105
II.1.b. Coexpression of spore coat proteins and pull down assay in <i>E. coli</i>	106
II.2. The <i>CD2399</i> gene	107
II.2.a. <i>CD2399</i> and <i>CD0596</i> are σ^K -controlled genes	107
II.2.b. <i>CD2399</i> is not required for sporulation	108
II.2.c. <i>CD2399</i> mutant spores have a germination delay	108
II.2.d. The inactivation of <i>CD2399</i> does not affect the ultrastructure and resistance of the spore	109
O₂ tolerance and ROS protection in <i>C. difficile</i>	111
I. Role of the revRbrs and the FDPs in <i>C. difficile</i> vegetative cells	113
I.1. Regulation of revRbrs (<i>CD1474</i> , <i>CD1524</i>) and FDPs (<i>CD1623</i> , <i>CD1157</i>) gene expression	113
I.2. FDP and revRbrs sequence analysis	114
I.3. Protein characterization and redox properties	114
I.4. <i>CD1474</i> and <i>CD1524</i> reduce both H ₂ O ₂ and O ₂ while <i>CD1157</i> reduces only O ₂	115

I.5. The function of the revRbrs and the FDPs, in the management of O ₂ tolerance.	116
II. Proteins produced under the control of σ^B are present in the spores	118
II.1. σ^B expression and activity during sporulation	118
II.2. Localization of σ^B - controlled proteins at the spore surface	119
Materials and methods	121
Supplementary tables and figures	132
Table S1. Bacterial strains and plasmids used in this study	132
Table S2: Oligonucleotides used in this study.	137
Discussion	140
I. The morphogenesis of the <i>C. difficile</i> spore coat	141
I.1. Role of CotL on <i>C. difficile</i> spore coat structure	141
I.2. The dual control of <i>cotL</i> gene expression	141
I.3. CotL properties and its localization in the spore	143
I.4. Interactions between coat proteins in <i>C. difficile</i>	144
I.5. Spore encasement dependent on CotL	145
I.6. Model for the assembly of the outermost layers of the <i>C. difficile</i> spore	146
II. Signaling pathway and σ^B activation in <i>C. difficile</i>	148
II.1. Role of the environmental signals in the activation of σ^B in <i>C. difficile</i>	148
II.2. Role of the energy signals in the activation of σ^B in <i>C. difficile</i>	149
II.3. Expression of <i>sigB</i> in <i>C. difficile</i>	149
II.4. Heterogeneity of gene expression of <i>sigB</i> and σ^B -targets	151
III. O₂ tolerance and ROS protection in <i>C. difficile</i>	153
III.1. Protective role of the <i>C. difficile</i> revRbrs and FDPs	153
III.2. Protection against H ₂ O ₂	154
III.3. O ₂ and ROS response in <i>B. subtilis</i> and clostridia	155
III.4. Protection against NO	156
III.5. Importance of O ₂ , ROS and NO detoxification pathways during colonization	157
IV. The role of σ^B and its targets during sporulation	158
IV.1. The negative role of σ^B in sporulation	158
IV.2. <i>sigB</i> expression in sporulating cells	158
IV.3. The hypothetical protective role of the σ^B -target genes	160
IV.3.a. Spore resistance	160
IV.3.b. Germination and Outgrowth	161
IV.3.c. Mother cell protection	161
V. Conclusion	163
Bibliography	164
Annexes	198
Article: The σ^B signalling activation pathway in the enteropathogen <i>Clostridium difficile</i>	199
Supplementary tables of the Article: CotL, a new morphogenetic spore coat protein of <i>Clostridium difficile</i>	234

Introduction

A



B

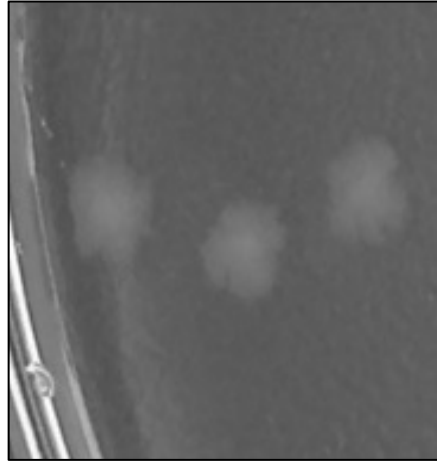


Figure 1: Morphology of *Clostridium difficile*. **A)** Phase-contrast microscopy image of *C. difficile* culture. **B)** *C. difficile* colonies on plate.

Chapter 1: The enteric pathogen *Clostridium difficile*

The human body contains a vast array of microorganisms but the highest density and diversity of microbial species inhabiting us is present in the intestine (10^{12-14} bacteria/gr in the colon). A typical human intestinal microbiota contains up to 1000 species of commensal, beneficial and pathogenic organisms (Qin et al. 2010). Most of these microorganisms belong to only two phyla: the Bacteroidetes (genus *Bacteroides*) and the Firmicutes (genus *Clostridium*, *Faecalibacterium*, *Lactobacillus*, *Ruminococcus*). Actinobacteria and Proteobacteria are also represented, but as minor constituents (Lozupone et al. 2012). A health-associated intestinal microbiota form a community that helps in food digestion, protects against enteropathogens and stimulate the immune system (Backhed et al. 2004, Littman and Pamer 2011, Stecher and Hardt 2011). The host, in turn, provides habitat and nutrients. Recent studies suggest that at least half of the bacterial genera found in the gut produce spores (Browne et al. 2016). Most of these spore formers present in gut correspond to clostridial species including *Clostridium difficile*.

I. *Clostridium difficile*

C. difficile is a gram-positive, toxin-producing and spore-forming anaerobe. *C. difficile* was identified and described for the first time in 1935 by Hall and O'Toole as part of the intestinal microflora in neonates (Hall and O'Toole 1935). At that time, the bacterium was described as an “actively motile, heavy-bodied rod with elongated subterminal or nearly terminal spores” (Figure 1A). This specie was named *Bacillus difficilis* to reflect the difficulties in its isolation and growth in the laboratory. *C. difficile* bacillus is between 3 and 15 μm long and 0.5 to 2 μm wide and colonies are opaque and irregular in Petri dish (Figure 1B). In 1970's, multiple studies provided evidence that *C. difficile* was the etiologic agent of antibiotic-associated diarrhea and colitis not only in animals, but also in humans (Carroll and Bartlett 2011). Nowadays, *C. difficile* is recognized as the leading cause of nosocomial antibiotic-associated diarrhea in developed countries (Smits et al. 2016). The development of *C. difficile* infection (CDI) is associated with different virulence factors, mainly with the release of two toxins, TcdA and TcdB, that play a crucial role in the pathogenicity of *C. difficile* (Voth and Ballard 2005, Aktories et al. 2017, Chandrasekaran and Lacy 2017).

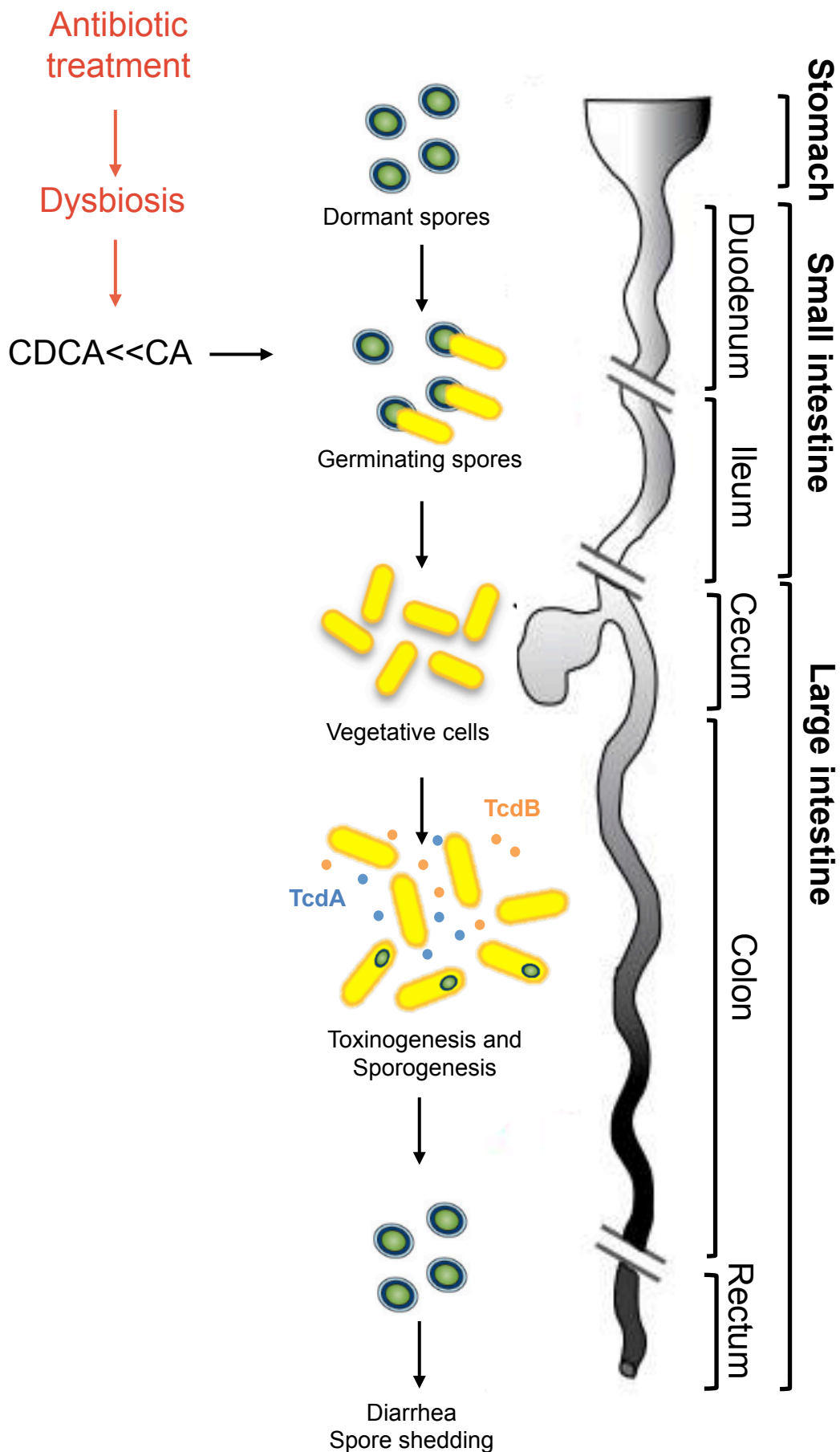


Figure 2: *C. difficile* life cycle in the gastrointestinal tract. Spores ingested from the environment survive to the acidic pH of the stomach and germinate in the small intestine. Antibiotic exposure induces dysbiosis, which creates a ratio of bile acids chenodeoxycholate (CDCA) vs cholate (CA) favorable for germination of the spores and growth of *C. difficile*. In the cecum and colon *C. difficile* produces toxins TcdA and TcdB and spores. The two toxins will cause severe damages to the epithelium and are the main direct causes of the disease symptoms. Shedding of the spores will allow their accumulation in the environment and the infection of new hosts.

C. difficile belongs to the cluster XI of clostridia with, among others, *Clostridium sticklandii* and *Clostridium sordelii* (Collins et al. 1994). In 2009, *C. difficile* and the related Cluster XI were reclassified into a family-level group, *Peptostreptococcaceae*, distinct from the current *Clostridiaceae* family. Later on, it was renamed *Peptoclostridium difficile* (Yutin and Galperin 2013). More recently, *C. difficile* was renamed *Clostridioides difficile* and is considered the type species of the genus *Clostridioides* (Lawson et al. 2016). For clarity in the manuscript, I will use the more familiar designation *Clostridium difficile* and *C. difficile*. The complete genome of *C. difficile* reference 630 strain was sequenced in 2006 (Sebahia et al. 2006). The chromosome is composed by 4 290 252 base pairs (bp) with a G+C content of 29%, and 3 776 coding sequences are present (Monot et al. 2011, Dannheim et al. 2017). *C. difficile* shares only 15% of its coding sequences with *Clostridium botulinum* and *Clostridium tetani*, and 50% of the coding sequences are unique to this bacterium. Moreover, 11% of the chromosome consists of mobile genetic elements (Sebahia et al. 2006). These mobile elements are responsible for the acquisition of genes that probably favors a better adaptation to the environment of the host's digestive tract, such as genes involved in resistance to antibacterial compounds, virulence or production of structures and surface proteins. For example, *C. difficile* resistance to antibiotics such as erythromycin, chloramphenicol or tetracycline is largely mediated by transposons present in the genome (Lyras et al. 2004, Hussain et al. 2005, Sebahia et al. 2006).

I.1. *C. difficile* infection cycle

C. difficile is transmitted via the oral-faecal route (Figure 2). Being a strict anaerobe, the vegetative form of *C. difficile* cannot survive in an oxygenated environment for long and is then unable to transmit the infection. The infectious potential of this bacterium is linked to its ability to produce spores that play a crucial role in *C. difficile* transmission and persistence (Deakin et al. 2012). Spores are metabolically inactive forms, highly resistant to extremes of temperature, desiccation, oxidative stress, antibiotics, the acidic environment of the stomach as well as to disinfectants such as hypochlorite and hydrogen peroxide used to eradicate and control dissemination (Nicholson et al. 2000, Baines et al. 2009, Oughton et al. 2009, Carroll and Bartlett 2011, Setlow 2014). *C. difficile* spores are widely distributed in the environment and can survive for long periods of time. They can be isolated from soil, water, food, hospital environment and the intestinal tract of both humans and domesticated animals (Weese 2010). When ingested, the spores survive the acidic pH of the stomach, and reach the intestine where

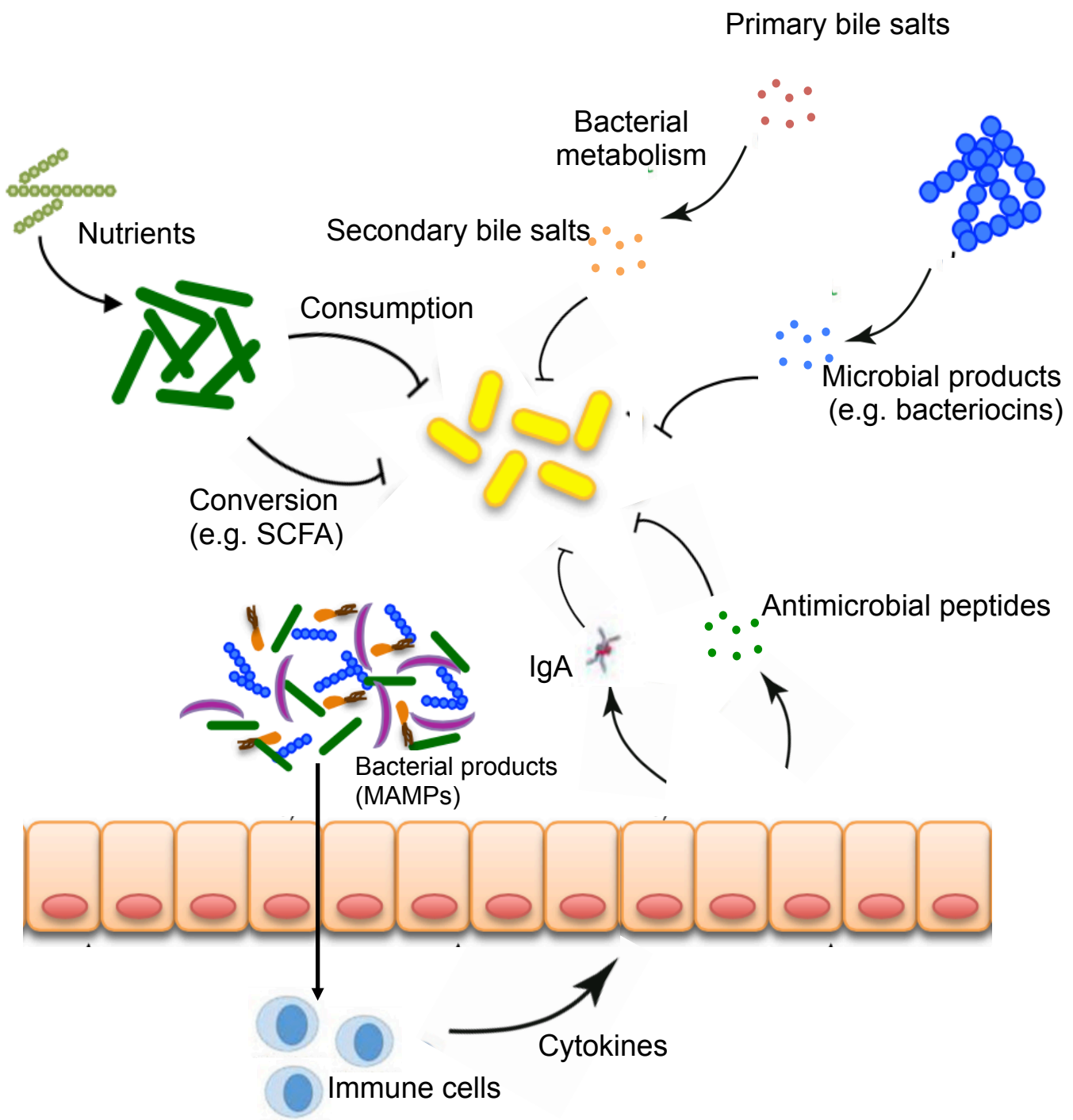


Figure 3: Potential mechanisms involved in colonization resistance against *C. difficile* in the gut. Direct inhibition of *C. difficile* by the gut microbiota can occur via the conversion of nutrients or host metabolites to compounds that are inhibitory to *C. difficile*, production of compounds with bacteriostatic activity (e.g. bacteriocins) and competition for nutrients. Indirect control of *C. difficile* expansion can occur via the stimulation of the host immune system through the production of microbial-associated molecular patterns (MAMPs). Detection of MAMPs by the host induces the activation of an host immune cascade and the production of innate (e.g. antimicrobial peptides) or adaptive (e.g. IgA) immune effectors. SCFA, short-chain fatty acids. Adapted from Britton and Young, 2012.

they are thought to attach to the epithelial cells in order to achieve efficient colonization. Indeed, recent studies have shown that attachment of the spore to the intestine seems to be essential for CDI development. Paredes-Sabja *et al* showed that the spore surface of *C. difficile* interacts with the surface of intestinal epithelial cells (Paredes-Sabja and Sarker 2012). More recently, it was demonstrated that the spore surface protein CotE enables binding of the spore to mucus by direct interaction with mucin (Hong *et al.* 2017). In the intestine, when the normal gut microbiota is disturbed, as during antibiotic treatment, the ratio of the bile acids derivatives cholate (CA) and chenodeoxycholate (CDCA) increases and the spores germinate (Sorg and Sonenshein 2008, Giel *et al.* 2010). Then vegetative cells multiply and colonize the cecum and the colon (Koenigsnecht *et al.* 2015). *C. difficile* will then produce the two major virulence factors: the TcdA and TcdB toxins (Carroll and Bartlett 2011). These two toxins will cause damage to intestinal epithelial cells and trigger a strong host inflammatory response that is responsible for diarrhea, colitis and colon perforation (Figure 2). In the large intestine, *C. difficile* also produces spores during infection that will be released into the environment during diarrheal episodes allowing transmission of *C. difficile* to a new host.

I.2. CDI risk factors and colonization resistance against *C. difficile*

The life cycle of *C. difficile* is strongly influenced by the gut microbiota of the host and its associated metabolites (Crobach *et al.* 2018, Samarkos *et al.* 2018). Individuals with a normal balanced microbiota are usually resistant to infection by *C. difficile* (Carroll and Bartlett 2011, Britton and Young 2012). This is because the microbial and metabolic environment of the gut is able to directly or indirectly prevent colonization by this pathogen (Figure 3) (Britton and Young 2012). One mechanism by which the gut microbiota prevents *C. difficile* invasion of the intestinal tract is via the transformation of bile acids (Figure 3 and 4). Humans secrete bile acids from cholesterol into the small intestine in response to consumption of meal. Two main primary bile acids are produced, CA and CDCA, that are conjugated to glycine or taurine amino acids (Figure 4). First, bile acids hydrolases produced by members of the intestinal microbiota deconjugate the bile acids from their amino acids in the intestinal lumen (Ridlon *et al.* 2006). Then, CA and CDCA are metabolized via the enzyme 7-dehydroxylase, into the secondary bile acids deoxycholate and lithocholate, respectively (Figure 4). This reaction is carried out by a small percentage of commensal bacteria such as *Clostridium scindens* (Wells and Hylemon 2000, Buffie *et al.* 2015). In fact, a

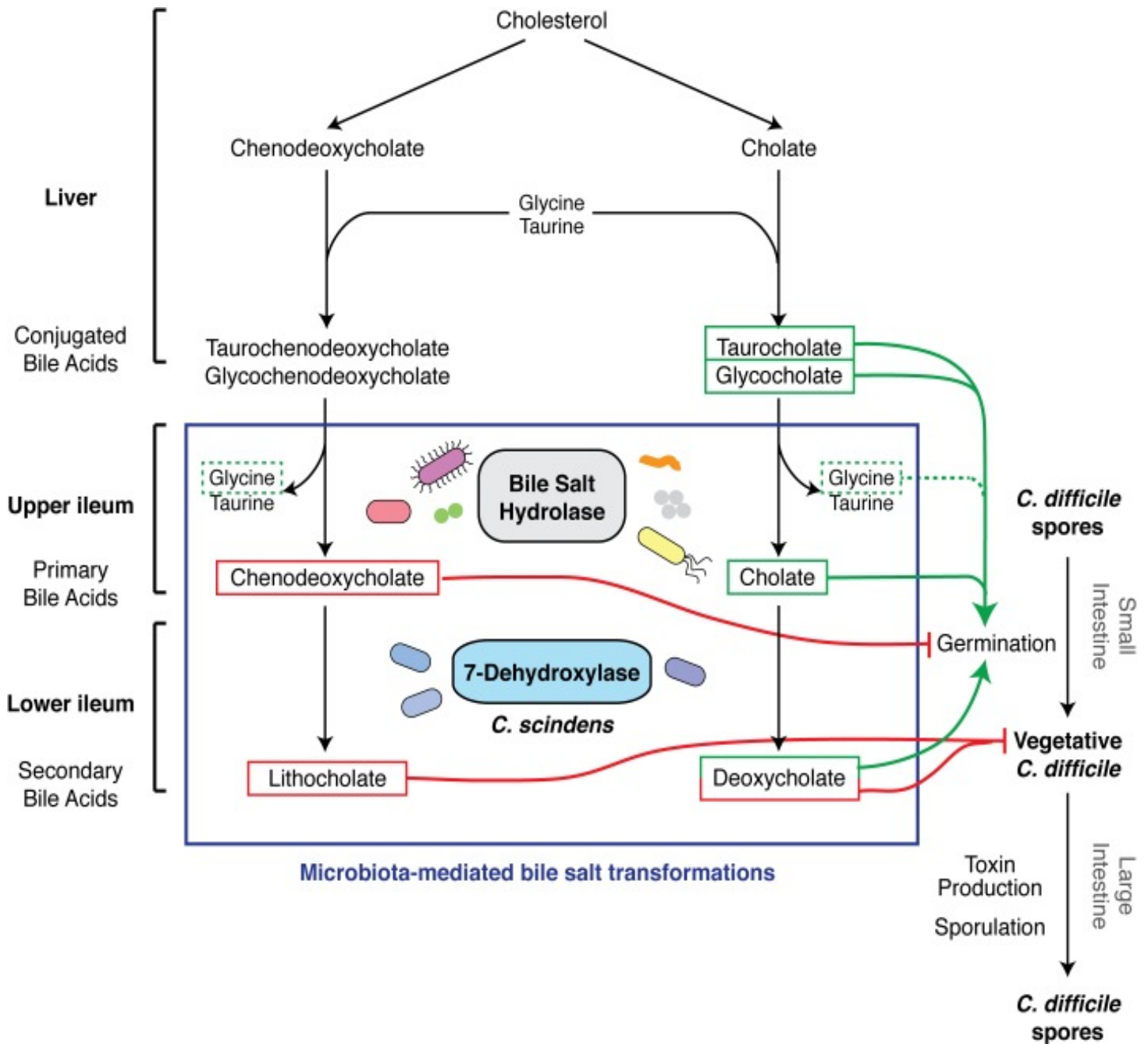


Figure 4: Effect of bile acid metabolism on the life cycle of *C. difficile*. The liver synthesizes bile acids from cholesterol and secretes them as conjugated bile acids. Ileum gut microbiota produces bile salt hydrolases that deconjugate bile acids to primary bile acids, chenodeoxycholate and cholate. Primary bile acids serve as substrates for 7-dehydroxylases, made by a small subset of clostridial organisms such as *C. scindens*, which generate secondary bile acids lithocholate and deoxycholate. Chenodeoxycholate and secondary bile acids are toxic to vegetative cells of *C. difficile* (red lines), while cholate derivatives promote germination when combined with amino acid co-germinants like glycine (dotted line). Shen *et al.*, 2015.

correlation between CDI resistance, the presence of *C. scindens* and elevated levels of secondary bile acids have been observed (Buffie et al. 2015). Combined with glycine, CA-derived bile acids such as taurocholate promote germination of *C. difficile* spores (Sorg and Sonenshein 2008). By contrast, CDCA inhibits spore germination and growth of *C. difficile* vegetative cells (Sorg and Sonenshein 2008, 2009), as well as the primary and secondary bile salt muricholates, which are present only in mice (Francis et al. 2013b). While deoxycholate found in humans and mice is a potent germinant, it is toxic, as the other secondary bile salts, for *C. difficile* vegetative cells (Sorg and Sonenshein 2008, Francis et al. 2013b). Therefore, in a healthy mouse or human host, intestinal microbiota promotes the presence of a small amount of primary bile salts and a high amount of secondary bile salts in the colon (Theriot and Young 2014, Buffie et al. 2015). This bile acids ratio leads a decrease in *C. difficile* spore germination and inhibition of vegetative cell growth (Figure 4) (Theriot et al. 2016). Antibiotic usage is the main risk factor for CDI (McFee 2009, Buffie et al. 2012) with the highest risk associated to the large spectrum antibiotics clindamycin, cephalosporins, penicillins, and fluoroquinolones (Slimings and Riley 2014, Spigaglia 2016). Indeed, in response to antibiotic treatment, the composition of the intestinal microbiota is strongly and differently altered (Theriot and Young 2014, Theriot et al. 2016). Treatment of mice with an antibiotic cocktail (ampicillin, gentamicin, metronidazole, neomycin and vancomycin) resulted in a decreased abundance of the Firmicutes phylum and increased persistence of Bacteroidetes and Proteobacteria (Hill et al. 2010). Other study, reported that after antibiotic treatment the gut community was dominated by the Proteobacteria phylum, *Enterobacteriaceae* family, whereas the Bacteroidetes and Firmicutes phyla only made up a small portion of the total population (Antonopoulos et al. 2009). In humans, studies defining the impact of antibiotherapy in the structure of the gastrointestinal tract are more limited. Antharam *et al* in 2013, compared fecal microbiota of healthy subjects and subjects with *C. difficile*-negative nosocomial diarrhea (CDN) or CDI. A decrease in bacterial diversity and species richness including *Ruminococcaceae*, *Lachnospiraceae* and butyrogenic bacteria was observed in the fecal microbiota of CDN and CDI patients compared to healthy controls (Antharam et al. 2013). A more recent study comparing the differences in gut microbiome among CDI patients, asymptomatic carriers and healthy individuals showed an overabundance of Proteobacteria in the two first groups, and a decrease in the abundance of Bacteroidetes and Firmicutes, especially butyrate producers was observed (Zhang et al. 2015). Antibiotic treatment results also in changes in the pools of certain metabolites. Among bile acids, Giel *et al* demonstrated that primary bile acids are the ones that predominant in the

mouse gut after antibiotic treatment (Giel et al. 2010). Moreover, it is known that CDCA, which inhibits germination, is absorbed by the small intestine 10 faster than the germinant CA of the *C. difficile* spores (Sorg and Sonenshein 2009). The increased amount of primary bile salts, promoting the germination of *C. difficile*, and the decreased level of secondary bile salts, which are toxic to *C. difficile*, favors the colonization of the digestive tract by this bacterium (Theriot et al. 2016). Antibiotherapy can also have an impact on certain bacteria from the microbiota that produces antimicrobial compounds that inhibit the growth of *C. difficile* (Figure 3). One example is the intestinal bacterium *Bacillus thurigiensis* that produces Thuricin CD, a bacteriocin with narrow spectrum activity against *C. difficile* (Rea et al. 2010). *C. scindens* and *Clostridium sordelli* secrete tryptophan-derived antibiotics, 1-acetyl- β -carboline and turbomycin A, respectively, that inhibit growth of *C. difficile* (Kang et al. 2018). Commensal bacteria may also contribute to inhibit *C. difficile* growth in the gut indirectly by mechanisms such as nutrient exhaustion or stimulation of the immune system. Gastrointestinal colonization of patients or hamsters by non-toxinogenic *C. difficile* strains can prevent colonization by toxinogenic *C. difficile* strains (Wilson and Sheagren 1983, Nagaro et al. 2013, Gerding et al. 2015). Also, the presence in the gut of microorganisms that consume simple sugars and sugars alcohols can reduce *C. difficile* colonization (Theriot and Young 2014, Fletcher et al. 2018). In fact, the antibiotic treatment decreases the level of glucose, free fatty acids and dipeptides. By contrast, sugar alcohols such as mannitol and sorbitol significantly increase after antibiotic treatment. Studies have also shown that a decreased microbial fermentation following antibiotic treatment, lowers the levels of short chain fatty acids (SCFAs) (Hoverstad et al. 1986b) and these conditions may provide a more favorable environment for *C. difficile* growth (Hoverstad et al. 1986a, Theriot and Young 2014). Finally, the commensal microbiota produces microbial associated molecular patterns (MAMPs) that stimulate the production of adaptative innate effectors by the host immune system preventing *C. difficile* expansion in the gut (Littman and Pamer 2011, Britton and Young 2012). Other risk factors to develop CDI exist, such as the number of administrated antibiotics, dose and duration of therapy. Previous hospitalization, use of proton pump inhibitors, inflammatory bowel disease and advanced age (>65 years), with the last case associated with a reduced efficacy of the immune system, are as well risk factors (Loo et al. 2011). All of them are associated with changes in the intestinal microbiota and ecosystem.

I.3. Epidemiology

C. difficile is a major cause of intestinal infection and diarrhea in individuals following antibiotic therapy (Rupnik et al. 2009, Smits et al. 2016). It is estimated that 7 to 17% of hospitalized patients carry toxinogenic strains of *C. difficile* (Poutanen and Simor 2004). CDI epidemiology has dramatically changed since the beginning of the 2000s. In the USA, between 2001 and 2010, the incidence of CDI among hospitalized adults approximately doubled (Reveles et al. 2014). *C. difficile* has become a major healthcare problem being responsible for half a million infections and 29.000 deaths each year, with a mortality rate estimated at 9.3% (Lessa et al. 2015). In Europe, the estimated number of cases is 124.000 per year (Zarb et al. 2012). However, CDI incidence is likely underestimated: on average, ~80 cases of CDI are missed per hospital per year in Europe (Davies et al. 2014). This is likely a result of a combination of factors such as the awareness of CDI among physicians and the type of methods/algorithm for CDI diagnosis implemented. In North America and in Europe, CDI outbreaks associated with increased severity of the disease and higher mortality rates are mainly linked to the emergence of strains belonging to the 027 ribotype and, to a lesser extent the 078 ribotype (Cartman et al. 2010, Smits et al. 2016). Potential mechanisms have been pointed for the increased severity of infections associated with 027 ribotype strains: increased toxin production (Warny et al. 2005), production of a binary toxin (Cowardin et al. 2016), fluoroquinolone resistance (He et al. 2013), increased efficiency of sporulation (Merrigan et al. 2010) and higher correlation with recurrent infection (Marsh et al. 2012). The duration of hospital stay resultant of CDI range from 2.7 to 21.3 days for hospital-acquired CDI (Gabriel and Beriot-Mathiot 2014).

Approximately 3%-4% of healthy adults are asymptotically colonized by *C. difficile*. High carriage rates (25-35%) are reported in infants (< 1 year of age) and the rate drops to 15% for ages 1-8 years (Enoch et al. 2011). However, infants are frequently asymptomatic carriers of *C. difficile*. This is thought to be related to an immature microbiome and immune system (Koenig et al. 2011, Backhed et al. 2015), protective maternal antibodies transferred in breast milk and/or the inability of the toxins to interact with the receptors and cause disease (Eglow et al. 1992, Rousseau et al. 2012). Recent epidemiological studies have shown increased rates of community-associated *C. difficile* disease, affecting groups not previously at risk (such as younger patients and patients who had no exposure to antibiotics in the 12 weeks before infection) (Khanna et al. 2012). In addition, *C. difficile* is frequently encountered in a diverse range of animals that includes both pets and those destined for

meat production such as pork, veal and horse (Gould and Limbago 2010, Alvarez-Perez et al. 2015, Warriner et al. 2017). To date, direct transmission of *C. difficile* from animals, food or the environment to humans is not clear. However, a recent study reported that asymptomatic farmers and their pigs can be colonized with clonal isolates of *C. difficile* 078, showing evidences that spread between animals and humans might occur (Knetsch et al. 2014). The increase incidence of community acquired *C. difficile* infection and the possible zoonotic transfer are a raising concern (Smits et al. 2016) and suggest additional and unrecognized risk factors for CDI.

I.4. Treatments of CDI

I.4.a. Conventional treatments

Initial therapy for CDI includes stopping the antibiotic therapy responsible for the emergence of *C. difficile*, if possible. If symptoms persist or worsen, antibiotic treatment against *C. difficile* is necessary. Metronidazole or vancomycin are used depending on the illness severity and co-morbidities. Metronidazole is the first line agent in the treatment of patients with mild-to-moderate CDI. Vancomycin is recommended for severe or complicated infections (Surawicz et al. 2013, Debast et al. 2014). Besides both antibiotics show similar cure rates in patients with mild-to-moderate infection, vancomycin is reserved for severe cases due to the growing concerns about antimicrobial-resistant microorganisms. In case of severe disease, vancomycin has higher cure rate (Kazanowski et al. 2014). One of the most challenging aspects of treating CDI is the recurrence of disease after a successful therapy. This makes recurrent CDI itself a significant risk factor. Recurrence can be caused by the initial infective strain or by spore reinfection from another strain acquired from the environment (Barbut et al. 2000). The risk increases significantly with each episode of recurrence: 20-30% after a first episode and up to 60% after a first recurrence (Shields et al. 2015). Treatment failures and recurrence of infection rates associated with the use of metronidazole and vancomycin were observed in the last years (Vardakas et al. 2012). Therefore, other antibiotics such as rifampicin and fidaxomicin have been proposed to treat CDI. Fidaxomicin became available for the treatment of CDI in 2011. This antibiotic has equivalent cure rates to vancomycin but lower rate of CDI recurrence (13% vs 25%) with strains other than 027 rybotype (Louie et al. 2011, Cornely et al. 2012). Contrary to vancomycin that has bacteriostatic activity against *C. difficile*, fidaxomicin is bactericidal (Kazanowski et al. 2014). Furthermore, it has a narrower spectrum compared to vancomycin

and metronidazole, and thus has a lower impact on the composition of the gut microbiota, in particular on *Bacteroides* species (Louie et al. 2012). However, the higher costs of fidaxomicin treatment compared to other therapeutic regimens may restrict its use. Alternative antimicrobials have been studied, such as the glycopeptide antibiotic teicoplanin. This compound has activity against Gram-positive anaerobes including *C. difficile*. A clinical trial has shown that teicoplanin was as effective as vancomycin and metronidazole for CDI. However, the higher cost associated with its use made it as a drug used for the treatment of repeated recurrences of CDI (Venugopal and Johnson 2012).

I.4.b. Faecal microbiota transplantation

The presence of *C. difficile*, either as an asymptomatic colonizer or as a pathogen, is associated with reduced microbiota diversity (Zhang et al. 2015). Similarly, patients with multiple episodes of CDI have a markedly reduced microbial diversity when compared to patients that suffered only a single episode of CDI (Chang et al. 2008). Thus, restoration of the complexity and diversity of the gut microbiota is required for *C. difficile* colonization resistance. Faecal microbiota transplantation (FMT) is a highly effective therapy that has gained much attention in the last years to treat recurrent CDI. The principle basis of FMT is that stools from a healthy donor contain a stable, viable, diverse and normal microbiota community. When introduced into the gut of a patient with CDI, they can restore their disrupted microbiota (Brandt 2012). Studies have shown that FMT resolves recurrent CDI in more than 90% of the cases (van Nood et al. 2013, Kelly et al. 2015b). A recent study on 18 patients shown a CDI healing rate of 94% after FMT (Konturek et al. 2016). Following successful transplantation, Bacteroidetes increased and Proteobacteria decreased in fecal microbiota (Seekatz et al. 2014). Interestingly, a recent study of five CDI patients showed that transfer of sterile filtrates from donor stool rather than fecal microbiota, was sufficient to eliminate symptoms. In most treated patients, the faecal filtrated transplantation was associated with a reduction of enterobacteracea. These results suggest that bacterial components, such as metabolites or bacteriophages might be sufficient but they cannot define the exact mechanism of action (Ott et al. 2017).

I.4.c. Immunotherapy

Since *C. difficile* TcdA and TcdB are the main factors responsible for CDI symptoms, most of the immune therapies that have been undertaken target these proteins. A monoclonal antibody raised against the toxin B, Zinplava, was recently approved by the FDA.

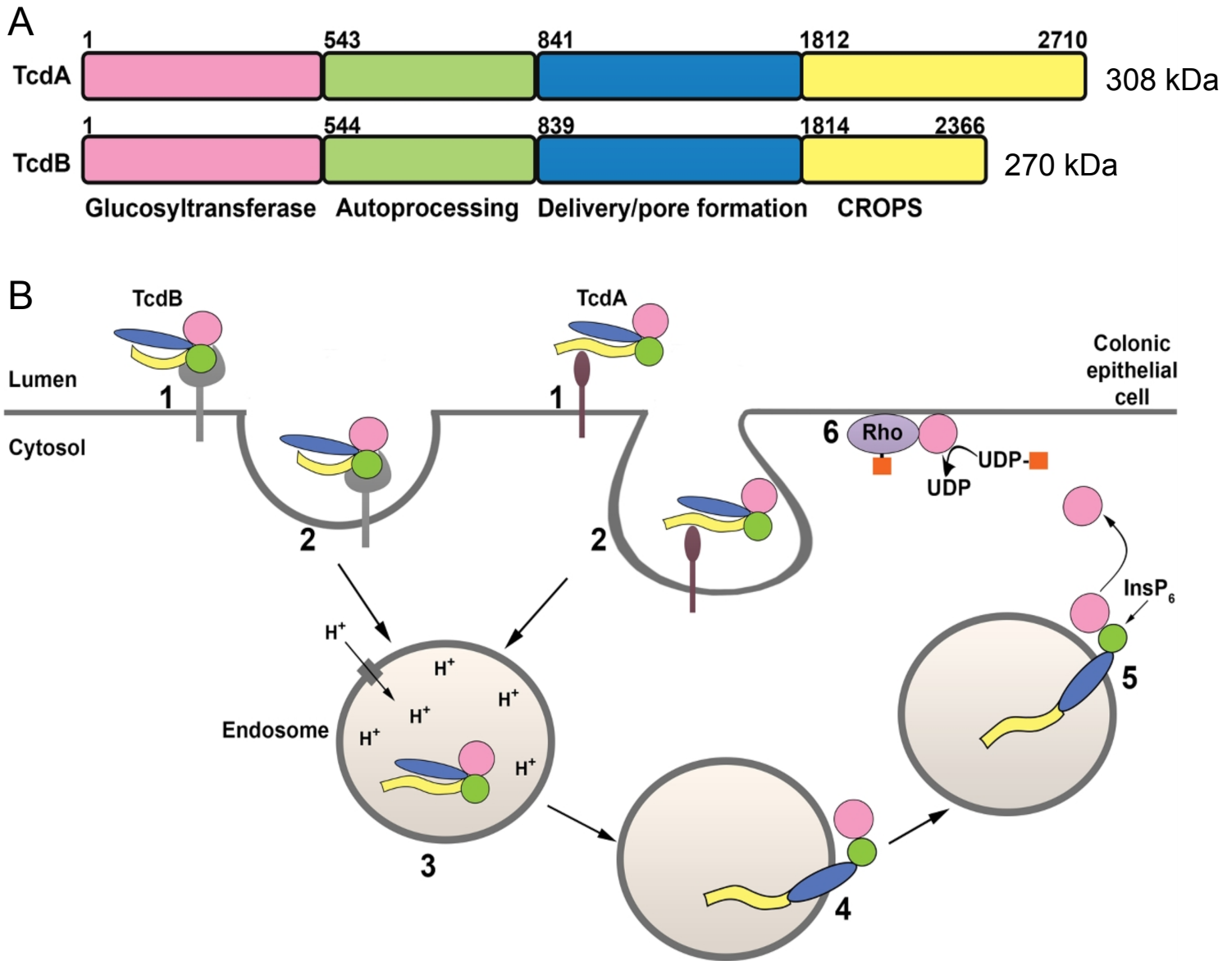


Figure 5: TcdA and TcdB primary structure and mechanism of action. A) TcdA and TcdB are organized into four functional domains: the glucosyltransferase domain (GTD; pink), the autoprocessing domain (APD; green), the delivery or pore-forming domain (blue) and the combined repetitive oligopeptides domain (CROPS; yellow). **B)** TcdA and TcdB bind different cell surface proteins or sugars on the colonic epithelium (step 1) and are internalized by distinct endocytic pathways (step 2). The toxins reach acidified endosomes (step 3) and the low pH triggers a conformational change in the toxin delivery domain, resulting in pore formation and translocation of the GTD (and likely the APD) into the cytosol (step 4). Inositol hexakisphosphate binds and activates the APD, resulting in the cleavage and release of the GTD (step 5). The GTD inactivates Rho family proteins by transferring the glucose moiety (orange squares) from UDP-glucose to the switch I region of the GTPase (step 6). Glucosylation disrupts GTPase signaling and leads to cytopathic ‘rounding’ effects and apoptotic cell death. Chandrasekaran and Lacy 2017.

Administration of Zinplava in combination with the standard antibacterial drugs (metronidazole, vancomycin or fidaxomicin) resulted in a lower rate of CDI recurrence (Wilcox et al. 2017). An antibody raised against toxin A (Actoxumab) was also developed but it provided no additional benefit over Zinplava. Active immunization has been also tested. An oral vaccination trial has been performed with spores of *Bacillus subtilis* expressing TcdA peptide repeats, which confer protection in a hamster model after challenge with the *C. difficile* 630 strain (Permpoonpattana et al. 2011a).

II. Virulence factors and colonization in *C. difficile*

II.1. The TcdA and TcdB toxins

II.1.a. Mechanism of action of TcdA and TcdB

C. difficile colonization can lead to asymptomatic carriage, or a wide range of symptoms, from mild diarrhea, abdominal pain, fever and leucocytosis, to more severe symptoms such as pseudomembranous colitis, toxic megacolon, bowel perforation, sepsis and death (Dawson et al. 2009, Rupnik et al. 2009). These symptoms are mainly caused by the large toxins TcdA and TcdB (Voth and Ballard 2005, Aktories et al. 2017, Chandrasekaran and Lacy 2017). The expression of the genes encoding TcdA (308 kDa) and TcdB (270 kDa) toxins is induced during stationary growth phase when nutrients become limited (Hundsberger et al. 1997). TcdA and TcdB have four domains: an N-terminal glucosyltransferase (GDT) domain that inactivates members of the Rho family of small GTPases (small regulatory proteins of the eukaryote actin cell cytoskeleton) by glucosylation; an autoprocessing (ADP) domain; a delivery/pore forming domain and a receptor-binding (CROPS) domain (Figure 5A). These domains contribute to a multistep mechanism of intoxication (Figure 5B). Once released, TcdA and TcdB bind to specific receptors on intestinal epithelial cells and are internalized by specific endocytic pathways. TcdA surface receptors are not clearly identified, however, TcdA is able to bind to glycoproteins such as Gp96 in the human colonocytes (Na et al. 2008) and to the sucrose-isomaltase located in the brush border of small intestines (Pothoulakis et al. 1996). After the identification of CSPG4 as a receptor for TcdB, two other reports were published showing that NECTIN3 (also termed poliovirus receptor-like protein (PVRL3)) and frizzled proteins 1, 2 and 7, function as colonic epithelial receptors for TcdB (LaFrance et al. 2015, Tao et al. 2016). The low pH in the endosome triggers a conformational change in the toxin delivery domain resulting in pore

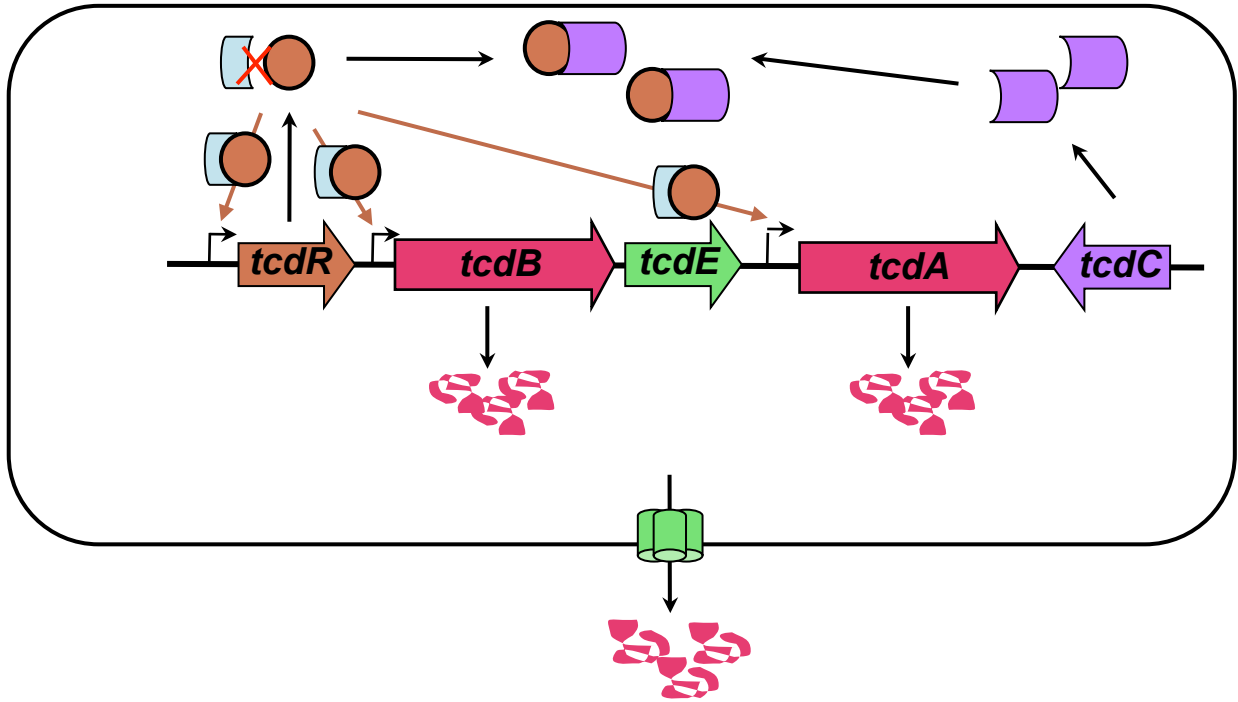


Figure 6: *C. difficile* pathogenicity locus (PaLoc). Both *tcdA* and *tcdB* genes are encoded on the 19.6-kb pathogenicity locus (PaLoc), together with *tcdR*, *tcdC* and *tcdE* genes. TcdR is an alternative sigma factor required for the transcription of *tcdA*, *tcdB* and *tcdR* itself. TcdC is an anti-sigma factor which sequesters TcdR preventing the transcription of the toxin genes. TcdE is a "holin" type bacteriophage protein required for toxin secretion.

formation that allows translocation of the GDT across the endosome membrane. GTD is autoprocessed and released to the cytosol where it catalyzes the glucosylation and hence the inactivation of Rho- and Ras- GTPases rendering them inactive (Just et al. 1995a, Just et al. 1995b). Consequences of this are disorganization of the cytoskeleton, cell rounding and eventually cell death by apoptosis (Figure 5B) (Warny et al. 2000, Nottrott et al. 2007). TcdB also induces necrosis by triggering the production of reactive oxygen species (ROS) through the assembly of the NADPH oxidase (NOX) complex on endosomes (Farrow et al. 2013). High levels of ROS promote cellular necrosis likely through DNA damage and protein oxidation. Additionally *C. difficile* toxins stimulate the production of pro-inflammatory cytokines by colonic epithelial cells which lead to an innate inflammatory response with neutrophil recruitment (Voth and Ballard 2005). Inflammation of the colon occurs with massive fluid loss into the large intestine, clinically presenting as diarrhea (Voth and Ballard 2005, Jank et al. 2007, Chandrasekaran and Lacy 2017). Despite the development of genetic tools, the relative contribution of the TcdA and TcdB in the pathogenesis of *C. difficile* is still relatively controversial. The combined deletion of both TcdA and TcdB completely abolish *in vivo* virulence (Kuehne et al. 2010, Kuehne et al. 2014). In order to understand the respective role of each toxin in the virulence process, a study performed in 2009 showed that TcdB, unlike TcdA, is essential for the virulence of *C. difficile* (Lyras et al. 2009). However, another study demonstrated that the presence of either TcdA or TcdB alone is sufficient to cause death in the hamster (Kuehne et al. 2010, Kuehne et al. 2014), suggesting that both toxins are capable of inducing disease. In agreement, some strains isolated from patients with classical symptoms of CDIs have been found to produce either TcdA or TcdB (Carter et al. 2012, Monot et al. 2015). Nevertheless, it appears that TcdB toxin is more important in the activation of the host immune system and the inflammatory response (Carter et al. 2015).

II.1.b. Regulation of *tcdA* and *tcdB* expression

The genes *tcdA* and *tcdB* encoding respectively TcdA and TcdB, are located in the 19.6-kb pathogenicity locus (PaLoc) (Figure 6) (Braun et al. 1996). In most non-toxigenic strains, the PaLoc is replaced by a 75–115 nucleotide non-coding sequence, while a 7.2-kb sequence of unknown function has been also found in some Tox⁻ strains (Braun et al. 1996, Monot et al. 2015). The PaLoc also carries three additional genes: *tcdE*, *tcdR* and *tcdC* (Figure 6). TcdE is a holin-like protein whose pore-forming activity is involved in the release of toxin (Govind and Dupuy, 2012). However the role of TcdE in the toxin secretion has been controversial (Govind and Dupuy 2012, Olling et al. 2012, Govind et al. 2015, Monot et al.

2015). Indeed, Olling et al., showed that toxin secretion was not affected by inactivation of the *tcdE* gene (Olling et al. 2012). Recently, it has been demonstrated that in response to specific environmental conditions toxin release is also mediated by an autolysin (Cwp19) and is associated by autolysis (Wydau-Dematteis et al. 2018). In addition they showed that both TcdE and bacteriolysis are coexisting mechanism for toxin release according to the growth condition. TcdR-encoding gene is positively regulated by σ^D , the σ factor controlling flagellum synthesis (El Meouche et al. 2013, McKee et al. 2013). TcdR is an alternative sigma factor that interacts with the core enzyme of the RNA polymerase (RNAP) to specifically recognize and activate transcription of toxin genes. TcdR also positively controls its own expression (Mani and Dupuy 2001). Finally, TcdC is an anti-sigma factor that negatively regulates toxin gene expression by interfering with the ability of the TcdR-containing RNAP to recognize the *tcdA* and *tcdB* promoters (Matamouros et al. 2007, Dupuy et al. 2008, Carter et al. 2011). Toxin expression is regulated by growth conditions and metabolic changes (Figure 7) (Martin-Verstraete et al. 2016). In fact, the presence of rapidly metabolizable carbon sources imported by the phosphotransferase-like system (PTS) such as glucose, fructose and mannitol represses the expression of toxin encoding genes (Dupuy and Sonenshein 1998). These repression is mediated by CcpA, the global regulator of the carbon catabolic repression system (Deutscher et al. 2006). CcpA interacts directly with the promoter region of several PaLoc genes, with the strongest affinity for the promoter region of *tcdR* (Antunes et al. 2012). The global transcriptional repressor CodY, which is involved in the adaptive response to nutrient deficiencies during entry in stationary phase, is responsible for the repression of toxin genes during the exponential growth phase (Dineen et al. 2007). The affinity of CodY to its targets genes is increased in the presence of branched-chain amino-acids (BCAA) and GTP (Ratnayake-Lecamwasam et al. 2001, Shivers and Sonenshein 2004). In these conditions, CodY negatively regulates toxin gene expression by binding to the *tcdR* promoter region (Dineen et al. 2007). Finally, in addition to the BCAAs, amino acids like proline, glycine and cysteine have a significant inhibitory effect on toxin production (Karlsson et al. 1999, Dubois et al. 2016). The impact of cysteine on *tcdA* and *tcdB* expression is mediated by the σ factor σ^L . σ^L is involved in the metabolism and virulence of Gram-positive bacteria (Okada et al. 2006). However, the absence of a consensus sequence for σ^L upstream of the PaLoc genes suggests an indirect effect on toxin expression. In *C. difficile*, σ^L controls the degradation of cysteine into pyruvate and sulfides, compounds that negatively affect the expression of toxins when they are added to the culture medium (Dubois et al. 2016). Since toxin production and sporulation take place during transition growth phase, the

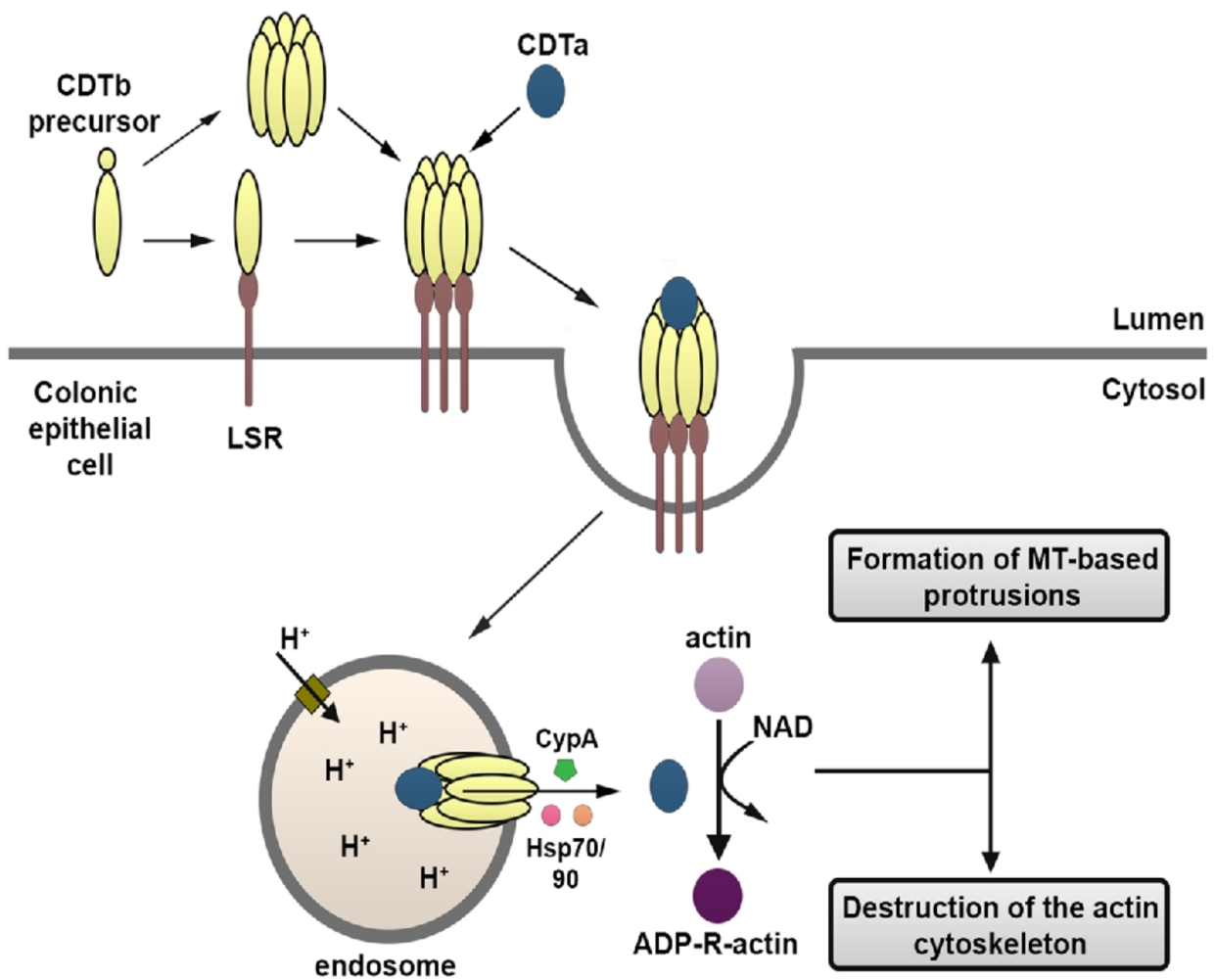


Figure 8: Schematic representation of the mechanism of action of CDT. The monomeric form of CDTb binds to its cell surface receptor, LSR. Thereafter, CDTb undergoes proteolytic activation and oligomerization on the cell surface. This process might also occur before binding. The oligomeric prepore binds CDTa, and the receptor-CDT complex is subsequently internalized into cells. As the endosome matures, the acidic pH triggers conformational changes in CDTb, resulting in membrane insertion and formation of a pore through which CDTa is translocated into the cytosol. Translocation of CDTa is facilitated by heat shock protein 70 (Hsp70), Hsp90 and cyclophilin A (CypA). In the cytosol, CDTa ADP-ribosylates actin at arginine-177. ADP-ribosylation of actin results in the eventual breakdown of the actin cytoskeleton and cytopathic cell rounding, and the formation of microtubule-based protrusions that enhance bacterial adherence. Chandrasekaran and Lacy 2017.

connection between the two mechanisms was studied (Underwood et al. 2009). The inactivation of *sigH*, coding for the key σ factor of the phase transition, results in increased expression of toxin encoding genes (Saujet et al. 2011). In addition, inactivation of the master regulator of sporulation *spo0A*, results in the upregulation of *tcdA* gene (Underwood et al. 2009, Pettit et al. 2014). The absence of the binding domain of Spo0A in the promoter region of toxin genes, suggests that Spo0A controls indirectly toxin genes transcription probably via one of the other factors that control toxin gene expression (Dineen et al. 2010, Antunes et al. 2011, Bouillaut et al. 2013). More recently, new links between sporulation and toxin synthesis have been demonstrated (Figure 7). RstA, a Rap-like protein, positively controls sporulation and negatively regulates toxin production (Edwards et al. 2016b). RstA negatively influences toxin production by repressing the transcription of *sigD*. Indeed, the inactivation of *rstA* leads to an increased expression of *sigD* and of σ^D -controlled genes (Edwards et al. 2016b).

II.2. The binary toxin CDT

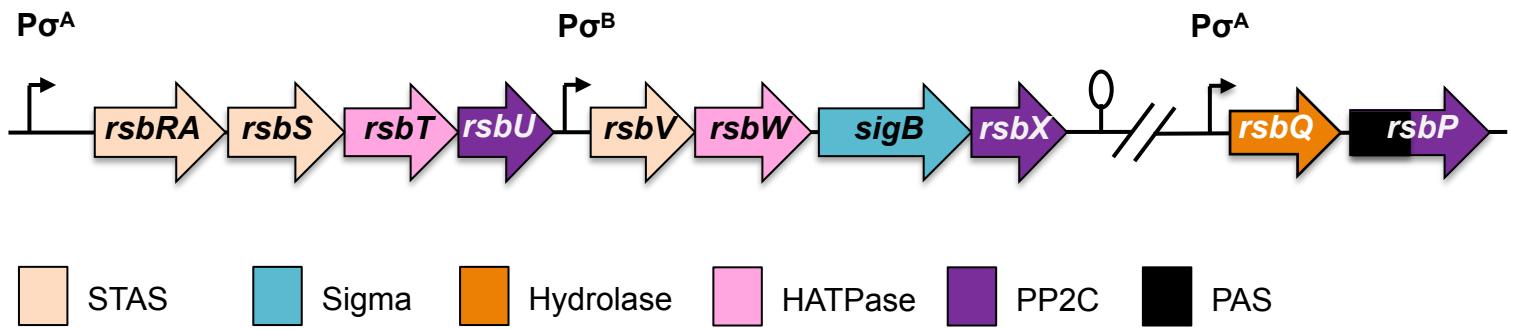
Some *C. difficile* strains, as those of PCR ribotypes 027 and 078, also produce a third toxin called *C. difficile* transferase CDT (Aktories et al. 2018). CDT belongs to the family of binary actin ADP-ribosylating toxins and is encoded by two genes, *cdtA* and *cdtB* located on a 6.2-kb chromosomal region (named the Cdt locus or CdtLoc). A third gene, *cdtR*, located in the same locus, encodes a regulator that positively controls CDT production (Carter et al. 2007) and in some *C. difficile* clinical strains regulates TcdA and TcdB production (Lyon et al. 2016). CDT-negative toxigenic strains typically contain a 2-kb deletion within the CdtLoc (Stare et al. 2007). As binary toxin, the CDTb component (100 kDa) binds to its membrane receptor, the lipolysis-stimulated lipoprotein receptor (LSR) (Figure 8). Then, proteolytic activation of CDTb occurs, which is necessary for oligomerization and formation of a heptamer. Alternatively, the monomeric form of CDTb may undergo proteolytic activation and oligomer formation before binding to LSR. Then, the catalytic component CDTa (50 kDa) interacts with CdtB and the LSR-CDT complex is endocytosed reaching an acidic endosomal compartment. The acidic pH of the endosome triggers conformational changes in CDTb, resulting in membrane insertion and formation of a pore that allows CDTa translocation to the cytosol. This process is supported by cytosolic chaperones such as the heat shock protein 70 (Hsp70), Hsp90 and cyclophilin A (CypA). In the cytosol, CDTa ADP ribosylates monomeric actin and this inhibits actin polymerization. Furthermore, depolymerization of actin favors the formation of microtubule-based protrusions that enhance adherence and colonization of *C.*

difficile (Figure 8) (Schwan et al. 2009, Chandrasekaran and Lacy 2017, Aktories et al. 2018). The environmental signals that regulate CDT production and the mechanism of toxin secretion have not yet been studied.

II.3. Other virulence factors: the colonization factors

Like many enteric pathogens, the vegetative cells of *C. difficile* are likely associate with the intestinal mucosa to begin the process of host colonization and establish infection. Therefore, adherence and motility must be important factors contributing to colonization efficiency and virulence of this pathogen (Awad et al. 2014). Studies have shown that *C. difficile* vegetative cells are able to bind to intestinal epithelial cells and, *in vitro*, interact with apical microvilli of differentiated Caco-2 cells (Eveillard et al. 1993, Karjalainen et al. 1994, Cerquetti et al. 2002). Moreover, the vegetative cells can also adhere *in vivo* to the mucosal epithelium of hamsters or mice (Borriello et al. 1988). The cell surface of *C. difficile* is covered by adhesion factors such as the S-layer proteins that facilitate binding to epithelial cells and to components of the extracellular matrix such as fibrinogen, laminin, fibronectin and collagen (Cerquetti et al. 2002, Spigaglia et al. 2013). It was shown that adherence of *C. difficile* to epithelial cells is greatly reduced on cell monolayers when they are pre-incubated with purified SlpA proteins, the major components of the S-layer (Merrigan et al. 2013). Several other proteins located at the cell surface play a role in adherence to intestinal epithelial cells: i.e., cell wall protein, such as Cwp66 with adhesive properties (Waligora et al. 2001); the fibronectin-binding protein Fbp68 (Hennequin et al. 2003); the lipoprotein CD0873 involved in adhesion to Caco2 cells (Kovacs-Simon et al. 2014) and the flagella composed of the flagellin FliC and the flagellar cap protein FliD, which are involved in mucus attachment (Tasteyre et al. 2001), and (iv). The role of FliC and FliD in adhesion to Caco-2 cells differs according to *C. difficile* strains. Indeed, the inactivation of *fliC* and *fliD* genes in the 630 Δ erm strain increased cell adhesion and virulence (Dingle et al. 2011, Baban et al. 2013) while the same inactivation in strain R20291 (ribotype 027) decreases adhesion (Baban et al. 2013).

A



B

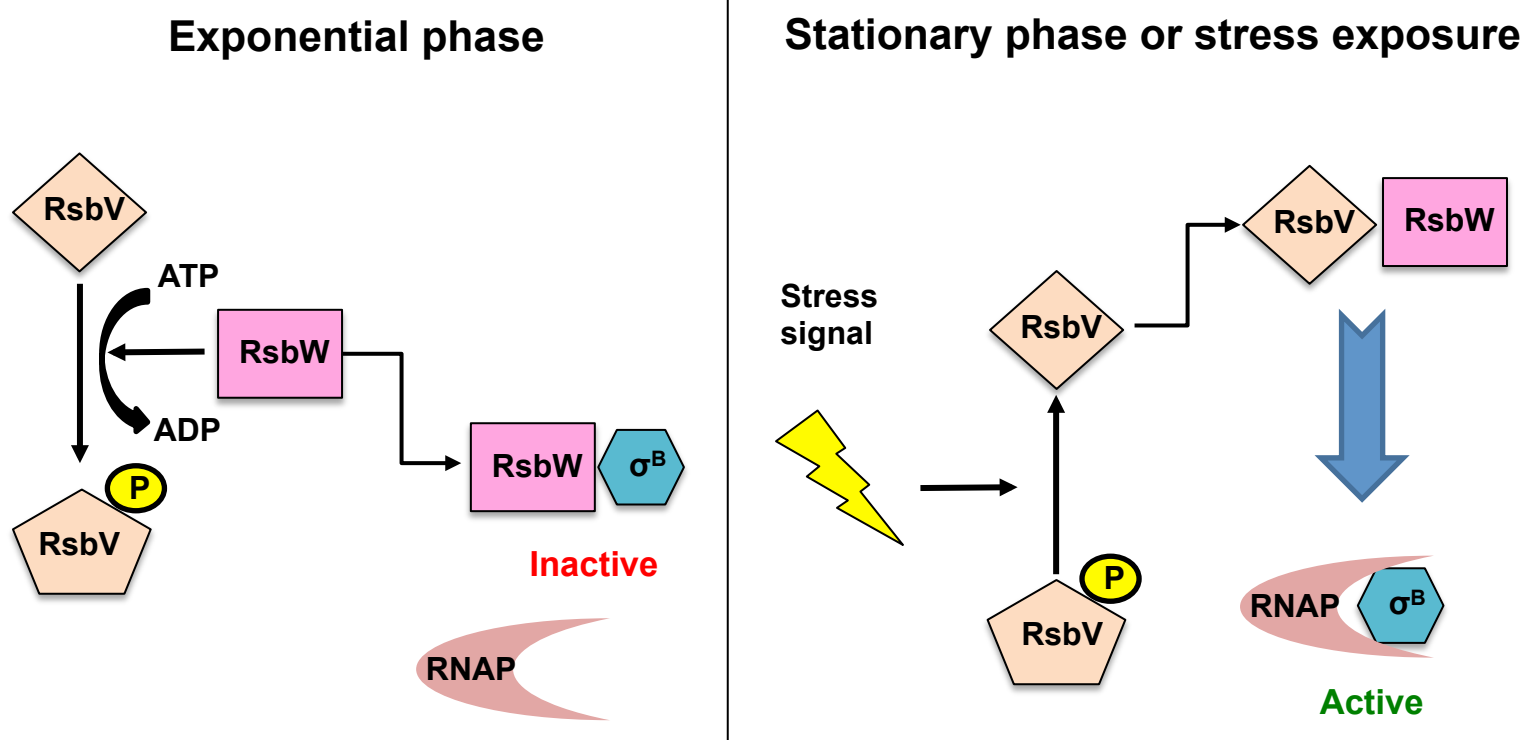


Figure 9: Organization of the *B. subtilis* *sigB* operon, genes encoding different regulators and model of σ^B activation. A) Open reading frames (arrows) and transcriptional start sites with promoters are indicated. Structurally and functionally conserved domains are color coded. Abbreviations: STAS (domain found in sulfate transporters and anti-sigma factor antagonists), Sigma (sigma factor), HATPase (kinase domain of two-component transmitter proteins), PP2C (Mn^{2+}/Mg^{2+} -dependent protein phosphatase 2C), PAS (Per-ARNT-Sim signal sensor domain implicated in the perception of redox, voltage, and/or, light signals). Adapted from Hecker et al., 2007. **B)** Partner switching mechanism involved in σ^B activation. In unstressed cells and during the exponential growth phase, the anti-sigma factor, RsbW, phosphorylates the anti-anti sigma, RsbV, and sequesters σ^B rendering it inactive. During stationary growth phase or after stress exposure, the non-phosphorylated form of RsbV interacts with RsbW, allowing σ^B release, its association with the RNA polymerase and transcription of its target genes.

Chapter 2: The stress response and the role of σ^B

I. Stresses encountered during gut infection

Pathogenic bacteria experience diverse stresses while spreading to and colonizing new hosts to cause infection. Enteric pathogens when ingested, must survive to the acidic pH of the stomach (Foster 1999). Within the intestinal lumen, bacteria encounters other stresses such as bile salts, free fatty acids, pH variations, hyperosmolarity, antibiotics, antimicrobial peptides and changing oxygen (O_2) tensions (Guiney 1997). Moreover, host inflammatory responses recruit phagocytic cells which subject pathogens to oxidative and nitrosative stress (Fang 2004). To survive to this hostile environment, bacteria have to develop mechanisms to sense these stresses and trigger appropriate responses that can allow their survival. Bacteria respond by altering their transcriptome and proteome in an adaptative manner.

II. σ^B , the alternative sigma factor of general stress response

The most effective response to a wide range of stresses and starvation conditions in several Firmicutes is mediated by σ^B , the alternative sigma factor of general stress response (Hecker et al. 2007). The σ^B -dependent responses are conserved in the genera *Bacillus*, *Staphylococcus*, *Listeria* and in a few clostridia. The *sigB* gene is usually associated with genes encoding the anti-anti-sigma factor, RsbV, and the sigma-factor, RsbW involved in the control of σ^B activity through a well-conserved post-translational mechanism, called partner switching (Alper et al. 1996).

II.1 σ^B in *B. subtilis*

II.1.a The role of σ^B and the mechanism of its activation

In *B. subtilis*, σ^B , RsbV, and RsbW are encoded within an eight-gene operon that is expressed constitutively from a σ^A -dependent promoter present upstream of *rsbRA* (Figure 9A) (Kalman et al. 1990, Wise and Price 1995). However, an internal σ^B -dependent promoter enhances expression of the four last genes of the operon (*rsbV*, *rsbW*, *sigB*, and *rsbX*) when σ^B is active (Kalman et al. 1990, Benson and Haldenwang 1993b). σ^B activity is controlled by a post-translational mechanism, in which interaction and activation of proteins are driven by

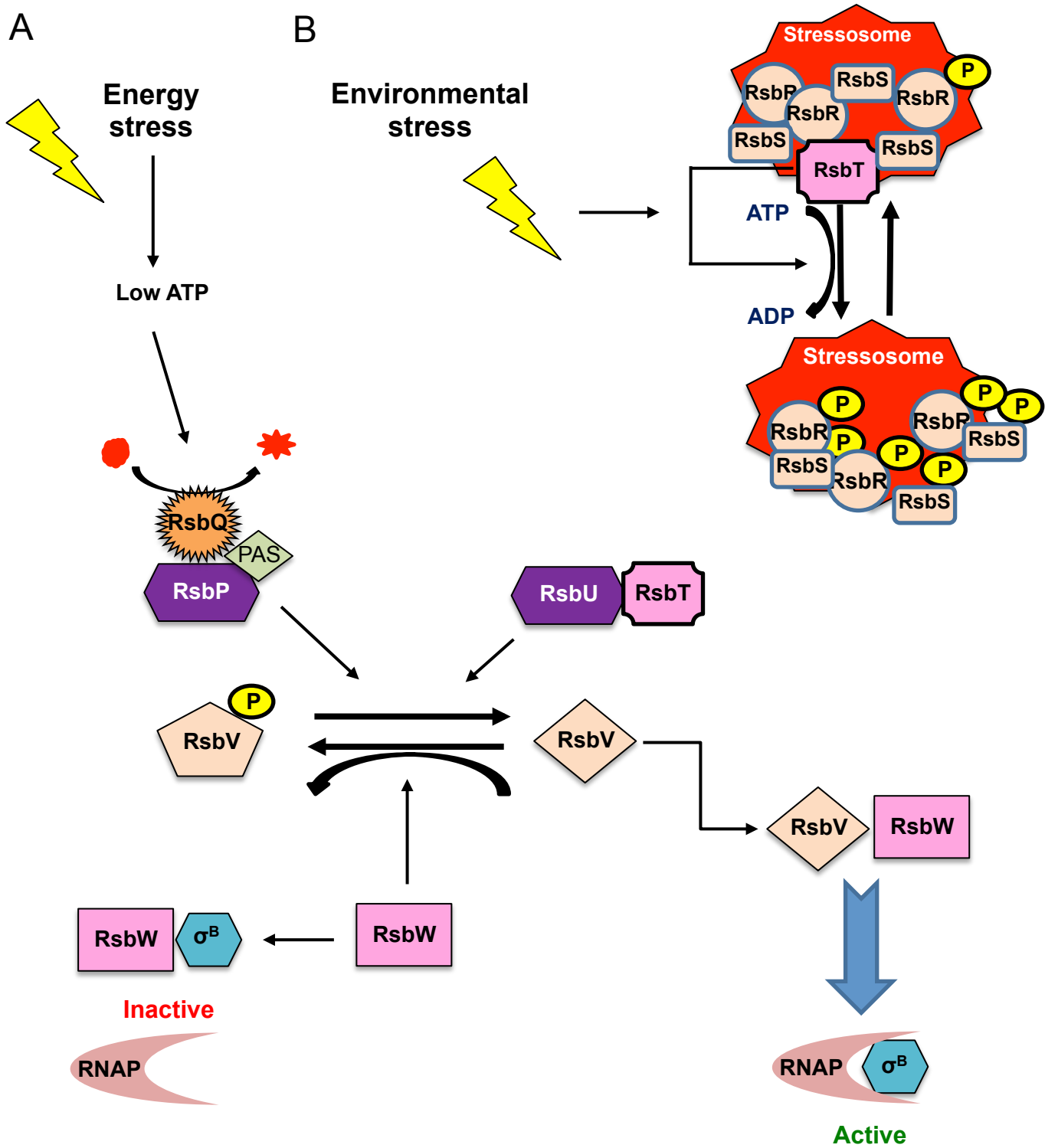


Figure 10: Model of the signal transduction leading to the activation of σ^B in *B. subtilis*.
A) Energy-stress mediated activation of RsbP phosphatase. **B)** Environmental stress-mediated activation of RsbT and its subsequent release from the stressosome.

reversible threonine and serine phosphorylation (Figure 9B) (Yang et al. 1996, Hecker et al. 2007). In fact, the phosphorylated state of the anti-anti-sigma factor, RsbV, is the key element of σ^B activation or silencing (Alper et al. 1996). In unstressed cells and during the exponential growth phase, the kinase RsbW, phosphorylates RsbV and sequesters as an anti-sigma factor, σ^B thereby preventing its association with the RNA polymerase (Benson and Haldenwang 1993a). When cells are exposed to a stress or in the stationary phase, a signal is transmitted to specific PP2C phosphatase(s) that dephosphorylate(s) RsbV and allows interaction of RsbV with RsbW, leading to the release and activation of σ^B (Figure 9B). The σ^B -containing holozyeme will ensure the recognition of appropriate promoters upstream of the controlled genes and their transcription.

II.1.b. The signal transduction pathway responsible for the activation of σ^B

Stress signals triggering phosphatase activation and σ^B release depend on the bacterial species. Stress stimuli include both high and low temperatures, salt, ethanol, acidic pH, hydrogen peroxide (H_2O_2), nitric oxide (NO), irradiation with blue light, presence of antibiotics inducing cell wall stress, and starvation for glucose, phosphate or O_2 . The carbonyl cyanide *m*-chlorophenylhydrazone (CCCP), which cause a deprivation of ATP and GTP levels can also triggers σ^B activation (Benson and Haldenwang 1993c, Boylan et al. 1993, Price et al. 2001, Helmann et al. 2003, Mascher et al. 2003, Moore et al. 2004, Zhang and Haldenwang 2005, Avila-Perez et al. 2006, Gaidenko et al. 2006, Hecker et al. 2007, Avila-Perez et al. 2010). In *B. subtilis*, σ^B can be activated via two main signaling pathways that respond to energy depletion or environmental stresses (Figure 10). For example, deficiency in glucose, phosphate, O_2 limitation or entry in stationary phase induces gene expression in a σ^B -dependent manner. All these conditions lead to a decrease in the amount of intracellular ATP (Maul et al. 1995, Antelmann et al. 2000, Hecker et al. 2007). Therefore, addition of CCCP or a high concentration of Mn^{2+} or Mg^{2+} (competitor ions used as a cofactor in ATP-generating reactions) that decreases the intracellular concentration of ATP increases the expression of σ^B -controlled genes (Voelker et al. 1996a, Zhang and Haldenwang 2005). RsbP is an RsbV-specific phosphatase that together with RsbQ senses energy limitation (Figure 10A). In addition to its catalytic PP2C-phosphatase domain, RsbP contains a PAS domain essential for its activity (Vijay et al. 2000). PAS domains are known to control interaction with other proteins, to detect changes in the energy level of the cells, or to sense the redox potential, light or O_2 concentration. Two models have been proposed for the RsbP activation (Nadezhdin et al. 2011). In the first model, RsbQ converts a small molecule into a product delivered to the

PAS domain of RsbP resulting in its conformational change. In the second model, RsbQ is directly associated with the PAS domain of RsbP and the transformation of a small molecule generates a conformational change in the PAS domain. In both cases, the conformational modification of the PAS domain activates the RsbP PP2C-phosphatase, which dephosphorylates RsbV~P, resulting in the activation of σ^B (Brody et al. 2009, Nadezhdin et al. 2011). In *B. subtilis*, environmental stresses that activate σ^B are recognized by a multicomponent protein complex, the stressosome, which transmits the signal to another PP2C-phosphatase, RsbU (Figure 10) (Voelker et al. 1996b, Yang et al. 1996). In growing cells, RsbU is inactive. Activation of RsbU is dependent on the binding and stimulation by the kinase, RsbT. However, under growing conditions, RsbT is captured by its antagonist RsbS. Together with RsbS and RsbR, RsbT is part of the stressosome. Upon environmental stress, the kinase activity of RsbT is stimulated by an unknown mechanism, and the stressosome components, RsbR and RsbS, are phosphorylated. Their phosphorylation promotes the dissociation of the RsbS-RsbT complex, releasing RsbT from the stressosome (Figure 10B) (Yang et al. 1996) and allows its association with RsbU. When bound to RsbT, the RsbU phosphatase domain is activated leading to the dephosphorylation of RsbV~P and the activation of σ^B . Finally, a third pathway of σ^B activation occurs during continuous growth at low temperature (Brigulla et al. 2003). However, this activation, which is RsbV-independent, is not yet well characterized.

II.2. Diversity of the mechanism of σ^B activation in other Firmicutes

Interestingly, while the role of RsbV and RsbW in σ^B activation is highly conserved, both signal and factors regulating σ^B activation upstream of RsbV differ considerably among Firmicutes. RsbQ and RsbP involved in sensing-energy branch are confined to *B. subtilis*. In *L. monocytogenes*, the pathway of σ^B activation by environmental stress such as acidic pH, osmotic and heat stresses, is similar to that observed in *B. subtilis* with the presence of the RsbRST proteins and a stressosome (Becker et al. 1998, Ferreira et al. 2001, Smith et al. 2013). Even if *L. monocytogenes* lacks RsbP and RsbQ, ATP depletion induces σ^B activity in an RsbT-dependent manner indicating that environmental and energy signals seem to be detected by the same pathway in this bacterium (Chaturongakul and Boor 2004, 2006). In *L. monocytogenes*, as in *B. subtilis* (Figure 9A), the *rsbVW-sigB-rsbX* genes are transcribed by a σ^B and *rsbRSTU* genes located upstream of *rsbV* are expressed from a σ^A -dependent promoter (Wise and Price 1995, Ferreira et al. 2004). In *S. aureus*, the stressosome components RsbR,

RrbS and RsbT as well as the proteins involved in the energy pathway, RsbP and RsbQ, are missing. Accordingly, depletion of ATP or an ethanol stress, triggering σ^B activation in *B. subtilis*, do not activate σ^B in *S. aureus* (Pane-Farre et al. 2006). In *S. aureus*, the activation of σ^B , which only involves RsbU, RsbV and RsbW (Giachino et al. 2001, Senn et al. 2005), is mainly activated upon entry into stationary phase or in the presence of alkaline stress (Giachino et al. 2001, Pane-Farre et al. 2006, Pane-Farre et al. 2009). Nevertheless, the mechanisms allowing the activation of RsbU in these conditions remain unknown. In this bacterium, the *rsbUWW-sigB* operon is transcribed from a σ^A -dependent promoter located upstream of *rsbU* and a σ^B -dependent promoter is present upstream of *rsbV* (Senn et al. 2005). In *B. cereus* group (*B. cereus*, *B. anthracis*, and *B. thuringiensis*), the absence of correlation between intracellular level of ATP and σ^B activation suggest that σ^B is not activated by energy depletion. In *B. cereus*, σ^B is activated during heat or osmotic shock and after ethanol exposure (van Schaik et al. 2004). This bacterium uses another phosphatase protein, RsbY and a sensor protein RsbK different from RsbQ and RsbT suggesting a specific mechanism of sensing environmental stresses (van Schaik et al. 2004, van Schaik et al. 2005). Despite differences in the *sigB* operon structure, all of these Firmicutes have a σ^B -dependent positive-feedback loop that regulates the transcription of the *sigB* and *rsb* genes.

II.3. The σ^B regulon

Large-scale transcriptomic and proteomic studies have been made to determine the genes controlled by σ^B . The σ^B regulon of *B. subtilis*, *L. monocytogenes* and *S. aureus* consists in approximately 150 genes positively regulated by σ^B (Petersohn et al. 2001, Price et al. 2001, Bischoff et al. 2004, Pane-Farre et al. 2006, van Schaik et al. 2007, Raengpradub et al. 2008, Oliver et al. 2010, Nannapaneni et al. 2012, Mujahid et al. 2013, Guldemann et al. 2016, Mader et al. 2016). Some σ^B -controlled genes are directly involved in the management of stresses, whereas others participate in various cellular processes such as metabolism, cell envelope homeostasis, biofilm formation and virulence (Guldemann et al. 2016). In addition, σ^B also positively and negatively controls the expression of genes encoding many regulators (about 20 in *B. subtilis*) and then indirectly regulates expression of their target genes and the adaptive responses associated. For example, σ^B transcribes the gene encoding the global regulator MgsR, which controls the expression of a sub-regulon involved in the oxidative stress response in *B. subtilis* (Reder et al. 2008). Among the MgsR targets is the transcriptional regulator NsrR involved in NO response resulting in a complex regulatory

cascade.

In bacilli, σ^B controls key functions involved in the response to heat, acid, starvation, NO or osmotic stress (Hecker et al. 2007, Nannapaneni et al. 2012, Reder et al. 2012b). In *Listeria*, σ^B participates in the responses to acid, oxidative, and energy stresses (Wiedmann et al. 1998, Ferreira et al. 2001, Chaturongakul and Boor 2004). In *S. aureus*, σ^B appears also to control cell wall metabolism, membrane transport and resistance to several clinically important antibiotics, such as methicillin and vancomycin (Pane-Farre et al. 2006, Schulthess et al. 2009). Indeed, overexpression or over-activation of σ^B induces in some *S. aureus* strains increased cell wall thickness and promotes increased resistance against teicoplanin, vancomycin and other antibiotics targeting bacterial wall like β -lactams (Bischoff and Berger-Bachi 2001, Morikawa et al. 2001, Schulthess et al. 2009). In addition, the phenotypes of a *sigB* mutant differ depending on the bacterial species, (Ferreira et al. 2001, Giachino et al. 2001, Bandow et al. 2002, Zhang et al. 2011, Reder et al. 2012c). The growth and survival of a *sigB* mutant of *B. subtilis* or *L. monocytogenes* is affected in presence of high osmolarity, low pH or high temperature (Volker et al. 1999, Ferreira et al. 2001, Wemekamp-Kamphuis et al. 2004). In agreement, σ^B of *B. subtilis* controls the transcription of genes required for the uptake of solutes (*opuD* and *opuE*) mediating osmoprotection (von Blohn et al. 1997), while in *L. monocytogenes*, many identified σ^B -controlled genes participate in the stress response to acidification (e.g., *gadCB*, *gadD*) or exposure to bile salts (e.g., *bsh*, *opuC*, *bilE*). This supports that σ^B is involved in multiple protective mechanisms against the challenges faced by *L. monocytogenes* during gastrointestinal infection and food processing (Sue et al. 2003, Sleator et al. 2005). An ethanol sensitivity for a *sigB* mutant is observed only in *B. subtilis* (Volker et al. 1999) while *sigB* inactivation in *B. cereus* causes a decreased temperature resistance (van Schaik et al. 2004). σ^B is also involved in the oxidative-stress response in *B. subtilis*, *L. monocytogenes* and *S. aureus*. Indeed, the viability of a *sigB* mutant of *L. monocytogenes* and *S. aureus* decreases when exposed to H_2O_2 or H_2O_2 -donor compounds (Ferreira et al. 2001, Cebrian et al. 2009). In *B. subtilis*, the *sigB* mutant is more sensitive to oxidative stress when cells are pre-adapted to a stress such as glucose starvation known to induce the activity of σ^B before exposure to H_2O_2 or paraquat (a superoxide donor) (Engelmann and Hecker 1996, Reder et al. 2012c). This was consistent with genes positively controlled by σ^B in *B. subtilis* encoding the KatB, KatX and YdbD catalases as well as thioredoxin TrxA, involved in thiol homeostasis (Scharf et al. 1998, Petersohn et al. 2001, Price et al. 2001). Moreover the gene encoding the Dps protein involved in DNA protection is

also controlled by σ^B (Antelmann et al. 1997, Wang et al. 2009b). However, the role of σ^B in the response to an NO stress stimuli is much less clear. Indeed, in *B. subtilis*, even if sodium nitroprusside (SNP), a NO donor or NO gas induces the expression of some σ^B -controlled genes under aerobic conditions (Moore et al. 2004, Rogstam et al. 2007), a *sigB* mutant is not more sensitive to SNP (Rogstam et al. 2007). Finally, in addition to stress response, σ^B can regulate the expression of virulence genes. A *sigB* mutant of *L. monocytogenes* shows a reduced virulence in a murine model, which suggested a role of σ^B in the pathogenesis of this bacterium (Wiedmann et al. 1998, Nadon et al. 2002). In fact, σ^B positively controls the expression of genes encoding the internalins InlA and InlB, which are involved in the internalization of this bacterium through interaction with E-cadherin or the Met and gC1qR receptors (Mengaud et al. 1996, Kazmierczak et al. 2003, Kim et al. 2005, Garner et al. 2006, McGann et al. 2007). In *S. aureus*, several genes involved in virulence seem to be under σ^B control including genes encoding several adhesins (Bischoff et al. 2004, Entenza et al. 2005).

As observed for the signaling pathway, considerable differences exist among species concerning the functions regulated by this alternative σ factor. In Firmicutes, the role of the σ^B regulon may have evolved to probably facilitate bacterial survival according with the lifestyle, the niche colonized and the stresses encountered by each species.

II.4. The role of σ^B in *C. difficile*

Not all Firmicutes have the *sigB*, *rsbV* and *rsbW* genes in their genome and σ^B is absent in most of the clostridia. The *sigB* gene is present only in the genome of a few clostridia including *C. thermocellum*, *C. cellulolyticum* (Cluster III), and in the members of the *Peptostreptococaceae* family such as *C. difficile*.

C. difficile encounters several stresses during all steps of the infectious cycle. First, in environment, spores face atmospheric O₂ (around 21% O₂) or disinfectant used for their eradication. Once ingested by the host, they are exposed to the acidic pH of the stomach and after germination in the gut, the *C. difficile* vegetative cells are exposed to antibiotics, bile salts, variations in pH or osmolarity and to cationic antimicrobial peptides (CAMPs) produced by the host and/or by the microbiota (Abt et al. 2016a). Indeed, several factors synthesized by *C. difficile* during infection (toxins, S-layer, flagellin) trigger inflammation, leading to the production of CAMPs but also of reactive oxygen and nitrogen species (ROS and RNS) that generate with the O₂ tension near the intestinal epithelium hostile growth conditions for this

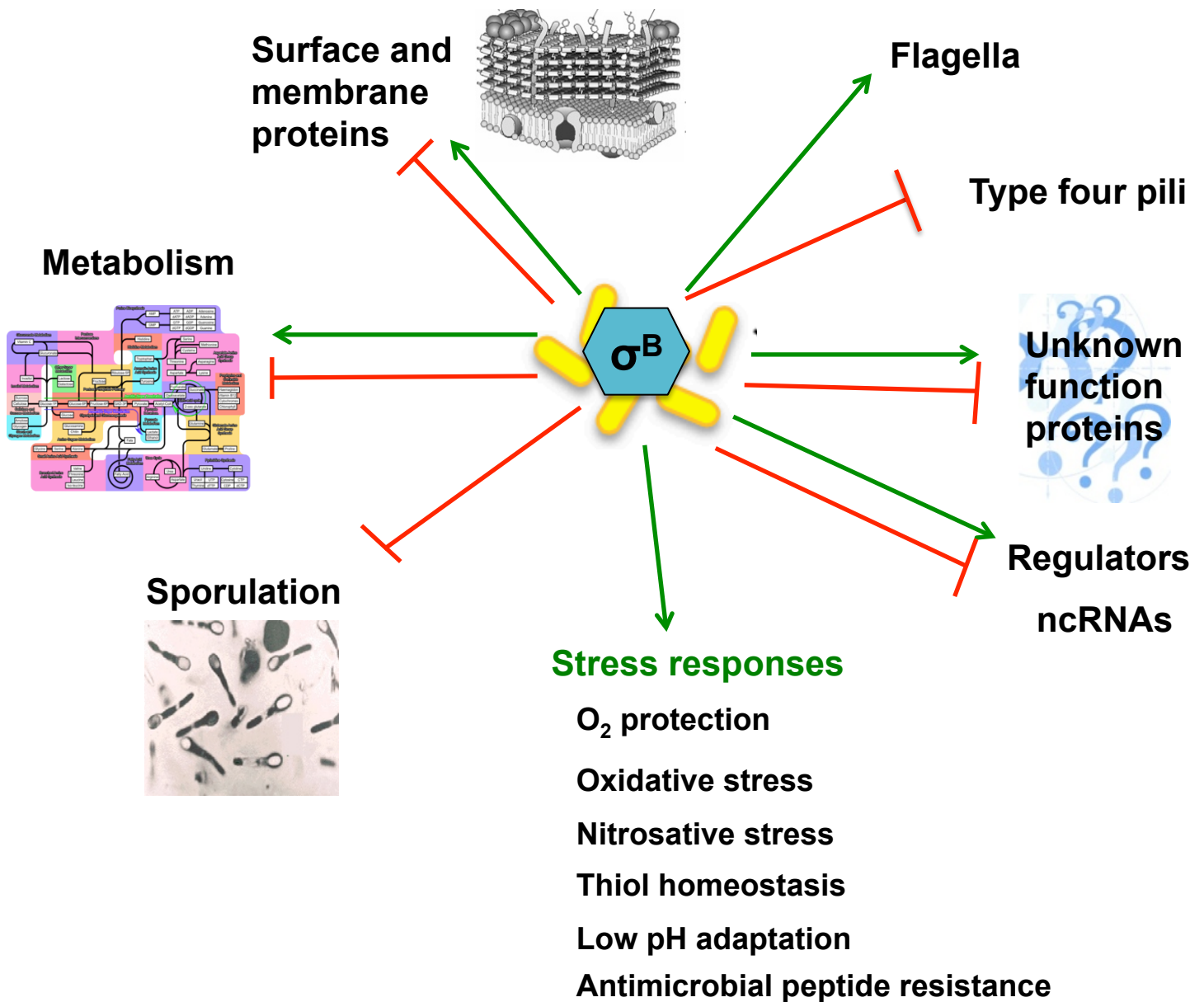


Figure 11: *C. difficile* σ^B has a pleiotropic role. Red and green arrows indicate respectively positive and negative control of σ^B under the different processes. σ^B positively regulates the expression of several genes involved in the management of stresses found by *C. difficile* during gut colonization: e.g. oxygen tolerance, oxidative and nitrosative stress, thiol homeostasis, low pH adaptation and antimicrobial peptide resistance.

strict anaerobic bacterium (see more in detail Chapter 3, section II. O₂ and ROS detoxification in *C. difficile*). To survive and ensure effective colonization of the digestive tract, *C. difficile* have to develop mechanisms to adapt to these conditions. Until recently, very little information was known about the responses developed by *C. difficile* against the different stresses encountered. Nowadays, we know that σ^B is crucial for the physiology of *C. difficile*, as for other Firmicutes, and its infectious cycle. σ^B positively and negatively controls the expression of about 1000 genes of *C. difficile* (about ~25% of genes) including genes involved in metabolism, motility, sporulation, cell surface biogenesis and stress management (Figure 11) (Kint et al. 2017). It was noted that 410 genes are positively controlled by σ^B corresponding to the largest number of genes when compared to the other Firmicutes (Bischoff et al. 2004, Nannapaneni et al. 2012, Guldimann et al. 2016, Mader et al. 2016).

Kint *et al.*, showed that a *sigB* mutant of *C. difficile* is more sensitive to acidification and CAMPs as well as to toxic compounds produced by the immune system such as H₂O₂, superoxide anion or NO (Kint et al. 2017). Moreover, it was shown for the first time in this bacterium, that σ^B plays a crucial role in O₂ tolerance. In agreement, σ^B positively controls genes encoding proteins potentially involved in O₂, ROS and NO detoxification. This includes *CD1157* and *CD1623* encoding flavodiiron proteins, two genes (*CD1125* and *CD0837*) encoding nitro-reductases, *CD0827* encoding a desulfoferrodoxin, *CD1474* and *CD1524* encoding reverse-rubrythrins, and *CD0176* encoding a protein similar to NADH-oxidoreductase (NADH-OR) supporting an important role of σ^B in the management of oxidative and nitrosative stress. This σ factor also controls thiol homeostasis and iron-sulfur clusters (Fe-S) biogenesis. Genes encoding proteins involved in thiol protection (*CD1690*- a thioredoxin (Trx), and *CD1822*- a thiol-peroxidase) and biogenesis of Fe-S centers (*CD1279* and *CD3670*, cysteine desulfurases) are also positively controlled by σ^B . These functions are important for maintenance of the metabolic activity of anaerobes that uses many Fe-S containing enzymes (Meyer 2000) and for counteracting the effects of oxidizing compounds.

In the proximal colon, the pH can reach acidic levels due to short-chain fatty-acid production (Nugent et al. 2001). The growth of the *sigB* mutant being severely affected at pH 5.0 suggests that σ^B controls, at least partly, genes involved in the acidic stress management and allow the *C. difficile* vegetative cells to cope with pH variations along the intestinal tract. However, the molecular mechanisms underlying the adaptation to acidic stress have yet to be elucidated in *C. difficile*. Additionally, σ^B seems to participate in the cell envelope homeostasis by controlling the expression of several genes encoding membrane- and cell

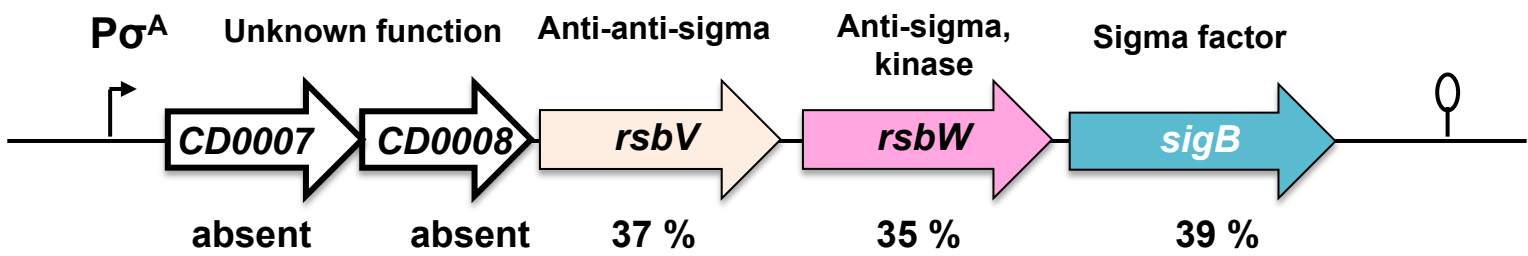


Figure 12: Organization of the *C. difficile* *sigB* operon. Open reading frames (arrows) and the transcriptional start site with the promoter recognized by σ^A are indicated. The function of proteins encoded by each gene is indicated above each gene. Percentage of identity with the *B. subtilis* proteins is indicated below each gene.

wall-associated proteins such as the S-layer precursor (*slpA*), autolysin (*CD2767-cwp19*) and putative autolysin (*CD2784-cwp6*) and two adhesins (*CD2831* and *CD3246*) anchored to the peptidoglycan. Proteins involved in cell wall metabolism are also controlled by σ^B . Importantly, *C. difficile sigB* mutant has a significant colonization defect in the axenic mouse when competing with the wild-type strain (Kint et al. 2017). The decreased ability of the *sigB* mutant to manage stresses encountered during gut colonization is probably responsible in part for the colonization defect. Moreover the control by σ^B of the genes encoding cell surface-associated proteins, whose some of them are involved in adhesion (Janoir 2016), might explain the failure to detect cells of the *sigB* mutant associated with the caecal mucosa. These results suggest a contribution of this sigma factor in the ability of *C. difficile* to adhere to intestinal cells (Kint et al. 2017). In conclusion, σ^B has been proposed as a key regulator of gut colonization by coordinating several processes likely required for adaptation, stress management and survival of bacteria within the gut (Kint et al. 2017).

II.4.a. Characterization of the σ^B signaling pathway in *C. difficile*

In *C. difficile*, *sigB* (*CD0011*) is the last gene of a five-gene operon that contains the genes encoding RsbV (*CD0009*) and RsbW (*CD0010*) (Figure 12). The two first genes of the operon, *CD0007* and *CD0008*, encode two small proteins of unknown function. RsbV and RsbW of *C. difficile* share 35% and 39% of identity with RsbV and RsbW of *B. subtilis*, respectively. In other firmicutes, genes near *sigB* gene usually encode proteins involved in the signaling pathway leading to the activation of σ^B (Hecker et al. 2007). However, in *C. difficile*, such proteins involved in the activation of σ^B are still unknown. I have participated in the study of the signaling pathway leading to the activation of σ^B in *C. difficile* in collaboration with Nicolas Kint (Kint *et al.*, in preparation; see Article in Annex). In this study, my main contribution was on the analysis of the expression of the *sigB* gene and its activity during vegetative growth, using transcriptional fusions and fluorescence microscopy (Kint *et al.*, in Annex).

Conservation of the partner switching mechanism

In this study, Nicolas Kint showed that the partner switching mechanism described in other Firmicutes (Figure 9B) is conserved in *C. difficile*. RsbW interacts with both RsbV and σ^B . Moreover, the overexpression of *rsbW* or the inactivation of *rsbV* increased the sensitivity of *C. difficile* to NO-donor compounds and decreased the tolerance to low O₂ tension. These phenotypes are reminiscent of those previously observed in the *sigB* mutant (Kint et al.

2017), confirming the involvement of these two proteins in σ^B activation. As in other Firmicutes, σ^B is kept inactive by RsbW (Figure 9B). In the presence of a stress signal, RsbV is dephosphorylated, binds to RsbW leading to the release of σ^B and the transcription of its targets. No obvious role for CD0007 and CD0008 was observed in σ^B activation under the tested conditions. The inactivation of *CD0007* and *CD0008* genes had no impact on the sensitivity of *C. difficile* to low O₂ tension or NO-donor compounds and did not modify the expression of σ^B -target genes at the onset of the stationary phase.

Players and signals in the activation of σ^B

The dephosphorylation of RsbV leading to the activation of σ^B is usually mediated by specific PP2C phosphatase(s) (Louie et al. 2009, Tannock et al. 2010, Petrella et al. 2012). The *C. difficile* genome encodes two PP2C phosphatases: CD2685 of unknown function, and CD3490 coding a phosphatase sharing 50% similarity with SpoIIE from *B. subtilis*, which is involved in early steps of the sporulation process. The inactivation of the *CD3490* gene (E. Cuenot, unpublished result) leads to an inability to sporulate suggesting a conservation of the function of this protein in *C. difficile*. In this study, CD2685, named RsbZ, was identified as a member of the signalling pathway responsible for *C. difficile* σ^B activation. RsbZ was shown to interact with RsbV and to dephosphorylate it, leading ultimately to the activation of σ^B . The *rsbZ* mutant has the same phenotype in terms of NO sensitivity and tolerance to low O₂ tensions as the *sigB* mutant (Kint et al. 2017). Moreover, the expression of σ^B -target genes decreased when the *rsbZ* gene was inactivated. In addition to its phosphatase domain, RsbZ has a GAF domain. The GAF domain of RsbZ might be involved in the detection of nutritional stresses in *C. difficile*.

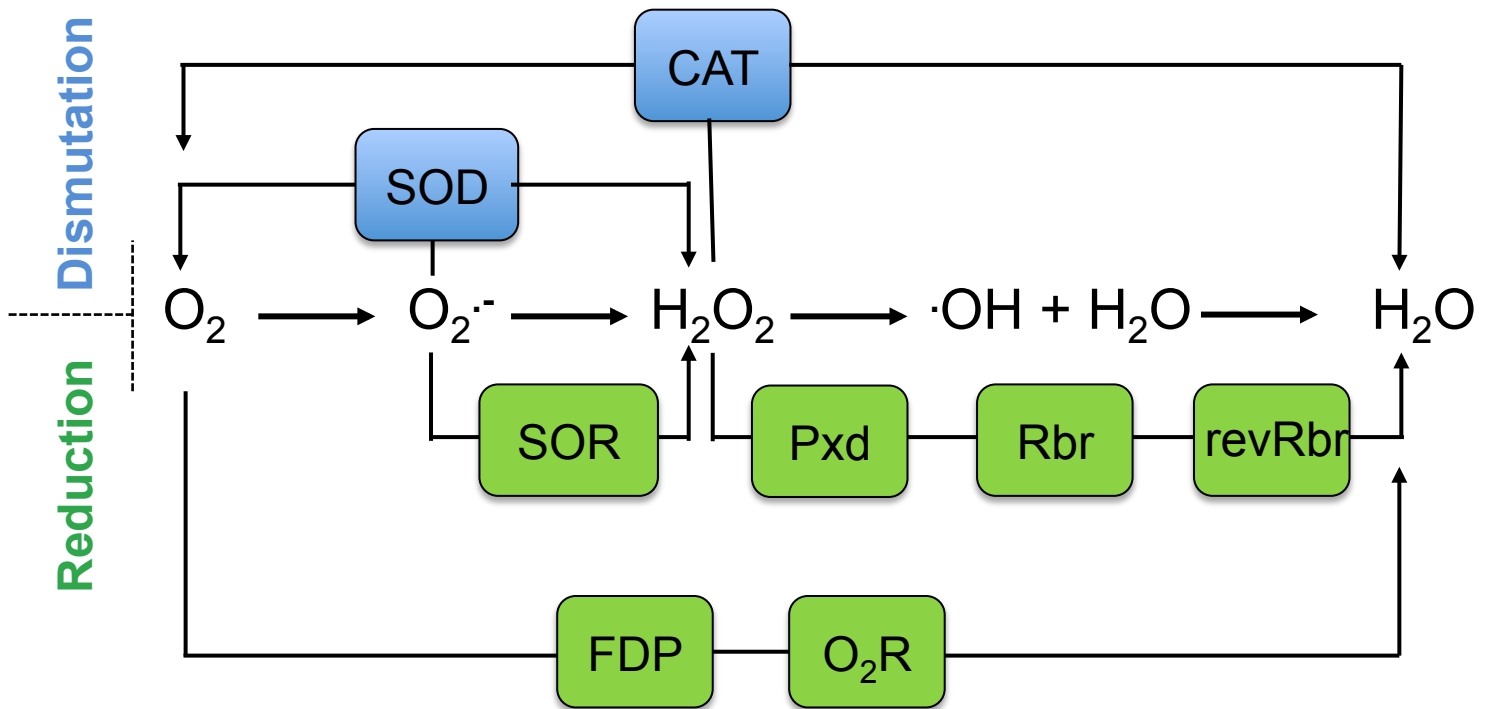


Figure 13: Enzymatic systems for detoxification of oxygen (O_2) and reactive oxygen species (ROS). SOD (superoxide dismutase), CAT (catalase), SOR (superoxide reductase), Pxd (peroxidase), Rbr (rubrerythrin), revRbr (reverse rubrerythrin), FDP (flavodiiron protein) and O_2R (respiratory O_2 reductase) are indicated.

Chapter 3: Oxygen and Reactive Oxygen Species detoxification

I. Cell defense mechanisms against these compounds present in bacteria

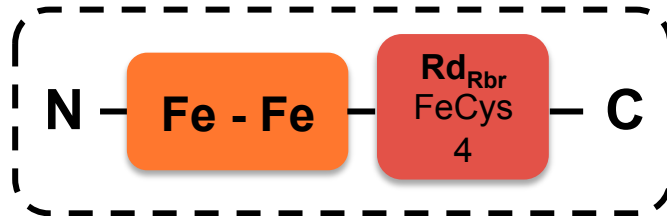
I.1. Catalases and superoxide dismutases

Mechanisms of cell defense against oxidative stress have been extensively studied in aerobic organisms. In this case, oxidative stress is a by-product of the aerobic lifestyle (Imlay 2003). Microorganisms typically deal with oxidative stress using two major enzymes: superoxide dismutases (SODs) and catalases. SODs catalyze the dismutation of the superoxide (O_2^-) into O_2 and H_2O_2 , a reaction requiring one proton per O_2^- reacted, but no external reductant. Then, H_2O_2 is degraded to O_2 and water by catalases (Figure 13). Some obligate anaerobes contain SOD and/or catalase, but the latter is less distributed among anaerobes than SOD (Brioukhanov and Netrusov 2004). The sulfate-reducing bacteria *Desulfovibrio gigas* contains both a SOD and a catalase, even if catalase activity does not seem to be present in all *Desulfovibrio* species (Dos Santos et al. 2000). *Desulfovibrio vulgaris* and *D. gigas* are catalase positive, and for the latter one long exposure times to O_2 lead to higher catalase activity (Fareleira et al. 2003). The obligate anaerobic gingival pathogenic *Porphyromonas gingivalis* also contains a SOD but lacks a catalase (Amano et al. 1986, Lynch and Kuramitsu 1999). In the genome of the strict anaerobe *C. acetobutylicum*, no catalase was annotated, and no function has been yet demonstrated for the annotated SODs (Nolling et al. 2001).

I.2. Alternative detoxification systems: NADH-dependent reductases

Production of O_2 by the SOD/catalases is obviously a disadvantage for anaerobes. Nevertheless, although strictly anaerobic, microorganisms such as *C. acetobutylicum* and *Clostridium perfringens* are considered to be aerotolerant anaerobes. *C. acetobutylicum* survives short periods of aeration (O'Brien and Morris 1971) while *C. perfringens* vegetative and stationary-phase cells can survive in a growth-arrested state in the presence of O_2 and/or low concentrations of O_2^- - or hydroxyl-radical-generating compounds (Briolat and Reysset 2002). This supported that alternative detoxification systems must exist. Indeed, anaerobic and microaerophilic bacteria use specific reduction pathways for ROS detoxification based

Rbr



revRbr

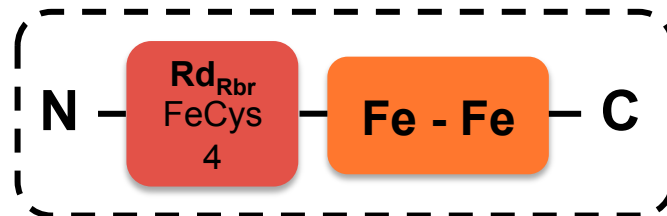


Figure 14: Schematic representation of a Rubrerythrin (Rbr) and a reverse Rubrerythrin (revRbr) domains. Rbr contains non-sulfur diiron center in the N-terminal part and a rubredoxin-type [FeCys₄] center, located at the C-terminal part. In a revRbr, the position of the two domains is switched.

mainly on NADH-dependent reductases that lead to water rather than O₂ production (Jenney et al. 1999, Lumppio et al. 2001, Hillmann et al. 2009b, Riebe et al. 2009). These organisms use superoxide reductases (SORs), rubrerythrins (Rbrs), reverse rubrerythrins (revRbrs) and flavodiiron proteins (FPDs) (Figure 13). These enzymes have been isolated and characterized from a number of organisms, including *D. vulgaris* (Wildschut et al. 2006), *P. gingivalis* (Lynch and Kuramitsu 1999, Sztukowska et al. 2002), *C. perfringens* (Jean et al. 2004) and *C. acetobutylicum* (Riebe et al. 2007). SORs, as SODs, are metalloenzymes. SORs catalyze the reduction of O₂⁻ to give H₂O₂, a reaction requiring two protons per O₂⁻ reacted, as well as an external reductant to provide the electron. In *C. acetobutylicum*, a desulfoferrodoxin (Dfx), which is a SOR homologue, was shown to be capable of reducing O₂⁻ to H₂O₂ (Riebe et al. 2007).

I.2.a. Rubrerythrins (Rbrs)

Rubrerythrins (Rbrs) constitute a family of proteins that are implicated in oxidative stress protection in anaerobic bacteria and archaea. These proteins contain two types of iron sites: an N-terminal non-sulfur diiron center and a rubredoxin-type [FeCys₄] center, located at the C-terminal part (Figure 14) (deMare et al. 1996). Reverse Rbr (revRbr) are enzymes in which the position of the diiron site and the rubredoxin domains are reversed (Figure 14). Both Rbr and revRbr have been shown to play a role as NAD(P)H:H₂O₂ oxidoreductase (Coulter et al. 1999, Weinberg et al. 2004). The reduced diiron site reacts directly with H₂O₂, while the [Fe(SCys)₄] site transfers electrons from an exogenous donor to the oxidized diiron site. NAD(P)H-dependent peroxidase activity was shown for classical Rbrs from *D. vulgaris* (Lumppio et al. 2001) and *Pyrococcus furiosus* (Weinberg et al. 2004). An O₂-reductase activity was also described for these proteins. However, the reactivity of these enzymes to O₂ is typically low relative to that with H₂O₂. *In vitro*, the *D. vulgaris* Rbr reduces H₂O₂ much more rapidly than O₂ (Coulter et al. 1999, Coulter and Kurtz 2001). An increased sensitivity to both O₂ and H₂O₂ was observed in Rbr-deletion mutant of *P. gingivalis* (Sztukowska et al. 2002). *C. acetobutylicum* genome encodes four proteins homologous to Rbrs: 2 normal Rbrs (RubY and RubZ) and 2 revRbrs (Rbr3B and Rbr3A whose encoding genes form an operon) (May et al. 2004). While normal Rbrs are upregulated upon oxygenation, revRbrs seem to be induced both upon oxygenation and oxidative stress (Hillmann et al. 2006). RubY has a peroxidase specific activity comparable to that of the revRbr *in vitro*, (May et al. 2004, Hillmann et al. 2006, Riebe et al. 2009), while the revRbrs, that are 99% identical, have both NADH

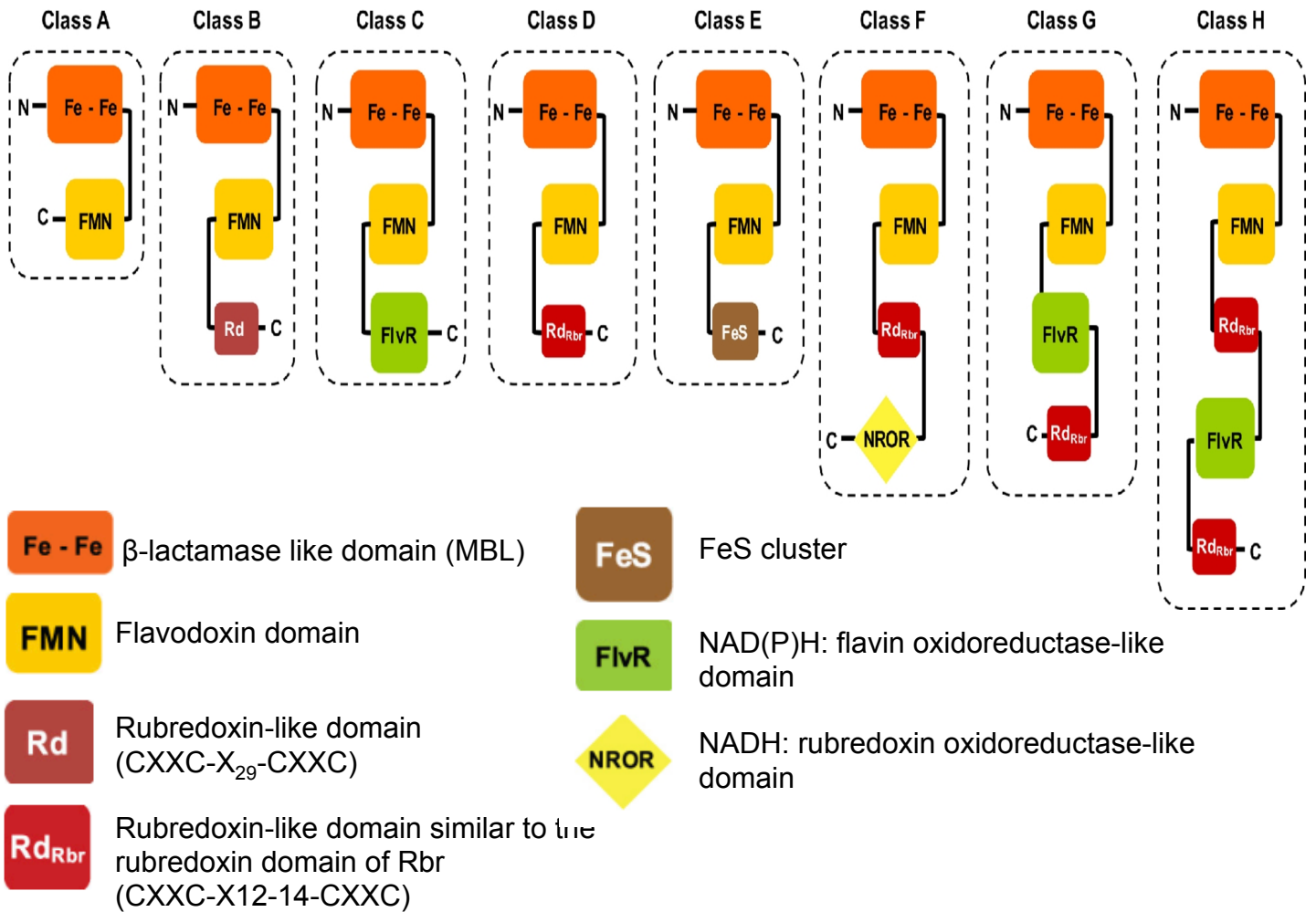


Figure 15: The FDP protein family. This scheme assumes a FDP family classification according to the known or proposed domain structure (deduced from their gene translated amino acid sequences). Structural domains are color coded. Adapted from Folgosa *et al.*, 2018.

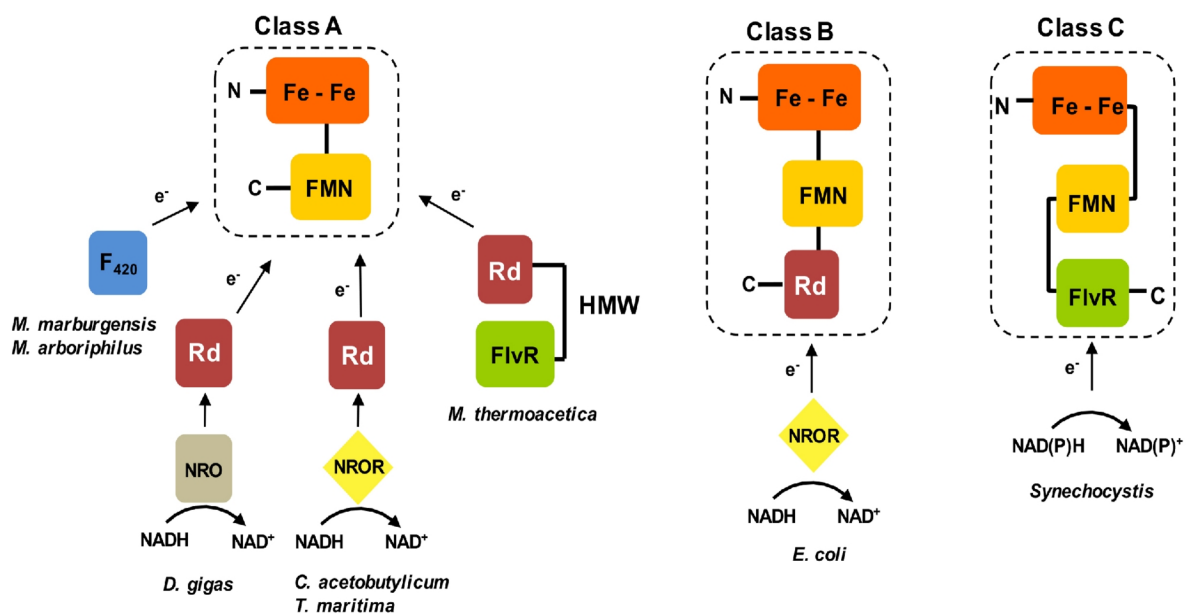


Figure 16: Schematic representation of the FDPs electron transfer chains comprising the known redox partners of FDPs. HMW—*Morella thermoacetica* high molecular weight rubredoxin; NRO—*Desulfovibrio gigas* NADH:rubredoxin oxidoreductase. Folgosa *et al.*, 2018.

peroxidase and oxidase activity (Kawasaki et al. 2004, May et al. 2004, Riebe et al. 2009). The overproduction of the Rbr3B showed significantly increased tolerance to O₂ and H₂O₂ exposure (Riebe et al. 2009). H₂O₂ and O₂ detoxification pathway in *C. acetobutylicum* involves a combination of several proteins i.e., Rbr or revRbr, rubredoxin (Rd) and NADH-rubredoxin oxidoreductase (NROR) that use NADH as an electron donor (Kawasaki et al. 2009, Riebe et al. 2009). Rbrs/revRbrs eliminate H₂O₂ and/or O₂ through their reduction to water (Kawasaki et al. 2004, May et al. 2004, Hillmann et al. 2006). Rd increases the NADH consumption rate by doing the electron-shuttle between NROR and Rbrs. In *C. acetobutylicum*, which does not have σ^B , the O₂ and H₂O₂ detoxification pathways are controlled by the negative regulator PerR, that senses H₂O₂ as a signal of oxygenation (Hillmann et al. 2008, Hillmann et al. 2009a). In fact, the inactivation of *perR* is related to an increased tolerance to O₂ and higher resistance to H₂O₂, leads to an increased expression of genes coding for proteins involved in the detoxification of O₂ and H₂O₂ (Hillmann et al. 2008).

I.2.b. Flavodiiron proteins (FDPs)

The flavodiiron proteins, called FDPs, are also involved in O₂ scavenging. FDPs have O₂ and/or NO reductase activity and belong to a family widespread in the three domains of life. These enzymes are found both in aerobic and anaerobic organisms. Based on their different domains, several classes of FDPs from A to H have been proposed (Figure 15) (Folgosa et al. 2018a). Class A FDPs contains only the minimal core composed of two domains: a metallo- β -lactamase-like domain, containing a diiron catalytic center, and a flavodoxin harboring a flavin mononucleotide (FMN). FDP activity requires also the participation of proteins involved in electron transfer such as Rds and NADH/FAD dependent oxidoreductases (Chen et al. 1993, Silaghi-Dumitrescu et al. 2003) or F₄₂₀ coenzyme in methanogens (Figure 16) (Seedorf et al. 2004). In some cases (see below), the Rd or the NADH/FAD dependent oxidoreductase domain are fused to the FDP core domain or present as independent proteins (Figure 15 and 16). Class A FDPs have either a clear preference for O₂ as observed for protozoal and archaeal enzymes (Seedorf et al. 2004, Smutna et al. 2009, Vicente et al. 2012) or exhibit a dual activity towards NO and O₂ as described for the enzymes of *M. thermoacetica* or *D. gigas* (Silaghi-Dumitrescu et al. 2003, Rodrigues et al. 2006). *C. acetobutylicum* possesses two FDPs, FprA1 and FprA2, with NADH:O₂ oxidoreductase activity that use NROR and a Rd as electron transporters (Hillmann et al. 2009b). FprA1 and FprA2 are more produced in the *perR* mutant strain (May et al. 2004) and

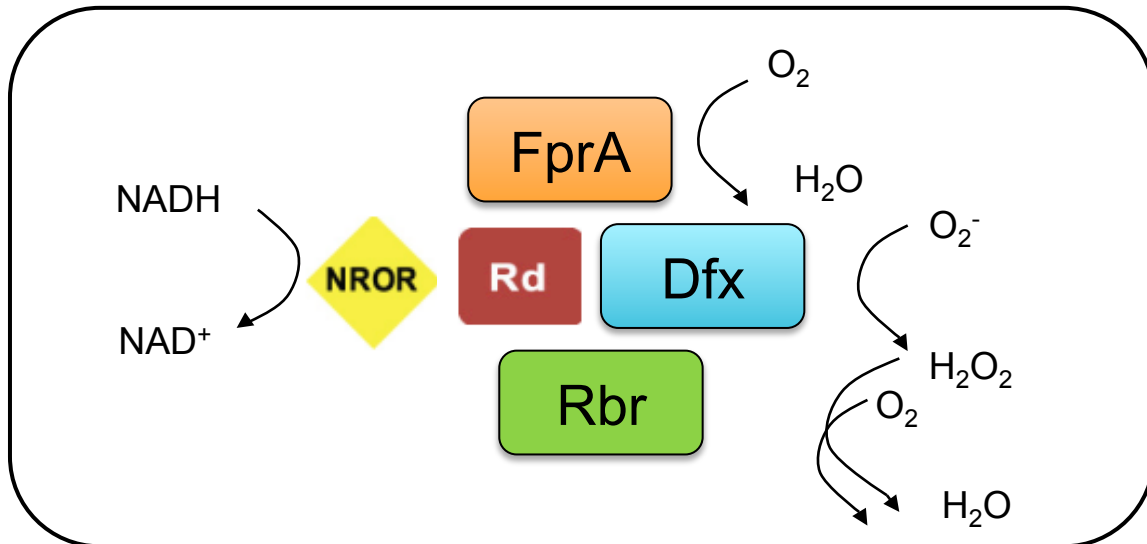


Figure 17: Oxygen and ROS detoxification system in *C. acetobutylicum*. Scheme of the NADH-dependent O₂, O₂⁻ and H₂O₂ detoxification complex composed of NADH-rubredoxin oxidoreductase (NROR), rubredoxin (Rd), flavoprotein (Fpr), desulfoferrodoxin (Dfx) and rubrerythrin (Rbr). Adapted from Kawasaki *et al.*, 2009.

their encoding genes are induced after O₂ exposure or during oxidative stress (Kawasaki et al. 2004, Kawasaki et al. 2005). Those proteins, together with the Rbrs and Dfx form an O₂ and H₂O₂ detoxification complex in *C. acetobutylicum* that is schematically represented in the Figure 17. The Class B FDPs, which includes NorV from *Escherichia coli*, is restricted to the Proteobacteria phylum. In addition to the core domain, NorV contains a Rd domain with a FeCys₄ center and for this reason was called flavorubredoxin (Figure 16) (Gomes et al. 2000, Gomes et al. 2002). This protein receives electrons from an NROR called NorW. *E. coli* NorV is the only example so far of an FDP with a clear preference for NO as a substrate (Vicente and Teixeira 2005, Vicente et al. 2007). It was shown that the transcriptional levels of the *norV* gene were higher after exposing *E. coli* cells to NO and NorV confers resistance to NO (Gardner et al. 2002, Justino et al. 2005). Finally, the Class C FDPs is widely distributed in cyanobacteria and contains a C-terminal flavin-binding domain. Class C FDP was isolated from *Synechocystis* sp and was shown to have NADH: O₂ oxidoreductase activity (Wasserfallen et al. 1998, Vicente et al. 2002). Class F FDPs occur mainly in Firmicutes, namely from the Clostridiales order and one example was recently characterized in *C. difficile* (see more in detail Chapter 3, section II. O₂ and ROS detoxification in *C. difficile*). For the remaining four classes of FDPs, their properties are deduced from the respective amino acid sequences, due to the lack of reported studies.

II. O₂ and ROS detoxification in *C. difficile*

II.1. The exposure of *C. difficile* to O₂, ROS and NO during infection

During its infectious cycle, *C. difficile* vegetative cells are gradually exposed to O₂ and oxidative stress. Indeed, the gut is not strictly anaerobic (Espey 2013) and an increasing gradient of O₂ exist from the intestinal lumen (anaerobic) to the mucosa (approximately 5% O₂). After an antibiotic treatment, the gradient of O₂ can be disturbed and cause an increase of O₂ tension in the gut (Rivera-Chavez et al. 2017). Indeed, the composition of gut-associated microbial communities is modified during antibiotherapy. For instance, a depletion of butyrate-producing microorganisms limits the production of butyrate and its oxidation by epithelial cells increasing diffusion of O₂ into the intestinal lumen (Figure 18) (Rivera-Chavez et al. 2016, Rivera-Chavez et al. 2017). Moreover, the inflammatory response triggered by *C. difficile* is a source of oxidative stress. When recruited to the infection site, immune cells such as macrophages and neutrophils ingest the invading bacteria and bombard them with oxidants.

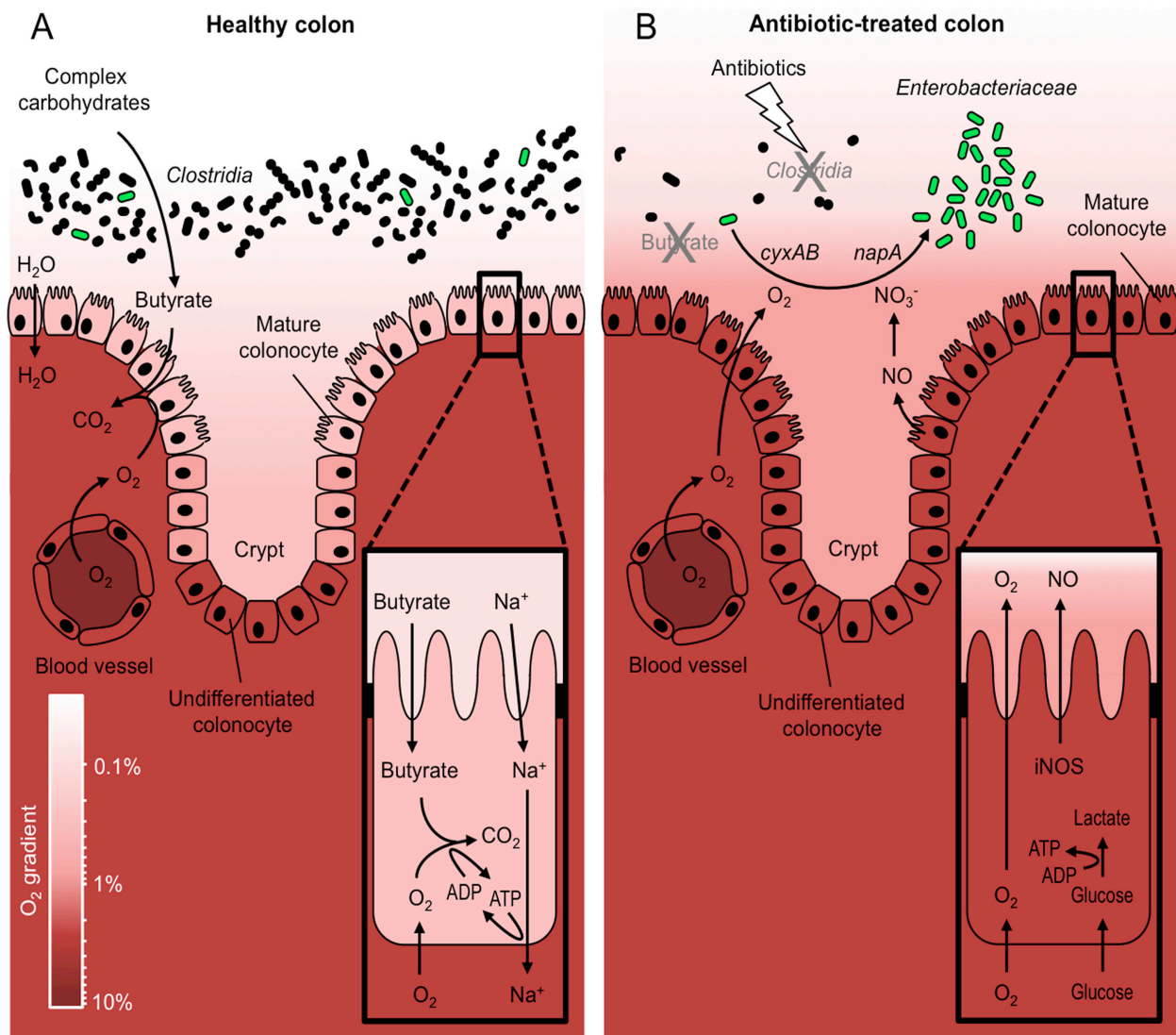


Figure 18: Oxygen tension in the colon before and after antibiotic treatment. A) O₂ tension and metabolic reactions in a healthy colon. The butyrate produced by the microbiota, and in particular by certain clostridia, is oxidized to CO₂ by mature colonocytes to produce energy (ATP). The consume of O₂ by mature colonocytes renders the epithelial surface hypoxic. **B)** Metabolic change and increase in O₂ pressure after antibiotic treatment. After antibiotic treatment, the intestinal microbiota is affected resulting in a decrease in butyrate production. In this case, mature colonocytes ferment glucose into lactate to obtain ATP. The use of this metabolism increases oxygenation of the epithelial surface. The resulting increased diffusion of O₂ into the intestinal lumen drives an aerobic expansion of organisms such as of *Enterobacteriaceae*. The color scale shown at the left bottom of the panel indicates the O₂ concentration signified by the coloring scheme of the schematic.

The host NADPH oxidase NOX2 complex activated by both phagocytosis of bacteria and by TcdB produce ROS such as O_2^- and H_2O_2 in the phagosome (Decoursey and Ligeti 2005). In addition, NO produced by nitric oxide synthases, mainly by iNOS, can react with O_2^- and form peroxynitrite ($ONOO^-$), nitrogen dioxide and other toxic RNS. Both ROS and RNS can react with multiple cellular components being deleterious to nearly all biomolecules. By mainly oxidizing Fe-S clusters, O_2^- can result in the inhibition of enzymatic activity and a release of iron that lead to oxidative stress through the fenton reaction (Imlay 2006). Moreover, H_2O_2 , which is able to penetrate lipid bilayers similar to that of water (Seaver and Imlay 2001), can oxidize lipids, cysteine residues of proteins and Fe-S clusters (Imlay 2003, Semchyshyn et al. 2005). Finally, NO can modify cysteine residues (S-nitrosylation) and react with transition metals (Vazquez-Torres and Baumler 2016), while $ONOO^-$ oxidizes thiols, DNA and the transition metal centers of metalloproteins (Radi 2013).

II.2. The response of *C. difficile* to O_2 and oxidative stress

The response of *C. difficile* to O_2 , oxidative and nitrosative stresses is poorly studied. Vegetative cells of this strictly anaerobic bacterium, are known to be highly sensitive to low levels of O_2 (Holy and Chmelar 2012). However, it has been recently demonstrated that this pathogen is able to grow in non-strict anaerobic conditions and to adapt to low O_2 tension. Indeed, this bacterium is able to grow under 2% O_2 (Giordano et al. 2018a) and 5% O_2 has only a moderate effect on *C. difficile* growth (Neumann-Schaal et al. 2018). However, the tolerance to O_2 seems to be strain-dependent. The survival of the 630 Δ *erm* reference strain is significantly reduced only after 3 hours of exposure to air and 12 hours are necessary to completely eliminate all vegetative cells. The "highly virulent" strain R20291 of 027 ribotype, as well as a clinical strain of 078 ribotype are less O_2 -tolerant with a survival that decreased sharply after 1 hour of exposure to air and no bacteria quantified after 3 hours of air exposure (Edwards et al. 2016a). In addition, *C. difficile* vegetative cells are sensitive to relative low concentrations of H_2O_2 (400 μ M). As observed with air, the sensitivity to H_2O_2 exposure is also strain-dependent. The 630 Δ *erm* strain is more resistant than strains of the 027 and 078 ribotypes (Edwards et al. 2016a). Nevertheless, the response of *C. difficile* to atmospheric O_2 and H_2O_2 exposure suggested that this pathogen has mechanisms to tolerate oxidizing conditions. However, the mechanisms used by *C. difficile* to resist exposure to H_2O_2 , air or O_2 and to detoxify these compounds are not yet clearly identified. It was demonstrated that σ^B plays a crucial role in this tolerance (Edwards et al. 2016a, Kint et al. 2017). Moreover, the

inactivation of the *gluD* gene encoding the glutamate dehydrogenase GluD (*CD0179*) responsible for the degradation of glutamate into α -ketoglutarate and NH_3 , increases the sensitivity of *C. difficile* to H_2O_2 (Girinathan et al. 2014). This effect might be due to a decreased concentration of α -ketoglutarate, a compound that might be able of capturing H_2O_2 (Mailloux et al. 2009). The deletion of the cysteine desulfurase encoding gene *iscS* involved in the Fe-S cluster (Isc) system cause a severe growth defect of *C. difficile* in the presence of 2% O_2 and the mutant fail to colonize a germ-free model (Giordano et al. 2018b). *C. difficile* very likely encodes other functions allowing the bacterium to tolerate and survive in the presence of low O_2 tensions and during oxidative stress. In 2008, Emerson *et al* performed a large-scale transcriptomic study that provided some insights into the response of this bacterium to air stress. The oxidative shock created by the exposure to air increased the expression of 98 genes in *C. difficile*, including several genes belonging to the σ^B regulon involved in oxido-reduction and electron transfers (Emerson et al. 2008). They found an increased expression of an operon encoding a reductase (*CD0174-76*) and of genes encoding a thiol peroxidase (*CD1822*), a Trx-Trx reductase system (*CD1690-91*) and a revRbr (*CD1524*). The high homology (96% identity) of the two genes encoding the revRbrs (*CD1474* and *CD1524*) did not allow determining if only one or both are upregulated. Expression of the two genes encoding the FDPs (*CD1623* and *CD1157*) probably involved in O_2 and/or NO reduction also increased in the presence of air (Emerson et al. 2008). However, in two more recent transcriptomic or multi-omic studies, no induction of these genes was observed under microaerophilic growth conditions (Giordano et al. 2018a, Neumann-Schaal et al. 2018). In those studies, the greatest expression changes concerned genes encoding proteins involved in sugar and amino acid metabolism. Changes in the reductive pathways of the Stickland reaction for the use of proline, glycine or leucine were observed. In addition, an induction of genes for the de-novo synthesis of cysteine was verified, likely associated with an important oxidation of cysteine in proteins in microaerophilic growth conditions. Carbon metabolism was also significantly modified with changes in the phosphotransferase system (PTS) facilitating uptake of sugars and a repression of the synthesis of enzymes involved in glycolysis and butyrate fermentation. A temporary induction in the synthesis of cofactor riboflavin was also detected possibly due to a demand for FMN and FAD in redox reactions (Neumann-Schaal et al. 2018).

Because *C. difficile* is exposed to low O_2 tensions and high concentrations of ROS in the gut, elucidate the mechanisms of stress response is of major concern. The *C. difficile*

genome encodes a SOD (SodA-CD1631) and three catalases (CotCB-CD0598, CotD-CD2401 and CotG-CD1567). However, the genes encoding these proteins are only expressed during sporulation and likely transcribed by the late sporulation sigma factors (σ^G and σ^K) (Fimlaid et al. 2013, Permpoonpattana et al. 2013, Saujet et al. 2013). Moreover, those proteins are located at the surface of *C. difficile* spore (Lawley et al. 2009b, Abhyankar et al. 2013, Diaz-Gonzalez et al. 2015).

Nevertheless, the presence in the *C. difficile* genome of genes encoding proteins sharing similarities with revRbrs and FDPs from *C. acetobutylicum* suggests the presence of O₂ and ROS alternative detoxification pathways in this bacterium. The *C. difficile* genome encodes a desulfoferrodoxin (CD0827), two revRbrs (CD1524 and CD1474), two Rbrs (CD0825 and CD2845), two FDPs proteins (CD1157 and CD1623) and several OR (CD0176, CD1623 and others). With the exception of the two Rbrs, all of these proteins are encoded by genes controlled by σ^B and a σ^B -dependent promoter is mapped or identified *in silico* upstream of all these genes (Kint et al. 2017). These data were in agreement with the control by σ^B on the resistance to ROS and the tolerance to low O₂ tensions (Kint et al. 2017). A very recent study has functionally characterized CD1623 as an NADH:O₂ reductase that might contribute to the survival of *C. difficile* in the gut (Folgosá et al. 2018b) (Figure 15). This protein belongs to the Class F of FDPs and contains a diiron center and an FMN in the core domain, a FeCys₄ center at a short spaced rubredoxin domain (as in classical Rbrs) and a NROR domain (binding a FAD) at the C-terminal (Figure 15). It is worth noting that CD1623 carries into a single polypeptide a complete electron transfer chain that enables coupling directly O₂ reduction to the oxidation of the electron donor NAD(P)H. This enzyme has a clear preference to O₂ as a substrate. Except for CD1623, the role of the other *C. difficile* proteins with a possible function in O₂ and ROS detoxification has not been studied. In the framework of my PhD goals, I studied the O₂ and ROS detoxification pathways in *C. difficile*, focusing mainly on the enzymatic characterization of the other FDP, CD1157, and the two revRbrs CD1474 and CD1524, and their role for this anaerobic pathogen.

Chapter 4: Sporulation and Germination

I. General stress response and sporulation: two survival mechanisms in *C. difficile*

Bacterial cell entry into stationary phase implies changes in metabolism and physiology. σ^B , the known sigma factor of general stress response, participates in the reprogramming of *C. difficile* cellular metabolism in stressful environments or at the onset of the stationary phase (Kint et al. 2017). When cells enter stationary phase (~10 h), it was shown that σ^B controls the expression of approximately 25% of *C. difficile* genes (Kint et al. 2017). Moreover, the sigma factor σ^H , which plays a crucial role in *C. difficile* during transition phase, controls the expression of several genes involved in metabolism, motility and sporulation (Saujet et al. 2011). Thus, σ^B together with σ^H , control around 49% of the genes induced at the onset of the stationary phase and are the major sigma factors in decision making during post-exponential growth (Saujet et al. 2011, Kint et al. 2017). Interestingly, genes involved in oxidative- and nitrosative-stress responses are controlled by σ^B , but not by σ^H . On the contrary, σ^H represses the expression of *C. difficile* toxin genes, whereas σ^B does not play any role in toxinogenesis. Moreover, σ^B and σ^H inversely control the sporulation process (Saujet et al. 2011, Kint et al. 2017). σ^B negatively controls the expression of more than 200 genes transcribed by the different sporulation-specific σ factors. In agreement, a *sigB* mutant sporulates more efficiently and/or earlier than the wild-type strain (Kint et al. 2017). By contrast, σ^H positively controls several genes required for sporulation and, accordingly, *sigH* inactivation results in an asporogeneous phenotype (Saujet et al. 2011). During transition from exponential to stationary growth phase, cells will activate a complex regulatory network to promote the more suitable choice to make in response to the given conditions. Thus, under stress conditions, such as entering stationary phase, *C. difficile* must quickly choose between a rapid adaptative response mediated by σ^B , or an irreversible and slower differentiation process leading to the formation of spores whose initiation is controlled by σ^H . Sporulation is predominantly the last resource for cells experiencing nutrient limitation.

II. The sporulation process

Endospores are formed by three classes of low G+C Gram positive bacteria (bacilli, clostridia and negativicutes), as a strategy to survive to unfavorable conditions. Bacterial

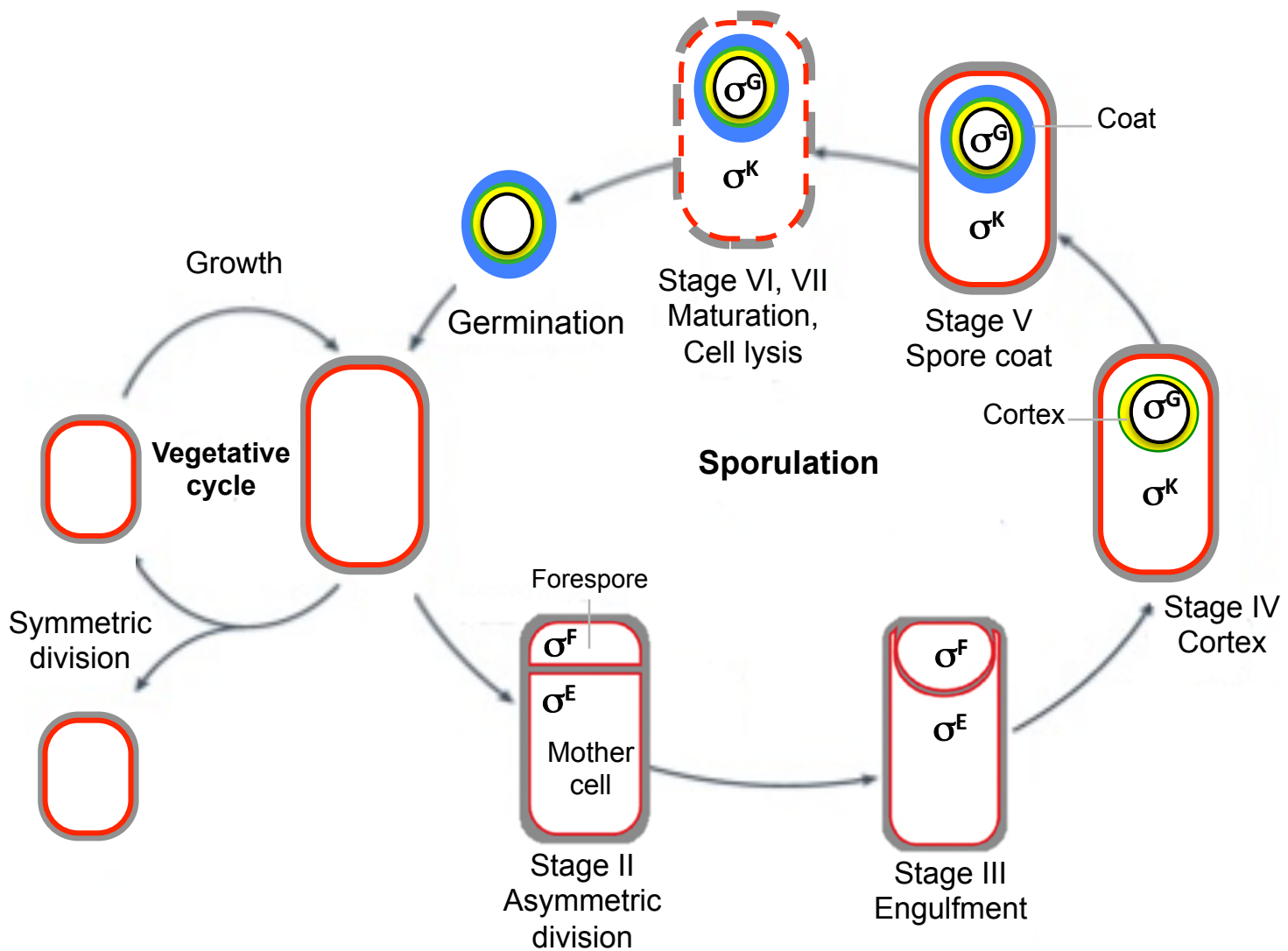


Figure 19: Formation of spores by endospore-forming bacteria and compartmentalization of gene expression. The main morphogenetic stages of the sporulation process are represented in the scheme. The compartment and main periods of activity of the sporulation σ^F , σ^E , σ^G and σ^K sigma factors are indicated in the respective morphological stages. Adapted from Errington *et al.*, 2003.

spores resist to extremes of physical and chemical parameters that would rapidly destroy vegetative cells, being the most resistant cellular structure known (Setlow 2007). Spore forming bacteria include important organisms in several fields. Certain species such as *Clostridium acetobutylicum*, a saprophyte clostridium able to undertake useful biotransformations while others are important animal and human pathogens responsible for diseases such as anthrax, botulism, diarrhea, gas gangrene or tetanus (Al-Hinai et al. 2015). For pathogenic bacteria, sporulation is crucial to survive during transmission from one host to another. Sporulation is a process of cellular differentiation allowing the conversion of a vegetative cell into a mature spore through several morphological stages (Figure 19). The main morphological stages are conserved between species (Piggot and Coote 1976, Fimlaid and Shen 2015). Stage 0 corresponds to the stage where the cells are undergoing normal vegetative growth by binary fission. When the growth conditions are unfavorable, the bacteria enter Stage I during which the chromosome is replicated and segregated in a polar way. Then, sporulation starts when an asymmetric division occurs near to one pole of the vegetative cell, resulting in the formation of a smaller cell, the forespore (FS) and a larger cell, the mother cell (MC). Each compartment contains a copy of the chromosome (Stage II). Evidences have indicated that the division can take place either in the “old“ or the “new“ cell pole (Veening et al. 2009). The sporulation septum contains a thinner layer of peptidoglycan (PG) separating the two compartments. After asymmetric division the MC engulfs the FS in a phagocytic-like manner (Stage III). During stage IV, the spore cortex is formed between the two membranes of the MC and the FC. Stage V corresponds to the assembly of the spore coat and stage VI is the maturation of the spore layers, cortex and coat. At the end (Stage VII), the mature spore is released to the environment through lysis of the MC (Hilbert and Piggot 2004). Although sporulation takes about 8-10 hours, vegetative growth is resumed in only a few minutes, as soon as the spore senses its germinants, following a process called germination (see more in detail Chapter 4, section III. Germination).

II.1. Regulation of sporulation in *B. subtilis*

Sporulation initiation is controlled by the master regulator Spo0A, present in all spore formers (Paredes et al. 2005, de Hoon et al. 2010, Galperin et al. 2012, Abecasis et al. 2013). In bacilli and clostridia, the development program of sporulation is mainly governed by four cell-type specific sigma factors: σ^F , σ^E , σ^G or σ^K . In *B. subtilis*, the first sigma factors, σ^F in the FS and σ^E in the MC, are activated soon after asymmetric division and control early stages

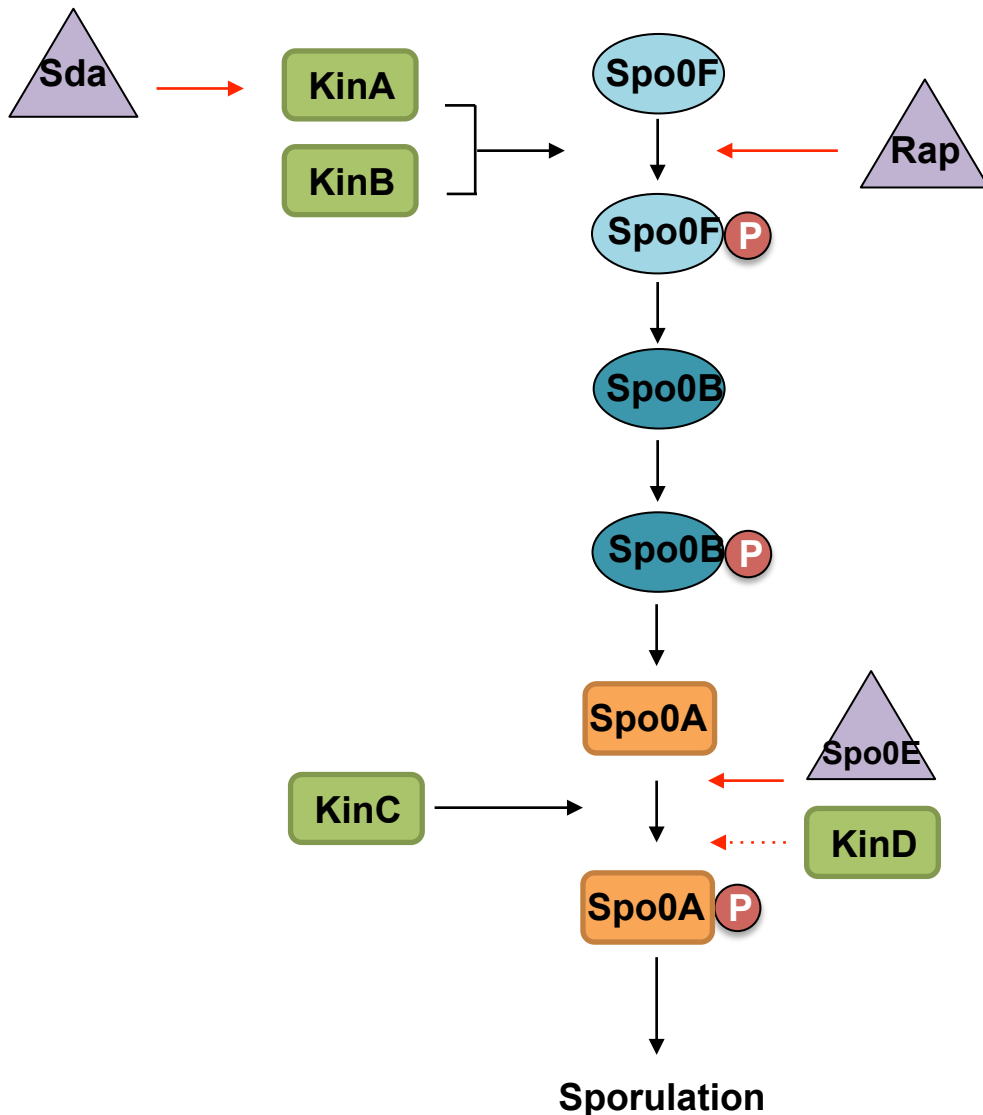


Figure 20: Activation of Spo0A in *B. subtilis*. Spo0A phosphorylation is controlled by a phosphorelay that depends on the activity of several kinases and other intermediaries. Interactions that ultimately lead to Spo0A phosphorylation are indicated in black, while the ones working against it are in red. The KinA and KinB kinases respond to yet not known signals by autophosphorylating and subsequently transferring phosphate to Spo0F. Spo0F phosphorylates Spo0B, which passes phosphate on to Spo0A. A third kinase, KinC, bypasses the phosphorelay and acts directly on Spo0A. Phosphatases, including RapA, B and E and Spo0E, and kinase inhibitors (Sda) act at various steps in the pathway to directly or indirectly antagonize Spo0A phosphorylation.

of spore development (Figure 19). σ^G and σ^K replace σ^F and σ^E in their respective compartments and control gene expression following engulfment completion (Figure 19) (Stragier and Losick 1996, Hilbert and Piggot 2004, Higgins and Dworkin 2012). Therefore, inactivation of both *sigF* and *sigE* blocks the sporulation process soon after asymmetric division generating cells presenting a disporic phenotype, while inactivation of *sigG* and *sigK* results in a blockage of the process after engulfment completion (Piggot and Coote 1976, Stragier and Losick 1996). The activation of σ^G and σ^K requires the preceding σ^F and σ^E factors to be active in the respective cell compartment (Stragier and Losick 1996, Errington 2003, Hilbert and Piggot 2004, Higgins and Dworkin 2012). Thus, after asymmetric division two parallel programs of gene expression define the FS and the MC lines of gene expression. In *B. subtilis*, six transcriptional regulators (SpoIIID, GerR, GerE, SpoVT, RfsA and YlyA) work in association with the different σ factors to modulate the expression of their targets (Figure 20) (de Hoon et al. 2010, Higgins and Dworkin 2012).

II.1.a Initiation of sporulation

Nutrient starvation has been pointed as the triggering factor to start the sporulation process in many endospore formers, notably in *B. subtilis* and other bacilli (Stephens 1998). Previous studies revealed that the nutritional sensor protein, CodY, negatively regulates sporulation (Ratnayake-Lecamwasam et al. 2001, Molle et al. 2003, Piggot and Hilbert 2004) by controlling genes directly involved in sporulation initiation, including *spo0A*, *rapA*, *rapC*, *rapE*, *sinIR*, *sigH* and *kinB* genes (Ratnayake-Lecamwasam et al. 2001, Molle et al. 2003, Chateau et al. 2013). The *spo0A* gene is transcribed from both σ^A - and σ^H - dependent promoters. Then, phosphorylation of Spo0A (Spo0A-P), leading to its dimerization, dramatically increases its affinity to its target sites on the DNA (Lewis et al. 2002). The unphosphorylated form of Spo0A is inactive but phenotypic differentiation processes can come from the extent of Spo0A phosphorylation and abundance. Spo0A phosphorylated at low level induces biofilm development and nutrient scavenging (i.e. cannibalism) (Hamon and Lazazzera 2001, Gonzalez-Pastor et al. 2003). By opposition, higher levels of Spo0A-P induce sporulation (Fujita et al. 2005). In *B. subtilis*, Spo0A phosphorylation is mediated by a phosphorelay that depends on the activity of five sensor histidine kinases (HK) KinA, KinB, KinC, KinD and KinE (Figure 20) (Perego 2001, Higgins and Dworkin 2012). KinA and KinB respond to a signal by autophosphorylating and subsequently phosphorylates Spo0F. Spo0F transfer the phosphate to Spo0B, which in turn transfers it to Spo0A that can activate transcription of sporulation genes (Figure 20). KinA is the major kinase responsible for

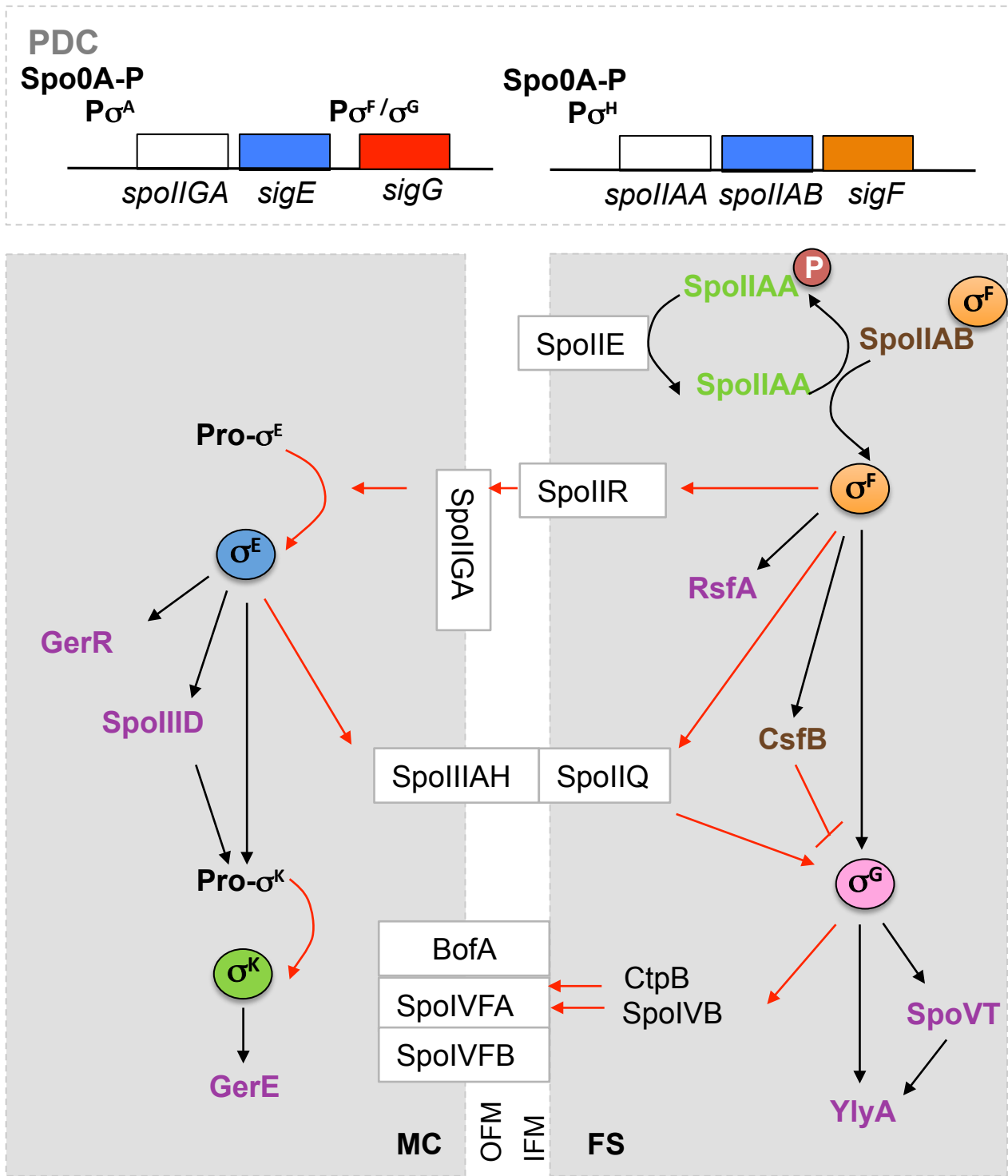


Figure 21: The sporulation network of *B. subtilis*. Temporal progression of sporulation is shown from top to bottom. Boxes represent the predivisive cell (PDC), mother cell (MC) and forespore (FS), the two cell compartments formed after asymmetric division. Membranes separating the FS and the MC are indicated (OFM: outer forespore membrane; IFM: inner forespore membrane). Sigma factors are shown colored and bold, with the precursor proteins indicated as $pro-\sigma^E/\sigma^K$, transcriptional regulators are shown in purple and anti-sigma factors in brown. Proteins associated with the membranes or located into the intermembrane space are in square. Black solid arrows indicate activation at the transcriptional level. Red arrows indicate the intercellular signal pathways involved in the sigma factor activation.

initiation of sporulation (Fujita and Losick 2005). It has three PAS domains that in other proteins sense changes in O₂ levels and redox potential. However, the specific physiological signal(s) that stimulate KinA remain unclear. KinC uses its PAS sensory domains to respond to small-molecule-directed potassium leakage and is able to bypass the phosphorelay, to phosphorylate directly Spo0A (Lopez et al. 2009) (Higgins and Dworkin 2012). KinD was shown to delay the onset of sporulation. How KinD affects Spo0A it is not known but it was hypothesized that KinD functions as a phosphatase (Aguilar et al. 2010). Kinase inhibitors (KipI and Sda), phosphatases (Spo0E, YnzD and YisI) and Rap proteins act at various steps of the pathway and can directly or indirectly influence the Spo0A phosphorylation (Figure 20). The Sda protein regulates KinA activity by binding to it and preventing its autophosphorylation (Rowland et al. 2004). Damage to DNA or block in DNA replication induce *sda* expression, and consequently Sda prevents activation of Spo0A by the phosphorelay (Burkholder et al. 2001). The phosphatase Spo0E directly dephosphorylates Spo0A. The Rap proteins A, B and E, dephosphorylate Spo0F-P and thereby reduce the level of Spo0A~P (Smits et al. 2007). Initially, the Rap proteins were thought to function as phosphatases, but evidences suggest that these proteins may cause dephosphorylation of Spo0F-P by binding to it and stimulating its autophosphatase activity, rather than by functioning directly as phosphatases.

II.1.b. The forespore line of gene expression: σ^F and σ^G

When Spo0A-P levels reaches a threshold, Spo0A-P activates sporulation genes such as the *spoIIAA-spoIIAB-spoIIAC* operon and the *spoIIIE* gene. *spoIIAC* encodes σ^F , the first sporulation-specific sigma factor to be activated in the FS compartment. The expression of the *spoIIA* operon is controlled by both Spo0A-P and σ^H (Figure 21) (Wu et al. 1989, Burbulys et al. 1991). Although produced in the predivisional cell, σ^F becomes active only after the formation of the asymmetric septum (Gholamhoseinian and Piggot 1989). In the predivisional cell, the anti-sigma factor SpoIIAB that binds to σ^F , phosphorylates the anti-anti-sigma factor SpoIIAA and held σ^F inactive. SpoIIIE, a serine phosphatase localized to the asymmetric septum, dephosphorylates SpoIIAA-P. Then, SpoIIAA will bind to SpoIIAB releasing an active σ^F after completion of asymmetric cell division (Figure 21) (Barak and Youngman 1996, Feucht et al. 1996, Hilbert and Piggot 2004). Several mechanisms have been proposed to explain the preferential dephosphorylation of SpoIIAA-P in the FS compartment. The larger surface area-to-volume ratio of the FS compartment allows dephosphorylated SpoIIAA to reach up a critical level to effectively bind all of SpoIIAB, thus activating σ^F (Iber et al.

2006). Also, a preferential localization of SpoIIE to the FS face of the septum has been pointed for the key activation of σ^F (Guberman et al. 2008). The other mechanism is related with transient chromosome asymmetry of *spoIIAB* gene, and with the relative instability of SpoIIAB protein. Upon asymmetric cell division, only the origin-proximal one third of the chromosome is trapped into the FS compartment (Wu et al. 1998). The *spoIIAB* gene is almost opposite to the *oriC* region on the chromosome leading to its transient exclusion from the FS compartment. This, in combination with the proteolysis of the SpoIIAB protein reduces the level of anti- σ^F relative to σ^F (Dworkin 2003). σ^F transcribes around 50 genes (Steil et al. 2005, Wang et al. 2006). Among these are i) *gpr* encoding a protease important for the degradation of small acid soluble proteins (SASPs) during germination (Sussman and Setlow 1991), ii) *spoIIR* encoding a protein required for the activation of σ^E (Figure 21) (Hofmeister et al. 1995, Karow et al. 1995), iii) *spoIIQ* encoding a protein required for engulfment and also for the activation of σ^G (Figure 21) (Broder and Pogliano 2006) and iv) *rsfA* encoding the RsfA regulator that activates some σ^F -transcribed genes and represses others (such as *spoIIR*) (Wu and Errington 2000, Wang et al. 2006). σ^F also transcribes the expression of *spoIIIG*, encoding σ^G , which replaces σ^F in the FS (Figure 21) (Sun et al. 1991, Wang et al. 2006). In *B. subtilis*, *spoIIIG* (*sigG*) gene is located downstream of the *spoIIIGA-spoIIIGB* (*sigE*) operon (Figure 21) (de Hoon et al. 2010). Transcription of *sigG* was thought to be delayed in comparison with the expression of other σ^F -controlled genes. However, a very recent study reported that *sigG* is transcribed by σ^F but at very low levels as a consequence of several intrinsic features on the *sigG* regulatory and coding sequence that dampen its transcription and translation (Mearls et al. 2018). Accordingly, a model suggests that *sigG* is first transcribed by σ^F , but the majority of *sigG* transcription occurs later under the control of σ^G itself (Mearls et al. 2018). σ^G can be detected in the FS towards the end of the engulfment, but it is active only after engulfment completion. Activation of σ^G depends on the formation of a channel connecting the MC and the FS compartment (Figure 21). This channel is composed of components encoded by genes transcribed by both σ^F and σ^E (Illing and Errington 1990, Camp and Losick 2008, 2009, Doan et al. 2009, Fredlund et al. 2013). SpoIIQ (σ^F -controlled) and the eight SpoIIIAA-AH proteins (σ^E -controlled) form a complex known as the « feeding tube » that allows the MC to nurse the FS and to maintain a metabolic potential that still permits transcription and macromolecular synthesis after engulfment completion (Camp and Losick 2009). The feeding tube has homology to secretion systems and also transports small molecules into the FS that are necessary for σ^G activation but remain unidentified (Camp and Losick 2009, Doan et al. 2009, Fredlund et al. 2013). Pre-engulfment

activity of σ^G in the FS is prevented by the FS anti-sigma factor, CsfB, which binds to and inactivates σ^G (Serrano et al. 2011). σ^G transcribes 95 FS-specific genes encoding proteins that contribute to spore morphogenesis, germination and protection of DNA from damages (SASPs) (Steil et al. 2005, Wang et al. 2006) (Setlow and Setlow 1988). Among them, PdaA is required for modification of the cortex peptidoglycan (Fukushima et al. 2002), the SpoVA is involved in dipicolinic acid (DPA) uptake and release, and GerA, GerB and GerK proteins are important for spore germination (Paidhungat et al. 2002). σ^G is also involved in the expression of genes coding for the membrane-embedded metalloprotease SpoIVB and CtpB involved in the processing and activation of σ^K , the last sigma factor of sporulation (Figure 21) (Campo and Rudner 2007, Mastny et al. 2013). Additionally, σ^G transcribes the *spoVT* gene, coding for a transcriptional regulator that controls positively or negatively the expression of about half of the σ^G -controlled genes (Figure 21) (Bagyan et al. 1996, Wang et al. 2006). σ^G together with SpoVT control the expression of *ylyA* gene, encoding the last FS-specific regulator. YlyA modulates the transcription of certain σ^G -controlled genes, including genes involved in germination (Traag et al. 2013).

II.1.c. The mother cell line of gene expression: σ^E and σ^K

B. subtilis MC-specific σ factors are synthesized as inactive pro-proteins and activated by proteolytic cleavage (Errington 2003, Hilbert and Piggot 2004, Higgins and Dworkin 2012). σ^E is the first σ factor to be activated in the MC compartment (LaBell et al. 1987). Pro- σ^E is encoded by *spoIIGB*, the second gene of the *spoIIG* operon whose transcription depends on a σ^A -specific promoter that is activated by Spo0A-P (Kenney et al. 1988). Processing of pro- σ^E into σ^E in the MC is mediated by the membrane-bound SpoIIGA protease, encoded by the first gene of the *spoIIG* operon (Stragier et al. 1988). This processing requires the product of the σ^F -dependent *spoIIR* gene (Figure 21). The SpoIIR protein produced in the FS is localized in the intermembrane space, where it triggers the proteolysis of pro- σ^E into σ^E by SpoIIGA (Figure 21) (Hofmeister et al. 1995, Karow et al. 1995, Fujita and Losick 2002). When activated, σ^E controls the expression of 262 genes in the MC (Eichenberger et al. 2003, Steil et al. 2005). The σ^E -dependent genes are involved in the control of the FS engulfment through the transcription of three genes: *spoIID*, *spoIIM* and *spoIIP* (Eichenberger et al. 2001). SpoIID, SpoIIM and SpoIIP (DMP complex) form a PG degradation complex located at the engulfment membrane together with the PG synthesis machinery of the FS. Additionally, σ^E controls the expression of the coat morphogenetic proteins *spoVM*, *spoIVA*, *spoVID*, *safA* and *cotE* (see more in detail Chapter 5, section III.2.a. Coat

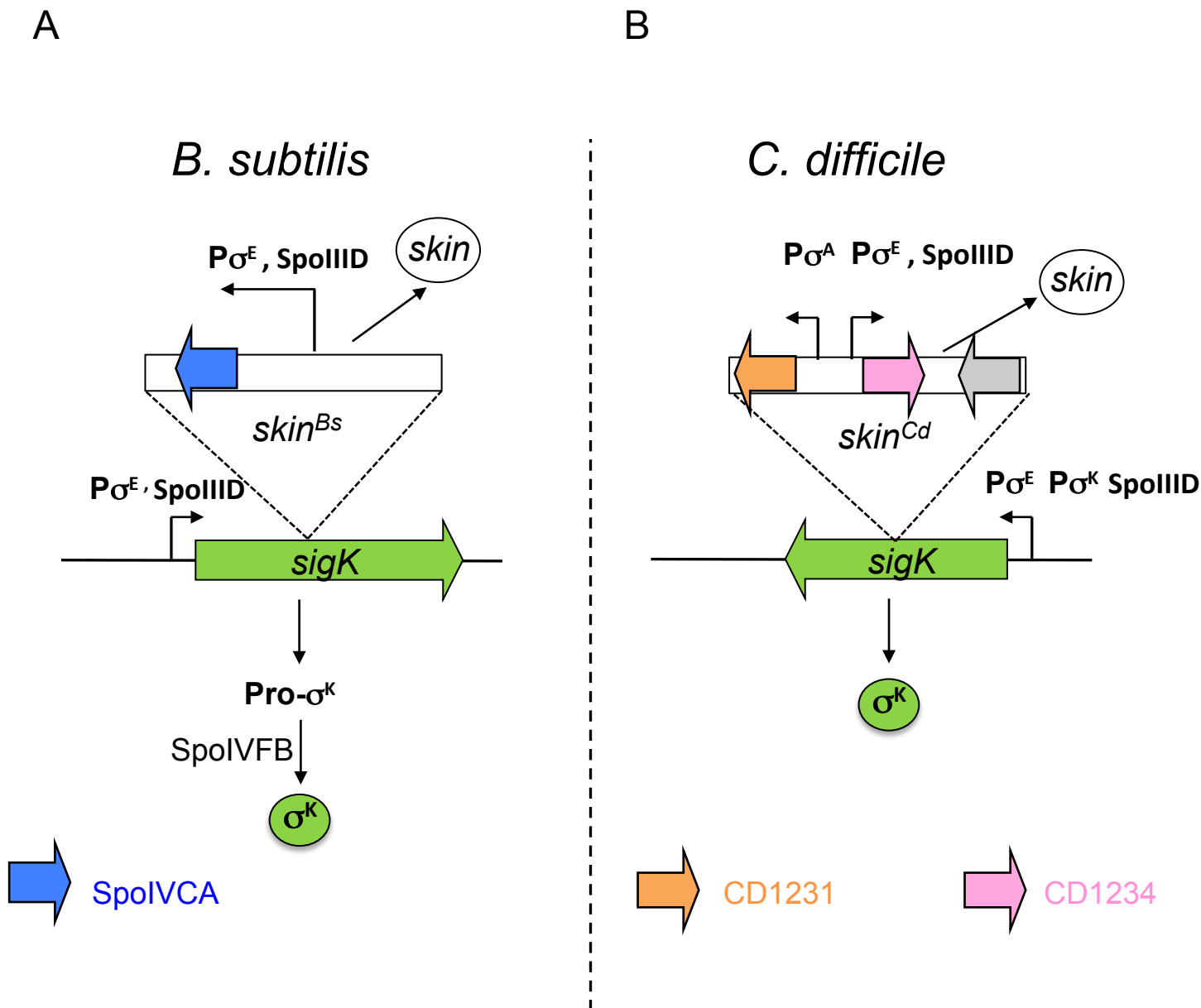


Figure 22: Regulation of σ^K activity in *B. subtilis* and in *C. difficile*. A prophage-like *skin* element must excise from genomic DNA prior to form a functional *sigK* gene. **A)** In *B. subtilis*, *skin* excision is mediated by the recombinase SpoIVCA. Then, σ^E and the SpoIIID regulator control *sigK* expression. σ^K is produced as an inactive pro- σ^K that undergoes proteolytic activation via the SpoIVFB protease. **B)** In *C. difficile*, the recombination directionality factor, CD1234, produced in the MC forms a complex with the recombinase CD1231 to catalyze *skin* excision. The rearrangement of the *sigK* gene leads to the production of an intact and functional sigma factor. Adapted from Fimlaid and Shen 2015.

morphogenetic proteins) (McKenney and Eichenberger 2012). σ^E drives the activation of σ^G in the FS through the synthesis of the SpoIIAA-AH proteins (Aung et al. 2007, Chastanet and Losick 2007) as well as both the synthesis and activation of the late MC sigma factor, σ^K (Figure 21). σ^E also transcribes the *spoIIID* and *gerR* genes encoding two transcriptional regulators (Figure 21) (Kunkel et al. 1989, Eichenberger et al. 2003). SpoIIID positively or negatively regulates σ^E -controlled genes (Halberg and Kroos 1994, Eichenberger et al. 2004), while GerR acts as a repressor of some σ^E -controlled genes and an activator of some σ^K -dependent genes (Eichenberger et al. 2004, Cangiano et al. 2010). Moreover, SpoIIID together with σ^E activates the transcription of the σ^K encoding gene, *sigK* (Figure 21) (Eichenberger et al. 2004). In fact, σ^K is controlled both at the transcriptional and post-translational level. In *B. subtilis*, as in other spore formers, the *sigK* gene is interrupted by a 48 kb prophage-like element called *skin*, which is excised during sporulation (Kunkel et al. 1990, Haraldsen and Sonenshein 2003). Excision of the *skin*^{Bs} is mediated by the site-specific recombinase, SpoIVCA, whose gene is present within the *skin*^{Bs} element (Figure 22A) (Kunkel et al. 1990, Popham and Stragier 1992). The *spoIVCA* gene, as *sigK*, is expressed under the dual control of σ^E and SpoIIID in the MC limiting *skin*^{Bs} excision to this compartment (Eichenberger et al. 2004). After the *skin* excision, σ^K is synthesized as an inactive precursor, pro- σ^K , which will be then processed by SpoIVFB, a membrane-localized protease. SpoIVFB is itself helded inactive in a complex with two other membrane proteins SpoIVFA and BofA (Figure 21). Removal of the pro-sequence requires a FS protein SpoIVB produced under σ^G control (Figure 21). SpoIVB is localized into the intermembrane space and cleave the inhibitory protein SpoIVFA. SpoIVFB is thereby activated to process pro- σ^K (Figure 21) (Campo and Rudner 2007). σ^K control the expression of about 75 genes (Eichenberger et al. 2004, Steil et al. 2005). Most of them encode spore coat proteins or proteins required for spore maturation. Among the members of the σ^K regulon is the gene for the last regulator of the sporulation cascade, GerE. This regulator represses the transcription of over half of the σ^K -target genes, while switching on 36 others (Figure 21) (Zheng et al. 1992, Eichenberger et al. 2004).

II.2. Regulation of sporulation in clostridia

Even if the Spo0A regulator and the four cell-type sporulation specific σ factors σ^F , σ^E , σ^G and σ^K are present in clostridial genomes, substantial differences exist in the sporulation molecular programs between bacilli and clostridia as well as among clostridia (Paredes et al. 2005, Galperin et al. 2012, Abecasis et al. 2013, Saujet et al. 2013, Al-Hinai et

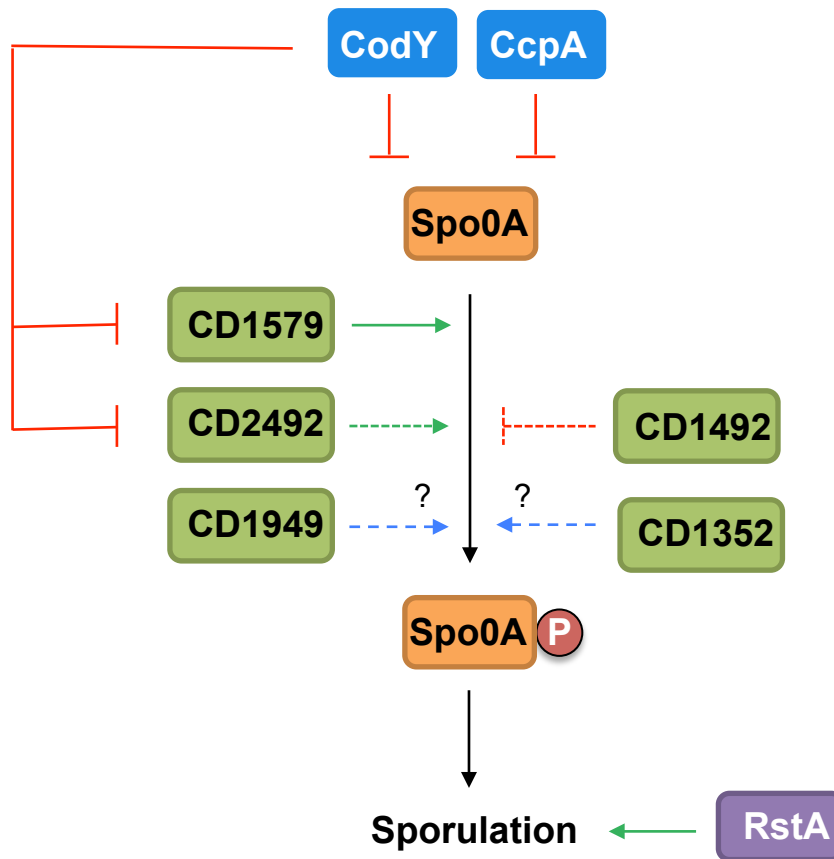


Figure 23: Activation of *C. difficile* Spo0A. The RstA regulator positively controls sporulation through an undetermined regulatory pathway. CodY and CcpA negatively regulate sporulation, by repressing the expression of *spo0A*. Additionally, CodY negatively controls the expression of the Spo0A-histidine kinases, CD1579 and CD2492. CD1579 directly phosphorylates Spo0A. CD2492 and CD1492 have a positive and a negative effect on sporulation, respectively, through a not yet known mechanism. The effect of CD1352 and CD1949 kinases on the phosphorylation state of Spo0A and in sporulation is currently unknown. Green, red and blue arrows represent respectively positive, negative or undetermined role of each protein on sporulation. Dashed arrows represent non demonstrated kinase or phosphatase activity for the HKs.

al. 2015, Fimlaid and Shen 2015). Genes encoding orthologues of the *B. subtilis* sensor HK, KinA-KinE, as well as the phosphorelay components Spo0B and Spo0F (Figure 20) are absent in clostridial genomes (Worner et al. 2006, Steiner et al. 2011). Furthermore, evidences point that phosphorylation of Spo0A results from two-component system activity rather than a multicomponent phosphorelay mechanism as observed in bacilli. Several orphan HKs that directly phosphorylate Spo0A have been identified in *C. acetobutylicum* (Steiner et al. 2011), *C. difficile* (Underwood et al. 2009) and *C. botulinum* (Worner et al. 2006). In addition, the regulation and activation of the four sporulation σ factors display different patterns among clostridia. For instance, σ^F and σ^E are active prior to asymmetric division in *C. acetobutylicum* and *C. perfringens*. In *C. acetobutylicum*, the σ^F regulon is quite different from that of *B. subtilis* and a *sigF* mutant cannot initiate the asymmetric division (Paredes et al. 2004, Jones et al. 2011). Moreover, σ^K plays a dual role in sporulation, one before asymmetric division, and one in the very late stages of spore maturation (Jones et al. 2008, Bi et al. 2011, Jones et al. 2011, Al-Hinai et al. 2015). Genome-wide analysis have demonstrated that in *C. difficile*, a weaker connection between the MC and the FS lines of gene expression exists when compared to *B. subtilis* (Pereira et al. 2013, Saujet et al. 2013).

II.2.a. Sporulation in *C. difficile*

Initiation of sporulation

In *C. difficile*, Spo0A plays a central role in the initiation of sporulation (Deakin et al. 2012) and controls the expression of 321 genes, involved not only in sporulation, but also in virulence and colonization (Pettit et al. 2014). *spo0A* is transcribed from both σ^A - and σ^H -dependent promoters (Saujet et al. 2011). As in *B. subtilis*, *spo0A* inactivation leads to an asporogenic phenotype (Underwood et al. 2009). Five putative orphan HKs (CD1352, CD1492, CD1579, CD1949 and CD2492) are present in *C. difficile* genome. The HKs CD1492, CD1579 and CD2492 share some sequence identity with KinA-E of *B. subtilis* (Underwood et al. 2009). CD1579 was shown to autophosphorylate and transfer its phosphate directly to Spo0A (Underwood et al. 2009) and the inactivation of CD2492 decreases 3.5-fold sporulation efficiency (Underwood et al. 2009). This suggests a role of both kinases in sporulation initiation (Figure 23). In contrast, CD1492 seems to have a negative effect on sporulation since its inactivation increases spore production (Childress et al. 2016). The signals or molecules triggering sporulation in *C. difficile* have not been identified yet. However, environmental stimuli such as nutrient limitation and other stress factors might be

involved. This is consistent with the impact of the CodY and CcpA regulators that negatively control sporulation in *C. difficile* (Figure 23) (Dineen et al. 2010, Antunes et al. 2012). Indeed, both *codY* and *ccpA* mutants sporulate more effectively than the wild-type strain (Antunes et al. 2012, Nawrocki et al. 2016). CcpA, the catabolite control protein, is implicated in the repression of genes involved in the control of the first stages of sporulation like *spo0A* and *spoIIA* operon (Antunes et al. 2012), while CodY was found to negatively controls the expression of *spo0A* as well as the two HKs *CD1579* and *CD2492* (Figure 23) (Dineen et al. 2010, Nawrocki et al. 2016). A study performed by Edwards *et al* suggested that *C. difficile* initiates sporulation in response to nutrient availability and uptake (Edwards et al. 2014). In agreement, an increased sporulation was observed when genes encoding two oligopeptide permeases, Opp and App, were inactivated, likely due to the inability to import small peptides as a nutrient source. In other Gram positive bacteria, Opp and App are also involved in the import of small quorum sensing peptides, which control physiological processes such as sporulation, toxin expression and production of other virulence factors (Perego et al. 1991, Rudner et al. 1991, Solomon et al. 1996, Gominet et al. 2001). However, it remains unclear whether *C. difficile* employs quorum sensing to regulate sporulation initiation. Recently, the regulator RstA was found to positively control sporulation initiation in *C. difficile*, while repressing motility and toxin production (Figure 23) (Edwards et al. 2016b).

Sigma factors and transcriptional regulators

In *B. subtilis*, hierarchical regulatory cascades such as $\sigma^F \rightarrow \text{RsfA} / \sigma^G \rightarrow \text{SpoVT} \rightarrow \text{YlyA}$ in the FS and $\sigma^E \rightarrow \text{GerR} / \text{SpoIIID} \rightarrow \sigma^K \rightarrow \text{GerE}$ in the MC (Figure 21) describe the programs of gene expression within each compartment (Eichenberger et al. 2004, Wang et al. 2006). These two lines of gene expression are connected by intercellular signalling pathways (Figure 21). In *C. difficile*, the sporulation σ factors exhibit compartment-specific activation similar to *B. subtilis*, with σ^F and σ^G activity being restricted to the FS and σ^E and σ^K activity being restricted to the MC (Fimlaid et al. 2013, Pereira et al. 2013). Similarly, the inactivation of *sigF* and *sigE* in *C. difficile* blocks the sporulation process after asymmetric division forming mutants with disporic forms. The *sigG* and *sigK* mutants are blocked after engulfment completion (Fimlaid et al. 2013, Pereira et al. 2013). *sigG* mutant does not make cortex while deposition of coat-like electron-dense material around the FS was observed contrary to what was detected in *B. subtilis*. *C. difficile sigK* mutant produces FS with a cortex layer but the coat layer is absent (Fimlaid et al. 2013, Pereira et al. 2013). This suggests that in *C.*

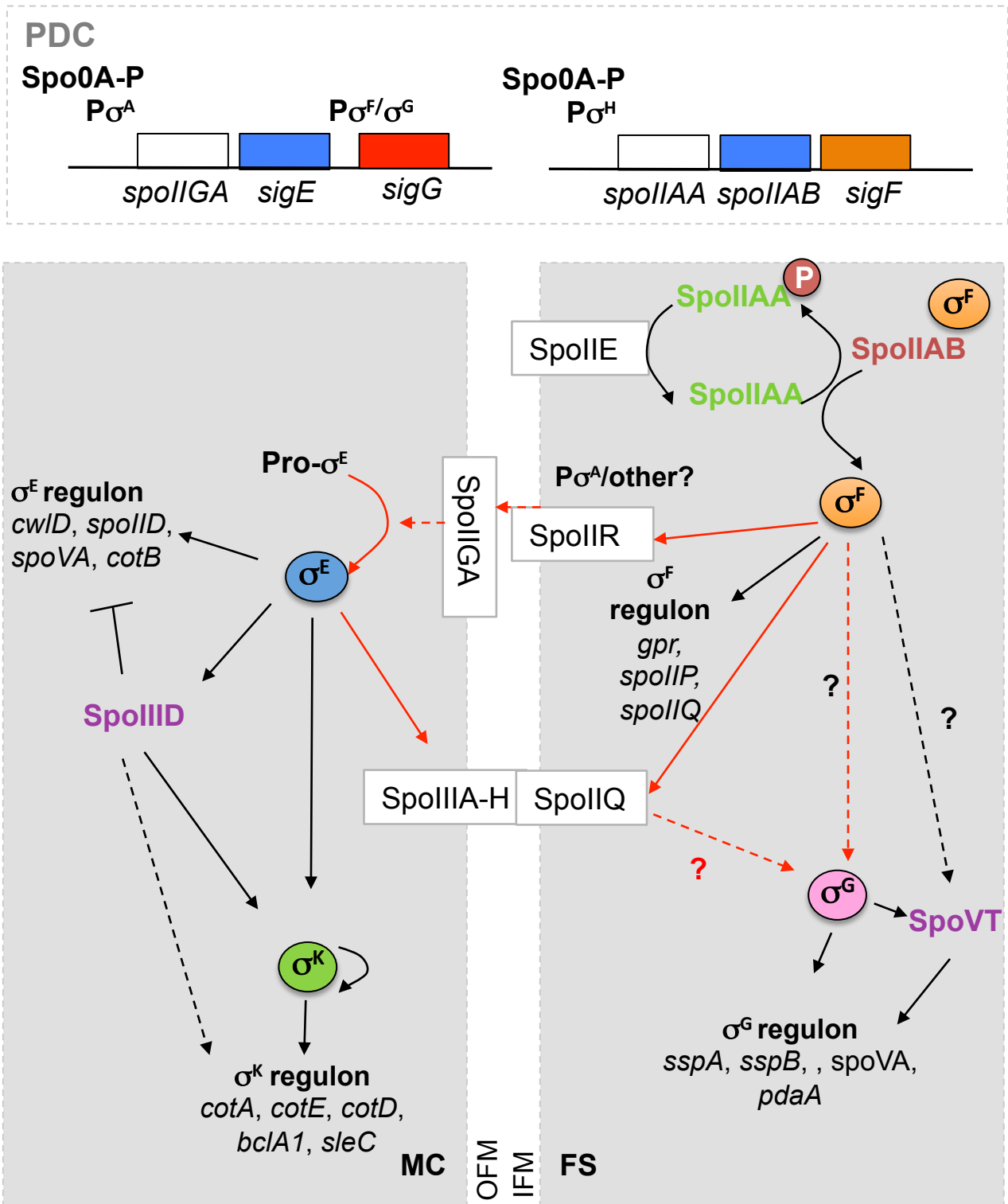


Figure 24: Model of the regulatory network controlling sporulation in *C. difficile*. Temporal progression of sporulation is shown from top to bottom. Boxes represent the predivisive cell (PDC), mother cell (MC) and forespore (FS), the two cell compartments formed after asymmetric division. Membranes separating the FS and the MC are indicated (OFM: outer forespore membrane; IFM: inner forespore membrane). Sigma factors are colored and bold, the precursor protein of σ^E is indicated as pro- σ^E . Transcriptional regulators are shown in purple. Proteins associated with the membranes or located into the intermembrane space are in square. Black solid arrows indicate activation at the transcriptional level. Red arrows indicate the intercellular signal pathways required for sigma factor activity. Broken arrows with a question mark represent mechanisms that are not yet fully understood. Adapted from Saujet *et al.*, 2013.

difficile, σ^K is dispensable for cortex development and controls coat polymerization, similar to *B. subtilis*. Even if the main functions and periods of activity of the sporulation specific sigma factors are conserved in *C. difficile*, a less tight communication between the FS and the MC compartment and a weaker connection between morphogenesis and expression are observed (Fimlaid et al. 2013, Pereira et al. 2013, Saujet et al. 2013). Moreover, only two regulators, SpoVT in the FS and SpoIIID in the MC, are found in *C. difficile* (Pishdadian et al. 2015). Compared to *B. subtilis*, in *C. difficile* (i) the σ^E regulon is not strictly under the control of σ^F although SpoIIR is essential for pro- σ^E cleavage; (ii) σ^E is dispensable for σ^G activation; (iii) σ^G is dispensable for σ^K activation; and (iv) σ^K does not undergo proteolytic activation in *C. difficile* (Fimlaid et al. 2013, Pereira et al. 2013, Saujet et al. 2013).

The forespore regulatory network: σ^F and σ^G

The *spoIIAA-spoIIAB-sigF* operon is transcribed by σ^H and positively controlled by Spo0A (Figure 24) (Saujet et al. 2011, Rosenbusch et al. 2012). σ^F , the first σ factor of the FS, is expressed before and after asymmetric division in both compartments, but the expression of its targets is observed only in the FS indicating that σ^F is active only in the smaller compartment (Pereira et al. 2013). As in *B. subtilis*, the mechanism of activation of σ^F is probably dependent on the anti- σ SpoIIAB, the anti-anti- σ factor SpoIIAA and the phosphatase SpoIIE (Figure 24) (Duncan and Losick 1993, Fimlaid and Shen 2015). Once activated, σ^F controls the expression of about 25 genes. Among them are *spoIIR*, *spoIIQ* and *spoIIP*. Similarly to *B. subtilis*, SpoIIQ and SpoIIP are critical for the engulfment completion (Serrano et al. 2016a, Dembek et al. 2018, Ribis et al. 2018). However, in *B. subtilis*, *spoIIP* is part of the σ^E regulon. In *C. difficile*, σ^F is also required to transcribe the *gpr* gene encoding a protease probably important for degradation of SASPs during germination (Sussman and Setlow 1991, Fimlaid et al. 2013, Saujet et al. 2013). Moreover, σ^F also controls the expression of genes thought to be involved in PG metabolism: *sleB*, *CD2141* and *CD1229* encoding a spore cortex hydrolysing enzyme, a DAla-DAla carboxypeptidase and a PG glycosyltransferase, respectively. Like in *B. subtilis*, the *spoIIGA*, *sigE* and *sigG* genes are clustered in *C. difficile* (Figure 24) (de Hoon et al. 2010). In *C. difficile*, *sigG* gene is likely transcribed from two promoters, one recognized by σ^A upstream of the *spoIIGA* gene and one upstream of the *sigG* gene recognized by σ^F and/or σ^G , since a promoter with both FS σ factor consensus sequences have been mapped (Saujet et al. 2011, Saujet et al. 2013). In *B. subtilis*, the onset of σ^G activity coincides with engulfment completion and requires the activity of σ^E . However, in *C. difficile*, σ^G activation does not require engulfment to be completed and is

independent of σ^E (Pereira et al. 2013, Saujet et al. 2013) suggesting that the feeding tube is dispensable for σ^G activity. In *C. difficile*, since a *sigF* mutant produces wild-type levels of σ^G but decreased levels of the σ^G -target genes, σ^G seems to require σ^F for post-translational activation via an unknown mechanism (Figure 24) (Fimlaid et al. 2013). σ^G controls the expression of 50 FS-specific genes including genes encoding the SASPs and the *spoVA* operon, which is required for the import of DPA from the MC to the FS (Donnelly et al. 2016). Additionally, genes encoding proteins that might be involved in protection against oxidative stress are controlled by σ^G . This includes *CD1567* (CotG), *CD1631* (SodA) and *CD2845*, which encode a catalase, a SOD and a rubrerythrin, respectively, as mentioned earlier in Chapter 3 (Permpoonpattana et al. 2013, Saujet et al. 2013). Genes involved in cell wall synthesis and cortex formation are also controlled by this σ factor (Fimlaid et al. 2013, Saujet et al. 2013). *CD1430* (PdaA1) encodes a N-acetylmuramic acid deacetylase involved in the formation of muramic- δ -lactam in the spore cortex PG (Coullon et al. 2018, Diaz et al. 2018). In addition, *CD1291* (*dacF*), which encodes a D-Ala-D-Ala carboxypeptidase likely regulating the degree of cross-linking of the spore PG was also positively controlled by σ^G . Finally, the *spoVT* gene encoding the SpoVT regulator is probably transcribed under the dual control of σ^F and σ^G (Fimlaid et al. 2013, Saujet et al. 2013). SpoVT is involved in the regulation of σ^G -targets such as *sspA* and *sspB* encoding the SASPs (Figure 24). Additionally, SpoVT seems to negatively regulate *spoIIR* and *gpr*, suggesting that, in *C. difficile*, this regulator might play the role of RsfA in the negative control of σ^F targets (Saujet et al. 2013).

The mother cell regulatory network: σ^E and σ^K

The *sigE* gene is transcribed from a σ^A -dependent promoter and positively controlled by Spo0A (Figure 24) (Saujet et al. 2011, Rosenbusch et al. 2012). In *C. difficile*, σ^F was found to positively regulate the expression of *spoIIR*. Whereas in *B. subtilis* σ^E maturation in the MC after asymmetric division is strictly dependent on σ^F , in *C. difficile*, such maturation is partially independent of this FS σ factor. Indeed, in *C. difficile* the synthesis of SpoIIR, that triggers the proteolysis of pro- σ^E into σ^E by SpoIIGA is partially independent on σ^F (Figure 24) (Saujet et al. 2013). The σ^E regulon comprises around 97 genes and is the largest regulon among the four sporulation specific σ factors as observed in *B. subtilis*. σ^E transcribes genes encoding proteins involved in engulfment control, formation of the feeding tube, synthesis of the cortex, germination and initiation of coat assembly (Fimlaid et al. 2013, Saujet et al. 2013). The *spoIID* gene encoding a PG hydrolase required for the engulfment of the FS is controlled by σ^E as well as the *cwlD* gene, encoding a N-acetylmuramoyl-L-alanine amidase

that together with the FS-controlled PdaA1 generates muramic- δ -lactam (Saujet et al. 2013, Diaz et al. 2018). As in *B. subtilis*, σ^E activates the expression of the *spoIIAA* operon. The genes of the *csp* operon, encoding the germinant receptor (CspC) and the proteases responsible for the activation of cortex-lytic enzymes (CspAB) during germination, are also under the control of σ^E (Adams et al. 2013, Francis et al. 2013a, Saujet et al. 2013). Additionally, a σ^E -dependent promoter was mapped upstream of *spoIVA*, *sipL* and *cotB* genes, all encoding spore coat proteins (Permpoonpattana et al. 2011a, Putnam et al. 2013, Saujet et al. 2013). Finally, σ^E transcribes the genes encoding σ^K and the transcriptional regulator SpoIIID, which negatively controls the transcription of members of the σ^E regulon (such as *spoIVA*, *sipL*, *cotB* and the *spoIIA* operon) and positively controls the expression of some members of the σ^K regulon (Figure 24) (Fimlaid et al. 2013, Pereira et al. 2013). In *C. difficile*, the *sigK* gene is transcribed from two different promoters: one dependent on σ^E and the other dependent on σ^K and positively controlled by SpoIIID (Fimlaid et al. 2013, Pereira et al. 2013, Saujet et al. 2013, Pishdadian et al. 2015). The positive control of SpoIIID under σ^K -controlled genes is due either to a direct binding of the regulator or via the positive control that SpoIIID exerts on *sigK* transcription. While σ^K is synthesized in *B. subtilis* as an inactive pre-protein, σ^K of *C. difficile* lacks a pro-sequence and the cleavage proteins (Figure 24 and 22B). Therefore, in *C. difficile*, σ^K is produced directly in its mature form. Accordingly, the absence of a cleavage process at the end of the engulfment, avoids a dependency of σ^G on σ^K activity in this bacterium (Pereira et al. 2013, Saujet et al. 2013).

The skin^{Cd} element

As observed in *B. subtilis*, a *skin^{Cd}* element is also present in the *sigK* gene of *C. difficile* (Figure 22B) (Stragier et al. 1989, Kunkel et al. 1990, Haraldsen and Sonenshein 2003). Compared with *B. subtilis*, the *skin^{Cd}* differs in size, gene content, site of insertion and orientation suggesting independent integrations into *sigK* gene during evolution (Haraldsen and Sonenshein 2003). The *skin^{Cd}* element has 19 open reading frames and a cassette of the CRISPR system used for protection against foreign DNA (Monot et al. 2011, Soutourina et al. 2013). Two proteins, CD1231 and CD1234, encoded by genes located within the *skin^{Cd}* are required for the excision of this element (Figure 22B) (Serrano et al. 2016b). CD1231 is a recombinase interacting with CD1234, a recombination directionality factor, to excise the *skin^{Cd}* element in the MC while only CD1231 is necessary for *skin^{Cd}* integration (Serrano et al. 2016b). Interestingly, the *CD1231* gene is constitutively expressed contrary to *spoIVCA* encoding the recombinase of the *skin^{Bs}*. By contrast, the expression of the *CD1234* gene is

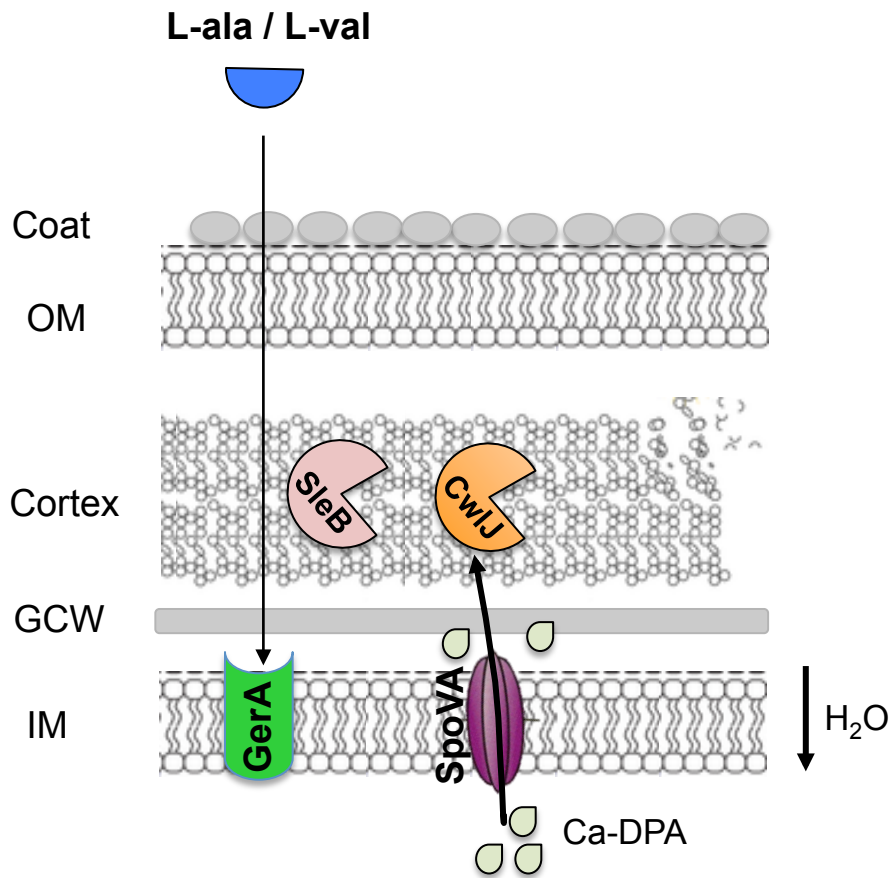


Figure 25: *B. subtilis* spore germination. Germinants such as L-alanine (or L-valine) interact with the GerA germinant receptor complex. The SpoVA channel is then activated and it releases Ca-DPA from the spore core. Released of Ca-DPA activates the CwlJ cortex hydrolase triggering cortex hydrolysis. OM, GCW and IM correspond to outer membrane, germ cell wall and inner membrane, respectively.

dependent on both σ^E and SpoIIID which results in the production of CD1234 only in the MC (Serrano et al. 2016b). The late production of CD1234 delays and restricts skin^{Cd} excision to the terminal MC. Thus, in *C. difficile*, the crucial element regulating σ^K activity is the skin^{Cd} excision (Serrano et al. 2016b). Then, the *sigK* gene is reconstituted, transcribed and translated. Global transcription profiling revealed that σ^K controls the transcription of 56 genes encoding proteins involved in processes such as synthesis of DPA, the assembly of the spore coat and exosporium as well as in the lysis of the MC (Figure 24) (Fimlaid et al. 2013, Saujet et al. 2013). The *dpaA* and *dpaB* genes encoding the DPA synthase are controlled by σ^K (Donnelly et al. 2016). In addition, genes encoding coat proteins such as CotA, CotE or the YabG protease are also positively controlled by σ^K . This is also the case for the *bclA1*, *bclA2* and *bclA3* genes encoding exosporium proteins and of two genes encoding N-acetylmuramic acid L-alanine amidases (*CD1898* and *CD2184*) that are possibly involved in MC lysis. Finally, *sleC* encoding the major spore cortex lytic enzyme is also a member of σ^K regulon.

III. Germination

The process by which the spores reinitiate growth is called germination. Germination usually occurs in response to environmental signals including amino acids and cell wall PG mucopeptides derived from growing cells (Setlow 2003, Shah et al. 2008). Since CDI is mediated by toxin producing vegetative cells, germination of *C. difficile* spores is an important initial step for the disease process (Howerton et al. 2013). Indeed, *C. difficile* strains presenting a defected germination are associated to a decreased virulence (Francis et al. 2013a, Fimlaid et al. 2015).

III.1. Germination in *B. subtilis*

In *B. subtilis*, nutrient germinants are sensed by Ger-type germinant receptors (GRs) synthesized in the FS under σ^G control, and localized at the inner membrane of the spore (Figure 25) (Paredes-Sabja et al. 2011). The germinants must pass through the spore coat, the FS outer membrane and the cortex to access the GRs. Thus, it is possible that there are specialized mechanisms to facilitate germinants access into the spore. In some bacilli, the GerP proteins located in the spore coat may play this function (Carr et al. 2010, Butzin et al. 2012). In bacilli and some clostridia, the binding of the germinant to the GRs, triggers the release of the DPA chelated to calcium (Ca-DPA) and of the monovalent ions (H^+ , Na^+ and K^+) stored in the spore core. During sporulation, DPA is initially synthesized in the MC

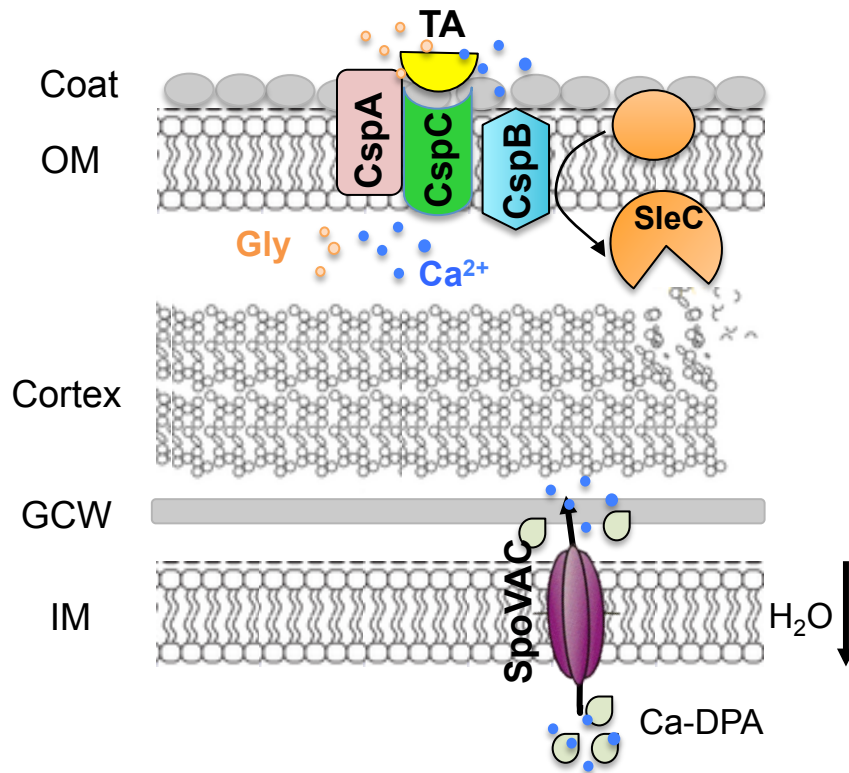


Figure 26: *Clostridium difficile* germination. CspC senses bile salts such as taurocholate and the co-germinants Ca²⁺ or Glycine. Csp protein-protein interactions lead to processing of pro-SleC to an active form. Cortex hydrolysis begins and SpoVAC releases CaDPA. OM, GCW and IM correspond to outer membrane, germ cell wall and inner membrane, respectively.

(Daniel and Errington 1993, Orsburn et al. 2010) and then transported into the core of the FS by a two step transport mechanism. DPA is first translocated into the intermembrane space by the FS outer membrane protein SpoVV (*ylbJ*, a σ^E regulated gene) and then is transferred into the spore core by the SpoVA complex located in the inner spore membrane (Tovar-Rojo et al. 2002, Ramirez-Guadiana et al. 2017). The same SpoVA channel is involved in the release of Ca-DPA during germination (Vepachedu and Setlow 2007). In *B. subtilis*, the Ca-DPA released binds to the cortex hydrolase CwlJ as a cofactor leading to the CwlJ activity (Figure 25) (Paidhungat et al. 2001). SleB is other cortex lytic enzyme which seems to be activated by cortex deformation (Paidhungat et al. 2001). The cortex degradation allows core hydration and resumption of metabolism in this compartment that results in the formation of the vegetative cell (Paidhungat et al. 2001, Vepachedu and Setlow 2007).

III.2. Germination in *C. difficile*

C. difficile genome lacks orthologs of GerA, GerB and GerK receptors involved in germination in *B. subtilis* (Sebaihia et al. 2006) suggesting that this bacterium responds to different environmental signals than those identified in bacilli. In fact, *C. difficile* spores germinate in response to a combination of specific bile salts (i.e., cholate and its derivatives [taurocholate, glycocholate and deoxycholate]). In addition, both L-glycine and divalent cations such as Ca^{2+} and Mg^{2+} can also act as co-germinants (Kochan et al. 2017). A recent study showed that Ca^{2+} present within the gastrointestinal tract play a major role in inducing germination *in vivo*. Ca^{2+} depletion of the ileal mouse contents reduced spore germination from 630 *C. difficile* strain by 90% (Kochan et al. 2017). The *C. difficile* genome encodes an operon of subtilisin-like proteases, *cspBAC*, controlled by σ^E that is essential for germination (Saujet et al. 2013, Kevorkian and Shen 2017). CspC was identified as the bile salt GR of *C. difficile* and it is located in the spore coat/ FS outer membrane (Figure 26) (Francis et al. 2013a). Moreover, the first evidence that CspC senses the different classes of co-germinants in addition to bile salts was recently showed (Rohlfing et al., 2018, bioRxiv, doi: <https://doi.org/10.1101/461657>). The CspB and CspA proteins also contribute to germination. Initially produced as a fusion, CspBA is processed by the YabG protease into CspB and CspA prior to incorporation into the spore (Kevorkian and Shen 2017). Then, CspA will be required for the incorporation of CspC into the mature spore (Kevorkian et al. 2016, Kevorkian and Shen 2017). The germination model supports the idea that upon germinants sensing, CspC activates the protease CspB, the only Csp protein with an intact catalytic triad

(Figure 26). CspB is required for the activation of the cortex lytic enzyme SleC, by cleavage of the inactive pro-SleC into SleC. Once activated, SleC initiates degradation of the cortex PG (Figure 26) (Burns et al. 2010, Adams et al. 2013, Kevorkian and Shen 2017). SleC is thought to recognize the cortex-specific modification muramic- δ -lactam (Burns et al. 2010, Gutelius et al. 2014). Contrary to *B. subtilis*, the hydrolysis of the cortex in *C. difficile*, precedes DPA release (Francis et al. 2015, Wang et al. 2015). Swelling of the core after cortex hydrolysis leads to DPA release through SpoVAC most likely by a mechanosensing mechanism (Francis and Sorg 2016). The role of the co-germinants and the events that lead to CspB activation are the major weakness of the model. A study showed that Ca^{2+} is required for CspB-mediated SleC cleavage (Kochan et al. 2017). Ca^{2+} from the spore core or from the external environment might bind to and activates CspB, with subsequent SleC activation and cortex hydrolysis. Another hypothesis is that CspC activates CspB by protein-protein interaction. Other proteins like GerG, GerS and CD3298 are also involved in the germination process. All of them are encoded by genes controlled by σ^E . GerS is a lipoprotein recently shown to be necessary for CwID-mediated cortex modification (Fimlaid et al. 2015, Diaz et al. 2018). GerS and CwID directly interact and CwID mediates GerS incorporation into mature spores. The cortex modifications are required for an efficient cortex hydrolysis by the lytic enzyme SleC (Diaz et al. 2018). Another protein required for *C. difficile* germination is GerG. Since *gerG* mutant produces spores lacking Csp proteins, the hypothesis is that GerG is required for optimal incorporation of CspA, CspB and CspC into spores (Donnelly et al. 2017). CD3298 is an ATPase likely involved in transport of Ca-DPA across the FS outer membrane (Kochan et al. 2017).

A

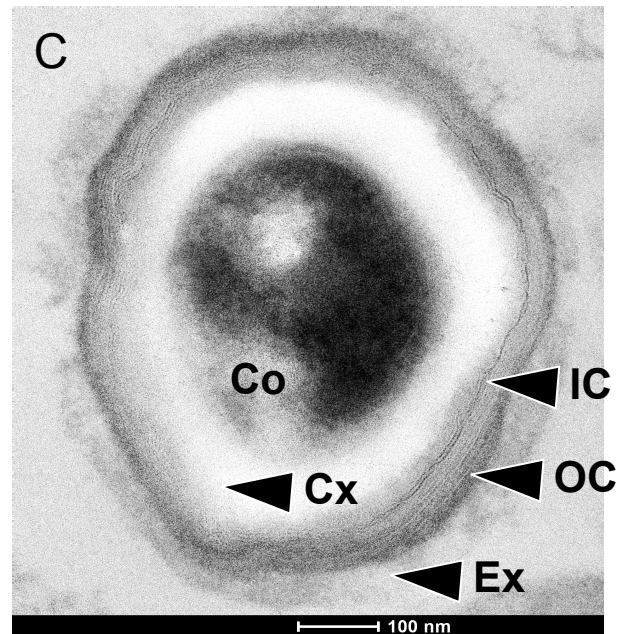
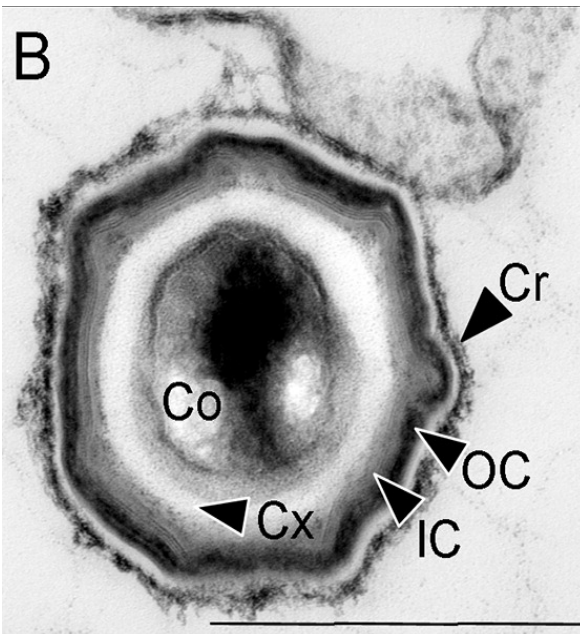
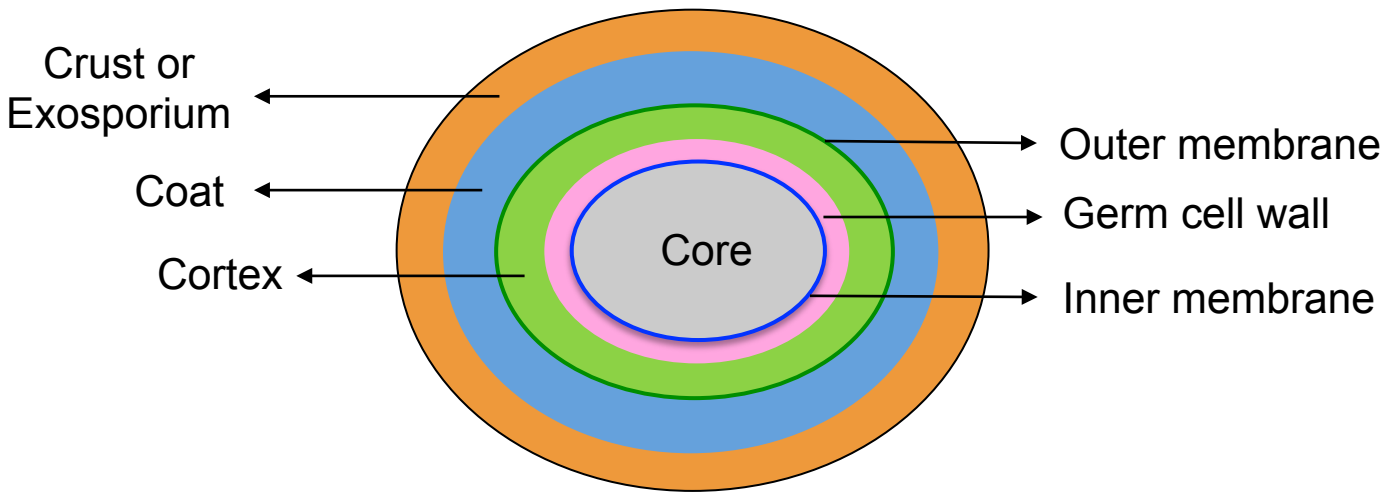


Figure 27: Structure of a bacterial spore. A) The main layers of the spore are represented. The most external layer, either crust or exosporium, is not present in all spore formers. Transmission electron microscopy of a *B. subtilis* spore (B) and a *C. difficile* spore (C). Co, Cx, IC, OC, Cr and Ex are abbreviations for core, cortex, inner coat, outer coat, crust and exosporium, respectively (*B. subtilis* picture was adapted from McKenney *et al.*, 2010).

Chapter 5: The spore

I. Structure of the spore

The overall architecture of the spore is conserved among endospore-forming bacteria. The spore is a spherical or roughly ovoid structure composed by concentric layers, surrounding the core in its center (Figure 27A). The spore core harbors the chromosomal DNA, maintained in a highly compact state by the SASPs that are believed to block transcription and protect the DNA (Setlow 2007, Moeller et al. 2008, Paredes-Sabja et al. 2008, Setlow 2014). The core also contains DPA in a 1:1 complex with divalent cations, mostly Ca^{2+} . The core is delimited by an inner membrane that retards the diffusion of water and serves as permeability barrier against chemicals (Setlow 2003, Sunde et al. 2009, Knudsen et al. 2016). In many species, this membrane houses the germinant receptors (Paredes-Sabja et al. 2011). The inner membrane will become the plasma membrane after germination. Around the FS inner membrane is a PG-containing germ cell wall that will become the cell wall for the emerging cell during outgrowth. The germ cell wall is surrounded by the spore cortex layer and the outer membrane. The cortex plays a major role in maintaining the dehydrated state of the core by constricting the core's volume. The cortex is a modified PG-containing layer, where the N-acetyl muramic acid is replaced by muramic- δ -lactam (Meador-Parton and Popham 2000). This modification is essential for specific hydrolysis by cortex lytic enzymes during germination, which degrade only the cortex layer and not the germ cell wall. Concomitantly with cortex formation, the proteinaceous spore coat layer is deposited at the surface of the outer membrane. This layer is universally present but varies in composition and morphology among species (Aronson and Fitz-James 1976, Henriques and Moran 2000, Giorno et al. 2007, Driks and Eichenberger 2016). In the case of *B. subtilis*, the spore coat is enfolded by the crust (Figure 27B) (McKenney et al. 2010). In other species such as *B. anthracis* and *C. difficile*, the most external spore layer is the exosporium (Figure 27C) (Stewart 2015). Most of these spore structures are rapidly lost during germination i.e., the cortex is degraded by cell wall hydrolases and the coat is shed. The fate of the outer spore membrane is less clear.

II. Spore resistance

Spores are metabolically dormant and partially dehydrated, which are likely

characteristics that allow their survival in nutrient-free and harsh environments (Setlow 2006, 2014). They exhibit extraordinary resistance properties including resistance to ultraviolet (UV) radiation, chemicals (such as H₂O₂ and hypochlorite), extreme heat and other stresses. Therefore, high level of Ca-DPA and partial dehydration of the spore core, a functional cortex, RecA-dependent DNA repair machinery and SASPs are important requirements for resistance to extreme heat (Setlow 2006, 2007, Paredes-Sabja et al. 2008, Donnelly et al. 2016). During late stages of sporulation, most of the water in the spore core is replaced with Ca-DPA, and mutants deficient in Ca-DPA do not survive desiccation.

II.1. Functions of the spore coat

The coat protects against a wide range of assaults, including digestion by predatory microbes and challenges by various chemicals (Nicholson et al. 2000, Riesenman and Nicholson 2000, Klobutcher et al. 2006, Setlow 2014). For example, intact *B. subtilis* spores can survive ingestion by *Tetrahymena thermophila*. However, coat disruption results in a digestion of the cortex by the protozoa (Klobutcher et al. 2006). Resistance to these organisms is likely due to exclusion of microbial degradative enzymes by sieving. For instance, the spore coat protects the underlying spore cortex, which is susceptible to PG-degrading enzymes such as lysozyme.

It seems reasonable to assume that the coat acts as a barrier, passively excluding degradative enzymes (Setlow 2006). However, the spore coat is not impermeable, because germinants can pass through it en route to the GRs in the inner membrane (Setlow et al. 2017). The coat also protects against several types of reactive chemicals, such as chlorine dioxide, hypochlorite, ozone, peroxyxynitrite and H₂O₂ (Setlow 2006, 2014). *B. subtilis* spores lacking the CotE protein essential for coat morphogenesis are more sensitive to H₂O₂ and hypochlorite (Riesenman and Nicholson 2000, Henriques and Moran 2007). Therefore, more specific resistance properties, like those directed against oxidative compounds, might be provided by catalases and other enzymes present in the coat. A Mn²⁺-dependent SOD (SodA) and at least two Mn²⁺ pseudocatalases, CotJC and YjqC, are associated with the *B. subtilis* coat layers. However, a possible role in protection against ROS has never been shown (Henriques et al. 1995, Henriques et al. 1998). In *C. difficile*, CotCB, CotD and CotG catalases are present in the surface layers of spores and *cotD* mutant spores showed a reduction in catalase activity compared to the wild-type strain (Permpoonpattana et al. 2013). Protection against UV radiation and H₂O₂ seems to be provided in part by CotA, a copper-

dependent laccase present in the outer coat of *B. subtilis*, which generates a melanin-like dark brown pigment that accumulates in the spores (Hullo et al. 2001, Martins et al. 2002). In addition, spore coat components might react with and detoxify some chemicals before they reach and attack their targets further within the spore (Riesenman and Nicholson 2000, Henriques and Moran 2007, Setlow 2014).

An integral coat seems to be also required for an efficient germination. In *B. subtilis*, the assembly of the cortex lytic enzyme CwlJ is dependent on the coat protein GerQ and the spores of the *gerQ* mutant germinate poorly (Bagyan and Setlow 2002). The inactivation of the *gerP* operon, mentioned earlier in the Chapter 4, section III.1 Germination in *B. subtilis*, also blocks germination prior to cortex hydrolysis in *B. subtilis* and *B. cereus*. GerP proteins seems to play a crucial role producing a permeable coat to small hydrophilic germinants to gain access to their receptors in the inner layers of the spore (Behravan et al. 2000, Butzin et al. 2012).

III. Spore surface layers of bacilli and clostridia

III.1. Conservation of proteins

The most internal spore compartments, core and cortex, do not usually display interspecies differences that are distinguishable by electron microscopy. Moreover, genes encoding proteins involved in the formation of the spore cortex, *spoVB*, *spoVD*, *spoVE*, *yabP*, *yabQ*, *ylbJ*, *yqfC* and *yqfD* in *B. subtilis* are conserved in spore forming bacteria, suggesting a conservation of the cortex biosynthesis (Fawcett et al. 2000, Asai et al. 2001, Eichenberger et al. 2003). By contrast, considerable diversity is observed in the structure of the most external layers such as the spore coat. About 80% of the spore coat proteins are conserved between *B. subtilis* and *B. anthracis*. In addition, 16 coat proteins appear to be unique to *B. subtilis* such as the *cgeAB* and *cgeCDE* operons encoding spore coat maturation proteins (Henriques and Moran 2007). In clostridia, conservation of *B. subtilis* coat proteins is even more limited (Henriques and Moran 2007, de Hoon et al. 2010, Permpoonpattana et al. 2011b, Galperin et al. 2012). Only about 20 genes of the *B. subtilis* encoding coat structural proteins have their homologs in the sequenced clostridial genomes. Considering that the spore surface represents the interface between spores and the environment, and given the diversity in coat structure and composition among species, it seems reasonable to speculate that this diversity is driven by adaptation of spore forming bacteria to variety of niches.

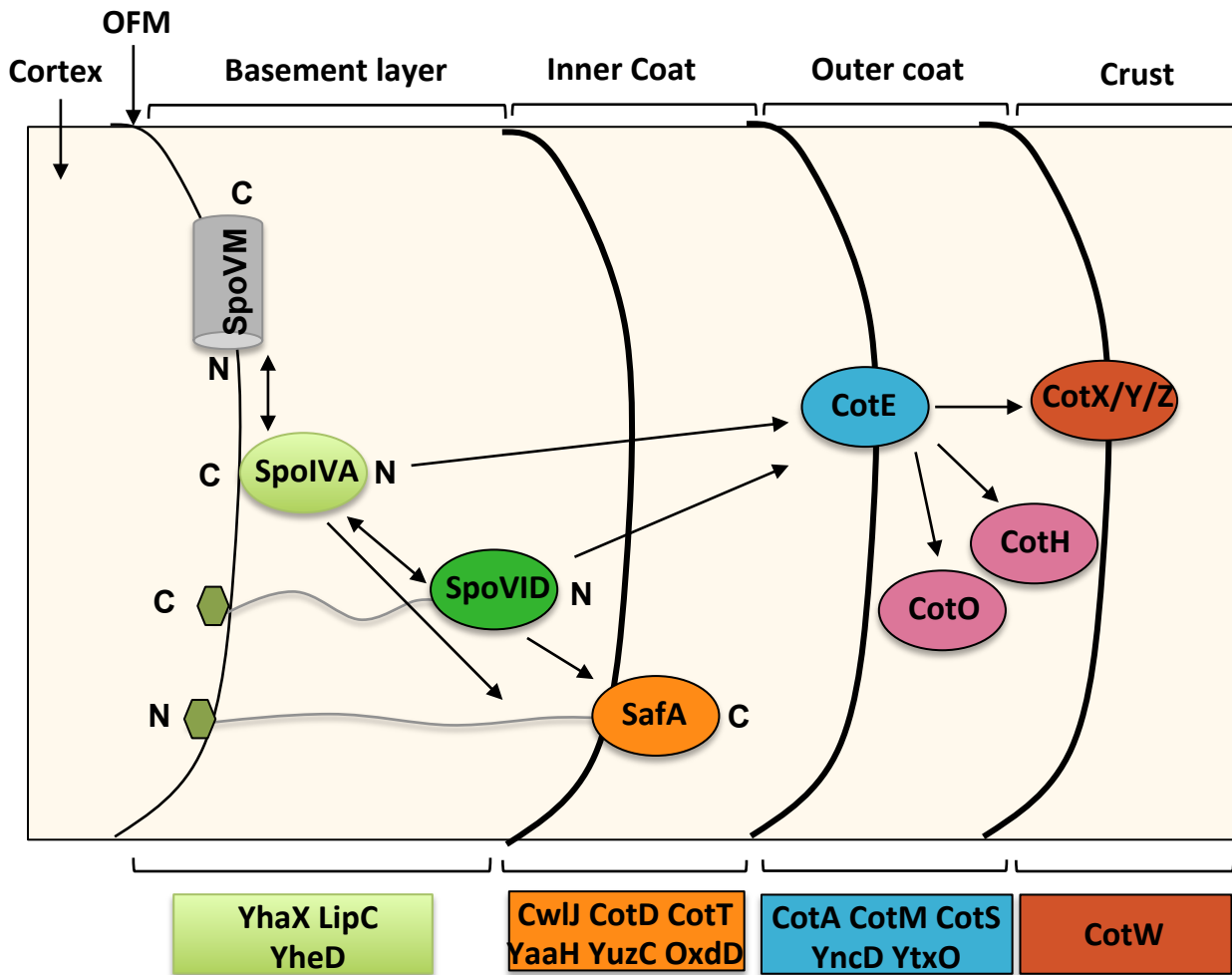


Figure 28: The *B. subtilis* coat interaction network. Morphogenetic proteins are indicated on the upper part of the figure and are located where their main function is exerted. The hexagon represent the LysM domain. Arrows indicate the interactions between the different morphogenetic coat and crust proteins. Examples of coat proteins, which proper location is dependent on the respective morphogenetic protein are indicated on the bottom of the figure. Assembly of each layer may be driven by the multimerization of the indicated morphogenetic protein. Polymerization of a morphogenetic protein would, presumably, create the necessary binding sites for each of the individual coat proteins that make up each layer. It remains to be determined whether and how the proteins of the individual layers interact with adjacent layers and how adjacent layers interact to form the mature spore coat. Adapted from Henriques and Moran 2007 and McKenney *et al.*, 2013.

III.2. Spore coat organization in *B. subtilis*

The spore coat of *B. subtilis* is a multilayered proteinaceous structure, composed at least by 70 proteins with a range in size from 6 kDa to larger than 70 kDa (Henriques and Moran 2007, McKenney et al. 2013, Driks and Eichenberger 2016). Proteins found in the coat layers can be extracted from purified spores by treatment with reducing agents in the presence of detergents (Henriques and Moran 2007). This spore layer is divided in an undercoat or basement layer, a lamellar inner coat and an electrodense outer coat (Figure 28) (McKenney and Eichenberger 2012). The inner and outer coat gained these designations due to the differences observed using TEM and osmium tetroxide staining i.e., the inner coat was more lightly and contained multiple concentric dark lamellae and the outer coat was electrodense and darkly stained (Warth et al. 1963, Giorno et al. 2007, Henriques and Moran 2007). Both coat layers are packed closely together and appear thicker at the spore poles. The factors that determine the pattern of each layer is not known but most likely reflects the successive overlay of the coat proteins during the assembly and their physical properties. The basement layer, is not distinguishable by TEM, but corresponds to the innermost layer atop which the rest of the coat assembles. It contains several coat proteins required to initiate coat assembly such as SpoIVA, SpoVM and SpoVID (Figure 28). These proteins help bridging the coat to the cortex layer (Driks and Eichenberger 2016). Indeed, some mutants with deficiencies in coat assembly (e.g., *cotE*) have undercoat regions that do not properly adhere to the underlying cortex (Zheng et al. 1988, Aronson et al. 1992, Driks and Eichenberger 2016).

III.2.a. Coat morphogenetic proteins

In *B. subtilis*, the formation of the coat layers is governed by the morphogenetic factors SpoVM, SpoIVA, SpoVID, SafA, and CotE (Figure 28) (Henriques and Moran 2007, McKenney et al. 2013). They were named morphogenetic proteins as they play a major role in coat morphogenesis without affecting gene expression. A combination of genetic and electron microscopy analyses was used to infer the locations of the morphogenetic proteins. Only SpoIVA is present in all bacilli and clostridia. SpoIVA is produced in the MC under the control of σ^E , and is essential for the assembly of both the spore cortex and coat layers (Piggot and Coote 1976, Roels et al. 1992, Stevens et al. 1992, Catalano et al. 2001). SpoIVA binds and hydrolyses ATP to form highly stable polymers that encase the FS (Ramamurthi and Losick 2008, Wu et al. 2015). The localization of SpoIVA requires SpoVM, also produced under the control of σ^E (Figure 28) (Price and Losick 1999). Both proteins were found to

localize early to the MC face of the FS outer membrane and were observed tracking along with the engulfing FS membrane forming a full spherical shell that encases the spore in a step known as “spore encasement” (Driks et al. 1994, Pogliano et al. 1995, Price and Losick 1999, van Ooij and Losick 2003). To this end, the C-terminal part of SpoIVA interacts with the N-terminal region of SpoVM and then polymerizes and surrounds the FS (Figure 28) (Ramamurthi et al. 2006). SpoVM is a 26-amino-acid-long protein that recognizes the positive curvature of the FS outer membrane and embeds itself there (Levin et al. 1993, Ramamurthi et al. 2009, Gill et al. 2015). Both *spoIVA* and *spoVM* mutants fail to make cortex, and the coat accumulates as swirls floating in the MC cytoplasm (Roels et al. 1992, Levin et al. 1993). Even if coat assembly and cortex formation are events that occur in different compartments, MC and intermembrane space respectively, SpoIVA and SpoVM are required for both processes. At this initial stage of coat formation, a quality control mechanism is present that prevents cortex formation if SpoIVA fails to encase the FS (Tan et al. 2015). It is dependent on the CmpA protein and the ClpXP protease. In the presence of spore coat defects, CmpA binds to improperly localized SpoIVA and delivers it to ClpXP for degradation (Tan et al. 2015). After elimination of SpoIVA, cortex formation is inhibited and the sporulating cell eventually lyses. In the absence of defect, CmpA is eliminated by ClpXP-mediated proteolysis. SpoIVA and SpoVM finish spore encasement as soon as engulfment is completed (McKenney and Eichenberger 2012). However, SpoIVA does not complete encasement in the absence of another coat morphogenetic protein SpoIVD (Wang et al. 2009a) whose production is also under the control of σ^E (Beall et al. 1993). SpoIVA proper assembly requires SpoIVD, but SpoIVA is also required for the localization of SpoVID to the surface of the developing spore (Figure 28) (Beall et al. 1993, Driks et al. 1994). This mutual dependency is supported by the evidence that SpoIVA interacts with the SpoVID’s N terminus (Figure 28). The phenotype of *spoVID* mutant cells is reminiscent of the observed in the *spoIVA* and *spoVM* mutants (Beall et al. 1993). However, SpoVID seems to be specifically devoted to the spore coat layer, since *spoVID* mutant is able to form the cortex layer (Beall et al. 1993). The swirls of coat material that accumulate in the MC cytoplasm of these three mutants, suggests that coat proteins are capable of self assembly even in the absence of the SpoIVA, SpoVM and SpoIVD localization (Aronson et al. 1992). Therefore, the assembly of the basement layer of the coat requires the combined contributions of these three proteins (Figure 28). Assembly of the coat layers beyond the basement layer is dependent on additional morphogenetic proteins (Driks et al. 1994). Among them, SafA and CotE are respectively the morphogenetic proteins of the inner and outer coat (Figure 28) and

are produced under the control of σ^E , while *cotE* has also a promoter recognized by σ^K (Zheng et al. 1988, Ozin et al. 2000). Recruitment of both SafA and CotE is dependent on SpoIVA and SpoVID (Figure 28) (Mullerova et al. 2009, de Francesco et al. 2012). An interaction between SafA and CotE has not been observed. SafA, located in the inner coat (Figure 28) (Takamatsu et al. 1999) interacts with both SpoIVA and SpoVID but the interaction with this last protein is stronger (Ozin et al. 2000, Mullerova et al. 2009). In the spore, CotE is located at the interface between the inner and outer coats (Figure 28) (Driks et al. 1994). The assembly of the two coat layers seems to occur independently, since *safA* mutant spores lack an inner coat but retain a seemingly unaffected outer coat and *cotE* mutant spores retain the lamellar structure of the inner coat but lack an outer coat (Zheng et al. 1988, Takamatsu et al. 1999, Henriques and Moran 2007). However, CotE appears to contribute to the attachment of the coat to the spore surface. The assembly of the outer coat involves the cooperation of CotE with additional morphogenetic proteins well documented in *B. subtilis*, such as CotH and CotO (Figure 28) (Naclerio et al. 1996, Zilhao et al. 1999, McPherson et al. 2005, Kim et al. 2006). Both proteins interact with CotE, and their absence results in a disorganized outer coat structure. However, unlike CotE, they do not appear to play a role in attachment of the coat to the FS (Zilhao et al. 1999, Little and Driks 2001, McPherson et al. 2005).

B. subtilis spores do not contain an exosporium. However, analysis using ruthenium red, which stains mainly acid polysaccharides, revealed the presence of filaments on the surface of *B. subtilis* spores (Waller et al. 2004). Since polysaccharides and proteins have been detected in spore surface extracts, these filaments are probably glycoprotein in nature. Therefore, this layer intimately connected to the outer coat and hardly observable by TEM, was named the spore crust (Figure 28) (Chada et al. 2003, Waller et al. 2004, McKenney et al. 2010). Three proteins, CotX, CotY and CotZ were shown to play a morphogenetic role in the assembly of the crust and are recruited in a CotE-dependent manner (Figure 28) (McKenney et al. 2010, Imamura et al. 2011). CotY and CotZ are cysteine-rich proteins that were shown to directly interact and may be subjected to cross-linking by formation of disulfide bonds (Zhang et al. 1993, Krajcikova et al. 2009). The function of the spore crust is not yet clear since mutants without spore crust are resistant to heat and lysozyme treatment (Zhang et al. 1993). However, *cotXYZ* mutant spores have an unusual outer coat that is readily disrupted during fixation, embedding, or sectioning for electron microscopy suggesting that the spore crust might contribute to the tight packing of the outer coat (Zhang et al. 1993).

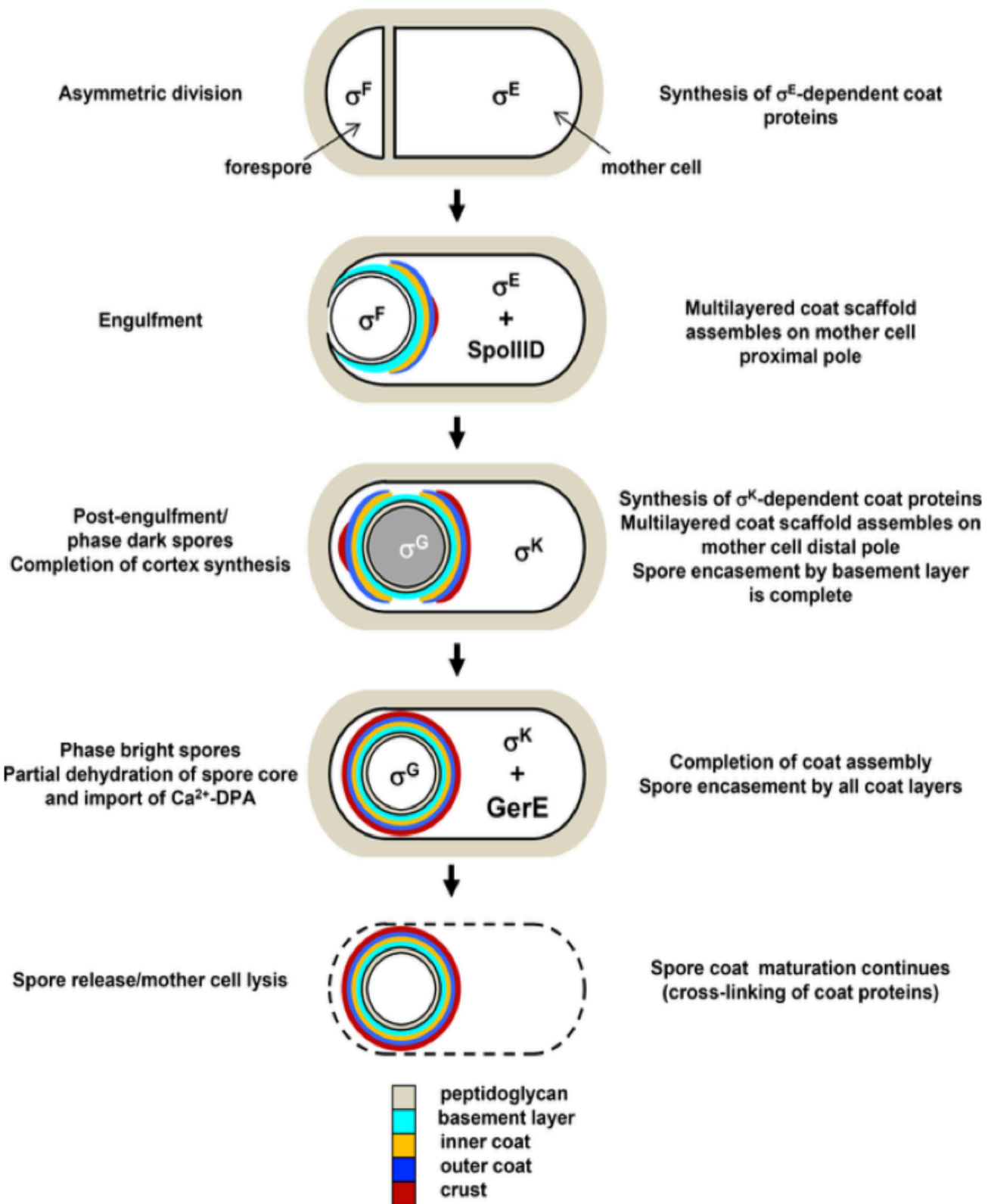


Figure 29: Model of spore coat assembly during *B. subtilis* sporulation. In the left column, are listed the stages of sporulation. The center column contains diagrams of spore coat morphogenesis. Layers of the spore coat are color coded (cyan = basement layer; yellow = inner coat; blue = outer coat; maroon = crust). In the right column, are listed the stages of spore coat assembly. DPA, dipicolinic acid. Driks 2016.

III.2.b. Coat assembly

Fluorescence microscopy using GFP-tagged coat proteins allowed to map genetic dependencies for the assembly of the coat and to define a network of interactions (Kim et al. 2006, McKenney et al. 2010). The coat proteins fused to GFP whose localization is dependent on SafA (i.e., CwlJ, CotD, CotT, YaaH, YuzC and OxD), were assigned to the inner coat while those whose localization is dependent on CotE (CotA, CotM, CotS, YncD and YtxO) were thought to reside in the outer layer (Figure 28). An approximately equal number of coat proteins were assigned to the inner and outer layers (Imamura et al. 2010, McKenney et al. 2010). The subset of CotE-dependent proteins shown to be also dependent on CotXYZ, were therefore categorized as crust proteins (CotW) (Figure 28) (Imamura et al. 2010, McKenney et al. 2010). There is also an additional subset of proteins such as YhaX, LipC and YheD, whose localization is dependent on SpoIVA and SpoVM, but independent on both SafA and CotE. The organization of the coat interaction network is highly hierarchical. Each morphogenetic protein is connected to many coat proteins. SpoIVA is at the top of the hierarchy for recruitment of coat proteins, being crucial for the localization of both SafA and CotE on the surface of the developing spore. In contrast, SpoVM and SpoVID are at the top of the spore encasement hierarchy (Figure 28). Encasement of SafA-GFP and CotE-GFP is dependent on SpoVM and SpoVID, and SpoVID interacts directly with SafA and CotE (Figure 28) (Costa et al. 2006, Mullerova et al. 2009, Wang et al. 2009a, de Francesco et al. 2012). The molecular mechanism driving encasement remains unknown but seems to occur in successive coordinated waves, beginning with proteins of the inner coat, followed by the outer coat and finally the crust.

III.2.c. Coat morphogenesis in real time

Apart from the role played by the morphogenetic proteins, transcriptional regulation has important consequences for the production and the dynamic of localization of coat proteins in the MC (Costa et al. 2007). Coat and crust/exosporium assembly takes about 6 h and is mainly governed by the MC. Specific sigma factors and transcription factors creates an hierarchical organization of gene expression that results in successive waves of protein synthesis crucial for proper spore coat assembly (Eichenberger et al. 2004, Henriques and Moran 2007, McKenney et al. 2013, Driks and Eichenberger 2016). The major coat morphogenetic proteins are expressed in an appropriate order (Figure 29). The cascade is initiated by σ^E that control genes encoding the regulatory proteins SpoIID and GerR (Figure

21). Later, σ^E is replaced by σ^K , which regulates GerE-encoding gene (Errington 2003, Piggot and Hilbert 2004). The combination of σ^E with the regulators SpoIIID and GerR, and of σ^K with the regulator GerE, produces a series of coherent and incoherent feedforward loops that result in different temporal patterns (prolonged, delayed, pulsed) of expression for different sets of genes (Figure 29) (Eichenberger et al. 2004). For instance, SpoIIID regulates some genes of the σ^E regulon, both positively and negatively, resulting in three waves of gene expression: the first wave is σ^E -dependent and will be later repressed by SpoIIID including *spoIVA* whose product (SpoIVA) is known to finish encasement at the end of engulfment. The second wave is also under the control of σ^E alone but unaffected by SpoIIID (including *safA*), and the third wave that is σ^E -dependent and further activated by SpoIIID (Roels et al. 1992, Price and Losick 1999, Takamatsu et al. 1999, Eichenberger et al. 2004). In the case of the crust protein operon, *cotYZ* is initially transcribed at a modest level under the control of σ^E , and then transcribed at a high level during late sporulation under the dual control of σ^K and GerE (Zhang et al. 1993, Eichenberger et al. 2004). The encasement by CotZ begins only after the spore becomes visible by phase contrast microscopy. The timing of gene expression is crucial and critical to spore coat morphology. For example, *cotE* is expressed in two pulses, first from a σ^E -dependent promoter that is shut off by SpoIIID and then from a promoter recognized by σ^K and is repressed at later stages by GerE (Zheng et al. 1988, Eichenberger et al. 2004). However, a delayed expression of this gene produced spores on which CotE, but not other proteins of the outer layer, was assembled (Costa et al. 2007).

In summary, SpoIVA is recruited to the FS outer membrane by SpoVM (Figure 28). SpoIVA then recruits SpoVID, whose LysM domain at the C-terminal facilitates its binding to the cortex PG beneath the FS outer membrane (Figure 28). SpoIVA, SpoVM and SpoVID marks the MC proximal pole as the site of coat attachment and the three proteins finish spore encasement as soon as engulfment is completed (Figure 29) (McKenney and Eichenberger 2012). SafA is targeted to the MC proximal pole first in a SpoVID-independent way, which probably depends on its LysM domain present at the N-terminal (Figure 28). CotE recruitment is most likely mediated by SpoIVA. Therefore, a scaffold organized in multiple layers is assembled on one pole of the FS (Figure 29). Subsequently, the coat encases the spore in multiple coordinated waves. Importantly, additional coat proteins can be added to this scaffold even after completion of encasement. This property implies that the coat remains permeable to proteins of a certain size until late stages in sporulation. For instance, the coat protein CotD is among the last to be produced (class VI), but eventually localizes to the inner

A

B

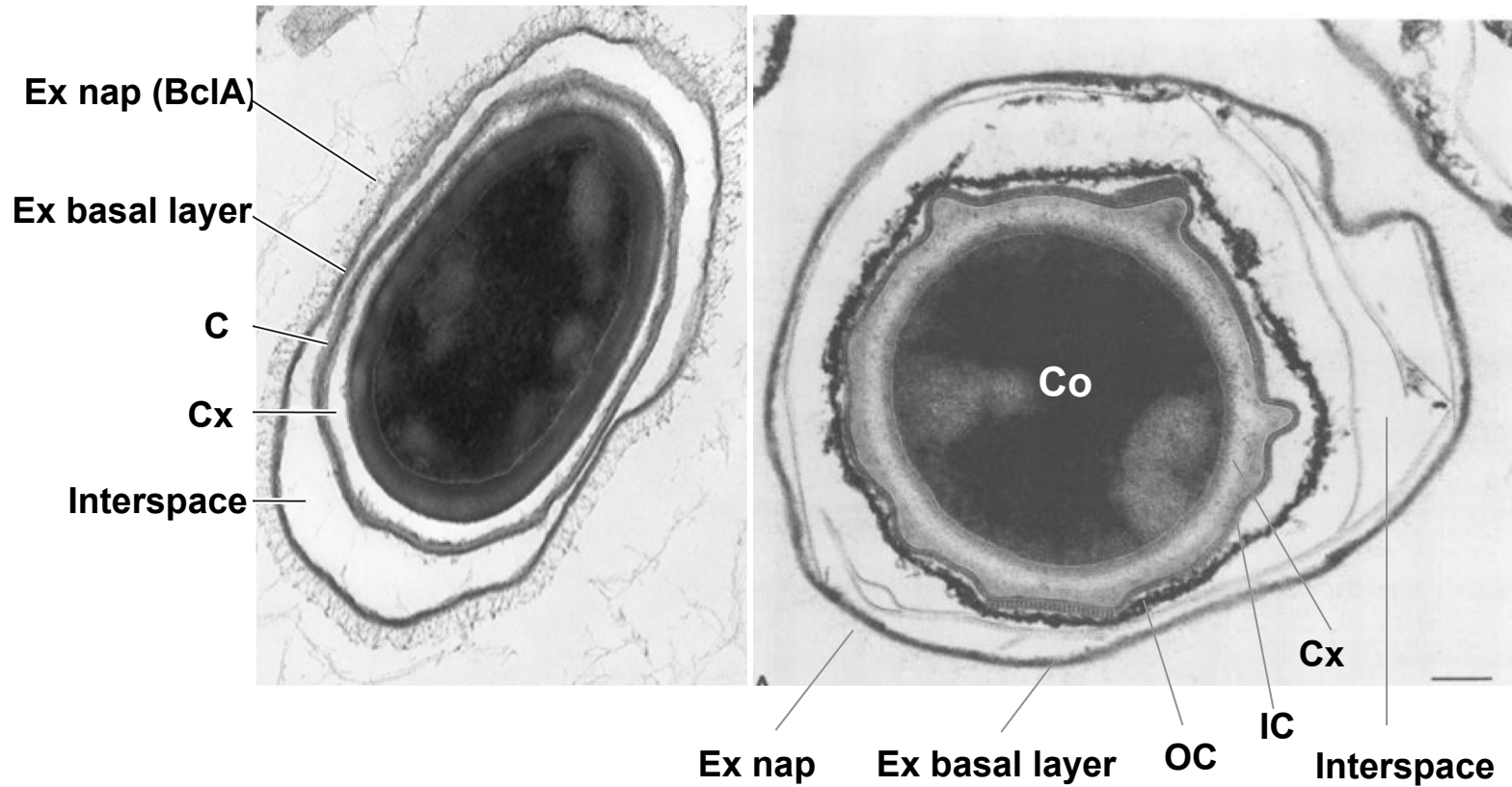


Figure 30: Thin-sectioned spores of *B. anthracis* (A) and *B. thuringiensis* (B). The main layers of the spore are represented. Co, Cx, IC, OC, C and Ex are abbreviations for core, cortex, inner coat, outer coat, coat and exosporium, respectively. The exosporium is the outermost protective layer of the spore. Exosporium contains hair-like projections mainly composed by the BclA protein. Exosporium is separated from the rest of the spore by a interspace. *B. anthracis* picture was adapted from Stewart 2015; *B. thuringiensis* picture was adapted from Gerhardt *et al.*, 1976.

coat and will have to cross the nascent outer coat layer to reach its final destination (McKenney and Eichenberger 2012).

III.3. Spore coat of *B. cereus* group

Differences in the appearance and thickness of the coat layers among spores of various bacilli strains or species are observed. The *B. cereus* group includes *B. anthracis* and *B. thuringiensis*. The coat of *B. cereus* and *B. anthracis* is thinner and more compact than those of *B. subtilis* (Figure 30A) (Chada et al. 2003). In *B. thuringiensis*, the inner coat is laminated but consists of a patchwork of striated packets, appearing either stacked or comb-like, and the outer coat is granular (Figure 30B) (Gerhardt et al. 1976). *B. subtilis* and *B. anthracis* group have a similar number of coat proteins. However, differences in the electrophoretic patterns suggest that the biochemical composition of the coat is different (Kuwana et al. 2002, Lai et al. 2003, Redmond et al. 2004). Since all bacilli contain the morphogenetic proteins SpoIVA, SpoVM and CotE, and almost all have SpoVID and SafA (Lai et al. 2003, Liu et al. 2004, Giorno et al. 2007), it is tempting to speculate that nearly all bacilli share the mechanisms of coat assembly. Indeed, *B. anthracis* and *B. subtilis* use some of the same proteins to direct assembly of their coat. SpoIVA is necessary to anchor the coat to the FS surface and for cortex formation in both species (Roels et al. 1992, Giorno et al. 2007). However, in *B. anthracis*, CotE plays only a modest role in coat formation, but a major role for proper assembly of the outermost layer, the exosporium. In this bacterium, it is rather CotH that directs the assembly of an important subset of coat proteins. Accordingly, *cotH* deletion has a more severe impact on coat assembly than *cotE* inactivation (Giorno et al. 2007). In *B. cereus*, *exsA* is the equivalent of *B. subtilis safA* and the gene organizations around both are identical. The location of ExsA has not been determined but it possesses an N-terminal LysM domain, as SafA, although the rest of the sequence is less conserved. ExsA, which controls coat and exosporium assembly in *B. cereus*, appears to have a more severe impact on the *B. cereus* coat assembly than does *safA* in *B. subtilis* (Bailey-Smith et al. 2005).

III.4. The Exosporium layer

The exosporium is the outermost layer of the *B. cereus* spores and those of its close relatives *B. anthracis* and *B. thuringiensis* (Stewart 2015). The exosporium is a hydrophobic, balloon-like glycoprotein layer separated from the spore coat by a gap called the interspace (Figure 30) (Henriques and Moran 2007, Giorno et al. 2009, Kailas et al. 2011). It consists of

a paracrystalline basal layer adorned with hair-like projections (Figure 30) (Gerhardt and Ribi 1964, Wehrli et al. 1980). In *B. cereus* group, the exosporium composition and structure are very similar (Ball et al. 2008) and is anchored to the coat layer via a number of protein-protein interactions. Proteins implicated in exosporium attachment include CotE, CotY, ExsA, ExsB, ExsY and ExsM (Bailey-Smith et al. 2005, Boydston et al. 2006, Johnson et al. 2006, McPherson et al. 2010, Stewart 2015). The basal layer of the exosporium contains over a dozen different integral proteins including CotY, ExsY, ExsFA and ExsFB (Redmond et al. 2004, Stewart 2015). The hair-like projections are attributed to the presence of the collagen-like glycoprotein, BclA, which is the major component of *B. anthracis* exosporium and is homogeneously distributed at the spore surface (Figure 30A) (Sylvestre et al. 2002). The N-terminus of BclA is covalently attached to the basal layer while the C-terminus of BclA is oriented to the exosporium surface (Boydston et al. 2005). Localization of *B. anthracis* BclA is mediated in part by the basal proteins ExsFA, ExsFB proteins (Sylvestre et al. 2005, Thompson et al. 2011). As for the *B. subtilis* spore crust, cysteine-rich proteins are also essential for the assembly of the exosporium. ExsY and CotY of *B. anthracis* and *B. cereus* are orthologues of the *B. subtilis* CotZ protein (Boydston et al. 2006, Johnson et al. 2006, Imamura et al. 2011). Whether the crust is functionally equivalent to the surface of the exosporium and whether crust-like layers are found on the outer spore coat in exosporium-containing spores are questions that remains unanswered. Some studies have proposed that the role of the exosporium is to protect the spore against degradative enzymes, antibodies, and macrophages (NO), while others suggest that the exosporium helps to regulate spore germination and adherence to abiotic and biotic surfaces (Tauveron et al. 2006, Weaver et al. 2007, Faille et al. 2010, Stewart 2015). Present in the exosporium layer, an Alanine racemase that converts L-alanine (a germinant for *B. anthracis*) to D-alanine (an inhibitor of germination) may function to inhibit premature germination under suboptimal growth conditions (Chesnokova et al. 2009). An Arginase activity is also present at the surface of *B. anthracis* spores (Raines et al. 2006), which could compete with the macrophage nitric oxide synthase (NOS2) that use L-arginine substrate to produce NO (Weaver et al. 2007). In addition, two spore SODs, Sod15 and SodA1, are present in the exosporium and their activity can afford *B. anthracis* protection against oxidative stress (Cybulski et al. 2009). While interactions between the exosporium protein BclA and the host integrin Mac-1 (CR3) allow entry of *B. anthracis* spores into phagocytic host cells (Oliva et al. 2008), the exosporium protects the spores from macrophage-mediated killing (Weaver et al. 2007). Finally, the metalloprotease InhA1 present in the exosporium of *B. cereus* allow bacterium to escape from

macrophages (Ramarao and Lereclus 2005).

A balloon-like exosporium has been also observed in clostridia such as *Clostridium sporogenes* and *Clostridium sordellii*. However, very different structure and protein compositions were identified when compared to *B. cereus* group (Janganan et al. 2016, Rabi et al. 2018). *C. sordellii* exosporium is composed by a thick inner layer and a thin outer layer, do not possess hair-like projections and is open at the spore poles (Rabi et al. 2017). Apertures in the exosporium and a balloon-like exosporium seem to be a characteristic of clostridial spores. Indeed, an opening in the exosporium has also been reported in *C. sporogenes* and *C. botulinum* (Stevenson and Vaughn 1972, Brunt et al. 2015, Rabi et al. 2017). The function of an open exosporium remains unclear but it very likely allows entry of larger molecules into the exosporium rather than acting as a protective barrier. In *C. sporogenes*, newly formed vegetative bacteria were shown to emerge through the pre-existing aperture in the exosporium openings upon germination (Brunt et al. 2015).

III.5. Spore surface layers of *C. difficile*

TEM studies indicate that the coat of *C. difficile* comprises two layers, consisting of an inner lamellar coat and a more electron-dense outer coat (Figure 27C) (Lawley et al. 2009b, Permpoonpattana et al. 2011b, Paredes-Sabja et al. 2012, Rabi et al. 2017). The stability of the exosporium was for a long time a matter of controversy. Several reports suggest that this layer is fragile and easily lost (Permpoonpattana et al. 2011b, Permpoonpattana et al. 2013), whereas other reports indicate that it is a stable layer that is only removed by proteases and/or sonication treatments (Joshi et al. 2012, Barra-Carrasco et al. 2013, Escobar-Cortes et al. 2013, Pizarro-Guajardo et al. 2014). Nowadays, it become clear that the stability of this layer could be related with the strain or to proteases used during spore purification procedures (Escobar-Cortes et al. 2013, Pizarro-Guajardo et al. 2016). *C. difficile* exosporium is a proteinaceous layer that contributes to the hydrophobicity of the spore surface (Diaz-Gonzalez et al. 2015). In contrast to the spore coat, the exosporium can be removed by enzymatic treatment with proteases (i.e., trypsin or proteinase K) or by sonication (Escobar-Cortes et al. 2013). Several studies showed that the morphology of the exosporium is strain-dependent (Joshi et al. 2012, Escobar-Cortes et al. 2013, Pizarro-Guajardo et al. 2016). Whereas spores of the 630 strain have an electron-dense compact exosporium layer, in most of others *C. difficile* strains studied (R20291, M120, TL176, and TL178), the exosporium layer have hair-like extensions similar as those observed in spore of the *B. cereus* group

(Chada et al. 2003, Paredes-Sabja et al. 2014, Pizarro-Guajardo et al. 2016). In contrast to other spore formers, during sporulation *C. difficile* forms two distinct exosporium morphotypes (Pizarro-Guajardo et al. 2016). These morphotypes include either spores with a thick or a thinner-exosporium layer as determined by the thickness of the electron-dense material surrounding the coat (Pizarro-Guajardo et al. 2016). Notably, the exosporium layer of *C. difficile* spores differs from that of spores of the *B. cereus* group (Stewart 2015, Pizarro-Guajardo et al. 2016, Rabi et al. 2017). In fact, *C. difficile* lacks many exosporium proteins of the *B. cereus* group's spores as well as the frequently observed gap that separates the spore coat from the exosporium. Instead, the exosporium of *C. difficile* spores is in direct contact with the spore coat layers in a similar way as the crust of *B. subtilis* spores (Barra-Carrasco et al. 2013, Paredes-Sabja et al. 2014, Diaz-Gonzalez et al. 2015, Calderon-Romero et al. 2018).

III.5.a. Morphogenesis of the *C. difficile* spore coat

Only 25% of the *B. subtilis* spore coat proteins have homologs in *C. difficile* and most of the morphogenetic proteins identified in *B. subtilis* or other bacilli are absent in *C. difficile*. This suggests that the components that govern spore coat assembly in *C. difficile* are divergent to those defined for *B. subtilis* and/or the *B. cereus* group (Henriques and Moran 2007, Lawley et al. 2009b). Among spore coat morphogenetic proteins, only SpoIVA is present in all bacilli and clostridia (Galperin et al. 2012). Since SpoVM is very short (less than 30 aa), it is difficult to identify its encoding gene from genome annotation. In addition, the absence of SpoIVD, SafA and CotE in clostridia suggests major differences in the assembly of the bacilli and clostridia surface layers (Galperin et al. 2012). In *C. difficile*, homologs for SpoIVA and SpoVM have been identified (Galperin et al. 2012). It is reasonable to propose that the SpoVM-SpoIVA-dependent mechanism for attaching the coat to the FS outer membrane was common in the two groups of spore forming bacteria. Consistent with this, *C. difficile* SpoIVA was shown to be essential for coat localization around the FS as observed in *B. subtilis* (Putnam et al. 2013). Indeed, in a *spoIVA* mutant, the coat is mislocalized and detected in the MC cytoplasm as in *B. subtilis*, where distinct coat layers are observed in the mislocalized coat swirls. This suggested that coat can still assemble, but SpoIVA is required to localize the coat around the FS. However, in contrast to *B. subtilis*, *C. difficile* SpoIVA is dispensable for cortex synthesis (Roels et al. 1992, Putnam et al. 2013). The *spoVM* gene of *C. difficile* encodes a small protein that like in *B. subtilis* is expressed in the MC under the control of σ^E . Moreover, many of the residues previously identified to be critical for the function of *B. subtilis* SpoVM are conserved in SpoVM of *C. difficile*.

However, contrary to what we observed in *B. subtilis*, *C. difficile* SpoVM was found to be dispensable for spore formation/maturation (Ribis et al. 2017). The inactivation of *spoVM* leads to morphological defects in a small percentage of cells, such as coat detachment from the FS or abnormal cortex thickness. It has been shown that *C. difficile* SpoVM and SpoIVA directly interact as observed in *B. subtilis*. However, SpoIVA is still able to polymerize on the surface of FS in the *spoVM* mutant and to encase the FS (Ribis et al. 2017). Even if the spore coat layers of *B. subtilis* and *C. difficile* are morphologically similar, the absence of SpoVID, SafA and CotE homologues in *C. difficile*, suggest that different proteins replace these morphogenetic proteins involved in the spore coat assembly. A functional homolog of *B. subtilis* SpoVID (CD3567) has been identified in *C. difficile*. This protein, contains a C-LysM domain (like SpoVID) that was shown to directly interact with the Walker A ATP-binding motif of SpoIVA, suggesting that CD3567 and SpoIVA form a complex that may drive coat assembly around the FS (Putnam et al. 2013). CD3567 was then renamed SipL for “SpoIVA interacting protein L”. However, the mechanism by which SpoIVA recognizes SipL fundamentally differs from that of SpoIVA recognizing SpoVID in *B. subtilis*. In addition, a *sipL* mutant shows a phenotype reminiscent of the *spoIVA* mutant, where the spore coat is tethered and mislocalized to the MC cytoplasm (Putnam et al. 2013). SipL, as SpoVID, might play a role in the encasement step, helping in the transition of the coat from the MC proximal pole (MCP) to full spherical shell around the spore (Wang et al. 2009a, McKenney and Eichenberger 2012). Whether the LysM domain tethers SipL to the FS by interacting with the cortex in addition to its presumed interaction with SpoIVA is still unknown.

III.5.b. Spore coat and exosporium proteins

Proteomic studies allow identifying spore proteins localized at the surface layers of *C. difficile* spores i.e., coat and exosporium (Permpoonpattana et al. 2011b, Abhyankar et al. 2013, Permpoonpattana et al. 2013, Diaz-Gonzalez et al. 2015). For several proteins, their presence at the spore surface was confirmed using antibodies raised against them either by immunofluorescence or by Western blot. CotA (CD1613) and CotB (CD1511) were identified at the surface of *C. difficile* spore. The *cotA* mutant spores exhibited major morphological defects and lacked the outer coat layer for half of them and were more sensitive to lysozyme (Permpoonpattana et al. 2013). By contrast, no detectable differences in spore ultrastructure or lysozyme resistance were observed for the *cotB* mutant spores. CotF (CD0597) is a tyrosine-rich protein homolog to *B. subtilis* CotJB, likely a structural component of the inner layers of the coat (Henriques et al. 1995, Seyler et al. 1997). CotF is located at the spore

surface but its role remains to be investigated (Permpoonpattana et al. 2013). CotCB (CD0598), CotD (CD2401), and CotG (CD1567) are a group of proteins predicted to have Mn^{2+} catalase activity (Permpoonpattana et al. 2011b, Permpoonpattana et al. 2013). Indeed, catalase activity was observed for the recombinant proteins for CotD and CotG while no activity was found for CotCB (Permpoonpattana et al. 2013). CotCB and CotD are homologs to the *B. subtilis* outer coat protein CotJC (Henriques et al. 1995, Seyler et al. 1997). As for *cotJC* mutant of *B. subtilis* (Henriques et al. 1995), no ultrastructural defects were observed in *cotD* and *cotCB* mutant spores (Permpoonpattana et al. 2013). Other proteins with enzymatic activities are present at the surface of *C. difficile* spores, such as SodA (CD1631), a homolog of the *B. subtilis* superoxide dismutase (SodA) and CotE, a bifunctional protein with peroxiredoxin reductase (N-terminal) and chitinase (C-terminal) activities. Even if the recombinant SodA protein carries high levels of SOD activity, the loss of *C. difficile* *sodA* had no effect on spore ultrastructure or spore resistance (Permpoonpattana et al. 2013). There are also no obvious ultrastructural defects in spores of a *cotE* mutant (Permpoonpattana et al. 2011b, Permpoonpattana et al. 2013). Chitinase and a low level of peroxidase activities were detected with recombinant CotE^C and CotE^N, respectively (Permpoonpattana et al. 2013). Interestingly, it was found recently that CotE plays an important role in spore attachment to the gut mucosa via direct interaction with mucin and the chitinase activity of CotE contributes to mucin degradation (Hong et al. 2017). It is important to note that *C. difficile* CotE bears no sequence or functional homology to the *B. subtilis* outer coat morphogenetic protein CotE (McKenney et al. 2013).

Discrimination of spore proteins localization within the coat or the exosporium of *C. difficile* spores was difficult until the establishment of methods that allow to separate these two layers. The development of exosporium removal methods, that maintain the spore coat intact, combined with mass spectrometry allowed the study of the proteomic composition of the exosporium of *C. difficile* spores (Escobar-Cortes et al. 2013, Diaz-Gonzalez et al. 2015). CotA, CotB, CotD and CotE are among the proteins that were identified in the exosporium extracts (Diaz-Gonzalez et al. 2015). However, analysis of untreated and proteinase K-treated spores revealed that CotA and CotB are surface exposed and accessible to antibodies but that most of these proteins are insensitive to proteinase K treatment confirming their localization in the spore coat (Diaz-Gonzalez et al. 2015). BclA proteins, as well as the cysteine-rich proteins CdeC, CdeM and CdeA are mainly located in the exosporium layer since these proteins are almost absent from the surface of proteinase K- treated spores (Diaz-Gonzalez et al. 2015). In

C. difficile, three paralogs of the *B. anthracis* collagen-like glycoprotein (i.e., BclA) are encoded in the genome of the 630 strain (i.e., *bclA1* [CD0332], *bclA2* [CD3230], and *bclA3* [CD3349]). These genes are expressed in the MC under σ^K control (Pizarro-Guajardo et al. 2014). The BclA proteins contain three domains: an N-terminal domain that localizes BclA to the exosporium, a collagen-like domain, and a C-terminal domain facing to the surface of the exosporium (Pizarro-Guajardo et al. 2014). BclA1 undergoes post-translational cleavage and forms high molecular complexes with other spore proteins, suggesting that it is assembled in the spore surface through cleavage and/or crosslinking to other exosporium proteins (Pizarro-Guajardo et al. 2014). No homologues of ExsFA and ExsFB proteins involved in the localization of BclA and the stability of the exosporium (Sylvestre et al. 2005) are encoded in the *C. difficile* genome. Additionally no conserved motifs were found in the N-terminal domain of all three BclAs suggesting that the assembly mechanism is different in *C. difficile* (Sebahia et al. 2006). The inactivation of *bclA1* and *bclA2* genes causes aberrations in the spore coat, and spores of all three independent *bclA* mutants showed reduced surface hydrophobicity and a faster germination rate (Phetcharaburanin et al. 2014). Glycosylation of the *C. difficile* BclA3 protein at the spore surface have been demonstrated. This is consistent with the presence of the *sgtA* gene located immediately upstream of the *bclA3*, which encodes a glycosyltransferase involved in the biosynthesis of surface-associated glycan components (Strong et al. 2014).

Unlike 630 spores, R20291 and CD196 strains have a pseudogene *bclA1* due to the appearance of an early stop codon. As consequence, the 027 strains encode a BclA1 protein of approximately 6 kDa that still can assemble at the spore surface (Stabler et al. 2009, Phetcharaburanin et al. 2014).

III.5.c. Morphogenetic proteins of *C. difficile* exosporium

As in bacilli, cysteine-rich proteins are also present at the surface of *C. difficile* spores. A previous study performed in R20291 strain, demonstrated that the *C. difficile* exosporium cysteine-rich protein “CdeC” (CD1067), is required for exosporium morphogenesis and coat assembly (Barra-Carrasco et al. 2013). Very recently, new insights into the mechanism of *C. difficile* exosporium assembly were brought with the study of CdeC and CdeM in the 630 strain (Calderon-Romero et al. 2018). *cdeC* and *cdeM* are transcribed by σ^K . While *cdeC* is conserved in related *Peptostreptococcaeae* family members, *cdeM* is unique to *C. difficile*. These two cysteine-rich proteins have different role in the integrity of the spore surface layers. Both proteins are required for the correct formation of the exosporium layer. However,

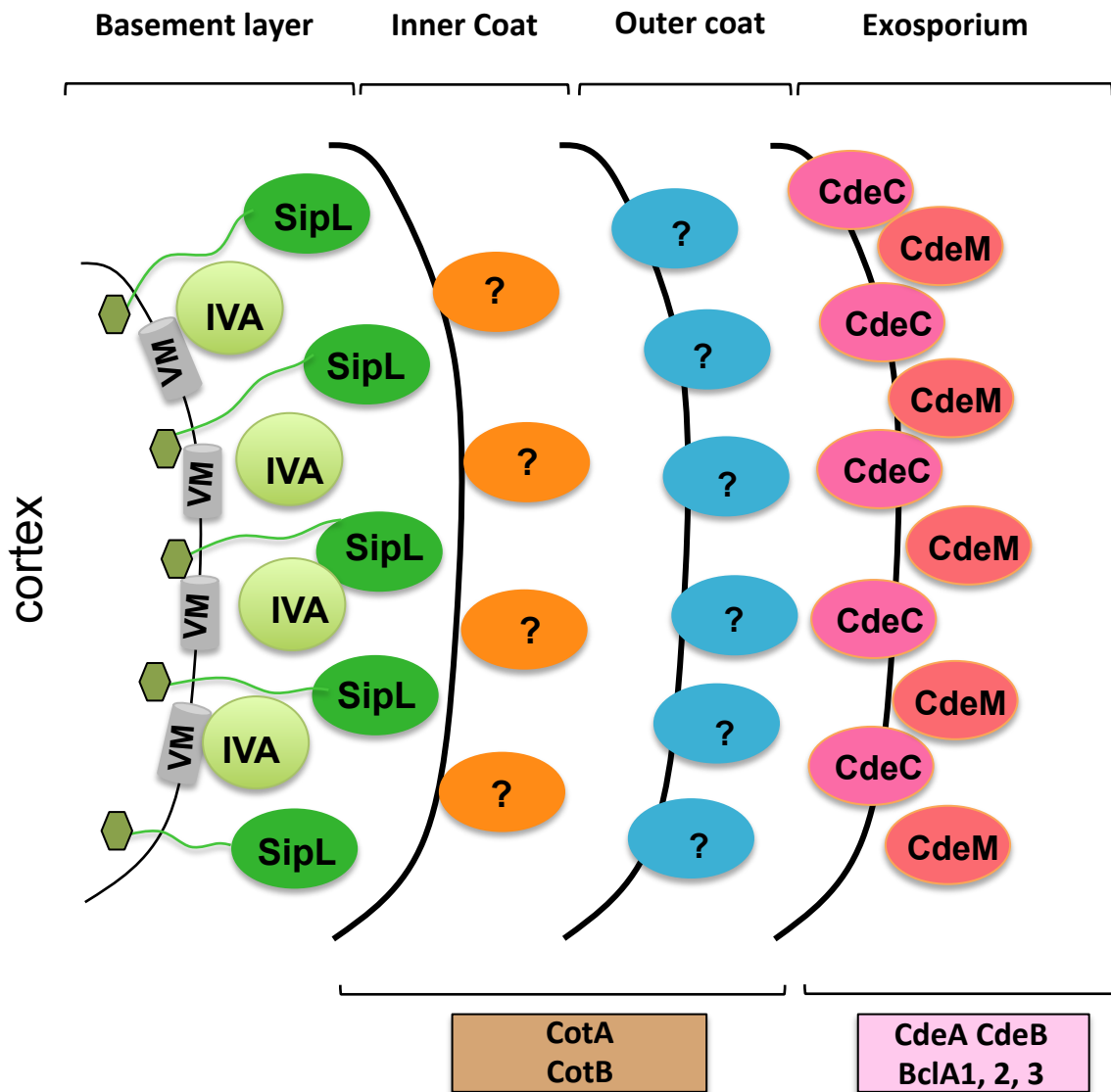


Figure 31: Schematic representation of proteins of the spore surface layers of *C. difficile*. Morphogenetic proteins are indicated on the upper part of the figure and are located where their main function is exerted. The hexagon represent the LysM domain. CotA and CotB are proposed to be located in the inner spore coat layers, whereas BclA and Cde proteins are in the exosporium. Adapted from Calderon-Romero *et al.*, 2018.

the *cdeC* mutant was also defective in spore coat assembly, more permeable to lysozyme or ethanol and more susceptible to inactivation by heat and macrophages (Calderon-Romero et al. 2018). CdeC and CdeM are both required for the presence at the spore surface of CotA, CotB and BclA1. In addition, the amount of CdeC at the spore surface seems to be dependent on the presence of CdeM.

III.5.d. Representative model of the proteins at the spore surface layers

The current model of assembly of the *C. difficile* spore surface layers coat and exosporium is presented in Figure 31 (Putnam et al. 2013, Paredes-Sabja et al. 2014, Ribis et al. 2017, Calderon-Romero et al. 2018). The morphogenetic proteins SpoIVA and SipL are located close to the FS outer membrane, forming a basement layer. These proteins interact and are required during the initial steps of spore coat assembly to ensure coat localization around the FS (Putnam et al. 2013). In *C. difficile*, SpoVM seems to be dispensable for spore formation (Ribis et al. 2017). CotA and CotB are proposed to be located in the inner spore coat layers (Figure 31) (Diaz-Gonzalez et al. 2015), whereas BclA and Cde proteins are in the exosporium (Pizarro-Guajardo et al. 2014, Diaz-Gonzalez et al. 2015). CdeC acts as a morphogenetic anchoring protein at the interface of the outer spore coat and exosporium while CdeM seems to be uniquely located on the exosporium layer (Calderon-Romero et al. 2018). How CdeC and CdeM recruits the remaining exosporium proteins remains unclear. In *B. subtilis*, SpoIVA and SpoVID are required for the recruitment of the next coat morphogenetic factors SafA and CotE (McKenney and Eichenberger 2012). However, since homologs of these proteins are absent in *C. difficile*, further research is needed to identify the morphogenetic proteins recruited by SpoIVA and SipL in this bacterium. As in the model organism *B. subtilis*, most of the proteins located at the spore surface layers of *C. difficile* are encoded by genes expressed in the MC compartment under the control of σ^E and σ^K . *spoVM*, *spoIVA*, *sipL* and *cotB* are controlled by σ^E (Fimlaid et al. 2013, Saujet et al. 2013), while *cotA*, *cotCB*, *cotD*, *cotE*, *bclA1*, *bclA2*, *bclA3*, *cdeC*, and *cdeM* genes are expressed under the control of σ^K (Fimlaid et al. 2013, Saujet et al. 2013). Few exceptions are CotG and SodA, which are controlled by σ^G . Among the genes whose expression is controlled by the MC specific σ factors, we identified *CD1065*, encoding a protein of unknown function with no homologs in bacilli. In this work, I studied the role of CD1065 in the spore morphogenesis of *C. difficile*.

Objectives of the thesis

During its infectious cycle, *C. difficile* is exposed to various stresses. In the environment, spores face atmospheric O₂ and disinfectants used for their eradication. Then, inside the host both spores and vegetative cells are exposed, among other stresses, to O₂ and reactive oxygen species produced by the host cells during inflammation. Therefore, *C. difficile* must be able to protect itself and survive in these hostile environments. The spore surface layers typically enable spore survival in the presence of predatory enzymes and chemical compounds found in the gastrointestinal tract. However, even if some progress has been made in understanding the biology of *C. difficile* spore formation, many questions remain about morphogenesis of the spore surface layers and the mechanisms used by spores to protect against toxic compounds. In the gut, once spore germination is complete, vegetative cells need to protect against low O₂ tensions as well as oxidative and nitrosative conditions. However, little is still known about the proteins involved in the ability of *C. difficile* to tolerate O₂, ROS and RNS. *C. difficile* genome encodes both revRbrs and FDPs, suggesting the existence of O₂ and ROS detoxification pathways in this bacterium. Interestingly, some of these proteins were detected in the proteome of the spore surface layers, which suggests that such detoxification can also be done by spores.

The first objective of my thesis is to study some members of the σ^K -regulon, including both *CD1065* and *CD2399* genes, and their role in the spore formation of *C. difficile*.

The second objective is 1) to study the expression of the genes encoding the revRbrs and FDPs during both vegetative growth and sporulation; 2) to characterize the enzymatic reactions catalyzed by some of them; and 3) to study the role of these proteins in the management of *C. difficile* O₂ tolerance.

Results

Spore coat morphogenesis

I. Article: CotL, a new morphogenetic spore coat protein of

Clostridium difficile

C. difficile spores play a central role in the infectious cycle, contributing to transmission, infection and persistence (Lawley et al. 2010, Deakin et al. 2012). The spore surface layers i.e., the coat and exosporium, enable spore resistance to enzymatic degradation and chemicals present in the host gastrointestinal tract (Nicholson et al. 2000, Riesenman and Nicholson 2000, Klobutcher et al. 2006, Setlow 2014). Additionally, the spore surface is likely the primary site of spore-host interactions (Stewart 2015). Therefore, understanding fundamental aspects on morphogenesis of the spore surface layers and their functional properties is a matter of great interest.

The structure of *C. difficile* spore is similar to that of the other spore-forming bacteria. However, the protein composition of the spore surface layers differs from that of bacilli (Lawley et al. 2009b, Permpoonpattana et al. 2011b, Abhyankar et al. 2013, Diaz-Gonzalez et al. 2015). In fact, only 25% of the *C. difficile* coat proteins have homologs in the spore former model *B. subtilis* (Henriques and Moran 2007, Permpoonpattana et al. 2011b, Permpoonpattana et al. 2013). In *B. subtilis*, the spore surface is primarily composed of proteins produced in the MC under the control of first σ^E and later σ^K (Henriques and Moran 2007, McKenney et al. 2013). In this bacterium, the formation of the coat layers is governed by the morphogenetic factors SpoVM, SpoIVA, SpoVID, SafA, and CotE (Henriques and Moran 2007, McKenney et al. 2013). In the basement layer of the coat, the SpoVM, SpoIVA and SpoVID proteins are required to start the coat localization around the FS surface. Recruitment of SafA, the inner coat morphogenetic protein, and of CotE, the morphogenetic protein of the outer coat, is dependent on SpoIVA and SpoVID (McKenney et al. 2013). Both SpoVM and SpoIVA homologs are present in *C. difficile* (Galperin et al. 2012). In this bacterium, SpoIVA was shown to be essential for coat localization around the FS (Putnam et al. 2013). However, contrary to the observed in *B. subtilis*, SpoVM was found to be dispensable for spore formation/maturation. No homologs of *B. subtilis* SpoVID, SafA and CotE were found in *C. difficile*. However, a functional homolog of SpoVID, SipL, was identified in *C. difficile*. As SpoVID, SipL interacts with SpoIVA and might form a complex

that drive coat assembly around the FS (Putnam et al. 2013). The morphogenetic proteins for the inner and outer coat layers of *C. difficile* are still unknown.

Among the genes whose expression is controlled by the specific σ factors of MC, it was identified *CDI065* (later renamed *cotL*) encoding CotL protein of unknown function with no homologs in bacilli. In this work, we then demonstrated that CotL is an important morphogenetic factor of the coat layer of *C. difficile* spores. The *cotL* gene was expressed in the MC compartment under the dual control of the sporulation sigma factors, σ^E and σ^K . CotL is present in the spore coat and the *cotL* mutant spores lack most of the spore coat layers and are more sensitive to lysozyme. Using translational SNAP fusions with several coat and exosporium proteins, we showed that CotL is required for the assembly of these proteins around the FS surface during sporulation. Finally, *cotL* mutant spores were impaired in germination, a phenotype likely to be associated with the structurally altered coat. Our results bring insights on a new morphogenetic partner important for coat assembly of *C. difficile* spores.

To make the reading easier, supplementary tables S1, S3 and S4 from this article are in Annex. Due to the large amount of raw data, the table S2 concerning the comparative analysis of the spore coat/exosporium proteome from the wild-type and the *cotL* mutant is not included in paper format in the manuscript. The supplementary figures S1, S2, S3, S4, S5 and S6 are in the text after all the main figures.

CotL, a new morphogenetic spore coat protein of *Clostridium difficile*

Carolina Alves Feliciano^{1,2}, Thibaut Douché³, Quentin Gai Gianetto^{3,4}, Mariette Matondo³, Isabelle Martin-Verstraete^{1,2 *} and Bruno Dupuy^{1,2 *}

¹ Laboratoire Pathogénèse des Bactéries Anaérobies, Institut Pasteur, Paris, France;

² University Paris Diderot, Sorbonne Paris Cité, Paris, France;

³ Plateforme Protéomique, Unité de Spectrométrie de Masse pour La Biologie, CNRS USR 2000, Institut Pasteur, Paris, France.

⁴ Bioinformatics and Biostatistics HUB, C3BI, CNRS USR 3756, Institut Pasteur, Paris, France.

*Corresponding authors: Laboratoire Pathogénèse des Bactéries Anaérobies, Institut Pasteur, and University Paris Diderot, Sorbonne Paris Cité, Paris, France

email: bdupuy@pasteur.fr and isabelle.martin-verstraete@pasteur.fr.

Key words: *Clostridium difficile*, spore, coat, morphogenesis, CotL

Summary

The strict anaerobe *Clostridium difficile* is the most common cause of antibiotic-associated diarrhoea. The oxygen-resistant *C. difficile* spores play a central role in the infectious cycle, contributing to transmission, infection and recurrence. The spore surface layers, the coat and exosporium, enable the spores to resist physical and chemical stress. However, little is known about the mechanisms of their assembly. In this study, we characterized a new spore protein, CotL, which is required for the assembly of the spore coat. The *cotL* gene was expressed in the mother cell compartment under the dual control of the RNA polymerase sigma factors, σ^E and σ^K . CotL was localized in the spore coat, and the spores of the *cotL* mutant had a major morphologic defect at the level of the coat/exosporium layers. Therefore, the mutant spores contained a reduced amount of several coat/exosporium proteins and a defect in their localization in sporulating cells. Finally, *cotL* mutant spores were more sensitive to lysozyme and were impaired in germination, a phenotype likely to be associated with the structurally altered coat. Collectively, these results strongly suggest that CotL is a morphogenetic protein essential for the assembly of the spore coat in *C. difficile*.

Introduction

Clostridioides difficile, commonly known as *Clostridium difficile*, is a Gram-positive, spore-forming obligate anaerobic bacterium that is currently considered to be the leading cause of antibiotic-associated diarrhoea (Kelly and LaMont 2008, Rupnik et al. 2009). The incidence and severity of *C. difficile* infection (CDI) have been increasing in North America and Europe (Rupnik et al. 2009, Wiegand et al. 2012). Spores, which are the primary infectious form, play a crucial role in transmission, infection and recurrence (Lawley et al. 2010, Deakin et al. 2012). As an obligate anaerobic bacterium, vegetative cells are unable to grow in an aerobic environment, and the metabolically dormant spore has a central role in the resistance outside the host. After ingestion, the earliest CDI events correspond to spore germination upon sensing specific bile salts in the gastrointestinal tract, followed by the growth of vegetative cells and gut colonization (Sorg and Sonenshein 2008). The vegetative cells then produce two toxins, TcdA and TcdB, which are the primary virulence factors required for the development of CDI symptoms. Spores are also produced in the gut and cause both spreading into the environment and relapse (Deakin et al. 2012, Janoir et al. 2013). The resistance to extreme environmental conditions and chemical compounds, including oxygen, antibiotics and disinfectants, makes the spores difficult to eradicate (Rupnik et al. 2009, Edwards et al. 2016a).

The process of sporulation is an ancient bacterial developmental programme that has been extensively studied in the model organism *Bacillus subtilis* (Hilbert and Piggot 2004, Higgins and Dworkin 2012). Spore morphogenesis starts with the formation of an asymmetric septum, which produces a smaller forespore (FS) and a larger mother cell (MC). The MC then engulfs the FS and directs the formation of the spore protective layers that are the cortex, coat and exosporium (Henriques and Moran 2007, McKenney and Eichenberger 2012). After a period of spore maturation, the MC undergoes autolysis to release the spore. The programmes of gene expression in the FS and MC compartments are defined by the cell type-specific RNA polymerase sigma (σ) factors: σ^F in the FS and σ^E in the MC control the early stages of sporulation and are replaced following engulfment completion by σ^G and σ^K in the respective compartment (Galperin et al. 2012, Abecasis et al. 2013). In *C. difficile*, as observed in *B. subtilis*, σ^F and σ^G activity is restricted to the FS, and σ^E and σ^K govern development events in the MC (Pereira et al. 2013, Saujet et al. 2013). Interestingly, significant deviations from the *B. subtilis* paradigm concerning the regulatory circuit leading to the σ factor activation are observed with a reduced communication between the MC and the FS and a weaker connection between gene expression and morphogenesis (Pereira et al. 2013, Saujet et al. 2013). *C.*

difficile spore structure is similar to that of other spore-forming bacteria. From the internal to external side, the spores are comprised of a dehydrated central core surrounded by the inner FS membrane, a germ cell wall, a modified peptidoglycan cortex layer, an outer membrane, a proteinaceous layer known as the spore coat and an outermost layer named the exosporium (Henriques and Moran 2007, Paredes-Sabja et al. 2014). However, the protein composition of the spore surface layers in *C. difficile* differs from that of other bacilli and clostridia (Lawley et al. 2009b, Permpoonpattana et al. 2011b, Abhyankar et al. 2013, Diaz-Gonzalez et al. 2015). The exosporium is absent in *B. subtilis*, and only 25% of the coat proteins have homologs in *C. difficile* (Henriques and Moran 2007, Permpoonpattana et al. 2011b, Permpoonpattana et al. 2013). The spore surface of the bacilli is primarily composed of proteins produced in the MC under the control of first σ^E and later σ^K (Henriques and Moran 2007, McKenney et al. 2013). In addition to transcriptional regulation, coat assembly depends on the ordered synthesis and recruitment of proteins that are encased at the FS surface forming a basement layer, an inner coat and an outer coat. In *B. subtilis*, the formation of these three layers is governed by morphogenetic proteins, such as SpoVM, SpoIVA, SpoVID, SafA and CotE (McKenney et al. 2013). Homologs for SpoIVA and SpoVM are present in *C. difficile* (Galperin et al. 2012). The SpoIVA of *C. difficile* is a morphogenetic protein essential for coat localization around the FS at the early development stages of sporulation (Putnam et al. 2013). The *C. difficile* SpoIVA directly interacts with SpoVM even if SpoVM is not essential to encase SpoIVA in the FS. SpoVM is also dispensable for spore formation (Ribis et al. 2017) in contrast to that observed in *B. subtilis*. SipL has been identified as a morphogenetic protein specific to *C. difficile*. SipL, together with SpoIVA, interacts and drives coat assembly around the *C. difficile* FS (Putnam et al. 2013). SipL is likely to be a functional homologue of SpoVID of *Bacillus* sp., a protein that helps in the transition of the spore coat from the mother cell proximal (MCP) pole to full encasement (Wang et al. 2009a, McKenney and Eichenberger 2012). In *B. subtilis*, SpoIVA recruits the morphogenetic protein from the inner coat, SafA, while both SpoIVA and SpoVID are required for the recruitment of CotE, an outer coat morphogenetic protein (de Francesco et al. 2012, McKenney et al. 2013). In *C. difficile*, the absence of homologs for *B. subtilis* SafA and CotE suggests that different proteins are involved in the assembly of the spore surface layers (Galperin et al. 2012).

In *C. difficile*, as in *B. subtilis*, the spore surface layers are comprised of proteins produced by the MC under the control of σ^E and/or σ^K (Pereira et al. 2013, Saujet et al. 2013, Pishdadian et al. 2015). In a previous study, transcriptome analyses combined with a genome-

wide transcriptional start site mapping allowed the definition of the regulons of the four σ factors of sporulation, σ^F , σ^E , σ^G and σ^K in *C. difficile* (Saujet et al. 2013). Among the genes whose expression is controlled by the MC specific σ factors, we identified *CD1065* encoding a lysine-rich protein of unknown function with no homologs in bacilli. The expression of the *CD1065* gene is down-regulated in a *sigE* and *sigK* mutant (Fimlaid et al. 2013, Saujet et al. 2013) and is induced during the infection of axenic mice (Janoir et al. 2013). In this study, we showed that the *CD1065* gene is transcribed by σ^E and σ^K during endospore development. We determined that the *CD1065* mutant forms spores lacking most of the spore coat and exosporium proteins, while the level of gene expression or protein production of the coat/exosporium components was similar in the sporulating cells of the *CD1065* mutant and the wild-type strain. In addition, *CD1065* spores are sensitive to lysozyme and impaired in germination. These studies characterize a new coat protein crucial for the assembly of the spore surface layers in *C. difficile* and provide new information about the assembly partners of the spore coat in this bacterium.

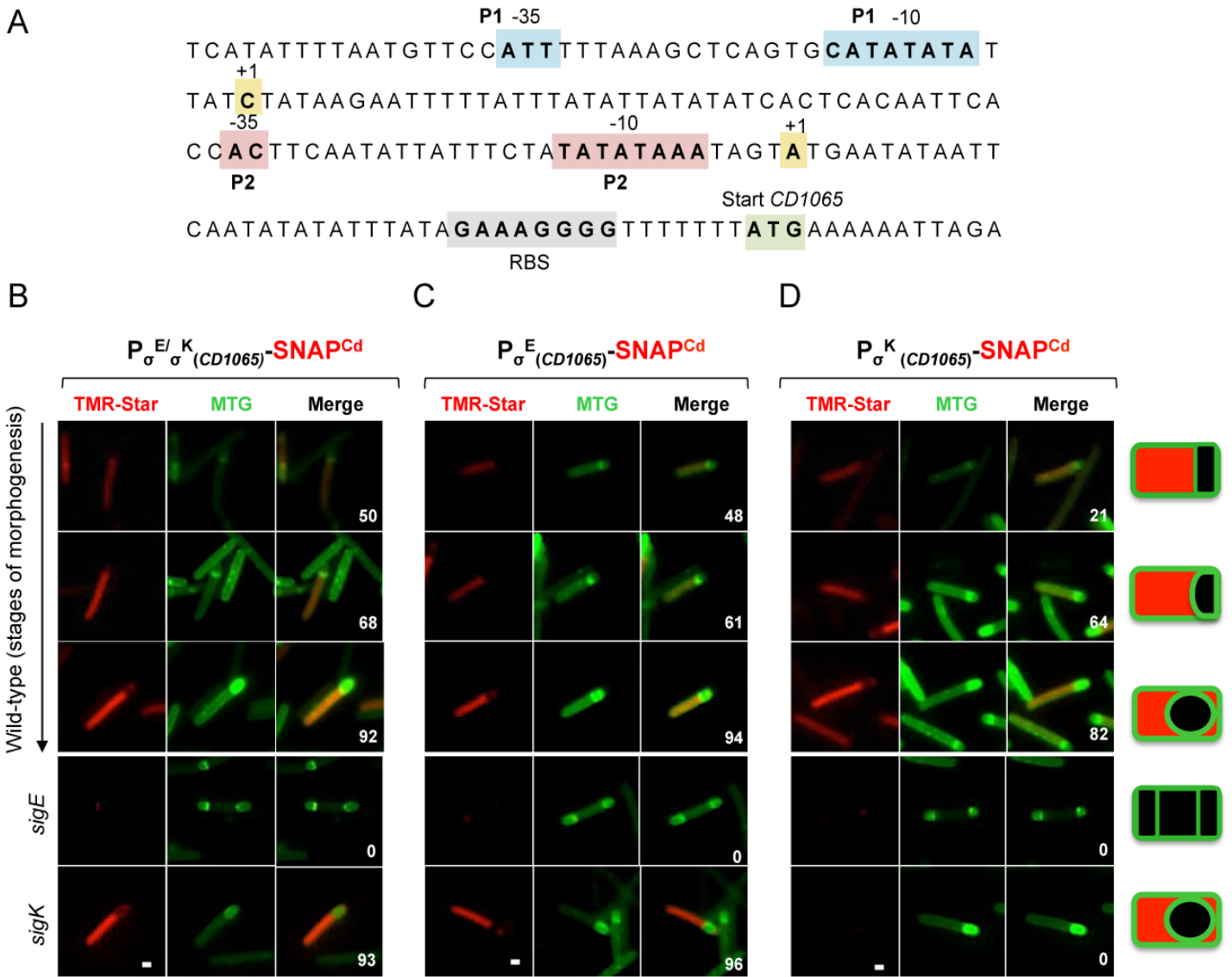


Figure 1: Mother cell specific expression of *CD1065*. **A**) Promoter region of the *CD1065* gene. The mapped transcriptional start sites (+1, yellow), and the -10 and -35 promoter elements corresponding to the consensus for the promoters recognized by σ^E (P1 blue boxes) and σ^K (P2 red boxes) are indicated. The possible ribosome-binding site (RBS) and the start codon of *CD1065* are indicated as grey and green boxes, respectively. **B, C and D**) Temporal and cell type-specific expression of *CD1065* during sporulation. Microscopy analysis of the cells carrying $P_{\sigma^{E/K}(CD1065)}\text{-SNAP}^{Cd}$ (**B**), $P_{\sigma^E(CD1065)}\text{-SNAP}^{Cd}$ (**C**) or $P_{\sigma^K(CD1065)}\text{-SNAP}^{Cd}$ (**D**) transcriptional fusions in the wild-type 630 Δ *erm* strain and in the *sigE* or *sigK* mutant. The cells were collected after 24 h of growth in liquid SM, stained with TMR-Star and the membrane dye MTG, and examined using fluorescence microscopy. The merged images showed the overlap between the TMR-Star (red) and the MTG (green) channels. The panels are representative of the expression patterns observed for different stages of sporulation and are ordered from early to late stages for the wild-type strains. For the *sigE* and *sigK* mutants, a morphological stage characteristic of each mutant is indicated. The data shown are representative of at least three independent experiments. The numbers represent the percentage of cells at the indicated stage expressing the reporter fusion. For each stage, the number of cells analysed (n) is as follows: asymmetric division, n=20-30; engulfment, n=40-60; cortex/coat maturation, n= 90-100. For *sigE* and *sigK* mutants, n= 30-40. Scale bar, 1 μ m.

Results

Expression of *CDI065* in the mother cell compartment is under the dual control of the sporulation sigma factors σ^E and σ^K

In *C. difficile*, σ^K is essential for the assembly of the spore surface layers (Fimlaid et al. 2013, Pereira et al. 2013, Saujet et al. 2013). In the genome-wide analysis of cell type-specific transcription during spore formation, *CDI065* appears as a member of the σ^K regulon (Saujet et al. 2013). As expected, the expression of *CDI065* decreases 17- and 3-fold in the *sigE* and *sigK* mutants, respectively, in qRT-PCR experiments (Saujet et al. 2013). In this study, we identified two transcriptional start sites (TSSs) located 116 nt (promoter P1) and 42 nt (promoter P2) upstream of the translational start site of *CDI065* (Fig. 1A). A canonical -10 box (CATATATA) for promoters recognized by σ^E is present upstream of the TSS corresponding to P1, and an ATT sequence 14 bp upstream from the -10 box could match the -35 motif. Upstream of the second TSS (P2), we found a -10 (TATATAAA) and a -35 (AC) box close to the consensus of the σ^K -dependent promoters (Fig. 1A).

The σ^E - and σ^K -dependent promoters identified upstream of *CDI065* suggested that this gene might be expressed in the MC compartment from the early to late stages of sporulation as demonstrated for *sigK* expression itself (Pereira et al. 2013, Serrano et al. 2016b). To monitor the *CDI065* expression during sporulation, the promoter region containing both the σ^E - and the σ^K -dependent promoters was cloned into pFT47, a vector carrying the gene encoding a fluorescent reporter SNAP^{Cd} (Pereira et al. 2013, Cassona et al. 2016). After 24 h of growth in sporulation medium (SM), cells expressing the transcriptional P _{$\sigma^E/\sigma^K(CDI065)$} -SNAP^{Cd} fusion were doubly labeled with TMR-Star and the membrane dye MTG to allow identification of the different stages of sporulation. Fluorescence microscopy revealed that the expression of the P _{$\sigma^E/\sigma^K(CDI065)$} -SNAP^{Cd} fusion was confined to the MC (Fig. 1B). *CDI065* expression was detected immediately after asymmetric division in 50% of the cells, increasing to 68% of the cells during engulfment and to 92% of the cells after engulfment completion. No *CDI065* expression was observed in the FS. To investigate the impact of each σ factor on *CDI065* expression, we introduced the transcriptional fusion into *sigE* and *sigK* mutants. The expression of P _{$\sigma^E/\sigma^K(CDI065)$} -SNAP^{Cd} was abolished in the *sigE* mutant (Fig. 1B). In contrast, *sigK* inactivation did not suppress the expression of this fusion, since fluorescence was detected similarly to the wild-type 630 Δ *erm* strain after engulfment. When we monitored the SNAP production by a Western blot using an anti-SNAP antibody, no signal was detected in the *sigE* background (Fig. S1A). However, a decrease in the

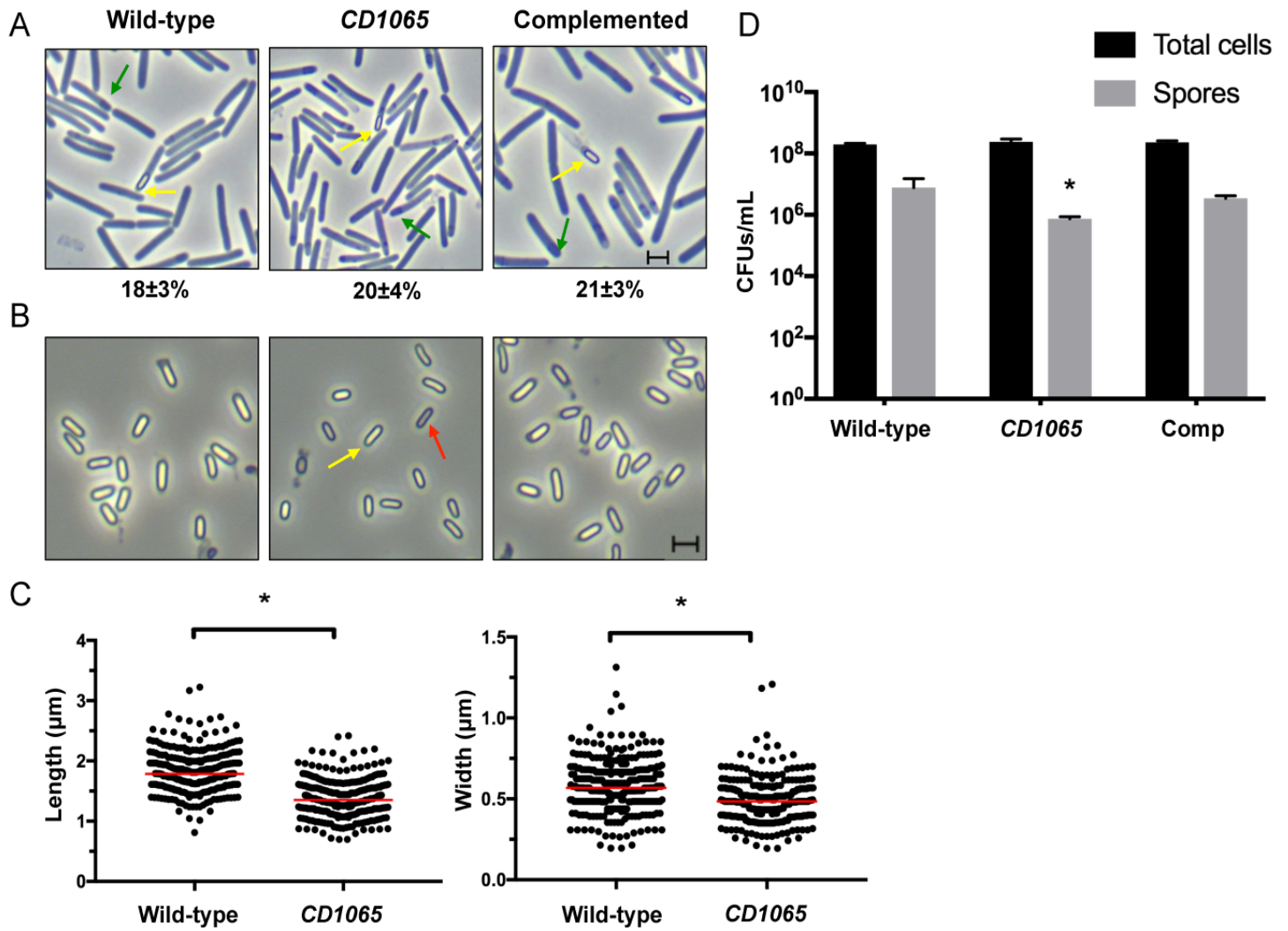


Figure 2: The *CD1065* mutant is able to sporulate. Phase-contrast microscopy of sporulating cells (**A**) and purified spores (**B**) of the wild-type, *CD1065* mutant and complemented strains after 24 h of growth in liquid SM. Yellow arrows mark the mature phase-bright spores; red arrows indicate the phase-grey spores, and green arrows indicate the immature, phase-dark forespores. In panel A, the numbers represent the percentage of sporulating cells. Scale bar, 2 μm . **C**) Spore length and width of the wild-type and *CD1065* mutant strains. The red line indicates the median. $n=300$. Statistical analysis was conducted using a Wilcoxon test, $*P < 0.05$. **D**) Counts (CFUs/mL) of total cells (black) and heat-resistant spores (grey) for the wild-type, *CD1065* mutant and complemented strains grown for 24 h in SM and plated on BHI with 0.1% TA. Data represent the average of four biological replicates. Statistical analysis was conducted using a Wilcoxon test, $*P < 0.05$.

abundance of the SNAP protein was observed in the *sigK* mutant compared to the wild-type strain (Fig. S1A). This result was consistent with the decreased level of the *CDI065* transcript detected by qRT-PCR in the *sigK* mutant (Saujet et al. 2013) even if we failed to detect this decrease by analysing the $P_{\sigma^E/\sigma^K(CDI065)}\text{-SNAP}^{\text{Cd}}$ fusion using microscopy. To study the respective roles of σ^E and σ^K in the complex pattern of expression of *CDI065* in more detail, we constructed two additional transcriptional fusions with the individual promoters: $P_{\sigma^E(CDI065)}\text{-SNAP}^{\text{Cd}}$ and $P_{\sigma^K(CDI065)}\text{-SNAP}^{\text{Cd}}$. Fluorescence expression from the $P_{\sigma^E(CDI065)}\text{-SNAP}^{\text{Cd}}$ fusion was similar to that observed for the $P_{\sigma^E/\sigma^K(CDI065)}\text{-SNAP}^{\text{Cd}}$ fusion, and a signal was only detected in the *sigK* mutant sporulating cells (Fig. 1C). Regarding the $P_{\sigma^K(CDI065)}\text{-SNAP}^{\text{Cd}}$ fusion, we detected a significantly lower fluorescent signal at the initial stage of morphogenesis with 21% of cells detected after asymmetric division instead of the 50% for the $P_{\sigma^E/\sigma^K(CDI065)}\text{-SNAP}^{\text{Cd}}$ fusion (Fig. 1D). Since it is known that σ^E is active earlier than σ^K , the decreased number of cells expressing fluorescence immediately after asymmetric division might be a result of the delayed expression of the SNAP from the $P_{\sigma^K(CDI065)}\text{-SNAP}^{\text{Cd}}$ fusion when compared to the $P_{\sigma^E/\sigma^K(CDI065)}\text{-SNAP}^{\text{Cd}}$ fusion (Pereira et al. 2013, Saujet et al. 2013). No signal was detected in both the *sigE* and *sigK* mutants with the $P_{\sigma^K(CDI065)}\text{-SNAP}^{\text{Cd}}$ fusion (Fig. 1D), which is consistent with the requirement of σ^E for *sigK* expression (Pereira et al. 2013, Saujet et al. 2013). Samples of cultures expressing each fusion collected after 24 h of growth in SM were also analysed using Western blot. A reduced amount of the SNAP protein was detected when the gene is controlled by either σ^E or σ^K (Fig. S1B) suggesting that both σ factors contribute to *CDI065* expression. Together, these results strongly suggested that *CDI065* transcription is initiated from P1 by σ^E at early stage of sporulation and is maintained or increased during the late stages by the use of both P1 and P2 recognized by σ^E and σ^K , respectively.

CDI065 is required for efficient germination

To test whether *CDI065* plays a role in sporulation and/or germination, we inserted a group II intron into the *CDI065* gene in the $630\Delta erm$ strain in a sense orientation immediately after the 123rd nucleotide in its coding sequence (Fig. S2) (Heap et al. 2007, Heap et al. 2009). We cloned the *CDI065* gene expressed from both P1 and P2 into the plasmid pMTL84121 for complementation studies. After 24 h of growth in SM, phase-contrast microscopy analysis revealed that the mutant can sporulate. The frequency of spore formation was 20% of the sporulating cells for the mutant compared with 18% for the wild-type strain (Fig. 2A). We purified the spores to analyse their morphology. While the wild-type

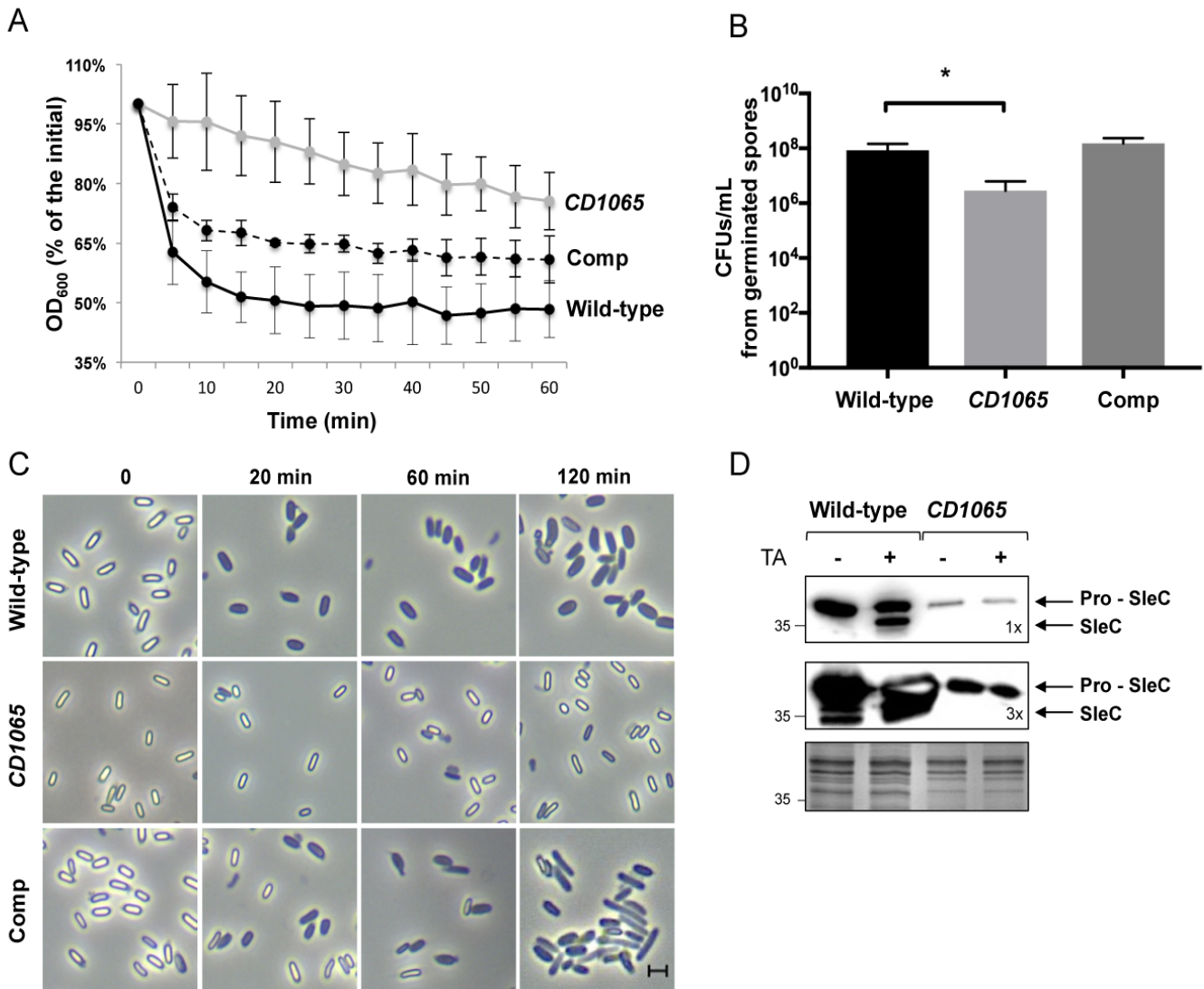


Figure 3: *CD1065* mutant spores are defective in the earliest stages of germination. A) Change in the OD_{600nm} of the spores of the wild-type, *CD1065* mutant and complemented strains after the addition of 1% TA. OD_{600nm} measurements were taken every 5 min. **B)** CFUs/mL obtained after plating the purified spores on BHI with 0.1% TA. Data represent the average of four biological replicates. Statistical analysis was conducted using a Wilcoxon test, $*P < 0.05$. **C)** Purified spores incubated in BHI in the presence of 1% TA were fixed in formaldehyde and visualized using phase-contrast microscopy. Scale bar, 2 μm . **D)** Processing of the SleC in response to TA. The spores were suspended for 20 min in BHI containing 1% TA, and the SleC cleavage was tested by Western blot analysis using anti-SleC antibody. The volume of protein extract applied on the gel was increased three-fold for the second Western blot. Coomassie gel was used as the loading control.

strain forms only phase-bright spores, the *CDI065* mutant produces both mature phase-bright spores and a small proportion (8%) of phase-grey immature spores (Fig. 2B, red arrow). In addition, mutant spores appeared smaller than the wild-type spores. Measurements of the length and width of the spores showed that the mutant spores are thinner and shorter (Fig. 2C). After 24 h of growth in SM, the titre of the heat resistant spores was also assessed by plating them in BHI containing 0.1% of the germinant taurocholate (TA). The *CDI065* mutant produced 10-fold fewer heat resistant spores than the wild-type strain. Complementation partially restored the heat resistant spore formation (Fig. 2D). Since the *CDI065* mutant can sporulate, the reduction in heat resistant spores detection might be due to a defect in germination. The addition of a germinant, such as TA, results in a change from refractive phase-bright spores to phase-dark spores due to cortex hydrolysis, calcium dipicolinic acid (Ca-DPA) release and subsequent rehydration of the core leading to a decrease in the optical density (OD_{600nm}) (Setlow 2003, Donnelly et al. 2016). To study the role of *CDI065* in germination, we monitored the decrease in the OD_{600nm} of wild-type and mutant spore suspensions after the addition of TA. When incubated with 1% TA at 37°C for 1 h, we observed a decrease of 50% and 20% in the OD_{600nm} of the wild-type and mutant spores, respectively (Fig. 3A). The germination rate was partially restored in the complemented strain (Fig. 3A). In addition, when plated in BHI containing 0.1% TA, purified *CDI065* mutant spores exhibited a 30-fold defect in spore germination efficiency compared to the wild-type and complemented strains (Fig. 3B). The germination efficiency did not increase after a prolonged incubation (48 h) for both the wild-type and the mutant spores. This result is consistent with the inability of some mutant spores to germinate after 24 h in the presence of 0.1% TA as observed by phase-contrast microscopy (data not shown). These results indicated that *CDI065* inactivation likely impairs germination rather than sporulation.

We further monitored the germination process using phase-contrast microscopy. We showed that in the presence of 1% TA, most of the phase-bright spores of the wild-type strain were converted to phase-dark spores after 20 min (Fig. 3C). In contrast, the majority of the mutant spores were still phase-bright after 2 h, suggesting that the *CDI065* mutant spores are defective in cortex hydrolysis, the first germination step in *C. difficile* (Francis et al. 2015). It has been shown that Ca-DPA release occurs immediately after the cortex hydrolysis of the *C. difficile* spores (Francis et al. 2015). We tested whether *CDI065* mutant spores could release Ca-DPA in response to 1% TA. While the wild-type spores released ~80% of the stored Ca-DPA in response to TA (Fig. S3), only ~20% of the stored Ca-DPA was released under similar conditions for the *CDI065* spores. Together, these results suggest that *CDI065* mutant

Table 1. Spore surface proteins less abundant in the *CD1065* mutant compared to the wild-type strain.

Protein (Gene)	MW [kDa]	Function	Fold-change (WT/ <i>CD1065</i>)	p-value (LIMMA t-test)	Know/predicted σ factor needed for expression
CspBA (<i>CD2247</i>)	125	Serine protease processes Pro-SleC into SleC	2	1,7E-05	σ^E
SleC (<i>CD0551</i>)	47	Spore cortex-lytic enzyme	10	8,5E-08	σ^K
SpoIVA (<i>CD2629</i>)	56	Morphogenetic coat protein	3	6,2E-08	σ^E
SipL (<i>CD3567</i>)	59	SpoIVA-Interacting protein	3	6,5E-08	σ^E
CotA (<i>CD1613</i>)	34	Coat protein	2	6,4E-06	σ^K
CotB (<i>CD1511</i>)	35	Outer coat layer protein	45	1,1E-10	σ^E
CotE (<i>CD1433</i>)	81	Coat protein Peroxiredoxin/chitinase	3	1,1E-06	σ^K
CotG (<i>CD1567</i>)	25	Coat protein Manganese catalase	3	3,7E-06	σ^G
CD0596	9	Hypothetical protein	7	1,3E-09	σ^K
CotF (<i>CD0597</i>)	11	Spore coat protein	8	9,9E-09	σ^K
CotCB (<i>CD0598</i>)	22	Coat protein manganese catalase	3	1,1E-07	σ^K
CD2399	8	Hypothetical protein (CotJA superfamily)	9	2,9E-06	σ^K
CD2400	11	Spore coat assembly protein CotJB2	6	3,1E-06	σ^K
CotD (<i>CD2401</i>)	21	Coat protein manganese catalase	2	6,6E-06	σ^K
Rbr (<i>CD2845</i>)	22	Rubrerhythrin	4	3,6E-06	σ^G
SodA (<i>CD1631</i>)	27	Superoxide dismutase	44	2,0E-10	σ^G
CD3580	29	Hypothetical protein	7	1,3E-09	σ^K
CdeC (<i>CD1067</i>)	45	Cysteine-rich exosporium morphogenetic protein	3	1,5E-05	σ^K
CdeM (<i>CD1581</i>)	19	Conserved hypothetical protein	3	6,7E-07	σ^K
BclA1 (<i>CD0332</i>)	68	Exosporium glycoprotein	4	3,1E-06	σ^K

spores are defective in the earliest stages of germination.

The germination-signalling pathway of *C. difficile* is markedly different from that of the other spore-forming bacteria (Bhattacharjee et al. 2016). *C. difficile*, which lacks the inner membrane germinant receptors from the Ger family known to sense amino acids and sugars, uses a CspC pseudoprotease located in the coat extractable fraction to sense bile acid germinants, such as TA (Sorg and Sonenshein 2008, Paredes-Sabja et al. 2011, Francis et al. 2013a). When CspC senses the germinant, it activates the serine protease CspB that will cleave Pro-SleC in SleC, the cortex hydrolase. Cortex hydrolysis triggers Ca-DPA release from the spore, leading to hydration of the core and to the initiation of outgrowth (Adams et al. 2013, Francis et al. 2015). Our results prompted us to investigate whether the CspB-mediated proteolytic activation of SleC is affected in the *CDI065* mutant (Adams et al. 2013). To test this hypothesis, purified spores of the wild-type and the *CDI065* mutant strains were treated with 1% TA for 20 min at 37°C. Pro-SleC cleavage was then analysed by Western blotting using an antibody raised against SleC. Interestingly, the amount of Pro-SleC was strongly reduced in the coat of the mutant compared to that of the wild-type strain (Fig. 3D). After TA treatment, Pro-SleC was cleaved in the spores of the wild-type (Fig. 3D) but not in the *CDI065* mutant, even when we increased 3-fold the amount of protein. This result suggests that the *CDI065* inactivation interferes with Pro-SleC maturation in response to TA.

Inactivation of *CDI065* affects the abundance of major proteins in the spore surface

The lower amount of the pro-SleC protein in the coat extract of the *CDI065* mutant spores led us to investigate whether the content of the spore surface layers of this mutant was different from that in the wild-type strain. SDS-PAGE analysis of the spore coat plus exosporium extracts obtained from purified spores showed that several protein bands were absent or present at reduced levels in the mutant spores (Fig. S4A, red arrows). To have a global view of the spore surface proteome of the *CDI065* mutant, proteins extracted from the coat/exosporium of spores of the wild-type strain and the mutant were analysed using mass spectrometry. The analysis revealed that the abundance of several spore surface proteins decreased drastically in the *CDI065* mutant spores (Table 1). The abundance of the early morphogenetic proteins SpoIVA and SipL (Putnam et al. 2013) and the coat proteins, CotaA and CotB (Permpoonpattana et al. 2013), was reduced in the mutant. Among the proteins identified as less abundant in the spore surface layers of the *CDI065* mutant when compared to the wild-type strain, we identified two catalases CotD and CotG, the superoxide dismutase SodA, the rubrerythrin CD2845 likely involved in protection against oxidative stress and

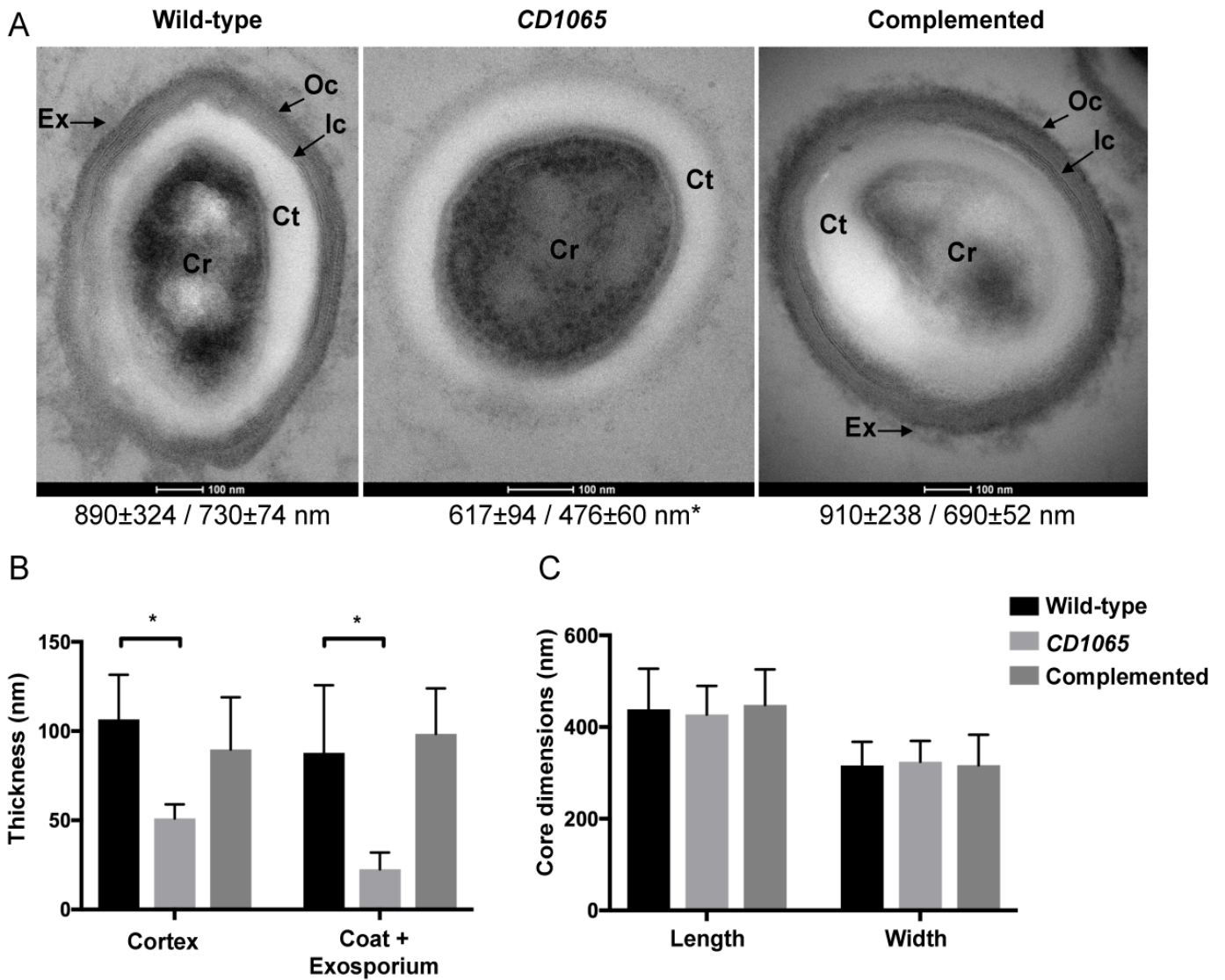


Figure 4: *CD1065* mutant spores have a defective spore coat layer. A) Thin sections of the wild-type, *CD1065* mutant and complemented spores were analysed using TEM as described in the Materials and Methods. Ex, exosporium, Oc, outer coat, Ic, inner coat, Ct, cortex, Cr, core. Scale bars are shown in each figure. The numbers on the bottom of each figure represent the spore dimensions for each strain (length and width) based on the analysis of at least 10 individual spores. Statistical significance was determined using a Wilcoxon test ($*P < 0.05$). **B)** The thickness of the exosporium, the outer/inner coat layers, and the cortex layer of the spores from the three strains were measured. Error bars denote standard errors of the means of at least 10 individual spores. Statistical significance was determined using a Wilcoxon test ($*P < 0.05$). **C)** Size of the spore core of the wild-type, the *CD1065* mutant and the complemented strains. The length and width of the core was measured. Error bars denote the standard errors of the means of at least 10 individual spores.

CotE, which has peroxiredoxin and chitinase activity (Table 1). The abundance of the exosporium morphogenetic cysteine-rich proteins, CdeC (Barra-Carrasco et al. 2013, Calderon-Romero et al. 2018) and CdeM ((Diaz-Gonzalez et al. 2015, Calderon-Romero et al. 2018), as well as the exosporium glycoprotein BelA1 (Pizarro-Guajardo et al. 2014) also decreased in the coat extract of the mutant (Table 1). The abundance of other σ^K -controlled coat proteins, such as CD3580, CD2400 and CD0597, was also reduced from the coat extract of the *CDI065* mutant (Abhyankar et al. 2013). A reduced amount of germination-related proteins, such as the protease CspB and the spore cortex-lytic enzyme SleC, was detected in the mutant, while no differences were observed in the amount of the germinant receptor CspC and the lipoprotein GerS between the wild-type and mutant coat extracts. To validate these results, we performed Western blot experiments using antibodies raised against coat and exosporium proteins. In agreement with the mass spectrometry data, a decreased level of SipL, CotB, CdeC, CdeM, CspB and Pro-SleC was observed in the coat extracts of the mutant spores (Fig. S4B). Both full-length (80 kDa) and cleaved CotE proteins (40 kDa) were detected in the wild-type spores, while the cleaved protein was absent in the coat extract of the mutant spores. Contrary to what we observed by mass spectrometry that we cannot yet explain, a slight decreased level of CspC was detected in the coat extract of the *CDI065* mutant spores by Western blot (Fig. S4B). Complementation of the *CDI065* mutant restored partially or totally the wild-type levels of these proteins. Together, these results suggest that *CDI065* mutation has an effect on the pattern of proteins from the spore surface layers.

***CDI065* gene disruption affects the assembly of the surface layers of *C. difficile* spores**

To assess the effect of *CDI065* inactivation on the structure of the spore surface layers, the morphology of the *CDI065* mutant spores was analysed using transmission electron microscopy (TEM). Previous TEM studies have revealed that the *C. difficile* spore outermost layers comprise an inner lamellar and an outer electrodense coat layer surrounded by an exosporium (Lawley et al. 2009b, Permpoonpattana et al. 2011b). *CDI065* mutant spores analysed by TEM exhibited a major morphological defect. A strong reduction of the surface layers (coat plus exosporium) was observed, although the cortex was maintained (Fig. 4A). On average, the size of the mutant spores (length 617 ± 94 nm/width 476 ± 60 nm) was also smaller than that of the wild-type strain (length 890 ± 324 nm/width 730 ± 74 nm). These data confirmed the first observation performed using phase-contrast microscopy (Fig. 2BC). The surface layers and the cortex of the mutant spores were 4-fold and 2-fold thinner, respectively, than those of the wild-type spores (Fig. 4B). The production of the phase-grey

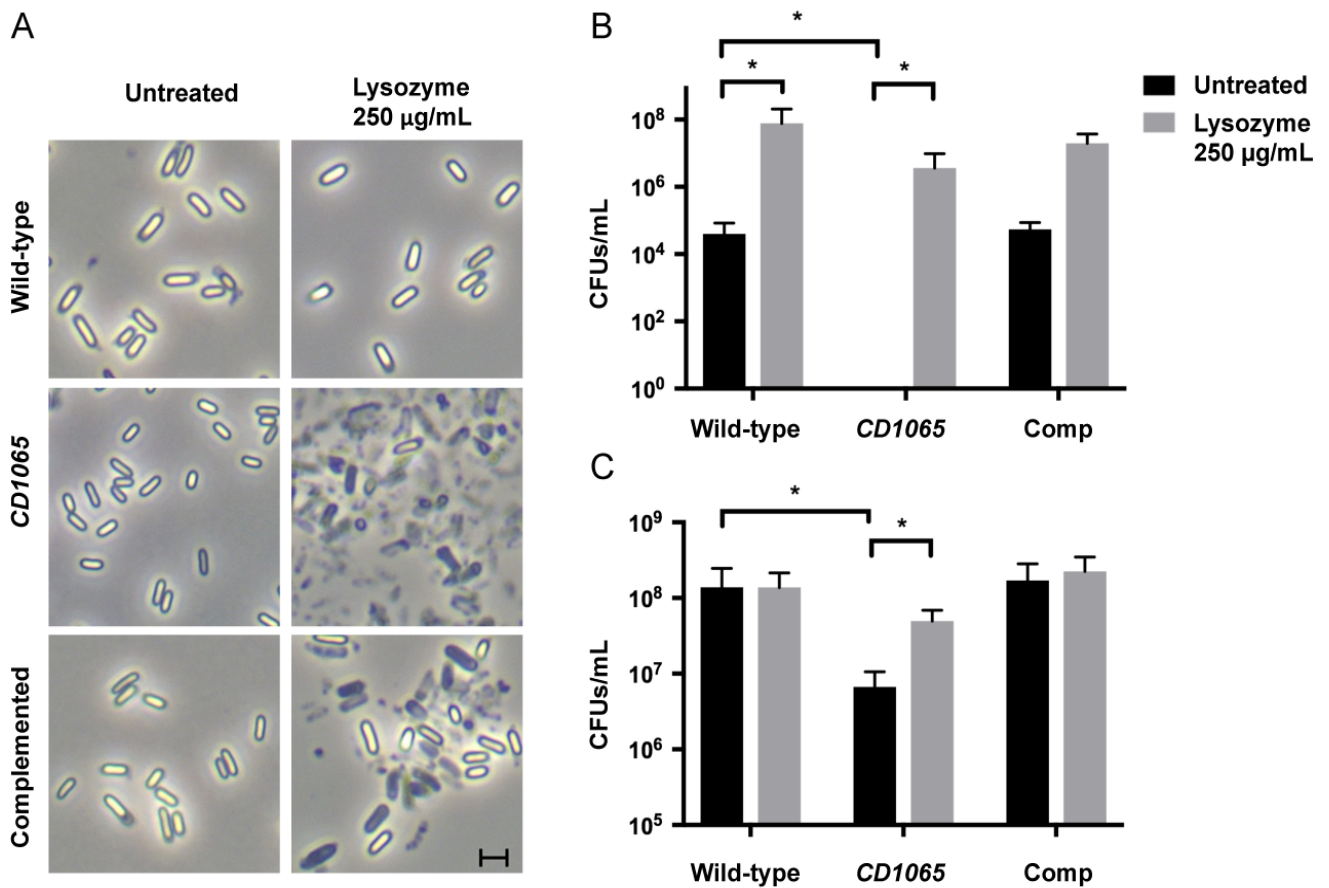


Figure 5: Lysozyme triggers germination of *CD1065* mutant spores. **A)** Phase-contrast microscopy of the wild-type, *CD1065* mutant and complemented spores treated with or without 250 µg/mL of lysozyme for 1 h at 37°C. Scale bar, 2 µm. **B and C)** CFU/mL obtained of the wild-type, *CD1065* mutant and complemented spores untreated (black) and lysozyme-treated (grey) after plating onto BHI agar (**B**) or BHI agar containing 0.1% TA (**C**). Data represent the average of the results of at least three independent experiments, and the error bars represent standard errors of the means. Statistical analysis was conducted using a Wilcoxon test, **P* < 0.05.

mutant spores observed using phase-contrast microscopy might be related to the decrease in the thickness of the cortex layer. By contrast, no differences were observed in the size of the spore core (Fig. 4C). Importantly, the complementation of *CD1065* restored the assembly of the spore coat and exosporium. In summary, these observations suggested that CD1065 plays an essential role in spore coat assembly and spore morphology.

Disruption of *CD1065* increases spore coat permeability

The defective spore coat structure observed in the *CD1065* mutant suggested that these spores could have reduced resistance properties. Since the coat layer protects *C. difficile* spores against lysozyme (Escobar-Cortes et al. 2013), we treated spores of the wild-type, mutant and complemented strains with 250 $\mu\text{g}/\text{mL}$ of lysozyme for 1 h. We observed that most of the wild-type spores remained phase-bright after this treatment (Fig. 5A). In contrast, the mutant spores lost the phase-bright property, suggesting that the absence of an intact coat in the *CD1065* mutant leads to cortex degradation by lysozyme. Consistent with these results, untreated and lysozyme-treated spores were plated in BHI. Contrary to the wild-type and complemented spores, the *CD1065* mutant spores were unable to form colonies on BHI. However, once in the presence of lysozyme, we restored a level of germination almost similar to that observed in the wild-type or complemented spores (Fig. 5B). These results suggested that lysozyme itself can trigger *CD1065* mutant spores germination even in the absence of TA. For the complemented strain, we observed only a partial complementation after lysozyme treatment under the microscope (Fig. 5A). A decreased level of some coat proteins at the spore surface (Fig S4) might slightly affect the coat permeability allowing the lysis of the cortex in at least a fraction of the complemented spores. In addition, by plating the spore suspensions after lysozyme treatment in BHI containing TA, we observed a significant increase of the germination of the *CD1065* mutant spores but not in the wild-type and the complemented strains (Fig. 5C). Together, these results suggested that the *CD1065* mutant spores are more permeable to lysozyme, which can trigger germination by directly degrading the spore-peptidoglycan cortex.

***CD1065* mutation does not block the expression of the σ^E - and σ^K -target genes**

To explain how the CD1065 protein is required for the coat formation, we first tested if CD1065 could be a regulatory protein required for the expression of the genes encoding coat/exosporium proteins. For this purpose, we used qRT-PCR to compare the expression of sporulation-controlled genes in the *CD1065* mutant and the wild-type strain after 14 h or 24 h

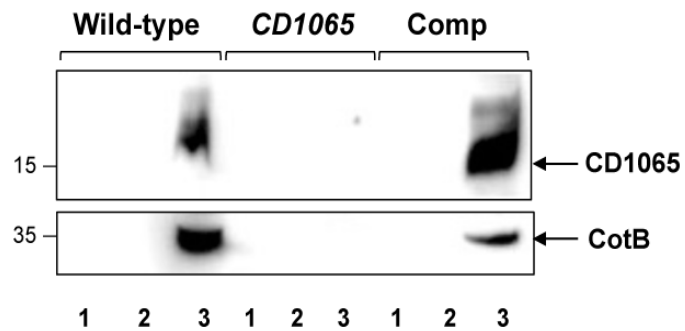


Figure 6: CD1065 protein is localized in the coat/exosporium layer of *C. difficile* spores. Western blot analyses of coat/exosporium (3) and decoated spore lysate (1 and 2) fractions from the wild-type, *CD1065* mutant and complemented strains. The decoated lysate contains the spore core and cortex layers untreated (1) or lysozyme-treated to separate the cortex layer of the core (2). CotB was used as a control for a coat protein.

of growth in SM. No differences were observed between the two strains in the expression level of different target genes of the sporulation σ factors (Saujet et al. 2013) suggesting that CD1065 is not involved in the regulation of the genes encoding spore coat proteins (Table S4). By using Western blotting, we further analysed the amount of the σ^E and σ^K -controlled proteins in the crude extracts of sporulating cells harvested after 14 h or 24 h of growth. Sporulating cells of the *CD1065* mutant produced wild-type levels of the σ^E -targets (SipL, CotB, CspBA, CspC) and the σ^K -targets (SleC, CotE, CdeC and CdeM) (Fig. S4C). These results showed that the deficiencies observed in the coat content of the spores of the *CD1065* mutant (Fig. S4B) are not associated with a reduction in the expression of the encoding genes or in protein production. Since this mutant is impaired in its ability to incorporate coat proteins at the spore surface, CD1065 might be a morphogenetic protein required for the presence of key components of the spore coat and exosporium.

CD1065 localizes in the spore surface layers of *C. difficile*

To determine whether the CD1065 protein is located within the spore envelope, we subjected wild-type and *CD1065* mutant spores to a decoating treatment to separate a coat/exosporium soluble fraction and a pellet fraction, which include the core and cortex layers. The pellet was treated with or without lysozyme to hydrolyse the cortex. We performed Western blotting of the different fractions using an antibody raised against the CD1065 protein. This experiment revealed that CD1065 is located only in the coat/exosporium fraction, as CotB used as a coat control (Fig. 6) (Permpoonpattana et al. 2011b). The absence of the signal in the other two fractions indicates that CD1065 is not located in the most internal layers. As CD1065 is found in the coat fraction of mature spores and is rich in lysine, we decided to rename it CotL. Then, we monitored the subcellular localization of this protein during the process of sporulation. We created a C-terminal SNAP-tag translational fusion by cloning a fragment encompassing the two promoters and the coding sequence of the *cotL* gene ($P_{\sigma^E/\sigma^K(cotL)}-cotL$ -SNAP^{Cd}) into pFT58 (Pereira et al. 2013, Cassona et al. 2016). The resulting plasmid was introduced in the wild-type strain. Samples of cultures harbouring this translational fusion were collected after 24 h of growth in SM, and the cells were labeled with TMR-Star. Different patterns of CotL localization were detected according to the stages of spore morphogenesis. The fluorescent signal of the $P_{\sigma^E/\sigma^K(cotL)}-cotL$ -SNAP^{Cd} was detected in the MC compartment during the engulfment and in sporulating cells with phase-dark FS, in 65% and 26% of all the cells in the population with signal, respectively (Fig. 7A). Fluorescent signal around the spore was detected in cells with phase-

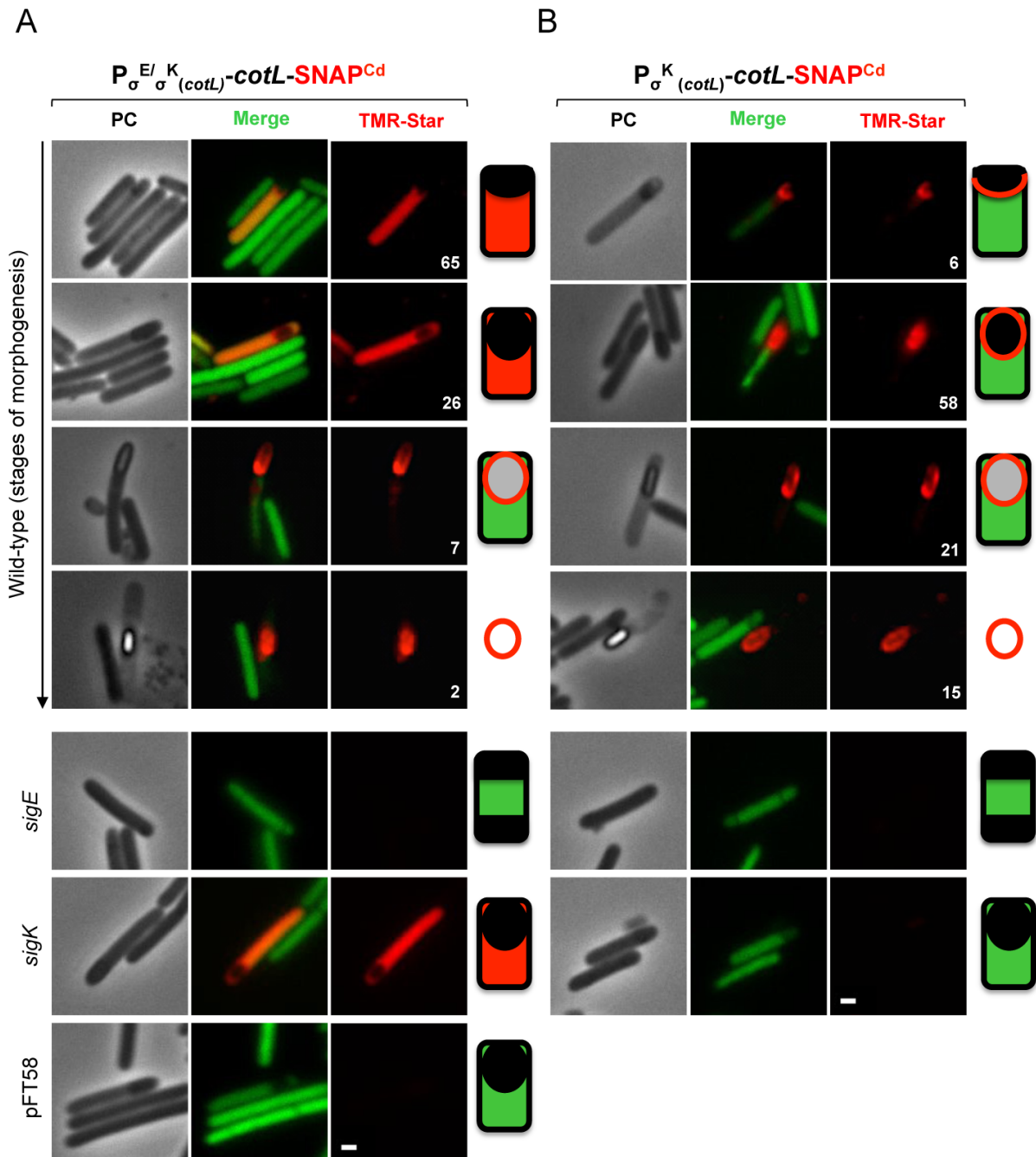


Figure 7: Subcellular localization of the CotL protein fused to SNAP^{Cd}. Microscopy analysis of *C. difficile* cells harboring $P_{\sigma^{E/\sigma^K(cotL)}}-cotL-SNAP^{Cd}$ (A) or $P_{\sigma^K(cotL)}-cotL-SNAP^{Cd}$ (B) translational fusions in the wild-type strain and the *sigE* or *sigK* mutant. The cells were collected after 24 h of growth in liquid SM, stained with TMR-Star and examined by phase-contrast (PC) and fluorescence microscopy to monitor the SNAP production. The merged images show the overlap between the TMR-Star (red) and the autofluorescence (green) channels. Wild-type carrying pFT58 was used as the negative control. A schematic representation of the location pattern of the CotL-SNAP^{Cd} protein is shown on the right side of each panel, ordered from early to late stages. Among the cells with signal, the numbers represent the percentage of sporulating cells/spores showing the corresponding pattern of coat protein location. The data shown are representative of three independent experiments. At least 100 cells were analysed for each strain. Scale bar, 1 μ m.

grey FS (7%) and free spores (2%) (Fig. 7A). No signal was detected in the sporulating cells harbouring only pFT58 (Fig. 7A). To investigate how the inactivation of *sigE* and *sigK* influences CotL location, we introduced the $P_{\sigma^E/\sigma^K(cotL)}-cotL-SNAP^{Cd}$ translational fusion in the respective mutants. As expected, no fluorescent signal was detected in the *sigE* mutant (Fig. 7A). However, in the *sigK* mutant, the SNAP fluorescence was detected only in the MC cytoplasm (Fig. 7A), suggesting that the CotL protein cannot be placed and assembled around the FS in the absence of σ^K . This is consistent with previous studies showing that the *sigK* mutant produce spores with no detectable coat layers (Pereira et al. 2013, Pishdadian et al. 2015). Since σ^E is active earlier than σ^K , we also monitored the location of CotL according to its timing of production. For this, we constructed a second translational fusion containing only the σ^K -dependent promoter ($P_{\sigma^K(cotL)}-cotL-SNAP^{Cd}$). Interestingly, no accumulation of the CotL-SNAP^{Cd} protein was observed in the MC compartment (Fig. 7B). Instead, the fluorescence signal in the sporulating cells was detected first as a cap in the MCP pole during engulfment (6%), and later around the spore in cells with phase-dark and phase-grey FS (58% and 21%, respectively) (Fig. 7B). In free spores (15%), the fluorescent signal was detected around the spore (Fig. 7B). In addition, no fluorescent signal was detected in the *sigK* mutant but also in the *sigE* mutant, since σ^E is required for *sigK* expression (Fig. 7B) (Pereira et al. 2013).

Spore coat and exosporium proteins are mis-localized in the *cotL* mutant cells

To determine the role of CotL in the location of different coat proteins, we constructed C-terminal SNAP-tag translational fusions with known spore coat/exosporium proteins and introduced the resulting plasmids into the wild-type and *cotL* mutant strains. After 24 h of growth in SM, we determined their patterns of subcellular localization in sporulating cells. As early-synthesized coat proteins belonging to the σ^E -regulon, we selected SpoIVA and CotB (Permpoonpattana et al. 2013, Putnam et al. 2013). In the wild-type strain, a signal for the SpoIVA-SNAP^{Cd} signal was detected only in cells with visible phase-dark FS either as a dot, a single cap-like structure in the MCP pole or around the FS (49%, 46% and 5%, respectively) (Fig. 8A). No fluorescent signal was found in free spores (Fig. 8A). The more internal localization of SpoIVA in the spore coat might prevent its detection in mature free spores. In the *cotL* mutant, the SpoIVA-SNAP^{Cd} protein was found to accumulate either as a dot in the MCP pole of phase-dark FS (88%) or also as dots in the MCP pole and the MC compartment (7%) (Fig.8A). The position of the red dots overlaps with an apparent accumulation of material visible by phase-contrast microscopy at the MCP pole of the FS. In the *cotL* mutant,

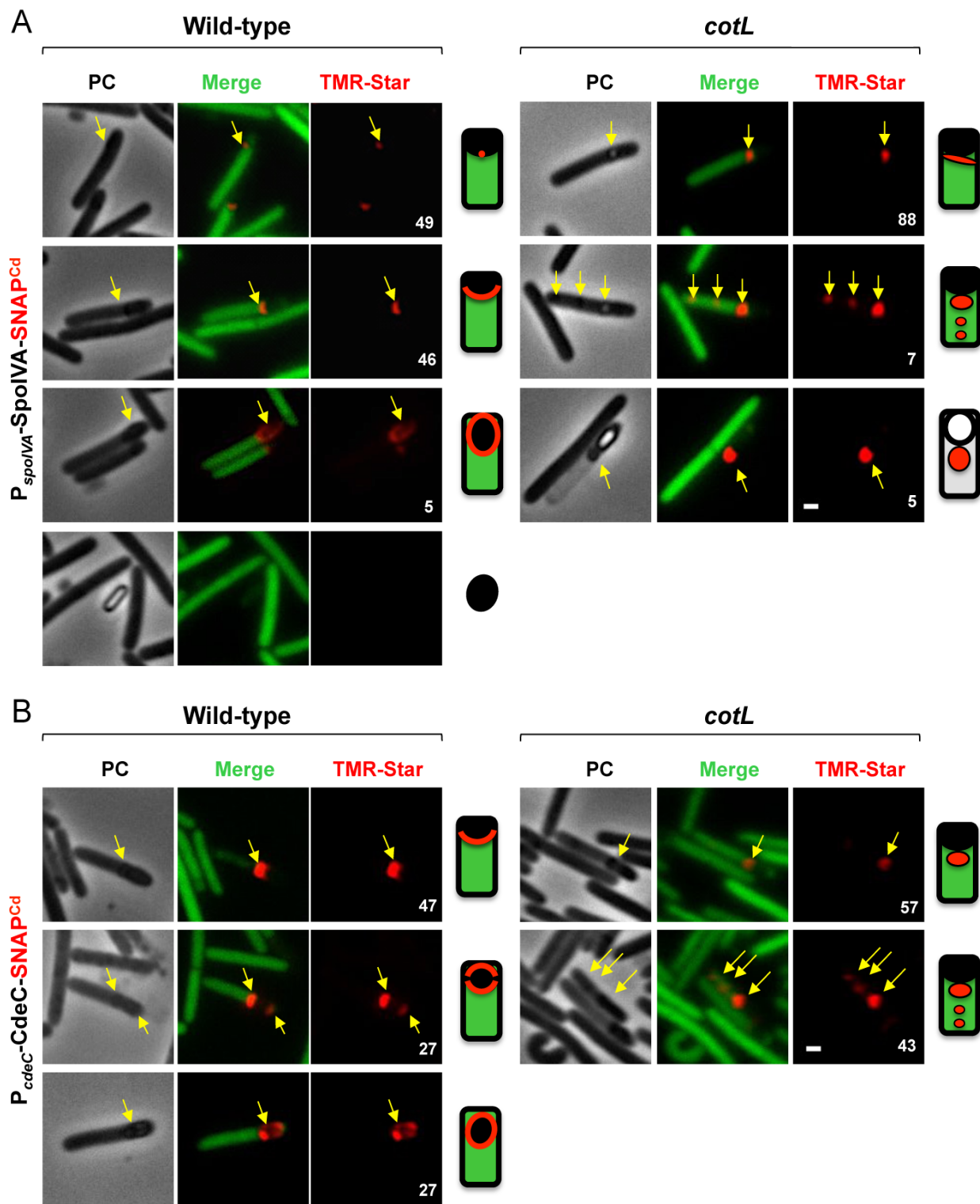


Figure 8: Fluorescence localization of coat proteins fused to SNAP^{Cd} . Microscopy analysis of the wild-type and *cotL* mutant cells carrying (A) SpoIVA- and (B) CdeC- SNAP^{Cd} translational fusions. The cells were collected after 24 h of growth in liquid SM, stained with TMR-Star and examined by phase-contrast (PC) and fluorescence microscopy to monitor the SNAP production. The merged images show the overlap between the TMR-Star (red) and the autofluorescence (green) channels. The yellow arrows point the fluorescent signal. A schematic representation of the location pattern of the different proteins fused to SNAP^{Cd} is shown on the right side of each panel. Among the cells with signal, the numbers represent the percentage of sporulating cells/spores showing the corresponding pattern of coat protein location. The data shown are representative of three independent experiments. For each strain, 100 cells were analysed. Scale bar, 1 μm .

completely free spores were not found. However, contrary to the observed in the wild-type strain, in phase-bright spores of the *cotL* mutant, a fluorescent signal for the SpoIVA-SNAP^{Cd} fusion was detected in one of the poles (5%) (Fig. 8A, yellow arrow). This signal is consistent with an accumulation of material at the spore pole also visible by phase-contrast microscopy (Fig. 8A). The CotB-SNAP^{Cd} protein fusion was detected in the wild-type strain as a single cap-like structure in the MCP pole (81%), at both FS poles (7%) and around free spores (2%) (Fig S5). In the *cotL* mutant, CotB-SNAP^{Cd} was mainly found as a dot in the MCP pole of phase-dark FS (97% of the cases). As for the SpoIVA-SNAP^{Cd} fusion, an accumulation of material was detected by phase-contrast microscopy in the same place (Fig. S5). In phase-bright spores, this SNAP protein fusion was observed at one pole of the spore (Fig. S5, yellow arrow). These results suggest that *cotL* inactivation seems to impair the proper assembly around the FS of at least these two σ^E -target proteins.

Concerning coat proteins synthesized under σ^K control, we selected three proteins, CdeC, CotD and CotE for the construction of translational SNAP fusions (Fig. 8B and S6). The CdeC-SNAP^{Cd} and CotD-SNAP^{Cd} protein fusions were detected in three different patterns in the wild-type strain, i.e., as single cap-like structure in the MCP pole (47% and 50%, respectively), as a double cap in the MCP and mother cell distal (MCD) poles (27% and 17%, respectively), or around the entire FS in sporulating cells with phase-dark FS for CdeC (27%) and around free spores in the case of CotD (33%) (Fig. 8B and S6A). In the *cotL* mutant, CdeC-SNAP^{Cd} and CotD-SNAP^{Cd} proteins were detected in 57% and 38% of the sporulating cells as a dot in the MCP pole, respectively (Fig. 8B and S6A). In the other sporulating cells with signal, CdeC-SNAP^{Cd} accumulated in dots in the MCP pole and in the MC compartment (43%). In the *cotL* mutant free spores, CotD-SNAP^{Cd} fusion was detected at one pole of the spore (Fig. 8B and S6A). For CotE, a non-morphogenetic protein associated with the *C. difficile* spore surface (Paredes-Sabja et al. 2014), inactivation of *cotL* resulted in spots in the MCP pole of the FS (64%) and in MC cytoplasm of cells with either phase-grey or phase-bright spores (17% and 19%, respectively), in contrast to the cap-like pattern seen at the MCP in the wild-type strain (Fig. S6B).

Altogether, the results show that the inactivation of *cotL* gene leads to modifications in the location pattern of both σ^E and σ^K target proteins suggesting that CotL is required to properly encase the coat proteins around the FS during sporulation.

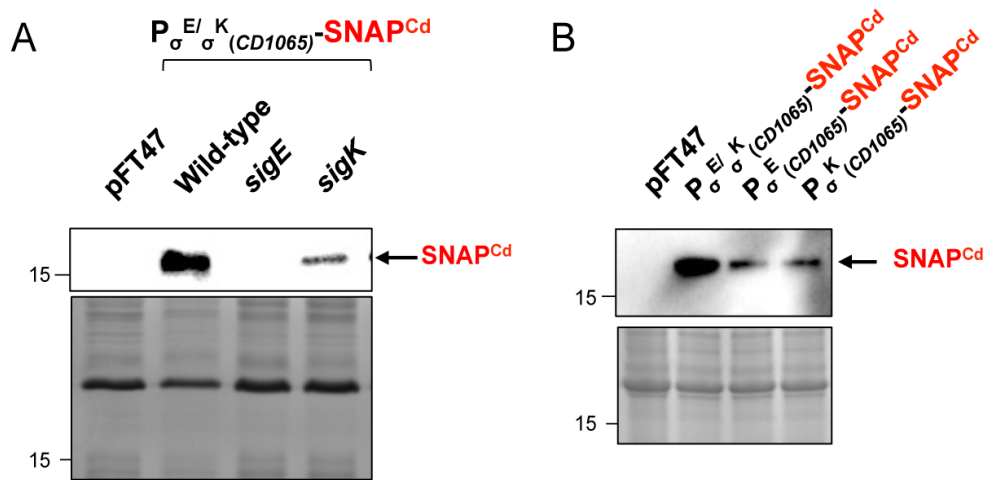


Figure S1: Detection of SNAP production from *CD1065-SNAP^{Cd}* transcriptional fusion using native or truncated promoters and different backgrounds. The accumulation of SNAP^{Cd} in extracts produced from sporulating cells of the wild-type 630Δ*erm* strain, *sigE* or *sigK* mutants harboring P_{σ^E/σ^K(CD1065)}-SNAP^{Cd} fusion (A) or the wild-type strain harboring P_{σ^E/σ^K(CD1065)}-SNAP^{Cd}, P_{σ^E(CD1065)}-SNAP^{Cd} or P_{σ^K(CD1065)}-SNAP^{Cd} fusions (B). 630Δ*erm* carrying pFT47 was used as a negative control. Proteins in whole cells lysates were resolved by SDS-PAGE and subjected to immunoblot analysis using an anti-SNAP antibody. A section of the corresponding Coomassie-stained gel is shown as a loading control. The position of molecular mass markers (kDa) is shown on the left side of the panels. The experiment was repeated at least three times with different samples.

Discussion

Despite the increased knowledge on the regulatory network controlling sporulation in *C. difficile*, relatively little is known about the spore composition and the mechanisms that orchestrate the assembly of its surface layers. Except for SpoIVA (Putnam et al. 2013) and SpoVM (Ribis et al. 2017), the key differences in the morphogenetic coat proteins of *B. subtilis* and *C. difficile* make extrapolation difficult. In this study, we propose that the *C. difficile* coat-associated protein, CotL, is a new morphogenetic coat protein essential for the efficient assembly of the coat and exosporium layers. Spore morphogenetic proteins are key components of the ordered assembly of coat proteins at the spore surface. We observed by TEM analysis that *cotL* inactivation resulted in a substantial defect in the spore morphogenesis with a strong reduction of the coat and an absence of exosporium layers. Congruently, the abundance of several spore coat and exosporium proteins is strongly decreased in extracts of the spore surface layers of the *cotL* mutant compared to those of the wild-type strain (Table 1 and Fig. S4B). However, *cotL* inactivation did not impair the transcription of sporulation-related genes, or the protein production in sporulating cells. Thus, we infer that CotL plays a morphogenetic rather than a regulatory role in coat formation. Indeed, we observe that some coat proteins produced under the control of σ^E such as SpoIVA and CotB, or of σ^K such as CdeC, CotD and CotE are mis-localized in the *cotL* mutant. In this mutant, they accumulate mainly in the MCP pole or as spots in the MC cytoplasm rather than around the FS. These results suggest that the CotL protein is required to correctly guide and incorporate spore surface proteins around the spore.

The structurally defected coat of the *cotL* mutant spores has a strong impact on spore function, particularly in their sensitivity to lysozyme and their germination properties. An impaired coat structure strongly affects germination efficiency and spore resistance to lysozyme as observed for the *B. subtilis* *spoVID*, *safA* and *cotE* mutants (Zheng et al. 1988, Beall et al. 1993, Takamatsu et al. 1999, Costa et al. 2007). Coat-less spores of *Clostridium perfringens* also do not respond to germinants, but lysozyme can induce germination (Cassier and Ryter 1971). In *C. difficile*, the morphologic defect of the surface layers of the *cotL* mutant is probably responsible for an increased spore permeability of lysozyme that can trigger germination by accessing and hydrolysing the spore cortex. The observed germination defect in the *cotL* mutant is very likely an indirect consequence of a misassembled spore coat and of the reduced amount of CspC, CspB and Pro-SleC proteins in the surface layers of this mutant. The decrease of Csp proteins likely results in a defected maturation of the cortex hydrolase SleC. The inactivation of *cotL* also leads to the production of a thinner spore cortex

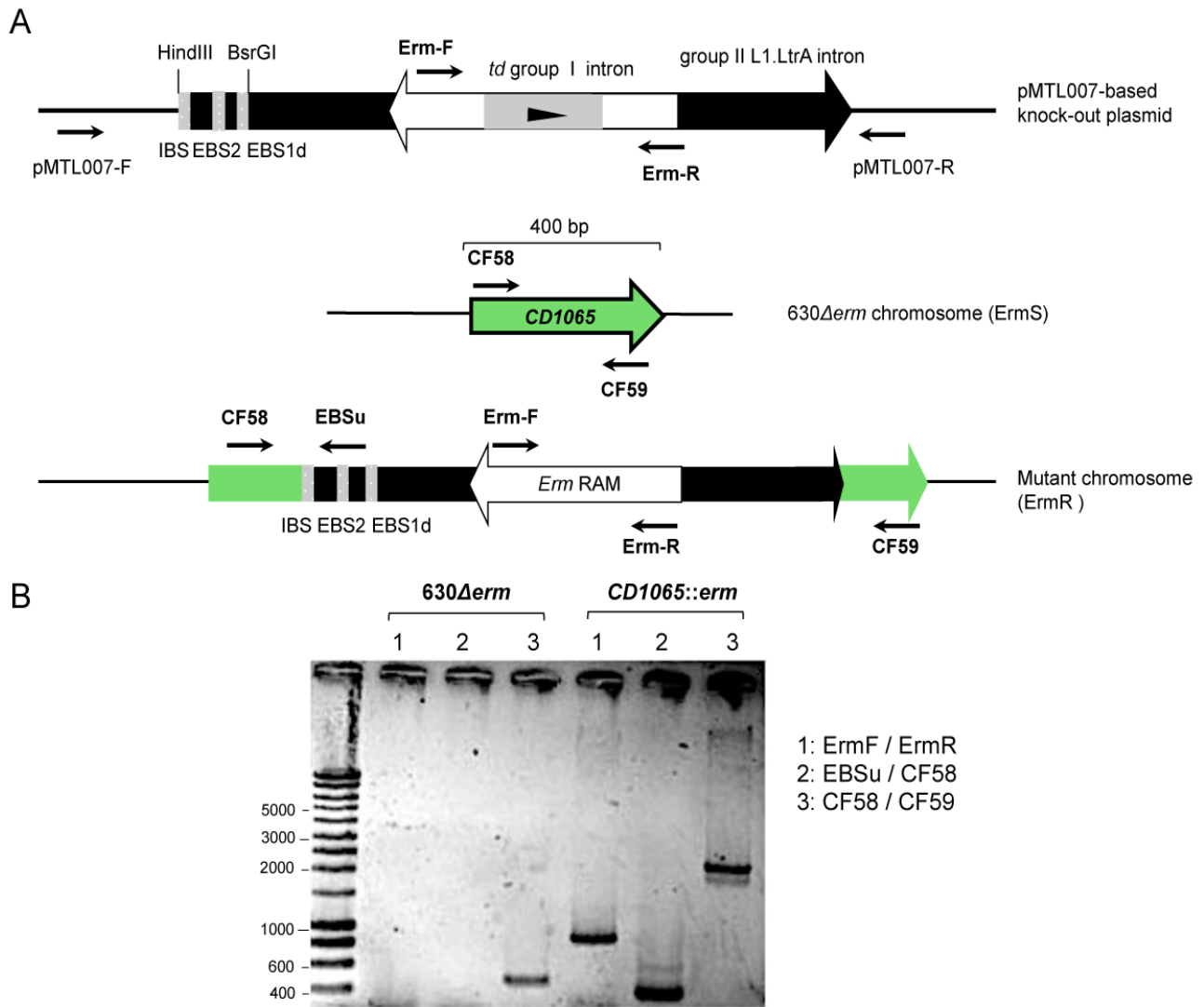


Figure S2: Construction of the *CD1065* mutant in *C. difficile*. **A)** Schematic representation of the inactivation strategy for the *CD1065* gene using the ClosTron technology. Primers were designed to re-target the group II intron of pMTL0007-CE5 to insert it into the *CD1065* gene in a sense orientation immediately after the 123rd nucleotide of its coding sequence. **B)** Verification of the L1.LtrB intron integration into the *CD1065* gene in the 630 Δ erm strain. PCRs were performed with DNA of the 630 Δ erm strain and the *CD1065* mutant using primers (CF58/CF59) flanking the insertion site in *CD1065* (lane 3), one primer flanking the insertion site in *CD1065* (CF58) and the intron primer EBSu (lane 2) or primers (Erm-F/Erm-R) amplifying the erythromycin cassette (lane 1).

compared to what is seen in the wild-type spores. This is consistent with a slight decrease on heat resistance at 80°C observed for the *cotL* mutant spores (data not shown).

The expression of the *cotL* gene is restricted to the MC as expected for a coat protein, and this gene is transcribed under the dual control of the two specific σ factors of the MC, σ^E and σ^K . The transcription of *cotL* is initiated by σ^E early during sporulation after asymmetric division, suggesting a potential role of CotL in early FS development, as already observed for SpoIVA and SipL (Putnam et al. 2013). In addition, the transcription of *cotL* by σ^K probably allows the maintenance or increased expression of *cotL* during the late sporulation stages. Congruently, we observed a reduced abundance of the SNAP protein when produced under the control of the σ^E - or σ^K -dependent promoter alone compared to its production under the control of both σ^E and σ^K . In addition, when the *cotL*-SNAP^{Cd} translational fusion is uniquely transcribed by σ^K likely at a reduced level, the CotL-SNAP^{Cd} protein is immediately assembled at the FS surface, while the CotL-SNAP^{Cd} produced under the dual control of σ^E and σ^K first accumulates in the MC and then assembles around the FS (Fig. 7A and B). The microscopy results also revealed that the CotL-SNAP^{Cd} protein produced under the control of its native promoter is not assembled around the FS in the *sigK* mutant (Fig. 7A). Consistently with this, the *sigK* mutant itself is defective in coat polymerization and localization (Pereira et al. 2013, Pishdadian et al. 2015). However, it has been shown that CotB-SNAP^{Cd} (σ^E -target) is located at the FS surface in the *sigK* mutant (Pereira et al. 2013), suggesting that *C. difficile* coat assembly starts at an early sporulation stage, as in *B. subtilis* (Henriques and Moran 2007). Our observations raise the hypothesis that CotL assembly might be dependent on the presence of a σ^K -regulated gene product even if we cannot completely exclude that the reduced amount of CotL expressed solely under the control of σ^K might be responsible for its direct assembly without accumulation in the MC.

Previously published proteomic studies (Lawley et al. 2009b, Abhyankar et al. 2013, Diaz-Gonzalez et al. 2015) and our proteomic analysis failed to detect the CotL protein in the spore or in the spore surface layers. However, we successfully detected CotL at the spore surface either by fluorescence microscopy using CotL-SNAP^{Cd} fusion or by Western blot analysis of the coat/exosporium extract using an antibody raised against CotL. Since CotL is a lysine-rich protein (24% of the amino acids), this feature might hinder its detection by bottom-up mass spectrometry-based proteomics. Proteins are usually digested into peptides with trypsin, an enzyme that cleaves after lysine and arginine residues and the generated peptides are therefore too small or not suitable with their further identification by mass spectrometry.

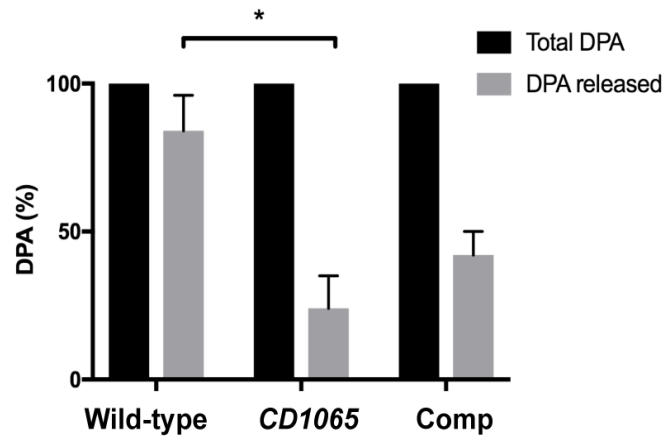


Figure S3: Dipicolinic acid (DPA) release by spores of the wild-type, the *CD1065* mutant and the complemented strains. Spores of the indicated strains were suspended in PBS supplemented with TA (1%) and glycine (10 mM). After 1 h exposure, the amount of DPA in the germination solution was determined as indicated in the Materials and Methods. The data represent the average and standard deviation from three biological replicates. Statistical significant difference relative to the wild-type was determined using a Wilcoxon test, $*P < 0.05$.

In *C. difficile*, coat assembly around the FS is driven by the morphogenetic proteins SpoIVA and SipL (Putnam et al. 2013). In the corresponding mutants, the sporulating cells exhibit defects in coat localization, spore coat swirls are detected in the MC cytoplasm, and the spores cannot be purified (Putnam et al. 2013). CdeC and CdeM are the morphogenetic factors of the exosporium of *C. difficile* spores. *cdeC* mutant spores, but not *cdeM* mutant spores, exhibit a thinner coat (Calderon-Romero et al. 2018). Our results indicate that the *cotL* mutant has a less severe defect in spore formation than the *spoIVA* or *sipL* mutant but a more severe than the *cdeC* mutant. We could purify *cotL* mutant spores, however most of the spore coat and the entire exosporium layer are lacking. The localization of CotL in the coat layers of *C. difficile* spore remains to be determined more precisely. However, our results strongly suggest a hierarchical organization of the coat layers in which CotL seems to play a role downstream of the morphogenetic factors, SpoIVA and SipL, but upstream of CdeC. In addition, the *spoIVA* and *sipL* genes are transcribed by σ^E while the *cdeC* gene is transcribed by σ^K . The dual genetic control of the *cotL* gene by σ^E and σ^K suggests a crucial role for CotL production during transition from the early to late sporulation stages. In *B. subtilis*, the *cotE* gene encoding the outer coat morphogenetic protein is similarly expressed first from a σ^E -dependent promoter and later from a σ^K -dependent promoter (Zheng and Losick 1990). CotE is located at the interface of the inner and outer spore coat layers. A *cotE* mutant retains a lamellar inner coat but lacks an outer coat (Zheng et al. 1988). SafA is the inner coat morphogenetic protein of *B. subtilis*. The *safA* gene is expressed under σ^E control, and *safA* mutant spores lack an inner coat but still retain the outer coat (Takamatsu et al. 1999). In *C. difficile*, a few coat materials are detected around the purified spores of the *cotL* mutant, but no lamellar or electron-dense layers are observed (Fig. 4). These data suggest that the inactivation of *cotL* in *C. difficile* has a stronger impact on spore morphogenesis than the inactivation of *safA* or *cotE* gene in *B. subtilis*. This is consistent with the observation that the early coat proteins, SpoIVA and CotB, are not correctly assembled around FS of the *cotL* mutant suggesting that CotL is an important player in starting coat assembly. In addition, a mis-assembly of early coat proteins in the *cotL* mutant, most likely hinders the correct localization of late coat proteins such as CdeC, CotD and CotE.

Interestingly, from the inside out of the spore, a conservation of coat morphogenetic proteins in the *Peptostreptococcaceae* family is observed. While SpoIVA and SpoVM are conserved in all spore-formers, CotL, as CdeC, is conserved in all the *C. difficile* strains sequenced so far. Both CotL and CdeC are also present in other members of the *Peptostreptococcaceae* family such as *Clostridioides manganotti*, *Terrisporobacter*

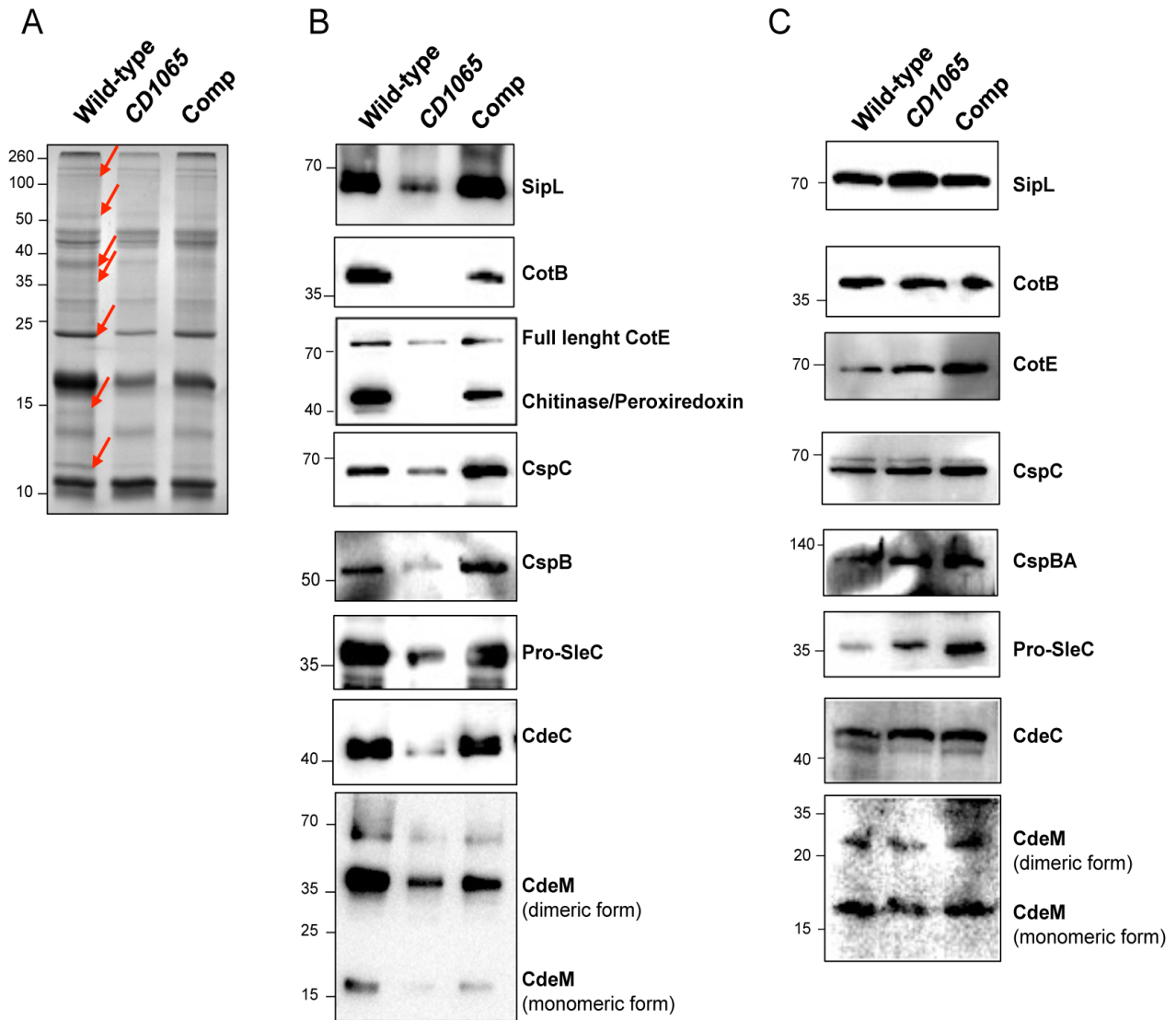


Figure S4: *CD1065* inactivation affects the abundance of the major proteins of the spore surface. **A)** Coat/exosporium extracts from purified spores of the wild-type, the *CD1065* mutant, and the complemented strains were loaded on acrylamide gel and stained with Coomassie brilliant blue. Red arrows highlight the major differences in the protein bands. **B and C)** Western blot analyses using coat/exosporium extracts of purified spores (**B**) or extracts of sporulating cells (**C**) using antibodies raised against different spore coat or exosporium proteins (SipL, CotB, CotE, CspC, CspBA, SleC, CdeC and CdeM). Experiments were repeated at least three times with independent samples.

glycolicus, *Paraclostridium bifermentans*, and *Intestinibacter bartlettii* (Calderon-Romero et al. 2018). However, the exosporium protein CdeM is specific to *C. difficile*. Considering that the spore surface is the interface between spores and the environment, this reflects an adaptation of *C. difficile* to its specific ecologic niche.

In summary, our study brings new insights into the coat composition and assembly of *C. difficile* spores. We propose that a new protein, CotL, plays a morphogenetic role in coat assembly around the FS. Further studies to address the precise role of CotL in coat assembly as well as the determination of possible direct interactions of CotL with SpoIVA, SpoVM, SipL or even CdeC will be relevant to address in future work.

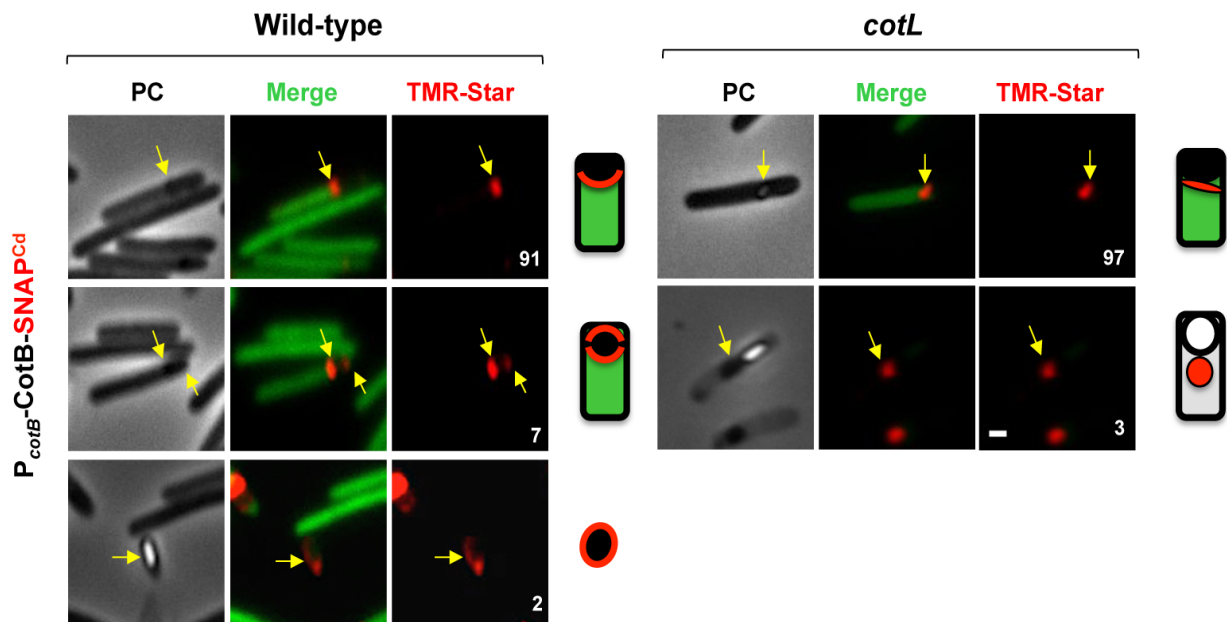


Figure S5: Fluorescence localization of CotB-SNAP^{Cd}. Microscopic analysis of the wild-type and *cotL* mutant cells carrying a CotB-SNAP^{Cd} translational fusion. The cells were collected after 24 h of growth in liquid SM, stained with TMR-Star and examined using fluorescence microscopy. The cells were collected after 24 h of growth in liquid SM, stained with TMR-Star and examined by phase-contrast (PC) and fluorescence microscopy to monitor the SNAP production. The merged images show the overlap between the TMR-Star (red) and the autofluorescence (green) channels. The yellow arrows point the fluorescent signal. A schematic representation of the location pattern of the different proteins fused to SNAP^{Cd} is shown on the right side of each panel. Among the cells with signal, the numbers represent the percentage of sporulating cells/spores showing the corresponding pattern of coat protein location. The data shown are representative of three independent experiments. For each strain, 100 cells were analysed. Scale bar, 1 μ m.

Experimental procedures

Bacterial strains and growth conditions

The bacterial strains used in this study are listed in Table S1. Luria-Bertani (LB) medium (1% bacto-tryptone, 0.5% yeast extract, and 0.5% NaCl, pH 7.0) was used for the growth of *Escherichia coli*. When indicated, ampicillin (100 µg/mL) or chloramphenicol (15 µg/mL) was added to the culture medium. *C. difficile* strains were grown anaerobically (5% H₂, 5% CO₂ and 90% N₂) at 37°C in brain heart infusion (BHI) medium (Difco). Sporulation assays were performed in sporulation medium (SM) (Wilson et al. 1982). To produce spores, we used an SMC medium containing (per liter): 90 g of Bacto peptone (Bacto™ 211677), 5 g of Proteose peptone (82450, Sigma-Aldrich), 1 g of (NH₄)₂SO₄ and 1.5 g of Tris. When necessary, cefoxitin (25 µg/mL), thiamphenicol (15 µg/mL) and erythromycin (2.5 µg/mL) were added to the *C. difficile* cultures. All the primers used in this study are listed in Table S3.

Construction of *C. difficile* strains

The ClosTron gene knockout system (Heap et al. 2007, Heap et al. 2009) was used to inactivate the gene in 630Δ*erm*. Using the Targetron design software (Sigma-Aldrich), we designed primers to retarget the group II intron of pMTL007-CE5 into the *cotL* gene in the sense orientation immediately after the 123rd nucleotide in the coding sequence (Table S3). *E. coli* HB101(RP4) containing pMTL007-CE5-*cotL*-123s (pDIA6563) was mated with *C. difficile* 630Δ*erm*. *C. difficile* transconjugants were selected by sub-culturing on BHI agar containing thiamphenicol and cefoxitin and plated on BHI agar containing erythromycin. After extraction of the chromosomal DNA of transconjugants, PCRs were realized to verify the integration of the intron into the *cotL* gene and the splicing of the group I intron after integration (Fig. S2 and Table S3). This experiment produced strain CDIP782 (630Δ*erm cotL::erm*, Table S1). To complement this mutant, we amplified *cotL* coding sequence and its promoter region (positions -243 to +438 from the translational start site) using genomic DNA as the template. The PCR product was cloned between the *EcoRI* and *NotI* sites of plasmid pMTL84121 (Heap et al. 2009), to produce pDIA6626. This plasmid was transferred by conjugation into *C. difficile cotL::erm* producing CDIP952 strain (Table S1).

Mapping of the 5' terminus of *cotL* mRNA

The 5' end of the *cotL* mRNA was mapped by primer extension using the 5' Rapid Amplification of cDNA Ends (RACE) System (Invitrogen) according to the manufacturer's

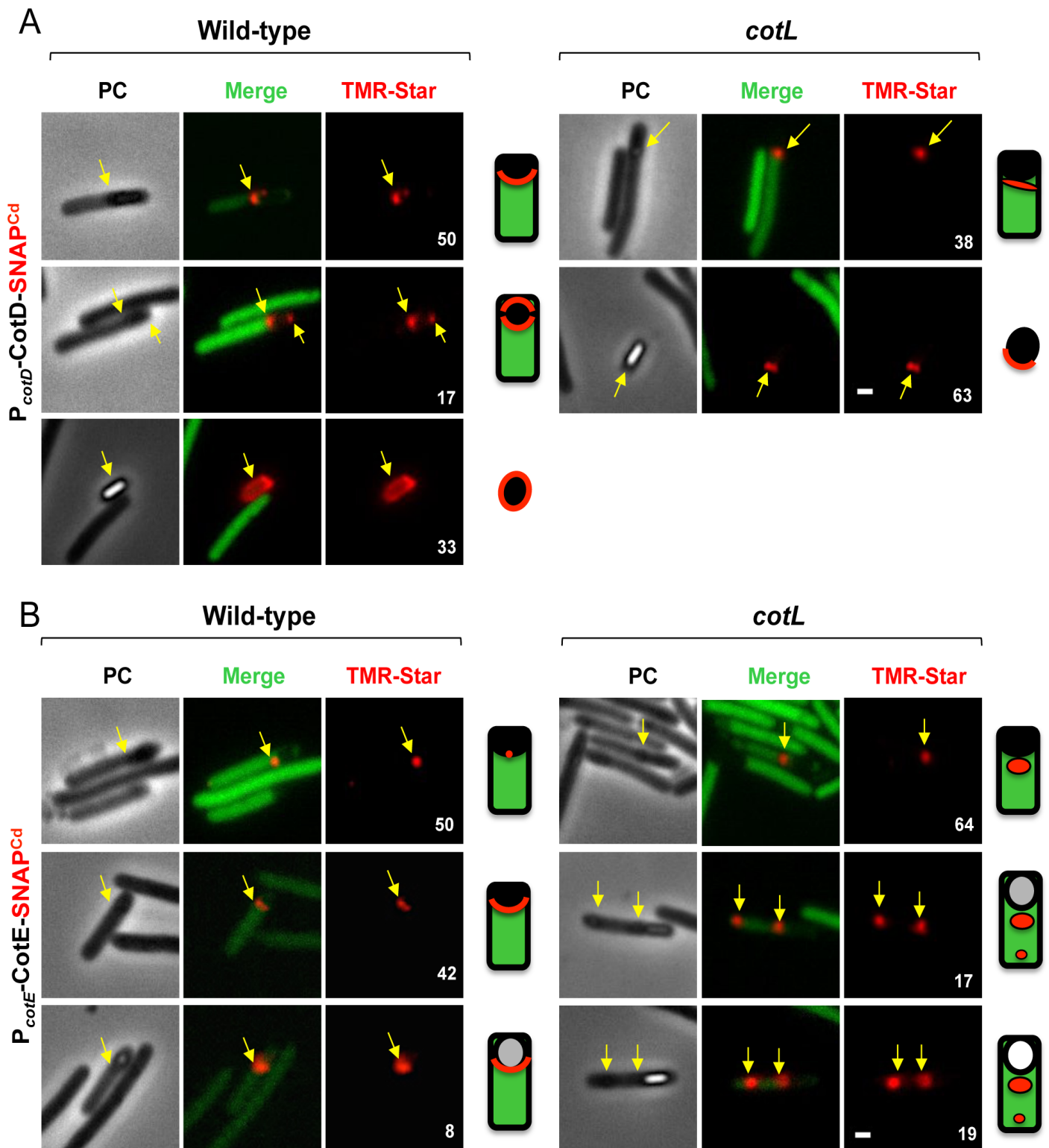


Figure S6: Fluorescence localization of coat proteins fused to SNAP^{Cd}. Microscopy analysis of the wild-type and *cotL* mutant cells carrying (A) CotD- and (B) CotE-SNAP^{Cd} translational fusions. The cells were collected after 24 h of growth in liquid SM, stained with TMR-Star and examined by phase-contrast (PC) and fluorescence microscopy to monitor the SNAP production. The merged images show the overlap between the TMR-Star (red) and the autofluorescence (green) channels. The yellow arrows point the fluorescent signal. A schematic representation of the location pattern of the different proteins fused to SNAP^{Cd} is shown on the right side of each panel. Among the cells with signal, the numbers represent the percentage of sporulating cells/spores showing the corresponding pattern of coat protein location. The data shown are representative, of three independent experiments. One hundred cells were analysed for each strain. Scale bar, 1 μ m.

recommendations. CF127 primer (Table S3) was used to synthesise the first cDNA strand, using the RNAs extracted from 630 Δ *erm* after 14 h and 24 h of growth in SM as templates. The CF131 primer was used for the PCR of the dC-tailed cDNA. The products of the primer extension were analysed by electrophoresis in 1.5% agarose gel. Two different-size products were detected, and TA cloning was used to discriminate the two inserts analysed by sequencing.

RNA extraction and quantitative RT-PCR analysis

To study σ^E - or σ^F -targets, we harvested the cells from 630 Δ *erm* and *cotL* mutant after 14 h of growth in SM medium, while σ^G - and σ^K -targets were analysed after 24 h of growth. RNA was extracted using the FastRNA Pro Blue Kit (MP Biomedicals), according to the manufacturer's instructions. cDNAs synthesis and real-time quantitative PCR were performed as previously described (Saujet et al. 2011, Soutourina et al. 2013). In each sample, the quantity of cDNAs for each gene was normalized to the quantity of cDNAs of the DNAPolIII gene. The relative transcript changes were calculated using the $2^{-2\Delta\Delta Ct}$ method as previously described (Livak and Schmittgen 2001). The primers used for each marker are listed in Table S3.

Transcriptional and translational SNAP^{Cd} fusions

To construct transcriptional fusions, pFT47 containing the SNAP^{Cd} sequence was used (Pereira et al. 2013, Cassona et al. 2016). The promoter region of the *cotL* gene (P1 plus P2) was PCR amplified using genomic DNA and primer pairs CF120/CF121 to produce a 250 bp PCR product (position -243 to +19 from the TSS of P2). To construct the fusion bearing only P2, the σ^K -dependent promoter of *cotL*, a 90 bp region was amplified using the CF133/CF121 primer pairs (position -75 to +19 from the TSS of P2). The DNA fragments were inserted between the *EcoRI* and *XhoI* sites of pFT47 to obtain pDIA6561 and pDIA6613 (Table S1). To construct the fusion bearing only promoter P1, we removed promoter P2 by inverse PCR using pDIA6561 as a template and the CF206/CF207 primer pair. To create a C-terminal SNAP-tag translational fusion, the promoter (P1 plus P2 or P2 alone) and coding regions of *cotL* were amplified from genomic DNA using primer pairs CF126/CF127 (positions -243 to +438 from the translational start site) or CF189/CF127 (positions -75 to +438 from the translational start site). The resulting PCR products were inserted into pFT58 using Gibson Assembly yielding pDIA6617 and pDIA6663 and verified by sequencing. Plasmids were

introduced in *E. coli* HB101 (RP4) and transferred to *C. difficile* 630 Δ *erm*, *sigE* and *sigK* mutant strains by conjugation. To create other C-terminal SNAP-tag fusions, the promoter and coding regions of *CD2629* (SpoIVA), *CD1511* (CotB), *CD1433* (CotE) and *CD1067* (CdeC) were amplified from genomic DNA using adapted primer pairs (Table S3). CF124/CF202 and CF203/CF204 pairs were used to amplify the promoter present upstream of *CD2399* the first gene of the *cotD* operon and the coding region of *CD2401* (*cotD*), respectively. The PCR products were inserted into pFT58 using Gibson Assembly. The plasmids obtained were introduced in *E. coli* HB101 (RP4) and transferred by conjugation to the *C. difficile* 630 Δ *erm* and *cotL::erm* mutant strains (Table S1).

Fluorescence microscopy and image analysis

For SNAP labelling, the TMR-Star substrate (New England Biolabs) was added to the cells at a final concentration of 250 nM, and the mixture was incubated for 30 min in the dark and in anaerobiosis. After labelling, the cells were collected by centrifugation (4000xg for 3 min at room temperature), washed 3 times with 1 mL of PBS, and finally resuspended in 1 mL of PBS containing or lacking the membrane dye Mitotracker Green (MTG; 0.5 μ g/mL) (Molecular Probes, Invitrogen). For phase-contrast and fluorescence microscopy, spores or cells were mounted on 1.7% agarose-coated glass slides to keep the cells immobilized and to obtain sharper images (Glaser *et al.*, 1997). The images were taken with exposure times of 200 ms for MTG and 600 ms for SNAP. Concerning the transcriptional fusions, cells were observed using a Nikon Eclipse TI-E microscope 60x Objective and captured with a CoolSNAP HQ2 Camera. For the translational fusions, cells were observed using a Delta Vision Elite microscope equipped with an Olympus 100x objective and captured with sCMOS camera. The images were analysed using ImageJ.

Spore production and sporulation tests

SMC liquid medium inoculated with *C. difficile* was incubated overnight at 37°C. Two hundred microlitres from this culture plated in SMC agar were incubated at 37°C for 7 days. Spores scraped off with water were incubated for 7 days at 4°C. Cell fragments and spores were separated by centrifugation using a HistoDenz (Sigma-Aldrich) gradient (Dembek *et al.* 2013). Suspensions (>99% of spores) are free of vegetative cells, sporulating cells and cell debris as determined by phase-contrast microscopy. The spore suspension was quantified by measuring the OD_{600nm}.

Overnight cultures grown at 37°C in BHI were used to inoculate SM media at a dilution of

1:200. At specific time points, 1 mL of culture was withdrawn, serially diluted in BHI and plated before and after heat treatment (30 min, at 60°C), in order to determine the total and heat-resistant colony forming units (CFU). Samples were plated onto BHI supplemented with 0.1% TA (Sigma-Aldrich) to promote efficient spore germination (Wilson et al. 1982).

Germination assay

Approximately 10^8 spores (equivalent of 0.4 OD_{600nm} units) were resuspended in 200 µL of water. The spore suspension was heat-treated at 65°C during 10 min, and serial dilutions were plated on BHI containing 0.1% TA to determine the number of spores that are able to germinate. The CFU were monitored at 24 h and 48 h. At least three biological replicates were performed using at least two independent spore preparations.

The germination of the spores was also monitored by OD_{600nm} as previously described (Donnelly et al. 2016) and by phase-contrast microscopy as described previously (Kong et al. 2011). For optical measurement, spores resuspended in BHI were exposed to 1% TA, and the OD_{600nm} was measured every 5 min for 1 h. For the phase-contrast microscopy, purified spores were resuspended to an OD_{600nm} of 0.4 in BHI containing 1% TA and incubated under anaerobic conditions for 2 h at 37°C. At each time point, samples were pelleted by centrifugation, washed with PBS and fixed with 2% paraformaldehyde for 15 min at room temperature. Fixed samples were washed with PBS once more and dried onto glass slides. Phase-contrast microscopy was conducted using an Axioskop microscope (Zeiss) with a 100x oil immersion lens. The images were captured using an Axiocam 105 colour (Zeiss).

Ca-DPA release and SleC cleavage assays and lysozyme resistance tests

Measurement of the DPA release was performed as previously described (Francis et al. 2013a) from purified spores incubated at 37°C in PBS supplemented with 1% TA and 10 mM glycine for 1 h. Equal aliquots were incubated at 100°C as a measure of 100% DPA release (positive control) or incubated at 37°C in PBS without the germinants (negative control). SleC cleavage assay was performed as previously described (Kevorkian et al. 2016) from spores suspended for 20 min in BHI containing 1% TA. Lysozyme resistance of *C. difficile* spores was measured by suspending 10^8 spores in 200 µL of PBS in the presence or absence of 250 µg/mL of lysozyme. Spores were incubated for 1 h at 37°C with shaking (300 rpm), and the samples were visualized by phase-contrast microscopy and plated onto BHI agar containing 0.1% TA and incubated anaerobically for 24 h at 37°C.

Transmission electron microscopy

To analyse the ultrastructure by TEM, purified spores of the wild-type, *cotL* mutant and complemented strains were fixed with 2.5% of glutaraldehyde (Sigma Aldrich) in 0.1 M HEPES, pH 7.2. Post fixation was conducted with 1% osmium tetroxide (Merck) and 1.5% ferro-cyanide (Sigma Aldrich) in 0.1 M HEPES. After dehydration by a graded series of ethanol, spores were infiltrated with epoxy resin. Seventy-nanometer sections were collected on formvar coated slot grids (EMS) and were contrasted with 4% uranyl acetate and Reynolds lead citrate. The stained sections were observed using a Tecnai spirit FEI operated at 120 kV. The images were acquired using an FEI Eagle digital camera.

Coat extraction and Western blot analysis

To analyse the profile of the coat and exosporium proteins, *C. difficile* spores were resuspended in extraction buffer (0.125 mM Tris-HCl, 5% β -mercaptoethanol, 2% SDS, 0.5 mM dithiothreitol (DTT) and 5% glycerol, pH 6.8) containing 0.025% bromophenol blue and boiled as previously described (Costa et al. 2006). For coat and cortex fractionation, the spores were first resuspended in extraction buffer, boiled and centrifuged to recover the supernatant corresponding to the coat fraction (including the coat and exosporium layers). Pellets were treated with or without 2 mg/mL of lysozyme for 2 h at 37°C. For sporulating cells, whole cell lysates were prepared as described previously (Fagan and Fairweather 2011). Briefly, sporulating cultures of *C. difficile* were harvested by centrifugation at 5000 rpm for 10 min at 4°C, and the pellets were frozen at -20°C. The bacteria were thawed and resuspended in PBS containing 0.12 μ g/mL of DNase I to an OD_{600nm} of 40. An equal volume of 2X extraction buffer containing 0.025% bromophenol blue was added to the protein samples (Laemmli 1970), which were resolved by SDS-PAGE and visualized by Coomassie brilliant blue R-250 staining (Bio-Rad). Proteins were transferred to a PVDF membrane (0.45 μ m) and subjected to immunoblot analyses as described previously (Serrano et al. 1999). Mouse polyclonal antibody raised against CotL and rabbit polyclonal antibodies raised against CspC (1:2000), CspBA (1:2500), SleC (1:5000) (Adams et al. 2013), CdeM (1:40000) (A. O. Henriques), CdeC (1:1000), CotB (1:5000), CotE (1:1000), SipL (1:2500) (Putnam et al. 2013) and anti-SNAP (1:1000) (NEB) were used. Anti-rabbit or anti-mouse secondary antibodies conjugated to horseradish peroxidase (Sigma) were used at a 1:5000 dilution. Immunoblots were developed with enhanced chemiluminescence reagents (Thermo Scientific).

Antibody production

To construct *cotL* expression the plasmid, the coding sequencing of the *cotL* gene was PCR amplified using genomic DNA and primer pairs CF184/CF185 to produce a 500 bp PCR product. The DNA fragment was cloned between the *NdeI* and *XhoI* sites of pET20 to obtain pDIA6636 (Table S1). After verification by sequencing, the plasmid was introduced in *E. coli* BL21 (DE3) yielding ECO832 (Table S1). The anti-CotL antibody used in this study was raised in mice by Agro-Bio. CotL-His₆ was purified on Co²⁺ affinity resin from *E. coli* strain 832. Cultures were grown and protein expression was induced in Terrific broth (TB) medium (Thermo Scientific) for 16h at 37°C. *E. coli* cells were harvested, resuspended in lysis buffer buffer A (50 mM NaH₂PO₄, 300 mM NaCl, 10 mM imidazole) containing 1X Bug buster (Novagen), 40 µg/mL Dnase and 50 µg/mL lysozyme) and lysed at RT for 40 min. Cell extracts were centrifuged, the supernatant was passed through a 0.2 µm filter and used to affinity purify CotL-His₆. Elution was performed using buffer B (50 mM NaH₂PO₄, 300 mM NaCl, 300 mM imidazole).

Mass spectrometry of the spore coat and exosporium layers

C. difficile spores were resuspended in extraction buffer and boiled as previously described (Costa et al. 2006). Coat and exosporium proteins were recovered by centrifugation and precipitated with 10% TCA. For spore protein digestion, protein pellets were resuspended in urea 8 M and NH₄HCO₃ 100 mM and sonicated on ice. Subsequently, 50 µg of total proteins were reduced with TCEP 10 mM (646547 - Sigma) for 30 min and then alkylated with iodoacetamide 20 mM (I114 - Sigma) for 1 h. Proteins were digested with rLys-C 1 µg (V1671, Promega) for 4 h at 37°C and then digested with trypsin 1 µg (V5111, Promega) overnight at 37°C. The digestion was terminated with formic acid 4%, and the peptides were desalted using a C18 Sep-Pak Cartridge (WAT054955, Waters). The peptides were eluted successively with 50% Acetonitrile (ACN)/0.1% Formic acid (FA) and 80% ACN/0.1% FA before being dried in a vacuum centrifuge. The peptides were resuspended in 2% ACN /0.1% FA.

For LC-MS/MS analysis, a nanochromatographic system (Proxeon EASY-nLC 1000, Thermo Fisher Scientific) was coupled online to a Q ExactiveTM HF Mass Spectrometer (Thermo Fisher Scientific). For each sample, 1 µg of peptides was injected onto a 50-cm homemade C18 column (1.9 µm particles, 100 Å pore size, ReproSil-Pur Basic C18, Dr. Maisch GmbH) and separated with a multi-step gradient from 2 to 45% ACN in 105 min at a

flow rate of 250 nL/min over 132 min. The column temperature was set to 60°C. The data were acquired as previously described (Lago et al. 2017).

Raw data were analysed using MaxQuant software version 1.5.5.1 (Cox and Mann 2008) and the Andromeda search engine (Cox et al. 2011). The MS/MS spectra were searched against an internal *C. difficile* database containing 3 957 proteins, and the contaminant file included in MaxQuant. The database search parameters were fixed as described (Lago et al. 2017). For the quantification, skip normalization option was used. For the statistical analysis of one biological condition *versus* the other, it was used the same data analysis pipeline than in (Jeannin et al. 2018). Exceptionally, the proteins exhibiting lower than 2 LFQ value in both conditions were discarded from the list to avoid misidentified proteins (Jeannin et al. 2018). The mass spectrometry proteomics data have been deposited to the ProteomeXchange Consortium via the PRIDE partner repository with the dataset identifier PXD010359 (Vizcaino et al. 2016).

Acknowledgements

We thank Maryse Moya-Nilges for performing transmission electron microscopy, Jost Enniga and Giulia Manina for access to the fluorescence microscope, Adriano Henriques for providing the plasmids carrying the SNAP^{Cd} reporter gene and the antibody raised against CdeM, Aimee Shen for helpful discussion and providing the antibodies, Nigel Minton for the ClosTron system and Julian Garneau for the bioinformatics analysis. Research in this study for the CAF fellowship was funded by the Institut Pasteur and ITN Marie Curie, Clospore (H2020-MSCA-ITN-2014 642068).

References

- Abecasis, A.B., Serrano, M., Alves, R., Quintais, L., Pereira-Leal, J.B., and Henriques, A.O. (2013) A genomic signature and the identification of new sporulation genes. *J Bacteriol* **195**: 2101-2115.
- Abhyankar, W., Hossain, A.H., Djajasaputra, A., Permpoonpattana, P., Ter Beek, A., Dekker, H.L. et al. (2013) In pursuit of protein targets: proteomic characterization of bacterial spore outer layers. *J Proteome Res* **12**: 4507-4521.
- Adams, C.M., Eckenroth, B.E., Putnam, E.E., Doublet, S., and Shen, A. (2013) Structural and functional analysis of the CspB protease required for Clostridium spore germination. *PLoS Pathog* **9**: e1003165.
- Barra-Carrasco, J., Olguin-Araneda, V., Plaza-Garrido, A., Miranda-Cardenas, C., Cofre-Araneda, G., Pizarro-Guajardo, M. et al. (2013) The Clostridium difficile exosporium cysteine (CdeC)-rich protein is required for exosporium morphogenesis and coat assembly. *J Bacteriol* **195**: 3863-3875.
- Beall, B., Driks, A., Losick, R., and Moran, C.P., Jr. (1993) Cloning and characterization of a gene required for assembly of the Bacillus subtilis spore coat. *J Bacteriol* **175**: 1705-1716.
- Bhattacharjee, D., McAllister, K.N., and Sorg, J.A. (2016) Germinants and Their Receptors in Clostridia. *J Bacteriol* **198**: 2767-2775.
- Calderon-Romero, P., Castro-Cordova, P., Reyes-Ramirez, R., Milano-Cespedes, M., Guerrero-Araya, E., Pizarro-Guajardo, M. et al. (2018) Clostridium difficile exosporium cysteine-rich proteins are essential for the morphogenesis of the exosporium layer, spore resistance, and affect C. difficile pathogenesis. *PLoS Pathog* **14**: e1007199.
- Cassier, M., and Ryter, A. (1971) [A Clostridium perfringens mutant producing coatless spores by lysozyme-dependent germination]. *Ann Inst Pasteur (Paris)* **121**: 717-732.
- Cassona, C.P., Pereira, F., Serrano, M., and Henriques, A.O. (2016) A Fluorescent Reporter for Single Cell Analysis of Gene Expression in Clostridium difficile. *Methods Mol Biol* **1476**: 69-90.
- Costa, T., Isidro, A.L., Moran, C.P., Jr., and Henriques, A.O. (2006) Interaction between coat morphogenetic proteins SafA and SpoVID. *J Bacteriol* **188**: 7731-7741.
- Costa, T., Serrano, M., Steil, L., Volker, U., Moran, C.P., Jr., and Henriques, A.O. (2007) The timing of cotE expression affects Bacillus subtilis spore coat morphology but not lysozyme resistance. *J Bacteriol* **189**: 2401-2410.
- Cox, J., and Mann, M. (2008) MaxQuant enables high peptide identification rates, individualized p.p.b.-range mass accuracies and proteome-wide protein quantification. *Nat Biotechnol* **26**: 1367-1372.
- Cox, J., Neuhauser, N., Michalski, A., Scheltema, R.A., Olsen, J.V., and Mann, M. (2011) Andromeda: a peptide search engine integrated into the MaxQuant environment. *J Proteome Res* **10**: 1794-1805.
- de Francesco, M., Jacobs, J.Z., Nunes, F., Serrano, M., McKenney, P.T., Chua, M.H. et al. (2012) Physical interaction between coat morphogenetic proteins SpoVID and CotE is necessary for spore encasement in Bacillus subtilis. *J Bacteriol* **194**: 4941-4950.
- Deakin, L.J., Clare, S., Fagan, R.P., Dawson, L.F., Pickard, D.J., West, M.R. et al. (2012) The Clostridium difficile spo0A gene is a persistence and transmission factor. *Infect Immun* **80**: 2704-2711.
- Dembek, M., Stabler, R.A., Witney, A.A., Wren, B.W., and Fairweather, N.F. (2013) Transcriptional analysis of temporal gene expression in germinating Clostridium difficile 630 endospores. *PLoS One* **8**: e64011.
- Diaz-Gonzalez, F., Milano, M., Olguin-Araneda, V., Pizarro-Cerda, J., Castro-Cordova, P., Tzeng, S.C. et al. (2015) Protein composition of the outermost exosporium-like layer of Clostridium difficile 630 spores. *J Proteomics* **123**: 1-13.
- Donnelly, M.L., Fimlaid, K.A., and Shen, A. (2016) Characterization of Clostridium difficile Spores Lacking Either SpoVAC or Dipicolinic Acid Synthetase. *J Bacteriol* **198**: 1694-1707.
- Edwards, A.N., Karim, S.T., Pascual, R.A., Jowhar, L.M., Anderson, S.E., and McBride, S.M. (2016) Chemical and Stress Resistances of Clostridium difficile Spores and Vegetative Cells. *Front Microbiol* **7**: 1698.

- Escobar-Cortes, K., Barra-Carrasco, J., and Paredes-Sabja, D. (2013) Proteases and sonication specifically remove the exosporium layer of spores of *Clostridium difficile* strain 630. *J Microbiol Methods* **93**: 25-31.
- Fagan, R.P., and Fairweather, N.F. (2011) *Clostridium difficile* has two parallel and essential Sec secretion systems. *J Biol Chem* **286**: 27483-27493.
- Fimlaid, K.A., Bond, J.P., Schutz, K.C., Putnam, E.E., Leung, J.M., Lawley, T.D., and Shen, A. (2013) Global analysis of the sporulation pathway of *Clostridium difficile*. *PLoS Genet* **9**: e1003660.
- Francis, M.B., Allen, C.A., and Sorg, J.A. (2015) Spore Cortex Hydrolysis Precedes Dipicolinic Acid Release during *Clostridium difficile* Spore Germination. *J Bacteriol* **197**: 2276-2283.
- Francis, M.B., Allen, C.A., Shrestha, R., and Sorg, J.A. (2013) Bile acid recognition by the *Clostridium difficile* germinant receptor, CspC, is important for establishing infection. *PLoS Pathog* **9**: e1003356.
- Galperin, M.Y., Mekhedov, S.L., Puigbo, P., Smirnov, S., Wolf, Y.I., and Rigden, D.J. (2012) Genomic determinants of sporulation in Bacilli and Clostridia: towards the minimal set of sporulation-specific genes. *Environ Microbiol* **14**: 2870-2890.
- Heap, J.T., Pennington, O.J., Cartman, S.T., and Minton, N.P. (2009) A modular system for *Clostridium* shuttle plasmids. *J Microbiol Methods* **78**: 79-85.
- Heap, J.T., Pennington, O.J., Cartman, S.T., Carter, G.P., and Minton, N.P. (2007) The ClosTron: a universal gene knock-out system for the genus *Clostridium*. *J Microbiol Methods* **70**: 452-464.
- Henriques, A.O., and Moran, C.P., Jr. (2007) Structure, assembly, and function of the spore surface layers. *Annu Rev Microbiol* **61**: 555-588.
- Higgins, D., and Dworkin, J. (2012) Recent progress in *Bacillus subtilis* sporulation. *FEMS Microbiol Rev* **36**: 131-148.
- Hilbert, D.W., and Piggot, P.J. (2004) Compartmentalization of gene expression during *Bacillus subtilis* spore formation. *Microbiol Mol Biol Rev* **68**: 234-262.
- Janoir, C., Deneve, C., Bouttier, S., Barbut, F., Hoys, S., Caleechum, L. et al. (2013) Adaptive strategies and pathogenesis of *Clostridium difficile* from in vivo transcriptomics. *Infect Immun* **81**: 3757-3769.
- Jeannin, P., Chaze, T., Gai Gianetto, Q., Matondo, M., Gout, O., Gessain, A., and Afonso, P.V. (2018) Proteomic analysis of plasma extracellular vesicles reveals mitochondrial stress upon HTLV-1 infection. *Sci Rep* **8**: 5170.
- Kelly, C.P., and LaMont, J.T. (2008) *Clostridium difficile*--more difficult than ever. *N Engl J Med* **359**: 1932-1940.
- Kevorkian, Y., Shirley, D.J., and Shen, A. (2016) Regulation of *Clostridium difficile* spore germination by the CspA pseudoprotease domain. *Biochimie* **122**: 243-254.
- Kong, L., Zhang, P., Wang, G., Yu, J., Setlow, P., and Li, Y.Q. (2011) Characterization of bacterial spore germination using phase-contrast and fluorescence microscopy, Raman spectroscopy and optical tweezers. *Nat Protoc* **6**: 625-639.
- Laemmli, U.K. (1970) Cleavage of structural proteins during the assembly of the head of bacteriophage T4. *Nature* **227**: 680-685.
- Lago, M., Monteil, V., Douche, T., Guglielmini, J., Criscuolo, A., Maufrais, C. et al. (2017) Proteome remodelling by the stress sigma factor RpoS/sigma(S) in *Salmonella*: identification of small proteins and evidence for post-transcriptional regulation. *Sci Rep* **7**: 2127.
- Lawley, T.D., Croucher, N.J., Yu, L., Clare, S., Sebahia, M., Goulding, D. et al. (2009) Proteomic and genomic characterization of highly infectious *Clostridium difficile* 630 spores. *J Bacteriol* **191**: 5377-5386.
- Lawley, T.D., Clare, S., Deakin, L.J., Goulding, D., Yen, J.L., Raisen, C. et al. (2010) Use of purified *Clostridium difficile* spores to facilitate evaluation of health care disinfection regimens. *Appl Environ Microbiol* **76**: 6895-6900.
- Livak, K.J., and Schmittgen, T.D. (2001) Analysis of relative gene expression data using real-time quantitative PCR and the 2(-Delta Delta C(T)) Method. *Methods* **25**: 402-408.
- McKenney, P.T., and Eichenberger, P. (2012) Dynamics of spore coat morphogenesis in *Bacillus subtilis*. *Mol Microbiol* **83**: 245-260.
- McKenney, P.T., Driks, A., and Eichenberger, P. (2013) The *Bacillus subtilis* endospore: assembly and functions of the multilayered coat. *Nat Rev Microbiol* **11**: 33-44.

- Paredes-Sabja, D., Setlow, P., and Sarker, M.R. (2011) Germination of spores of Bacillales and Clostridiales species: mechanisms and proteins involved. *Trends Microbiol* **19**: 85-94.
- Paredes-Sabja, D., Shen, A., and Sorg, J.A. (2014) Clostridium difficile spore biology: sporulation, germination, and spore structural proteins. *Trends Microbiol* **22**: 406-416.
- Pereira, F.C., Saujet, L., Tome, A.R., Serrano, M., Monot, M., Couture-Tosi, E. et al. (2013) The spore differentiation pathway in the enteric pathogen Clostridium difficile. *PLoS Genet* **9**: e1003782.
- Permpoonpattana, P., Tolls, E.H., Nadem, R., Tan, S., Brisson, A., and Cutting, S.M. (2011) Surface layers of Clostridium difficile endospores. *J Bacteriol* **193**: 6461-6470.
- Permpoonpattana, P., Phetcharaburanin, J., Mikelson, A., Dembek, M., Tan, S., Brisson, M.C. et al. (2013) Functional characterization of Clostridium difficile spore coat proteins. *J Bacteriol* **195**: 1492-1503.
- Pishdadian, K., Fimlaid, K.A., and Shen, A. (2015) SpoIID-mediated regulation of sigmaK function during Clostridium difficile sporulation. *Mol Microbiol* **95**: 189-208.
- Pizarro-Guajardo, M., Olguin-Araneda, V., Barra-Carrasco, J., Brito-Silva, C., Sarker, M.R., and Paredes-Sabja, D. (2014) Characterization of the collagen-like exosporium protein, BclA1, of Clostridium difficile spores. *Anaerobe* **25**: 18-30.
- Putnam, E.E., Nock, A.M., Lawley, T.D., and Shen, A. (2013) SpoIVA and SipL are Clostridium difficile spore morphogenetic proteins. *J Bacteriol* **195**: 1214-1225.
- Ribis, J.W., Ravichandran, P., Putnam, E.E., Pishdadian, K., and Shen, A. (2017) The Conserved Spore Coat Protein SpoVM Is Largely Dispensable in Clostridium difficile Spore Formation. *mSphere* **2**.
- Rupnik, M., Wilcox, M.H., and Gerding, D.N. (2009) Clostridium difficile infection: new developments in epidemiology and pathogenesis. *Nat Rev Microbiol* **7**: 526-536.
- Saujet, L., Monot, M., Dupuy, B., Soutourina, O., and Martin-Verstraete, I. (2011) The key sigma factor of transition phase, SigH, controls sporulation, metabolism, and virulence factor expression in Clostridium difficile. *J Bacteriol* **193**: 3186-3196.
- Saujet, L., Pereira, F.C., Serrano, M., Soutourina, O., Monot, M., Shelyakin, P.V. et al. (2013) Genome-wide analysis of cell type-specific gene transcription during spore formation in Clostridium difficile. *PLoS Genet* **9**: e1003756.
- Serrano, M., Zilhao, R., Ricca, E., Ozin, A.J., Moran, C.P., Jr., and Henriques, A.O. (1999) A Bacillus subtilis secreted protein with a role in endospore coat assembly and function. *J Bacteriol* **181**: 3632-3643.
- Serrano, M., Kint, N., Pereira, F.C., Saujet, L., Boudry, P., Dupuy, B. et al. (2016) A Recombination Directionality Factor Controls the Cell Type-Specific Activation of sigmaK and the Fidelity of Spore Development in Clostridium difficile. *PLoS Genet* **12**: e1006312.
- Setlow, P. (2003) Spore germination. *Curr Opin Microbiol* **6**: 550-556.
- Sorg, J.A., and Sonenshein, A.L. (2008) Bile salts and glycine as cogermnants for Clostridium difficile spores. *J Bacteriol* **190**: 2505-2512.
- Soutourina, O.A., Monot, M., Boudry, P., Saujet, L., Pichon, C., Sismeiro, O. et al. (2013) Genome-wide identification of regulatory RNAs in the human pathogen Clostridium difficile. *PLoS Genet* **9**: e1003493.
- Takamatsu, H., Kodama, T., Nakayama, T., and Watabe, K. (1999) Characterization of the yrbA gene of Bacillus subtilis, involved in resistance and germination of spores. *J Bacteriol* **181**: 4986-4994.
- Vizcaino, J.A., Csordas, A., Del-Toro, N., Dianes, J.A., Griss, J., Lavidas, I. et al. (2016) 2016 update of the PRIDE database and its related tools. *Nucleic Acids Res* **44**: 11033.
- Wang, K.H., Isidro, A.L., Domingues, L., Eskandarian, H.A., McKenney, P.T., Drew, K. et al. (2009) The coat morphogenetic protein SpoVID is necessary for spore encasement in Bacillus subtilis. *Mol Microbiol* **74**: 634-649.
- Wiegand, P.N., Nathwani, D., Wilcox, M.H., Stephens, J., Shelbaya, A., and Haider, S. (2012) Clinical and economic burden of Clostridium difficile infection in Europe: a systematic review of healthcare-facility-acquired infection. *J Hosp Infect* **81**: 1-14.
- Wilson, K.H., Kennedy, M.J., and Fekety, F.R. (1982) Use of sodium taurocholate to enhance spore recovery on a medium selective for Clostridium difficile. *J Clin Microbiol* **15**: 443-446.
- Zheng, L.B., and Losick, R. (1990) Cascade regulation of spore coat gene expression in Bacillus subtilis. *J Mol Biol* **212**: 645-660.

Zheng, L.B., Donovan, W.P., Fitz-James, P.C., and Losick, R. (1988) Gene encoding a morphogenic protein required in the assembly of the outer coat of the *Bacillus subtilis* endospore. *Genes Dev* **2**: 1047-1054.

Table 1: Determination of the interaction of CotL with other different spore coat proteins using bacterial adenylate cyclase two hybrid (BACTH).

CotL + SipL		pUT18C		pUT18		
		CotL	SipL	CotL	SipL	-
pKT25	CotL		1136±758		960±788	
	SipL	742±425		1526±475		
pKNT25	CotL		767±394		212±78	
	SipL	134±17		134±14		
	-					110±23

CotL + CotB		pUT18C		pUT18		
		CotL	CotB	CotL	CotB	-
pKT25	CotL		127±3		139±14	
	CotB	120±8		127±7		
pKNT25	CotL		151±7		947±428	
	CotB	129±3		134±19		
	-					93±45

CotL + CotA		pUT18C		pUT18		
		CotL	CotA	CotL	CotA	-
pKT25	CotL		164±48		114±34	
	CotA	88±31		113±61		
pKNT25	CotL		76±28		140±10	
	CotA	ND		ND		
	-					124±6

CotL + CotE		pUT18C		pUT18		
		CotL	CotE	CotL	CotE	-
pKT25	CotL		112±86		69±32	
	CotE	125±14		53±5		
pKNT25	CotL		161±151		324±153	
	CotE	143±16		128±27		
	-					106±42

CotL + CdeC		pUT18C		pUT18		
		CotL	CdeC	CotL	CdeC	-
pKT25	CotL		128±17		134±13	
	CdeC	71±18		135±21		
pKNT25	CotL		172±28		144±17	
	CdeC	144±25		138±18		
	-					110±23

CotL + CotL		pUT18C	pUT18	
		CotL	CotL	-
pKT25	CotL	101±52	107±44	
pKNT25	CotL	98±45	211±11	
	-			126±3

Values shown are the average β -galactosidase activities (in Miller unit) of the indicated pair-wise fusions. Each value corresponds to the mean and the standard deviation of 4 or 5 independent experiments from double transformants. Positive interactions are indicated in orange.

II. Complementary results on Spore coat morphogenesis

II.1. Investigation of potential CotL partners

Our study revealed that CotL is an important morphogenetic factor of the *C. difficile* spore. In fact, CotL is located in the spore surface layers coat/exosporium and is required for the proper localization of several coat proteins around the FS during spore development. We showed that CotL is not apparently involved in the regulation of genes encoding coat proteins, since a *cotL* mutant is able to produce wild-type levels of any of the coat proteins tested. Altogether, our results showed that CotL protein is crucial for the assembly of the spore coat, playing a morphogenetic rather than a regulatory role in the spore formation.

Spore coat morphogenetic proteins of *B. subtilis* are typically known to interact with and recruit other coat components (Henriques and Moran 2007, McKenney et al. 2013). SpoIVA localization to the spore occurs through a direct interaction with SpoVM (Price and Losick 1999). Moreover, SpoIVA interacts with SpoVID, and a physical association between this last protein and the morphogenetic proteins of the inner and outer coat layers, SafA and CotE, also occurs (Ramamurthi et al. 2006, Mullerova et al. 2009).

The requirement of *C. difficile* CotL for proper localization of several coat proteins at the spore surface suggests that this protein might interact and recruit these coat components. In *C. difficile*, SpoIVA was recently shown to interact with SpoVM (Ribis et al. 2017) and SipL (Putnam et al. 2013). However, the lack of *B. subtilis* SafA and CotE homologs in *C. difficile* suggests that different factors are involved in the morphogenesis of the coat layer in this pathogen. Present in the coat layer and required for the assembly of proteins around the FS surface, CotL might play the role of morphogenetic proteins similar to *B. subtilis* SafA and CotE and to analyse it, we decided to search for potential CotL partners.

II.1.a. Identification of proteins interacting with CotL by BACTH

The inactivation of *cotL* leads to an almost uncoated spore and SpoIVA and SipL are the first proteins starting the assembly of the coat layer. Therefore, we decided to test first whether CotL could interact with these two proteins. Then, we investigated possible interactions between CotL and other coat components such as CotB and CotA, whose expression is controlled by σ^E and σ^K , respectively and present mainly in the coat layer; CotE, controlled by σ^K , which is an enzymatic component of the spore exosporium; and lastly

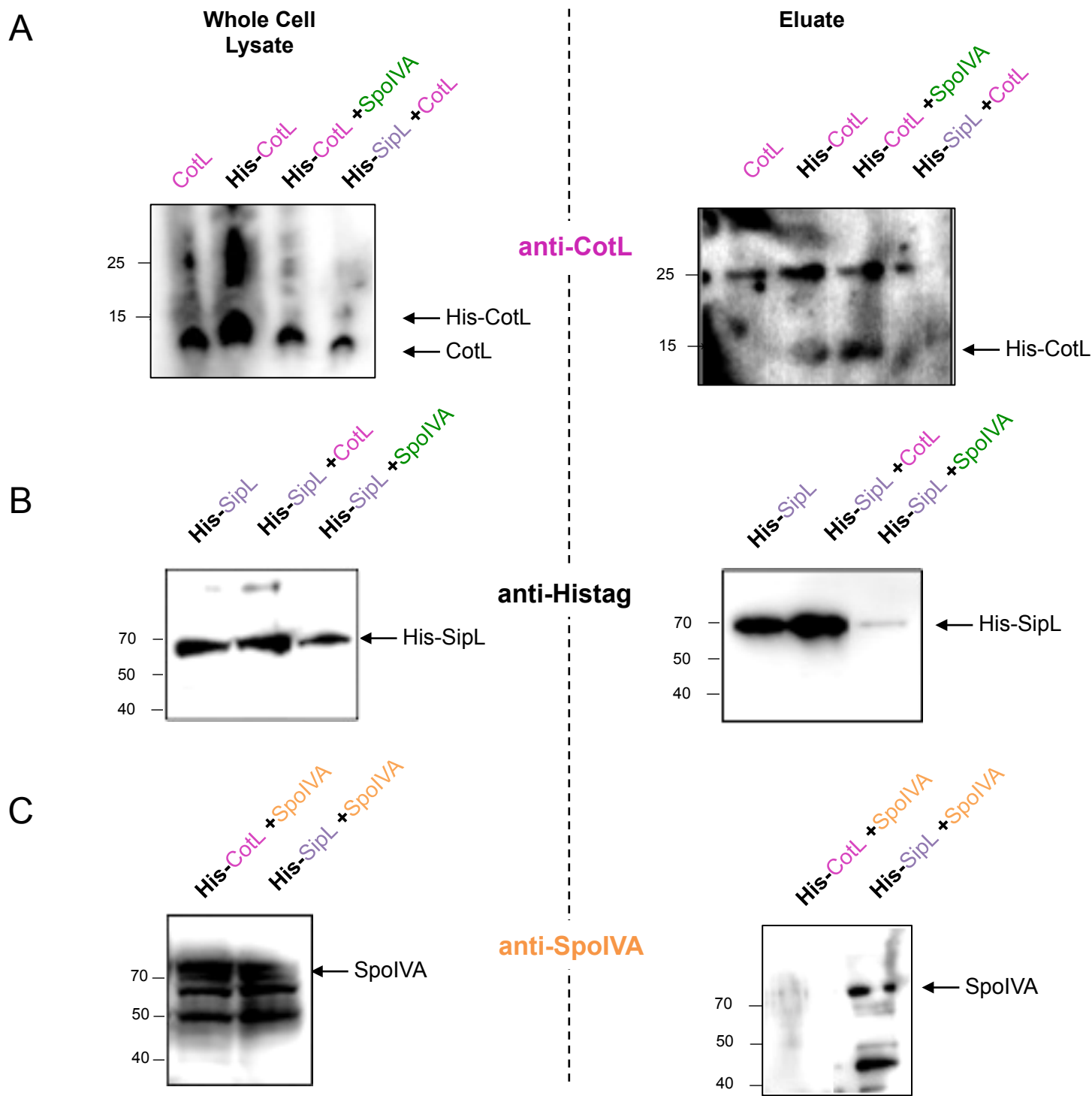


Figure 32: CotL-SipL and CotL-SpoIVA pull down assays. Whole cell lysate and eluated fractions were tested by Western blotting using anti-CotL (A), anti-Histag (to detect SipL) (B) or anti-SpoIVA (C) antibodies. The indicated proteins were produced in *E. coli* upon induction with IPTG. Aliquots were removed, pelleted, and lysed to generate the whole-cell lysate sample. The lysate was applied into a Co^{2+} affinity resin, eluted from the resin, and resolved on a 12% SDS-PAGE gel.

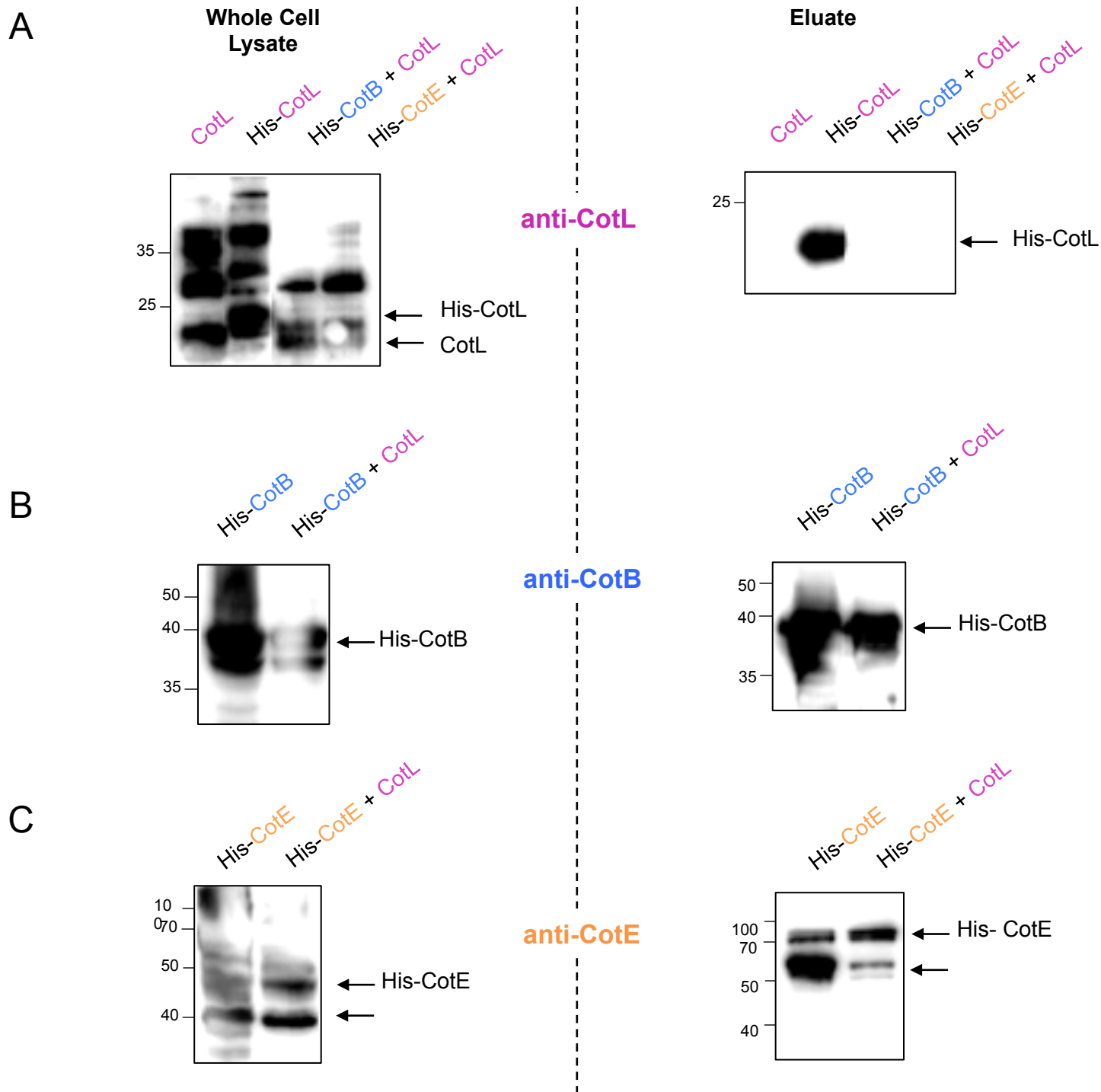


Figure 33: CotL-CotB and CotL-CotE pull down assays. Whole cell lysate and eluated fractions were tested by Western blotting using anti-CotL (**A**), anti-CotB (**B**) or anti-CotE (**C**) antibodies. The indicated proteins were produced in *E. coli* upon induction with IPTG. Aliquots were removed, pelleted, and lysed to generate the whole-cell lysate sample. The lysate was applied into a Co^{2+} affinity resin, eluted from the resin, and resolved on a 12% SDS-PAGE gel.

CdeC, a member of the σ^K regulon required as a morphogenetic protein of the exosporium. We investigated possible interactions between CotL and these *C. difficile* spore proteins by using a bacterial two hybrid system (BACTH). This system is based on the reconstitution of an adenylate-cyclase from the N-terminal (T25 fragment) and C-terminal (T18 fragment) parts when the two proteins fused to these parts interact to each other (Karimova et al. 1998). The production of cAMP by the reconstituted enzyme leads to the expression of *lacZ* allowing detection of the interaction. CotL, SipL, CotB, CotA, CotE and CdeC were fused to T18 and T25 both in N- and C-terminal positions. Unfortunately, we were unable to construct the plasmids to test the interaction between CotL and SpoIVA proteins. The interaction of fusion partners was investigated by testing β -galactosidase activity. Negative control experiments were carried out using the empty plasmids pKNT25 and pUT18 (Table 1). According to the quantification of the different combinations tested, β -galactosidase activity resulting from an interaction between CotL and SipL was detected in five different combinations out of eight (Table 1). A possible interaction between CotL and CotB, and between CotL and CotE has been detected only in one combination, and in both of them, the C-terminal part of CotL is fused to the T25 part. No β -galactosidase activity was detected in any combination of the CotL-CotA and CotL-CdeC. A CotL self-interaction was also investigated but no β -galactosidase activity was detected. These results suggest that CotL might interact with SipL and CotB and CotE might be possible partners of this protein to a lesser extent. Finally, no interaction was observed within CotL and between CotL and CotA or CdeC.

II.1.b. Coexpression of spore coat proteins and pull down assay in *E. coli*

In order to confirm the positive interactions obtained using the BACTH system, we decided to use another biochemical assay. We used for this task the pETDuet system that allow to coexpress genes encoding two proteins, that make possible interaction inside the cells and consequently purification of the protein complex. In this case, one protein carries the polyhistidine-tag and could be purified by affinity on a Cobalt (Co^{2+}) column and the second is produced as a native protein and can be pulled down. We used this assay to search for interactions between CotL and SipL, CotB or CotE. We also analysed a possible interaction between CotL and SpoIVA. As positive control, we coexpressed *spoIVA* and *sipL* since these proteins have been previously shown to interact (Putnam et al. 2013). Immunoblot analysis of *E. coli* whole cells lysates using antibodies raised against the His-tag or specific coat protein confirmed that all proteins were produced in *E. coli* (Figure 32 and 33). To identify potential

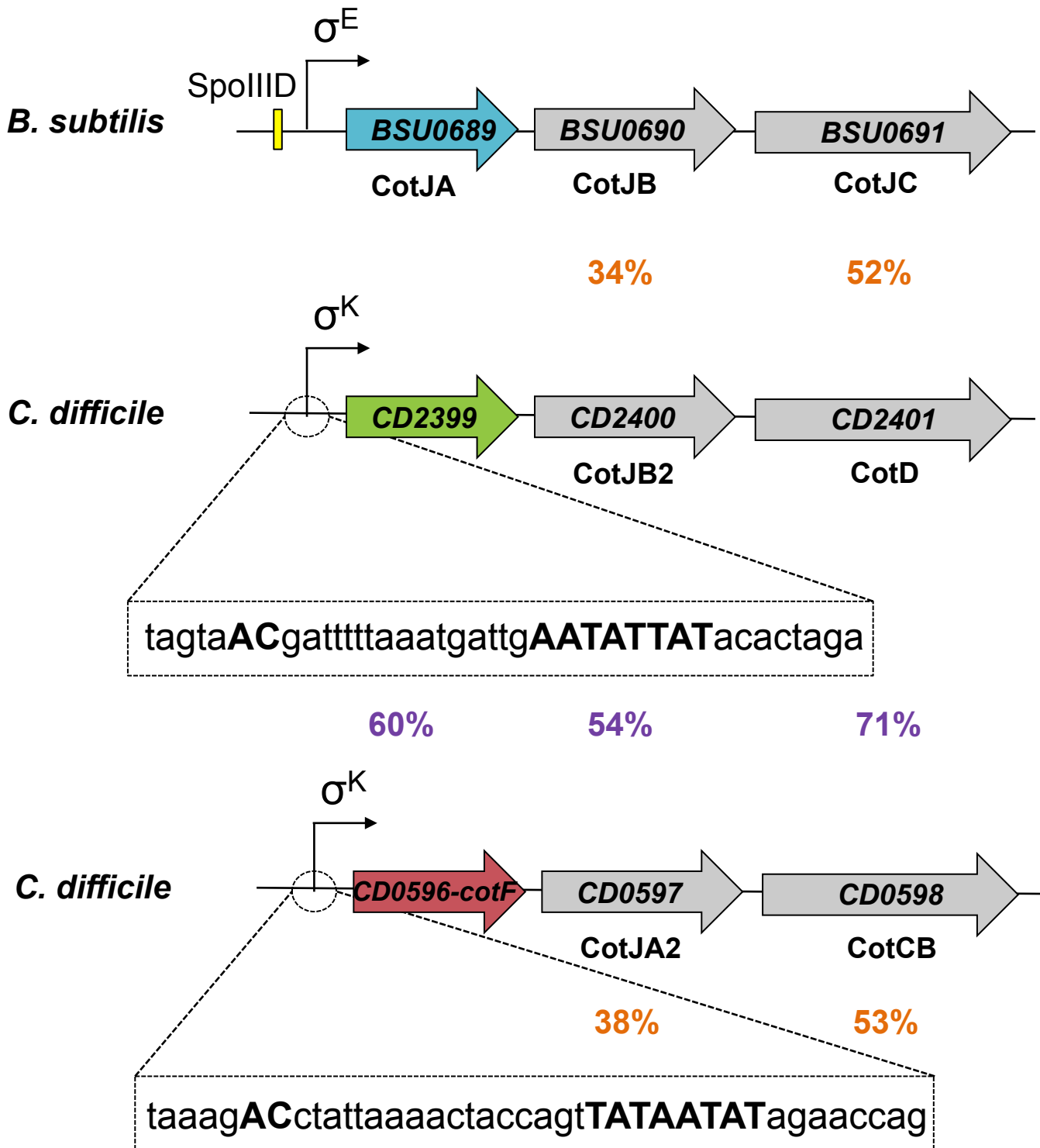


Figure 34: Organization of the *cotJ* operons in *B. subtilis* and *C. difficile*. Open reading frames (arrows) and transcriptional start sites with promoters recognized by the sigma factors are indicated. The SpolIID binding box in *B. subtilis* promoter is indicated in yellow. The percentage of amino acid identity between *B. subtilis* and *C. difficile* proteins is indicated in orange. In purple, is indicated the percentage of amino acid identity between *C. difficile* proteins from the two *cotJ* operons. σ^K consensus elements were found upstream of CD2399 and CD0596. The positions of the -10 and -35 boxes are indicated in bold.

interactions, the proteins after purification on Co²⁺ Sepharose were analyzed by Western blotting (Figure 32 and 33). While native CotL was detected in crude extracts from *E. coli*, this protein was not detected in the elution fraction when produced without His-tag (Figure 32A and 33A). By contrast, His-tagged CotL proteins were always detected in the elution fractions, showing a specific binding onto the affinity column. The obtained results showed that, in our conditions, SpoIVA was pulled down with His-tagged SipL after coexpression of both genes in *E. coli* (Figure 32C). However, CotL was not pulled down when co-produced with His-SipL (Figure 32A and B), His-CotB (Figure 33A and B) or His-CotE (Figure 33A and C). In addition, SpoIVA was not pulled down with His-CotL (Figure 32A and C). Thus, even if a positive interaction was detected by BACTH assay, we were not able to confirm this result using pull down assays.

II.2. The CD2399 gene

II.2.a. CD2399 and CD0596 are σ^K -controlled genes

The expression of most of the genes encoding proteins required for coat synthesis and assembly in *C. difficile* are transcribed by σ^E and σ^K and regulated by the DNA binding protein SpoIIID (Fimlaid et al. 2013, Saujet et al. 2013). In order to identify additional genes whose products might play a role in spore coat, we selected another gene, *CD2399*, which belongs to the σ^K regulon (Saujet et al. 2013). *CD2399* is conserved in several *C. difficile* strains (CD630, CDR20291 and CD0196) and is only present in members of the *Peptostreptococcaceae* family such as *Paraclostridium bifermentans* and *Intestinibacter bartletti*. *CD2399* (69 aa) is a paralogue of *CD0596* (renamed as CotF; 73 aa) sharing 60% identity (Figure 34). Both proteins contain a CotJA superfamily domain of spore proteins suggesting that they could function as *B. subtilis* CotJA (Henriques et al. 1995, Seyler et al. 1997). Both *CD2399* and *CD0596* proteins were detected in the proteome of *C. difficile* spore and particularly in the spore coat/exosporium extracts (Lawley et al. 2009a, Abhyankar et al. 2013). In *B. subtilis*, *cotJA* is the first gene of a tricistronic operon *cotJA-cotJB-cotJC* encoding spore coat proteins (Figure 34). This operon is transcribed by σ^E and contains a SpoIIID binding box. The two genes downstream of the *C. difficile* *CD2399* gene, *CD2400* and *CD2401*, encode spore coat proteins and share 34% and 52% identity to CotJB and CotJC of *B. subtilis*, respectively. *CD2400* is an 11 kDa protein named CotJB2, and *CD2401-CotD* is a manganese catalase (Figure 34). Downstream of *CD0596* gene, the two genes *CD0597* and *CD0598* also encode spore coat proteins named CotJA2 and CotCB and they share 38%

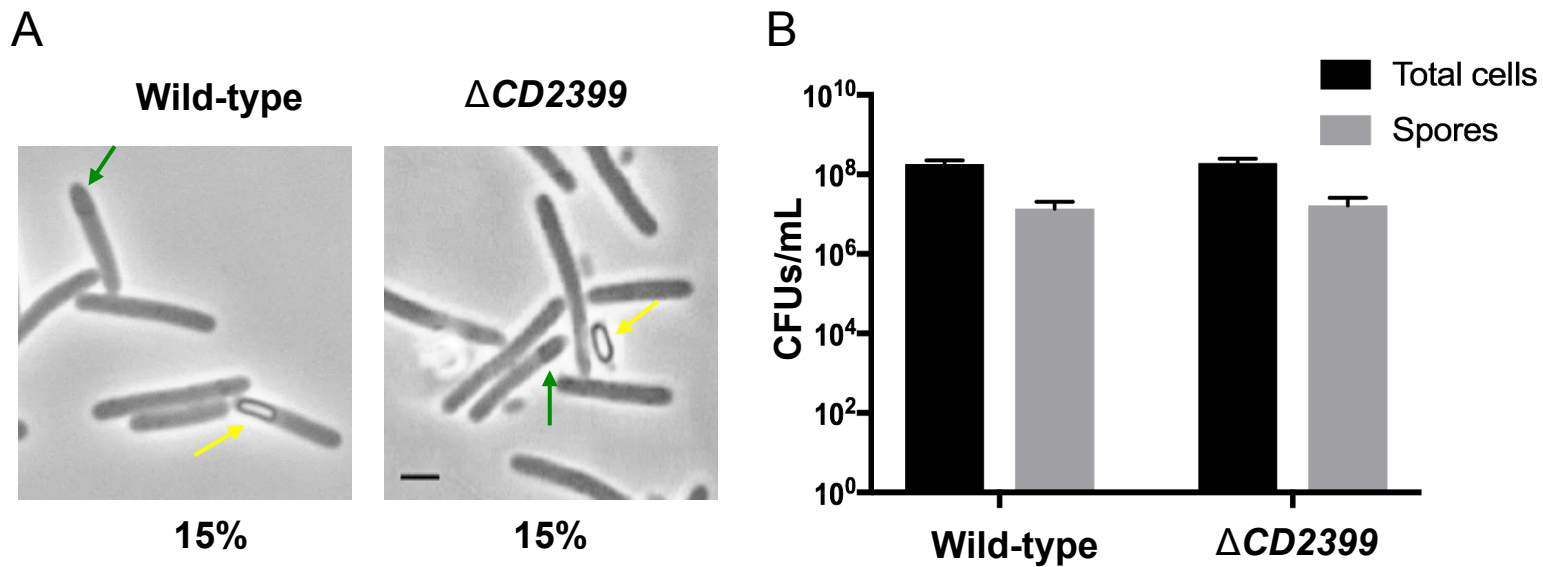


Figure 35: The $CD2399$ mutant is able to sporulate. **A)** Phase-contrast microscopy of sporulating cells of the wild-type and the $CD2399$ mutant strains after 24 h of growth in liquid SM. Yellow arrows mark mature phase-bright spores and red arrows indicate immature, phase-dark forespores. The numbers represent the percentage of sporulating cells. Scale bar, 2 μ m. **B)** Counts (CFUs/mL) of total cells (black) and heat-resistant spores (grey) for the wild-type and the $CD2399$ mutant grown for 24 h in SM and plated on BHI with 0.1% TA. Data represent the average of four biological replicates.

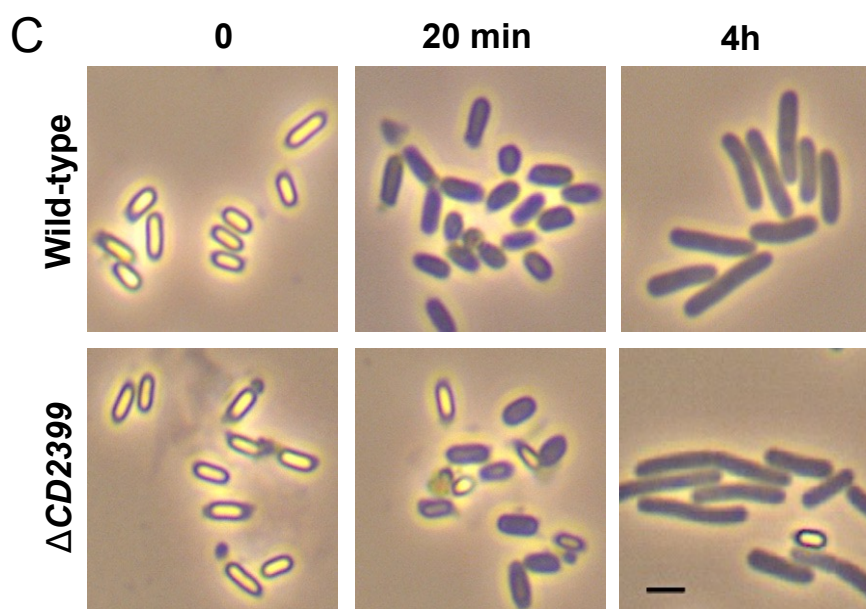
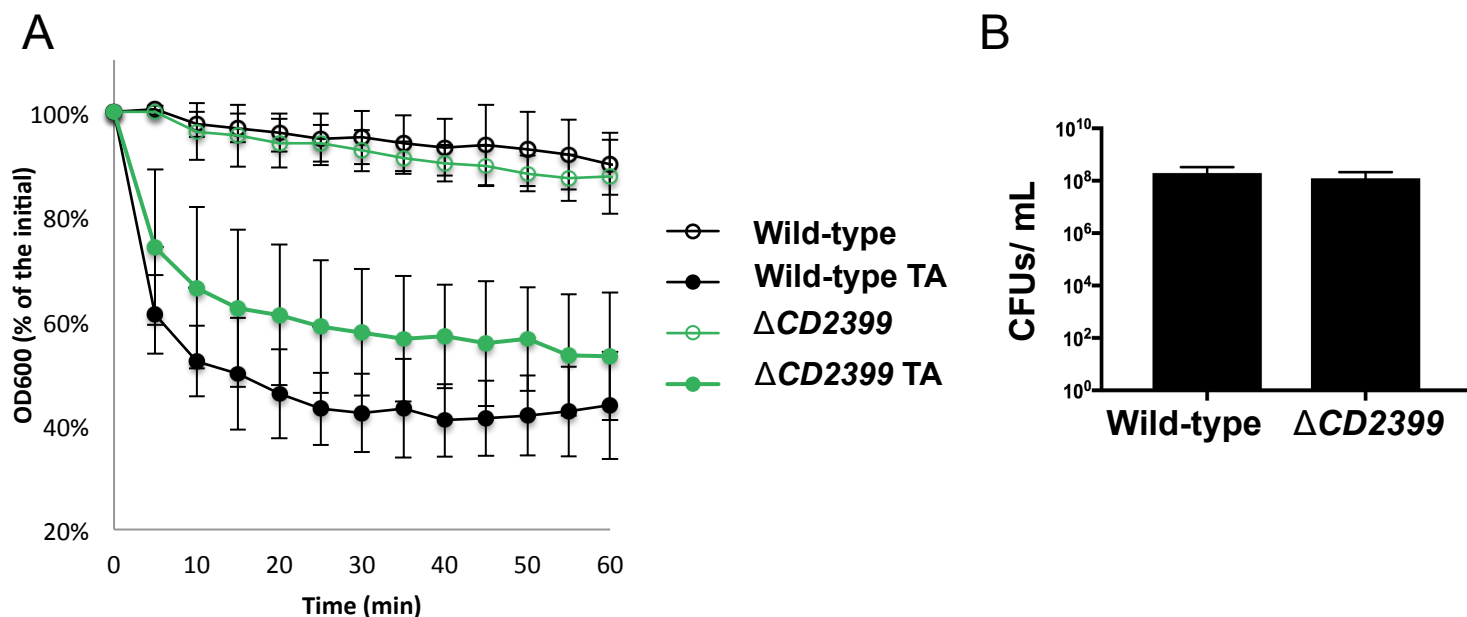


Figure 36: $CD2399$ mutant spores have a germination delay. **A)** Change in the OD_{600nm} of the spores of the wild-type and $CD2399$ mutant strains after the addition of 1% TA. OD_{600nm} measurements were taken every 5 min. **B)** CFUs/mL obtained after plating the purified spores on BHI with 0.1% TA. Data represent the average of four biological replicates. **C)** Kinetics of germination. Purified spores incubated in BHI in the presence of 1% TA were fixed in formaldehyde and visualized using phase-contrast microscopy. Scale bar, 2 μ m.

and 53% identity to CotJB and CotJC of *B. subtilis*, respectively. CD0597 protein is removed from the spore surface by sonication and the inactivation of its encoding gene does not affect the ultrastructure of the spore suggesting that this spore protein is located in the exosporium layer (Permpoonpattana et al. 2013, Diaz-Gonzalez et al. 2015). We noted that CotCB (CD2400) and CotD (CD0598) share 71% of identity.

Previous transcriptome studies showed that the expression of *CD2399*, *cotJB2* and *cotD* in one hand and *CD0596*, *cotJB1* and *cotCB* in other hand is 100- and 50-fold down-regulated in a *sigK* mutant compared to the wild-type strain, respectively (Saujet et al. 2013). These results combined with the presence of a sequence similar to σ^K consensus elements upstream of the transcriptional start site of both *CD2399* and *CD0596* genes strongly suggest that their expression is controlled by σ^K (Figure 34) (Saujet et al. 2013). Since no promoter was identified upstream of *cotJB2-cotD* genes and of *cotJB1-cotCB*, *CD2399-coJB2-cotD* and *CD0596-coJB1-cotCB* might form two tricistronic operons.

II.2.b. CD2399 is not required for sporulation

In order to test the role of CD2399 in the spore formation, the encoding gene *CD2399* was inactivated using the allele couple exchange (ACE) mutagenesis system (Cartman et al. 2012). When we analyzed the morphology of the strain by phase contrast microscopy after 24 h of growth in sporulation medium (SM), we observed a similar percentage of sporulating cells between the *CD2399* mutant and wild-type strains (Figure 35A). The efficiency of heat-resistant spore formation was also tested and the wild-type and the *CD2399* mutant produced 1.37×10^7 and 1.67×10^7 heat-resistant spores/ml, respectively (Figure 35B). These data suggest that the *CD2399* mutant sporulates similarly than the wild-type strain.

II.2.c. CD2399 mutant spores have a germination delay

We also evaluated whether inactivation of *CD2399* affected spore germination. We monitored the decrease in the OD_{600nm} of the wild-type and mutant spore suspensions after the addition of 1% taurocholate (TA). After 5 min in the presence of TA, we observed a decrease of 40% in the OD_{600nm} of the wild-type spores, while the decrease is of 25% for the *CD2399* mutant suggesting a delay in the germination rate (Figure 36A). However, the colony formation efficiency of *CD2399* mutant spores in BHI agar plates with TA was similar to that of the wild-type strain (Figure 36B). We further monitored the germination process using phase contrast microscopy. In the wild-type strain, only phase dark spores were observed after

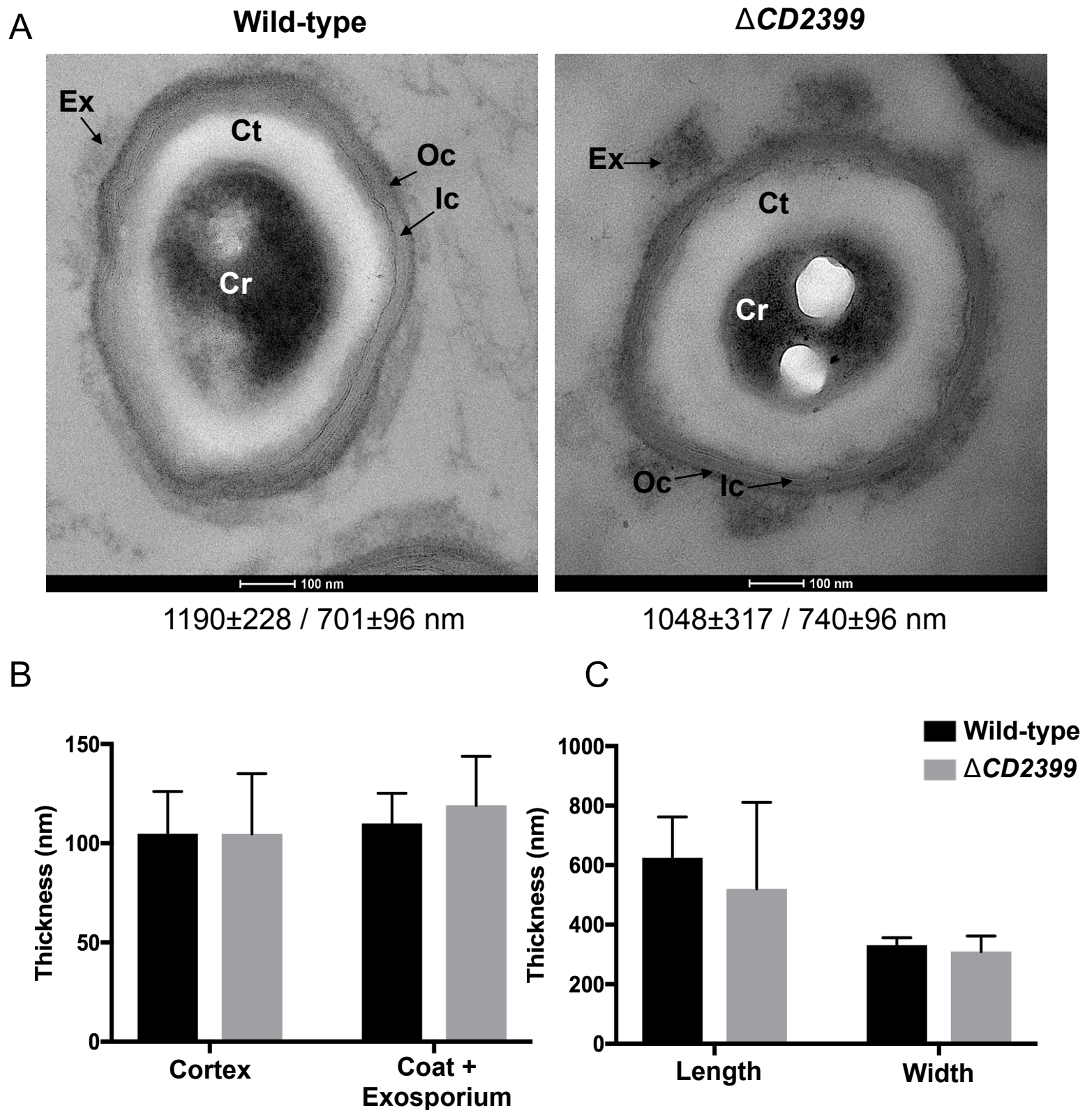


Figure 37: Morphology of the spores of the wild-type strain and the CD2399 mutant. A) Thin sections of the spores were analysed using TEM as described in the Materials and Methods. Ex, exosporium, Oc, outer coat, Ic, inner coat, Ct, cortex, Cr, core. Scale bars are shown in each figure. The numbers on the bottom of each figure represent the spore dimensions for each strain (length and width) based on the analysis of at least 8 individual spores. **B)** The thickness of the cortex layer and the exosporium plus the outer/inner coat layers of the spores from the two strains were measured. Error bars denote standard errors of the means of at least 8 individual spores. **C)** Size of the spore core of the wild-type and the CD2399 mutant. The length and width of the core was measured. Error bars denote the standard errors of the means of at least 8 individual spores.

20 min in the presence of the germinant. However, in the same conditions, only 75% of the *CD2399* mutant spores were converted into phase dark spores (Figure 36C). Moreover, four hours after germination induction, outgrowth was observed in both strains but few phase bright spores were still detected in the *CD2399* mutant. Altogether these results suggest that part of the *CD2399* mutant spores have a germination delay, whereas they are able to germinate since no differences are observed when the same amount of wild-type and *CD2399* mutant spores are plated in BHI supplemented with TA.

II.2.d. The inactivation of *CD2399* does not affect the ultrastructure and resistance of the spore

Because σ^K plays an important role in the assembly of the spore coat and *CD2399* gene is a member of the σ^K regulon, we compared the ultrastructure and the polypeptide composition of the spore surface layers of the wild-type and the *CD2399* mutant. Spores from the wild-type and *CD2399* mutant were first purified and analysed by transmission electron microscopy (TEM). TEM analysis showed that *CD2399* mutant spores have the same size and a structure similar to the wild-type; moreover no obvious differences were observed in the spore coat layers, in the cortex and in the core (Figure 37). Spore surface proteins were then extracted and we found no significant difference of the protein profiles between the *CD2399* mutant and the wild-type (Figure 38A). We further analyzed by Western blot the amount of some spore coat and exosporium proteins, such as the cortex hydrolase SleC, the peroxiredoxin-chitinase CotE and the exosporium morphogenetic protein CdeM, and we observed a slight decrease of the level of these proteins in the $\Delta CD2399$ mutant when compared to the wild-type strain (Figure 38B). Altogether, these observations suggest that the deletion of *CD2399* does not affect the assembly of the spore surface layers, even if the amount of the tested coat/exosporium proteins slightly decreased in the mutant. When we tested the resistance of the wild-type and the *CD2399* mutant spores to lysozyme, ethanol and to a higher temperature (80 °C), we observed that *CD2399* mutant spores are as resistant as the wild-type spores to these conditions tested (Figure 39).

Evidences suggest that all products of the operon to which *CD2399* belongs are components of the *C. difficile* spore coat. In fact in *B. subtilis*, the members of the similar *cotJ* operon (*cotJA* and *cotJC*) encode spore coat proteins located at the undercoat/basement layer. However the exact localization of *CD2399* in the coat layers of *C. difficile* is not yet clear. Moreover the differences in the genetic control of the two operons, i.e., controlled by σ^E and

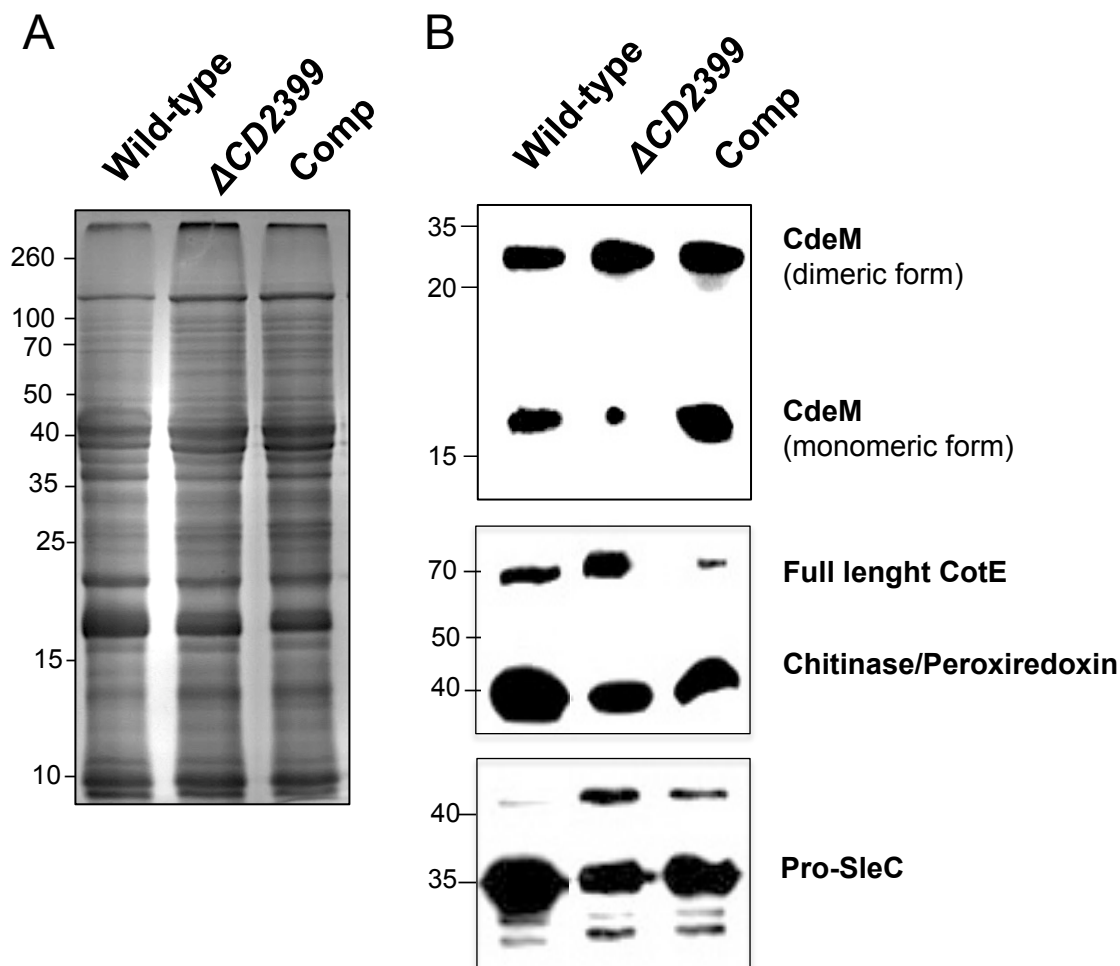


Figure 38: Protein profile of *C. difficile* spore coat/exosporium in the absence of CD2399. **A)** Coat/exosporium extracts from purified spores of the wild-type, the *CD2399* mutant and the complemented strains were loaded on acrylamide gel and stained with Coomassie brilliant blue. **B)** Western blot using antibodies raised against CdeM, CotE or SleC. Experiments were repeated at least two times with independent samples.

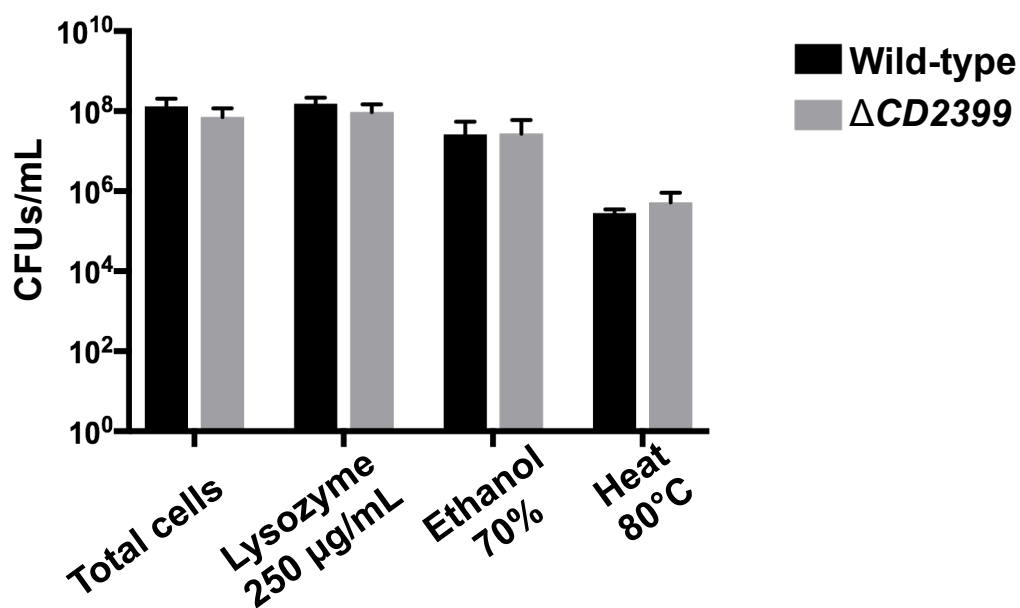


Figure 39: Sensitivity of the wild-type and the *CD2399* mutant spores to lysozyme, ethanol and heat. CFU/mL obtained of the wild-type and *CD2399* mutant spores after plating onto BHI agar containing 0.1% TA. Data represent the average of the results of three independent experiments, and the error bars represent standard errors of the means.

SpoIIID in *B. subtilis* and likely controlled by σ^K in *C. difficile* suggest an earlier production of the *B. subtilis* CotJ proteins. Consequently, *B. subtilis* CotJ-encoded products may be involved in earlier stages of coat assembly. Our initial data indicated that CD2399 is not required for spore formation. The CD2399 mutant spores are structurally similar and present the same resistance properties to lysozyme, heat and ethanol than that of the wild-type strain. The only differences observed in the CD2399 mutant when compared to the wild-type strain, concerned both the small delay in germination and the slight decrease in the level of some coat proteins. In *B. subtilis*, the inactivation of any of the members from *cotJ* operon results in the formation of spores with a normal morphology and no detectable resistance deficiency (Henriques et al. 1995, Seyler et al. 1997). However, in *B. subtilis*, CotJA and CotJC proteins are not detected in the coat of the *cotJC* and the *cotJA* mutants respectively, suggesting that CotJA might interact with CotJC for their assembly into the spore coat (Seyler et al. 1997). In fact, an interaction between CotJA and CotJC has been observed (Seyler et al. 1997). It has been also noted that CotJC from *B. subtilis* carries a motif found in manganese catalases but enzymatic activity has never been demonstrated for this protein. The analysis of the localization of the *C. difficile* CotD protein similar to CotJC in the CD2399 mutant cells, and its assembly at the spore surface might be an interesting point to address in future work.

So far, the role of CD2399 on the spore coat of *C. difficile* is not yet clear. Nonetheless, the presence of the paralogue CD0596 in the spore coat might suggest functional redundancy. Inactivation of the CD0596 gene in a CD2399 mutant background might bring new insights about the role of these two proteins in the assembly of the spore coat of *C. difficile*.

O₂ tolerance and ROS protection in *C. difficile*

After spore germination, *C. difficile* vegetative cells multiply and colonize the intestine. Then, the cells produce virulence factors including the two toxins, TcdA and TcdB, which cause the pathology associated with CDI. These toxins are responsible for alterations in the actin cytoskeleton of the intestinal epithelial cells, inducing intestinal-cell lysis and triggering an important inflammation (Abt et al. 2016a, Janoir 2016). The inflammation process results in the production of ROS, NO and RNS at bactericidal concentrations by the host immune system (Britton and Young 2014, Theriot and Young 2015). Apart from the oxidative stress, O₂ is also an important stress that *C. difficile* might face during gut colonization. Indeed, although a healthy gastrointestinal tract with a diverse microbiota is regarded as mainly anoxic, an increasing O₂ gradient from the lumen of the colon toward the intestinal epithelium is present (Marteyn et al. 2011, Kelly et al. 2015a). Additionally, antibiotic-induced disruption of the host microbiota leads to an increase in O₂ within the gut (Kelly et al. 2015a, Rivera-Chavez et al. 2016). Thus, O₂ concentration fluctuations in the gastrointestinal tract presents a challenge to anaerobic bacteria such as *C. difficile* (Marteyn et al. 2011). Recently it was demonstrated that *C. difficile* is capable of growth in non-strict anaerobic conditions (1-3% O₂) (Kint et al. 2017, Giordano et al. 2018a) indicating this bacterium encodes an arsenal of proteins involved in O₂ detoxification and protection.

However, we still know little about the proteins involved in the ability of *C. difficile* to tolerate O₂. In other organisms, both flavodiiron proteins (FDPs) and rubrerythrines (Rbrs) have been shown to play an important role protecting the cells from O₂, oxidative or nitrosative stress, suggesting that those proteins might play a role in these responses in *C. difficile* (Sztukowska et al. 2002, Wildschut et al. 2006, Hillmann et al. 2009b, Riebe et al. 2009). FDPs are enzymes composed of a minimal core containing both a non-heme diiron catalytic center and a flavodoxin FMN-containing domain located at the N-terminal and C-terminal part of the protein, respectively (Romao et al. 2016, Folgosa et al. 2018a). These enzymes have substrate-specificity to O₂ or NO but some FDPs have dual activity. Two genes encoding FDPs, *CD1623* and *CD1157*, are present in *C. difficile*. On the other hand, Rbrs are composed by two types or iron sites: a N-terminal non-sulfur diiron center and a rubredoxin-like [Fe(SCys)₄] domain in the C-terminal part (deMare et al. 1996, Kurtz 2006). Reverse Rbrs (revRbrs) are enzymes in which the position of the diiron site and the rubredoxin domains are reversed. The genome of *C. difficile* encodes two revRbrs, *CD1474* and *CD1524*.

The main activity for Rbrs and revRbrs is as peroxidase, linked to NAD(P)H oxidation, but O₂-reductase activity has been also reported (Coulter et al. 1999, Weinberg et al. 2004, Kurtz 2006). To shuttle electrons, both FDPs and revRbrs require other proteins like a rubredoxin (Rd) and NADH/FAD dependent oxidoreductases (Kawasaki et al. 2009, Riebe et al. 2009). Interestingly, the genes encoding both revRbrs and FDPs are positively controlled by σ^B (Kint et al. 2017). This sigma factor is crucial for the management of oxidative and nitrosative stresses and to O₂ tolerance (Kint et al. 2017). From all enzymes protecting the cells from O₂, oxidative or nitrosative stress, only the FDP protein, CD1623, has been functionally characterised as an O₂-reductase (Folgosa et al. 2018b).

In the present study, we sought to functionally characterize the second FDP, CD1157, and the two revRbrs of *C. difficile* and to determine the physiological role of these proteins in O₂ tolerance and oxidative stress resistance of this anaerobic pathogen.

I. Role of the revRbrs and the FDPs in *C. difficile* vegetative cells

I.1. Regulation of revRbrs (*CD1474*, *CD1524*) and FDPs (*CD1623*, *CD1157*) gene expression

The genome-wide transcriptional start site (TSS) mapping study (Soutourina et al. 2013) identified a solely TSS for *CD1474*, *CD1524* and *CD1623* and two different potential TSS for *CD1157*. The promoter sequence upstream of the *CD1474* TSS harbors a classical consensus sequence (WGWTT-N₁₃₋₁₇-(G/T)GGTAWA) recognized by σ^B in *C. difficile* (Kint et al. 2017). A σ^B consensus sequence was also identified in the promoter region of the *CD1524*, *CD1623* and *CD1157* genes upstream of the TSSs (Figure 40A, B and Figure 41A, respectively). Moreover, upstream the second TSS of *CD1157*, we detected a promoter harboring a canonical -10 box (TATATT) of the σ^A -dependent promoter and a less conserved -35 box (Figure 41A).

The expression of *CD1474* has been showed to be only σ^B -dependent (Kint *et al.*, in Annex). To analyse the expression of *CD1524* and *CD1623*, the promoter region of each gene was fused to the gene encoding a fluorescent reporter SNAP^{Cd} into the vector pFT47 (Pereira et al. 2013, Cassona et al. 2016). The resulting plasmids were transferred into the wild-type strain and the *sigB* mutant. After 16 h of growth in BHI, cells were labelled with TMR-Star. Following labelling, we observed an expression of the P_(CD1524)- and the P_(CD1623)-SNAP^{Cd} fusions in the wild-type strain in 82% and 58% of the cells, respectively (Figure 40C and D). By contrast, no fluorescent signal was detected in the cells of the *sigB* mutant.

The presence of two promoters upstream of the *CD1157* gene suggests that its expression might be controlled by both σ^A and σ^B . To monitor the expression of *CD1157*, we engineered a transcriptional fusion between the entire promoter region containing both promoters and the SNAP^{Cd} gene (Pereira et al. 2013, Cassona et al. 2016) and transferred the resulting plasmid into the wild-type strain and the *sigB* mutant. We observed an expression of the P _{$\sigma^A \sigma^B$ (CD1157)}-SNAP^{Cd} fusion in 12% of the cells in the wild-type strain after 16 h of growth in BHI (Figure 41B), while in the *sigB* mutant, the expression of P _{$\sigma^A \sigma^B$ (CD1157)}-SNAP^{Cd} is observed, but to a lower extent (2% of cells) (Figure 41B). To confirm the dual control of *CD1157* expression, we fused the promoter region harboring either the σ^A consensus sequence P _{σ^A (CD1157)} or the σ^B consensus sequence P _{σ^B (CD1157)} to the SNAP^{Cd} encoding gene. The expression of P _{σ^A (CD1157)}-SNAP^{Cd} was observed in both the wild-type and the *sigB* mutant strains in 12% and 2% of the cells, respectively (Figure 41C). By contrast, no fluorescence was detected for P _{σ^B (CD1157)}-

MSKVFEVKKDIYFTGVVDEGLKVFDIIMETFGT **TYNSYLIKDEKTVLFD** 50
TVKANFKDEFLSNLSEVTDIAKIDYVVIH**HTEPDH**AGSLKYLLDINPNIE
 VYCTKAAKLYLDGQINRPFNCHVIKDGEILNIGKRNLRFITAPFL**HWVDT** 150
MFTYIEEDKTLLTCD**DAFGCHFASVDAEVVNSE**DYLSAKHYDCIVKPF
AKHVLSAVDKVVGLNIEFDTILTS**H**GPMLTKDPMMAAVKRYVEWSTEAVN 250
 TTNQNQV**SIFYLSAYSNTLEMAKKIKEGLDKEGAKAELYDLE**
DMTLTEMHDTLVVSKVILLGSPTINKTMVKPMWDLFSVID 350
PMANQGGKIAGVFGSFGWSGEGITMAETLLK**SMSFKMPVES**
LKKKFFPSEETLKECMAFGAEFAKLVK 397

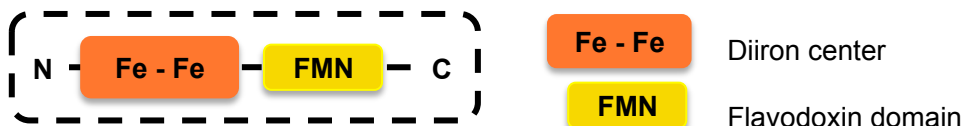


Figure 42: Amino acid sequence of the FDP CD1157. The diiron center (35-224 aa) is represented in orange and the flavodoxin FMN domain (257-389 aa) in yellow. Amino acid residues that coordinate the catalytic iron atoms are in blue.

MKKFV**CTVCGYI**HEGDAA**PAQCPVCKV**GADKFEEMKGEKNWADEHRIGVA 50
 MKKFV**CTVCGYI**HEGDAA**PAQCPVCKV**GADKFEEMKGEMVWADEHRIGVA

 QGVDEE**IIIEGLRANFV**GECTEVGM**YLA**MSRQADREGYP**EVGEAYKRI**ALE 100
 QGVDAE**IIIEGLRANFT**GECTEVGM**YLA**MSRQADREGYP**VAEAYKRI**A

 EAEHAAKFAELLGEVVADTKENLRVRVDAEY**GATDGK**LKLAKKAKELGL 150
 EAEHAAKFAELLGEVVADTKENLRVRVDAEY**GATDGK**LKLAKRAKELGL

 DAIHDTVHEMCKDEARHGKAFLG**LLNR**YFGK CD1474 181
 DAIHDTVHEMCKDEARHGKAFLG**LLNR**HFGK CD1524 **96 % identity**

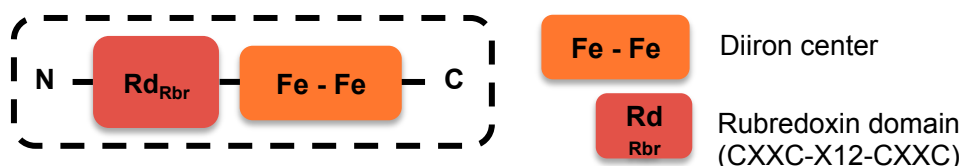


Figure 43: Amino acid sequence alignment of the two revRbrs CD1474 and CD1524. The rubredoxin domain (3-35aa) is represented in red and the diiron center (56-179 aa) in orange. The two CysxxCys motifs from the FeCys4 center of the Rd domain are highlighted in yellow. The alignment was performed in ClustalW.

SNAP^{Cd} in the *sigB* mutant (Figure 41D) whereas the expression from this fusion was observed in the 7% of the cells of the wild-type strain. Altogether, these results indicate that *CD1157* expression is related to both the σ^A - and σ^B -dependent promoters while *CD1524* and *CD1623* expression is only σ^B -dependent as already observed for *CD1474* encoding the other revRbr (Kint *et al.*, in Annex).

I.2. FDP and revRbrs sequence analysis

The *CD1157* gene encodes a Class A FDP (see Introduction, chapter 3, section: 1.2.b Flavodiiron proteins) with 397 amino acid residues harbouring the minimal core that is common to all FDPs so far analysed (Folgosa *et al.* 2018a). The N-terminal part shares similarities with the fold of metallo- β -lactamase and contains a non-heme diiron center, which is the catalytic site involved in the reduction of O₂ or NO. The C-terminal part is composed of a flavodoxin FMN-containing domain ensuring the electron transfer (Figure 42). Amino acids involved in the coordination of the diiron center in FDPs, including histidines (His⁸³, His⁸⁸, His¹⁴⁹, His²²⁹) aspartates (Asp⁸⁷, Asp¹⁶⁸) and glutamates (Glu⁸⁵) are conserved in CD1157. As other FDPs, CD1157 likely receives electrons from a NAD(P)H-OR to reduce O₂ and/or NO.

The two revRbrs, CD1474 and CD1524, share 96% of amino acid identity (Figure 43). Two domains, found in inverted position in classical Rbrs, compose these proteins: an electron transfer Rd domain binding a Fe(Cys)₄ center at the N-terminal and a diiron catalytic center at the C-terminal part (deMare *et al.* 1996). The Rd domain of 33 amino acids contains two CysXXCys motifs (Cys6/Cys9, Cys22/Cys25) separated by 12 residues, which is typical of short-spaced Rd domain found in Rbrs (Cardenas *et al.* 2016).

I.3. Protein characterization and redox properties

The FDP CD1157, and the two revRbrs, CD1474 and CD1524, were produced as non-tagged proteins in *E. coli* grown in M9 medium supplemented with iron in the presence of IPTG. The proteins were then purified through several chromatographic steps. The molecular masses determined from the SDS-PAGE, ~ 45 kDa for CD1157 and ~ 22 kDa for the two revRbrs, were in agreement with those calculated from the respective amino acids sequence, 44 and 20 kDa (Figure 44). Gel filtration of the purified recombinant proteins (data not shown) revealed that CD1157 behaves as a homodimer in solution, presenting a molecular mass of ~ 74.7 kDa while both revRbrs are isolated as tetramers in solution with determined molecular masses of ~ 79.2 kDa for the CD1474 and ~ 79.8 kDa for the CD1524. FDPs so far

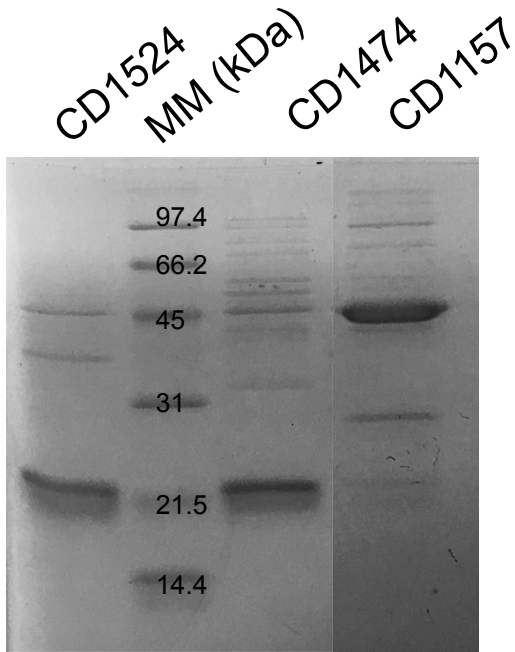


Figure 44: SDS-PAGE gel from the two revRbrs CD1524 and CD1474, and the FDP CD1157. Low-range molecular mass marker is indicated.

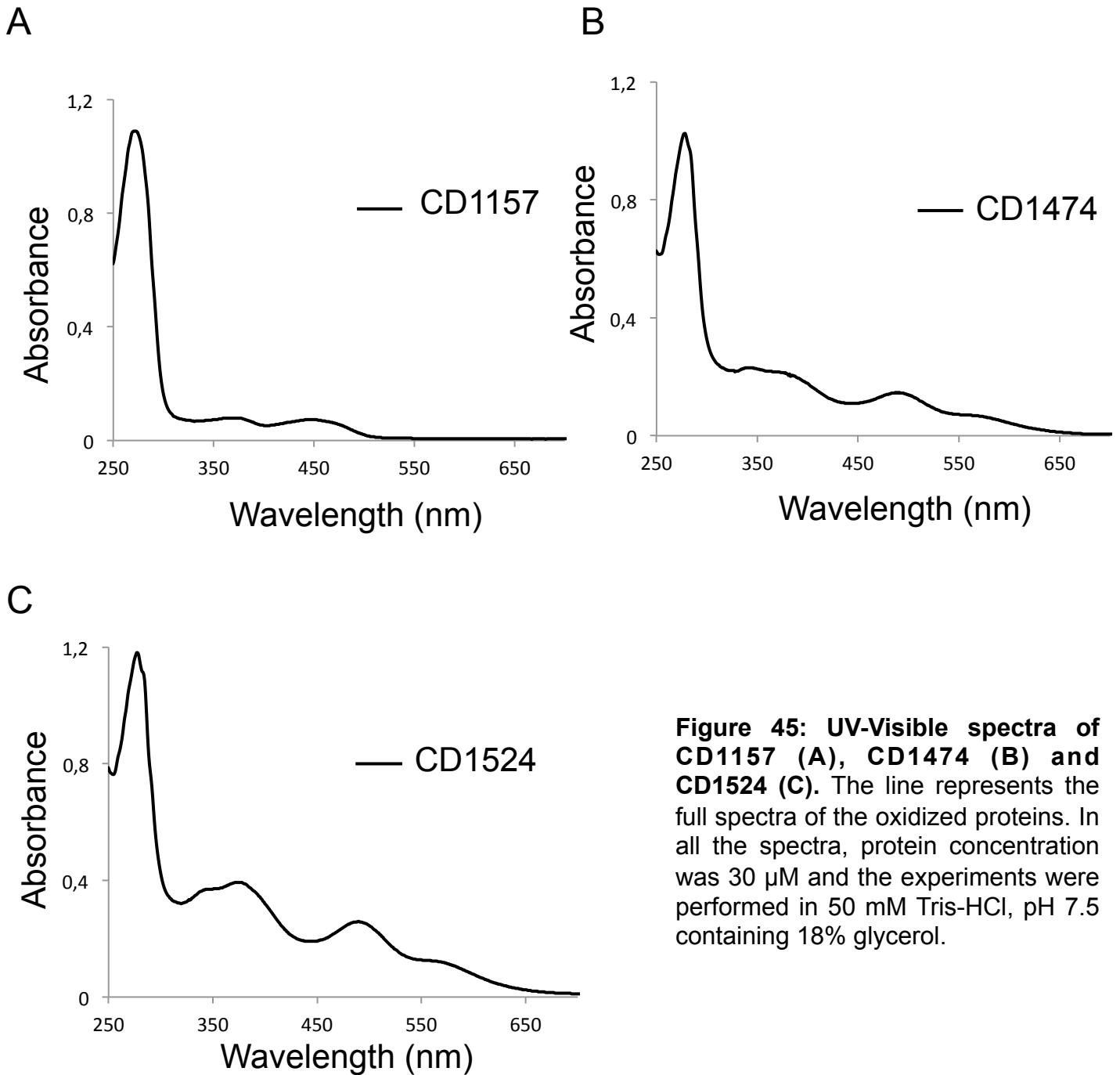


Figure 45: UV-Visible spectra of CD1157 (A), CD1474 (B) and CD1524 (C). The line represents the full spectra of the oxidized proteins. In all the spectra, protein concentration was 30 μ M and the experiments were performed in 50 mM Tris-HCl, pH 7.5 containing 18% glycerol.

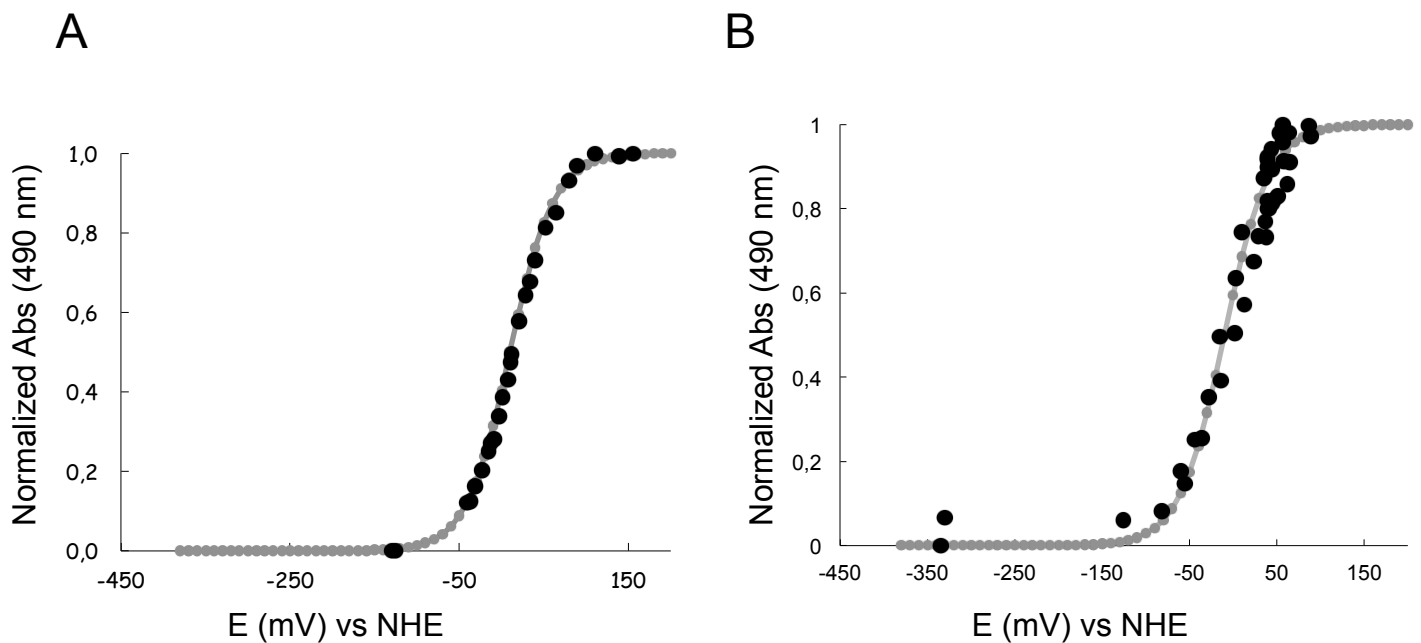


Figure 46: Anaerobic redox titration curves of the revRbrs CD1474 (A) and (B) CD1524. Panels correspond to the normalized intensities measured at 490 nm. In both titrations, protein concentration was 30 μM and the experiments were performed in 50 mM Tris-HCl, pH 7.5 containing 18% glycerol. The solid lines correspond to Nernst equations adjusted as described in the text, with the following reduction potentials: CD1474, +10 mV, CD1524, -10 mV.

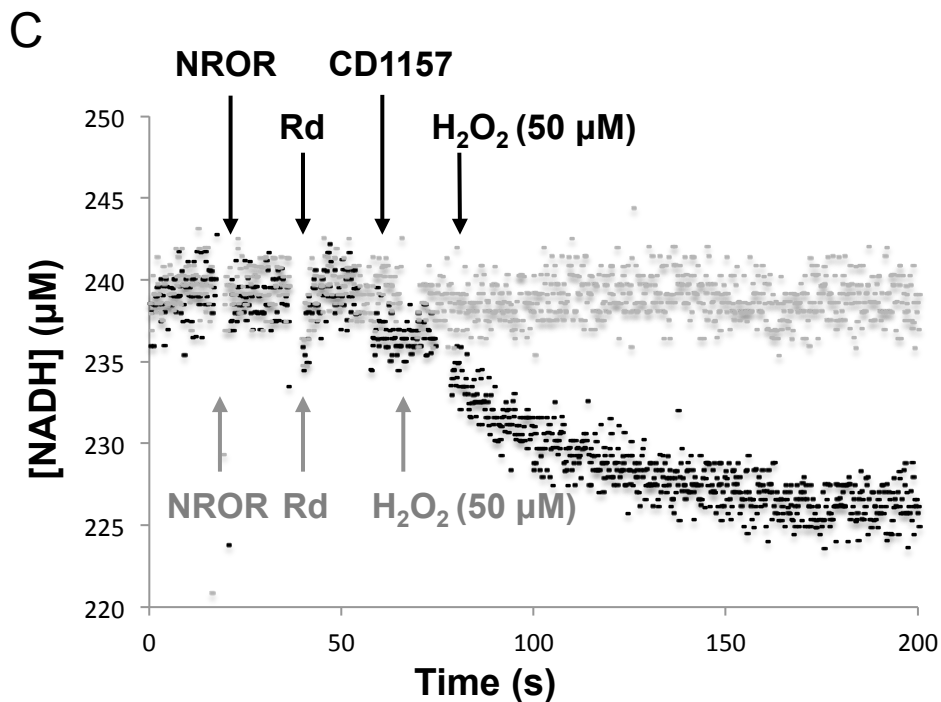
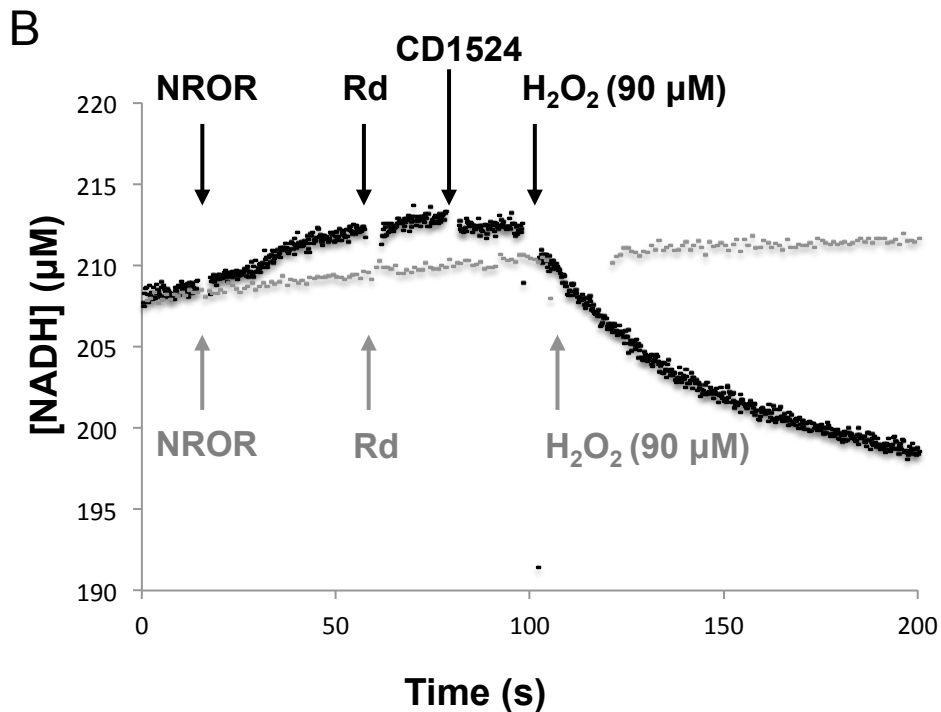
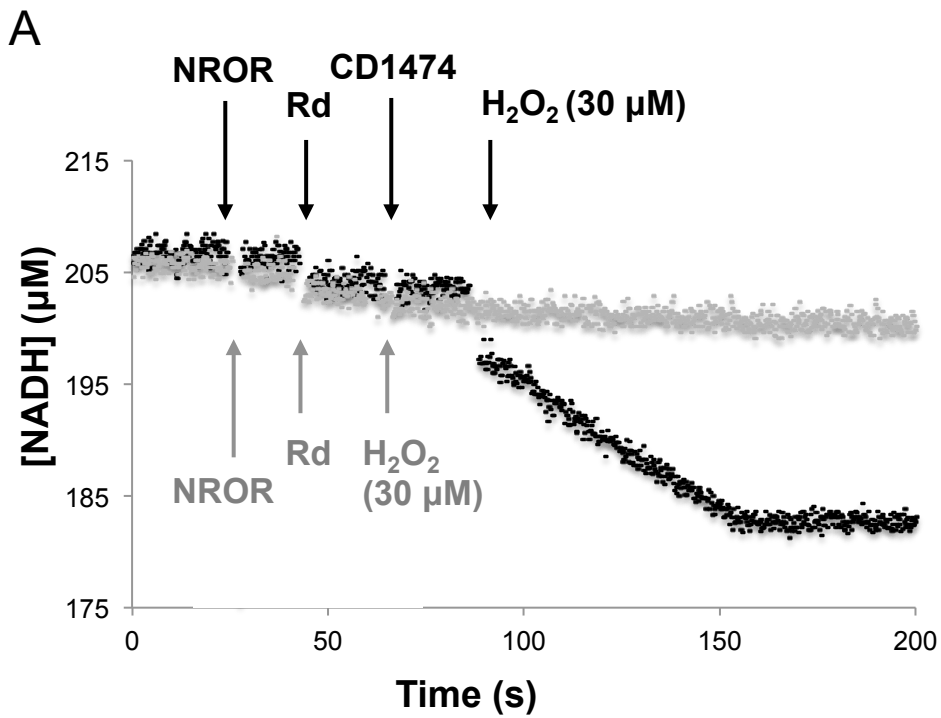


Figure 47: H₂O₂- reductase activities of the two revRbrs, CD1474 and CD1524, and the FDP CD1157. The reaction was performed anaerobically and monitored at 340 nm, following NADH (around 0.2 mM) consumption. Protein concentrations were 800 nM for the NADH rubredoxin oxidoreductase (NROR), 5 µM for the Rd (Rubredoxin), 100 nM for CD1474 (**A**) and 30 nM for CD1524 (**B**) in 50 mM Tris-HCl, pH 7.5 containing 18% glycerol. For the FDP assay, were used 1.6 µM of NROR, 10 µM of Rd and 1 µM of CD1157 in 50 mM Tris-HCl, pH 7.5 containing 18% glycerol. Black and grey curve represent the reaction in the presence or absence of the revRbrs or FDP, respectively.

characterized appear in solution as homodimers or homotetramers, an essential configuration for efficient electron transfer between the FMN of one monomer and the diiron center of the other (Folgosá et al. 2018a). The same configuration, homodimers or homotetramers is usually found in Rbrs (Tempel et al. 2004, Pinto et al. 2011). Reverse phase HPLC analysis identified FMN as the flavin cofactor of CD1157 (data not shown), which is usually observed in the flavodoxin core domain of FDPs (Romao et al. 2016, Folgosá et al. 2018a). In addition, the UV-visible absorbance spectrum of CD1157 is characteristic of a protein containing flavin as cofactor, exhibiting maxima at 380 nm and 450 nm (Figure 45A). By contrast, the UV-visible absorbance spectra of CD1474 and CD1524 are characteristic of proteins containing a Rd center, exhibiting maxima at 380 nm and 490 nm (Figure 45B and C). For all proteins analyzed, the presence of a diiron site is not detected due to its low molar absorptivity (Solomon et al. 2000).

Finally, analyses of CD1157 showed a ratio for iron/FMN/protein monomer of 1/0.3/1. These values are lower than expected (2/1/1) suggesting an incomplete incorporation of iron and FMN in the protein even after FMN supplementation following purification. CD1474 and CD1524 showed an iron/protein monomer ratio of 1.3/1 and 2.8/1.1, respectively. CD1524 appeared to be fully loaded with iron while the ratio was lower than expected for CD1474.

The reduction potentials of the Rd center for the revRbrs CD1474 and CD1524 were obtained by redox titrations monitored by visible spectroscopy (Figure 46) in an anaerobic chamber at pH 7.5. The Rd site was monitored at 490 and 556 nm and a potential of -10 mV and +10 mV were obtained respectively for CD1524 and CD1474. Redox titration of the flavin center of CD1157 will be done in future experiments.

I.4. CD1474 and CD1524 reduce both H₂O₂ and O₂ while CD1157 reduces only O₂

Having established the presence of the FMN and iron cofactors and determined the redox properties of each protein, we addressed the catalytic activities of CD1157 and of the two revRbrs. The O₂⁻ and H₂O₂-reductase activities of the three enzymes were determined using NADH as the primary electron donor. Purified CD1157, CD1474 and CD1524 (at 30 μM) alone did not show detectable NADH oxidase activity (data not shown). Since the *C. difficile* physiological electron donors of these proteins are still unknown, external partners were used to perform the assays. We found that a NROR and a Rd from *E. coli* were able to

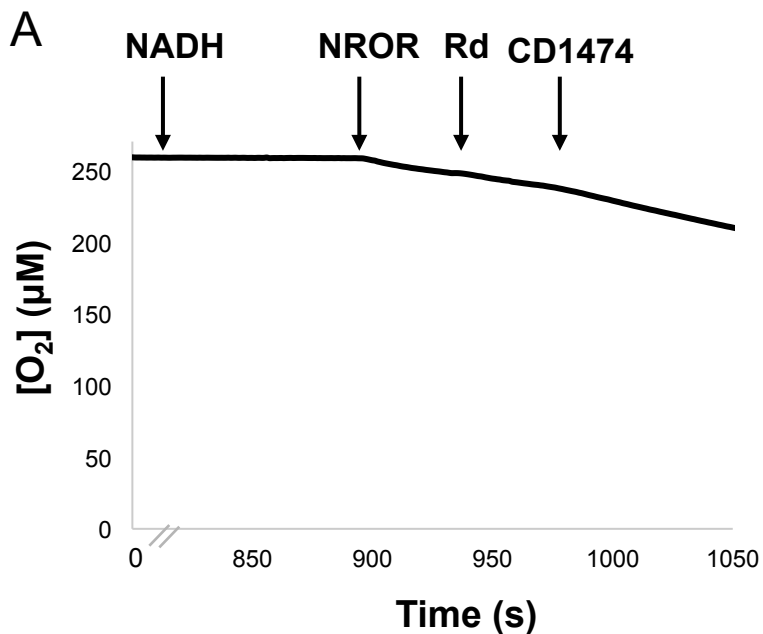
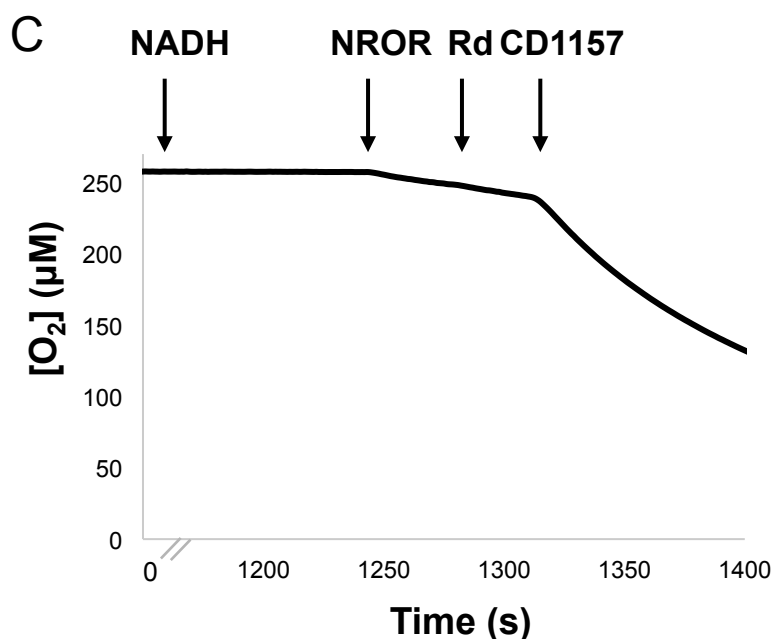
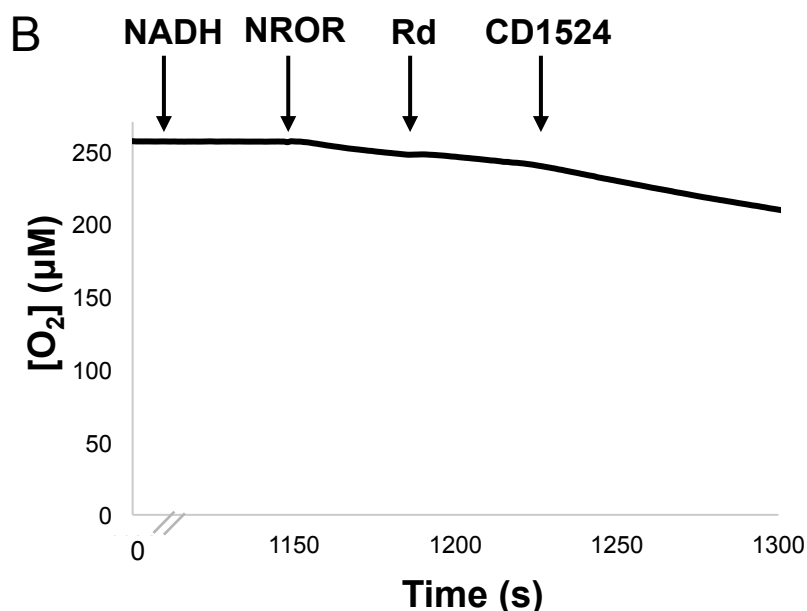


Figure 48: O₂-reductase activities of the revRbrs, CD1474 and CD1524, and the FDP CD1157. Assays were performed using a O₂ electrode. Protein concentrations were 800 nM for the NADH rubredoxin oxidoreductase (NROR), 5 µM for the Rd (Rubredoxin), 100 nM for the CD1474 (**A**) and the CD1524 (**B**) and 1 µM for CD1157 (**B**), in 50 mM Tris-HCl, pH 7.5 containing 18% glycerol. NADH (5 mM) was used as reductant. Arrows indicate the time points of protein additions.



reduce CD1157 and the two revRbrs in the presence of NADH (data not shown). To test H₂O₂-reductase activity, NADH consumption was measured spectrophotometrically, upon addition of H₂O₂ to a premix containing NADH, NROR, Rd and either CD1157, CD1474 or CD1524. A clear H₂O₂-reductase activity was observed for the two revRbrs with a rate of $2.1 \pm 0.15 \text{ s}^{-1}$ and $7.6 \pm 0.62 \text{ s}^{-1}$ for CD1474 and CD1524, respectively (Figure 47A and B). By contrast, we detected only a negligible H₂O₂-reductase activity with a rate of $0.27 \pm 0.03 \text{ s}^{-1}$ for CD1157 (Figure 47C). To test O₂-reductase activity, we directly measured O₂ consumption using an O₂ Clark-type selective electrode. CD1157, CD1474 or CD1524 was added to an O₂-saturated buffer ($\sim 260 \mu\text{mol l}^{-1}$ of O₂) containing NADH, NROR and Rd from *E. coli*. O₂-reductase activity was observed for CD1157, CD1474 and CD1524 with a rate of $1.4 \pm 0.31 \text{ s}^{-1}$, $1.2 \pm 0.14 \text{ s}^{-1}$ and $2.0 \pm 0.38 \text{ s}^{-1}$, respectively (Figure 48). From these results, we conclude that CD1157 acts as an NADH:O₂-reductase and that both revRbrs CD1524 and CD1474 act as NADH:H₂O₂-reductase and NADH:O₂-reductase.

I.5. The function of the revRbrs and the FDPs, in the management of O₂ tolerance

To study in *C. difficile* the physiological role of the two revRbrs and the two FDPs, including the CD1623, already characterized as an O₂-reductase (Folgosa et al. 2018b), we generated the corresponding mutants. We inactivated the *CD1157* gene using the Clostron system, which enabled the insertion of a type I intron after the 225th nucleotide in sense orientation (Figure S1). Using the allele chromosomal exchange (ACE), we deleted the *CD1474*, *CD1524* and *CD1623* open reading frames yielding $\Delta CD1474$, $\Delta CD1524$ and $\Delta CD1623$ single mutants. We also generated $\Delta CD1474$ - $\Delta CD1524$ and $\Delta CD1623$ -*CD1157* double mutants (Figure S1). As the four proteins under study possess an O₂-reductase activity, we assessed the ability of the different mutants to grow when exposed to low O₂ tension. Concerning the revRbrs, no difference in growth between the wild-type and the double $\Delta CD1474$ - $\Delta CD1524$ mutant strains was observed in anaerobiosis or when exposed to 0.1 % of O₂ (Figure 49). By contrast, a growth defect was observed for the $\Delta CD1474$ - $\Delta CD1524$ double mutant in the presence of 0.2 % of O₂ (Figure 49). The growth of this mutant was even more affected when exposed to 0.4 % of O₂, when compared to the wild-type. Of note, we did not observe any growth defect for the $\Delta CD1474$ or $\Delta CD1524$ single mutant whatever the O₂ tension used suggesting a functional redundancy between these two proteins. Accordingly, complementation of the $\Delta CD1474$ - $\Delta CD1524$ double mutant by either *CD1474* or *CD1524*

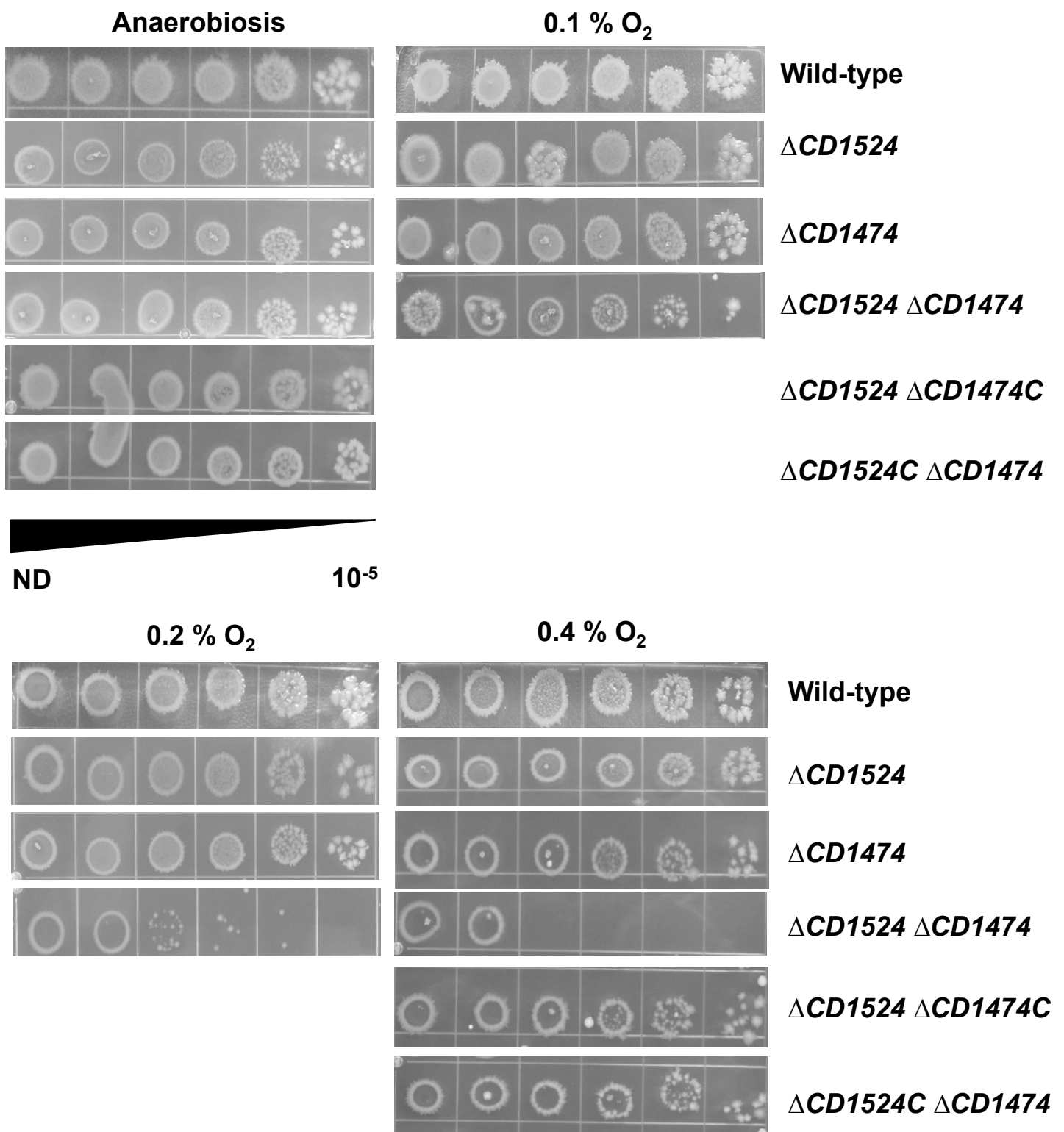


Figure 49: Role of the two revRbRs in low O₂ tension tolerance. Serial dilutions of the wild-type strain, ΔCD1524, ΔCD1474 mutants, ΔCD1524-ΔCD1474 double mutant, and the double mutant complemented with one or the one Rbr were spotted on TY taurocholate plates. Plates were then incubated 64 h either in anaerobic atmosphere (control) or in the presence of 0.1, 0.2 or 0.4 % O₂.

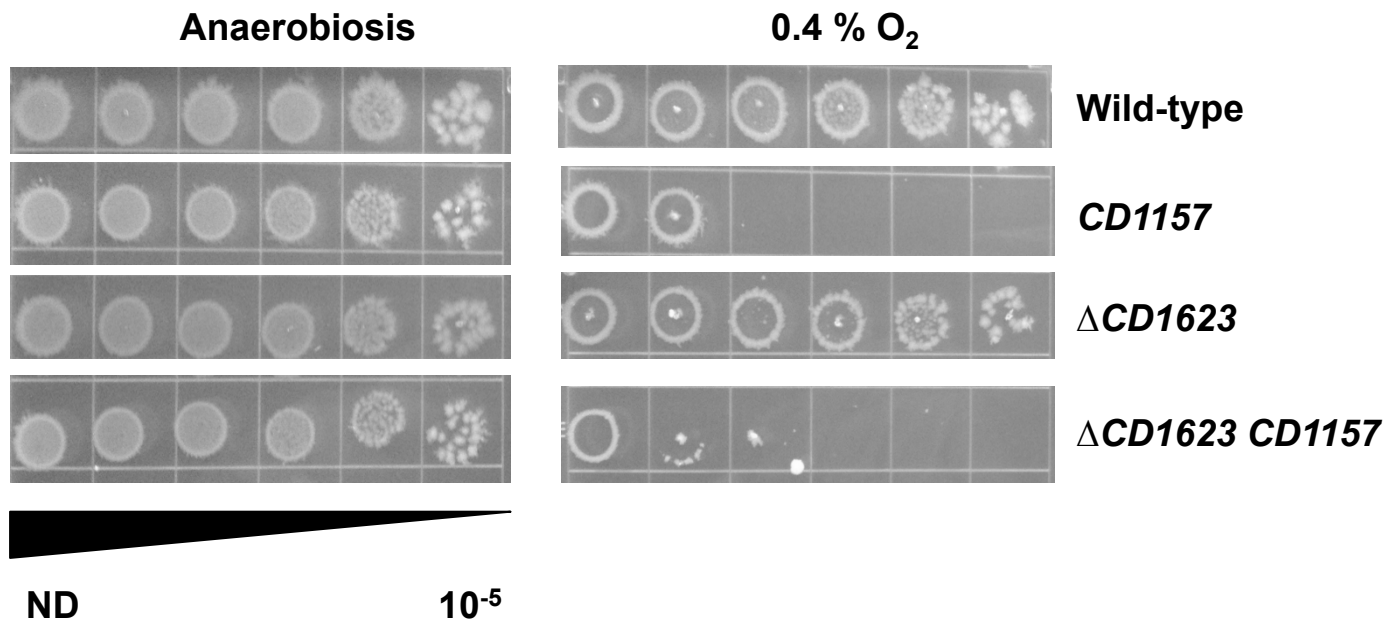


Figure 50: Role of the two FDPs in low O₂ tension tolerance. Serial dilutions of the wild-type strain, *CD1157*, Δ *CD1623* mutants and the Δ *CD1623-CD1157* double mutant were spotted on TY taurocholate plates. Plates were then incubated 64 h either in anaerobic atmosphere (control) or in the presence of 0.4 % O₂.

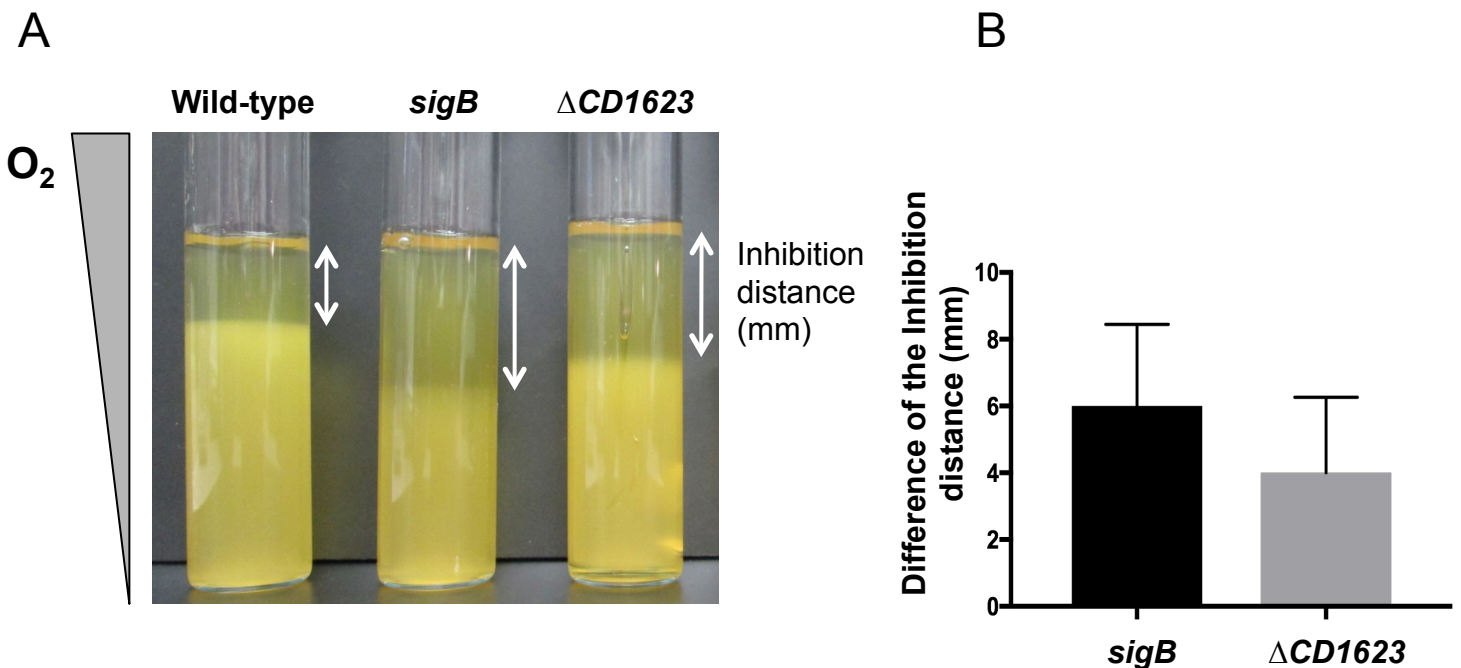


Figure 51: Air sensitivity of the Δ *CD1623* mutant. **A)** The air tolerant assay in soft agar tubes. The white arrows indicate the zone of growth inhibition. **B)** The histograms represent the difference of the growth inhibition difference between each mutant and the wild-type strain, which was used as reference (0). The data represent the average and standard deviation from at least three biological replicates.

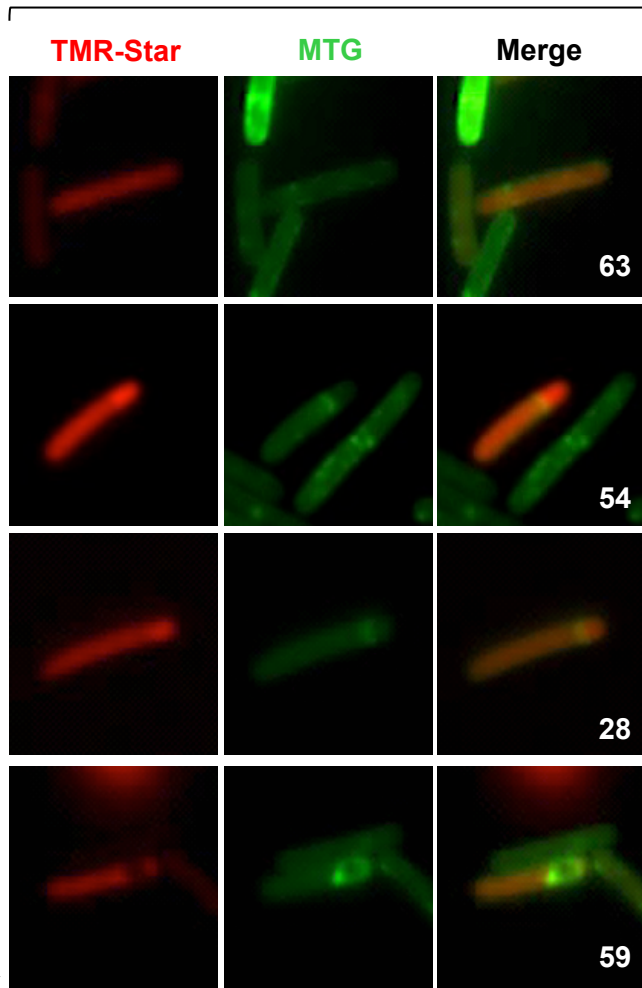
wild-type gene was enough to fully restore the growth in presence of low O₂ tension (Figure 49). For the FDPs, a growth defect was observed for the *CD1157* mutant in the presence of 0.4 % of O₂ (Figure 50). In the same conditions, even if no major growth defect was observed for the Δ *CD1623* mutant, cells seem to be affected since they did not grow in the middle of the spot for some dilutions. To assess if O₂-reductase activity of CD1157 and CD1623 could be additive, the Δ *CD1623-CD1157* double mutant was exposed to 0.4% O₂. The growth of the double mutant was almost abolished with only slightly different from the Δ *CD1157* mutant under the same conditions tested. We did not observe a growth defect for any of the strains in anaerobiosis (Figure 50). We also tested the effect of these genes inactivation on the growth of *C. difficile* in TY soft agar tubes incubated in the presence of air for 24h. As control, we used the *sigB* mutant previously showed to be less tolerant to air (Kint et al. 2017). The Δ *CD1474*, Δ *CD1524* and *CD1157* single mutants and the Δ *CD1474-CD1524* double mutant were able to grow as the wild-type strain (data not shown). By contrast, we observed a higher growth inhibition zone for the Δ *CD1623* mutant compared to that of the wild-type strain (Figure 51A). The difference between the growth inhibition distance between the *sigB* and Δ *CD1623* mutants and the wild-type strain was 6 and 4 mm, respectively (Figure 51B). The air sensitivity of the Δ *CD1623-CD1157* double mutant will be addressed in future experiments.

Altogether these results indicate that the two FDPs, CD1157 and CD1623, and the two RevRbrs, CD1474 and CD1524, play an important role for the O₂ tolerance in *C. difficile*. We can also conclude that CD1474 and CD1524 are functionally redundant in their ability to reduce O₂. Work is currently in progress in the laboratory to construct multi-mutants of both the FDPs and revRbrs genes and to complement the mutants inactivated with the respective genes.

A

 $P_{(sigB)}-SNAP^{Cd}$

Wild-type (stages of morphogenesis)



B

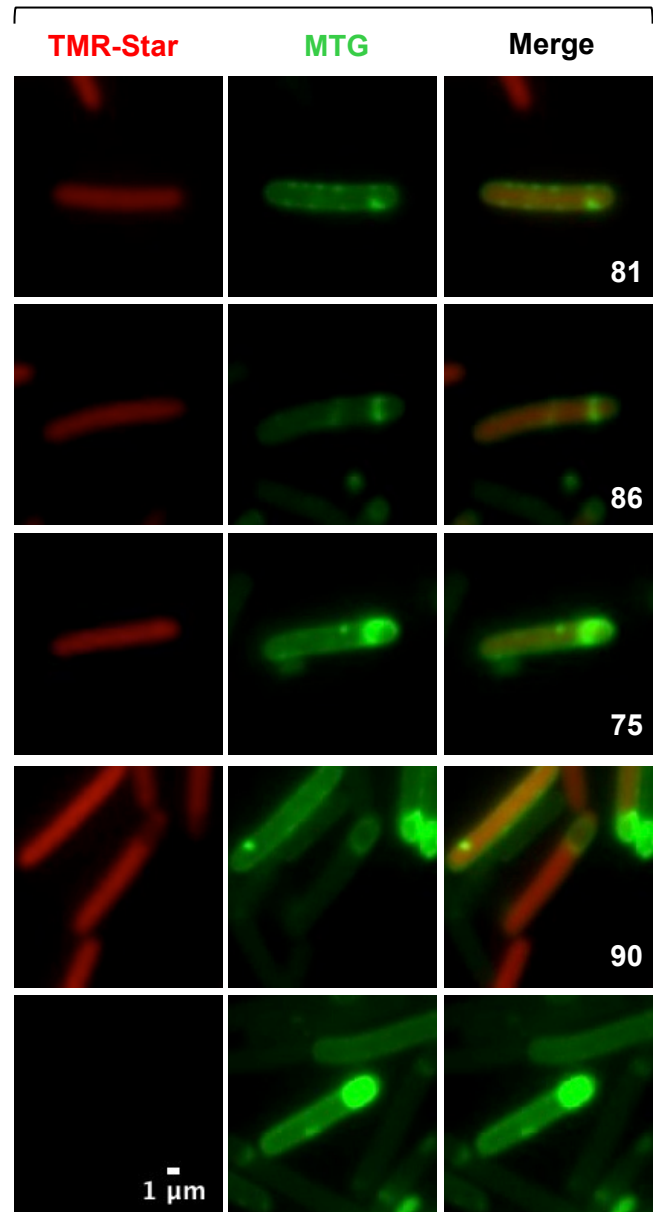
 $P_{(CD1474)}-SNAP^{Cd}$ *sigB*

Figure 52: Expression of the *sigB* gene and its target gene, *CD1474*, during sporulation. Temporal and cell type-specific expression of *sigB* (A) and of *CD1474* (B) during sporulation. The cells were collected after 24 h of growth in liquid SM, stained with TMR-Star and the membrane dye MTG, and examined using fluorescence microscopy. The merged images showed the overlap between the TMR-Star (red) and the MTG (green) channels. The numbers represent the percentage of cells at the indicated stage that show expression of the reporter fusion. The panels are representative of the expression patterns observed for different stages of sporulation, ordered from early to late for the wild-type strains. Scale bar, 1 μ m.

II. Proteins produced under the control of σ^B are present in the spores

In *C. difficile*, the alternative sigma factor σ^B plays a pleiotropic and crucial role regulating numerous genes involved in biological processes such as motility, sporulation, cell wall metabolism and stress responses (Kint et al. 2017). However, while σ^B positively controls stress response, the sporulation genes are negatively controlled by this sigma factor. The majority of the genes of the σ^F , σ^E and σ^G regulons (84%, 96% and 96%, respectively) were up-regulated in the *sigB* mutant (Kint et al. 2017). However, only 38% of the σ^K regulon was derepressed in the *sigB* mutant, a rate probably underestimated due to the timing of cell sampling used in the transcriptomic study (10 h) that did not allow detection of the expression of later sporulation genes controlled by σ^B . In agreement, the inactivation of *sigB* resulted in a higher sporulation efficiency compared with the wild-type strain (Kint et al. 2017).

II.1. σ^B expression and activity during sporulation

Most of the proteins located at the spore surface are encoded by genes transcribed in the MC by σ^E and σ^K . Interestingly, several proteomic studies revealed the presence of proteins at the spore surface that are not synthesized under the control of sporulation-specific sigma factors. In particular, the revRbrs, CD1474 and CD1524, the FDP CD1623 and the OR CD0176, has been identified in spore coat proteomes (Lawley et al. 2009b, Abhyankar et al. 2013, Diaz-Gonzalez et al. 2015, Kint et al. 2017). The corresponding genes are transcribed by σ^B (Kint et al. 2017). Therefore, we decided to explore both the synthesis of σ^B and its activity during sporulation. To monitor its expression during sporulation, the promoter region of the *sigB* operon located upstream of the *CD0007* was fused to the SNAP^{Cd} gene (Pereira et al. 2013, Cassona et al. 2016). The resulting plasmid was transferred into the 630 Δ *erm* strain. After 24 h of growth in sporulation medium (SM), cells expressing the transcriptional P_{*sigB*}-SNAP^{Cd} fusion were doubly labeled with TMR-Star and the membrane dye MTG to allow identification of the different stages of sporulation. The expression of the P_{*sigB*}-SNAP^{Cd} fusion was detected in 63% of pre-divisional cells (Figure 52A). Moreover, fluorescence was detected in both MC and FS compartment after asymmetric division and during engulfment morphological steps in 54% and 28% of the cells, respectively (Figure 52A). Interestingly, at the end of sporulation after engulfment completion, the expression of the P_{*sigB*}-SNAP^{Cd} fusion was confined to the MC compartment, in 59% of the cells (Figure 52A). To check the activity of σ^B along sporulation, we used the revRbr-encoding gene *CD1474* as a σ^B -target gene.

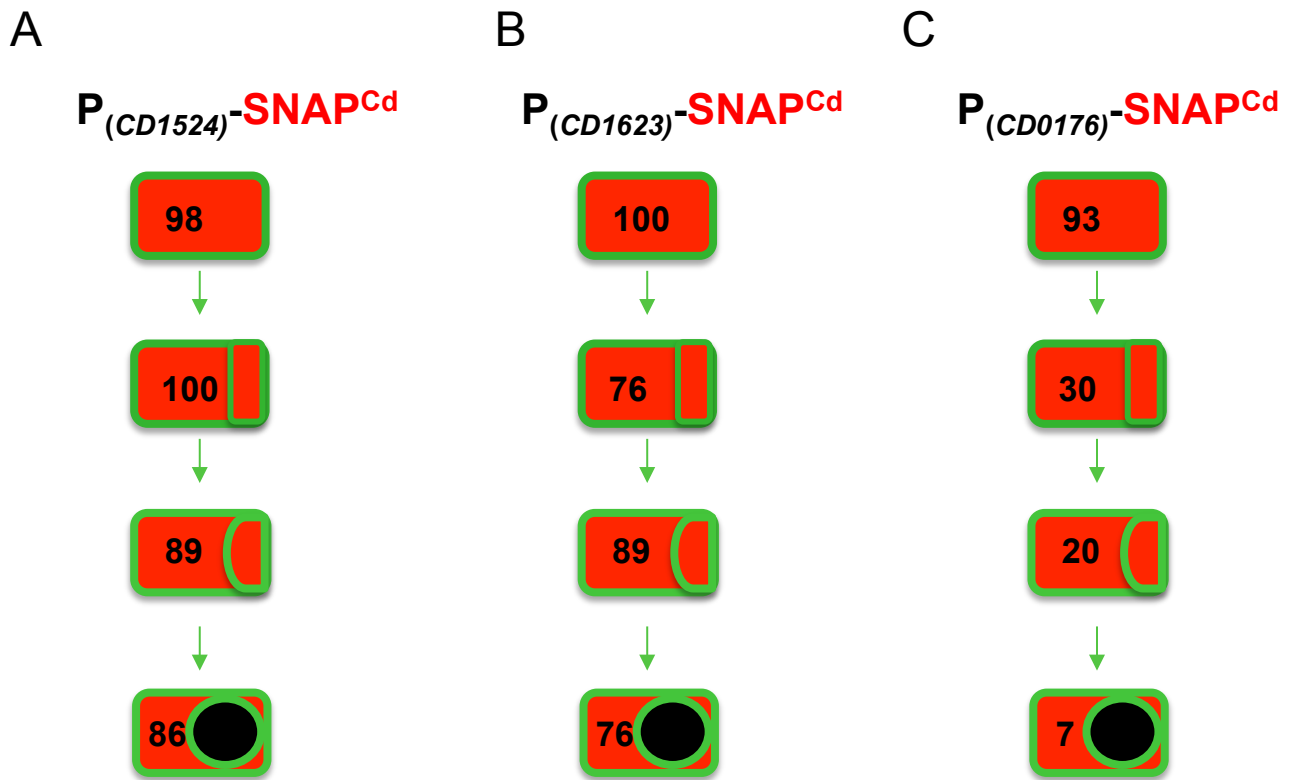


Figure 53: Expression of the *CD1524*, *CD1623* and *CD0176* genes during sporulation.

Schematic representation of the temporal and cell type-specific expression of *CD1524* (A), *CD1623* (B) and of *CD0176* (C) during sporulation. The cells were collected after 24 h of growth in liquid SM, stained with TMR-Star and the membrane dye MTG, and examined using fluorescence microscopy. The numbers represent the percentage of cells at the indicated stage that show expression of the reporter fusion.

Indeed, this gene is a good candidate to study σ^B activity since a unique σ^B -dependent promoter was mapped by TSS analysis upstream of the *CDI474* gene, and its expression is completely abolished in the *sigB* mutant during vegetative growth (Soutourina et al. 2013, Kint et al. 2017) (Kint *et al.*, in Annex). The promoter region of *CDI474* was fused to the SNAP^{Cd} gene and the resulting plasmid transferred into the 630 Δ *erm* strain and the *sigB* mutant. The expression of P_{CDI474}-SNAP^{Cd} fusion was found in 81% of the pre-divisional cells but also in 86% of the cells after asymmetric division and in 75% of the cells during engulfment process in both MC and FS compartments. After engulfment completion, fluorescence signal was detected in 90% of the cells and again only in the MC compartment as observed for the P_{sigB}-SNAP^{Cd} fusion. In addition, no signal was detected in the *sigB* mutant (Figure 52B). Similar results were observed with the *CDI524* and the *CDI623* genes (Figure 53A and B). Interestingly, for the *CDI0176* gene, even if we observed the same compartmentalization of the σ^B activity, the percentage of cells expressing P_{CDI0176}-SNAP^{Cd} fusion was much more low comparing with the other tested genes (Figure 53C). After engulfment completion, only 7% of the cells showed fluorescent signal. Importantly, for all the genes, no signal was detected in the *sigB* mutant strain. Altogether, these observations showed that both *sigB* and the σ^B -controlled genes, *CDI474*, *CDI524*, *CDI623* and *CDI0176* are expressed during sporulation and that this expression is surprisingly restricted to the MC compartment after engulfment completion. The absence of fluorescence in the *sigB* background indicates that even during sporulation, their expression is exclusively controlled by σ^B .

II.2. Localization of σ^B - controlled proteins at the spore surface

The detection of σ^B activity in the MC during sporulation is in agreement with the identification of σ^B -targets at the surface of the spore. Analysis of the ultrastructure of *sigB* mutant spores using TEM revealed that the *sigB* mutant produce spores similar to the wild-type strain, with intact spore coat and exosporium layers surrounding the cortex (Figure 54A). However, in order to confirm the presence of σ^B -target proteins at the spore surface, we compared the proteome of the spore surface layers of the wild-type and *sigB* mutant strains. First, a SDS-PAGE analysis of the spore coat plus exosporium extracts obtained from purified spores did not reveal major differences in the protein profile of the *sigB* mutant compared with the wild-type strain (Figure 54B). To have a global view of the spore surface proteome of the *sigB* mutant, proteins extracted from the coat/exosporium of spores of the wild-type

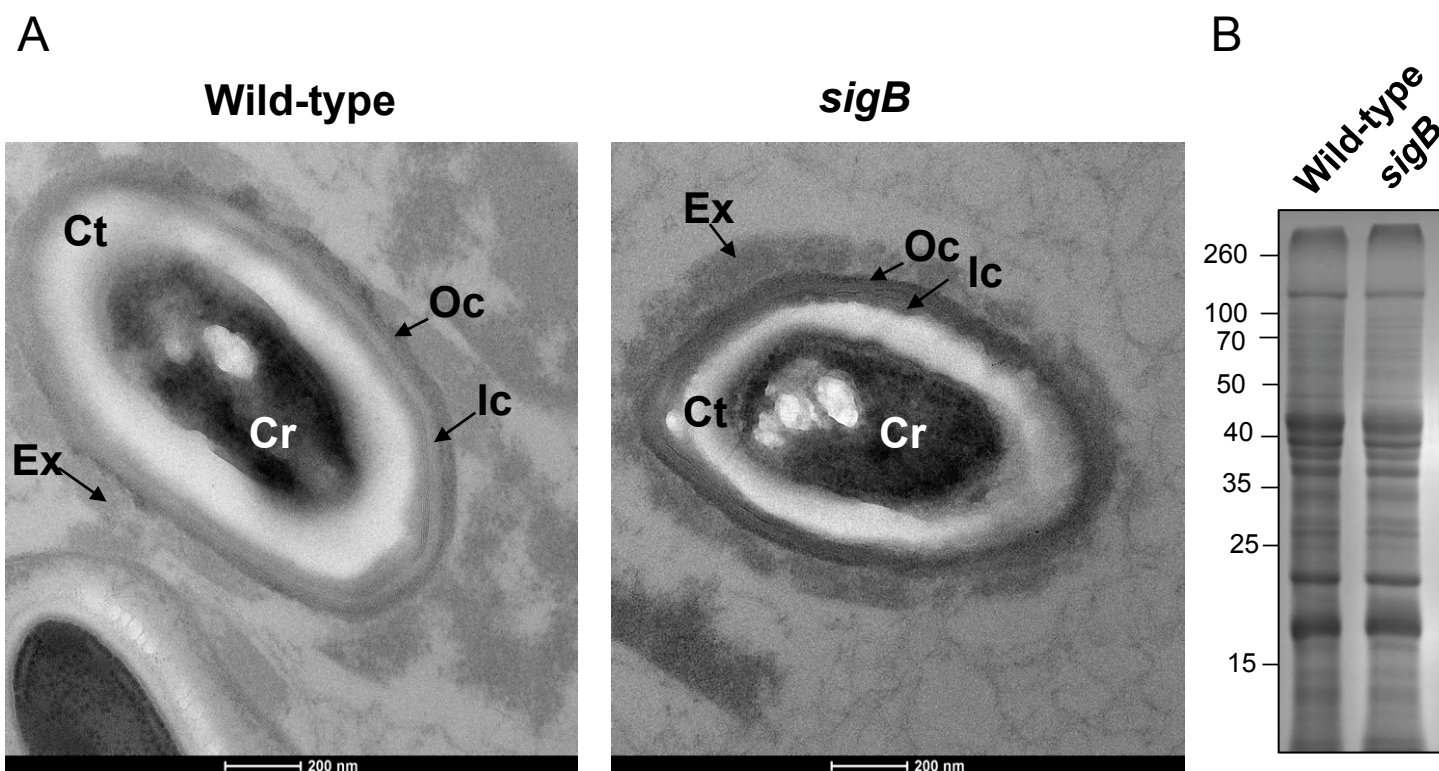


Figure 54: Wild-type and *sigB* mutant spores. A) Morphology of the spores of the wild-type and *sigB* mutant. Thin sections of the spores were analysed using TEM as described in the Material and Methods. Ex, exosporium, Oc, outer coat, Ic, inner coat, Ct, cortex, Cr, core. Scale bars are shown in each figure. B) Coat/exosporium extracts from purified spores of the wild-type and the *sigB* mutant strains were loaded on acrylamide gel and stained with Coomassie brilliant blue.

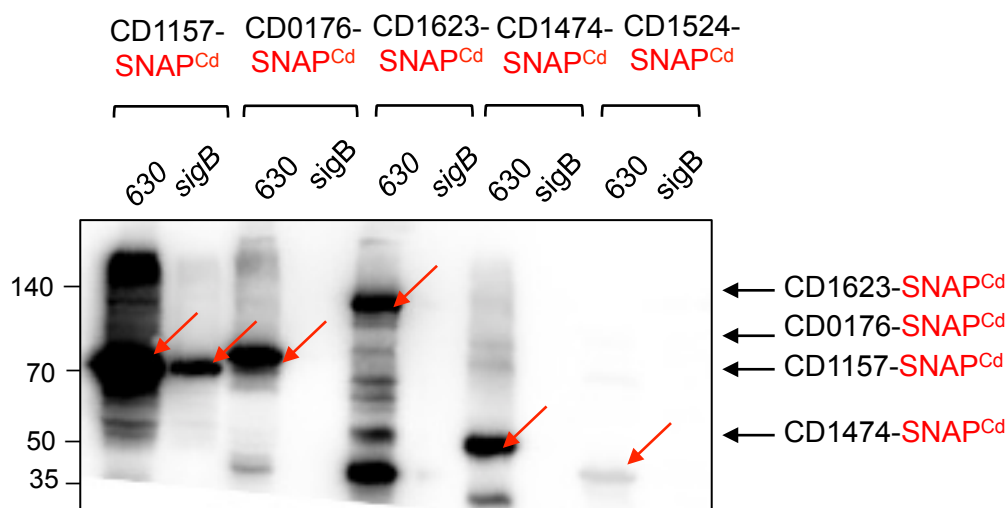


Figure 55: Detection of proteins produced under the control of σ^B in the coat extract. Western blot analyses of coat/exosporium from the wild-type and *sigB* mutant strain carrying a CD1157-, CD0176-, CD1623-, CD1474- or CD1524-SNAP^{Cd} fusion.

strain and the mutant were analysed using mass spectrometry. This analysis revealed that the abundance of proteins previously found at the spore surface layers whose synthesis is under the control of σ^B , decreased in the *sigB* mutant spores compared with the wild-type strain (Table 2). For instance, the abundance of the revRbrs CD1474 and CD1524 and the FDP CD1623 was around 8-, 3- and 4- fold reduced, respectively, in the *sigB* mutant. The abundance of the oxidoreductase CD0176 also decreased 7-fold in the coat extract of the *sigB* mutant. The nitroreductase CD1125, produced under the control of σ^B , was also present at a reduced level in the coat extract of this mutant. In contrast, some proteins, such as the Rbr CD2845, were detected in a higher abundance in the coat extract of the *sigB* mutant compared to the wild-type strain. The *CD2845* gene is controlled by the late FS sigma factor σ^G (Table 2). Except for CD2845, we did not observe differences in the abundance of other spore coat proteins. We noted that contrary to other proteomic studies on *C. difficile* spores, we detected the FDP CD1157 in the coat extract of the wild-type strain. Moreover, no significant differences were observed in the abundance of this protein in the coat extract of the *sigB* mutant compared to the wild-type and strain (Table 2).

In order to confirm the localization of some of the proteins in the spore surface layers, we constructed C-terminal SNAP-tag translational fusions with some σ^B -controlled genes. These fusions were introduced into the wild-type and *sigB* mutant strains. Spores carrying the translational fusions were purified. The spore coat/exosporium was extracted in order to be analysed by Western blotting using an antibody raised against the SNAP protein. We have thus confirmed the presence of the revRbrs, CD1474 and CD1524, the FDP CD1623 and the OR CD0176 at the spore surface layers of the wild-type strain while these protein fusions were not detected in the coat/exosporium extract of the *sigB* mutant (Figure 55). The FDP CD1157 was detected in both wild-type and *sigB* mutant in agreement with the data of the proteome of the spore surface (Figure 55). However, a decreased amount of CD1157 was observed in the spore surface layers of the *sigB* mutant background in agreement with the expression of the *CD1157* gene under the dual control of a σ^A - and a σ^B -dependent promoter. Further experiments will be required in order to determine the role of these proteins in the spore and to decipher the molecular mechanisms involved to restrict the activity of σ^B in the MC compartment at late stages of sporulation.

Table 2. Comparative analysis of the spore coat/exosporium proteome from the wild-type and the *sigB* mutant. Relevant proteins are indicated with an asterisk.

Protein (Gene)	MW [kDa]	Function	Fold-change (WT/ <i>CD1065</i>)	-LOG(p-value)	Know/predicted σ factor needed for expression
Down in the <i>sigB</i> mutant					
CD0174	68.1	Carbon monoxide dehydrogenase cooS	12.4	6.4	σ^B
CD0175	17.8	oxidoreductase, Fe-S subunit	6.6	3.8	σ^B
CD0176*	45.7	Oxidoreductase, NAD/FAD binding subunit	7.1	2.3	σ^B
CD1125*	32.7	Nitroreductase-family protein	4.6	3.8	σ^B
CD1474*	20.0	Reverse Rubrerythrin	7.6	4.6	σ^B
CD1524*	20.0	Reverse Rubrerythrin	2.6	2.3	σ^B
CD1623*	94.3	Oxidoreductase	4.3	6.0	σ^B
CD2373	53.0	Carbon starvation protein	3.2	3.4	σ^B
CD2820	17.7	Hypothetical protein	4.6	2.1	
CD2996	27.4	Hypothetical protein	3.4	2.8	
CD3614	24.0	Hypothetical protein	4.1	1.8	
CD1176	6.5	Uncharacterized protein	3.9	2.0	
CD1404	66.6	Oligopeptide transporter	3.5	3.8	
CD1479	78.2	Ferrous iron transport protein B	3.8	4.3	
Up in the <i>sigB</i> mutant					
CD1396	29.7	Amino acid amidase	0.1	3.7	
CD1543	8.1	FMN-dependent NADH-azoreductase	0.1	2.5	σ^G
CD2575	24.2	Ribulose-phosphate 3-epimerase	0.2	2.3	
CD2841	60.2	Putative amidohydrolase	0.3	2.4	σ^B
CD2845*	22.4	Rubrerythrin	0.3	2.5	σ^G
CD3490	88.5	Stage II sporulation protein E SpoIIE	0.4	3.3	σ^A

CD3499	20.0	Stage V sporulation protein T SpoVT	0.3	2.8	σ^G
CD1796	34.4	Nitrite and sulfite reductase subunit	0.3	2.5	σ^A
CD0275	39.9	Accessory gene regulator agrB	0.3	2.0	
CD0684	52.3	ATP-dependent peptidase	0.2	1.6	σ^B
CD1698	44.9	Riboflavin biosynthesis protein	0.1	4.2	
CD1700	41.2	Riboflavin biosynthesis protein	0.4	4.5	
CD1914	32.1	ethanolamine ammonia-lyase small subunit	0.4	2.8	
CD2156	52.1	Thiamine biosynthesis protein ThiH	0.3	3.7	
CD2934	14.8	Hypothetical protein	0.3	3.3	
CD2936	38.6	Hypothetical protein	0.1	3.2	
CD2945	19.2	Phage protein	0.1	4.0	
CD2947	8.2	Hypothetical protein	0.1	2.2	
CD3010	47.7	Cytochrome C assembly protein	0.4	2.7	
CD3033	12.0	Thioredoxin	0.04	4.2	

Materials and methods

Bacterial strains and growth conditions

The bacterial strains used in this study are listed in Table S1. *E. coli* strains were grown in LB broth (1% bacto-tryptone, 0.5% yeast extract, and 0.5% NaCl, pH 7.0) or in M9 minimal medium. When indicated, ampicillin (100 µg/ml), chloramphenicol (15 µg/ml) or kanamycin (30 µg/ml) was added to the culture medium. *C. difficile* strains were grown anaerobically (5% H₂, 5% CO₂ and 90% N₂) at 37°C in brain heart infusion (BHI) medium (Difco), in TY (Bacto tryptone 30 g.l⁻¹, yeast extract 20 g.l⁻¹, pH 7.4) or in *C. difficile* minimal medium (CDMM). For solid media, agar was added to a final concentration of 17 g.l⁻¹. Sporulation assays were performed in sporulation medium (SM) (Wilson et al. 1982). To produce spores, we used an SMC medium containing (per liter): 90 g of Bacto peptone (Bacto™ 211677), 5 g of Proteose peptone (82450, Sigma-Aldrich), 1 g of (NH₄)₂SO₄ and 1.5 g of Tris. When necessary, cefoxitin (25 µg/ml), thiamphenicol (15 µg/ml) and erythromycin (2.5 µg/ml) were added to the *C. difficile* cultures. All the primers used in this study are listed in Table S2.

Construction of *C. difficile* strains

The $\Delta CD2399$, $\Delta CD1474$, $\Delta CD1524$ and $\Delta CD1623$ knock-out mutants were obtained using the *codA*-mediated allele exchange method (Cartman et al. 2012, Peltier et al. 2015). Briefly, for all these genes, 1.5 kb fragments located upstream and downstream of the gene to be deleted were PCR amplified from 630 Δerm genomic DNA using primers CF14/CF15 and CF16/CF17, IMV917/NK70 and NK71/IMV918, IMV919/NK64 and NK65/IMV920, IMV914/NK58 and NK59/IMV915 (Table S2) for $\Delta CD2399$, $\Delta CD1474$, $\Delta CD1524$ and $\Delta CD1623$, respectively. Purified PCR fragments were introduced into the pMTLSC7315 plasmid using BamHI and XhoI restriction sites in case of $\Delta CD2399$, and using the Gibson Assembly® Master Mix (Biolabs) for the other genes. The sequences of the resulting plasmids were verified by sequencing. The plasmids obtained were introduced in HB101/RP4 *E. coli* strain allowing the transfer by conjugation into the *C. difficile* 630 Δerm strain. Transconjugants were selected on BHI plates supplemented with Tm and *Clostridium difficile* selective supplement (SR0096, Oxoid). Isolation of faster growing single-crossover integrants was performed by serial restreaking on BHI plates supplemented with Cfx and Tm. Single-crossover integrants were then restreaked on CDMM plates supplemented with fluorocytosine

(50 µg/ml) allowing the isolation of double crossover events (Cartman et al. 2012). To confirm the plasmid loss, fluorocytosine resistant clones were restreaked on BHI plates supplemented with Cfx and Tm. The Tm sensitive clones were checked by PCR for the presence of the expected deletion (Figure S1). Steps in *C. difficile* were repeated in each different mutant in order to generate double-mutants, CDIP714 for the two revRbrs and CDIP1370 for the two FDPs (Table S1).

The ClosTron gene knockout system (Heap et al. 2007, Heap et al. 2009) was used to inactivate the *CD1157* gene in 630 Δ *erm*, yielding strain 630 Δ *erm* *CD1157::erm* (CDIP588). We designed with the Targetron design software (Sigma-Aldrich) primers to retarget the group II intron of pMTL0007 to insert into the *CD1157* gene in sense orientation immediately after the 225th nucleotide in the coding sequence (Table S2). The PCR product generated by overlap extension was cloned between the HindIII and BsrG1 sites of pMTL007 to obtain pDIA6374. *E. coli* HB101(RP4) containing pDIA6374 was mated with *C. difficile* 630 Δ *erm*. *C. difficile* transconjugants were selected by sub-culturing on BHI agar containing Tm and Cfx and then plated on BHI agar containing Erm. Chromosomal DNA of transconjugants was isolated as previously described (Antunes et al. 2011). PCR was realized to verify the integration of the intron into the *CD1157* gene and the splicing of the group I intron from the group II intron after integration (Figure S1).

To complement *CD2399*, *CD1474* and *CD1524*, both the promoter region and the open reading frame of the corresponding gene were amplified by PCR using pairs of oligonucleotides, CF117/CF118, CF115/CF116, CF113/ CF114 for *CD2399*, *CD1474* and *CD1524*, respectively. The PCR products were cloned into pMTL84121 to produce pDIA6534, pDIA6538 and pDIA6537 (Table S1). *E. coli* HB101 (RP4) strain containing each plasmid was mated with every single or double mutant (Table S1). For *CD2399* complementation, the plasmid was transferred by conjugation into *C. difficile* Δ *CD2399* (Table S1).

Bacterial adenylate cyclase two hybrid system (BACTH) and β -galactosidase assays

Protein-protein interactions were analysed using the BACTH system (Euromedex). All the procedures for plasmid constructions and *E. coli* co-transformations were performed according to the manufacturer's instruction. Briefly, this system is based on the catalytic domain of the adenylate cyclase from *Bordetella pertussis* (CyA) that is composed of two

different fragments, T25 and T18. When T25 and T18 are separated, CyA is not active. However, when these fragments are fused with interacting proteins, the heterodimerization of these hybrid proteins allows a functional complementation and so the production of cyclic AMP (cAMP) leading to *lacZ* gene expression. The open reading frames of *cotL*, *sipL*, *cotB*, *cotA*, *cotE* and *cdeC* were cloned into plasmids containing T18 or T25 either in C-terminal or N-terminal position. The BTH101 *E. coli* strain was co-transformed by the different combinations of T18 and T25 fusion plasmids (Table S1). Co-transformation with the T25 and T18 expressing plasmids was used as control for the basal β -galactosidase activity. The β -galactosidase activity was measured after an overnight culture of co-transformants in the presence of 0.5 mM of IPTG (isopropyl- β -D-thiogalacto-pyranoside). 100 μ l of overnight cultures was mixed with 500 μ l of Z buffer (Na_2HPO_4 0.06 M, NaH_2PO_4 0.04 M, KCl 0.01M, MgSO_4 0.001 M, DTT 0.001 M and SDS 0.0037%) and 400 μ l of M63 medium. After addition of 20 μ l of chloroform, the tubes were mixed for 10 s. The tubes were pre-incubated 5 min at 28 °C and 200 μ l ONPG (4 mg.ml⁻¹) was added. When the yellow coloration appeared, 500 μ l of Na_2CO_3 (1 M) was added to the tube to stop the reaction. After centrifugation to eliminate cells fragments, the supernatants were recovered to measure the OD_{420nm}. β -galactosidase activity was quantified as Miller unit [1000 x (OD_{420nm}/(time of incubation (min) x volume of extract (ml) x OD_{600nm} of the overnight culture)].

His-tag pull down assays

To construct the different plasmids, fragments were amplified from chromosomal DNA. For His-tagged protein construction, the fragments were cloned into petDuet using EcoRI and NotI restriction enzyme sites. For untagged proteins the fragments were cloned using Nde and XhoI (Table S2). Ligation products were transformed into NEB and confirmed by sequencing. The resulting plasmids were transformed into BL21 (DE3) cells for protein production. *E. coli* BL21 (DE3) strains (see Table S1) were grown to mid-log phase in 2YT (5 g NaCl, 10 g yeast extract, and 15 g tryptone per liter), induced with IPTG, and grown overnight at 19°C. Cultures were pelleted, resuspended in lysis buffer (300 mM NaCl, 50 mM Na_2HPO_4 pH 8), and lysed by freeze-thawing and sonication. Cell extracts were batch affinity purified using Co^{2+} affinity resin (TALON resin, Clontech Laboratoires) and eluted by using imidazole buffer (300 mM NaCl, 50 mM Na_2HPO_4 pH 8, 250 mM imidazole). The resulting eluates were resolved by SDS-PAGE (12%) and visualized by Coomassie brilliant blue R-250 staining (Bio-Rad) or transferred onto a PVDF membrane for Western blot analysis, as

described above.

Transcriptional SNAP^{Cd} fusions

To construct SNAP transcriptional fusions, we used pFT47, a pMTL84121 plasmid derivative containing a synthetic SNAP^{Cd} sequence (Pereira et al. 2013, Cassona et al. 2016). To construct a *sigB*-SNAP^{Cd} transcriptional fusion, pDIA6325 used for *sigB* complementation containing both the sequence located upstream of *CD0007* (position -120 to +50 from the TSS) and the *sigB* gene was digested by XhoI and StuI to remove the *sigB* gene and keep the σ^A -dependent promoter present upstream of *CD0007*. The SNAP^{Cd} gene was PCR amplified using pFT47 DNA and primers pairs NK155/NK156. The DNA fragment was digested by DpnI to remove the pFT47 plasmid trace and inserted between the XhoI and StuI sites of pDIA6325 to obtain pDIA6589. The resulting plasmid was then transferred into the 630 Δ *erm* strain and the *sigB* mutant.

To construct the transcriptional SNAP^{Cd} fusion with the complete promoter region of *CD1157*, a fragment (position -308 to +114 from the start codon) was amplified using genomic DNA and the primer pair IMV949/IMV950 to produce a 423 bp PCR product. The DNA fragment was inserted between the EcoRI and XhoI sites of pFT47 to obtain pDIA6517. To construct the fusion bearing only the σ^A - or the σ^B -dependent promoter, promoters regions of *CD1157* (position -308 to -64 and -104 to +114 from the start codon) were amplified with IMV949/IMV977 and IMV976/IMV950, respectively. The DNA fragments were then introduced between the EcoRI and XhoI sites of pFT47 yielding pDIA6670 and pDIA6669 for σ^A - or the σ^B -dependent promoter, respectively. To construct the *CD1474*-, the *CD1524*- and the *CD1623*- transcriptional SNAP^{Cd} fusions, the promoter regions (-206 to +19, -190 to +30 and -202 to +14 from the transcriptional start site) were amplified using primer pairs CF19/CF20, CF23/CF24 and CF21/CF22 to generate a 225 bp, a 221 bp and a 216 bp PCR product, respectively. The DNA fragment was then inserted into pFT47 between the EcoRI and XhoI sites to obtain pDIA6457, pDIA6459 and pDIA6458. To construct the *CD0176*-transcriptional SNAP^{Cd} fusion, the promoter region (-248 to -23 from the ATG start codon upstream of the first gene of the operon *CD0174*) was amplified using the primer pairs CF25/CF26 to generate a 231 bp PCR product. The DNA fragment was then inserted into pFT47 between the EcoRI and XhoI sites to obtain pDIA6460. The sequence of the inserts was checked by sequencing. The plasmids were introduced into *E. coli* HB101 (RP4) and then transferred by conjugation into *C. difficile* 630 Δ *erm* strain and the *sigB* mutant (Table S1).

Translational SNAP^{Cd} fusions

To obtain C-terminal SNAP-tag translational fusions, we used pFT58 (Pereira et al. 2013, Cassona et al. 2016). pFT58 digested with EcoRI was amplified by inverse PCR using CF95/CF96. The promoter and coding regions of *CD1474*, *CD1157* or *CD1623* were amplified from genomic DNA using primer pairs CF99/CF100, CF107/CF108 and CF101/CF102. For *CD0176*-SNAP translational fusion, the promoter was amplified using CF103/CF104 and the *CD0176* coding sequencing with CF105/CF106. The PCR products were inserted into pFT58 using Gibson Assembly yielding pDIA6497, pDIA6498, pDIA6499 and pDIA6503. The inserts of these plasmids were verified by sequencing. Plasmids were introduced in *E. coli* HB101 (RP4) and transferred to *C. difficile* 630 Δ *erm* and *sigB* mutant strains by conjugation (Table S1).

Fluorescence microscopy and image analysis

For SNAP labelling, the TMR-Star substrate (New England Biolabs) was added to the cells at a final concentration of 250 nM, and the mixture was incubated for 30 min in the dark. After labelling, the cells were collected by centrifugation (4000xg for 3 min at room temperature), washed 3 times with 1 ml of PBS, and finally resuspended in 1 ml of PBS containing or lacking the membrane dye Mitotracker Green (MTG; 0.5 μ g/ml) (Molecular Probes, Invitrogen). For phase-contrast and fluorescence microscopy, spores or cells were mounted on 1.7% agarose-coated glass slides to keep the cells immobilized and to obtain sharper images (Glaser *et al.*, 1997). The images were taken with exposure times of 200 ms for MTG and 600 ms for SNAP. Cells were observed using a Nikon Eclipse TI-E microscope 60x Objective and captured with a CoolSNAP HQ2 Camera. The images were analysed using ImageJ.

Spore production and sporulation tests

SMC liquid medium inoculated with *C. difficile* was incubated overnight at 37°C. A sample (200 μ l) of this culture was plated in SMC agar and incubated at 37°C for 7 days. Spores scraped off with water were incubated for 7 days at 4°C. Cell fragments and spores were separated by centrifugation using a HistoDenz gradient (Sigma-Aldrich) (Dembek et al. 2013). Suspensions (>99% of spores) are free of vegetative cells, sporulating cells and cell debris as determined by phase-contrast microscopy. The spore suspension was quantified by measuring the OD_{600nm}.

Overnight cultures grown at 37°C in BHI were used to inoculate SM media at a dilution of 1:200. At specific time points, 1 ml of culture was withdrawn, serially diluted in BHI and plated before and after heat treatment (30 min, at 60°C), in order to determine the total and heat-resistant colony forming units (CFU). Samples were plated onto BHI supplemented with 0.1% TA (Sigma-Aldrich) to promote efficient spore germination (Wilson et al. 1982).

Germination assay

Approximately 10^8 spores (equivalent of 0.4 OD_{600nm} units) were resuspended in 200 µl of water. The spore suspension was heat-treated at 65°C during 10 min, and serial dilutions were plated on BHI containing 0.1% TA to determine the number of spores that are able to germinate. The CFU were monitored 24 h and 48 h after plating. At least three biological replicates were performed using at least two independent spore preparations. The germination of the spores was also monitored by OD_{600nm} (Donnelly et al. 2016) and by phase-contrast microscopy (Kong et al. 2011). Spores resuspended in BHI were exposed to 1% TA, and the OD_{600nm} was measured every 5 min for 1 h. For the phase-contrast microscopy, purified spores were resuspended to an OD_{600nm} of 0.4 in BHI containing 1% TA and incubated under anaerobic conditions for 4 h at 37°C. At each time point, samples were pelleted by centrifugation, washed with PBS and fixed with 2% paraformaldehyde for 15 min at room temperature. Fixed samples were washed with PBS once more and dried onto glass slides. Phase-contrast microscopy was conducted using an Axioskop microscope (Zeiss) with a 100X oil immersion lens. The images were captured using an Axiocam 105 colour (Zeiss).

Spore resistance treatments

Lysozyme resistance of spores was measured by suspending 10^8 spores in 200 µl of PBS in the presence of 250 µg/ml of lysozyme. Ethanol resistance of spores was measured by resuspending the spores in 200 µl of 70% ethanol. Heat resistance of *C. difficile* spores was determined at 80°C. For each condition, spores were incubated for 1 h at 37°C with shaking (300 rpm), and the samples were plated onto BHI agar containing 0.1% TA and incubated anaerobically for 24 h at 37°C.

Transmission electron microscopy

To analyse the ultrastructure by TEM, purified spores were fixed with 2.5% of glutaraldehyde (Sigma Aldrich) in 0.1 M HEPES (4-(2-hydroxyethyl)-1-piperazineethanesulfonic acid), pH 7.2. Post fixation was conducted with 1% osmium

tetroxide (Merck) and 1.5% ferro-cyanide (Sigma Aldrich) in 0.1 M HEPES. After dehydration by a graded series of ethanol, spores were infiltrated with epoxy resin. Seventy-nanometer sections were collected on formvar coated slot grids (EMS) and were contrasted with 4% uranyl acetate and Reynolds lead citrate. The stained sections were observed using a Tecnai spirit FEI operated at 120 kV. The images were acquired using an FEI Eagle digital camera.

Coat extraction and Western blot analysis

To analyse the profile of the coat and exosporium proteins, *C. difficile* spores were resuspended in extraction buffer (0.125 mM Tris-HCl, 5% β -mercaptoethanol, 2% SDS, 0.5 mM dithiothreitol (DTT) and 5% glycerol, pH 6.8) containing 0.025% bromophenol blue and boiled as previously described (Costa et al. 2006). For vegetative and sporulating cells, whole cell lysates were prepared as described previously (Fagan and Fairweather 2011). Briefly, sporulating cultures of *C. difficile* were harvested by centrifugation at 5000 rpm for 10 min at 4°C, and the pellets were frozen at -20°C. The bacteria were thawed and resuspended in PBS containing 0.12 μ g/ml of DNase I to an OD_{600nm} of 40. An equal volume of 2X extraction buffer containing 0.025% bromophenol blue was added to the protein samples (Laemmli 1970), which were resolved by SDS-PAGE and visualized by Coomassie brilliant blue R-250 staining (Bio-Rad). Proteins were transferred to a PVDF membrane (0.45 μ m) and subjected to immunoblot analyses as described previously (Serrano et al. 1999). Rabbit polyclonal antibodies raised against CspC (1:2000), CspBA (1:2500), SleC (1:5000) (Adams et al. 2013), CdeM (1:40000) (A. O. Henriques), CdeC (1:1000), CotB (1:5000), CotE (1:1000), SipL (1:2500) (Putnam et al. 2013) and anti-SNAP (1:1000) (NEB) were used. Anti-rabbit or anti-mouse secondary antibodies conjugated to horseradish peroxidase (Sigma) were used at a 1:5000 dilution. Immunoblots were developed with enhanced chemiluminescence reagents (Thermo Scientific).

Mass spectrometry of the spore coat and exosporium layers

C. difficile spores were resuspended in extraction buffer and boiled as previously described (Costa et al. 2006). Coat and exosporium proteins were recovered by centrifugation and precipitated with 10% TCA. Protein pellets were resuspended in urea 8 M and NH₄HCO₃ 100 mM and sonicated on ice. Subsequently, 50 μ g of total proteins were reduced with TCEP 10 mM (646547 - Sigma) for 30 min and then alkylated with iodoacetamide 20 mM (I114 -

Sigma) for 1 h. Proteins were digested with rLys-C 1 μg (V1671, Promega) for 4 h at 37°C and then digested with trypsin 1 μg (V5111, Promega) overnight at 37°C. The digestion was terminated with formic acid 4%, and the peptides were desalted using a C18 Sep-Pak Cartridge (WAT054955, Waters). The peptides were eluted successively with 50% Acetonitrile (ACN)/0.1% Formic acid (FA) and 80% ACN/0.1% FA before being dried in a vacuum centrifuge. The peptides were resuspended in 2% ACN /0.1% FA.

For LC-MS/MS analysis, a nanochromatographic system (Proxeon EASY-nLC 1000, Thermo Fisher Scientific) was coupled online to a Q ExactiveTM HF Mass Spectrometer (Thermo Fisher Scientific). For each sample, 1 μg of peptides was injected onto a 50-cm homemade C18 column (1.9 μm particles, 100 Å pore size, ReproSil-Pur Basic C18, Dr. Maisch GmbH) and separated with a multi-step gradient from 2 to 45% ACN in 105 min at a flow rate of 250 nl/min over 132 min. The column temperature was set to 60°C. The data were acquired as previously described (Lago et al. 2017).

Raw data were analyzed using MaxQuant software version 1.5.1.2 (Cox and Mann 2008) and the Andromeda search engine (Cox et al. 2011). The MS/MS spectra were searched against an internal *C. difficile* database containing 3 957 proteins, and the contaminant file included in MaxQuant. The database search parameters were fixed as described (Lago et al. 2017). Output proteinGroup file was integrated into Perseus (Tyanova et al. 2016) to perform data filtering and statistical tests. First, contaminants, reverse identifications and proteins only identified by site were excluded. A protein filtering was set for the validation process such as a protein was integrated in the final list only if this one was identified in at least two replicates of a condition. Second, LFQ intensities were log₂ transformed and missing values were imputed and replaced by random Log₂ LFQ intensities that are drawn from a normal distribution at the low detection level. Third, a two-sided T-tests of the Log transformed LFQ intensities with a permutation-based FDR calculation at 5% and S₀=0.5 (Tusher et al. 2001) were applied to determine statistically significant proteins.

Protein expression and purification

The coding region of CD1474 and CD1524 were PCR amplified using genomic DNA and primer pairs IMV970/IMV971 and IMV968/IMV969 to produce a 540 bp PCR product. The resulting PCR products were cloned into pET20 (Novagen) yielding pDIA6635 and pDIA6671. The amino acid sequence of CD1157 was used to synthesize its encoding gene at GenScript Inc. USA, codon optimized for expression in *E. coli*. The sequence was cloned into pET24a (Novagen). After verification by sequencing, the plasmids were introduced in *E. coli*

BL21 (DE3). These strains were used for overexpression of the respective proteins. Overexpression of CD1524, CD1474 and CD1157 was performed by growing the strains aerobically at 37 °C at 150 rpm in M9 minimal medium, with 20 mM glucose, 0.1 mM FeSO₄, and 100 µg/ml ampicillin (for CD1474 and CD1524), or 50 µg/ml kanamycin (for CD1157) until an optical density at 600 nm of approximately 0.4 was reached. At that time, 0.1 mM of FeSO₄ was added and protein expression was induced either by 1 mM of IPTG for *CD1524* and *CD1474* or 100 µM for *CD1157*. After 6 h of growth at 30°C, cells were harvested by centrifugation, resuspended in a buffer containing 20 mM (Tris)-HCl (pH 7.5) and stored at - 20 °C. Cells were disrupted by at least 3 cycles in a French Press apparatus at 16.000 psi (Thermo) in the presence of DNase (Applichem). The crude extract was cleared by low-speed centrifugation at 25.000xg for 25 min and then at 138.000xg for 1 h 30 min at 4 °C to remove cell debris and membrane fraction, respectively. The soluble extract was dialyzed overnight at 4 °C against buffer A (20 mM Tris-HCl, pH 7.5, 18% Glycerol) and was subsequently loaded onto a Q-Sepharose Fast Flow column (65 mL, GE Healthcare) previously equilibrated with buffer A. Proteins were eluted with a linear gradient from buffer A to buffer B (buffer A containing 500 mM NaCl). The eluted fractions were followed throughout the purification process by SDS-PAGE and UV-visible spectroscopy. Fractions containing the desired protein were pooled and concentrated. For CD1474 and CD1524, the concentrated fraction was then loaded onto a size exclusion Superdex S75 column (330 ml, GE Healthcare), equilibrated with buffer A containing 150 mM NaCl. The fractions containing the protein were pooled and concentrated. For the CD1474, the last fraction was loaded onto a Fractogel column (20 ml, Merck Millipore), previously equilibrated with buffer A and eluted with a linear gradient from buffer A to buffer B. After purification, CD1157 was incubated overnight at 4°C in the presence of 1 mM of flavin mononucleotide (FMN) and subsequently applied onto a PD-10 desalting column to eliminate unbound FMN. Fractions containing purified proteins were verified by SDS-PAGE (Figure 44).

Protein, metal and flavin quantification

Purified protein samples were quantified using the Bicinchoninic Acid Kit (Thermo) and bovine serum albumin as standard. Iron content was determined by the phenanthroline colorimetric method. Protein samples were incubated for 15 min with 1 M HCl and for further 30 min with 10% trichloroacetic acid at room temperature, centrifuged at 5,000 g for 20 min and neutralized with the addition of 15% of ammonium acetate. Samples were then incubated

with 10% hydroxylamine and 0.3% 1-10-phenanthroline. The absorbance spectrum was measured, and iron content quantified using $\epsilon_{510\text{nm}} = 11.2 \text{ mM}^{-1}\cdot\text{cm}^{-1}$. The flavin type was analysed as previously described (Folgoša et al. 2018b).

Oligomeric State Determination

The oligomeric state of the proteins was determined by size exclusion chromatography. Proteins were loaded onto a 25 ml Superdex S200 10/300 GL column (GE Healthcare), previously equilibrated with buffer A containing 150 mM NaCl. We used as standards a mixture containing aldolase (158 kDa), ferritin (440 kDa), conalbumin (75 kDa), carbonic anhydrase (29 kDa) and cytochrome c (12.4 kDa), and dextran blue (2000 kDa) as void volume marker.

Redox titrations

The diiron center of CD1157, CD1524 and CD1474, and the corresponding reduction potentials were investigated by EPR spectroscopy, using a Bruker EMX spectrometer equipped with an Oxford Instruments ESR-900 continuous flow helium cryostat, and a high sensitivity perpendicular mode rectangular cavity. The reduction potentials of the FMN from CD1157, and of the rubredoxin domain from the revRbr were determined by redox titrations monitored by visible absorption spectroscopy, in a Shimadzu UV-1603 spectrophotometer. Protein samples (30 μM in buffer C, 50 mM Tris-HCl, pH 7.5 and 18% glycerol) were anaerobically titrated, inside an anaerobic chamber (Coy Lab Products), by stepwise addition of a buffered sodium dithionite solution in the presence of a mixture of redox mediators (1 μM each): 1,2-naphthoquinone-4-sulfonic acid ($E'^{\circ} = +215 \text{ mV}$), trimethylhydroquinone ($E'^{\circ} = +115 \text{ mV}$), 1,4-naphthoquinone ($E'^{\circ} = +60 \text{ mV}$), menadione ($E'^{\circ} = 0 \text{ mV}$), plumbagin ($E'^{\circ} = -40 \text{ mV}$), indigo trisulfonate ($E'^{\circ} = -70 \text{ mV}$), indigo disulfonate ($E'^{\circ} = -110 \text{ mV}$), 2-hydroxy-1,4-naphthoquinone ($E'^{\circ} = -152 \text{ mV}$) and anthraquinone-2-sulfonate ($E'^{\circ} = -225 \text{ mV}$). A combined Pt electrode (Ag/AgCl in 3.5 M KCl, as reference) was used and calibrated at 20°C against a saturated quinhydrone solution (pH 7). The reduction potentials are reported with the standard hydrogen electrode as a reference. All experimental data was manually adjusted to appropriate Nernst equations as described in the Results section: monoelectronic Nernst equations for the rubredoxin site, and Nernst equations for two consecutive monoelectronic transitions for the flavins, weighted according to the relative absorption intensities and concentrations of each cofactor.

Oxygen tolerance assays

O₂ tolerance assays were performed as indicated below. Five microliters of different serial dilutions (from 10⁰ to 10⁻⁵) of *C. difficile* strains grown for 7 h in the TY medium were spotted on TY plates supplemented with 0.05% of taurocholate. Plates were then incubated in the presence of different O₂ tensions while a control plate was incubated in anaerobiosis. The last dilution allowing growth was recorded after incubation at 37°C for 64 h.

Spectrophotometric measurements of the H₂O₂ reductase activity

Because the physiological electron donor to the *C. difficile* CD1524, CD1474 and CD1157 is unknown, we used an artificial electron-donating system: a mixture of a NADH:rubredoxin oxidoreductase (NROR) and a rubredoxin from *E. coli*. The *E. coli* proteins were purified as previously described (Gomes et al. 2000, Vicente et al. 2007). The enzymatic activity for H₂O₂ was determined by UV-Visible spectroscopy, inside an anaerobic chamber (Coy Lab Products). The assays were performed in buffer C. The reaction was monitored at 340 nm, observing the NADH consumption ($\epsilon_{340} = 6220 \text{ mM}^{-1} \text{ cm}^{-1}$). A mixture of buffer, 200 μM of NADH, NROR, rubredoxin and each protein of interest was prepared inside a cuvette, after which the reaction was initiated by the addition of H₂O₂. Concentrations of CD1524, CD1474 or CD1157 were 0.03 μM , 0.1 μM and 1 μM respectively.

Measurement of O₂ reductase activity

The O₂ reductase activity of the proteins was measured amperometrically with Clark-type electrodes selective for O₂ (Oxygraph-2K, Oroboros Instruments, Innsbruck, Austria). The assays were performed in buffer C. The O₂ reductase activity was evaluated at 25 °C in air equilibrated buffer (~250 μM of O₂), in the presence of 5 mM NADH, NROR (810 nM) and rubredoxin (5 μM) from *E. coli*. The reaction was initiated by addition of CD1524 or CD1474 (0.1 μM) or CD1157 (1 μM). Assays were performed in the presence of catalase (640 nM) and superoxide dismutase (240 nM).

Supplementary tables and figures

Table S1. Bacterial strains and plasmids used in this study.

Strains	Genotypes	Origin
<i>E. coli</i>		
10-beta	<i>F⁻ mcrA D(mrr-hsdRMS-mcrBC) f80lacZDM15 DlacX74 deoR, recA1 araD139 D(ara-leu)7697 galK rpsL(Str^R) endA1 nupG</i>	NEB
HB101 (RP4)	<i>supE44 aa14 galK2 lacY1 D(gpt-proA) 62 rpsL20 (Str^R) xyl-5 mtl-1 recA13 D(mcrC-mrr) hsdS_B(r_B⁻m_B⁻) RP4 (Tra⁺ IncP Ap^R Km^R Tc^R)</i>	Laboratory stock
BTH101	<i>F⁻ cya-99 araD139 galE15 galK16 rpsL1 (Str^R) hsdR2 mcrA1 mcrB1</i>	Euromedex®
BL21 (DH3)	<i>fhuA2 (lon) ompT gal (λ DE3) (dcm) ΔhsdS λ DE3= λ sBamHlo ΔEcoRI-B int:::(lacI::PlacUV5::T7 gen1) i21 Δnin5 / E.coli</i> strain for T7 expression, protease deficient B strain	NEB
ECO501	BTH101 + pKNT25 + pUT18	This work
ECO831	BL21 (DE3) pET20- <i>CD1474</i>	This work
ECO860	BL21 (DE3) pET20- <i>CD1524</i>	This work
ECO949	BTH101 + pUT18- <i>cotL</i> + pKNT25- <i>sipL</i>	This work
ECO950	BTH101 + pUT18- <i>cotL</i> + pKT25- <i>sipL</i>	This work
ECO951	BTH101 + pUT18C- <i>cotL</i> + pKNT25- <i>sipL</i>	This work
ECO952	BTH101 + pUT18C- <i>cotL</i> + pKT25- <i>sipL</i>	This work
ECO953	BTH101 + pKNT- <i>cotL</i> + pUT18- <i>sipL</i>	This work
ECO954	BTH101 + pKNT- <i>cotL</i> + pUT18C- <i>sipL</i>	This work
ECO955	BTH101 + pKT- <i>cotL</i> + pUT18- <i>sipL</i>	This work
ECO956	BTH101 + pKT- <i>cotL</i> + pUT18C- <i>sipL</i>	This work
ECO957	BTH101 + pUT18- <i>cotL</i> + pKNT25- <i>cotB</i>	This work
ECO958	BTH101 + pUT18- <i>cotL</i> + pKT25- <i>cotB</i>	This work
ECO959	BTH101 + pUT18C- <i>cotL</i> + pKNT25- <i>cotB</i>	This work
ECO960	BTH101 + pUT18C- <i>cotL</i> + pKT25- <i>cotB</i>	This work
ECO961	BTH101 + pKNT25- <i>cotL</i> + pUT18- <i>cotB</i>	This work
ECO962	BTH101 + pKNT25- <i>cotL</i> + pUT18C- <i>cotB</i>	This work
ECO963	BTH101 + pKT25- <i>cotL</i> + pUT18- <i>cotB</i>	This work

ECO964	BTH101 + pKT25- <i>cotL</i> + pUT18C- <i>cotB</i>	This work
ECO965	BTH101 + pUT18- <i>cotL</i> + pKNT25- <i>cdeC</i>	This work
ECO966	BTH101 + pUT18- <i>cotL</i> + pKT25- <i>cdeC</i>	This work
ECO967	BTH101 + pUT18C- <i>cotL</i> + pKNT25- <i>cdeC</i>	This work
ECO968	BTH101 + pUT18C- <i>cotL</i> + pKT25- <i>cdeC</i>	This work
ECO969	BTH101 + pKNT25- <i>cotL</i> + pUT18- <i>cdeC</i>	This work
ECO970	BTH101 + pKNT25- <i>cotL</i> + pUT18C- <i>cdeC</i>	This work
ECO971	BTH101 + pKT25- <i>cotL</i> + pUT18- <i>cdeC</i>	This work
ECO972	BTH101 + pKT25- <i>cotL</i> + pUT18C- <i>cdeC</i>	This work
ECO974	BTH101 + pUT18- <i>cotL</i> + pKNT25- <i>cotE</i>	This work
ECO975	BTH101 + pUT18- <i>cotL</i> + pKT25- <i>cotE</i>	This work
ECO976	BTH101 + pUT18C- <i>cotL</i> + pKNT25- <i>cotE</i>	This work
ECO977	BTH101 + pUT18C- <i>cotL</i> + pKT25- <i>cotE</i>	This work
ECO978	BTH101 + pKNT25- <i>cotL</i> + pUT18- <i>cotE</i>	This work
ECO979	BTH101 + pKNT25- <i>cotL</i> + pUT18C- <i>cotE</i>	This work
ECO980	BTH101 + pKT25- <i>cotL</i> + pUT18- <i>cotE</i>	This work
ECO981	BTH101 + pKT25- <i>cotL</i> + pUT18C- <i>cotE</i>	This work
ECO1007	BTH101 + pKT25- <i>cotL</i> + pUT18C- <i>cotA</i>	This work
ECO1008	BTH101 + pKT25- <i>cotL</i> + pUT18- <i>cotA</i>	This work
ECO1009	BTH101 + pKNT25- <i>cotL</i> + pUT18C- <i>cotA</i>	This work
ECO1010	BTH101 + pKNT25- <i>cotL</i> + pUT18- <i>cotA</i>	This work
ECO1011	BTH101 + pUT18C- <i>cotL</i> + pKT25- <i>cotA</i>	This work
ECO1012	BTH101 + pUT18- <i>cotL</i> + pKT25- <i>cotA</i>	This work
ECO1017	BTH101 + pKT25- <i>cotL</i> + pUT18C- <i>cotL</i>	This work
ECO1018	BTH101 + pKNT25- <i>cotL</i> + pUT18C- <i>cotL</i>	This work
ECO1019	BTH101 + pKT25- <i>cotL</i> + pUT18- <i>cotL</i>	This work
ECO1020	BTH101 + pKNT25- <i>cotL</i> + pUT18- <i>cotL</i>	This work
ECO1030	BL21 (DE3) + pDIA6838	This work
ECO1031	BL21 (DE3) + pDIA6839	This work

ECO1033	BL21 (DE3) + pDIA6840	This work
ECO1035	BL21 (DE3) + pDIA6841	This work
ECO1036	BL21 (DE3) + pDIA6842	This work
ECO1037	BL21 (DE3) + pDIA6843	This work
ECO1038	BL21 (DE3) + pDIA6844	This work
ECO1039	BL21 (DE3) + pDIA6845	This work
ECO1041	BL21 (DE3) + pDIA6846	This work
ECO1042	BL21 (DE3) + pDIA6847	This work
<i>C. difficile</i>		
CDIP546	630 Δ erm sigB::erm	Kint <i>et al</i> , 2017
CDIP588	630 Δ erm CD1157::erm	This work
CDIP658	630 Δ erm + pDIA6458	This work
CDIP659	630 Δ erm + pDIA6459	This work
CDIP661	630 Δ erm + pDIA6457	This work
CDIP666	630 Δ erm + pDIA6460	This work
CDIP668	630 Δ erm sigB::erm + pDIA6457	This work
CDIP669	630 Δ erm sigB::erm + pDIA6458	This work
CDIP670	630 Δ erm sigB::erm + pDIA6459	This work
CDIP671	630 Δ erm sigB::erm + pDIA6460	This work
CDIP691	630 Δ erm Δ CD1524	This work
CDIP697	630 Δ erm Δ CD1474	This work
CDIP714	630 Δ erm Δ CD1524 Δ CD1474	This work
CDIP717	630 Δ erm Δ CD2399	This work
CDIP734	630 Δ erm pFT47	This work
CDIP740	630 Δ erm sigB::erm + pDIA6497	This work
CDIP742	630 Δ erm + pDIA6503	This work
CDIP743	630 Δ erm sigB::erm + pDIA6503	This work
CDIP744	630 Δ erm + pDIA6499	This work
CDIP745	630 Δ erm sigB::erm + pDIA6499	This work
CDIP774	630 Δ erm sigB::erm + pDIA6517	This work
CDIP750	630 Δ erm + pDIA6497	This work
CDIP751	630 Δ erm + pDIA6498	This work
CDIP752	630 Δ erm sigB::erm + pDIA6498	This work
CDIP753	630 Δ erm pFT58	This work
CDIP767	630 Δ erm + pDIA6517	This work
CDIP798	630 Δ erm Δ CD2399 + pDIA6534 (complementation)	This work
CDIP799	630 Δ erm Δ CD1524 + pDIA6537	This work
CDIP800	630 Δ erm Δ CD1524 Δ CD1474 + pDIA6537	This work
CDIP801	630 Δ erm Δ CD1474 + pDIA6538 (complementation)	This work
CDIP802	630 Δ erm Δ CD1524 Δ CD1474 + pDIA6538	This work
CDIP843	630 Δ erm + pDIA6589	This work
CDIP845	630 Δ erm sigB::erm + pDIA6589	This work
CDIP1045	630 Δ erm + pDIA6669	This work
CDIP1046	630 Δ erm + pDIA6670	This work
CDIP1047	630 Δ erm sigB::erm + pDIA6669	This work
CDIP1048	630 Δ erm sigB::erm + pDIA6670	This work
CDIP1136	630 Δ erm cdeM::erm + pDIA6617	This work
CDIP1137	630 Δ erm cdeM::erm + pDIA6663	This work
CDIP1369	630 Δ erm Δ CD1623	This work

CDIP1370	630 Δ erm CD1157::erm Δ CD1623	This work
Plasmids	Relevant properties	Origin
pKT25	Kan ^R	Euromedex®
pKNT25	Kan ^R	Euromedex®
pUT18	Amp ^R	Euromedex®
pUT18C	Amp ^R	Euromedex®
pET20	<i>E. coli</i> expressing vector (Amp ^R)	Novagen
pET24a	<i>E. coli</i> expressing vector (Kan ^R)	Novagen
pFT47	pMTL84121-SNAP ^{Cd} (for transcriptional fusions) (Cm ^R /Tm ^R)	Pereira <i>et al.</i> , 2013
pETDuet	(Amp ^R)	Novagen
pFT58	pMTL84121-linker-SNAP ^{Cd} (for translational fusions) (Cm ^R /Tm ^R)	Pereira <i>et al.</i> , 2013
pMTL-SC7315	(Cm ^R /Tm ^R)	Cartman <i>et al.</i> , 2012
pMTL007	group II intron, ErmBtdRAM2 and <i>ltrA</i> of pMTL20lacZ-TTErm ;BtdRAM2, Cm ^R /Tm ^R	Heap <i>et al.</i> , 2007
pMTL84121	<i>Clostridium</i> modular plasmid containing <i>catP</i> (Cm ^R /Tm ^R)	Heap <i>et al.</i> , 2009
pDIA6325	P _{σB(sigB)} - <i>sigB</i> (complementation)	Kint <i>et al.</i> , 2017
pDIA6374	pMTL007- CD1157 Cm ^R -Tm ^R	This work
pDIA6427	pMTL-SC7315 Δ CD2399	This work
pDIA6429	pMTL-SC7315- Δ CD1524 Cm ^R -Tm ^R	This work
pDIA6457	pFT47 P _{CD1474} -SNAP ^{Cd}	This work
pDIA6458	pFT47 P _{CD1623} -SNAP ^{Cd}	This work
pDIA6459	pFT47 P _{CD1524} -SNAP ^{Cd}	This work
pDIA6460	pFT47 P _{CD0176} -SNAP ^{Cd}	This work
pDIA6474	pMTL-SC7315- Δ CD1474 Cm ^R -Tm ^R	This work
pDIA6497	pFT58 P _{CD1157} -SNAP ^{Cd}	This work
pDIA6498	pFT58 P _{CD1474} -SNAP ^{Cd}	This work
pDIA6499	pFT58 P _{CD1623} -SNAP ^{Cd}	This work
pDIA6503	pFT58 P _{CD0176} -SNAP ^{Cd}	This work
pDIA6517	pFT47 P _{CD1157} -SNAP ^{Cd}	This work
pDIA6534	pMTL84121-CD2399 Cm ^R -Tm ^R (complementation)	This work
pDIA6537	pMTL84121-CD1524 Cm ^R -Tm ^R (complementation)	This work
pDIA6538	pMTL84121-CD1474 Cm ^R -Tm ^R (complementation)	This work
pDIA6589	pFT47 P _{sigB} -SNAP ^{Cd}	This work
PDIA6617	pFT58 P _{σE/σK(cotL)} -cotL-SNAP ^{Cd}	This work
pDIA6635	pET20-CD1474	This work
pDIA6663	pFT58 P _{σK(cotL)} -cotL-SNAP ^{Cd}	This work
PDIA6669	P(σ^B CD1157)-SNAP ^{Cd}	This work
pDIA6670	P(σ^A CD1157)-SNAP ^{Cd}	This work
pDIA6671	pET20-CD1524	This work
pDIA6700	pKT25- <i>cotL</i>	This work
pDIA6701	pKNT25- <i>cotL</i>	This work
pDIA6702	pUT18- <i>cotL</i>	This work
pDIA6703	pUT18C- <i>cotL</i>	This work
pDIA6704	pKT25- <i>sipL</i>	This work

pDIA6705	pKNT25- <i>sipL</i>	This work
pDIA6706	pUT18- <i>sipL</i>	This work
pDIA6707	pUT18C- <i>sipL</i>	This work
pDIA6708	pKT25- <i>cotB</i>	This work
pDIA6709	pKNT25- <i>cotB</i>	This work
pDIA6710	pUT18- <i>cotB</i>	This work
pDIA6711	pUT18C- <i>cotB</i>	This work
pDIA6737	pKT25- <i>cotE</i>	This work
pDIA6738	pKNT25- <i>cotE</i>	This work
pDIA6739	pUT18- <i>cotE</i>	This work
pDIA6740	pUT18C- <i>cotE</i>	This work
pDIA6741	pKT25- <i>cdeC</i>	This work
pDIA6742	pKNT25- <i>cdeC</i>	This work
pDIA6743	pUT18- <i>cdeC</i>	This work
pDIA6744	pUT18C- <i>cdeC</i>	This work
pDIA6830	pUT18- <i>cotA</i>	This work
pDIA6831	pUT18C- <i>cotA</i>	This work
pDIA6832	pKT25- <i>cotA</i>	This work
pDIA6838	pETDuet His- <i>cotE</i> + <i>cotL</i>	This work
pDIA6839	pETDuet <i>cotL</i>	This work
pDIA6840	pETDuet His- <i>cotL</i>	This work
pDIA6841	pETDuet His- <i>cotB</i> + <i>cotL</i>	This work
pDIA6842	pETDuet His- <i>sipL</i> + <i>cotL</i>	This work
pDIA6843	pETDuet His- <i>sipL</i>	This work
pDIA6844	pETDuet His- <i>cotL</i> + <i>spoIVA</i>	This work
pDIA6845	pETDuet His- <i>sipL</i> + <i>spoIVA</i>	This work
pDIA6846	pETDuet His- <i>cotE</i>	This work
pDIA6847	pETDuet His- <i>cotB</i>	This work
pDIA6893	pMTL-SC7315- Δ CD1623 Cm ^R -Tm ^R	This work

The *erm* gene encodes the erythromycin resistance cassette. The *cat* gene encodes the chloramphenicol resistance cassette leading to resistance to chloramphenicol, Cm^R and to thiamphenicol, Tm^R. Amp^R and Kan^R means that the plasmid harbors a resistance cassette responsible for ampicillin and kanamycin resistance, respectively.

Table S2: Oligonucleotides used in this study.^aRestriction sites and tails used for Gibson assembly cloning are underlined.

Primer	Sequence (5' to 3') ^a	Description
CF14	CGCGGATCCACCCTTTCCAATTGTTTATAGTG	ACE 5' <i>CD2399</i> PCR1 BamHI
CF15	GGAATTCCTCCTTGTTGTAATAGATAGGTAA	ACE 3' <i>CD2399</i> PCR1 EcoRI
CF16	GGAATTCCTAGAGTCTGAAATGTACAACAAAG	ACE 5' <i>CD2399</i> PCR2 EcoRI
CF17	CCGCTCGAGTTACTATTTGATTGATACCTGCTT	ACE 3' <i>CD2399</i> PCR2 XhoI
CF19	GGAATTCGCTCATAGATTAAGTACCATATC	5' <i>CD1474</i> promoter EcoRI
CF20	CCGCTCGAGAATTTT TTATTTATTAAGTTAGTC	3' <i>CD1474</i> promoter XhoI
CF21	GGAATTCGTT TAG ACA AAG ATT TAG ATG TTA C	5' <i>CD1623</i> promoter EcoRI
CF22	CCGCTCGAG TAA AAT AGT TAT TTA GTC TCT T	3' <i>CD1623</i> promoter XhoI
CF23	GGAATTCAGAGGAGTCTTCATTAGAAA G	5' <i>CD1524</i> promoter EcoRI
CF24	CCGCTCGAGAATTTTAT TTTTAAGTTTAATA	3' <i>CD1524</i> promoter XhoI
CF25	GGAATTCGTATTG GATGGAAGTGAGAAGGAT	5' <i>CD0176</i> promoter EcoRI
CF26	CCGCTCGAGTATTTTATATTAATAAAGTAGAT TA	3' <i>CD0176</i> promoter XhoI
CF30	TAT AAA TAT CAA AAC CAA CAT TA	<i>CD1474</i> sequencing
CF31	TTA TTA GTG GTA AGT ATG CTT ATA	<i>CD1623</i> sequencing
CF39	TTC TTC AAT TCC AGA TGC CT	<i>CD1524</i> sequencing
CF95	CGTAATCATGGTCATATGGATA	pFT58-adjacent EcoRI
CF96	GGATCCGCAGCTGCTGATAAAGA	pFT58-adjacent BamHI
CF99	TATCCATATGACCATGATTACGGCTCATAGATTAAGTAC CATATC	5' <i>CD1474</i> promoter
CF100	TCTTTATCAGCAGCTGCGGATCCTTTTCCAAAATATCTA TTTAATAATC	3' <i>CD1474</i>
CF101	TATCCATATGACCATGATTACGGTTTAGACAAAGATTTA GATG TTAC	5' <i>CD1623</i> promoter
CF102	TCTTTATCAGCAGCTGCGGATCCTAGTATATCAGCCTTC ATAAT	3' <i>CD1623</i>
CF103	TATCCATATGACCATGATTACGGTATTGGATGGAAGTGA GAAGGAT	5' <i>CD0176</i> promoter
CF104	TATTTTATATTAATAAAGTAGATTA	3' <i>CD0176</i> promoter
CF105	TAATCTACTTTTAAATATAAATAACAGAAGGAGGAA AATGATGAATTA	5' <i>CD0176</i>
CF106	TCTTTATCAGCAGCTGCGGATCCTACACTATAACAAAAT TCTCC	3' <i>CD0176</i>
CF107	TATCCATATGACCATGATTACGTATACACGATAAAAATAT TTTCTAT	5' <i>CD1157</i> promoter
CF108	TCTTTATCAGCAGCTGCGGATCCTTAACTAATTTTGCA AATTCTGC	3' <i>CD1157</i>
CF113	TCCCCCGGGCAGAGGAGTCTTCATTAGAAAG	Complementation <i>CD1524</i> 5' XmaI
CF114	CCGCTCGAGTTATTTTCCAAAATGTCTGTTTAA	Complementation <i>CD1524</i> 3' XhoI
CF115	GGAATTCGCTCATAGATTAAGTACCATATC	Complementation <i>CD1474</i> 5' EcoRI
CF116	ATAAGAATGCGGCCGCTTATTTTCCAAAATATCTATTTA ATAATC	Complementation <i>CD1474</i> 3' NotI
CF117	GGAATTCCTTACAAAAAAGTCTACCTTCATC	Complementation <i>CD2399</i> 5' EcoRI

CF118	CCGCTCGAGTTCATTATCTTCTACCTCCTCTAT	Complementation <i>CD2399</i> 3' XhoI
CF211	CGCGGATCCTATGAAAAAATTAGATACAGA	BACTH 5' <i>cotL</i> BamHI
CF212	CGAATTCCTATTCATGAGGGTTAGACTT	BACTH 3' <i>cotL</i> EcoRI pKT25, pUT18C
CF213	CGAATTCGATTCATGAGGGTTAGACTTT	BACTH 3' <i>cotL</i> EcoRI pNT25, pUT18
CF217	CGCGGATCCTATGATAGATAATCAAAAATATGT	BACTH 5' <i>cotB</i> BamHI
CF218	CGAATTCCTTACATGTTTTTATAACTCTCCAATATT	BACTH 3' <i>cotB</i> EcoRI pKT25, pUT18C
CF219	CGAATTCGACATGTTTTTATAACTCTCCAATATT	BACTH 3' <i>cotB</i> EcoRI pNT25, pUT18
CF220	CGCGGATCCTATGGAATTAATTAAGATGTAAT	BACTH 5' <i>sipL</i> BamHI
CF221	CGAATTCCTTAATCTACTAATACGACTTTTTTTTTCT	BACTH 3' <i>sipL</i> EcoRI pKT25, pUT18C
CF222	CGAATTCGAATCTACTAATACGACTTTTTTTTTCT	BACTH 3' <i>sipL</i> EcoRI pNT25, pUT18
CF223	CGCGGATCCAATGCAAGATTATAAAAAAATAAAA	BACTH 5' <i>cdeC</i> BamHI
CF224	CGAATTCCTATCTGTGGCAACTTGGCT	BACTH 3' <i>cdeC</i> EcoRI pKT25, pUT18C
CF225	CGAATTCGATCTGTGGCAACTTGGCTT	BACTH 3' <i>cdeC</i> EcoRI pNT25, pUT18
CF226	CGCGGATCCGGTGATTTACATGCCAAA	BACTH 5' <i>cotE</i> BamHI
CF227	CGAATTCCTTAGAATTGCCATAAATACCTT C	BACTH 3' <i>cotE</i> EcoRI pKT25, pUT18C
CF228	CGAATTCGAGAATTGCCATAAATACCTTCA	BACTH 3' <i>cotE</i> EcoRI pNT25, pUT18
CF229	CGCGGATCCCGTGGAATAATAAATGTA	BACTH 5' <i>cotA</i> BamHI
CF230	CGAATTCCTATGCAATATAATCTATAGAATCTAC	BACTH 3' <i>cotA</i> EcoRI pKT25, pUT18C
CF231	CGAATTCGATGCAATATAATCTATAGAATCTACA	BACTH 3' <i>cotA</i> EcoRI pNT25, pUT18
CF236	GGAATTCCTATGAAAAAATTAGATACAGA	petDuet 5' <i>cotL</i> EcoRI
CF130	ATAAGAATGCGGCCGCTATTCATGAGGGTTAGACTTTT T	petDuet 3' <i>cotL</i> NotI
CF184	GGAATTCATATGAAAAAATTAGATACAGAGTCA	petDuet 5' <i>cotL</i> NdeI
CF237	CCGCTC GAGCTATTCATGAGGGTTAGACTTTTT	petDuet 3' <i>cotL</i> XhoI
CF238	G GAATTCCTATGATAGATAATCAAAAATATGT	petDuet 5' <i>cotB</i> EcoRI
CF239	ATAAGAATGCGGCCGCTTACATGTTTTTATAACTCTCCA ATATT	petDuet 3' <i>cotB</i> NotI
CF244	GGAATTCGGTGATTTACATGCCAAA	petDuet 5' <i>cotE</i> EcoRI
CF245	ATAAGAATGCGGCCGCTTAGAATTGCCATAAATACCTT C	petDuet 3' <i>cotE</i> NotI
CF248	GGAATTCCTATGGAATTAATTAAGATGTAATTA	petDuet 5' <i>sipL</i> EcoRI
CF249	ATAAGAATGCGGCCGCTTAATCTACTAATACGACTTTTT TT	petDuet 3' <i>sipL</i> NotI
CF254	GGAATTCATATGTATAGGAGGAATAATATGAAT	petDuet 5' <i>spoIVA</i> NdeI
CF255	CCGCTC GAG TTATAACAAAATAGTTATAATATTAGA	petDuet 3' <i>spoIVA</i> XhoI
IMV699	CCGCTCGAGAAAAGGGAACGTATTG	Complementation <i>CD1623</i> 5' XhoI
IMV700	CGGGATCCTTAAACCTATGTATGTA	Complementation <i>CD1623</i> 3' BamHI
IMV844	CTTTACTGGAGTAGTAGATGAA	Verification intron <i>CD1157</i>
IMV845	GACCATCTAAGTATAGTTTAGCA	Verification intron <i>CD1157</i>
IMV914	TCATGAGATTATCAAAAAGGGGACAATTTATCTTGATT CTAG	ACE <i>CD1623</i> 5' PCR1 rev comp vector
IMV915	GTAGAAATACGGTGTTTTTTCACTTGAGTAAAGTCAGGA TT	ACE <i>CD1623</i> 3' PCR2 rev comp vector
IMV917	TCATGAGATTATCAAAAAGGGATAGACTTCTAAATATTTC	ACE <i>CD1474</i> 5' PCR1 rev

	CC	comp vector
IMV918	GTAGAAATACGGTGTTTTTTTAGCACAACTAACACTATAA TTC	ACE <i>CD1474</i> 3' PCR2 rev comp vector
IMV919	TCATGAGATTATCAAAAGGAAGGAGGGGGCTTTATTGA AA	ACE <i>CD1524</i> 5' PCR1 rev comp vector
IMV920	GTAGAAATACGGTGTTTTTTTGTTTCATGGCAACAGTAACA TC	ACE <i>CD1524</i> 3' PCR2 rev comp vector
IMV949	AGGAATTCCTCCAAACAAGCTCTT	5' P σ^A -(<i>CD1157</i>) EcoRI
IMV950	CCGCTCGAGAGTTGTAAGTTGTCCCAA	3' P σ^B -(<i>CD1157</i>) XhoI
IMV968	GGAATTCATATGAAGAAATTTGTTTGTACAG	5' <i>CD1474</i> pET20 NdeI
IMV969	CCGCTCGAGTTATTATTTTCCAAAATATCTATTTAATAA TC	3' <i>CD1474</i> pET20 XhoI (stop)
IMV970	GGAATTCATATGAAAAAATTTGTTTGTACAG	5' <i>CD1524</i> pET20 NdeI
IMV971	CCGCTCGAGTTATTATTTTCCAAAATGTCTGTTTAA	3' <i>CD1524</i> pET20 XhoI (stop)
IMV976	AGGAATTCATAAAACTATTGTTTTACATGA	5' P σ^B -(<i>CD1157</i>) EcoRI
IMV977	CCGCTCGAGAAAAGATGTCATGATAAGTCA	3' P σ^A -(<i>CD1157</i>) XhoI
NK58	GTTATTTAGTCTCTTTATACCCTGCTTG	ACE <i>CD1623</i> 3' PCR1
NK59	CAAGCAGGGTATAAAGAGACTAAATAACGATTTTGAGG ATATTATGAAGGCTG	ACE <i>CD1623</i> 5' PCR2 rev comp NK58
NK64	GGTGCAGCATCTCCTTCATGTATA	ACE <i>CD1524</i> 3' PCR1
NK65	TATACATGAAGGAGATGCTGCACCCTTAGGATTATTAA ACAGACATTTTGG	ACE <i>CD1524</i> 5' PCR2 rev comp NK64
NK70	ATTTCTTCATAATTACTTTTCTCCTAAA	ACE <i>CD1474</i> 3' PCR1
NK71	TTTAGGAGGAAAGTAATTATGAAGAAAGAAGCTAGACA TGGTAAAGCATTTC	ACE <i>CD1474</i> 5' PCR2 rev comp NK70
NK155	GATCAGGCCTATGGATAAAGATTGTGAAATGA	pFT47 5' StuI
NK156	GATCCTCGAGTTATTCTTACCCAAGTCCT	pFT47 3' XhoI

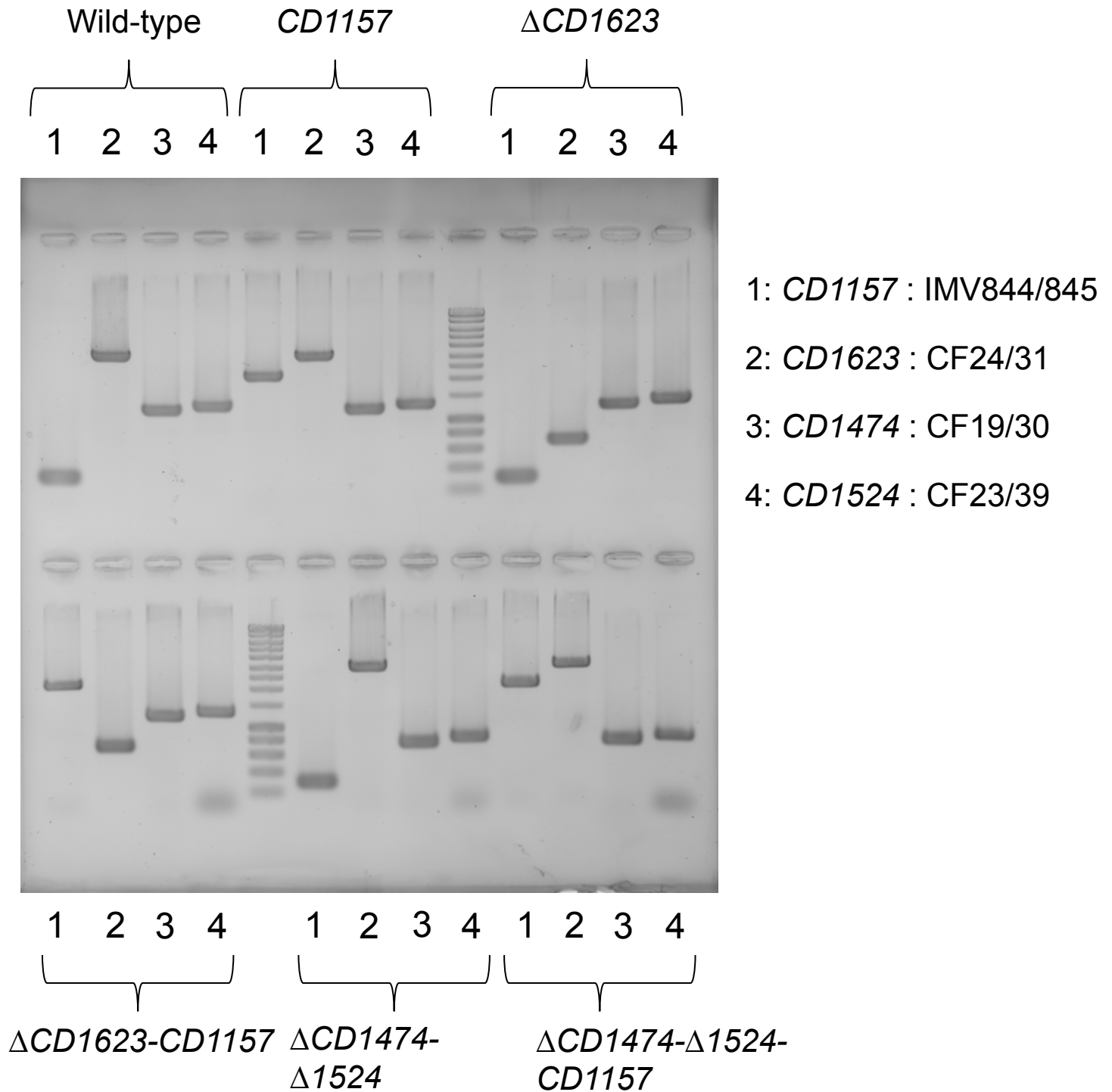


Figure S1: Construction of *C. difficile* single and multi-mutants for the FDPs- and revRbs-encoding genes. For the *CD1157* Clostron mutant, the verification of the L1.LtrB intron integration into the *CD1157* gene was performed by using primers IMV844/IMV845 flanking the insertion site in *CD1157*. For the ACE mutants, the verification of the deletion of *CD1623*, *CD1474* and *CD1524* genes in the different backgrounds was performing using CF24/CF31, CF19/CF30 and CF23/CF39 respectively.

Discussion

I. The morphogenesis of the *C. difficile* spore coat

Spores play a key role in the pathogenesis of *C. difficile*. This metabolically inactive structure allows transmission, and its accumulation inside the host ensures persistence and recurrence. The anatomy of the spore comprises a series of specialized concentric shells, each of which provides specific functions (Setlow 2006, 2014). A critical protective structure is the coat, a proteinaceous layer that encases bacilli and clostridia spores and provides a barrier against degradative enzymes and chemical compounds (Nicholson et al. 2000, Riesenman and Nicholson 2000, Klobutcher et al. 2006, Setlow 2014). Unlike *B. subtilis*, *C. difficile* possesses an exosporium, which is the outermost spore layer. The exosporium provides the first site of interaction with the host. Several proteins have been identified in the spore coat and exosporium layers of *C. difficile* and the function of some of them was already studied (Permpoonpattana et al. 2011b, Abhyankar et al. 2013, Permpoonpattana et al. 2013, Diaz-Gonzalez et al. 2015). However, additional studies are still needed to define the proteins and the mechanisms that guide deposition of these components in the outermost layers of *C. difficile* spores and the interactions between them. Here, we have elucidated a new protein, CotL that controls the assembly of the spore coat layers in *C. difficile*.

I.1. Role of CotL on *C. difficile* spore coat structure

SpoIVA (Putnam et al. 2013) and SpoVM (Ribis et al. 2017), are the only conserved morphogenetic proteins between *B. subtilis* and *C. difficile*. In this study, we showed that the *C. difficile* coat-associated protein, CotL, is a new morphogenetic protein essential for the efficient assembly of the coat layers. Indeed, the assembly of early- and late-coat proteins occurs in a CotL-dependent manner and CotL is required for the appearance of the spore coat. Consistent with this, the amount of most of the spore coat and exosporium proteins is strongly decreased in the spore surface layers of the *cotL* mutant when compared to the wild-type strain. However, *cotL* inactivation impaired neither the transcription of sporulation-related genes, nor the protein production in sporulating cells. Thus, we have concluded that CotL plays a morphogenetic rather than a regulatory role in coat formation.

I.2. The dual control of *cotL* gene expression

Our data shows that the CotL protein resides within the outermost layers of the spore, in agreement with the expression of *cotL* gene in the MC compartment under the dual control

of σ^E and σ^K . The *cotL* gene is transcribed by σ^E early during sporulation suggesting a potential role of CotL in early FS development, as already observed for SpoIVA and SipL (Putnam et al. 2013). Then, the transcription of the *cotL* gene by σ^K probably allows the maintenance or an increased expression of this gene that might be needed during the late sporulation stages. The timing of *cotL* expression has consequences on the assembly of CotL itself around the FS. Using SNAP translational fusions, we observed that when CotL is produced only under the control of σ^K leading to a delayed and likely a reduced amount of its production, CotL seems to be immediately assembled at the FS surface. By contrast, when produced under the dual control of σ^E and σ^K , CotL first accumulates in the MC and then assembles around the FS. Moreover, the CotL protein produced under the control of its native promoter is not assembled around the FS in the *sigK* mutant. It has been shown that synthesis of coat proteins is usually controlled either by σ^E or by σ^K , but it is only when σ^K becomes active that the coat layers start gaining their characteristic appearance as viewed by electron microscopy (Henriques and Moran 2007). Consistent with this, the *sigK* mutant itself is defective in coat polymerization and localization (Pereira et al. 2013, Pishdadian et al. 2015). However, it has been shown that the CotB-SNAP^{Cd} protein (a σ^E -target) is located at the FS surface in the *sigK* mutant (Pereira et al. 2013), suggesting that *C. difficile* coat assembly can start at early sporulation stage as in *B. subtilis* (Henriques and Moran 2007). Our observations raised the hypothesis that CotL assembly might be dependent on the presence of a still uncharacterized σ^K -regulated gene product even if we cannot exclude that the reduced amount of CotL when expressed solely under the control of σ^K might be directly assembled without accumulation in the MC. The analysis of the CotL localization in different mutants inactivated for coat proteins is an interesting point to address in future work.

A continuous expression of *cotL* gene during sporulation suggests that the timing of CotL production may have an impact in the assembly of the other coat components around the FS. *B. subtilis* CotE, the outer coat morphogenetic protein located at the interface of the inner and outer spore coat layers, is an example of how the timing of protein synthesis is essential to determine a correct morphogenesis of the spore. As for *C. difficile cotL*, the *cotE* gene of *B. subtilis* is similarly expressed first from a σ^E -dependent promoter (P1) and later from a σ^K -dependent promoter (P2) (Zheng and Losick 1990). The P1 promoter is shut off by SpoIIID at the early stages of the morphogenesis while the P2 promoter is shut off by GerE during the latest stages of morphogenesis. The *cotE* mutant retains the inner coat but lacks the outer coat layer (Zheng et al. 1988). Additionally, the early expression of *cotE* is essential for outer coat

assembly since a later expression of this gene under the control of the σ^K - dependent (*gerE*) or GerE-dependent (*cotG*) promoter, respectively does not allow assembly of a visible outer coat structure. In our case, we observed that *C. difficile* CotL is required for the correct encasement of the basement layer protein SpoIVA around the FS suggesting that the early synthesis of CotL is likely essential for the assembly of the *C. difficile* spore layers. How does CotL localizes in *spoIVA* mutant sporulating cells is an information that would give clues about its role in spore coat assembly.

I.3. CotL properties and its localization in the spore

The previous proteomic studies (Lawley et al. 2009b, Abhyankar et al. 2013, Diaz-Gonzalez et al. 2015) in addition to our proteomic analysis failed to detect the CotL protein in the spore or in the spore surface layers. However, we successfully detected CotL in the coat/exosporium extract of *C. difficile* spores by Western blot analysis using an antibody raised against CotL. The feature of CotL as a lysine-rich protein might hinder its detection by bottom-up mass spectrometry-based proteomics. Indeed, proteins are usually digested into peptides with trypsin, an enzyme that cleaves after lysine and arginine residues and the generated peptides of CotL digestion might be therefore too small or not suitable with their further identification by mass spectrometry.

The exact location of CotL within these spore layers still remains to be determined more precisely. In *C. difficile*, coat assembly around the FS is driven by SpoIVA and SipL (Putnam et al. 2013). In the corresponding mutants, the sporulating cells exhibit defects in coat localization, spore coat swirls are detected in the MC cytoplasm, and the spores cannot be purified (Putnam et al. 2013). CdeC and CdeM were identified as morphogenetic factors of the exosporium (Barra-Carrasco et al. 2013, Calderon-Romero et al. 2018). Spores of the *cdeC* mutant, but not that of *cdeM* mutant, exhibit a thinner coat (Calderon-Romero et al. 2018). Our results indicate that the defect in spore formation of *cotL* mutant is less severe than that of *spoIVA* or *sipL* mutant but is more severe when compared to that of the *cdeC* mutant. We can purify *cotL* mutant spores, even if most of the coat and the exosporium layers are lacking. All this together suggests a hierarchical organization of the coat layers in which CotL might play a role downstream of the morphogenetic factors, SpoIVA and SipL, but upstream of CdeC and CdeM. To analyse if the inactivation of the *cdeM* gene interferes with the localization of CotL protein, we introduced the $P_{\sigma^E/\sigma^K(cotL)}-cotL-SNAP^{Cd}$ or $P_{\sigma^K(cotL)}-cotL-SNAP^{Cd}$ translational fusions in the *cdeM* mutant. In both wild-type and *cdeM* mutant strains,

A

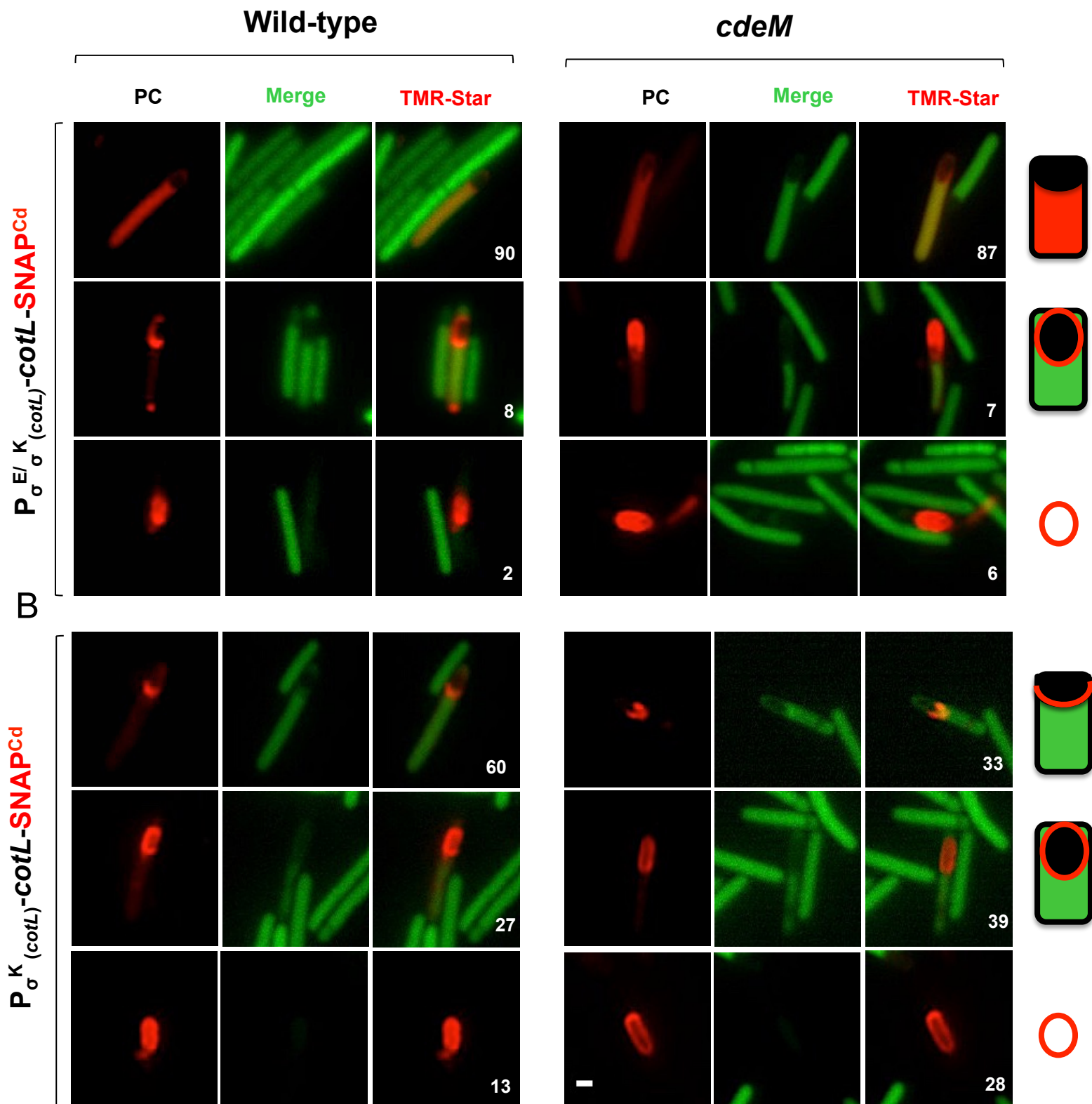


Figure 56: Subcellular localization of the CotL protein fused to SNAP^{Cd}. Microscopy analysis of *C. difficile* wild-type (A) and *cdeM* mutant (B) cells harboring $P_{\sigma^{E/\sigma K(cotL)}}-cotL-SNAP^{Cd}$ or $P_{\sigma K(cotL)}-cotL-SNAP^{Cd}$ translational fusions. The cells were collected after 24 h of growth in liquid SM, stained with TMR-Star and examined by fluorescence microscopy to monitor the SNAP production. The merged images show the overlap between the TMR-Star (red) and the autofluorescence (green) channels. A schematic representation of the location pattern of the CotL-SNAP^{Cd} protein is shown on the right side ordered from early to late stages. Among the cells with signal, the numbers represent the percentage of sporulating cells/spores showing the corresponding pattern of coat protein location. Scale bar, 1 μ m.

the $P_{\sigma^E/\sigma^K}_{(cotL)-cotL-SNAP^{Cd}}$ was detected in the MC compartment (90% and 87%, respectively), around the spore in both the sporulating cells (8% and 7%) and in the free spores (2% and 6%) (Figure 56A). In contrast, the $P_{\sigma^K}_{(cotL)-cotL-SNAP^{Cd}}$ fluorescence signal was detected either as a cap in the MCP pole (60% and 33%) or around the spore in both the sporulating cells (27% and 39%) and the free spores (13% and 26%) (Figure 56B). In agreement with our hypothesis, this data showed that CotL localization is not affected in the absence of CdeM (Figure 56). As mentioned above, how the inactivation of *spoVM*, *spoIVA*, *sipL* and/or *cdeC* genes influences the pattern of CotL localization is an interesting point to address in future work. Comparing with the *B. subtilis* model, our results suggest that *C. difficile* CotL acts earlier in coat morphogenesis than SafA and CotE. The *safA* mutant spores lack an inner coat but still retain the outer coat (Takamatsu et al. 1999). However, the *cotE* mutant spores lack an outer coat and retain the inner coat (Zheng et al. 1988), while the basement layer does not properly adhere to the underlying cortex (Henriques and Moran 2007). In *C. difficile*, few coat materials are detected around the purified spores of the *cotL* mutant and no lamellar or electrodense layers are observed, suggesting a stronger impact of the inactivation of *cotL* on spore morphogenesis than inactivation of the *safA* or the *cotE* genes in *B. subtilis*. Consistent with the observation that SpoIVA is not correctly assembled around FS in the *cotL* mutant, we proposed that CotL is an important player in starting coat assembly.

I.4. Interactions between coat proteins in *C. difficile*

The spore coat assembly requires a complex protein interaction network (Kim et al. 2006, McKenney and Eichenberger 2012). Morphogenetic proteins make an initial structure from which the coat grown around the spore by the polymerization of individual proteins and addition of other components. In *C. difficile*, very little is known about interaction between spore coat proteins. So far, interactions between SpoIVA and SpoVM or SipL proteins were the only ones demonstrated (Putnam et al. 2013, Ribis et al. 2017). However, the binding of other coat proteins to SpoIVA and/or SipL remains unknown. The requirement of CotL for the encasement of other proteins at the spore outermost layers lead us to test possible interactions between CotL and coat and/or exosporium proteins such as SipL, CotA, CotB, CotE and CdeC. From all proteins tested, our experiments using the bacterial two hybrid system (BACTH) only suggested that CotL might interact with SipL. However, we were unable to confirm this result using pull down assays. In collaboration with Aimee Shen's

group, we also tried to pull down CotL using a SipL-3xFlag fusion in *C. difficile* but we did not have more success. Concerning CotB and CotE, the interactions with CotL were weak and detected in one out of eight combinations only when CotL was fused to the T25 part of the adenylate cyclase through its C-terminal part. Whether in the other constructions, CotL contact regions might be blocked by the adenylate cyclase domains is a question that remains to be addressed. However, none positive confirmation of possible interactions came from the pull down assays. In addition, no interaction was revealed by the BACTH analysis between CotL and CotA or CdeC suggesting an absence of interaction. However, we cannot exclude that CotA or CdeC fusions were poorly synthesized, or that their stability and/or solubility were low in *E. coli*. Fail attempts to overexpress coat proteins in *E. coli* have been already reported (Krajcikova et al. 2017). A CotG self-interaction and a direct contact between CotG and CotB from *B. subtilis* was detected using a yeast two hybrid system (Zilhao et al. 2004) while no interaction was revealed for CotG by BACTH analysis. It seems that overexpression of *cotG* in *E. coli* failed, explaining the lack of any observable CotG interaction using this system. Difficulties in over-expressing exosporium proteins under soluble conditions have been also reported. For instance, the *C. difficile* exosporium protein, CdeC, requires *E. coli* strains providing an oxidative environment for optimal soluble expression conditions (Brito-Silva et al. 2018). In addition, false positive and negative results can be generated by the BACTH system, which requires that verification must be done using other methods. As we observed for SipL, even if interactions were detected in *E. coli*, it might not mean that they indeed exist at the spore surface. Used as control, SipL and SpoIVA were shown to interact using pull down assays (Putnam et al. 2013) and we were able to reproduce this result. Unfortunately, we were unable to make the SpoIVA constructs to show an interaction between SpoIVA and SipL by BACTH. To address and facilitate the screening of coat protein-protein interactions additional tools are required. Since bacterial- and yeast-two hybrid assays can give different results, we need in the future to optimize the overproduction and solubilization of coat/exosporium proteins in each organism. In *C. difficile*, the identification of partners of CotL might be possible by using a CotL-3xFlag fusion.

I.5. Spore encasement dependent on CotL

We showed that encasement of early- and late-proteins around the FS occurs in a CotL-dependent manner. However, no direct interaction between CotL and all the analysed proteins has been demonstrated so far. In *B. subtilis*, a large group of outer coat proteins

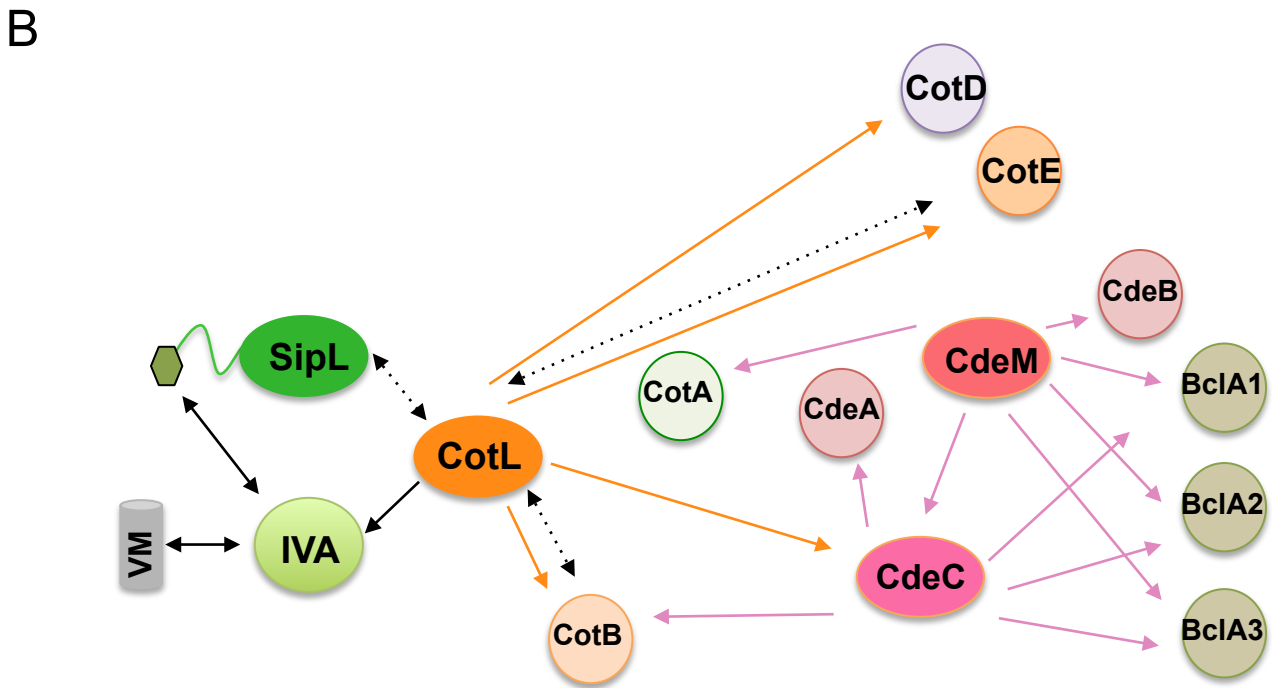
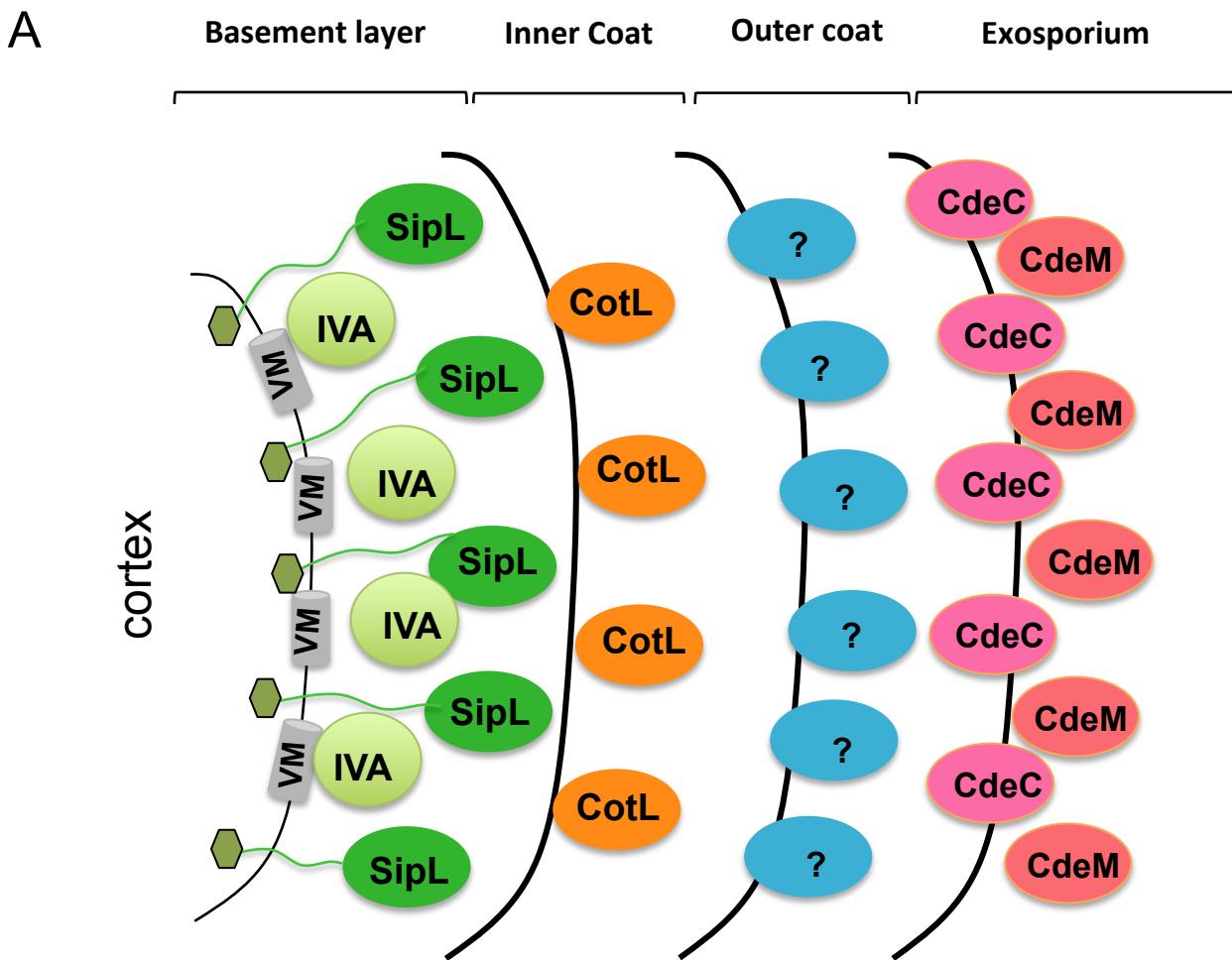


Figure 57: Model of the morphogenetic proteins of the outermost layers of the *C. difficile* spore. A) Preliminary model of the localization of the spore coat (SpoVM, SpoIVA, SipL and CotL) and exosporium (CdeC and CdeM) morphogenetic proteins. The hexagon represents the LysM domain. **B)** Proteins interaction network. Confirmed protein interactions are represented by a double arrow. Double dotted arrows represent positive interactions determined by BACTH. One-way orange arrows indicate proteins which assembly or recruitment at the FS is dependent on CotL. One-way pink arrows indicate proteins which abundance in the spore coat/exosporium is dependent on CdeC or CdeM.

requires CotE for localization. However, only a very few such as CotC, CotU and CotH interacts directly with CotE (Isticato et al. 2010, Isticato et al. 2015). In *C. difficile*, CotB, CotE and CdeC might be part of the CotL network, which does not necessarily require direct interaction. In fact, we cannot rule out the possibility that CotL might need the assistance of another unidentified factor essential for the physical contact between these proteins. Additionally, an interesting point in CotL protein is its amino acid composition. The positively charged amino acid, lysine, correspond to 24% of the CotL residues. Among the spore coat proteins of *B. subtilis*, the outer coat component, CotO, contains 16% of lysine residues. Interestingly, CotO is a morphogenetic protein, which assembly is CotE-dependent. CotO directs the deposition of a subset of coat proteins and is needed to form a morphologically normal outer coat (McPherson et al. 2005). Whether the high percentage of lysines is important for the function of CotO in *B. subtilis* has not been addressed. However, the high level of this charged amino acid might be relevant for the assembly of the coat layers. At physiological pH, we deduce that *C. difficile* CotL is positively charged (pI 9.76) while most of the spore coat proteins are negatively charged. This unique property of CotL might be relevant to mediate electrostatic interactions with other structural components and could contribute to the formation of a tough layer and the mechanical resistance of the spore coat. Since we found by BACTH positive interactions between CotL and SipL, and to a lesser extent with CotB or CotE, if these interactions are mainly electrostatic salt concentration and pH are probably important factors to take into account to optimize the pull down assays.

I.6. Model for the assembly of the outermost layers of the *C. difficile* spore

Altogether, our results allow to elaborate a preliminary model for the assembly and organization of the outermost layers, coat and exosporium in *C. difficile* spores (Figure 57A). In a basement layer, SpoIVA and SipL interact and might form a complex that drive coat assembly around the FS (Putnam et al. 2013). Similar to *B. subtilis*, SpoVM probably recognizes the positive curvature of the FS and embed itself within the MC-derived membrane. Since SpoVM is largely dispensable for SpoIVA encasement in the *C. difficile* FS, SpoIVA may independently interact with the FS membrane (Ribis et al. 2017). Alternatively, SipL or another factor could help SpoIVA to surround the FS in the absence of SpoVM (Figure 57A). TEM allowed to distinguish an inner lamellar and an outer electrodense coat in *C. difficile* spores (Permpoonpattana et al. 2011b, Barra-Carrasco et al. 2013). However, it remains unclear whether each distinct layers are associated to specific morphogenetic proteins

like in *B. subtilis*. Based on our results including the early and late expression of *cotL* gene during sporulation, the morphology of the *cotL* mutant spores and the requirement of CotL for the localization of other spore coat proteins, we propose that CotL may be located in the inner coat layer. In *B. subtilis*, SpoIVA and SpoVID interact with CotE and SafA. Since no homologs of these proteins are present in *C. difficile*, further research is needed to identify additional morphogenetic spore coat proteins recruited by SpoIVA, SipL, SpoVM and/or CotL.

The morphogenetic proteins of the exosporium, CdeC and CdeM, direct the assembly of the most external layer (Calderon-Romero et al. 2018). CdeC might be at the interface of the spore coat and exosporium layers. However, CdeM seems to be located uniquely in the exosporium layer (Figure 57A). Coupling our findings with previous localization studies (Diaz-Gonzalez et al. 2015), we can propose putative locations for the other spore surface proteins identified (Figure 57B). CotA and CotB are located in the spore coat layers (Diaz-Gonzalez et al. 2015) while the CotE, CotD, BclA and Cde proteins are located in the exosporium (Pizarro-Guajardo et al. 2014). The CotL-dependent proteins, defined as those that were mis-assembled in the *cotL* mutant FS, include SpoIVA, CotB, CotD, CotE and CdeC (Figure 57B) and cannot be precisely located. In fact, the mis-assembly of early coat proteins in the *cotL* mutant, most likely hinders the correct localization of late coat proteins such as CdeC, CotD and CotE and consequently the assembly of the exosporium layer. Finally CdeC is required for the assembly of CdeA, CotB and the high molecular complex BclA1 and BclA3, while CdeM-dependent proteins include CotA and CdeB, the low molecular mass complex formed by BclA1, BclA2, BclA3 and CdeB (Figure 57B).

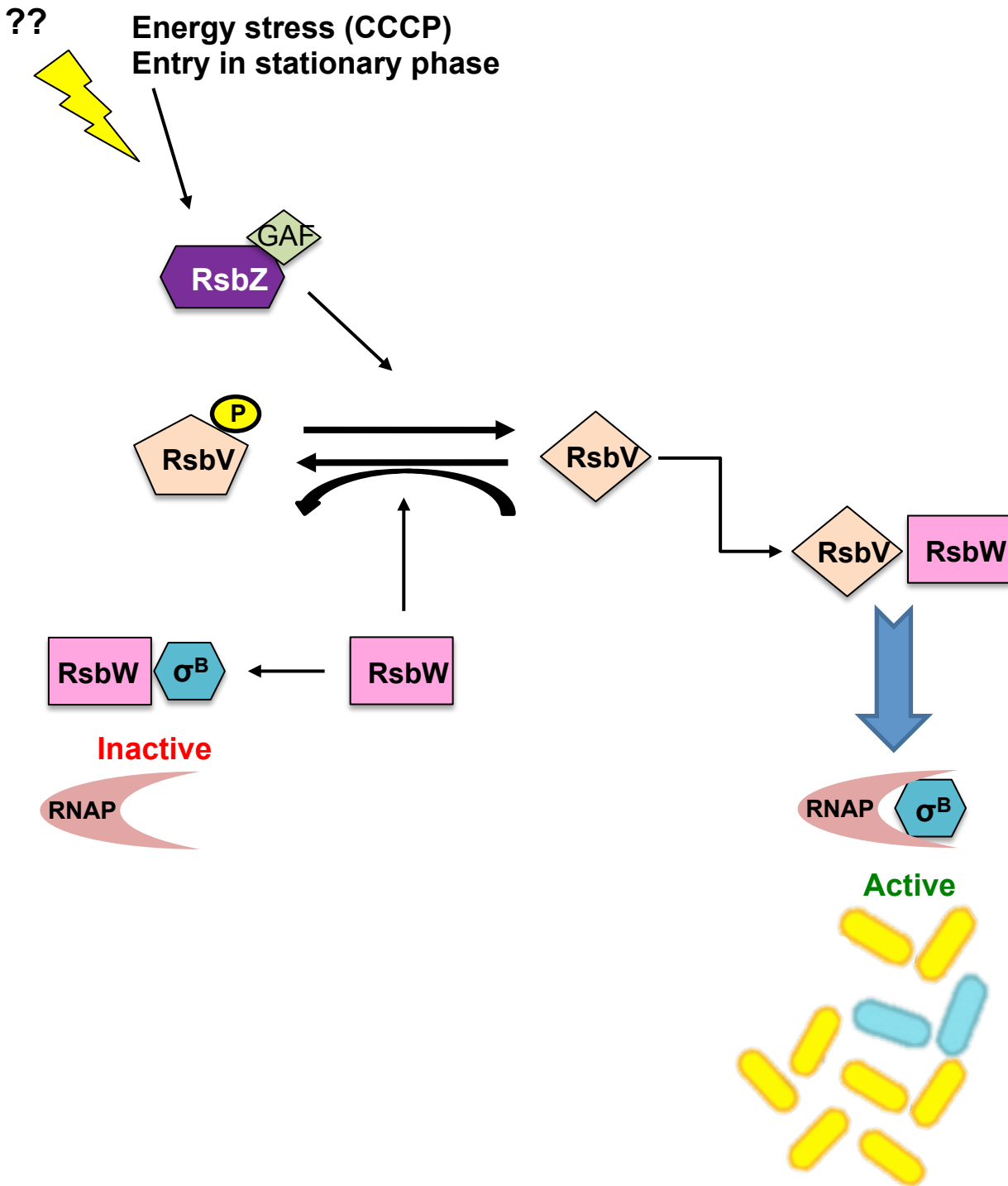


Figure 58: Model of the signal transduction leading to the activation of σ^B in *C. difficile*. Partner switching mechanism of σ^B activation is conserved in *C. difficile*. During stationary growth phase or after stress exposure, the RsbZ phosphatase dephosphorylate RsbV, which interacts with RsbW, allowing σ^B release, its association with the RNA polymerase and transcription of its targets genes. Stress signals triggering phosphatase activation in *C. difficile* are not know but exposure to CCCP and entry into stationary phase activate σ^B activity.

II. Signaling pathway and σ^B activation in *C. difficile*

Bacterial cells respond to stress or starvation by expressing a set of genes whose products are necessary to cope with the adverse environmental conditions and ensure survival of the cell (Kjelleberg et al. 1993). In *C. difficile*, the alternative sigma factor σ^B controls genes involved in stress response (Kint et al. 2017). σ^B equips the cells with a protective and preventive machinery conferring stress resistance (Hecker et al. 2007, Kint et al. 2017). During my thesis, I participated with Nicolas Kint in the study of the signaling pathway leading to the activation of σ^B in *C. difficile*. My main contribution in this work was in the analysis of both *sigB* expression and σ^B activity during vegetative growth (Kint *et al*, in Annex).

II.1. Role of the environmental signals in the activation of σ^B in *C. difficile*

In this study, Nicolas Kint showed the conservation of the partner switching mechanism, involving RsbV and RsbW, in the activation of σ^B in *C. difficile*. He also demonstrated that the phosphorylation state of RsbV, and later on the activation of σ^B , is dependent on the activity of the newly identified PP2C phosphatase CD2685/RsbZ (Figure 58). However, stress signals triggering phosphatase activation in *C. difficile* remain unknown. In addition, no typical environmental stresses tested induce σ^B activity. Indeed, exposure to bile salts, acidic pH, ROS or NO-donor compounds that correspond to stresses encountered within the gut did not increase the expression of σ^B -target genes. When we tested a combination of NO-donor compounds with H₂O₂ or a superoxide donor, mimicking the conditions encountered by *C. difficile* during inflammation, we did not observed induction of σ^B activity. In other Firmicutes, exposure to environmental stresses typically induces the activation of σ^B (Hecker et al. 2007). In *B. subtilis* and *L. monocytogenes*, these signals are detected via the stressosome by an unknown mechanism (Pane-Farre et al. 2017). In *B. cereus*, the stressosome is absent, and the activation of σ^B by environmental signals appears to be mediated by the kinase RsbK (de Been et al. 2010). The absence of homologues of the stressosome components or RsbK in *C. difficile* might explain the absence of induction of σ^B activity in response to the various environmental stresses tested. However, we cannot exclude the possibility that the conditions used to test σ^B induction are not drastic enough to promote the activation of this sigma factor in *C. difficile*.

II.2. Role of the energy signals in the activation of σ^B in *C. difficile*

As in other Firmicutes, the activity of σ^B in *C. difficile* increases at the onset of the stationary phase (Kint et al. 2017) and several σ^B -targets are more expressed at 10h compared to 4h (Saujet et al. 2011). At the entry in stationary phase, energy deficiency occurs in consequence of the decreased intracellular concentration of ATP. In *B. subtilis* or *L. monocytogenes*, the addition of ionophore carbonyl cyanide m-chlorophenylhydrazone (CCCP) leading to a drop of the ATP pool as well as the growth in starvation conditions of glucose, phosphate or in limitation in O₂ availability that likely result in ATP drop also allows the activation of σ^B (Hecker et al. 2007). Nicolas Kint showed that the addition of CCCP induces the activity of σ^B in *C. difficile* in a RbsZ-dependent manner (Figure 58). Since exposure to CCCP and entry into stationary phase are able to trigger σ^B target expression, it is quite possible that σ^B activation is mediated by an energy stress (Figure 58). Additional experiments to decipher the mechanism leading to the σ^B activation in response to CCCP are currently being performed in the laboratory.

From a physiologic point of view, the activation of σ^B through an energetic pathway raises some questions. Studies have shown that in dysbiotic mice there is an increase in the concentration of compounds required for growth and multiplication of vegetative cells of *C. difficile* (Theriot et al. 2014, Theriot and Young 2014). These compounds include amino acids such as glycine, cysteine or proline, as well as mannitol and sorbitol (Theriot et al. 2014). These data suggest that *C. difficile* does not face a nutrient-deficient environment during gut colonization. On the other hand, most of the *C. difficile* proteins involved in energy metabolism and maintenance of oxidation-reduction potential contain cysteines and Fe-S clusters. These molecules are extremely sensitive to oxidation and are the main targets of the oxidizing agents found during the infectious cycle such as O₂ and/or ROS, NO or RNS produced during inflammation (Py et al. 2011). Therefore, it is possible that the activation of σ^B through energy stress is due to an indirect effect of the oxidative environment encountered by *C. difficile* during its infectious cycle including the inactivation of enzymes involved in the central metabolism of the bacterium. Further studies will be performed to decipher the role of the energy metabolism and the mechanisms involved on σ^B activation in *C. difficile*.

II.3. Expression of *sigB* in *C. difficile*

In most Firmicutes, a basal expression of the *sigB* operon is mediated by a promoter recognized by σ^A . σ^B is produced at a basal level, sequestered by RsbW and is eventually

turned active following stress. However, the presence of an internal promoter upstream of the *rsbV* gene recognized by σ^B promotes a rapid increase in the production of RsbV, RsbW and σ^B when the bacteria are exposed to a stress (Hecker et al. 2007). Contrary to the other Firmicutes, σ^B of *C. difficile* is not auto-regulated but only constitutively expressed throughout the growth via a σ^A -dependent promoter. In agreement, we demonstrated by qRT-PCR and monitoring the expression of a P_{sigB} -SNAP^{Cd} fusion, that *sigB* gene is expressed similarly in the wild-type and the *sigB* mutant strains during growth. In *B. subtilis* and *L. monocytogenes*, the last gene of the *sigB* operon, *rsbX*, codes for a PP2C phosphatase that allows the "reset" of the stressosome, decreasing the activity of σ^B . This mechanism prevents excessive activation of σ^B , which can be toxic to the bacteria (Eymann et al. 2011, Xia et al. 2015). Similarly, in *B. cereus*, a mechanism mediated by RsbK and RsbM modulates the activity of σ^B , preventing its permanent activation (Chen et al. 2012). None of the genes encoding these proteins are present in the *C. difficile* genome, suggesting that none of these systems exists for σ^B in this bacterium. These results are consistent with the fact that the overexpression of *rsbZ* causes a growth defect and that overexpression of *sigB* is toxic in *C. difficile*. Therefore, the absence of an auto-regulation of σ^B in *C. difficile* might be a mechanism used by this bacterium to prevent over-activation of σ^B , potentially toxic to the cell.

In addition, the fact that the overexpression of the *rsbZ* gene induces a stronger activation of σ^B , suggests that some phosphatase might be active even in the absence of a stress. Interestingly, during exponential growth, a fraction of the total RsbV is dephosphorylated in *C. difficile* (Kint *et al*, in Annex) as observed in *S. aureus* and *B. subtilis* (Eymann and Hecker 2001, Pane-Farre et al. 2009). It seems possible that RsbZ has a basal activity allowing the dephosphorylation of RsbV~P and therefore the activation of σ^B in the absence of a stress exposure. This hypothesis is in agreement with our data obtained from SNAP fusions with genes strictly dependent on σ^B for their expression, showing that σ^B is active during the exponential growth phase at least in a fraction of the cells as already observed in *S. aureus* and *L. monocytogenes* (Pane-Farre et al. 2009, Utratna et al. 2012, Guldimann et al. 2017). The activation of σ^B during the exponential growth phase without previous exposure to stress probably promotes a rapid adaptation of the bacterium when it copes a hostile environment. Under these conditions, early activation of σ^B could be essential during the infectious cycle to resist the various stresses encountered in the host. However, we also observed that the revRbr *CDI474* gene expression level increases during growth,

confirming an increased σ^B activity at the stationary phase, as observed in other Firmicutes, and in previous transcriptomic data of *C. difficile* comparing the expression profiles between exponential and stationary growth phase (Saujet et al. 2011).

II.4. Heterogeneity of gene expression of *sigB* and σ^B -targets

Interestingly, we observed that the expression of the *sigB* gene was heterogeneous within a population of vegetative cells. Using a P_{sigB} -SNAP^{Cd} fusion, we showed that *sigB* is only expressed in a small fraction (between 10 and 20 %) of *C. difficile* cells during both exponential (4 h) and at the onset of the stationary growth phase (10 h) in both the wild-type and *sigB* mutant strains (Kint *et al.*, in Annex). This is in agreement with the fact that *C. difficile sigB* expression is not autoregulated, and with the transcriptomic analysis that do not reveal differences in the expression of this gene whatever the growth stages (Saujet et al. 2011) (Kint *et al.*, in Annex). As observed for the *sigB* gene, the expression of the flavodiiron protein (FDP) gene *CD1157* under the control of the dual promoter σ^A/σ^B or only through the σ^A - or σ^B - dependent promoters, was also detected in a very few number of cells during stationary phase. However, no major differences were observed in the percentage of cells expressing *CD1157* under the control of σ^A/σ^B or σ^A alone. Nevertheless, the number of cells expressing *CD1157* under σ^B control is even lower suggesting that the expression of the *CD1157* gene may be below the fluorescence detection limit. The same heterogeneity of expression was observed for genes encoding the reverse rubrerythrins (*revRbrs*, *CD1474* and *CD1524*) and the second FDP (*CD1623*) during stationary phase, which support that the activation of σ^B is heterogeneous. We noted that the expression of these genes was detected in a higher percentage of cells than the expression of *sigB* itself. Because these genes are only under the control of σ^B , it is possible that the level of expression of the P_{sigB} -SNAP^{Cd} fusion may be below the fluorescence detection limit. Finally, it would be interesting to verify if the cells expressing *sigB* show the same σ^B activity by using different reporter genes. Additionally, the analysis of the expression of other σ^B -controlled genes at the single cell level will be important to confirm the heterogeneity of σ^B activity.

Such heterogeneity of σ^B expression and activity may be a strategy to increase the chances of part of the population to survive when the environmental conditions become adverse (Eldar and Elowitz 2010, Guldimann et al. 2017). Heterogeneity of gene expression during stationary phase was recently showed for the *C. difficile* toxins, where only a fraction of the population expresses *tcdA* (Ransom et al. 2018b). This suggests that within a bacterial

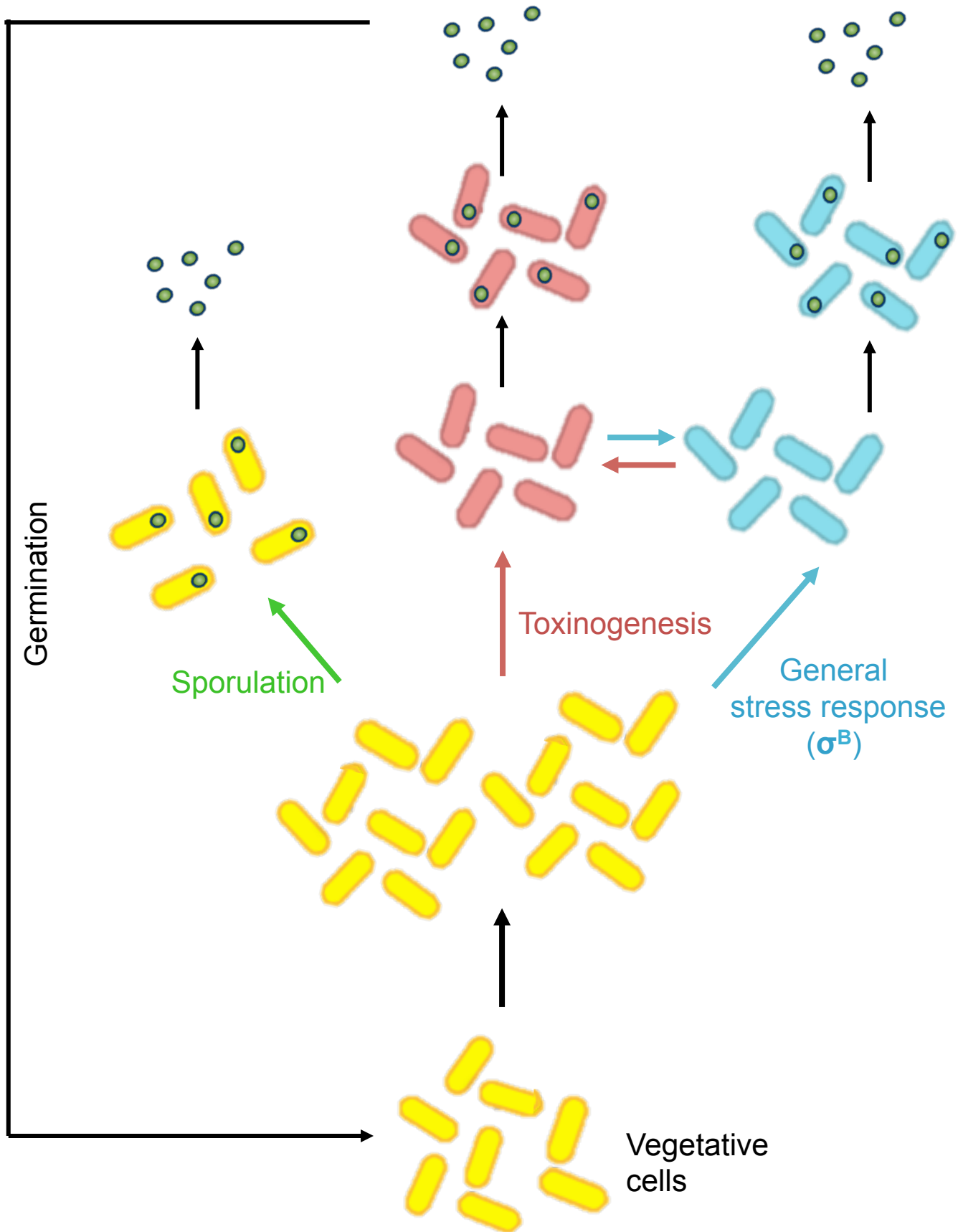


Figure 59: Heterogeneity of *C. difficile* gene expression. At stationary phase, the *C. difficile* bacterial population likely specialize into distinct subpopulations responsible for sporulation, σ^B -mediated stress response and toxin production. The two last subpopulations can survive as vegetative cells or eventually sporulate allowing the activations of σ^B or the toxin production in sporulating cells.

population, subpopulations could be responsible for different physiological functions through “bet-hedging” strategies in order to maximize the chances of survival in hostile conditions. Each *C. difficile* sub-population would invest in functions such as survival, toxin production or dissemination (Figure 59). This mechanism of “bet-hedging” might be important in *C. difficile* for an efficient colonization of the intestinal tract (Kint et al. 2017). However, the study of Ramson *et al*, and our data indicate that sporulation, toxin production and σ^B -dependent response are not exclusive processes. Toxin gene expression and sporulation can occur in the same cell and σ^B is active in sporulating cells, as it will be discussed more in detail below. These suggest that under stressful conditions, a sub-population of cells might directly initiate sporulation, while other sub-populations develop mechanisms of stress response mediated by σ^B or use their energetic sources to produce the toxins (Figure 59). In the presence of a currently unknown stimulus, these two last groups of cells can survive as vegetative cells or eventually might enter into sporulation. Whether σ^B activity and toxin production occur in the same cell is not yet known. In order to address this point, an interesting strategy would be to use different fluorescent reporter genes fused to promoters involved in stress response and toxin synthesis to study gene expression within a bacterial population by fluorescence microscopy.

III. O₂ tolerance and ROS protection in *C. difficile*

III.1. Protective role of the *C. difficile* revRbrs and FDPs

Previous results demonstrated an increased expression of genes encoding revRbrs and FDPs when *C. difficile* is exposed to air (Emerson et al. 2008). Surprisingly, in recent transcriptomic studies of *C. difficile* grown under microaerophilic conditions, these genes were not among the subset of upregulated genes (Giordano et al. 2018a, Neumann-Schaal et al. 2018). However, the *in vivo* results obtained in this work indicate that these proteins confer tolerance to O₂, and this protection most likely arises from their ability to scavenge O₂. A *C. difficile* double mutant inactivated for the two revRbrs and a mutant inactivated for the FDP CD1157 showed decreased tolerance to low O₂ tension. Accordingly, our complementary *in vitro* results showed that the revRbrs, CD1474 and CD1524, or the FDP CD1157 from *C. difficile*, in association with a NROR and a Rd from *E. coli*, function as NADH oxidase, reducing O₂ to water. Interestingly, the genes encoding the two revRbrs, Rbr3B and Rbr3A, and the two FDPs, FprA1 and FprA2, from *C. acetobutylicum* are upregulated after O₂ exposure and function as NADH oxidases (Kawasaki et al. 2004, Kawasaki et al. 2005). However, the oxidase specific activities of FprA1/ FprA2 are at least 100-fold higher than that of the revRbrs (Hillmann et al. 2009b, Riebe et al. 2009). In *C. difficile*, the NADH oxidase activities of the FDP and the revRbrs were almost similar (Table 3). Additionally, using the same artificial system described above (NROR and Rd from *E. coli*), we showed that the revRbrs CD1474 and CD1524 also have NADH peroxidase activity. As observed in *C. acetobutylicum*, the *C. difficile* revRbrs can use both O₂ and H₂O₂ as electron acceptors, but H₂O₂ is the preferred substrate. For both activities, the electron transfer pathway did not absolutely require the Rd from *E. coli*, but its presence increased the NADH peroxidase and oxidase activities. The physiological electron donors of both revRbrs and the FDP CD1157 from *C. difficile* remain unknown. However, since the genome of the *C. difficile* 630 strain does not contain genes encoding Rds, the NAD(P)H- oxidoreductases (ORs) in this strain most likely directly reduce the [Fe(SCys)₄] site of the revRbrs or the FMN domain of the FDP. Possible candidates for ORs in *C. difficile* might be the CD0176, the NADH oxidase CD2540 and a NADH-dependent flavin OR CD2709. In the laboratory, we have constructed a CD0176 deletion mutant. However, the inactivation of this gene did not result in a clear effect on the sensitivity of *C. difficile* to several stresses such as O₂ or H₂O₂. The enzymatic role of CD0176 is currently under study by our collaborators in Portugal. In addition, an interesting

Table 3. Reductase activities of the two revRbrs CD1474 and CD1524, and the two FDPs CD1157 and CD1623 to the substrates O₂, H₂O₂ and NO.

Enzyme	Enzymatic Activitiy (s⁻¹)		
	O₂	H₂O₂	NO
CD1474	1.15 ± 0.14	2.09 ± 0.15	0.02 ± 0.001
CD1524	1.98 ± 0.38	7.56 ± 0.62	0.03 ± 0.005
CD1157	1.36 ± 0.31	0.27 ± 0.03	0.19 ± 0.062
CD1623	16.0 ± 1.3	2.4 ± 0.5	0.20 ± 0.01

possibility that could be tested is whether the NROR and the Rd domains of the FDP CD1623 are able to reduce the revRbrs and/or the FDP CD1157.

In a previous study, FDP CD1623 showed an O₂-reductase activity (Folgosa et al. 2018b). The O₂ reductase activity of this enzyme was higher than the observed for the revRbrs and FDP CD1157 (Table 3). However, while we observed a decreased tolerance of the $\Delta CD1474\text{-}\Delta CD1524$ double mutant and the *CD1157* mutant to 0.4 % O₂, only a small difference was observed for the $\Delta CD1623$ mutant when compared to the wild-type. At 0.4 % O₂, the $\Delta CD1623\text{-}CD1157$ double mutant was only slightly different from the *CD1157* mutant. Future experiments at lower and higher percentages of O₂ will be performed in order to test more precisely the differences in O₂ tolerance between the mutants. When exposed to air, we observed a slight increased sensitivity of the $\Delta CD1623$ mutant, while no differences were observed for the other mutants. The reason why the $\Delta CD1474\text{-}\Delta CD1524$ double mutant and the *CD1157* mutant are more sensitive to low O₂ tension but not to air is not yet clear. The determination of the K_m of each enzyme will give additional information that might help to explain these differences.

The CD1623 protein contains all the domains necessary to oxidize the NADH and to directly reduce the substrate. By contrast, it is noteworthy that an artificial system of electron transfer was used to determine the revRbrs and CD1157 activities and can lead to an underestimation of the physiological activities. In addition, only half of the CD1157 purified protein was actually active due to an incomplete association with iron and FMN that are important cofactors for the enzymatic activity. Based on these data, we cannot exclude the possibility that the O₂-reductase activity determined for our proteins might be underestimated.

III.2. Protection against H₂O₂

Despite the different attempts and methods we tried to analyse the role of the revRbrs and the FDPs in H₂O₂ protection in *C. difficile*, we were unable to observe differences between the various mutants and the wild-type strain when exposed to this toxic compound. Therefore, even if an H₂O₂-reductase activity was observed for the two revRbrs and for the FDP CD1623 (Folgosa et al. 2018b), the absence of a phenotype for the corresponding mutants suggests functional redundancy. We showed that the *C. difficile sigB* mutant is more sensitive to H₂O₂ (Kint et al. 2017). In addition to the revRbrs and FDP CD1623, σ^B positively controls additional genes encoding proteins such as the glutamate dehydrogenase

GluD (Girinathan et al. 2014), and thioredoxins involved in thiol homeostasis (Kint et al. 2017). These proteins, together with the revRbrs and the FDP CD1623 might contribute to the *C. difficile* resistance against H₂O₂. Moreover, *C. difficile* genome encodes two classical Rbrs: CD2845 and CD0825. *CD2845* is expressed under the control of the sporulation-specific sigma factor σ^G and is likely not expressed during vegetative growth (Saujet et al. 2013). However, *CD0825* gene is part of an operon containing genes encoding the PerR regulator, a desulfoferrodoxin and a glutamate synthetase. A σ^A -dependent promoter is present upstream of the *CD0825* gene, but the control of the expression of this operon by PerR remains to be determined. A peroxidase activity of the classical Rbr from *C. difficile*, as well as the presence of other proteins able to scavenge H₂O₂, might still protect *C. difficile* against these compound, even in the absence of the revRbrs. To confirm these hypothesis, we plan to analyse in collaboration with Prof. Miguel Teixeira's group (ITQB, Portugal) the NADH oxidase and peroxidase activities of the crude extracts of the different single and multi-mutants, as it has been performed in *C. acetobutylicum* (Hillmann et al. 2008). We can speculate that if the peroxidase activity of crude extracts of the mutant inactivated for the two revRbrs is similar to the one observed in the wild-type strain, it would suggest that other proteins can have such activity in addition to that of the revRbrs. Additionally, this experiment might allow us to better compare the activity of the different revRbrs and FDPs enzymes without using artificial electron partners.

III.3. O₂ and ROS response in *B. subtilis* and clostridia

In *C. acetobutylicum*, σ^B is absent, and PerR is involved in H₂O₂ and O₂ resistance through the regulation of the expression of the genes encoding the revRbrs, among others (Hillmann et al. 2008). In this bacterium, the inactivation of *perR* leads to prolonged aerotolerance and higher resistance to H₂O₂ (Hillmann et al. 2008). An increased tolerance to H₂O₂ exposure was also observed in a strain overexpressing the genes encoding the revRbrs (Riebe et al. 2009). Interestingly, the authors were not able to inactivate the genes encoding the revRbrs suggesting that these genes are essential and required for the survival of *C. acetobutylicum* (Hillmann et al. 2006). Since we did not observe difference in the protection against H₂O₂ between the *C. difficile* wild-type strain and both the double $\Delta CDI474$ - $\Delta CDI524$ and single *CDI623* mutant, it would be interesting to test H₂O₂ sensitivity using the complemented strains where we expect an overexpression of each gene through a multicopy plasmid. In *B. subtilis*, the oxidative stress resistance can be mediated by catalases controlled



Figure 60: Amino acid sequence alignment of FDPs. The *C. difficile* FDPs CD1157 and CD1623 were aligned against the FDPs from *Thermotoga maritima*, *Entamoeba histolytica*, *Giardia intestinalis*, *Methanothermobacter marburgensis*, *Escherichia coli*, *Moorella thermoacetica* and *Desulfovibrio gigas*. Green arrows indicate the residues in positions 1 and 2. The selectivity for O₂ or NO is also indicated.

by either PerR (KatA) or σ^B (KatB and KatX). In this way, the response induced by oxidative stress would be either specific through PerR or mediated by a general stress response via σ^B (Hecker et al. 2007). In *C. difficile*, PerR and σ^B are present like in *B. subtilis*. However no induction of σ^B activity has been observed to date in the presence of ROS and the H₂O₂ protection mediated by σ^B is probably unspecific. Concerning the role of PerR and its targets in *C. difficile*, nothing has been yet studied, as the effect of H₂O₂ on gene expression. Further work will be needed to determine the targets of PerR and the connection that both PerR and σ^B might have to protect this bacterium from oxidative stress.

III.4. Protection against NO

Some FDPs have been shown to scavenge nitric oxide (NO) (Silaghi-Dumitrescu et al. 2003, Silaghi-Dumitrescu et al. 2005, Folgosa et al. 2018a). CD1157 belongs to the class A FDP. These FDPs typically have a clear preference for O₂ (Seedorf et al. 2004, Smutna et al. 2009, Vicente et al. 2012), or a dual reductase activity for NO and O₂, as observed for example for the FprA2 from *C. acetobutylicum* (Silaghi-Dumitrescu et al. 2003, Rodrigues et al. 2006, Hillmann et al. 2009b). Contrary to FprA2, only O₂-reductase activity was observed for CD1157 (Table 3). In addition, the *C. difficile* CD1623 of the class F FDP is clearly an O₂-reductase and does not have NO-reductase activity (Folgosa et al. 2018b). To date, the determinants of substrate specificity of the FDPs remains unclear, although it has been shown in *Entamoeba histolytica* that some amino acids in the catalytic center of the FDP can modulate its enzymatic activity (Goncalves et al. 2014). The alignment of *C. difficile* CD1157 with FDPs from other organisms reveals the conservation of Lys⁵³ and Tyr²⁶³ that are characteristic of FDPs with a preference for O₂ as substrate (Figure 60). The presence of a Lys⁵⁵ and a His²⁶⁷ in CD1623 suggested a specificity of this enzyme to O₂ (Figure 60). This is in agreement with the enzymatic activities found for these two enzymes mainly as O₂-reductases. Regarding the two revRbrs, they did not show NO-reductase activity. So far, no report of Rbrs with NO-reductase activity has been documented. The sensitivity of our different revRbrs and FDPs mutants to NO-donor compounds was analysed but no differences were observed when compared to the wild-type strain. This result was not surprising since none of the proteins seems able to efficiently use NO as substrate. Among genes positively controlled by σ^B in *C. difficile*, some encode proteins that may intervene in NO detoxification pathways. These proteins include a hydroxylamine reductase (CD2168) and two nitro-reductases (CD1125 and CD0837). A consensus sequence recognized by σ^B was found *in*

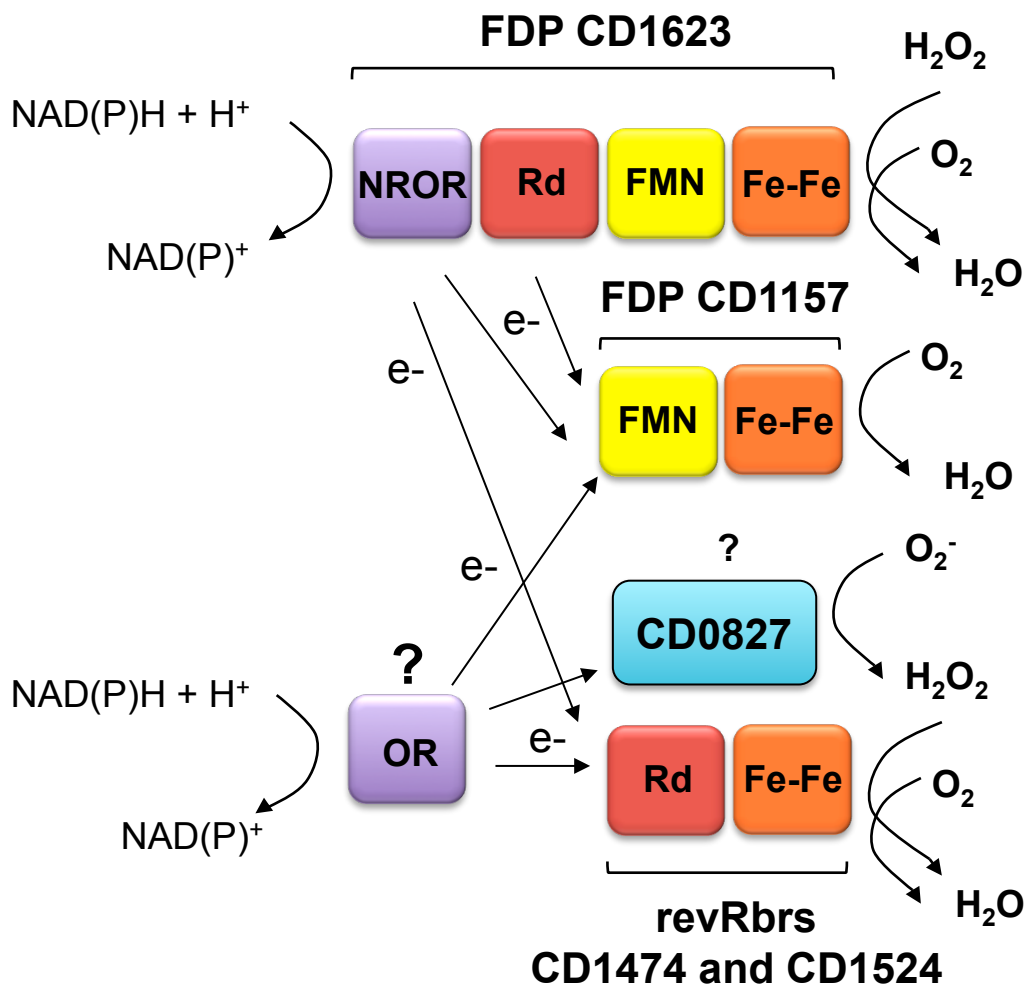


Figure 61: Model of the O_2 and ROS detoxification pathway in *C. difficile*. Scheme of the NAD(P)H-dependent O_2 , O_2^- and H_2O_2 detoxification complex. Structural domains are color coded. NROR (NADH rubredoxin oxidoreductase), OR (oxidoreductase), Rd (Rubredoxin domain), FMN (flavodoxin domain) and Fe-Fe (diiron center). Arrows indicate electron transference. Candidates for the OR may be CD0176, CD2540 and CD2709. The CD0827 desulfoferrodoxin is a candidate for the reduction of the O_2^- .

silico in the promoter regions of the *CD1125* and *CD0837* genes suggesting that σ^B directly controls their transcription. The role of these proteins in NO detoxification should be addressed in the future.

Altogether, our results clearly demonstrate that the two revRbrs and the two FDPs play an important role scavenging O_2 . Additionally, the two revRbrs are probably part of a subset of proteins that confers resistance to oxidative stress by scavenging H_2O_2 . Further studies will be needed to address additional candidates that combined with these proteins, constitute the reductive scavenging system for O_2 and ROS in *C. difficile*. Figure 61 summarizes the proposed ROS and O_2 detoxification pathways involving revRbrs, FDPs and yet non-identified proteins. Candidates for ORs might be CD0176, CD2540 and CD2709. In addition, we propose that the desulfoferrodoxin CD0827, is a candidate for the reduction of the superoxide anion in *C. difficile*.

III.5. Importance of O_2 , ROS and NO detoxification pathways during colonization

The inactivation of genes encoding proteins playing oxidative protective roles, results in a decrease in the virulence or colonization of the host. *Candida albicans* cells lacking a superoxide dismutase (SOD) are more susceptible to macrophage attack and had attenuated virulence in mice (Hwang et al. 2002). In *Streptococcus agalactiae*, SodA contributes to the virulence of the bacterium (Poyart et al. 2001). Despite the important role played by FDPs and Rbrs in scavenging O_2 , H_2O_2 and NO, studies showing their specific roles *in vivo* colonization are still limited. Mydel *et al* showed that the Rbr of *Porphyromonas gingivalis* ensures the proliferation of this pathogen in mice. However, the *in vivo* protection afforded by the Rbr was not associated with the oxidative burst responses but rather with protection against reactive nitrogen species (RNS) (Mydel et al. 2006). In *C. difficile*, the inactivation of *sigB* results in a major colonization defect. However, σ^B is a master regulator controlling a lot of different processes, including O_2 tolerance, ROS and NO protection (Kint et al. 2017). The specific role of the *C. difficile* revRbrs and the FDPs in colonization is a crucial point that will be addressed in future work.

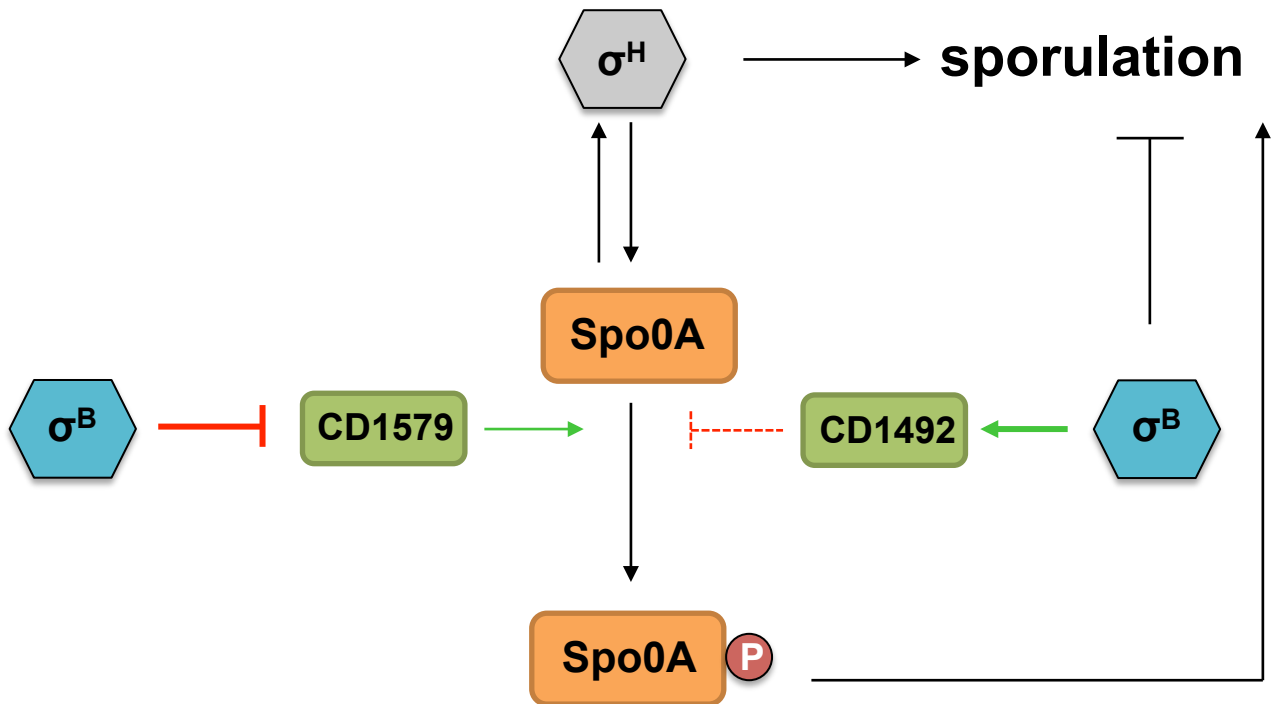


Figure 62: Model of the negative control of σ^B on *C. difficile* sporulation. The initiation of sporulation is dependent on σ^H , Spo0A and its phosphorylation state. σ^B negatively and positively controls the expression of the *CD1579* and the *CD1492* genes, respectively. σ^B negatively controls sporulation likely through regulation of the Spo0A phosphorylation. Green and red arrows represent positive or negative control respectively. A mechanism of phosphatase activity for CD1492 have not been characterized.

IV. The role of σ^B and its targets during sporulation

IV.1. The negative role of σ^B in sporulation

σ^B is the key regulator of the adaptive stress response in *C. difficile* vegetative cells. However, when all the alternative survival strategies fail, the last resource of this bacterium is to differentiate into a highly resistant dormant cell type, the endospore (Stephens 1998). In *C. difficile*, sporulation is negatively controlled by σ^B . The expression of more than 200 genes involved in sporulation are derepressed in a *sigB* mutant and this mutant sporulates more efficiently and/or earlier than the wild-type strain (Kint et al. 2017). In *B. subtilis*, the overexpression of *sigB* results in a decreased sporulation efficiency (Reder et al. 2012a, Reder et al. 2012b). Similarly, the inactivation of *rsbW* or *rsbX*, causing σ^B over-activation, inhibits the ability of *B. subtilis* to sporulate (Kalman et al. 1990, Benson and Haldenwang 1992). In this bacterium, σ^B seems to act at the initiation of the sporulation process by influencing the phosphorylation level of the master regulator of sporulation, Spo0A. Indeed, the *spo0E* gene, encoding a phosphatase involved in the dephosphorylation of Spo0A~P, has a promoter recognized by σ^B (Reder et al. 2012a). In *C. difficile*, σ^B negatively controls the expression of the *CD1579* gene, encoding a kinase of Spo0A. Additionally, σ^B positively controls the expression of the *CD1492* gene, encoding a phosphotransfer protein that seems to have a negative effect on sporulation since its inactivation increases spore production (Childress et al. 2016). These data support the idea that σ^B might lead to a decrease in Spo0A~P concentration resulting in the limitation of sporulation (Figure 62). Thus, to face stressful environments encountered during infection, *C. difficile* may use two strategies: 1) a rapid adaptive response to stress stimuli mediated by σ^B or 2) an irreversible and slower differentiation process leading to the formation of spores.

IV.2. *sigB* expression in sporulating cells

Surprisingly, we showed that even if σ^B represses sporulation, the *sigB* gene continues to be expressed during this developmental process. More importantly, σ^B is still active during sporulation since the genes encoding the two revRbrs, CD1474 and CD1524, the FDP CD1623, and the OR CD0176 are also expressed and proteins produced. We demonstrated actually that when the cells are grown in a medium that promotes sporulation, more than half of the vegetative cells express *sigB* and its targets genes (the revRbrs and the FDP CD1623) after 24 h of growth. Although these genes are expressed in both MC and FS compartments

from early sporulation steps until engulfment completion, both *sigB* and its targets will only be expressed in the MC compartment at the end of sporulation process. The mechanism behind this differential control of expression remains unknown. However, we noted that the expression of these genes during sporulation is still dependent on *sigB* and, that the *sigB* operon including *rsbV* and *rsbW* is transcriptionally regulated by σ^A and expressed during sporulation. Several studies in *B. subtilis* demonstrated that σ^A continued to be active during sporulation in both compartments (Fujita 2000, Li and Piggot 2001, Fukushima et al. 2003, Ohashi et al. 2003). Certain classes of housekeeping genes such as the *sacB* gene transcribed from a σ^A -dependent promoter are expressed in the FS and in the MC both before and after engulfment (Li and Piggot 2001). However, expression of σ^A -dependent motility genes or other genes involved in the synthesis of histidine, phenylalanine and serine were severely reduced after initiation of sporulation. These suggest that the expression of particular σ^A -dependent genes is subjected to additional regulatory mechanisms (Steil et al. 2005). Unfortunately, as far as I know, the expression of *B. subtilis sigB* gene has not been monitored during sporulation using fluorescence microscopy. However, based on our results we may hypothesize that in *C. difficile* additional regulators might be involved in the compartmentalization of σ^A -dependent gene expression. It is also possible that an unknown regulatory mechanism is involved in the control of *sigB* expression during sporulation. However, we cannot exclude other possibilities such as the binding of SASPs proteins to the FS DNA at the end of sporulation that might hinder the expression of certain genes in the FS, such as the *sigB* operon. The analysis of the expression of *C. difficile* housekeeping genes and genes under the dual control of σ^A and σ^B , such as *CD1157* encoding the FDP, during the different morphogenetic stages of sporulation will be an interesting point to address in the future. This would give new insights about the role of both σ^A and σ^B in sporulation.

Another interesting point to be discussed is the detection of the anti-sigma factor RsbV in the total proteome of the spore (Lawley et al. 2009b). Neither σ^B nor the anti-anti-sigma factor RsbW was detected. First, this fact might suggest an increased stability of RsbV over the others. Second, the undetected σ^B is in agreement with the absence of σ^B activity in the FS compartment after engulfment completion.

We also demonstrated that even if *sigB* was expressed in more than half of the cells after engulfment completion, the expression of the gene encoding the OR CD0176 was detected only in a few cells at the same stage. Since the expression of *CD0176* is also strictly dependent on σ^B , this data suggests that a targeted activity of σ^B might exist, associated to the

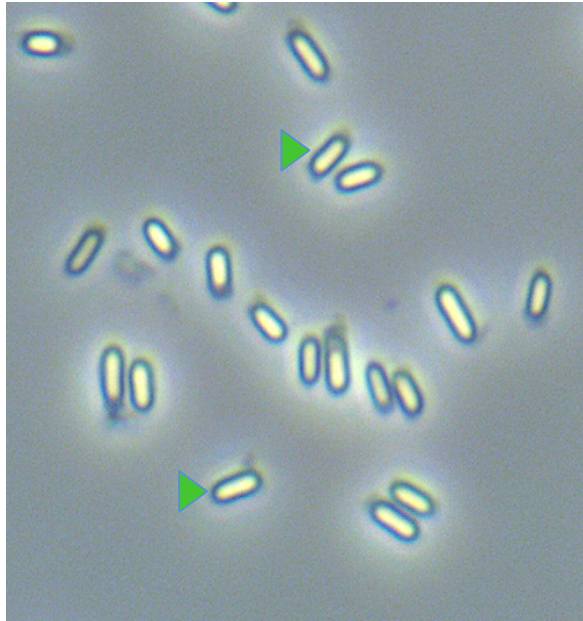
presence of additional regulation factors controlling the σ^B regulon during sporulation. The detailed mechanisms controlling the expression and activation of σ^B during sporulation will be addressed in future experiments.

IV.3. The hypothetical protective role of the σ^B -target genes

IV.3.a. Spore resistance

Spores are resistant to O_2 but also to H_2O_2 , hypochlorite and other disinfectants used in hospital (Fawley et al. 2007, Otter and French 2009). Several factors contribute to the protection of the spore against oxidizing agents, such as the DNA saturation by SASPs, the low permeability of the spore inner membrane and, the spore coat layer (Setlow 2014). The protective role of the spore coat is very likely related both with its barrier effect and with the presence of proteins able to detoxify oxidizing compounds before they reach more internal targets (Riesenman and Nicholson 2000). In *B. subtilis*, CotA protects spores from H_2O_2 (Hullo et al. 2001). However, a protective role against ROS by SodA and the catalases CotJC and YjqC present at the spore surface has not been shown (Henriques et al. 1995, Henriques et al. 1998). In *C. difficile*, catalase activity was observed for the recombinant catalases, CotD and CotG but not for CotCB. The *cotD* mutant spores showed a reduction in catalase activity compared to the wild-type strain (Permpoonpattana et al. 2013). The expression of the genes encoding the revRbrs and the FDP CD1623 in the MC compartment is in agreement with the localization of the corresponding proteins at the outermost layers of the spore. These proteins could contribute to the resistance of the spore to O_2 and ROS. Indeed, the revRbrs have O_2 - and H_2O_2 -reductase activities *in vitro*. However, contrary to the catalases that can perform their enzymatic reactions without needing other partners, the revRbrs need an electron transfer pathway and an electron donor, such as NADH. The FDP CD1623, which also has O_2 - and H_2O_2 -reductase activities, contains all the domains and can play its enzymatic role without partners, but still needs an electron donor. It should be noted that spores being metabolically inactive produce minimal if any levels of ATP and NADH (Korza et al. 2017, Setlow et al. 2017). Whether these proteins are active and play a protective role at the spore surface is still speculative and will be investigated. Therefore, it would be interesting to compare the peroxidase activity of the spores of the different revRbrs and FDPs mutants as well their resistance to H_2O_2 . It is also important to extend this study to other σ^B targets, detected or not in the proteome of the spore outermost layers. For instance, one of the two *C. difficile* thioredoxin systems composed by the thioredoxin-CD1690 and the thioredoxin

Wild-type



$\Delta CD1474\Delta CD1524$

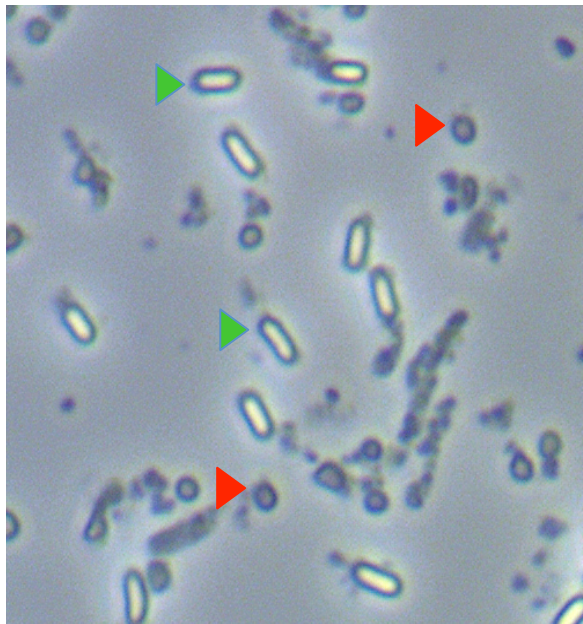


Figure 63: Phase-contrast microscopy of purified spores of the wild-type and the $\Delta CD1474\Delta CD1524$ double mutant strains. Green arrows mark mature phase-bright spores and red arrows indicate immature, phase-dark spores.

reductase-CD1691 is transcribed by σ^B . The thioredoxin reductase was detected in the proteome of the spore, but not to that of the spore surface layers (Lawley et al. 2009b, Abhyankar et al. 2013, Diaz-Gonzalez et al. 2015). The study of the expression of these genes and the localization of the encoding proteins might give clues about the role of σ^B and its targets in spore protection.

IV.3.b. Germination and Outgrowth

The expression of the genes encoding the two revRbrs, the FDP CD1623 and the OR CD0176 in the FS compartment during sporulation might suggest importance of their role in the future vegetative cell, particularly during outgrowth. *Clostridium novyi* spores contain mRNA encoding a thioredoxin reductase, a glutaredoxin, a glutathione peroxidase and a Rd (Bettegowda et al. 2006). Glutathione peroxidases have been implicated as major scavengers for H₂O₂ (Arthur 2000). Interestingly, transcripts encoding CD1631-SodA, two putative OR complexes with ferredoxin activity (CD2197-CD2199 and CD2427-CD2429), a NADH oxidase (CD2540) and a NADH-dependent flavin oxidoreductase (CD2709) have been found in *C. difficile* germinating spores. The presence of some σ^B -targets transcripts stored in the spore could also allow the spores to rapidly synthesize proteins that are required for germination and outgrowth in permissive oxidative environments. It would be interesting to monitor the expression of these genes during outgrowth from purified spores carrying the transcriptional SNAP fusions. In future work, the analysis of the germination efficiency of the different mutants will be also carried out in conditions mimicking the gut environment. Another interesting possibility to be addressed is whether the localization of the revRbrs, FDPs and the OR at the outermost layers of the spore are important during outgrowth as well. During germination and outgrowth, the spore coat layer is discarded to allow emergence of the vegetative form (Hamilton and Stubbs 1967, Abee et al. 2011). Because the revRbrs, FDPs and the OR proteins are part of the outermost layer, they might provide an arsenal that protects the cell during outgrowth, through the detoxification of toxic compounds in the surrounding environment.

IV.3.c. Mother cell protection

Recent results have raised another hypothesis for the role of σ^B during sporulation. Indeed, after 7 days of growth in sporulation medium, we observed that the double mutant inactivated for the two revRbrs produce less spores than the wild-type strain (Figure 63). Additionally, phase-contrast microscopy analysis revealed a mixture of immature phase-dark

and mature spores phase-bright spores for the double mutant purified spores, while mainly phase bright spores were observed in the wild-type strain. The reason for the high amount of phase-dark spores in the $\Delta CD1474\text{-}\Delta CD1524$ double mutant is not yet known. However, given the decreased tolerance of the double mutant to low O₂ tension and probably to other stresses, we hypothesize that the mutant cells might be more sensitive and more susceptible to lysis. During sporulation, the timing of the MC lysis is crucial to ensure the release of a mature spore (Sato et al. 2006). A premature lysis of the sporulating cell might typically prevent for a proper formation and maturation of the spore. This might explain, in part, the decreased spore yield for the double mutant inactivated for the two revRbrs. In the colon, *C. difficile* sporulates in conditions where the cells are exposed to inflammation. These proteins, not only protect the cell against O₂ and possibly H₂O₂ during growth, but they also might play an important protective role for the endospore during sporulation. The activity of σ^B and the production of the revRbrs in the MC until the last steps of spore formation might be important to protect the cell before the mature spore is formed and released to the environment. In order to address our hypothesis, we plan to monitor the sporulation of the double mutant during the 7 days in SMC plates and combine it with live/death cell microscopy experiment. In addition, we plan to test the effect of stressful compounds such as H₂O₂ on the sporulation process of the wild-type and the double mutant. Very few studies exist concerning the role of revRbrs. Two revRbrs of around 90% identical to the revRbrs (CD1474 and CD1524) of *C. difficile*, were identified in the exosporium of *C. sordelli* spores (Rabi et al. 2018). However, the mechanism behind their synthesis is not yet known. The *sigB* operon is conserved in this bacterium, however its role has not been yet studied. Studies on the expression and role of revRbrs in other spore forming bacteria will be important to help to elucidate their role during sporulation.

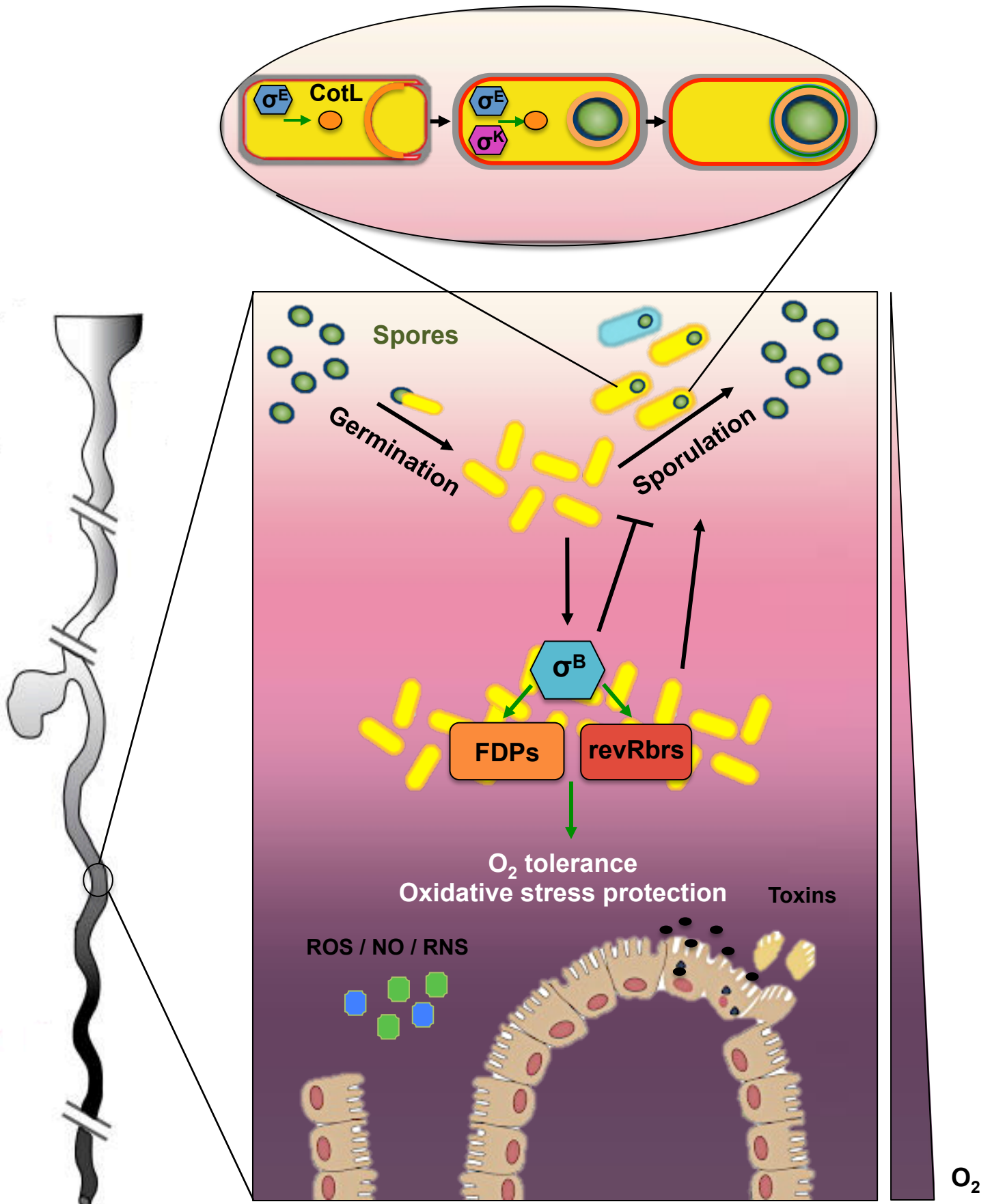


Figure 64: Model for the role of σ^B and sporulation during colonization of the gastrointestinal tract by *C. difficile*. After ingestion, *C. difficile* spores will germinate in the intestine. Once in the colon, vegetative cells are exposed to various stresses such as the increasing O_2 tension in the proximity of the epithelial cells. In addition, the host produces oxidizing compounds such as ROS/NO and RNS via the inflammatory process. The activation of σ^B and the synthesis of the FDPs and revRbrs proteins will allow bacteria to survive and proliferate in the colon. In the presence of a yet not known stimulus, *C. difficile* sporulates and in a sub-population of sporulating cells, σ^B is active. In the MC compartment, the spore coat protein CotL, which encoding gene is transcribed by both σ^E and σ^K , localizes first as a cap in the MC proximal pole and later around the spore. CotL is responsible for the encasement of other coat proteins around the FS, playing a key role in the morphogenesis of the *C. difficile* spore coat.

V. Conclusion

This work brought new information on 1) key enzymes used by *C. difficile* to scavenge O₂ and H₂O₂ and involved in oxidative stress tolerance and 2) the structure and morphogenesis of the *C. difficile* spore coat layers. Indeed, after spore germination in the small intestine, the vegetative cells of *C. difficile* will multiply and colonize the colon as a nutrient-rich environment, while being exposed to toxic compounds that can affect their growth (Figure 64). Moreover, the production and secretion of toxins by *C. difficile* lead to a strong inflammation process that promotes the production of antimicrobial oxidizing compounds by the host immune cells such as ROS, NO and RNS. In addition, an increasing gradient of O₂ exist from the intestinal lumen (anaerobic) to the mucosa (approximately 5% O₂), which can increase again and/or be disturb after an antibiotic treatment. The implementation of a stress response mediated by σ^B appears as a first survival strategy. σ^B , which is active in a fraction of the vegetative cells, inhibits sporulation and controls genes essential to guarantee an efficient colonization of the gut. Among them, are the revRbrs- and FDPs-encoding genes (Figure 64). In this work, we showed that these proteins are essential determinants for the ability of *C. difficile* to tolerate and survive in the presence of low O₂ tension. Whether these proteins play a role *in vivo* in the detoxification of H₂O₂ will be addressed in the future. When the conditions become too hostile, sporulation, a long and irreversible process, is then implemented to produce spores. Interestingly, even if σ^B represses sporulation, σ^B -mediated stress response and sporulation might not be mutually exclusive processes. The synthesis of the revRbrs in the MC compartment, controlled by σ^B during sporulation, might protect the cell against oxidizing components by inactivating them before the spore is ready to be released (Figure 64). The *C. difficile* spore is the highly infectious form of this bacterium and serves as means of survival during transmission from one host to another. In this work, we characterized a new spore protein, CotL that is essential for the assembly of the spore coat layers and ultimately, for the formation of a resistant spore (Figure 64). We found that CotL is located inside the coat of the *C. difficile* spore, and demonstrated that its role during coat assembly is to mediate the encasement of other coat components around the FS during sporulation. However important questions still remain and particularly on how CotL, together with SpoIVA and SipL, interact with all the proteins that they direct to the surface of the developing spore. Nevertheless, the present study has expanded our knowledge on *C. difficile* spore morphology, highlighting that the coat assembly pathway in *C. difficile* presents substantial differences relative to that of *B. subtilis*.

Bibliography

- Abecasis, A. B., M. Serrano, R. Alves, L. Quintais, J. B. Pereira-Leal, and A. O. Henriques. 2013. A genomic signature and the identification of new sporulation genes. *J Bacteriol* **195**:2101-2115.
- Abee, T., M. N. Groot, M. Tempelaars, M. Zwietering, R. Moezelaar, and M. van der Voort. 2011. Germination and outgrowth of spores of *Bacillus cereus* group members: diversity and role of germinant receptors. *Food Microbiol* **28**:199-208.
- Abhyankar, W., A. H. Hossain, A. Djajasaputra, P. Permpoonpattana, A. Ter Beek, H. L. Dekker, S. M. Cutting, S. Brul, L. J. de Koning, and C. G. de Koster. 2013. In pursuit of protein targets: proteomic characterization of bacterial spore outer layers. *J Proteome Res* **12**:4507-4521.
- Abram, F., E. Starr, K. A. Karatzas, K. Matlawska-Wasowska, A. Boyd, M. Wiedmann, K. J. Boor, D. Connally, and C. P. O'Byrne. 2008. Identification of components of the sigma B regulon in *Listeria monocytogenes* that contribute to acid and salt tolerance. *Appl Environ Microbiol* **74**:6848-6858.
- Abt, M. C., P. T. McKenney, and E. G. Pamer. 2016a. *Clostridium difficile* colitis: pathogenesis and host defence. *Nat Rev Microbiol* **14**:609-620.
- Abt, M. C., P. T. McKenney, and E. G. Pamer. 2016b. *Clostridium difficile* colitis: pathogenesis and host defence. *Nat Rev Microbiol* **14**:609-620.
- Adams, C. M., B. E. Eckenroth, E. E. Putnam, S. Double, and A. Shen. 2013. Structural and functional analysis of the CspB protease required for *Clostridium* spore germination. *PLoS Pathog* **9**:e1003165.
- Aguilar, C., H. Vlamakis, A. Guzman, R. Losick, and R. Kolter. 2010. KinD is a checkpoint protein linking spore formation to extracellular-matrix production in *Bacillus subtilis* biofilms. *MBio* **1**.
- Aktories, K., P. Papatheodorou, and C. Schwan. 2018. Binary *Clostridium difficile* toxin (CDT) - A virulence factor disturbing the cytoskeleton. *Anaerobe*.
- Aktories, K., C. Schwan, and T. Jank. 2017. *Clostridium difficile* Toxin Biology. *Annu Rev Microbiol*.
- Al-Hinai, M. A., S. W. Jones, and E. T. Papoutsakis. 2015. The *Clostridium* sporulation programs: diversity and preservation of endospore differentiation. *Microbiol Mol Biol Rev* **79**:19-37.
- Alper, S., A. Dufour, D. A. Garsin, L. Duncan, and R. Losick. 1996. Role of adenosine nucleotides in the regulation of a stress-response transcription factor in *Bacillus subtilis*. *J Mol Biol* **260**:165-177.
- Alvarez-Perez, S., J. L. Blanco, T. Pelaez, M. P. Lanzarot, C. Harmanus, E. Kuijper, and M. E. Garcia. 2015. Faecal shedding of antimicrobial-resistant *Clostridium difficile* strains by dogs. *J Small Anim Pract* **56**:190-195.
- Amano, A., H. Tamagawa, S. Shizukuishi, and A. Tsunemitsu. 1986. Superoxide dismutase, catalase and peroxidases in oral anaerobic bacteria. *J Osaka Univ Dent Sch* **26**:187-192.
- Antelmann, H., S. Engelmann, R. Schmid, A. Sorokin, A. Lapidus, and M. Hecker. 1997. Expression of a stress- and starvation-induced *dps/pexB*-homologous gene is controlled by the alternative sigma factor sigmaB in *Bacillus subtilis*. *J Bacteriol* **179**:7251-7256.
- Antelmann, H., C. Scharf, and M. Hecker. 2000. Phosphate starvation-inducible proteins of *Bacillus subtilis*: proteomics and transcriptional analysis. *J Bacteriol* **182**:4478-4490.
- Antharam, V. C., E. C. Li, A. Ishmael, A. Sharma, V. Mai, K. H. Rand, and G. P. Wang. 2013. Intestinal dysbiosis and depletion of butyrogenic bacteria in *Clostridium difficile* infection and nosocomial diarrhea. *J Clin Microbiol* **51**:2884-2892.
- Antonopoulos, D. A., S. M. Huse, H. G. Morrison, T. M. Schmidt, M. L. Sogin, and V. B. Young. 2009. Reproducible community dynamics of the gastrointestinal microbiota following antibiotic perturbation. *Infect Immun* **77**:2367-2375.
- Antunes, A., E. Camiade, M. Monot, E. Courtois, F. Barbut, N. V. Sernova, D. A. Rodionov, I. Martin-Verstraete, and B. Dupuy. 2012. Global transcriptional control by glucose and carbon regulator CcpA in *Clostridium difficile*. *Nucleic Acids Res* **40**:10701-10718.
- Antunes, A., I. Martin-Verstraete, and B. Dupuy. 2011. CcpA-mediated repression of *Clostridium difficile* toxin gene expression. *Mol Microbiol* **79**:882-899.
- Aravind, L., and C. P. Ponting. 1997. The GAF domain: an evolutionary link between diverse phototransducing proteins. *Trends Biochem Sci* **22**:458-459.

- Aronson, A. I., L. Ekanayake, and P. C. Fitz-James. 1992. Protein filaments may initiate the assembly of the *Bacillus subtilis* spore coat. *Biochimie* **74**:661-667.
- Aronson, A. I., and P. Fitz-James. 1976. Structure and morphogenesis of the bacterial spore coat. *Bacteriol Rev* **40**:360-402.
- Arthur, J. R. 2000. The glutathione peroxidases. *Cell Mol Life Sci* **57**:1825-1835.
- Asai, K., H. Takamatsu, M. Iwano, T. Kodama, K. Watabe, and N. Ogasawara. 2001. The *Bacillus subtilis* yabQ gene is essential for formation of the spore cortex. *Microbiology* **147**:919-927.
- Aung, S., J. Shum, A. Abanes-De Mello, D. H. Broder, J. Fredlund-Gutierrez, S. Chiba, and K. Pogliano. 2007. Dual localization pathways for the engulfment proteins during *Bacillus subtilis* sporulation. *Mol Microbiol* **65**:1534-1546.
- Avila-Perez, M., K. J. Hellingwerf, and R. Kort. 2006. Blue light activates the sigmaB-dependent stress response of *Bacillus subtilis* via YtvA. *J Bacteriol* **188**:6411-6414.
- Avila-Perez, M., J. B. van der Steen, R. Kort, and K. J. Hellingwerf. 2010. Red light activates the sigmaB-mediated general stress response of *Bacillus subtilis* via the energy branch of the upstream signaling cascade. *J Bacteriol* **192**:755-762.
- Awad, M. M., P. A. Johanesen, G. P. Carter, E. Rose, and D. Lyras. 2014. *Clostridium difficile* virulence factors: Insights into an anaerobic spore-forming pathogen. *Gut Microbes* **5**:579-593.
- Baban, S. T., S. A. Kuehne, A. Barketi-Klai, S. T. Cartman, M. L. Kelly, K. R. Hardie, I. Kansau, A. Collignon, and N. P. Minton. 2013. The role of flagella in *Clostridium difficile* pathogenesis: comparison between a non-epidemic and an epidemic strain. *PLoS One* **8**:e73026.
- Backhed, F., H. Ding, T. Wang, L. V. Hooper, G. Y. Koh, A. Nagy, C. F. Semenkovich, and J. I. Gordon. 2004. The gut microbiota as an environmental factor that regulates fat storage. *Proc Natl Acad Sci U S A* **101**:15718-15723.
- Backhed, F., J. Roswall, Y. Peng, Q. Feng, H. Jia, P. Kovatcheva-Datchary, Y. Li, Y. Xia, H. Xie, H. Zhong, M. T. Khan, J. Zhang, J. Li, L. Xiao, J. Al-Aama, D. Zhang, Y. S. Lee, D. Kotowska, C. Colding, V. Tremaroli, Y. Yin, S. Bergman, X. Xu, L. Madsen, K. Kristiansen, J. Dahlgren, and J. Wang. 2015. Dynamics and Stabilization of the Human Gut Microbiome during the First Year of Life. *Cell Host Microbe* **17**:852.
- Bagyan, I., J. Hobot, and S. Cutting. 1996. A compartmentalized regulator of developmental gene expression in *Bacillus subtilis*. *J Bacteriol* **178**:4500-4507.
- Bagyan, I., and P. Setlow. 2002. Localization of the cortex lytic enzyme CwlJ in spores of *Bacillus subtilis*. *J Bacteriol* **184**:1219-1224.
- Bailey-Smith, K., S. J. Todd, T. W. Southworth, J. Proctor, and A. Moir. 2005. The ExsA protein of *Bacillus cereus* is required for assembly of coat and exosporium onto the spore surface. *J Bacteriol* **187**:3800-3806.
- Baines, S. D., R. O'Connor, K. Saxton, J. Freeman, and M. H. Wilcox. 2009. Activity of vancomycin against epidemic *Clostridium difficile* strains in a human gut model. *J Antimicrob Chemother* **63**:520-525.
- Ball, D. A., R. Taylor, S. J. Todd, C. Redmond, E. Couture-Tosi, P. Sylvestre, A. Moir, and P. A. Bullough. 2008. Structure of the exosporium and sublayers of spores of the *Bacillus cereus* family revealed by electron crystallography. *Mol Microbiol* **68**:947-958.
- Bandow, J. E., H. Brotz, and M. Hecker. 2002. *Bacillus subtilis* tolerance of moderate concentrations of rifampin involves the sigma(B)-dependent general and multiple stress response. *J Bacteriol* **184**:459-467.
- Barak, I., and P. Youngman. 1996. SpoIIE mutants of *Bacillus subtilis* comprise two distinct phenotypic classes consistent with a dual functional role for the SpoIIE protein. *J Bacteriol* **178**:4984-4989.
- Barbut, F., A. Richard, K. Hamadi, V. Chomette, B. Burghoffer, and J. C. Petit. 2000. Epidemiology of recurrences or reinfections of *Clostridium difficile*-associated diarrhea. *J Clin Microbiol* **38**:2386-2388.
- Barra-Carrasco, J., V. Olguin-Araneda, A. Plaza-Garrido, C. Miranda-Cardenas, G. Cofre-Araneda, M. Pizarro-Guajardo, M. R. Sarker, and D. Paredes-Sabja. 2013. The *Clostridium difficile* exosporium cysteine (CdeC)-rich protein is required for exosporium morphogenesis and coat assembly. *J Bacteriol* **195**:3863-3875.

- Beall, B., A. Driks, R. Losick, and C. P. Moran, Jr. 1993. Cloning and characterization of a gene required for assembly of the *Bacillus subtilis* spore coat. *J Bacteriol* **175**:1705-1716.
- Becker, L. A., M. S. Cetin, R. W. Hutkins, and A. K. Benson. 1998. Identification of the gene encoding the alternative sigma factor sigmaB from *Listeria monocytogenes* and its role in osmotolerance. *J Bacteriol* **180**:4547-4554.
- Behravan, J., H. Chirakkal, A. Masson, and A. Moir. 2000. Mutations in the gerP locus of *Bacillus subtilis* and *Bacillus cereus* affect access of germinants to their targets in spores. *J Bacteriol* **182**:1987-1994.
- Benson, A. K., and W. G. Haldenwang. 1992. Characterization of a regulatory network that controls sigma B expression in *Bacillus subtilis*. *J Bacteriol* **174**:749-757.
- Benson, A. K., and W. G. Haldenwang. 1993a. *Bacillus subtilis* sigma B is regulated by a binding protein (RsbW) that blocks its association with core RNA polymerase. *Proc Natl Acad Sci U S A* **90**:2330-2334.
- Benson, A. K., and W. G. Haldenwang. 1993b. Regulation of sigma B levels and activity in *Bacillus subtilis*. *J Bacteriol* **175**:2347-2356.
- Benson, A. K., and W. G. Haldenwang. 1993c. The sigma B-dependent promoter of the *Bacillus subtilis* sigB operon is induced by heat shock. *J Bacteriol* **175**:1929-1935.
- Bettegowda, C., X. Huang, J. Lin, I. Cheong, M. Kohli, S. A. Szabo, X. Zhang, L. A. Diaz, Jr., V. E. Velculescu, G. Parmigiani, K. W. Kinzler, B. Vogelstein, and S. Zhou. 2006. The genome and transcriptomes of the anti-tumor agent *Clostridium novyi*-NT. *Nat Biotechnol* **24**:1573-1580.
- Bhattacharjee, D., K. N. McAllister, and J. A. Sorg. 2016. Germinants and Their Receptors in Clostridia. *J Bacteriol* **198**:2767-2775.
- Bi, C., S. W. Jones, D. R. Hess, B. P. Tracy, and E. T. Papoutsakis. 2011. SpoIIE is necessary for asymmetric division, sporulation, and expression of sigmaF, sigmaE, and sigmaG but does not control solvent production in *Clostridium acetobutylicum* ATCC 824. *J Bacteriol* **193**:5130-5137.
- Bischoff, M., and B. Berger-Bachi. 2001. Teicoplanin stress-selected mutations increasing sigma(B) activity in *Staphylococcus aureus*. *Antimicrob Agents Chemother* **45**:1714-1720.
- Bischoff, M., P. Dunman, J. Kormanec, D. Macapagal, E. Murphy, W. Mounts, B. Berger-Bachi, and S. Projan. 2004. Microarray-based analysis of the *Staphylococcus aureus* sigmaB regulon. *J Bacteriol* **186**:4085-4099.
- Borriello, S. P., A. R. Welch, F. E. Barclay, and H. A. Davies. 1988. Mucosal association by *Clostridium difficile* in the hamster gastrointestinal tract. *J Med Microbiol* **25**:191-196.
- Bouillaut, L., W. T. Self, and A. L. Sonenshein. 2013. Proline-dependent regulation of *Clostridium difficile* Stickland metabolism. *J Bacteriol* **195**:844-854.
- Boydston, J. A., P. Chen, C. T. Steichen, and C. L. Turnbough, Jr. 2005. Orientation within the exosporium and structural stability of the collagen-like glycoprotein BclA of *Bacillus anthracis*. *J Bacteriol* **187**:5310-5317.
- Boydston, J. A., L. Yue, J. F. Kearney, and C. L. Turnbough, Jr. 2006. The ExsY protein is required for complete formation of the exosporium of *Bacillus anthracis*. *J Bacteriol* **188**:7440-7448.
- Boylan, S. A., A. R. Redfield, M. S. Brody, and C. W. Price. 1993. Stress-induced activation of the sigma B transcription factor of *Bacillus subtilis*. *J Bacteriol* **175**:7931-7937.
- Boylan, S. A., A. Rutherford, S. M. Thomas, and C. W. Price. 1992. Activation of *Bacillus subtilis* transcription factor sigma B by a regulatory pathway responsive to stationary-phase signals. *J Bacteriol* **174**:3695-3706.
- Brandt, L. J. 2012. Fecal transplantation for the treatment of *Clostridium difficile* infection. *Gastroenterol Hepatol (N Y)* **8**:191-194.
- Braun, V., T. Hundsberger, P. Leukel, M. Sauerborn, and C. von Eichel-Streiber. 1996. Definition of the single integration site of the pathogenicity locus in *Clostridium difficile*. *Gene* **181**:29-38.
- Brigulla, M., T. Hoffmann, A. Krisp, A. Volker, E. Bremer, and U. Volker. 2003. Chill induction of the SigB-dependent general stress response in *Bacillus subtilis* and its contribution to low-temperature adaptation. *J Bacteriol* **185**:4305-4314.
- Briolat, V., and G. Reysset. 2002. Identification of the *Clostridium perfringens* genes involved in the adaptive response to oxidative stress. *J Bacteriol* **184**:2333-2343.

- Brioukhanov, A. L., and A. I. Netrusov. 2004. Catalase and superoxide dismutase: distribution, properties, and physiological role in cells of strict anaerobes. *Biochemistry (Mosc)* **69**:949-962.
- Brito-Silva, C., J. Pizarro-Cerda, F. Gil, and D. Paredes-Sabja. 2018. Identification of *Escherichia coli* strains for the heterologous overexpression of soluble *Clostridium difficile* exosporium proteins. *J Microbiol Methods* **154**:46-51.
- Britton, R. A., and V. B. Young. 2012. Interaction between the intestinal microbiota and host in *Clostridium difficile* colonization resistance. *Trends Microbiol* **20**:313-319.
- Britton, R. A., and V. B. Young. 2014. Role of the intestinal microbiota in resistance to colonization by *Clostridium difficile*. *Gastroenterology* **146**:1547-1553.
- Broder, D. H., and K. Pogliano. 2006. Forespore engulfment mediated by a ratchet-like mechanism. *Cell* **126**:917-928.
- Brody, M. S., V. Stewart, and C. W. Price. 2009. Bypass suppression analysis maps the signalling pathway within a multidomain protein: the RsbP energy stress phosphatase 2C from *Bacillus subtilis*. *Mol Microbiol* **72**:1221-1234.
- Brody, M. S., K. Vijay, and C. W. Price. 2001. Catalytic function of an alpha/beta hydrolase is required for energy stress activation of the sigma(B) transcription factor in *Bacillus subtilis*. *J Bacteriol* **183**:6422-6428.
- Browne, H. P., S. C. Forster, B. O. Anonye, N. Kumar, B. A. Neville, M. D. Stares, D. Goulding, and T. D. Lawley. 2016. Culturing of 'unculturable' human microbiota reveals novel taxa and extensive sporulation. *Nature* **533**:543-546.
- Brunt, J., K. L. Cross, and M. W. Peck. 2015. Apertures in the *Clostridium sporogenes* spore coat and exosporium align to facilitate emergence of the vegetative cell. *Food Microbiol* **51**:45-50.
- Buffie, C. G., V. Bucci, R. R. Stein, P. T. McKenney, L. Ling, A. Gobourne, D. No, H. Liu, M. Kinnebrew, A. Viale, E. Littmann, M. R. van den Brink, R. R. Jenq, Y. Taur, C. Sander, J. R. Cross, N. C. Toussaint, J. B. Xavier, and E. G. Pamer. 2015. Precision microbiome reconstitution restores bile acid mediated resistance to *Clostridium difficile*. *Nature* **517**:205-208.
- Buffie, C. G., I. Jarchum, M. Equinda, L. Lipuma, A. Gobourne, A. Viale, C. Ubeda, J. Xavier, and E. G. Pamer. 2012. Profound alterations of intestinal microbiota following a single dose of clindamycin results in sustained susceptibility to *Clostridium difficile*-induced colitis. *Infect Immun* **80**:62-73.
- Burbulys, D., K. A. Trach, and J. A. Hoch. 1991. Initiation of sporulation in *B. subtilis* is controlled by a multicomponent phosphorelay. *Cell* **64**:545-552.
- Burkholder, W. F., I. Kurtser, and A. D. Grossman. 2001. Replication initiation proteins regulate a developmental checkpoint in *Bacillus subtilis*. *Cell* **104**:269-279.
- Burns, D. A., J. T. Heap, and N. P. Minton. 2010. SleC is essential for germination of *Clostridium difficile* spores in nutrient-rich medium supplemented with the bile salt taurocholate. *J Bacteriol* **192**:657-664.
- Butzin, X. Y., A. J. Troiano, W. H. Coleman, K. K. Griffiths, C. J. Doona, F. E. Feeherry, G. Wang, Y. Q. Li, and P. Setlow. 2012. Analysis of the effects of a gerP mutation on the germination of spores of *Bacillus subtilis*. *J Bacteriol* **194**:5749-5758.
- Calderon-Romero, P., P. Castro-Cordova, R. Reyes-Ramirez, M. Milano-Cespedes, E. Guerrero-Araya, M. Pizarro-Guajardo, V. Olguin-Araneda, F. Gil, and D. Paredes-Sabja. 2018. *Clostridium difficile* exosporium cysteine-rich proteins are essential for the morphogenesis of the exosporium layer, spore resistance, and affect *C. difficile* pathogenesis. *PLoS Pathog* **14**:e1007199.
- Camp, A. H., and R. Losick. 2008. A novel pathway of intercellular signalling in *Bacillus subtilis* involves a protein with similarity to a component of type III secretion channels. *Mol Microbiol* **69**:402-417.
- Camp, A. H., and R. Losick. 2009. A feeding tube model for activation of a cell-specific transcription factor during sporulation in *Bacillus subtilis*. *Genes Dev* **23**:1014-1024.
- Campo, N., and D. Z. Rudner. 2007. SpoIVB and CtpB are both forespore signals in the activation of the sporulation transcription factor sigmaK in *Bacillus subtilis*. *J Bacteriol* **189**:6021-6027.

- Cangiano, G., A. Mazzone, L. Baccigalupi, R. Isticato, P. Eichenberger, M. De Felice, and E. Ricca. 2010. Direct and indirect control of late sporulation genes by GerR of *Bacillus subtilis*. *J Bacteriol* **192**:3406-3413.
- Cardenas, J. P., R. Quatrini, and D. S. Holmes. 2016. Aerobic Lineage of the Oxidative Stress Response Protein Rubrerythrin Emerged in an Ancient Microaerobic, (Hyper)Thermophilic Environment. *Front Microbiol* **7**:1822.
- Carr, K. A., B. K. Janes, and P. C. Hanna. 2010. Role of the gerP operon in germination and outgrowth of *Bacillus anthracis* spores. *PLoS One* **5**:e9128.
- Carroll, K. C., and J. G. Bartlett. 2011. Biology of *Clostridium difficile*: implications for epidemiology and diagnosis. *Annu Rev Microbiol* **65**:501-521.
- Carter, G. P., A. Chakravorty, T. A. Pham Nguyen, S. Mileto, F. Schreiber, L. Li, P. Howarth, S. Clare, B. Cunningham, S. P. Sambol, A. Cheknis, I. Figueroa, S. Johnson, D. Gerding, J. I. Rood, G. Dougan, T. D. Lawley, and D. Lyras. 2015. Defining the Roles of TcdA and TcdB in Localized Gastrointestinal Disease, Systemic Organ Damage, and the Host Response during *Clostridium difficile* Infections. *MBio* **6**:e00551.
- Carter, G. P., G. R. Douce, R. Govind, P. M. Howarth, K. E. Mackin, J. Spencer, A. M. Buckley, A. Antunes, D. Kotsanas, G. A. Jenkin, B. Dupuy, J. I. Rood, and D. Lyras. 2011. The anti-sigma factor TcdC modulates hypervirulence in an epidemic BI/NAP1/027 clinical isolate of *Clostridium difficile*. *PLoS Pathog* **7**:e1002317.
- Carter, G. P., D. Lyras, D. L. Allen, K. E. Mackin, P. M. Howarth, J. R. O'Connor, and J. I. Rood. 2007. Binary toxin production in *Clostridium difficile* is regulated by CdtR, a LytTR family response regulator. *J Bacteriol* **189**:7290-7301.
- Carter, G. P., J. I. Rood, and D. Lyras. 2012. The role of toxin A and toxin B in the virulence of *Clostridium difficile*. *Trends Microbiol* **20**:21-29.
- Cartman, S. T., J. T. Heap, S. A. Kuehne, A. Cockayne, and N. P. Minton. 2010. The emergence of 'hypervirulence' in *Clostridium difficile*. *Int J Med Microbiol* **300**:387-395.
- Cartman, S. T., M. L. Kelly, D. Heeg, J. T. Heap, and N. P. Minton. 2012. Precise manipulation of the *Clostridium difficile* chromosome reveals a lack of association between the tcdC genotype and toxin production. *Appl Environ Microbiol* **78**:4683-4690.
- Cassier, M., and A. Ryter. 1971. [A *Clostridium perfringens* mutant producing coatless spores by lysozyme-dependent germination]. *Ann Inst Pasteur (Paris)* **121**:717-732.
- Cassona, C. P., F. Pereira, M. Serrano, and A. O. Henriques. 2016. A Fluorescent Reporter for Single Cell Analysis of Gene Expression in *Clostridium difficile*. *Methods Mol Biol* **1476**:69-90.
- Catalano, F. A., J. Meador-Parton, D. L. Popham, and A. Driks. 2001. Amino acids in the *Bacillus subtilis* morphogenetic protein SpoIVA with roles in spore coat and cortex formation. *J Bacteriol* **183**:1645-1654.
- Cebrian, G., N. Sagarzazu, A. Aertsen, R. Pagan, S. Condon, and P. Manas. 2009. Role of the alternative sigma factor sigma on *Staphylococcus aureus* resistance to stresses of relevance to food preservation. *J Appl Microbiol* **107**:187-196.
- Cerquetti, M., A. Serafino, A. Sebastianelli, and P. Mastrantonio. 2002. Binding of *Clostridium difficile* to Caco-2 epithelial cell line and to extracellular matrix proteins. *FEMS Immunol Med Microbiol* **32**:211-218.
- Chada, V. G., E. A. Sanstad, R. Wang, and A. Driks. 2003. Morphogenesis of bacillus spore surfaces. *J Bacteriol* **185**:6255-6261.
- Chandrasekaran, R., and D. B. Lacy. 2017. The role of toxins in *Clostridium difficile* infection. *FEMS Microbiol Rev* **41**:723-750.
- Chang, J. Y., D. A. Antonopoulos, A. Kalra, A. Tonelli, W. T. Khalife, T. M. Schmidt, and V. B. Young. 2008. Decreased diversity of the fecal Microbiome in recurrent *Clostridium difficile*-associated diarrhea. *J Infect Dis* **197**:435-438.
- Chastanet, A., and R. Losick. 2007. Engulfment during sporulation in *Bacillus subtilis* is governed by a multi-protein complex containing tandemly acting autolysins. *Mol Microbiol* **64**:139-152.
- Chateau, A., W. van Schaik, P. Joseph, L. D. Handke, S. M. McBride, F. M. Smeets, A. L. Sonenshein, and A. Fouet. 2013. Identification of CodY targets in *Bacillus anthracis* by genome-wide in vitro binding analysis. *J Bacteriol* **195**:1204-1213.

- Chaturongakul, S., and K. J. Boor. 2004. RsbT and RsbV contribute to sigmaB-dependent survival under environmental, energy, and intracellular stress conditions in *Listeria monocytogenes*. *Appl Environ Microbiol* **70**:5349-5356.
- Chaturongakul, S., and K. J. Boor. 2006. SigmaB activation under environmental and energy stress conditions in *Listeria monocytogenes*. *Appl Environ Microbiol* **72**:5197-5203.
- Chen, L., M. Y. Liu, J. LeGall, P. Fareleira, H. Santos, and A. V. Xavier. 1993. Rubredoxin oxidase, a new flavo-hemo-protein, is the site of oxygen reduction to water by the "strict anaerobe" *Desulfovibrio gigas*. *Biochem Biophys Res Commun* **193**:100-105.
- Chen, L. C., J. C. Chen, J. C. Shu, C. Y. Chen, S. C. Chen, S. H. Chen, C. Y. Lin, C. Y. Lu, and C. C. Chen. 2012. Interplay of RsbM and RsbK controls the sigma(B) activity of *Bacillus cereus*. *Environ Microbiol* **14**:2788-2799.
- Chesnokova, O. N., S. A. McPherson, C. T. Steichen, and C. L. Turnbough, Jr. 2009. The spore-specific alanine racemase of *Bacillus anthracis* and its role in suppressing germination during spore development. *J Bacteriol* **191**:1303-1310.
- Childress, K. O., A. N. Edwards, K. L. Nawrocki, S. E. Anderson, E. C. Woods, and S. M. McBride. 2016. The Phosphotransfer Protein CD1492 Represses Sporulation Initiation in *Clostridium difficile*. *Infect Immun* **84**:3434-3444.
- Collins, M. D., P. A. Lawson, A. Willems, J. J. Cordoba, J. Fernandez-Garayzabal, P. Garcia, J. Cai, H. Hippe, and J. A. Farrow. 1994. The phylogeny of the genus *Clostridium*: proposal of five new genera and eleven new species combinations. *Int J Syst Bacteriol* **44**:812-826.
- Cornely, O. A., M. A. Miller, T. J. Louie, D. W. Crook, and S. L. Gorbach. 2012. Treatment of first recurrence of *Clostridium difficile* infection: fidaxomicin versus vancomycin. *Clin Infect Dis* **55 Suppl 2**:S154-161.
- Costa, T., A. L. Isidro, C. P. Moran, Jr., and A. O. Henriques. 2006. Interaction between coat morphogenetic proteins SafA and SpoVID. *J Bacteriol* **188**:7731-7741.
- Costa, T., M. Serrano, L. Steil, U. Volker, C. P. Moran, Jr., and A. O. Henriques. 2007. The timing of cotE expression affects *Bacillus subtilis* spore coat morphology but not lysozyme resistance. *J Bacteriol* **189**:2401-2410.
- Coullon, H., A. Rifflet, R. Wheeler, C. Janoir, I. G. Boneca, and T. Candela. 2018. N-Deacetylases required for muramic-delta-lactam production are involved in *Clostridium difficile* sporulation, germination and heat resistance. *J Biol Chem*.
- Coulter, E. D., and D. M. Kurtz, Jr. 2001. A role for rubredoxin in oxidative stress protection in *Desulfovibrio vulgaris*: catalytic electron transfer to rubrerythrin and two-iron superoxide reductase. *Arch Biochem Biophys* **394**:76-86.
- Coulter, E. D., N. V. Shenvi, and D. M. Kurtz, Jr. 1999. NADH peroxidase activity of rubrerythrin. *Biochem Biophys Res Commun* **255**:317-323.
- Cowardin, C. A., E. L. Buonomo, M. M. Saleh, M. G. Wilson, S. L. Burgess, S. A. Kuehne, C. Schwan, A. M. Eichhoff, F. Koch-Nolte, D. Lyras, K. Aktories, N. P. Minton, and W. A. Petri, Jr. 2016. The binary toxin CDT enhances *Clostridium difficile* virulence by suppressing protective colonic eosinophilia. *Nat Microbiol* **1**:16108.
- Cox, J., and M. Mann. 2008. MaxQuant enables high peptide identification rates, individualized p.p.b.-range mass accuracies and proteome-wide protein quantification. *Nat Biotechnol* **26**:1367-1372.
- Cox, J., N. Neuhauser, A. Michalski, R. A. Scheltema, J. V. Olsen, and M. Mann. 2011. Andromeda: a peptide search engine integrated into the MaxQuant environment. *J Proteome Res* **10**:1794-1805.
- Crobach, M. J. T., J. J. Vernon, V. G. Loo, L. Y. Kong, S. Pechine, M. H. Wilcox, and E. J. Kuijper. 2018. Understanding *Clostridium difficile* Colonization. *Clin Microbiol Rev* **31**.
- Cybulski, R. J., Jr., P. Sanz, F. Alem, S. Stibitz, R. L. Bull, and A. D. O'Brien. 2009. Four superoxide dismutases contribute to *Bacillus anthracis* virulence and provide spores with redundant protection from oxidative stress. *Infect Immun* **77**:274-285.
- Daniel, R. A., and J. Errington. 1993. Cloning, DNA sequence, functional analysis and transcriptional regulation of the genes encoding dipicolinic acid synthetase required for sporulation in *Bacillus subtilis*. *J Mol Biol* **232**:468-483.

- Dannheim, H., T. Riedel, M. Neumann-Schaal, B. Bunk, I. Schober, C. Sproer, C. M. Chibani, S. Gronow, H. Liesegang, J. Overmann, and D. Schomburg. 2017. Manual curation and reannotation of the genomes of *Clostridium difficile* 630Deltaerm and *C. difficile* 630. *J Med Microbiol* **66**:286-293.
- Davies, K. A., C. M. Longshaw, G. L. Davis, E. Bouza, F. Barbut, Z. Barna, M. Delmee, F. Fitzpatrick, K. Ivanova, E. Kuijper, I. S. Macovei, S. Mentula, P. Mastrantonio, L. von Muller, M. Oleastro, E. Petinaki, H. Pituch, T. Noren, E. Novakova, O. Nyc, M. Rupnik, D. Schmid, and M. H. Wilcox. 2014. Underdiagnosis of *Clostridium difficile* across Europe: the European, multicentre, prospective, biannual, point-prevalence study of *Clostridium difficile* infection in hospitalised patients with diarrhoea (EUCLID). *Lancet Infect Dis* **14**:1208-1219.
- Dawson, L. F., E. Valiente, and B. W. Wren. 2009. *Clostridium difficile*--a continually evolving and problematic pathogen. *Infect Genet Evol* **9**:1410-1417.
- de Been, M., C. Francke, R. J. Siezen, and T. Abee. 2011. Novel sigmaB regulation modules of Gram-positive bacteria involve the use of complex hybrid histidine kinases. *Microbiology* **157**:3-12.
- de Been, M., M. H. Tempelaars, W. van Schaik, R. Moezelaar, R. J. Siezen, and T. Abee. 2010. A novel hybrid kinase is essential for regulating the sigma(B)-mediated stress response of *Bacillus cereus*. *Environ Microbiol* **12**:730-745.
- de Francesco, M., J. Z. Jacobs, F. Nunes, M. Serrano, P. T. McKenney, M. H. Chua, A. O. Henriques, and P. Eichenberger. 2012. Physical interaction between coat morphogenetic proteins SpoVID and CotE is necessary for spore encasement in *Bacillus subtilis*. *J Bacteriol* **194**:4941-4950.
- de Hoon, M. J., P. Eichenberger, and D. Vitkup. 2010. Hierarchical evolution of the bacterial sporulation network. *Curr Biol* **20**:R735-745.
- Deakin, L. J., S. Clare, R. P. Fagan, L. F. Dawson, D. J. Pickard, M. R. West, B. W. Wren, N. F. Fairweather, G. Dougan, and T. D. Lawley. 2012. The *Clostridium difficile* spo0A gene is a persistence and transmission factor. *Infect Immun* **80**:2704-2711.
- Debast, S. B., M. P. Bauer, E. J. Kuijper, M. European Society of Clinical, and D. Infectious. 2014. European Society of Clinical Microbiology and Infectious Diseases: update of the treatment guidance document for *Clostridium difficile* infection. *Clin Microbiol Infect* **20 Suppl 2**:1-26.
- Decoursey, T. E., and E. Ligeti. 2005. Regulation and termination of NADPH oxidase activity. *Cell Mol Life Sci* **62**:2173-2193.
- deMare, F., D. M. Kurtz, Jr., and P. Nordlund. 1996. The structure of *Desulfovibrio vulgaris* rubrerythrin reveals a unique combination of rubredoxin-like FeS4 and ferritin-like diiron domains. *Nat Struct Biol* **3**:539-546.
- Dembek, M., A. Kelly, A. Barwinska-Sendra, E. Tarrant, W. A. Stanley, D. Vollmer, J. Biboy, J. Gray, W. Vollmer, and P. S. Salgado. 2018. Peptidoglycan degradation machinery in *Clostridium difficile* forespore engulfment. *Mol Microbiol*.
- Dembek, M., R. A. Stabler, A. A. Witney, B. W. Wren, and N. F. Fairweather. 2013. Transcriptional analysis of temporal gene expression in germinating *Clostridium difficile* 630 endospores. *PLoS One* **8**:e64011.
- Deutscher, J., C. Francke, and P. W. Postma. 2006. How phosphotransferase system-related protein phosphorylation regulates carbohydrate metabolism in bacteria. *Microbiol Mol Biol Rev* **70**:939-1031.
- Diaz, O. R., C. V. Sayer, D. L. Popham, and A. Shen. 2018. *Clostridium difficile* Lipoprotein GerS Is Required for Cortex Modification and Thus Spore Germination. *mSphere* **3**.
- Diaz-Gonzalez, F., M. Milano, V. Olguin-Araneda, J. Pizarro-Cerda, P. Castro-Cordova, S. C. Tzeng, C. S. Maier, M. R. Sarker, and D. Paredes-Sabja. 2015. Protein composition of the outermost exosporium-like layer of *Clostridium difficile* 630 spores. *J Proteomics* **123**:1-13.
- Dineen, S. S., S. M. McBride, and A. L. Sonenshein. 2010. Integration of metabolism and virulence by *Clostridium difficile* CodY. *J Bacteriol* **192**:5350-5362.
- Dineen, S. S., A. C. Villapakkam, J. T. Nordman, and A. L. Sonenshein. 2007. Repression of *Clostridium difficile* toxin gene expression by CodY. *Mol Microbiol* **66**:206-219.
- Dingle, T. C., G. L. Mulvey, and G. D. Armstrong. 2011. Mutagenic analysis of the *Clostridium difficile* flagellar proteins, FliC and FliD, and their contribution to virulence in hamsters. *Infect Immun* **79**:4061-4067.

- Doan, T., C. Morlot, J. Meisner, M. Serrano, A. O. Henriques, C. P. Moran, Jr., and D. Z. Rudner. 2009. Novel secretion apparatus maintains spore integrity and developmental gene expression in *Bacillus subtilis*. *PLoS Genet* **5**:e1000566.
- Donnelly, M. L., K. A. Fimlaid, and A. Shen. 2016. Characterization of *Clostridium difficile* Spores Lacking Either SpoVAC or Dipicolinic Acid Synthetase. *J Bacteriol* **198**:1694-1707.
- Donnelly, M. L., W. Li, Y. Q. Li, L. Hinkel, P. Setlow, and A. Shen. 2017. A *Clostridium difficile*-Specific, Gel-Forming Protein Required for Optimal Spore Germination. *MBio* **8**.
- Dos Santos, W. G., I. Pacheco, M. Y. Liu, M. Teixeira, A. V. Xavier, and J. LeGall. 2000. Purification and characterization of an iron superoxide dismutase and a catalase from the sulfate-reducing bacterium *Desulfovibrio gigas*. *J Bacteriol* **182**:796-804.
- Driks, A., and P. Eichenberger. 2016. The Spore Coat. *Microbiol Spectr* **4**.
- Driks, A., S. Roels, B. Beall, C. P. Moran, Jr., and R. Losick. 1994. Subcellular localization of proteins involved in the assembly of the spore coat of *Bacillus subtilis*. *Genes Dev* **8**:234-244.
- Dubois, T., M. Dancer-Thibonnier, M. Monot, A. Hamiot, L. Bouillaut, O. Soutourina, I. Martin-Verstraete, and B. Dupuy. 2016. Control of *Clostridium difficile* Physiopathology in Response to Cysteine Availability. *Infect Immun* **84**:2389-2405.
- Dufour, A., and W. G. Haldenwang. 1994. Interactions between a *Bacillus subtilis* anti-sigma factor (RsbW) and its antagonist (RsbV). *J Bacteriol* **176**:1813-1820.
- Duncan, L., and R. Losick. 1993. SpoIIAB is an anti-sigma factor that binds to and inhibits transcription by regulatory protein sigma F from *Bacillus subtilis*. *Proc Natl Acad Sci U S A* **90**:2325-2329.
- Dupuy, B., R. Govind, A. Antunes, and S. Matamouros. 2008. *Clostridium difficile* toxin synthesis is negatively regulated by TcdC. *J Med Microbiol* **57**:685-689.
- Dupuy, B., and A. L. Sonenshein. 1998. Regulated transcription of *Clostridium difficile* toxin genes. *Mol Microbiol* **27**:107-120.
- Dworkin, J. 2003. Transient genetic asymmetry and cell fate in a bacterium. *Trends Genet* **19**:107-112.
- Edwards, A. N., S. T. Karim, R. A. Pascual, L. M. Jowhar, S. E. Anderson, and S. M. McBride. 2016a. Chemical and Stress Resistances of *Clostridium difficile* Spores and Vegetative Cells. *Front Microbiol* **7**:1698.
- Edwards, A. N., K. L. Nawrocki, and S. M. McBride. 2014. Conserved oligopeptide permeases modulate sporulation initiation in *Clostridium difficile*. *Infect Immun* **82**:4276-4291.
- Edwards, A. N., R. Tamayo, and S. M. McBride. 2016b. A novel regulator controls *Clostridium difficile* sporulation, motility and toxin production. *Mol Microbiol* **100**:954-971.
- Eglow, R., C. Pothoulakis, S. Itzkowitz, E. J. Israel, C. J. O'Keane, D. Gong, N. Gao, Y. L. Xu, W. A. Walker, and J. T. LaMont. 1992. Diminished *Clostridium difficile* toxin A sensitivity in newborn rabbit ileum is associated with decreased toxin A receptor. *J Clin Invest* **90**:822-829.
- Ehsaan, M., S. A. Kuehne, and N. P. Minton. 2016. *Clostridium difficile* Genome Editing Using pyrE Alleles. *Methods Mol Biol* **1476**:35-52.
- Eichenberger, P., P. Fawcett, and R. Losick. 2001. A three-protein inhibitor of polar septation during sporulation in *Bacillus subtilis*. *Mol Microbiol* **42**:1147-1162.
- Eichenberger, P., M. Fujita, S. T. Jensen, E. M. Conlon, D. Z. Rudner, S. T. Wang, C. Ferguson, K. Haga, T. Sato, J. S. Liu, and R. Losick. 2004. The program of gene transcription for a single differentiating cell type during sporulation in *Bacillus subtilis*. *PLoS Biol* **2**:e328.
- Eichenberger, P., S. T. Jensen, E. M. Conlon, C. van Ooij, J. Silvaggi, J. E. Gonzalez-Pastor, M. Fujita, S. Ben-Yehuda, P. Stragier, J. S. Liu, and R. Losick. 2003. The sigmaE regulon and the identification of additional sporulation genes in *Bacillus subtilis*. *J Mol Biol* **327**:945-972.
- El Meouche, I., J. Peltier, M. Monot, O. Soutourina, M. Pestel-Caron, B. Dupuy, and J. L. Pons. 2013. Characterization of the SigD regulon of *C. difficile* and its positive control of toxin production through the regulation of tcdR. *PLoS One* **8**:e83748.
- Eldar, A., and M. B. Elowitz. 2010. Functional roles for noise in genetic circuits. *Nature* **467**:167-173.
- Emerson, J. E., R. A. Stabler, B. W. Wren, and N. F. Fairweather. 2008. Microarray analysis of the transcriptional responses of *Clostridium difficile* to environmental and antibiotic stress. *J Med Microbiol* **57**:757-764.
- Engelmann, S., and M. Hecker. 1996. Impaired oxidative stress resistance of *Bacillus subtilis* sigB mutants and the role of katA and katE. *FEMS Microbiol Lett* **145**:63-69.

- Enoch, D. A., M. J. Butler, S. Pai, S. H. Aliyu, and J. A. Karas. 2011. Clostridium difficile in children: colonisation and disease. *J Infect* **63**:105-113.
- Entenza, J. M., P. Moreillon, M. M. Senn, J. Kormanec, P. M. Dunman, B. Berger-Bachi, S. Projan, and M. Bischoff. 2005. Role of sigmaB in the expression of Staphylococcus aureus cell wall adhesins ClfA and FnbA and contribution to infectivity in a rat model of experimental endocarditis. *Infect Immun* **73**:990-998.
- Errington, J. 2003. Regulation of endospore formation in Bacillus subtilis. *Nat Rev Microbiol* **1**:117-126.
- Escobar-Cortes, K., J. Barra-Carrasco, and D. Paredes-Sabja. 2013. Proteases and sonication specifically remove the exosporium layer of spores of Clostridium difficile strain 630. *J Microbiol Methods* **93**:25-31.
- Espey, M. G. 2013. Role of oxygen gradients in shaping redox relationships between the human intestine and its microbiota. *Free Radic Biol Med* **55**:130-140.
- Eveillard, M., V. Fourel, M. C. Barc, S. Kerneis, M. H. Coconnier, T. Karjalainen, P. Bourlioux, and A. L. Servin. 1993. Identification and characterization of adhesive factors of Clostridium difficile involved in adhesion to human colonic enterocyte-like Caco-2 and mucus-secreting HT29 cells in culture. *Mol Microbiol* **7**:371-381.
- Eymann, C., and M. Hecker. 2001. Induction of sigma(B)-dependent general stress genes by amino acid starvation in a spo0H mutant of Bacillus subtilis. *FEMS Microbiol Lett* **199**:221-227.
- Eymann, C., S. Schulz, K. Gronau, D. Becher, M. Hecker, and C. W. Price. 2011. In vivo phosphorylation patterns of key stressosome proteins define a second feedback loop that limits activation of Bacillus subtilis sigmaB. *Mol Microbiol* **80**:798-810.
- Fagan, R. P., and N. F. Fairweather. 2011. Clostridium difficile has two parallel and essential Sec secretion systems. *J Biol Chem* **286**:27483-27493.
- Faille, C., Y. Lequette, A. Ronse, C. Slomianny, E. Garenaux, and Y. Guerardel. 2010. Morphology and physico-chemical properties of Bacillus spores surrounded or not with an exosporium: consequences on their ability to adhere to stainless steel. *Int J Food Microbiol* **143**:125-135.
- Fang, F. C. 2004. Antimicrobial reactive oxygen and nitrogen species: concepts and controversies. *Nat Rev Microbiol* **2**:820-832.
- Fareleira, P., B. S. Santos, C. Antonio, P. Moradas-Ferreira, J. LeGall, A. V. Xavier, and H. Santos. 2003. Response of a strict anaerobe to oxygen: survival strategies in Desulfovibrio gigas. *Microbiology* **149**:1513-1522.
- Farrow, M. A., N. M. Chumblor, L. A. Lapiere, J. L. Franklin, S. A. Rutherford, J. R. Goldenring, and D. B. Lacy. 2013. Clostridium difficile toxin B-induced necrosis is mediated by the host epithelial cell NADPH oxidase complex. *Proc Natl Acad Sci U S A* **110**:18674-18679.
- Fawcett, P., P. Eichenberger, R. Losick, and P. Youngman. 2000. The transcriptional profile of early to middle sporulation in Bacillus subtilis. *Proc Natl Acad Sci U S A* **97**:8063-8068.
- Fawley, W. N., S. Underwood, J. Freeman, S. D. Baines, K. Saxton, K. Stephenson, R. C. Owens, Jr., and M. H. Wilcox. 2007. Efficacy of hospital cleaning agents and germicides against epidemic Clostridium difficile strains. *Infect Control Hosp Epidemiol* **28**:920-925.
- Ferreira, A., M. Gray, M. Wiedmann, and K. J. Boor. 2004. Comparative genomic analysis of the sigB operon in Listeria monocytogenes and in other Gram-positive bacteria. *Curr Microbiol* **48**:39-46.
- Ferreira, A., C. P. O'Byrne, and K. J. Boor. 2001. Role of sigma(B) in heat, ethanol, acid, and oxidative stress resistance and during carbon starvation in Listeria monocytogenes. *Appl Environ Microbiol* **67**:4454-4457.
- Feucht, A., T. Magnin, M. D. Yudkin, and J. Errington. 1996. Bifunctional protein required for asymmetric cell division and cell-specific transcription in Bacillus subtilis. *Genes Dev* **10**:794-803.
- Fimlaid, K. A., J. P. Bond, K. C. Schutz, E. E. Putnam, J. M. Leung, T. D. Lawley, and A. Shen. 2013. Global analysis of the sporulation pathway of Clostridium difficile. *PLoS Genet* **9**:e1003660.
- Fimlaid, K. A., O. Jensen, M. L. Donnelly, M. B. Francis, J. A. Sorg, and A. Shen. 2015. Identification of a Novel Lipoprotein Regulator of Clostridium difficile Spore Germination. *PLoS Pathog* **11**:e1005239.

- Fimlaid, K. A., and A. Shen. 2015. Diverse mechanisms regulate sporulation sigma factor activity in the Firmicutes. *Curr Opin Microbiol* **24**:88-95.
- Fletcher, J. R., S. Erwin, C. Lanzas, and C. M. Theriot. 2018. Shifts in the Gut Metabolome and *Clostridium difficile* Transcriptome throughout Colonization and Infection in a Mouse Model. *mSphere* **3**.
- Folgosa, F., M. C. Martins, and M. Teixeira. 2018a. Diversity and complexity of flavodiiron NO/O₂ reductases. *FEMS Microbiol Lett* **365**.
- Folgosa, F., M. C. Martins, and M. Teixeira. 2018b. The multidomain flavodiiron protein from *Clostridium difficile* 630 is an NADH:oxygen oxidoreductase. *Sci Rep* **8**:10164.
- Foster, J. W. 1999. When protons attack: microbial strategies of acid adaptation. *Curr Opin Microbiol* **2**:170-174.
- Francis, M. B., C. A. Allen, R. Shrestha, and J. A. Sorg. 2013a. Bile acid recognition by the *Clostridium difficile* germinant receptor, CspC, is important for establishing infection. *PLoS Pathog* **9**:e1003356.
- Francis, M. B., C. A. Allen, and J. A. Sorg. 2013b. Muricholic acids inhibit *Clostridium difficile* spore germination and growth. *PLoS One* **8**:e73653.
- Francis, M. B., C. A. Allen, and J. A. Sorg. 2015. Spore Cortex Hydrolysis Precedes Dipicolinic Acid Release during *Clostridium difficile* Spore Germination. *J Bacteriol* **197**:2276-2283.
- Francis, M. B., and J. A. Sorg. 2016. Dipicolinic Acid Release by Germinating *Clostridium difficile* Spores Occurs through a Mechanosensing Mechanism. *mSphere* **1**.
- Fredlund, J., D. Broder, T. Fleming, C. Claussin, and K. Pogliano. 2013. The SpoIIQ landmark protein has different requirements for septal localization and immobilization. *Mol Microbiol* **89**:1053-1068.
- Fujita, M. 2000. Temporal and selective association of multiple sigma factors with RNA polymerase during sporulation in *Bacillus subtilis*. *Genes Cells* **5**:79-88.
- Fujita, M., J. E. Gonzalez-Pastor, and R. Losick. 2005. High- and low-threshold genes in the Spo0A regulon of *Bacillus subtilis*. *J Bacteriol* **187**:1357-1368.
- Fujita, M., and R. Losick. 2002. An investigation into the compartmentalization of the sporulation transcription factor sigmaE in *Bacillus subtilis*. *Mol Microbiol* **43**:27-38.
- Fujita, M., and R. Losick. 2005. Evidence that entry into sporulation in *Bacillus subtilis* is governed by a gradual increase in the level and activity of the master regulator Spo0A. *Genes Dev* **19**:2236-2244.
- Fukushima, T., S. Ishikawa, H. Yamamoto, N. Ogasawara, and J. Sekiguchi. 2003. Transcriptional, functional and cytochemical analyses of the veg gene in *Bacillus subtilis*. *J Biochem* **133**:475-483.
- Fukushima, T., H. Yamamoto, A. Atrih, S. J. Foster, and J. Sekiguchi. 2002. A polysaccharide deacetylase gene (pdaA) is required for germination and for production of muramic delta-lactam residues in the spore cortex of *Bacillus subtilis*. *J Bacteriol* **184**:6007-6015.
- Gabriel, L., and A. Beriot-Mathiot. 2014. Hospitalization stay and costs attributable to *Clostridium difficile* infection: a critical review. *J Hosp Infect* **88**:12-21.
- Gaidenko, T. A., T. J. Kim, A. L. Weigel, M. S. Brody, and C. W. Price. 2006. The blue-light receptor YtvA acts in the environmental stress signaling pathway of *Bacillus subtilis*. *J Bacteriol* **188**:6387-6395.
- Galperin, M. Y., S. L. Mekhedov, P. Puigbo, S. Smirnov, Y. I. Wolf, and D. J. Rigden. 2012. Genomic determinants of sporulation in Bacilli and Clostridia: towards the minimal set of sporulation-specific genes. *Environ Microbiol* **14**:2870-2890.
- Gardner, A. M., R. A. Helmick, and P. R. Gardner. 2002. Flavorubredoxin, an inducible catalyst for nitric oxide reduction and detoxification in *Escherichia coli*. *J Biol Chem* **277**:8172-8177.
- Garner, M. R., B. L. Njaa, M. Wiedmann, and K. J. Boor. 2006. Sigma B contributes to *Listeria monocytogenes* gastrointestinal infection but not to systemic spread in the guinea pig infection model. *Infect Immun* **74**:876-886.
- Gerding, D. N., T. Meyer, C. Lee, S. H. Cohen, U. K. Murthy, A. Poirier, T. C. Van Schooneveld, D. S. Pardi, A. Ramos, M. A. Barron, H. Chen, and S. Villano. 2015. Administration of spores of nontoxigenic *Clostridium difficile* strain M3 for prevention of recurrent *C. difficile* infection: a randomized clinical trial. *JAMA* **313**:1719-1727.

- Gerhardt, P., H. S. Pankratz, and R. Scherrer. 1976. Fine structure of the *Bacillus thuringiensis* spore. *Appl Environ Microbiol* **32**:438-440.
- Gerhardt, P., and E. Ribí. 1964. Ultrastructure of the Exosporium Enveloping Spores of *Bacillus Cereus*. *J Bacteriol* **88**:1774-1789.
- Gholamhoseinian, A., and P. J. Piggot. 1989. Timing of spoII gene expression relative to septum formation during sporulation of *Bacillus subtilis*. *J Bacteriol* **171**:5747-5749.
- Giachino, P., S. Engelmann, and M. Bischoff. 2001. Sigma(B) activity depends on RsbU in *Staphylococcus aureus*. *J Bacteriol* **183**:1843-1852.
- Giel, J. L., J. A. Sorg, A. L. Sonenshein, and J. Zhu. 2010. Metabolism of bile salts in mice influences spore germination in *Clostridium difficile*. *PLoS One* **5**:e8740.
- Gill, R. L., Jr., J. P. Castaing, J. Hsin, I. S. Tan, X. Wang, K. C. Huang, F. Tian, and K. S. Ramamurthi. 2015. Structural basis for the geometry-driven localization of a small protein. *Proc Natl Acad Sci U S A* **112**:E1908-1915.
- Giordano, N., J. L. Hastie, and P. E. Carlson. 2018a. Transcriptomic profiling of *Clostridium difficile* grown under microaerophilic conditions. *Pathog Dis* **76**.
- Giordano, N., J. L. Hastie, A. D. Smith, E. D. Foss, D. F. Gutierrez-Munoz, and P. E. Carlson, Jr. 2018b. Cysteine Desulfurase IscS2 Plays a Role in Oxygen Resistance in *Clostridium difficile*. *Infect Immun* **86**.
- Giorno, R., J. Bozue, C. Cote, T. Wenzel, K. S. Moody, M. Mallozzi, M. Ryan, R. Wang, R. Zielke, J. R. Maddock, A. Friedlander, S. Welkos, and A. Driks. 2007. Morphogenesis of the *Bacillus anthracis* spore. *J Bacteriol* **189**:691-705.
- Giorno, R., M. Mallozzi, J. Bozue, K. S. Moody, A. Slack, D. Qiu, R. Wang, A. Friedlander, S. Welkos, and A. Driks. 2009. Localization and assembly of proteins comprising the outer structures of the *Bacillus anthracis* spore. *Microbiology* **155**:1133-1145.
- Girinathan, B. P., S. E. Braun, and R. Govind. 2014. *Clostridium difficile* glutamate dehydrogenase is a secreted enzyme that confers resistance to H₂O₂. *Microbiology* **160**:47-55.
- Glaser, P., M. E. Sharpe, B. Raether, M. Perego, K. Ohlsen, and J. Errington. 1997. Dynamic, mitotic-like behavior of a bacterial protein required for accurate chromosome partitioning. *Genes Dev* **11**:1160-1168.
- Gomes, C. M., A. Giuffre, E. Forte, J. B. Vicente, L. M. Saraiva, M. Brunori, and M. Teixeira. 2002. A novel type of nitric-oxide reductase. *Escherichia coli* flavorubredoxin. *J Biol Chem* **277**:25273-25276.
- Gomes, C. M., J. B. Vicente, A. Wasserfallen, and M. Teixeira. 2000. Spectroscopic studies and characterization of a novel electron-transfer chain from *Escherichia coli* involving a flavorubredoxin and its flavoprotein reductase partner. *Biochemistry* **39**:16230-16237.
- Gominet, M., L. Slamti, N. Gilois, M. Rose, and D. Lereclus. 2001. Oligopeptide permease is required for expression of the *Bacillus thuringiensis* plcR regulon and for virulence. *Mol Microbiol* **40**:963-975.
- Goncalves, V. L., J. B. Vicente, L. Pinto, C. V. Romao, C. Frazao, P. Sarti, A. Giuffre, and M. Teixeira. 2014. Flavodiiron oxygen reductase from *Entamoeba histolytica*: modulation of substrate preference by tyrosine 271 and lysine 53. *J Biol Chem* **289**:28260-28270.
- Gonzalez-Pastor, J. E., E. C. Hobbs, and R. Losick. 2003. Cannibalism by sporulating bacteria. *Science* **301**:510-513.
- Gould, L. H., and B. Limbago. 2010. *Clostridium difficile* in food and domestic animals: a new foodborne pathogen? *Clin Infect Dis* **51**:577-582.
- Govind, R., and B. Dupuy. 2012. Secretion of *Clostridium difficile* toxins A and B requires the holin-like protein TcdE. *PLoS Pathog* **8**:e1002727.
- Govind, R., L. Fitzwater, and R. Nichols. 2015. Observations on the Role of TcdE Isoforms in *Clostridium difficile* Toxin Secretion. *J Bacteriol* **197**:2600-2609.
- Guberman, J. M., A. Fay, J. Dworkin, N. S. Wingreen, and Z. Gitai. 2008. PSICIC: noise and asymmetry in bacterial division revealed by computational image analysis at sub-pixel resolution. *PLoS Comput Biol* **4**:e1000233.
- Guiney, D. G. 1997. Regulation of bacterial virulence gene expression by the host environment. *J Clin Invest* **99**:565-569.

- Guldimann, C., K. J. Boor, M. Wiedmann, and V. Guariglia-Oropeza. 2016. Resilience in the Face of Uncertainty: Sigma Factor B Fine-Tunes Gene Expression To Support Homeostasis in Gram-Positive Bacteria. *Appl Environ Microbiol* **82**:4456-4469.
- Guldimann, C., V. Guariglia-Oropeza, S. Harrand, D. Kent, K. J. Boor, and M. Wiedmann. 2017. Stochastic and Differential Activation of sigmaB and PrfA in *Listeria monocytogenes* at the Single Cell Level under Different Environmental Stress Conditions. *Front Microbiol* **8**:348.
- Gutelius, D., K. Hokeness, S. M. Logan, and C. W. Reid. 2014. Functional analysis of SleC from *Clostridium difficile*: an essential lytic transglycosylase involved in spore germination. *Microbiology* **160**:209-216.
- Halberg, R., and L. Kroos. 1994. Sporulation regulatory protein SpoIID from *Bacillus subtilis* activates and represses transcription by both mother-cell-specific forms of RNA polymerase. *J Mol Biol* **243**:425-436.
- Hall, J. C., and E. O'Toole. 1935. Intestinal flora in new-born infants with a description of a new pathogenic anaerobic, *Bacillus difficilis*. *Am J Dis Child* **49**:390-402.
- Hamilton, W. A., and J. M. Stubbs. 1967. Comparison of the germination and outgrowth of spores of *Bacillus cereus* and *Bacillus polymyxa*. *J Gen Microbiol* **47**:121-129.
- Hamon, M. A., and B. A. Lazazzera. 2001. The sporulation transcription factor Spo0A is required for biofilm development in *Bacillus subtilis*. *Mol Microbiol* **42**:1199-1209.
- Haraldsen, J. D., and A. L. Sonenshein. 2003. Efficient sporulation in *Clostridium difficile* requires disruption of the sigmaK gene. *Mol Microbiol* **48**:811-821.
- He, M., F. Miyajima, P. Roberts, L. Ellison, D. J. Pickard, M. J. Martin, T. R. Connor, S. R. Harris, D. Fairley, K. B. Bamford, S. D'Arc, J. Brazier, D. Brown, J. E. Coia, G. Douce, D. Gerding, H. J. Kim, T. H. Koh, H. Kato, M. Senoh, T. Louie, S. Michell, E. Butt, S. J. Peacock, N. M. Brown, T. Riley, G. Songer, M. Wilcox, M. Pirmohamed, E. Kuijper, P. Hawkey, B. W. Wren, G. Dougan, J. Parkhill, and T. D. Lawley. 2013. Emergence and global spread of epidemic healthcare-associated *Clostridium difficile*. *Nat Genet* **45**:109-113.
- Heap, J. T., S. A. Kuehne, M. Ehsaan, S. T. Cartman, C. M. Cooksley, J. C. Scott, and N. P. Minton. 2010. The ClosTron: Mutagenesis in *Clostridium* refined and streamlined. *J Microbiol Methods* **80**:49-55.
- Heap, J. T., O. J. Pennington, S. T. Cartman, G. P. Carter, and N. P. Minton. 2007. The ClosTron: a universal gene knock-out system for the genus *Clostridium*. *J Microbiol Methods* **70**:452-464.
- Heap, J. T., O. J. Pennington, S. T. Cartman, and N. P. Minton. 2009. A modular system for *Clostridium* shuttle plasmids. *J Microbiol Methods* **78**:79-85.
- Hecker, M., J. Pane-Farre, and U. Volker. 2007. SigB-dependent general stress response in *Bacillus subtilis* and related gram-positive bacteria. *Annu Rev Microbiol* **61**:215-236.
- Helmann, J. D., M. F. Wu, A. Gaballa, P. A. Kobel, M. M. Morshedi, P. Fawcett, and C. Paddon. 2003. The global transcriptional response of *Bacillus subtilis* to peroxide stress is coordinated by three transcription factors. *J Bacteriol* **185**:243-253.
- Hennequin, C., C. Janoir, M. C. Barc, A. Collignon, and T. Karjalainen. 2003. Identification and characterization of a fibronectin-binding protein from *Clostridium difficile*. *Microbiology* **149**:2779-2787.
- Henriques, A. O., B. W. Beall, K. Roland, and C. P. Moran, Jr. 1995. Characterization of cotJ, a sigma E-controlled operon affecting the polypeptide composition of the coat of *Bacillus subtilis* spores. *J Bacteriol* **177**:3394-3406.
- Henriques, A. O., L. R. Melsen, and C. P. Moran, Jr. 1998. Involvement of superoxide dismutase in spore coat assembly in *Bacillus subtilis*. *J Bacteriol* **180**:2285-2291.
- Henriques, A. O., and C. P. Moran, Jr. 2000. Structure and assembly of the bacterial endospore coat. *Methods* **20**:95-110.
- Henriques, A. O., and C. P. Moran, Jr. 2007. Structure, assembly, and function of the spore surface layers. *Annu Rev Microbiol* **61**:555-588.
- Higgins, D., and J. Dworkin. 2012. Recent progress in *Bacillus subtilis* sporulation. *FEMS Microbiol Rev* **36**:131-148.
- Hilbert, D. W., and P. J. Piggot. 2004. Compartmentalization of gene expression during *Bacillus subtilis* spore formation. *Microbiol Mol Biol Rev* **68**:234-262.

- Hill, D. A., C. Hoffmann, M. C. Abt, Y. Du, D. Kobuley, T. J. Kirn, F. D. Bushman, and D. Artis. 2010. Metagenomic analyses reveal antibiotic-induced temporal and spatial changes in intestinal microbiota with associated alterations in immune cell homeostasis. *Mucosal Immunol* **3**:148-158.
- Hillmann, F., C. Doring, O. Riebe, A. Ehrenreich, R. J. Fischer, and H. Bahl. 2009a. The role of PerR in O₂-affected gene expression of *Clostridium acetobutylicum*. *J Bacteriol* **191**:6082-6093.
- Hillmann, F., R. J. Fischer, and H. Bahl. 2006. The rubrerythrin-like protein Hsp21 of *Clostridium acetobutylicum* is a general stress protein. *Arch Microbiol* **185**:270-276.
- Hillmann, F., R. J. Fischer, F. Saint-Prix, L. Girbal, and H. Bahl. 2008. PerR acts as a switch for oxygen tolerance in the strict anaerobe *Clostridium acetobutylicum*. *Mol Microbiol* **68**:848-860.
- Hillmann, F., O. Riebe, R. J. Fischer, A. Mot, J. D. Caranto, D. M. Kurtz, Jr., and H. Bahl. 2009b. Reductive dioxygen scavenging by flavo-diiron proteins of *Clostridium acetobutylicum*. *FEBS Lett* **583**:241-245.
- Hofmeister, A. E., A. Londono-Vallejo, E. Harry, P. Stragier, and R. Losick. 1995. Extracellular signal protein triggering the proteolytic activation of a developmental transcription factor in *B. subtilis*. *Cell* **83**:219-226.
- Holy, O., and D. Chmelar. 2012. Oxygen tolerance in anaerobic pathogenic bacteria. *Folia Microbiol (Praha)* **57**:443-446.
- Hong, H. A., W. T. Ferreira, S. Hosseini, S. Anwar, K. Hitri, A. J. Wilkinson, W. Vahjen, J. Zentek, M. Soloviev, and S. M. Cutting. 2017. The Spore Coat Protein CotE Facilitates Host Colonization by *Clostridium difficile*. *J Infect Dis* **216**:1452-1459.
- Hoverstad, T., B. Carlstedt-Duke, E. Lingaas, T. Midtvedt, K. E. Norin, H. Saxerholt, and M. Steinbakk. 1986a. Influence of ampicillin, clindamycin, and metronidazole on faecal excretion of short-chain fatty acids in healthy subjects. *Scand J Gastroenterol* **21**:621-626.
- Hoverstad, T., B. Carlstedt-Duke, E. Lingaas, E. Norin, H. Saxerholt, M. Steinbakk, and T. Midtvedt. 1986b. Influence of oral intake of seven different antibiotics on faecal short-chain fatty acid excretion in healthy subjects. *Scand J Gastroenterol* **21**:997-1003.
- Howerton, A., M. Patra, and E. Abel-Santos. 2013. A new strategy for the prevention of *Clostridium difficile* infection. *J Infect Dis* **207**:1498-1504.
- Hullo, M. F., I. Moszer, A. Danchin, and I. Martin-Verstraete. 2001. CotA of *Bacillus subtilis* is a copper-dependent laccase. *J Bacteriol* **183**:5426-5430.
- Hundsberger, T., V. Braun, M. Weidmann, P. Leukel, M. Sauerborn, and C. von Eichel-Streiber. 1997. Transcription analysis of the genes *tcdA-E* of the pathogenicity locus of *Clostridium difficile*. *Eur J Biochem* **244**:735-742.
- Hussain, H. A., A. P. Roberts, and P. Mullany. 2005. Generation of an erythromycin-sensitive derivative of *Clostridium difficile* strain 630 (630Deltaerm) and demonstration that the conjugative transposon Tn916DeltaE enters the genome of this strain at multiple sites. *J Med Microbiol* **54**:137-141.
- Hwang, C. S., G. E. Rhie, J. H. Oh, W. K. Huh, H. S. Yim, and S. O. Kang. 2002. Copper- and zinc-containing superoxide dismutase (Cu/ZnSOD) is required for the protection of *Candida albicans* against oxidative stresses and the expression of its full virulence. *Microbiology* **148**:3705-3713.
- Iber, D., J. Clarkson, M. D. Yudkin, and I. D. Campbell. 2006. The mechanism of cell differentiation in *Bacillus subtilis*. *Nature* **441**:371-374.
- Illing, N., and J. Errington. 1990. The *spoIIIA* locus is not a major determinant of prespore-specific gene expression during sporulation in *Bacillus subtilis*. *J Bacteriol* **172**:6930-6936.
- Imamura, D., R. Kuwana, H. Takamatsu, and K. Watabe. 2010. Localization of proteins to different layers and regions of *Bacillus subtilis* spore coats. *J Bacteriol* **192**:518-524.
- Imamura, D., R. Kuwana, H. Takamatsu, and K. Watabe. 2011. Proteins involved in formation of the outermost layer of *Bacillus subtilis* spores. *J Bacteriol* **193**:4075-4080.
- Imlay, J. A. 2003. Pathways of oxidative damage. *Annu Rev Microbiol* **57**:395-418.
- Imlay, J. A. 2006. Iron-sulphur clusters and the problem with oxygen. *Mol Microbiol* **59**:1073-1082.
- Isticato, R., A. Pelosi, M. De Felice, and E. Ricca. 2010. CotE binds to CotC and CotU and mediates their interaction during spore coat formation in *Bacillus subtilis*. *J Bacteriol* **192**:949-954.

- Isticato, R., T. Sirec, S. Vecchione, A. Crispino, A. Saggese, L. Baccigalupi, E. Notomista, A. Driks, and E. Ricca. 2015. The Direct Interaction between Two Morphogenetic Proteins Is Essential for Spore Coat Formation in *Bacillus subtilis*. *PLoS One* **10**:e0141040.
- Janganan, T. K., N. Mullin, S. B. Tzokov, S. Stringer, R. P. Fagan, J. K. Hobbs, A. Moir, and P. A. Bullough. 2016. Characterization of the spore surface and exosporium proteins of *Clostridium sporogenes*; implications for *Clostridium botulinum* group I strains. *Food Microbiol* **59**:205-212.
- Jank, T., T. Gieseemann, and K. Aktories. 2007. Rho-glucosylating *Clostridium difficile* toxins A and B: new insights into structure and function. *Glycobiology* **17**:15R-22R.
- Janoir, C. 2016. Virulence factors of *Clostridium difficile* and their role during infection. *Anaerobe* **37**:13-24.
- Janoir, C., C. Deneve, S. Bouttier, F. Barbut, S. Hoys, L. Caleechum, D. Chapeton-Montes, F. C. Pereira, A. O. Henriques, A. Collignon, M. Monot, and B. Dupuy. 2013. Adaptive strategies and pathogenesis of *Clostridium difficile* from in vivo transcriptomics. *Infect Immun* **81**:3757-3769.
- Jean, D., V. Briolat, and G. Reyssset. 2004. Oxidative stress response in *Clostridium perfringens*. *Microbiology* **150**:1649-1659.
- Jeannin, P., T. Chaze, Q. Giai Gianetto, M. Matondo, O. Gout, A. Gessain, and P. V. Afonso. 2018. Proteomic analysis of plasma extracellular vesicles reveals mitochondrial stress upon HTLV-1 infection. *Sci Rep* **8**:5170.
- Jenney, F. E., Jr., M. F. Verhagen, X. Cui, and M. W. Adams. 1999. Anaerobic microbes: oxygen detoxification without superoxide dismutase. *Science* **286**:306-309.
- Johnson, M. J., S. J. Todd, D. A. Ball, A. M. Shepherd, P. Sylvestre, and A. Moir. 2006. ExsY and CotY are required for the correct assembly of the exosporium and spore coat of *Bacillus cereus*. *J Bacteriol* **188**:7905-7913.
- Jones, S. W., C. J. Paredes, B. Tracy, N. Cheng, R. Sillers, R. S. Senger, and E. T. Papoutsakis. 2008. The transcriptional program underlying the physiology of clostridial sporulation. *Genome Biol* **9**:R114.
- Jones, S. W., B. P. Tracy, S. M. Gaida, and E. T. Papoutsakis. 2011. Inactivation of sigmaF in *Clostridium acetobutylicum* ATCC 824 blocks sporulation prior to asymmetric division and abolishes sigmaE and sigmaG protein expression but does not block solvent formation. *J Bacteriol* **193**:2429-2440.
- Jose, S., and R. Madan. 2016. Neutrophil-mediated inflammation in the pathogenesis of *Clostridium difficile* infections. *Anaerobe* **41**:85-90.
- Joshi, L. T., D. S. Phillips, C. F. Williams, A. Alyousef, and L. Baillie. 2012. Contribution of spores to the ability of *Clostridium difficile* to adhere to surfaces. *Appl Environ Microbiol* **78**:7671-7679.
- Just, I., J. Selzer, M. Wilm, C. von Eichel-Streiber, M. Mann, and K. Aktories. 1995a. Glucosylation of Rho proteins by *Clostridium difficile* toxin B. *Nature* **375**:500-503.
- Just, I., M. Wilm, J. Selzer, G. Rex, C. von Eichel-Streiber, M. Mann, and K. Aktories. 1995b. The enterotoxin from *Clostridium difficile* (ToxA) monoglucosylates the Rho proteins. *J Biol Chem* **270**:13932-13936.
- Justino, M. C., J. B. Vicente, M. Teixeira, and L. M. Saraiva. 2005. New genes implicated in the protection of anaerobically grown *Escherichia coli* against nitric oxide. *J Biol Chem* **280**:2636-2643.
- Kailas, L., C. Terry, N. Abbott, R. Taylor, N. Mullin, S. B. Tzokov, S. J. Todd, B. A. Wallace, J. K. Hobbs, A. Moir, and P. A. Bullough. 2011. Surface architecture of endospores of the *Bacillus cereus*/anthracis/thuringiensis family at the subnanometer scale. *Proc Natl Acad Sci U S A* **108**:16014-16019.
- Kalman, S., M. L. Duncan, S. M. Thomas, and C. W. Price. 1990. Similar organization of the sigB and spoIIA operons encoding alternate sigma factors of *Bacillus subtilis* RNA polymerase. *J Bacteriol* **172**:5575-5585.
- Kang, C. M., M. S. Brody, S. Akbar, X. Yang, and C. W. Price. 1996. Homologous pairs of regulatory proteins control activity of *Bacillus subtilis* transcription factor sigma(b) in response to environmental stress. *J Bacteriol* **178**:3846-3853.

- Kang, J. D., C. J. Myers, S. C. Harris, G. Kakiyama, I. K. Lee, B. S. Yun, K. Matsuzaki, M. Furukawa, H. K. Min, J. S. Bajaj, H. Zhou, and P. B. Hylemon. 2018. Bile Acid 7 α -Dehydroxylating Gut Bacteria Secrete Antibiotics that Inhibit *Clostridium difficile*: Role of Secondary Bile Acids. *Cell Chem Biol*.
- Karimova, G., J. Pidoux, A. Ullmann, and D. Ladant. 1998. A bacterial two-hybrid system based on a reconstituted signal transduction pathway. *Proc Natl Acad Sci U S A* **95**:5752-5756.
- Karjalainen, T., M. C. Barc, A. Collignon, S. Trolle, H. Boureau, J. Cotte-Laffitte, and P. Bourlioux. 1994. Cloning of a genetic determinant from *Clostridium difficile* involved in adherence to tissue culture cells and mucus. *Infect Immun* **62**:4347-4355.
- Karlsson, S., L. G. Burman, and T. Akerlund. 1999. Suppression of toxin production in *Clostridium difficile* VPI 10463 by amino acids. *Microbiology* **145** (Pt 7):1683-1693.
- Karow, M. L., P. Glaser, and P. J. Piggot. 1995. Identification of a gene, spoIIR, that links the activation of sigma E to the transcriptional activity of sigma F during sporulation in *Bacillus subtilis*. *Proc Natl Acad Sci U S A* **92**:2012-2016.
- Kawasaki, S., J. Ishikura, Y. Watamura, and Y. Niimura. 2004. Identification of O₂-induced peptides in an obligatory anaerobe, *Clostridium acetobutylicum*. *FEBS Lett* **571**:21-25.
- Kawasaki, S., Y. Sakai, T. Takahashi, I. Suzuki, and Y. Niimura. 2009. O₂ and reactive oxygen species detoxification complex, composed of O₂-responsive NADH:rubredoxin oxidoreductase-flavoprotein A2-desulfoferrodoxin operon enzymes, rubperoxin, and rubredoxin, in *Clostridium acetobutylicum*. *Appl Environ Microbiol* **75**:1021-1029.
- Kawasaki, S., Y. Watamura, M. Ono, T. Watanabe, K. Takeda, and Y. Niimura. 2005. Adaptive responses to oxygen stress in obligatory anaerobes *Clostridium acetobutylicum* and *Clostridium aminovalericum*. *Appl Environ Microbiol* **71**:8442-8450.
- Kazanowski, M., S. Smolarek, F. Kinnarney, and Z. Grzebieniak. 2014. *Clostridium difficile*: epidemiology, diagnostic and therapeutic possibilities-a systematic review. *Tech Coloproctol* **18**:223-232.
- Kazmierczak, M. J., S. C. Mithoe, K. J. Boor, and M. Wiedmann. 2003. *Listeria monocytogenes* sigma B regulates stress response and virulence functions. *J Bacteriol* **185**:5722-5734.
- Kelly, C. J., L. Zheng, E. L. Campbell, B. Saeedi, C. C. Scholz, A. J. Bayless, K. E. Wilson, L. E. Glover, D. J. Kominsky, A. Magnuson, T. L. Weir, S. F. Ehrentraut, C. Pickel, K. A. Kuhn, J. M. Lanis, V. Nguyen, C. T. Taylor, and S. P. Colgan. 2015a. Crosstalk between Microbiota-Derived Short-Chain Fatty Acids and Intestinal Epithelial HIF Augments Tissue Barrier Function. *Cell Host Microbe* **17**:662-671.
- Kelly, C. P., and J. T. LaMont. 2008. *Clostridium difficile*--more difficult than ever. *N Engl J Med* **359**:1932-1940.
- Kelly, C. R., S. Kahn, P. Kashyap, L. Laine, D. Rubin, A. Atreja, T. Moore, and G. Wu. 2015b. Update on Fecal Microbiota Transplantation 2015: Indications, Methodologies, Mechanisms, and Outlook. *Gastroenterology* **149**:223-237.
- Kenney, T. J., P. A. Kirchman, and C. P. Moran, Jr. 1988. Gene encoding sigma E is transcribed from a sigma A-like promoter in *Bacillus subtilis*. *J Bacteriol* **170**:3058-3064.
- Kevorkian, Y., and A. Shen. 2017. Revisiting the Role of Csp Family Proteins in Regulating *Clostridium difficile* Spore Germination. *J Bacteriol* **199**.
- Kevorkian, Y., D. J. Shirley, and A. Shen. 2016. Regulation of *Clostridium difficile* spore germination by the CspA pseudoprotease domain. *Biochimie* **122**:243-254.
- Khanna, S., D. S. Pardi, S. L. Aronson, P. P. Kammer, R. Orenstein, J. L. St Sauver, W. S. Harmsen, and A. R. Zinsmeister. 2012. The epidemiology of community-acquired *Clostridium difficile* infection: a population-based study. *Am J Gastroenterol* **107**:89-95.
- Kim, H., M. Hahn, P. Grabowski, D. C. McPherson, M. M. Otte, R. Wang, C. C. Ferguson, P. Eichenberger, and A. Driks. 2006. The *Bacillus subtilis* spore coat protein interaction network. *Mol Microbiol* **59**:487-502.
- Kim, H., H. Marquis, and K. J. Boor. 2005. SigmaB contributes to *Listeria monocytogenes* invasion by controlling expression of inlA and inlB. *Microbiology* **151**:3215-3222.
- Kint, N., C. Janoir, M. Monot, S. Hoys, O. Soutourina, B. Dupuy, and I. Martin-Verstraete. 2017. The alternative sigma factor sigmaB plays a crucial role in adaptive strategies of *Clostridium difficile* during gut infection. *Environ Microbiol* **19**:1933-1958.

- Kjelleberg, S., N. Albertson, K. Flardh, L. Holmquist, A. Jouper-Jaan, R. Marouga, J. Ostling, B. Svenblad, and D. Weichart. 1993. How do non-differentiating bacteria adapt to starvation? *Antonie Van Leeuwenhoek* **63**:333-341.
- Klobutcher, L. A., K. Ragkousi, and P. Setlow. 2006. The *Bacillus subtilis* spore coat provides "eat resistance" during phagocytic predation by the protozoan *Tetrahymena thermophila*. *Proc Natl Acad Sci U S A* **103**:165-170.
- Knetsch, C. W., T. R. Connor, A. Mutreja, S. M. van Dorp, I. M. Sanders, H. P. Browne, D. Harris, L. Lipman, E. C. Keessen, J. Corver, E. J. Kuijper, and T. D. Lawley. 2014. Whole genome sequencing reveals potential spread of *Clostridium difficile* between humans and farm animals in the Netherlands, 2002 to 2011. *Euro Surveill* **19**:20954.
- Knudsen, S. M., N. Cermak, F. F. Delgado, B. Setlow, P. Setlow, and S. R. Manalis. 2016. Water and Small-Molecule Permeation of Dormant *Bacillus subtilis* Spores. *J Bacteriol* **198**:168-177.
- Kochan, T. J., M. J. Somers, A. M. Kaiser, M. S. Shoshiev, A. K. Hagan, J. L. Hastie, N. P. Giordano, A. D. Smith, A. M. Schubert, P. E. Carlson, Jr., and P. C. Hanna. 2017. Intestinal calcium and bile salts facilitate germination of *Clostridium difficile* spores. *PLoS Pathog* **13**:e1006443.
- Koenig, J. E., A. Spor, N. Scalfone, A. D. Fricker, J. Stombaugh, R. Knight, L. T. Angenent, and R. E. Ley. 2011. Succession of microbial consortia in the developing infant gut microbiome. *Proc Natl Acad Sci U S A* **108 Suppl 1**:4578-4585.
- Koenigskecht, M. J., C. M. Theriot, I. L. Bergin, C. A. Schumacher, P. D. Schloss, and V. B. Young. 2015. Dynamics and establishment of *Clostridium difficile* infection in the murine gastrointestinal tract. *Infect Immun* **83**:934-941.
- Kong, L., P. Zhang, G. Wang, J. Yu, P. Setlow, and Y. Q. Li. 2011. Characterization of bacterial spore germination using phase-contrast and fluorescence microscopy, Raman spectroscopy and optical tweezers. *Nat Protoc* **6**:625-639.
- Konturek, P. C., J. Koziel, W. Dieterich, D. Haziri, S. Wirtz, I. Glowczyk, K. Konturek, M. F. Neurath, and Y. Zopf. 2016. Successful therapy of *Clostridium difficile* infection with fecal microbiota transplantation. *J Physiol Pharmacol* **67**:859-866.
- Korza, G., S. Abini-Agbomson, B. Setlow, A. Shen, and P. Setlow. 2017. Levels of L-malate and other low molecular weight metabolites in spores of *Bacillus* species and *Clostridium difficile*. *PLoS One* **12**:e0182656.
- Kovacs-Simon, A., R. Leuzzi, M. Kasendra, N. Minton, R. W. Titball, and S. L. Michell. 2014. Lipoprotein CD0873 is a novel adhesin of *Clostridium difficile*. *J Infect Dis* **210**:274-284.
- Krajcikova, D., V. Forgac, A. Szabo, and I. Barak. 2017. Exploring the interaction network of the *Bacillus subtilis* outer coat and crust proteins. *Microbiol Res* **204**:72-80.
- Krajcikova, D., M. Lukacova, D. Mullerova, S. M. Cutting, and I. Barak. 2009. Searching for protein-protein interactions within the *Bacillus subtilis* spore coat. *J Bacteriol* **191**:3212-3219.
- Kuehne, S. A., S. T. Cartman, J. T. Heap, M. L. Kelly, A. Cockayne, and N. P. Minton. 2010. The role of toxin A and toxin B in *Clostridium difficile* infection. *Nature* **467**:711-713.
- Kuehne, S. A., M. M. Collery, M. L. Kelly, S. T. Cartman, A. Cockayne, and N. P. Minton. 2014. Importance of toxin A, toxin B, and CDT in virulence of an epidemic *Clostridium difficile* strain. *J Infect Dis* **209**:83-86.
- Kunkel, B., L. Kroos, H. Poth, P. Youngman, and R. Losick. 1989. Temporal and spatial control of the mother-cell regulatory gene *spoIIID* of *Bacillus subtilis*. *Genes Dev* **3**:1735-1744.
- Kunkel, B., R. Losick, and P. Stragier. 1990. The *Bacillus subtilis* gene for the development transcription factor sigma K is generated by excision of a dispensable DNA element containing a sporulation recombinase gene. *Genes Dev* **4**:525-535.
- Kurtz, D. M., Jr. 2006. Avoiding high-valent iron intermediates: superoxide reductase and rubrerythrin. *J Inorg Biochem* **100**:679-693.
- Kuwana, R., Y. Kasahara, M. Fujibayashi, H. Takamatsu, N. Ogasawara, and K. Watabe. 2002. Proteomics characterization of novel spore proteins of *Bacillus subtilis*. *Microbiology* **148**:3971-3982.
- LaBell, T. L., J. E. Trempy, and W. G. Haldenwang. 1987. Sporulation-specific sigma factor sigma 29 of *Bacillus subtilis* is synthesized from a precursor protein, P31. *Proc Natl Acad Sci U S A* **84**:1784-1788.

- Laemmli, U. K. 1970. Cleavage of structural proteins during the assembly of the head of bacteriophage T4. *Nature* **227**:680-685.
- LaFrance, M. E., M. A. Farrow, R. Chandrasekaran, J. Sheng, D. H. Rubin, and D. B. Lacy. 2015. Identification of an epithelial cell receptor responsible for *Clostridium difficile* TcdB-induced cytotoxicity. *Proc Natl Acad Sci U S A* **112**:7073-7078.
- Lago, M., V. Monteil, T. Douche, J. Guglielmini, A. Criscuolo, C. Maufrais, M. Matondo, and F. Norel. 2017. Proteome remodelling by the stress sigma factor RpoS/sigma(S) in *Salmonella*: identification of small proteins and evidence for post-transcriptional regulation. *Sci Rep* **7**:2127.
- Lai, E. M., N. D. Phadke, M. T. Kachman, R. Giorno, S. Vazquez, J. A. Vazquez, J. R. Maddock, and A. Driks. 2003. Proteomic analysis of the spore coats of *Bacillus subtilis* and *Bacillus anthracis*. *J Bacteriol* **185**:1443-1454.
- Lawley, T. D., S. Clare, L. J. Deakin, D. Goulding, J. L. Yen, C. Raisen, C. Brandt, J. Lovell, F. Cooke, T. G. Clark, and G. Dougan. 2010. Use of purified *Clostridium difficile* spores to facilitate evaluation of health care disinfection regimens. *Appl Environ Microbiol* **76**:6895-6900.
- Lawley, T. D., S. Clare, A. W. Walker, D. Goulding, R. A. Stabler, N. Croucher, P. Mastroeni, P. Scott, C. Raisen, L. Mottram, N. F. Fairweather, B. W. Wren, J. Parkhill, and G. Dougan. 2009a. Antibiotic treatment of *clostridium difficile* carrier mice triggers a supershedder state, spore-mediated transmission, and severe disease in immunocompromised hosts. *Infect Immun* **77**:3661-3669.
- Lawley, T. D., N. J. Croucher, L. Yu, S. Clare, M. Sebahia, D. Goulding, D. J. Pickard, J. Parkhill, J. Choudhary, and G. Dougan. 2009b. Proteomic and genomic characterization of highly infectious *Clostridium difficile* 630 spores. *J Bacteriol* **191**:5377-5386.
- Lawson, P. A., D. M. Citron, K. L. Tyrrell, and S. M. Finegold. 2016. Reclassification of *Clostridium difficile* as *Clostridioides difficile* (Hall and O'Toole 1935) Prevot 1938. *Anaerobe* **40**:95-99.
- Lessa, F. C., L. G. Winston, L. C. McDonald, and C. d. S. T. Emerging Infections Program. 2015. Burden of *Clostridium difficile* infection in the United States. *N Engl J Med* **372**:2369-2370.
- Levin, P. A., N. Fan, E. Ricca, A. Driks, R. Losick, and S. Cutting. 1993. An unusually small gene required for sporulation by *Bacillus subtilis*. *Mol Microbiol* **9**:761-771.
- Lewis, R. J., D. J. Scott, J. A. Brannigan, J. C. Ladds, M. A. Cervin, G. B. Spiegelman, J. G. Hoggett, I. Barak, and A. J. Wilkinson. 2002. Dimer formation and transcription activation in the sporulation response regulator Spo0A. *J Mol Biol* **316**:235-245.
- Li, Z., and P. J. Piggot. 2001. Development of a two-part transcription probe to determine the completeness of temporal and spatial compartmentalization of gene expression during bacterial development. *Proc Natl Acad Sci U S A* **98**:12538-12543.
- Little, S., and A. Driks. 2001. Functional analysis of the *Bacillus subtilis* morphogenetic spore coat protein CotE. *Mol Microbiol* **42**:1107-1120.
- Littman, D. R., and E. G. Pamer. 2011. Role of the commensal microbiota in normal and pathogenic host immune responses. *Cell Host Microbe* **10**:311-323.
- Liu, H., N. H. Bergman, B. Thomason, S. Shallom, A. Hazen, J. Crossno, D. A. Rasko, J. Ravel, T. D. Read, S. N. Peterson, J. Yates, 3rd, and P. C. Hanna. 2004. Formation and composition of the *Bacillus anthracis* endospore. *J Bacteriol* **186**:164-178.
- Livak, K. J., and T. D. Schmittgen. 2001. Analysis of relative gene expression data using real-time quantitative PCR and the 2(-Delta Delta C(T)) Method. *Methods* **25**:402-408.
- Loo, V. G., A. M. Bourgault, L. Poirier, F. Lamothe, S. Michaud, N. Turgeon, B. Toye, A. Beaudoin, E. H. Frost, R. Gilca, P. Brassard, N. Dendukuri, C. Beliveau, M. Oughton, I. Brukner, and A. Dascal. 2011. Host and pathogen factors for *Clostridium difficile* infection and colonization. *N Engl J Med* **365**:1693-1703.
- Lopez, D., M. A. Fischbach, F. Chu, R. Losick, and R. Kolter. 2009. Structurally diverse natural products that cause potassium leakage trigger multicellularity in *Bacillus subtilis*. *Proc Natl Acad Sci U S A* **106**:280-285.
- Louie, T. J., K. Cannon, B. Byrne, J. Emery, L. Ward, M. Eyben, and W. Krulicki. 2012. Fidaxomicin preserves the intestinal microbiome during and after treatment of *Clostridium difficile*

- infection (CDI) and reduces both toxin reexpression and recurrence of CDI. *Clin Infect Dis* **55** **Suppl 2**:S132-142.
- Louie, T. J., J. Emery, W. Krulicki, B. Byrne, and M. Mah. 2009. OPT-80 eliminates *Clostridium difficile* and is sparing of bacteroides species during treatment of *C. difficile* infection. *Antimicrob Agents Chemother* **53**:261-263.
- Louie, T. J., M. A. Miller, K. M. Mullane, K. Weiss, A. Lentnek, Y. Golan, S. Gorbach, P. Sears, Y. K. Shue, and O. P. T. C. S. Group. 2011. Fidaxomicin versus vancomycin for *Clostridium difficile* infection. *N Engl J Med* **364**:422-431.
- Lozupone, C. A., J. I. Stombaugh, J. I. Gordon, J. K. Jansson, and R. Knight. 2012. Diversity, stability and resilience of the human gut microbiota. *Nature* **489**:220-230.
- Lumppio, H. L., N. V. Shenvi, A. O. Summers, G. Voordouw, and D. M. Kurtz, Jr. 2001. Rubrerythrin and rubredoxin oxidoreductase in *Desulfovibrio vulgaris*: a novel oxidative stress protection system. *J Bacteriol* **183**:101-108.
- Lynch, M. C., and H. K. Kuramitsu. 1999. Role of superoxide dismutase activity in the physiology of *Porphyromonas gingivalis*. *Infect Immun* **67**:3367-3375.
- Lyon, S. A., M. L. Hutton, J. I. Rood, J. K. Cheung, and D. Lyras. 2016. CdtR Regulates TcdA and TcdB Production in *Clostridium difficile*. *PLoS Pathog* **12**:e1005758.
- Lyras, D., V. Adams, I. Lucet, and J. I. Rood. 2004. The large resolvase TnpX is the only transposon-encoded protein required for transposition of the Tn4451/3 family of integrative mobilizable elements. *Mol Microbiol* **51**:1787-1800.
- Lyras, D., J. R. O'Connor, P. M. Howarth, S. P. Sambol, G. P. Carter, T. Phumoonna, R. Poon, V. Adams, G. Vedantam, S. Johnson, D. N. Gerding, and J. I. Rood. 2009. Toxin B is essential for virulence of *Clostridium difficile*. *Nature* **458**:1176-1179.
- Mader, U., P. Nicolas, M. Depke, J. Pane-Farre, M. Debarbouille, M. M. van der Kooi-Pol, C. Guerin, S. Derozier, A. Hiron, H. Jarmer, A. Leduc, S. Michalik, E. Reilman, M. Schaffer, F. Schmidt, P. Bessieres, P. Noirot, M. Hecker, T. Msadek, U. Volker, and J. M. van Dijl. 2016. *Staphylococcus aureus* Transcriptome Architecture: From Laboratory to Infection-Mimicking Conditions. *PLoS Genet* **12**:e1005962.
- Mailloux, R. J., R. Singh, G. Brewer, C. Auger, J. Lemire, and V. D. Appanna. 2009. Alpha-ketoglutarate dehydrogenase and glutamate dehydrogenase work in tandem to modulate the antioxidant alpha-ketoglutarate during oxidative stress in *Pseudomonas fluorescens*. *J Bacteriol* **191**:3804-3810.
- Mani, N., and B. Dupuy. 2001. Regulation of toxin synthesis in *Clostridium difficile* by an alternative RNA polymerase sigma factor. *Proc Natl Acad Sci U S A* **98**:5844-5849.
- Marles-Wright, J., T. Grant, O. Delumeau, G. van Duinen, S. J. Firbank, P. J. Lewis, J. W. Murray, J. A. Newman, M. B. Quin, P. R. Race, A. Rohou, W. Tichelaar, M. van Heel, and R. J. Lewis. 2008. Molecular architecture of the "stressosome," a signal integration and transduction hub. *Science* **322**:92-96.
- Marles-Wright, J., and R. J. Lewis. 2008. The *Bacillus subtilis* stressosome: A signal integration and transduction hub. *Commun Integr Biol* **1**:182-184.
- Marsh, J. W., R. Arora, J. L. Schlackman, K. A. Shutt, S. R. Curry, and L. H. Harrison. 2012. Association of relapse of *Clostridium difficile* disease with BI/NAP1/027. *J Clin Microbiol* **50**:4078-4082.
- Marteyn, B., F. B. Scorza, P. J. Sansonetti, and C. Tang. 2011. Breathing life into pathogens: the influence of oxygen on bacterial virulence and host responses in the gastrointestinal tract. *Cell Microbiol* **13**:171-176.
- Martin-Verstraete, I., J. Peltier, and B. Dupuy. 2016. The Regulatory Networks That Control *Clostridium difficile* Toxin Synthesis. *Toxins (Basel)* **8**.
- Martinez, L., A. Reeves, and W. Haldenwang. 2010. Stressosomes formed in *Bacillus subtilis* from the RsbR protein of *Listeria monocytogenes* allow sigma(B) activation following exposure to either physical or nutritional stress. *J Bacteriol* **192**:6279-6286.
- Martins, L. O., C. M. Soares, M. M. Pereira, M. Teixeira, T. Costa, G. H. Jones, and A. O. Henriques. 2002. Molecular and biochemical characterization of a highly stable bacterial laccase that occurs as a structural component of the *Bacillus subtilis* endospore coat. *J Biol Chem* **277**:18849-18859.

- Mascher, T., N. G. Margulis, T. Wang, R. W. Ye, and J. D. Helmann. 2003. Cell wall stress responses in *Bacillus subtilis*: the regulatory network of the bacitracin stimulon. *Mol Microbiol* **50**:1591-1604.
- Mastny, M., A. Heuck, R. Kurzbauer, A. Heiduk, P. Boisguerin, R. Volkmer, M. Ehrmann, C. D. Rodrigues, D. Z. Rudner, and T. Clausen. 2013. CtpB assembles a gated protease tunnel regulating cell-cell signaling during spore formation in *Bacillus subtilis*. *Cell* **155**:647-658.
- Matamouros, S., P. England, and B. Dupuy. 2007. *Clostridium difficile* toxin expression is inhibited by the novel regulator TcdC. *Mol Microbiol* **64**:1274-1288.
- Maul, B., U. Volker, S. Riethdorf, S. Engelmann, and M. Hecker. 1995. sigma B-dependent regulation of *gsiB* in response to multiple stimuli in *Bacillus subtilis*. *Mol Gen Genet* **248**:114-120.
- May, A., F. Hillmann, O. Riebe, R. J. Fischer, and H. Bahl. 2004. A rubrerythrin-like oxidative stress protein of *Clostridium acetobutylicum* is encoded by a duplicated gene and identical to the heat shock protein Hsp21. *FEMS Microbiol Lett* **238**:249-254.
- McFee, R. B. 2009. *Clostridium difficile*: emerging public health threat and other nosocomial or hospital acquired infections. *Introduction*. *Dis Mon* **55**:419-421.
- McGann, P., M. Wiedmann, and K. J. Boor. 2007. The alternative sigma factor sigma B and the virulence gene regulator PrfA both regulate transcription of *Listeria monocytogenes* internalins. *Appl Environ Microbiol* **73**:2919-2930.
- McKee, R. W., M. R. Mangalea, E. B. Purcell, E. K. Borchardt, and R. Tamayo. 2013. The second messenger cyclic Di-GMP regulates *Clostridium difficile* toxin production by controlling expression of *sigD*. *J Bacteriol* **195**:5174-5185.
- McKenney, P. T., A. Driks, and P. Eichenberger. 2013. The *Bacillus subtilis* endospore: assembly and functions of the multilayered coat. *Nat Rev Microbiol* **11**:33-44.
- McKenney, P. T., A. Driks, H. A. Eskandarian, P. Grabowski, J. Guberman, K. H. Wang, Z. Gitai, and P. Eichenberger. 2010. A distance-weighted interaction map reveals a previously uncharacterized layer of the *Bacillus subtilis* spore coat. *Curr Biol* **20**:934-938.
- McKenney, P. T., and P. Eichenberger. 2012. Dynamics of spore coat morphogenesis in *Bacillus subtilis*. *Mol Microbiol* **83**:245-260.
- McPherson, D. C., H. Kim, M. Hahn, R. Wang, P. Grabowski, P. Eichenberger, and A. Driks. 2005. Characterization of the *Bacillus subtilis* spore morphogenetic coat protein CotO. *J Bacteriol* **187**:8278-8290.
- McPherson, S. A., M. Li, J. F. Kearney, and C. L. Turnbough, Jr. 2010. ExsB, an unusually highly phosphorylated protein required for the stable attachment of the exosporium of *Bacillus anthracis*. *Mol Microbiol* **76**:1527-1538.
- Meador-Parton, J., and D. L. Popham. 2000. Structural analysis of *Bacillus subtilis* spore peptidoglycan during sporulation. *J Bacteriol* **182**:4491-4499.
- Mearls, E. B., J. Jackter, J. M. Colquhoun, V. Farmer, A. J. Matthews, L. S. Murphy, C. Fenton, and A. H. Camp. 2018. Transcription and translation of the *sigG* gene is tuned for proper execution of the switch from early to late gene expression in the developing *Bacillus subtilis* spore. *PLoS Genet* **14**:e1007350.
- Mengaud, J., H. Ohayon, P. Gounon, R. M. Mege, and P. Cossart. 1996. E-cadherin is the receptor for internalin, a surface protein required for entry of *L. monocytogenes* into epithelial cells. *Cell* **84**:923-932.
- Merrigan, M., A. Venugopal, M. Mallozzi, B. Roxas, V. K. Viswanathan, S. Johnson, D. N. Gerding, and G. Vedantam. 2010. Human hypervirulent *Clostridium difficile* strains exhibit increased sporulation as well as robust toxin production. *J Bacteriol* **192**:4904-4911.
- Merrigan, M. M., A. Venugopal, J. L. Roxas, F. Anwar, M. J. Mallozzi, B. A. Roxas, D. N. Gerding, V. K. Viswanathan, and G. Vedantam. 2013. Surface-layer protein A (SlpA) is a major contributor to host-cell adherence of *Clostridium difficile*. *PLoS One* **8**:e78404.
- Meyer, J. 2000. Clostridial iron-sulphur proteins. *J Mol Microbiol Biotechnol* **2**:9-14.
- Moeller, R., P. Setlow, G. Horneck, T. Berger, G. Reitz, P. Rettberg, A. J. Doherty, R. Okayasu, and W. L. Nicholson. 2008. Roles of the major, small, acid-soluble spore proteins and spore-specific and universal DNA repair mechanisms in resistance of *Bacillus subtilis* spores to ionizing radiation from X rays and high-energy charged-particle bombardment. *J Bacteriol* **190**:1134-1140.

- Molle, V., Y. Nakaura, R. P. Shivers, H. Yamaguchi, R. Losick, Y. Fujita, and A. L. Sonenshein. 2003. Additional targets of the *Bacillus subtilis* global regulator CodY identified by chromatin immunoprecipitation and genome-wide transcript analysis. *J Bacteriol* **185**:1911-1922.
- Monot, M., C. Boursaux-Eude, M. Thibonnier, D. Vallenet, I. Moszer, C. Medigue, I. Martin-Verstraete, and B. Dupuy. 2011. Reannotation of the genome sequence of *Clostridium difficile* strain 630. *J Med Microbiol* **60**:1193-1199.
- Monot, M., C. Eckert, A. Lemire, A. Hamiot, T. Dubois, C. Tessier, B. Dumoulard, B. Hamel, A. Petit, V. Lalande, L. Ma, C. Bouchier, F. Barbut, and B. Dupuy. 2015. *Clostridium difficile*: New Insights into the Evolution of the Pathogenicity Locus. *Sci Rep* **5**:15023.
- Moore, C. M., M. M. Nakano, T. Wang, R. W. Ye, and J. D. Helmann. 2004. Response of *Bacillus subtilis* to nitric oxide and the nitrosating agent sodium nitroprusside. *J Bacteriol* **186**:4655-4664.
- Morikawa, K., A. Maruyama, Y. Inose, M. Higashide, H. Hayashi, and T. Ohta. 2001. Overexpression of sigma factor, sigma(B), urges *Staphylococcus aureus* to thicken the cell wall and to resist beta-lactams. *Biochem Biophys Res Commun* **288**:385-389.
- Mujahid, S., R. H. Orsi, P. Vangay, K. J. Boor, and M. Wiedmann. 2013. Refinement of the *Listeria monocytogenes* sigmaB regulon through quantitative proteomic analysis. *Microbiology* **159**:1109-1119.
- Mullerova, D., D. Krajcikova, and I. Barak. 2009. Interactions between *Bacillus subtilis* early spore coat morphogenetic proteins. *FEMS Microbiol Lett* **299**:74-85.
- Mydel, P., Y. Takahashi, H. Yumoto, M. Sztukowska, M. Kubica, F. C. Gibson, 3rd, D. M. Kurtz, Jr., J. Travis, L. V. Collins, K. A. Nguyen, C. A. Genco, and J. Potempa. 2006. Roles of the host oxidative immune response and bacterial antioxidant rubrerythrin during *Porphyromonas gingivalis* infection. *PLoS Pathog* **2**:e76.
- Na, X., H. Kim, M. P. Moyer, C. Pothoulakis, and J. T. LaMont. 2008. gp96 is a human colonocyte plasma membrane binding protein for *Clostridium difficile* toxin A. *Infect Immun* **76**:2862-2871.
- Naclerio, G., L. Baccigalupi, R. Zilhao, M. De Felice, and E. Ricca. 1996. *Bacillus subtilis* spore coat assembly requires coH gene expression. *J Bacteriol* **178**:4375-4380.
- Nadezhdin, E. V., M. S. Brody, and C. W. Price. 2011. An alpha/beta hydrolase and associated Per-ARNT-Sim domain comprise a bipartite sensing module coupled with diverse output domains. *PLoS One* **6**:e25418.
- Nadon, C. A., B. M. Bowen, M. Wiedmann, and K. J. Boor. 2002. Sigma B contributes to PrfA-mediated virulence in *Listeria monocytogenes*. *Infect Immun* **70**:3948-3952.
- Nagaro, K. J., S. T. Phillips, A. K. Cheknis, S. P. Sambol, W. E. Zukowski, S. Johnson, and D. N. Gerding. 2013. Nontoxicogenic *Clostridium difficile* protects hamsters against challenge with historic and epidemic strains of toxigenic BI/NAP1/027 *C. difficile*. *Antimicrob Agents Chemother* **57**:5266-5270.
- Nannapaneni, P., F. Hertwig, M. Depke, M. Hecker, U. Mader, U. Volker, L. Steil, and S. A. van Hijum. 2012. Defining the structure of the general stress regulon of *Bacillus subtilis* using targeted microarray analysis and random forest classification. *Microbiology* **158**:696-707.
- Nawrocki, K. L., A. N. Edwards, N. Daou, L. Bouillaut, and S. M. McBride. 2016. CodY-Dependent Regulation of Sporulation in *Clostridium difficile*. *J Bacteriol* **198**:2113-2130.
- Neumann-Schaal, M., N. G. Metzendorf, D. Troitzsch, A. M. Nuss, J. D. Hofmann, M. Beckstette, P. Dersch, A. Otto, and S. Sievers. 2018. Tracking gene expression and oxidative damage of O2-stressed *Clostridioides difficile* by a multi-omics approach. *Anaerobe*.
- Ng, Y. K., M. Ehsaan, S. Philip, M. M. Collery, C. Janoir, A. Collignon, S. T. Cartman, and N. P. Minton. 2013. Expanding the repertoire of gene tools for precise manipulation of the *Clostridium difficile* genome: allelic exchange using pyrE alleles. *PLoS One* **8**:e56051.
- Nicholson, W. L., N. Munakata, G. Horneck, H. J. Melosh, and P. Setlow. 2000. Resistance of *Bacillus* endospores to extreme terrestrial and extraterrestrial environments. *Microbiol Mol Biol Rev* **64**:548-572.
- Nolling, J., G. Breton, M. V. Omelchenko, K. S. Makarova, Q. Zeng, R. Gibson, H. M. Lee, J. Dubois, D. Qiu, J. Hitti, Y. I. Wolf, R. L. Tatusov, F. Sabathe, L. Doucette-Stamm, P. Soucaille, M. J. Daly, G. N. Bennett, E. V. Koonin, and D. R. Smith. 2001. Genome sequence and

- comparative analysis of the solvent-producing bacterium *Clostridium acetobutylicum*. *J Bacteriol* **183**:4823-4838.
- Nottrott, S., J. Schoentaube, H. Genth, I. Just, and R. Gerhard. 2007. *Clostridium difficile* toxin A-induced apoptosis is p53-independent but depends on glucosylation of Rho GTPases. *Apoptosis* **12**:1443-1453.
- Nugent, S. G., D. Kumar, D. S. Rampton, and D. F. Evans. 2001. Intestinal luminal pH in inflammatory bowel disease: possible determinants and implications for therapy with aminosalicylates and other drugs. *Gut* **48**:571-577.
- O'Brien, R. W., and J. G. Morris. 1971. Oxygen and the growth and metabolism of *Clostridium acetobutylicum*. *J Gen Microbiol* **68**:307-318.
- Ohashi, Y., H. Ohshima, K. Tsuge, and M. Itaya. 2003. Far different levels of gene expression provided by an oriented cloning system in *Bacillus subtilis* and *Escherichia coli*. *FEMS Microbiol Lett* **221**:125-130.
- Okada, Y., N. Okada, S. Makino, H. Asakura, S. Yamamoto, and S. Igimi. 2006. The sigma factor RpoN (sigma54) is involved in osmotolerance in *Listeria monocytogenes*. *FEMS Microbiol Lett* **263**:54-60.
- Oliva, C. R., M. K. Swiecki, C. E. Griguer, M. W. Lisanby, D. C. Bullard, C. L. Turnbough, Jr., and J. F. Kearney. 2008. The integrin Mac-1 (CR3) mediates internalization and directs *Bacillus anthracis* spores into professional phagocytes. *Proc Natl Acad Sci U S A* **105**:1261-1266.
- Oliver, H. F., R. H. Orsi, M. Wiedmann, and K. J. Boor. 2010. *Listeria monocytogenes* {sigma}B has a small core regulon and a conserved role in virulence but makes differential contributions to stress tolerance across a diverse collection of strains. *Appl Environ Microbiol* **76**:4216-4232.
- Olling, A., S. Seehase, N. P. Minton, H. Tatge, S. Schroter, S. Kohlscheen, A. Pich, I. Just, and R. Gerhard. 2012. Release of TcdA and TcdB from *Clostridium difficile* cdi 630 is not affected by functional inactivation of the tcdE gene. *Microb Pathog* **52**:92-100.
- Orsburn, B. C., S. B. Melville, and D. L. Popham. 2010. EtfA catalyses the formation of dipicolinic acid in *Clostridium perfringens*. *Mol Microbiol* **75**:178-186.
- Ott, S. J., G. H. Waetzig, A. Rehman, J. Moltzau-Anderson, R. Bharti, J. A. Grasis, L. Cassidy, A. Tholey, H. Fickenscher, D. Seegert, P. Rosenstiel, and S. Schreiber. 2017. Efficacy of Sterile Fecal Filtrate Transfer for Treating Patients With *Clostridium difficile* Infection. *Gastroenterology* **152**:799-811 e797.
- Otter, J. A., and G. L. French. 2009. Survival of nosocomial bacteria and spores on surfaces and inactivation by hydrogen peroxide vapor. *J Clin Microbiol* **47**:205-207.
- Oughton, M. T., V. G. Loo, N. Dendukuri, S. Fenn, and M. D. Libman. 2009. Hand hygiene with soap and water is superior to alcohol rub and antiseptic wipes for removal of *Clostridium difficile*. *Infect Control Hosp Epidemiol* **30**:939-944.
- Ozin, A. J., A. O. Henriques, H. Yi, and C. P. Moran, Jr. 2000. Morphogenetic proteins SpoVID and SafA form a complex during assembly of the *Bacillus subtilis* spore coat. *J Bacteriol* **182**:1828-1833.
- Paidhungat, M., K. Ragkousi, and P. Setlow. 2001. Genetic requirements for induction of germination of spores of *Bacillus subtilis* by Ca(2+)-dipicolinate. *J Bacteriol* **183**:4886-4893.
- Paidhungat, M., B. Setlow, W. B. Daniels, D. Hoover, E. Papafragkou, and P. Setlow. 2002. Mechanisms of induction of germination of *Bacillus subtilis* spores by high pressure. *Appl Environ Microbiol* **68**:3172-3175.
- Pane-Farre, J., B. Jonas, K. Forstner, S. Engelmann, and M. Hecker. 2006. The sigmaB regulon in *Staphylococcus aureus* and its regulation. *Int J Med Microbiol* **296**:237-258.
- Pane-Farre, J., B. Jonas, S. W. Hardwick, K. Gronau, R. J. Lewis, M. Hecker, and S. Engelmann. 2009. Role of RsbU in controlling SigB activity in *Staphylococcus aureus* following alkaline stress. *J Bacteriol* **191**:2561-2573.
- Pane-Farre, J., M. B. Quin, R. J. Lewis, and J. Marles-Wright. 2017. Structure and Function of the Stressosome Signalling Hub. *Subcell Biochem* **83**:1-41.
- Paredes, C. J., K. V. Alsaker, and E. T. Papoutsakis. 2005. A comparative genomic view of clostridial sporulation and physiology. *Nat Rev Microbiol* **3**:969-978.
- Paredes, C. J., I. Rigoutsos, and E. T. Papoutsakis. 2004. Transcriptional organization of the *Clostridium acetobutylicum* genome. *Nucleic Acids Res* **32**:1973-1981.

- Paredes-Sabja, D., G. Cofre-Araneda, C. Brito-Silva, M. Pizarro-Guajardo, and M. R. Sarker. 2012. Clostridium difficile spore-macrophage interactions: spore survival. *PLoS One* **7**:e43635.
- Paredes-Sabja, D., D. Raju, J. A. Torres, and M. R. Sarker. 2008. Role of small, acid-soluble spore proteins in the resistance of Clostridium perfringens spores to chemicals. *Int J Food Microbiol* **122**:333-335.
- Paredes-Sabja, D., and M. R. Sarker. 2012. Adherence of Clostridium difficile spores to Caco-2 cells in culture. *J Med Microbiol* **61**:1208-1218.
- Paredes-Sabja, D., P. Setlow, and M. R. Sarker. 2011. Germination of spores of Bacillales and Clostridiales species: mechanisms and proteins involved. *Trends Microbiol* **19**:85-94.
- Paredes-Sabja, D., A. Shen, and J. A. Sorg. 2014. Clostridium difficile spore biology: sporulation, germination, and spore structural proteins. *Trends Microbiol* **22**:406-416.
- Peltier, J., H. A. Shaw, E. C. Couchman, L. F. Dawson, L. Yu, J. S. Choudhary, V. Kaeffer, B. W. Wren, and N. F. Fairweather. 2015. Cyclic diGMP regulates production of sortase substrates of Clostridium difficile and their surface exposure through ZmpI protease-mediated cleavage. *J Biol Chem* **290**:24453-24469.
- Peniche, A. G., T. C. Savidge, and S. M. Dann. 2013. Recent insights into Clostridium difficile pathogenesis. *Curr Opin Infect Dis* **26**:447-453.
- Perego, M. 2001. A new family of aspartyl phosphate phosphatases targeting the sporulation transcription factor Spo0A of Bacillus subtilis. *Mol Microbiol* **42**:133-143.
- Perego, M., C. F. Higgins, S. R. Pearce, M. P. Gallagher, and J. A. Hoch. 1991. The oligopeptide transport system of Bacillus subtilis plays a role in the initiation of sporulation. *Mol Microbiol* **5**:173-185.
- Pereira, F. C., L. Saujet, A. R. Tome, M. Serrano, M. Monot, E. Couture-Tosi, I. Martin-Verstraete, B. Dupuy, and A. O. Henriques. 2013. The spore differentiation pathway in the enteric pathogen Clostridium difficile. *PLoS Genet* **9**:e1003782.
- Permpoonpattana, P., H. A. Hong, J. Phetcharaburanin, J. M. Huang, J. Cook, N. F. Fairweather, and S. M. Cutting. 2011a. Immunization with Bacillus spores expressing toxin A peptide repeats protects against infection with Clostridium difficile strains producing toxins A and B. *Infect Immun* **79**:2295-2302.
- Permpoonpattana, P., J. Phetcharaburanin, A. Mikelsone, M. Dembek, S. Tan, M. C. Brisson, R. La Ragione, A. R. Brisson, N. Fairweather, H. A. Hong, and S. M. Cutting. 2013. Functional characterization of Clostridium difficile spore coat proteins. *J Bacteriol* **195**:1492-1503.
- Permpoonpattana, P., E. H. Tolls, R. Nadem, S. Tan, A. Brisson, and S. M. Cutting. 2011b. Surface layers of Clostridium difficile endospores. *J Bacteriol* **193**:6461-6470.
- Petersohn, A., M. Brigulla, S. Haas, J. D. Hoheisel, U. Volker, and M. Hecker. 2001. Global analysis of the general stress response of Bacillus subtilis. *J Bacteriol* **183**:5617-5631.
- Petrella, L. A., S. P. Sambol, A. Cheknis, K. Nagaro, Y. Kean, P. S. Sears, F. Babakhani, S. Johnson, and D. N. Gerding. 2012. Decreased cure and increased recurrence rates for Clostridium difficile infection caused by the epidemic C. difficile BI strain. *Clin Infect Dis* **55**:351-357.
- Pettit, L. J., H. P. Browne, L. Yu, W. K. Smits, R. P. Fagan, L. Barquist, M. J. Martin, D. Goulding, S. H. Duncan, H. J. Flint, G. Dougan, J. S. Choudhary, and T. D. Lawley. 2014. Functional genomics reveals that Clostridium difficile Spo0A coordinates sporulation, virulence and metabolism. *BMC Genomics* **15**:160.
- Phetcharaburanin, J., H. A. Hong, C. Colenutt, I. Bianconi, L. Sempere, P. Permpoonpattana, K. Smith, M. Dembek, S. Tan, M. C. Brisson, A. R. Brisson, N. F. Fairweather, and S. M. Cutting. 2014. The spore-associated protein BelA1 affects the susceptibility of animals to colonization and infection by Clostridium difficile. *Mol Microbiol* **92**:1025-1038.
- Piggot, P. J., and J. G. Coote. 1976. Genetic aspects of bacterial endospore formation. *Bacteriol Rev* **40**:908-962.
- Piggot, P. J., and D. W. Hilbert. 2004. Sporulation of Bacillus subtilis. *Curr Opin Microbiol* **7**:579-586.
- Pinto, A. F., S. Todorovic, P. Hildebrandt, M. Yamazaki, F. Amano, S. Igimi, C. V. Romao, and M. Teixeira. 2011. Desulforubrythrin from Campylobacter jejuni, a novel multidomain protein. *J Biol Inorg Chem* **16**:501-510.

- Pishdadian, K., K. A. Fimlaid, and A. Shen. 2015. SpoIID-mediated regulation of sigmaK function during *Clostridium difficile* sporulation. *Mol Microbiol* **95**:189-208.
- Pizarro-Guajardo, M., P. Calderon-Romero, P. Castro-Cordova, P. Mora-Urbe, and D. Paredes-Sabja. 2016. Ultrastructural Variability of the Exosporium Layer of *Clostridium difficile* Spores. *Appl Environ Microbiol* **82**:2202-2209.
- Pizarro-Guajardo, M., V. Olguin-Araneda, J. Barra-Carrasco, C. Brito-Silva, M. R. Sarker, and D. Paredes-Sabja. 2014. Characterization of the collagen-like exosporium protein, BclA1, of *Clostridium difficile* spores. *Anaerobe* **25**:18-30.
- Pogliano, K., E. Harry, and R. Losick. 1995. Visualization of the subcellular location of sporulation proteins in *Bacillus subtilis* using immunofluorescence microscopy. *Mol Microbiol* **18**:459-470.
- Popham, D. L., and P. Stragier. 1992. Binding of the *Bacillus subtilis* spoIVCA product to the recombination sites of the element interrupting the sigma K-encoding gene. *Proc Natl Acad Sci U S A* **89**:5991-5995.
- Pothoulakis, C., R. J. Gilbert, C. Cladaras, I. Castagliuolo, G. Semenza, Y. Hitti, J. S. Moncrief, J. Linevsky, C. P. Kelly, S. Nikulasson, H. P. Desai, T. D. Wilkins, and J. T. LaMont. 1996. Rabbit sucrase-isomaltase contains a functional intestinal receptor for *Clostridium difficile* toxin A. *J Clin Invest* **98**:641-649.
- Poutanen, S. M., and A. E. Simor. 2004. *Clostridium difficile*-associated diarrhea in adults. *CMAJ* **171**:51-58.
- Poyart, C., E. Pellegrini, O. Gaillot, C. Boumaila, M. Baptista, and P. Trieu-Cuot. 2001. Contribution of Mn-cofactored superoxide dismutase (SodA) to the virulence of *Streptococcus agalactiae*. *Infect Immun* **69**:5098-5106.
- Price, C. W., P. Fawcett, H. Ceremonie, N. Su, C. K. Murphy, and P. Youngman. 2001. Genome-wide analysis of the general stress response in *Bacillus subtilis*. *Mol Microbiol* **41**:757-774.
- Price, K. D., and R. Losick. 1999. A four-dimensional view of assembly of a morphogenetic protein during sporulation in *Bacillus subtilis*. *J Bacteriol* **181**:781-790.
- Putnam, E. E., A. M. Nock, T. D. Lawley, and A. Shen. 2013. SpoIVA and SipL are *Clostridium difficile* spore morphogenetic proteins. *J Bacteriol* **195**:1214-1225.
- Py, B., P. L. Moreau, and F. Barras. 2011. Fe-S clusters, fragile sentinels of the cell. *Curr Opin Microbiol* **14**:218-223.
- Qin, J., R. Li, J. Raes, M. Arumugam, K. S. Burgdorf, C. Manichanh, T. Nielsen, N. Pons, F. Levenez, T. Yamada, D. R. Mende, J. Li, J. Xu, S. Li, D. Li, J. Cao, B. Wang, H. Liang, H. Zheng, Y. Xie, J. Tap, P. Lepage, M. Bertalan, J. M. Batto, T. Hansen, D. Le Paslier, A. Linneberg, H. B. Nielsen, E. Pelletier, P. Renault, T. Sicheritz-Ponten, K. Turner, H. Zhu, C. Yu, S. Li, M. Jian, Y. Zhou, Y. Li, X. Zhang, S. Li, N. Qin, H. Yang, J. Wang, S. Brunak, J. Dore, F. Guarner, K. Kristiansen, O. Pedersen, J. Parkhill, J. Weissenbach, H. I. T. C. Meta, P. Bork, S. D. Ehrlich, and J. Wang. 2010. A human gut microbial gene catalogue established by metagenomic sequencing. *Nature* **464**:59-65.
- Rabi, R., S. Larcombe, R. Mathias, S. McGowan, M. Awad, and D. Lyras. 2018. *Clostridium sordellii* outer spore proteins maintain spore structural integrity and promote bacterial clearance from the gastrointestinal tract. *PLoS Pathog* **14**:e1007004.
- Rabi, R., L. Turnbull, C. B. Whitchurch, M. Awad, and D. Lyras. 2017. Structural Characterization of *Clostridium sordellii* Spores of Diverse Human, Animal, and Environmental Origin and Comparison to *Clostridium difficile* Spores. *mSphere* **2**.
- Radi, R. 2013. Peroxynitrite, a stealthy biological oxidant. *J Biol Chem* **288**:26464-26472.
- Raengpradub, S., M. Wiedmann, and K. J. Boor. 2008. Comparative analysis of the sigma B-dependent stress responses in *Listeria monocytogenes* and *Listeria innocua* strains exposed to selected stress conditions. *Appl Environ Microbiol* **74**:158-171.
- Raines, K. W., T. J. Kang, S. Hibbs, G. L. Cao, J. Weaver, P. Tsai, L. Baillie, A. S. Cross, and G. M. Rosen. 2006. Importance of nitric oxide synthase in the control of infection by *Bacillus anthracis*. *Infect Immun* **74**:2268-2276.
- Ramamurthi, K. S., K. R. Clapham, and R. Losick. 2006. Peptide anchoring spore coat assembly to the outer forespore membrane in *Bacillus subtilis*. *Mol Microbiol* **62**:1547-1557.

- Ramamurthi, K. S., S. Lecuyer, H. A. Stone, and R. Losick. 2009. Geometric cue for protein localization in a bacterium. *Science* **323**:1354-1357.
- Ramamurthi, K. S., and R. Losick. 2008. ATP-driven self-assembly of a morphogenetic protein in *Bacillus subtilis*. *Mol Cell* **31**:406-414.
- Ramarao, N., and D. Lereclus. 2005. The InhA1 metalloprotease allows spores of the *B. cereus* group to escape macrophages. *Cell Microbiol* **7**:1357-1364.
- Ramirez-Guadiana, F. H., A. J. Meeske, C. D. A. Rodrigues, R. D. C. Barajas-Ornelas, A. C. Kruse, and D. Z. Rudner. 2017. A two-step transport pathway allows the mother cell to nurture the developing spore in *Bacillus subtilis*. *PLoS Genet* **13**:e1007015.
- Ransom, E. M., G. M. Kaus, P. M. Tran, C. D. Ellermeier, and D. S. Weiss. 2018a. Multiple factors contribute to bimodal toxin gene expression in *Clostridioides (Clostridium) difficile*. *Mol Microbiol*.
- Ransom, E. M., G. M. Kaus, P. M. Tran, C. D. Ellermeier, and D. S. Weiss. 2018b. Multiple factors contribute to bimodal toxin gene expression in *Clostridioides (Clostridium) difficile*. *Mol Microbiol* **110**:533-549.
- Ratnayake-Lecamwasam, M., P. Serror, K. W. Wong, and A. L. Sonenshein. 2001. *Bacillus subtilis* CodY represses early-stationary-phase genes by sensing GTP levels. *Genes Dev* **15**:1093-1103.
- Rea, M. C., C. S. Sit, E. Clayton, P. M. O'Connor, R. M. Whittall, J. Zheng, J. C. Vederas, R. P. Ross, and C. Hill. 2010. Thuricin CD, a posttranslationally modified bacteriocin with a narrow spectrum of activity against *Clostridium difficile*. *Proc Natl Acad Sci U S A* **107**:9352-9357.
- Reder, A., D. Albrecht, U. Gerth, and M. Hecker. 2012a. Cross-talk between the general stress response and sporulation initiation in *Bacillus subtilis* - the sigma(B) promoter of *spo0E* represents an AND-gate. *Environ Microbiol* **14**:2741-2756.
- Reder, A., U. Gerth, and M. Hecker. 2012b. Integration of sigmaB activity into the decision-making process of sporulation initiation in *Bacillus subtilis*. *J Bacteriol* **194**:1065-1074.
- Reder, A., D. Hoper, U. Gerth, and M. Hecker. 2012c. Contributions of individual sigmaB-dependent general stress genes to oxidative stress resistance of *Bacillus subtilis*. *J Bacteriol* **194**:3601-3610.
- Reder, A., D. Hoper, C. Weinberg, U. Gerth, M. Fraunholz, and M. Hecker. 2008. The Spx paralogue MgsR (YqgZ) controls a subregulon within the general stress response of *Bacillus subtilis*. *Mol Microbiol* **69**:1104-1120.
- Redmond, C., L. W. Baillie, S. Hibbs, A. J. Moir, and A. Moir. 2004. Identification of proteins in the exosporium of *Bacillus anthracis*. *Microbiology* **150**:355-363.
- Reveles, K. R., G. C. Lee, N. K. Boyd, and C. R. Frei. 2014. The rise in *Clostridium difficile* infection incidence among hospitalized adults in the United States: 2001-2010. *Am J Infect Control* **42**:1028-1032.
- Ribis, J. W., K. A. Fimlaid, and A. Shen. 2018. Differential requirements for conserved peptidoglycan remodeling enzymes during *Clostridioides difficile* spore formation. *Mol Microbiol*.
- Ribis, J. W., P. Ravichandran, E. E. Putnam, K. Pishdadian, and A. Shen. 2017. The Conserved Spore Coat Protein SpoVM Is Largely Dispensable in *Clostridium difficile* Spore Formation. *mSphere* **2**.
- Ridlon, J. M., D. J. Kang, and P. B. Hylemon. 2006. Bile salt biotransformations by human intestinal bacteria. *J Lipid Res* **47**:241-259.
- Riebe, O., R. J. Fischer, and H. Bahl. 2007. Desulfoferrodoxin of *Clostridium acetobutylicum* functions as a superoxide reductase. *FEBS Lett* **581**:5605-5610.
- Riebe, O., R. J. Fischer, D. A. Wampler, D. M. Kurtz, Jr., and H. Bahl. 2009. Pathway for H₂O₂ and O₂ detoxification in *Clostridium acetobutylicum*. *Microbiology* **155**:16-24.
- Riesenman, P. J., and W. L. Nicholson. 2000. Role of the spore coat layers in *Bacillus subtilis* spore resistance to hydrogen peroxide, artificial UV-C, UV-B, and solar UV radiation. *Appl Environ Microbiol* **66**:620-626.
- Rivera-Chavez, F., C. A. Lopez, and A. J. Baumler. 2017. Oxygen as a driver of gut dysbiosis. *Free Radic Biol Med* **105**:93-101.
- Rivera-Chavez, F., L. F. Zhang, F. Faber, C. A. Lopez, M. X. Byndloss, E. E. Olsan, G. Xu, E. M. Velazquez, C. B. Lebrilla, S. E. Winter, and A. J. Baumler. 2016. Depletion of Butyrate-

- Producing Clostridia from the Gut Microbiota Drives an Aerobic Luminal Expansion of Salmonella. *Cell Host Microbe* **19**:443-454.
- Rodrigues, R., J. B. Vicente, R. Felix, S. Oliveira, M. Teixeira, and C. Rodrigues-Pousada. 2006. Desulfovibrio gigas flavodiiron protein affords protection against nitrosative stress in vivo. *J Bacteriol* **188**:2745-2751.
- Roels, S., A. Driks, and R. Losick. 1992. Characterization of spoIVA, a sporulation gene involved in coat morphogenesis in Bacillus subtilis. *J Bacteriol* **174**:575-585.
- Rogstam, A., J. T. Larsson, P. Kjelgaard, and C. von Wachenfeldt. 2007. Mechanisms of adaptation to nitrosative stress in Bacillus subtilis. *J Bacteriol* **189**:3063-3071.
- Romao, C. V., J. B. Vicente, P. T. Borges, C. Frazao, and M. Teixeira. 2016. The dual function of flavodiiron proteins: oxygen and/or nitric oxide reductases. *J Biol Inorg Chem* **21**:39-52.
- Rosenbusch, K. E., D. Bakker, E. J. Kuijper, and W. K. Smits. 2012. C. difficile 630Deltaerm Spo0A regulates sporulation, but does not contribute to toxin production, by direct high-affinity binding to target DNA. *PLoS One* **7**:e48608.
- Rousseau, C., I. Poilane, L. De Pontual, A. C. Maherault, A. Le Monnier, and A. Collignon. 2012. Clostridium difficile carriage in healthy infants in the community: a potential reservoir for pathogenic strains. *Clin Infect Dis* **55**:1209-1215.
- Rowland, S. L., W. F. Burkholder, K. A. Cunningham, M. W. Maciejewski, A. D. Grossman, and G. F. King. 2004. Structure and mechanism of action of Sda, an inhibitor of the histidine kinases that regulate initiation of sporulation in Bacillus subtilis. *Mol Cell* **13**:689-701.
- Rudner, D. Z., J. R. LeDeaux, K. Ireton, and A. D. Grossman. 1991. The spo0K locus of Bacillus subtilis is homologous to the oligopeptide permease locus and is required for sporulation and competence. *J Bacteriol* **173**:1388-1398.
- Rupnik, M., M. H. Wilcox, and D. N. Gerding. 2009. Clostridium difficile infection: new developments in epidemiology and pathogenesis. *Nat Rev Microbiol* **7**:526-536.
- Samarkos, M., E. Mastrogrianni, and O. Kampourpoulou. 2018. The role of gut microbiota in Clostridium difficile infection. *Eur J Intern Med*.
- Sato, N., K. Ohshima, M. Fukami, M. Okada, and T. Ogata. 2006. Kallmann syndrome: somatic and germline mutations of the fibroblast growth factor receptor 1 gene in a mother and the son. *J Clin Endocrinol Metab* **91**:1415-1418.
- Saujet, L., M. Monot, B. Dupuy, O. Soutourina, and I. Martin-Verstraete. 2011. The key sigma factor of transition phase, SigH, controls sporulation, metabolism, and virulence factor expression in Clostridium difficile. *J Bacteriol* **193**:3186-3196.
- Saujet, L., F. C. Pereira, M. Serrano, O. Soutourina, M. Monot, P. V. Shelyakin, M. S. Gelfand, B. Dupuy, A. O. Henriques, and I. Martin-Verstraete. 2013. Genome-wide analysis of cell type-specific gene transcription during spore formation in Clostridium difficile. *PLoS Genet* **9**:e1003756.
- Scharf, C., S. Riethdorf, H. Ernst, S. Engelmann, U. Volker, and M. Hecker. 1998. Thioredoxin is an essential protein induced by multiple stresses in Bacillus subtilis. *J Bacteriol* **180**:1869-1877.
- Schulthess, B., S. Meier, D. Homerova, C. Goerke, C. Wolz, J. Kormanec, B. Berger-Bachi, and M. Bischoff. 2009. Functional characterization of the sigmaB-dependent yabJ-spoVG operon in Staphylococcus aureus: role in methicillin and glycopeptide resistance. *Antimicrob Agents Chemother* **53**:1832-1839.
- Schwan, C., B. Stecher, T. Tzivelekidis, M. van Ham, M. Rohde, W. D. Hardt, J. Wehland, and K. Aktories. 2009. Clostridium difficile toxin CDT induces formation of microtubule-based protrusions and increases adherence of bacteria. *PLoS Pathog* **5**:e1000626.
- Seaver, L. C., and J. A. Imlay. 2001. Hydrogen peroxide fluxes and compartmentalization inside growing Escherichia coli. *J Bacteriol* **183**:7182-7189.
- Sebaihia, M., B. W. Wren, P. Mullany, N. F. Fairweather, N. Minton, R. Stabler, N. R. Thomson, A. P. Roberts, A. M. Cerdano-Tarraga, H. Wang, M. T. Holden, A. Wright, C. Churcher, M. A. Quail, S. Baker, N. Bason, K. Brooks, T. Chillingworth, A. Cronin, P. Davis, L. Dowd, A. Fraser, T. Feltwell, Z. Hance, S. Holroyd, K. Jagels, S. Moule, K. Mungall, C. Price, E. Rabinowitsch, S. Sharp, M. Simmonds, K. Stevens, L. Unwin, S. Whithead, B. Dupuy, G. Dougan, B. Barrell, and J. Parkhill. 2006. The multidrug-resistant human pathogen Clostridium difficile has a highly mobile, mosaic genome. *Nat Genet* **38**:779-786.

- Seedorf, H., A. Dreisbach, R. Hedderich, S. Shima, and R. K. Thauer. 2004. F420H₂ oxidase (FprA) from *Methanobrevibacter arboriphilus*, a coenzyme F420-dependent enzyme involved in O₂ detoxification. *Arch Microbiol* **182**:126-137.
- Seekatz, A. M., J. Aas, C. E. Gessert, T. A. Rubin, D. M. Saman, J. S. Bakken, and V. B. Young. 2014. Recovery of the gut microbiome following fecal microbiota transplantation. *MBio* **5**:e00893-00814.
- Semchyshyn, H., T. Bagnyukova, K. Storey, and V. Lushchak. 2005. Hydrogen peroxide increases the activities of soxRS regulon enzymes and the levels of oxidized proteins and lipids in *Escherichia coli*. *Cell Biol Int* **29**:898-902.
- Senn, M. M., P. Giachino, D. Homerova, A. Steinhuber, J. Strassner, J. Kormanec, U. Fluckiger, B. Berger-Bachi, and M. Bischoff. 2005. Molecular analysis and organization of the sigmaB operon in *Staphylococcus aureus*. *J Bacteriol* **187**:8006-8019.
- Serrano, M., A. D. Crawshaw, M. Dembek, J. M. Monteiro, F. C. Pereira, M. G. Pinho, N. F. Fairweather, P. S. Salgado, and A. O. Henriques. 2016a. The SpoIIQ-SpoIIAH complex of *Clostridium difficile* controls forespore engulfment and late stages of gene expression and spore morphogenesis. *Mol Microbiol* **100**:204-228.
- Serrano, M., N. Kint, F. C. Pereira, L. Saujet, P. Boudry, B. Dupuy, A. O. Henriques, and I. Martin-Verstraete. 2016b. A Recombination Directionality Factor Controls the Cell Type-Specific Activation of sigmaK and the Fidelity of Spore Development in *Clostridium difficile*. *PLoS Genet* **12**:e1006312.
- Serrano, M., G. Real, J. Santos, J. Carneiro, C. P. Moran, Jr., and A. O. Henriques. 2011. A negative feedback loop that limits the ectopic activation of a cell type-specific sporulation sigma factor of *Bacillus subtilis*. *PLoS Genet* **7**:e1002220.
- Serrano, M., R. Zilhao, E. Ricca, A. J. Ozin, C. P. Moran, Jr., and A. O. Henriques. 1999. A *Bacillus subtilis* secreted protein with a role in endospore coat assembly and function. *J Bacteriol* **181**:3632-3643.
- Setlow, B., and P. Setlow. 1988. Absence of transient elevated UV resistance during germination of *Bacillus subtilis* spores lacking small, acid-soluble spore proteins alpha and beta. *J Bacteriol* **170**:2858-2859.
- Setlow, P. 2003. Spore germination. *Curr Opin Microbiol* **6**:550-556.
- Setlow, P. 2006. Spores of *Bacillus subtilis*: their resistance to and killing by radiation, heat and chemicals. *J Appl Microbiol* **101**:514-525.
- Setlow, P. 2007. I will survive: DNA protection in bacterial spores. *Trends Microbiol* **15**:172-180.
- Setlow, P. 2014. Spore Resistance Properties. *Microbiol Spectr* **2**.
- Setlow, P., S. Wang, and Y. Q. Li. 2017. Germination of Spores of the Orders Bacillales and Clostridiales. *Annu Rev Microbiol* **71**:459-477.
- Seyler, R. W., Jr., A. O. Henriques, A. J. Ozin, and C. P. Moran, Jr. 1997. Assembly and interactions of cotJ-encoded proteins, constituents of the inner layers of the *Bacillus subtilis* spore coat. *Mol Microbiol* **25**:955-966.
- Shah, I. M., M. H. Laaberki, D. L. Popham, and J. Dworkin. 2008. A eukaryotic-like Ser/Thr kinase signals bacteria to exit dormancy in response to peptidoglycan fragments. *Cell* **135**:486-496.
- Shields, K., R. V. Araujo-Castillo, T. G. Theethira, C. D. Alonso, and C. P. Kelly. 2015. Recurrent *Clostridium difficile* infection: From colonization to cure. *Anaerobe* **34**:59-73.
- Shivers, R. P., and A. L. Sonenshein. 2004. Activation of the *Bacillus subtilis* global regulator CodY by direct interaction with branched-chain amino acids. *Mol Microbiol* **53**:599-611.
- Silaghi-Dumitrescu, R., E. D. Coulter, A. Das, L. G. Ljungdahl, G. N. Jameson, B. H. Huynh, and D. M. Kurtz, Jr. 2003. A flavodiiron protein and high molecular weight rubredoxin from *Moorella thermoacetica* with nitric oxide reductase activity. *Biochemistry* **42**:2806-2815.
- Silaghi-Dumitrescu, R., K. Y. Ng, R. Viswanathan, and D. M. Kurtz, Jr. 2005. A flavo-diiron protein from *Desulfovibrio vulgaris* with oxidase and nitric oxide reductase activities. Evidence for an in vivo nitric oxide scavenging function. *Biochemistry* **44**:3572-3579.
- Sleator, R. D., H. H. Wemekamp-Kamphuis, C. G. Gahan, T. Abee, and C. Hill. 2005. A PrfA-regulated bile exclusion system (BilE) is a novel virulence factor in *Listeria monocytogenes*. *Mol Microbiol* **55**:1183-1195.

- Slimings, C., and T. V. Riley. 2014. Antibiotics and hospital-acquired *Clostridium difficile* infection: update of systematic review and meta-analysis. *J Antimicrob Chemother* **69**:881-891.
- Smith, J. L., Y. Liu, and G. C. Paoli. 2013. How does *Listeria monocytogenes* combat acid conditions? *Can J Microbiol* **59**:141-152.
- Smits, W. K., C. Bongiorno, J. W. Veening, L. W. Hamoen, O. P. Kuipers, and M. Perego. 2007. Temporal separation of distinct differentiation pathways by a dual specificity Rap-Phr system in *Bacillus subtilis*. *Mol Microbiol* **65**:103-120.
- Smits, W. K., D. Lyras, D. B. Lacy, M. H. Wilcox, and E. J. Kuijper. 2016. *Clostridium difficile* infection. *Nat Rev Dis Primers* **2**:16020.
- Smutna, T., V. L. Goncalves, L. M. Saraiva, J. Tachezy, M. Teixeira, and I. Hrdy. 2009. Flavodiiron protein from *Trichomonas vaginalis* hydrogenosomes: the terminal oxygen reductase. *Eukaryot Cell* **8**:47-55.
- Solomon, E. I., T. C. Brunold, M. I. Davis, J. N. Kemsley, S. K. Lee, N. Lehnert, F. Neese, A. J. Skulan, Y. S. Yang, and J. Zhou. 2000. Geometric and electronic structure/function correlations in non-heme iron enzymes. *Chem Rev* **100**:235-350.
- Solomon, J. M., B. A. Lazazzera, and A. D. Grossman. 1996. Purification and characterization of an extracellular peptide factor that affects two different developmental pathways in *Bacillus subtilis*. *Genes Dev* **10**:2014-2024.
- Sorg, J. A., and A. L. Sonenshein. 2008. Bile salts and glycine as cogerminants for *Clostridium difficile* spores. *J Bacteriol* **190**:2505-2512.
- Sorg, J. A., and A. L. Sonenshein. 2009. Chenodeoxycholate is an inhibitor of *Clostridium difficile* spore germination. *J Bacteriol* **191**:1115-1117.
- Soutourina, O. A., M. Monot, P. Boudry, L. Saujet, C. Pichon, O. Sismeiro, E. Semenova, K. Severinov, C. Le Bouguenec, J. Y. Coppee, B. Dupuy, and I. Martin-Verstraete. 2013. Genome-wide identification of regulatory RNAs in the human pathogen *Clostridium difficile*. *PLoS Genet* **9**:e1003493.
- Spigaglia, P. 2016. Recent advances in the understanding of antibiotic resistance in *Clostridium difficile* infection. *Ther Adv Infect Dis* **3**:23-42.
- Spigaglia, P., A. Barketi-Klai, A. Collignon, P. Mastrantonio, F. Barbanti, M. Rupnik, S. Janezic, and I. Kansau. 2013. Surface-layer (S-layer) of human and animal *Clostridium difficile* strains and their behaviour in adherence to epithelial cells and intestinal colonization. *J Med Microbiol* **62**:1386-1393.
- Stabler, R. A., M. He, L. Dawson, M. Martin, E. Valiente, C. Corton, T. D. Lawley, M. Sebahia, M. A. Quail, G. Rose, D. N. Gerding, M. Gibert, M. R. Popoff, J. Parkhill, G. Dougan, and B. W. Wren. 2009. Comparative genome and phenotypic analysis of *Clostridium difficile* 027 strains provides insight into the evolution of a hypervirulent bacterium. *Genome Biol* **10**:R102.
- Stare, B. G., M. Delmee, and M. Rupnik. 2007. Variant forms of the binary toxin CDT locus and *tcdC* gene in *Clostridium difficile* strains. *J Med Microbiol* **56**:329-335.
- Stecher, B., and W. D. Hardt. 2011. Mechanisms controlling pathogen colonization of the gut. *Curr Opin Microbiol* **14**:82-91.
- Steil, L., M. Serrano, A. O. Henriques, and U. Volker. 2005. Genome-wide analysis of temporally regulated and compartment-specific gene expression in sporulating cells of *Bacillus subtilis*. *Microbiology* **151**:399-420.
- Steiner, E., A. E. Dago, D. I. Young, J. T. Heap, N. P. Minton, J. A. Hoch, and M. Young. 2011. Multiple orphan histidine kinases interact directly with Spo0A to control the initiation of endospore formation in *Clostridium acetobutylicum*. *Mol Microbiol* **80**:641-654.
- Stephens, C. 1998. Bacterial sporulation: a question of commitment? *Curr Biol* **8**:R45-48.
- Stevens, C. M., R. Daniel, N. Illing, and J. Errington. 1992. Characterization of a sporulation gene, *spoIVA*, involved in spore coat morphogenesis in *Bacillus subtilis*. *J Bacteriol* **174**:586-594.
- Stevenson, K. E., and R. H. Vaughn. 1972. Variability in ultrastructure of *Clostridium botulinum* spores. *Can J Microbiol* **18**:1717-1719.
- Stewart, G. C. 2015. The Exosporium Layer of Bacterial Spores: a Connection to the Environment and the Infected Host. *Microbiol Mol Biol Rev* **79**:437-457.

- Stragier, P., C. Bonamy, and C. Karmazyn-Campelli. 1988. Processing of a sporulation sigma factor in *Bacillus subtilis*: how morphological structure could control gene expression. *Cell* **52**:697-704.
- Stragier, P., B. Kunkel, L. Kroos, and R. Losick. 1989. Chromosomal rearrangement generating a composite gene for a developmental transcription factor. *Science* **243**:507-512.
- Stragier, P., and R. Losick. 1996. Molecular genetics of sporulation in *Bacillus subtilis*. *Annu Rev Genet* **30**:297-241.
- Strong, P. C., K. M. Fulton, A. Aubry, S. Foote, S. M. Twine, and S. M. Logan. 2014. Identification and characterization of glycoproteins on the spore surface of *Clostridium difficile*. *J Bacteriol* **196**:2627-2637.
- Sue, D., K. J. Boor, and M. Wiedmann. 2003. Sigma(B)-dependent expression patterns of compatible solute transporter genes *opuCA* and *lmo1421* and the conjugated bile salt hydrolase gene *bsh* in *Listeria monocytogenes*. *Microbiology* **149**:3247-3256.
- Sun, D. X., R. M. Cabrera-Martinez, and P. Setlow. 1991. Control of transcription of the *Bacillus subtilis* *spoIIIIG* gene, which codes for the forespore-specific transcription factor sigma G. *J Bacteriol* **173**:2977-2984.
- Sunde, E. P., P. Setlow, L. Hederstedt, and B. Halle. 2009. The physical state of water in bacterial spores. *Proc Natl Acad Sci U S A* **106**:19334-19339.
- Surawicz, C. M., L. J. Brandt, D. G. Binion, A. N. Ananthakrishnan, S. R. Curry, P. H. Gilligan, L. V. McFarland, M. Mellow, and B. S. Zuckerbraun. 2013. Guidelines for diagnosis, treatment, and prevention of *Clostridium difficile* infections. *Am J Gastroenterol* **108**:478-498; quiz 499.
- Sussman, M. D., and P. Setlow. 1991. Cloning, nucleotide sequence, and regulation of the *Bacillus subtilis* *gpr* gene, which codes for the protease that initiates degradation of small, acid-soluble proteins during spore germination. *J Bacteriol* **173**:291-300.
- Sylvestre, P., E. Couture-Tosi, and M. Mock. 2002. A collagen-like surface glycoprotein is a structural component of the *Bacillus anthracis* exosporium. *Mol Microbiol* **45**:169-178.
- Sylvestre, P., E. Couture-Tosi, and M. Mock. 2005. Contribution of ExsFA and ExsFB proteins to the localization of BclA on the spore surface and to the stability of the bacillus anthracis exosporium. *J Bacteriol* **187**:5122-5128.
- Sztukowska, M., M. Bugno, J. Potempa, J. Travis, and D. M. Kurtz, Jr. 2002. Role of rubrerythrin in the oxidative stress response of *Porphyromonas gingivalis*. *Mol Microbiol* **44**:479-488.
- Takamatsu, H., T. Kodama, T. Nakayama, and K. Watabe. 1999. Characterization of the *yrbA* gene of *Bacillus subtilis*, involved in resistance and germination of spores. *J Bacteriol* **181**:4986-4994.
- Tan, I. S., C. A. Weiss, D. L. Popham, and K. S. Ramamurthi. 2015. A Quality-Control Mechanism Removes Unfit Cells from a Population of Sporulating Bacteria. *Dev Cell* **34**:682-693.
- Tannock, G. W., K. Munro, C. Taylor, B. Lawley, W. Young, B. Byrne, J. Emery, and T. Louie. 2010. A new macrocyclic antibiotic, fidaxomicin (OPT-80), causes less alteration to the bowel microbiota of *Clostridium difficile*-infected patients than does vancomycin. *Microbiology* **156**:3354-3359.
- Tao, L., J. Zhang, P. Meraner, A. Tovaglieri, X. Wu, R. Gerhard, X. Zhang, W. B. Stallcup, J. Miao, X. He, J. G. Hurdle, D. T. Breault, A. L. Brass, and M. Dong. 2016. Frizzled proteins are colonic epithelial receptors for *C. difficile* toxin B. *Nature* **538**:350-355.
- Tasteyre, A., M. C. Barc, A. Collignon, H. Boureau, and T. Karjalainen. 2001. Role of FliC and FliD flagellar proteins of *Clostridium difficile* in adherence and gut colonization. *Infect Immun* **69**:7937-7940.
- Tauveron, G., C. Slomianny, C. Henry, and C. Faille. 2006. Variability among *Bacillus cereus* strains in spore surface properties and influence on their ability to contaminate food surface equipment. *Int J Food Microbiol* **110**:254-262.
- Tempel, W., Z. J. Liu, F. D. Schubot, A. Shah, M. V. Weinberg, F. E. Jenney, Jr., W. B. Arendall, 3rd, M. W. Adams, J. S. Richardson, D. C. Richardson, J. P. Rose, and B. C. Wang. 2004. Structural genomics of *Pyrococcus furiosus*: X-ray crystallography reveals 3D domain swapping in rubrerythrin. *Proteins* **57**:878-882.
- Theriot, C. M., A. A. Bowman, and V. B. Young. 2016. Antibiotic-Induced Alterations of the Gut Microbiota Alter Secondary Bile Acid Production and Allow for *Clostridium difficile* Spore Germination and Outgrowth in the Large Intestine. *mSphere* **1**.

- Theriot, C. M., M. J. Koenigsnecht, P. E. Carlson, Jr., G. E. Hatton, A. M. Nelson, B. Li, G. B. Huffnagle, Z. L. J, and V. B. Young. 2014. Antibiotic-induced shifts in the mouse gut microbiome and metabolome increase susceptibility to *Clostridium difficile* infection. *Nat Commun* **5**:3114.
- Theriot, C. M., and V. B. Young. 2014. Microbial and metabolic interactions between the gastrointestinal tract and *Clostridium difficile* infection. *Gut Microbes* **5**:86-95.
- Theriot, C. M., and V. B. Young. 2015. Interactions Between the Gastrointestinal Microbiome and *Clostridium difficile*. *Annu Rev Microbiol* **69**:445-461.
- Thompson, B. M., H. Y. Hsieh, K. A. Spreng, and G. C. Stewart. 2011. The co-dependence of BxpB/ExsFA and BclA for proper incorporation into the exosporium of *Bacillus anthracis*. *Mol Microbiol* **79**:799-813.
- Tovar-Rojo, F., M. Chander, B. Setlow, and P. Setlow. 2002. The products of the spoVA operon are involved in dipicolinic acid uptake into developing spores of *Bacillus subtilis*. *J Bacteriol* **184**:584-587.
- Traag, B. A., A. Ramirez-Peralta, A. F. Wang Erickson, P. Setlow, and R. Losick. 2013. A novel RNA polymerase-binding protein controlling genes involved in spore germination in *Bacillus subtilis*. *Mol Microbiol* **89**:113-122.
- Tusher, V. G., R. Tibshirani, and G. Chu. 2001. Significance analysis of microarrays applied to the ionizing radiation response. *Proc Natl Acad Sci U S A* **98**:5116-5121.
- Tyanova, S., T. Temu, P. Sinitcyn, A. Carlson, M. Y. Hein, T. Geiger, M. Mann, and J. Cox. 2016. The Perseus computational platform for comprehensive analysis of (prote)omics data. *Nat Methods* **13**:731-740.
- Underwood, S., S. Guan, V. Vijayashubhash, S. D. Baines, L. Graham, R. J. Lewis, M. H. Wilcox, and K. Stephenson. 2009. Characterization of the sporulation initiation pathway of *Clostridium difficile* and its role in toxin production. *J Bacteriol* **191**:7296-7305.
- Utratna, M., E. Cosgrave, C. Baustian, R. Ceredig, and C. O'Byrne. 2012. Development and optimization of an EGFP-based reporter for measuring the general stress response in *Listeria monocytogenes*. *Bioeng Bugs* **3**:93-103.
- Utratna, M., E. Cosgrave, C. Baustian, R. H. Ceredig, and C. P. O'Byrne. 2014. Effects of growth phase and temperature on sigmaB activity within a *Listeria monocytogenes* population: evidence for RsbV-independent activation of sigmaB at refrigeration temperatures. *Biomed Res Int* **2014**:641647.
- van Nood, E., A. Vrieze, M. Nieuwdorp, S. Fuentes, E. G. Zoetendal, W. M. de Vos, C. E. Visser, E. J. Kuijper, J. F. Bartelsman, J. G. Tijssen, P. Speelman, M. G. Dijkgraaf, and J. J. Keller. 2013. Duodenal infusion of donor feces for recurrent *Clostridium difficile*. *N Engl J Med* **368**:407-415.
- van Ooij, C., and R. Losick. 2003. Subcellular localization of a small sporulation protein in *Bacillus subtilis*. *J Bacteriol* **185**:1391-1398.
- van Schaik, W., M. H. Tempelaars, J. A. Wouters, W. M. de Vos, and T. Abee. 2004. The alternative sigma factor sigmaB of *Bacillus cereus*: response to stress and role in heat adaptation. *J Bacteriol* **186**:316-325.
- van Schaik, W., M. H. Tempelaars, M. H. Zwietering, W. M. de Vos, and T. Abee. 2005. Analysis of the role of RsbV, RsbW, and RsbY in regulating {sigma}B activity in *Bacillus cereus*. *J Bacteriol* **187**:5846-5851.
- van Schaik, W., M. van der Voort, D. Molenaar, R. Moezelaar, W. M. de Vos, and T. Abee. 2007. Identification of the sigmaB regulon of *Bacillus cereus* and conservation of sigmaB-regulated genes in low-GC-content gram-positive bacteria. *J Bacteriol* **189**:4384-4390.
- Vardakas, K. Z., K. A. Polyzos, K. Patouni, P. I. Rafailidis, G. Samonis, and M. E. Falagas. 2012. Treatment failure and recurrence of *Clostridium difficile* infection following treatment with vancomycin or metronidazole: a systematic review of the evidence. *Int J Antimicrob Agents* **40**:1-8.
- Vazquez-Torres, A., and A. J. Baumler. 2016. Nitrate, nitrite and nitric oxide reductases: from the last universal common ancestor to modern bacterial pathogens. *Curr Opin Microbiol* **29**:1-8.
- Veening, J. W., H. Murray, and J. Errington. 2009. A mechanism for cell cycle regulation of sporulation initiation in *Bacillus subtilis*. *Genes Dev* **23**:1959-1970.

- Venugopal, A. A., and S. Johnson. 2012. Current state of *Clostridium difficile* treatment options. *Clin Infect Dis* **55 Suppl 2**:S71-76.
- Vepachedu, V. R., and P. Setlow. 2007. Role of SpoVA proteins in release of dipicolinic acid during germination of *Bacillus subtilis* spores triggered by dodecylamine or lysozyme. *J Bacteriol* **189**:1565-1572.
- Vicente, J. B., C. M. Gomes, A. Wasserfallen, and M. Teixeira. 2002. Module fusion in an A-type flavoprotein from the cyanobacterium *Synechocystis* condenses a multiple-component pathway in a single polypeptide chain. *Biochem Biophys Res Commun* **294**:82-87.
- Vicente, J. B., F. M. Scandurra, J. V. Rodrigues, M. Brunori, P. Sarti, M. Teixeira, and A. Giuffrè. 2007. Kinetics of electron transfer from NADH to the *Escherichia coli* nitric oxide reductase flavorubredoxin. *FEBS J* **274**:677-686.
- Vicente, J. B., and M. Teixeira. 2005. Redox and spectroscopic properties of the *Escherichia coli* nitric oxide-detoxifying system involving flavorubredoxin and its NADH-oxidizing redox partner. *J Biol Chem* **280**:34599-34608.
- Vicente, J. B., V. Tran, L. Pinto, M. Teixeira, and U. Singh. 2012. A detoxifying oxygen reductase in the anaerobic protozoan *Entamoeba histolytica*. *Eukaryot Cell* **11**:1112-1118.
- Vijay, K., M. S. Brody, E. Fredlund, and C. W. Price. 2000. A PP2C phosphatase containing a PAS domain is required to convey signals of energy stress to the sigmaB transcription factor of *Bacillus subtilis*. *Mol Microbiol* **35**:180-188.
- Vizcaino, J. A., A. Csordas, N. Del-Toro, J. A. Dianas, J. Griss, I. Lavidas, G. Mayer, Y. Perez-Riverol, F. Reisinger, T. Ternent, Q. W. Xu, R. Wang, and H. Hermjakob. 2016. 2016 update of the PRIDE database and its related tools. *Nucleic Acids Res* **44**:11033.
- Voelker, U., T. Luo, N. Smirnova, and W. Haldenwang. 1997. Stress activation of *Bacillus subtilis* sigma B can occur in the absence of the sigma B negative regulator RsbX. *J Bacteriol* **179**:1980-1984.
- Voelker, U., A. Voelker, and W. G. Haldenwang. 1996a. Reactivation of the *Bacillus subtilis* anti-sigma B antagonist, RsbV, by stress- or starvation-induced phosphatase activities. *J Bacteriol* **178**:5456-5463.
- Voelker, U., A. Voelker, and W. G. Haldenwang. 1996b. The yeast two-hybrid system detects interactions between *Bacillus subtilis* sigmaB regulators. *J Bacteriol* **178**:7020-7023.
- Voelker, U., A. Voelker, B. Maul, M. Hecker, A. Dufour, and W. G. Haldenwang. 1995. Separate mechanisms activate sigma B of *Bacillus subtilis* in response to environmental and metabolic stresses. *J Bacteriol* **177**:3771-3780.
- Volker, U., B. Maul, and M. Hecker. 1999. Expression of the sigmaB-dependent general stress regulon confers multiple stress resistance in *Bacillus subtilis*. *J Bacteriol* **181**:3942-3948.
- von Blohn, C., B. Kempf, R. M. Kappes, and E. Bremer. 1997. Osmostress response in *Bacillus subtilis*: characterization of a proline uptake system (OpuE) regulated by high osmolarity and the alternative transcription factor sigma B. *Mol Microbiol* **25**:175-187.
- Voth, D. E., and J. D. Ballard. 2005. *Clostridium difficile* toxins: mechanism of action and role in disease. *Clin Microbiol Rev* **18**:247-263.
- Waligora, A. J., C. Hennequin, P. Mullany, P. Bourlioux, A. Collignon, and T. Karjalainen. 2001. Characterization of a cell surface protein of *Clostridium difficile* with adhesive properties. *Infect Immun* **69**:2144-2153.
- Waller, L. N., N. Fox, K. F. Fox, A. Fox, and R. L. Price. 2004. Ruthenium red staining for ultrastructural visualization of a glycoprotein layer surrounding the spore of *Bacillus anthracis* and *Bacillus subtilis*. *J Microbiol Methods* **58**:23-30.
- Wang, K. H., A. L. Isidro, L. Domingues, H. A. Eskandarian, P. T. McKenney, K. Drew, P. Grabowski, M. H. Chua, S. N. Barry, M. Guan, R. Bonneau, A. O. Henriques, and P. Eichenberger. 2009a. The coat morphogenetic protein SpoVID is necessary for spore encasement in *Bacillus subtilis*. *Mol Microbiol* **74**:634-649.
- Wang, S., A. Shen, P. Setlow, and Y. Q. Li. 2015. Characterization of the Dynamic Germination of Individual *Clostridium difficile* Spores Using Raman Spectroscopy and Differential Interference Contrast Microscopy. *J Bacteriol* **197**:2361-2373.

- Wang, S. T., B. Setlow, E. M. Conlon, J. L. Lyon, D. Imamura, T. Sato, P. Setlow, R. Losick, and P. Eichenberger. 2006. The forespore line of gene expression in *Bacillus subtilis*. *J Mol Biol* **358**:16-37.
- Wang, S. W., C. Y. Chen, J. T. Tseng, S. H. Liang, S. C. Chen, C. Hsieh, Y. H. Chen, and C. C. Chen. 2009b. orf4 of the *Bacillus cereus* sigB gene cluster encodes a general stress-inducible Dps-like bacterioferritin. *J Bacteriol* **191**:4522-4533.
- Warny, M., A. C. Keates, S. Keates, I. Castagliuolo, J. K. Zacks, S. Aboudola, A. Qamar, C. Pothoulakis, J. T. LaMont, and C. P. Kelly. 2000. p38 MAP kinase activation by *Clostridium difficile* toxin A mediates monocyte necrosis, IL-8 production, and enteritis. *J Clin Invest* **105**:1147-1156.
- Warny, M., J. Pepin, A. Fang, G. Killgore, A. Thompson, J. Brazier, E. Frost, and L. C. McDonald. 2005. Toxin production by an emerging strain of *Clostridium difficile* associated with outbreaks of severe disease in North America and Europe. *Lancet* **366**:1079-1084.
- Warriner, K., C. Xu, M. Habash, S. Sultan, and S. J. Weese. 2017. Dissemination of *Clostridium difficile* in food and the environment: Significant sources of *C. difficile* community-acquired infection? *J Appl Microbiol* **122**:542-553.
- Warth, A. D., D. F. Ohye, and W. G. Murrell. 1963. The composition and structure of bacterial spores. *J Cell Biol* **16**:579-592.
- Wasserfallen, A., S. Ragetli, Y. Jouanneau, and T. Leisinger. 1998. A family of flavoproteins in the domains Archaea and Bacteria. *Eur J Biochem* **254**:325-332.
- Weaver, J., T. J. Kang, K. W. Raines, G. L. Cao, S. Hibbs, P. Tsai, L. Baillie, G. M. Rosen, and A. S. Cross. 2007. Protective role of *Bacillus anthracis* exosporium in macrophage-mediated killing by nitric oxide. *Infect Immun* **75**:3894-3901.
- Weese, J. S. 2010. *Clostridium difficile* in food--innocent bystander or serious threat? *Clin Microbiol Infect* **16**:3-10.
- Wehrli, E., P. Scherrer, and O. Kubler. 1980. The crystalline layers in spores of *Bacillus cereus* and *Bacillus thuringiensis* studied by freeze-etching and high resolution electron microscopy. *Eur J Cell Biol* **20**:283-289.
- Weinberg, M. V., F. E. Jenney, Jr., X. Cui, and M. W. Adams. 2004. Rubrerythrin from the hyperthermophilic archaeon *Pyrococcus furiosus* is a rubredoxin-dependent, iron-containing peroxidase. *J Bacteriol* **186**:7888-7895.
- Wells, J. E., and P. B. Hylemon. 2000. Identification and characterization of a bile acid 7 α -dehydroxylation operon in *Clostridium* sp. strain TO-931, a highly active 7 α -dehydroxyating strain isolated from human feces. *Appl Environ Microbiol* **66**:1107-1113.
- Wemekamp-Kamphuis, H. H., J. A. Wouters, P. P. de Leeuw, T. Hain, T. Chakraborty, and T. Abee. 2004. Identification of sigma factor sigma B-controlled genes and their impact on acid stress, high hydrostatic pressure, and freeze survival in *Listeria monocytogenes* EGD-e. *Appl Environ Microbiol* **70**:3457-3466.
- Wiedmann, M., T. J. Arvik, R. J. Hurley, and K. J. Boor. 1998. General stress transcription factor sigmaB and its role in acid tolerance and virulence of *Listeria monocytogenes*. *J Bacteriol* **180**:3650-3656.
- Wiegand, P. N., D. Nathwani, M. H. Wilcox, J. Stephens, A. Shelbaya, and S. Haider. 2012. Clinical and economic burden of *Clostridium difficile* infection in Europe: a systematic review of healthcare-facility-acquired infection. *J Hosp Infect* **81**:1-14.
- Wilcox, M. H., D. N. Gerding, I. R. Poxton, C. Kelly, R. Nathan, T. Birch, O. A. Cornely, G. Rahav, E. Bouza, C. Lee, G. Jenkin, W. Jensen, Y. S. Kim, J. Yoshida, L. Gabryelski, A. Pedley, K. Eves, R. Tipping, D. Guris, N. Kartsonis, M. B. Dorr, I. Modify, and M. I. Investigators. 2017. Bezlotoxumab for Prevention of Recurrent *Clostridium difficile* Infection. *N Engl J Med* **376**:305-317.
- Wildschut, J. D., R. M. Lang, J. K. Voordouw, and G. Voordouw. 2006. Rubredoxin: oxygen oxidoreductase enhances survival of *Desulfovibrio vulgaris* hildenborough under microaerophilic conditions. *J Bacteriol* **188**:6253-6260.
- Wilson, K. H., M. J. Kennedy, and F. R. Fekety. 1982. Use of sodium taurocholate to enhance spore recovery on a medium selective for *Clostridium difficile*. *J Clin Microbiol* **15**:443-446.

- Wilson, K. H., and J. N. Sheagren. 1983. Antagonism of toxigenic *Clostridium difficile* by nontoxigenic *C. difficile*. *J Infect Dis* **147**:733-736.
- Wise, A. A., and C. W. Price. 1995. Four additional genes in the sigB operon of *Bacillus subtilis* that control activity of the general stress factor sigma B in response to environmental signals. *J Bacteriol* **177**:123-133.
- Worner, K., H. Szurmant, C. Chiang, and J. A. Hoch. 2006. Phosphorylation and functional analysis of the sporulation initiation factor Spo0A from *Clostridium botulinum*. *Mol Microbiol* **59**:1000-1012.
- Wu, I. L., K. Narayan, J. P. Castaing, F. Tian, S. Subramaniam, and K. S. Ramamurthi. 2015. A versatile nano display platform from bacterial spore coat proteins. *Nat Commun* **6**:6777.
- Wu, J. J., M. G. Howard, and P. J. Piggot. 1989. Regulation of transcription of the *Bacillus subtilis* spoIIA locus. *J Bacteriol* **171**:692-698.
- Wu, L. J., and J. Errington. 2000. Identification and characterization of a new prespore-specific regulatory gene, rsfA, of *Bacillus subtilis*. *J Bacteriol* **182**:418-424.
- Wu, L. J., A. Feucht, and J. Errington. 1998. Prespore-specific gene expression in *Bacillus subtilis* is driven by sequestration of SpoIIE phosphatase to the prespore side of the asymmetric septum. *Genes Dev* **12**:1371-1380.
- Wu, S., H. de Lencastre, and A. Tomasz. 1996. Sigma-B, a putative operon encoding alternate sigma factor of *Staphylococcus aureus* RNA polymerase: molecular cloning and DNA sequencing. *J Bacteriol* **178**:6036-6042.
- Wydaud-Dematteis, S., I. El Meouche, P. Courtin, A. Hamiot, R. Lai-Kuen, B. Saubamea, F. Fenaille, M. J. Butel, J. L. Pons, B. Dupuy, M. P. Chapot-Chartier, and J. Peltier. 2018. Cwp19 Is a Novel Lytic Transglycosylase Involved in Stationary-Phase Autolysis Resulting in Toxin Release in *Clostridium difficile*. *MBio* **9**.
- Xia, Y., Y. Xin, X. Li, and W. Fang. 2015. To Modulate Survival under Secondary Stress Conditions, *Listeria monocytogenes* 10403S Employs RsbX To Downregulate sigmaB Activity in the Poststress Recovery Stage or Stationary Phase. *Appl Environ Microbiol* **82**:1126-1135.
- Xia, Y., Y. Xin, X. Li, and W. Fang. 2016. To Modulate Survival under Secondary Stress Conditions, *Listeria monocytogenes* 10403S Employs RsbX To Downregulate sigmaB Activity in the Poststress Recovery Stage or Stationary Phase. *Appl Environ Microbiol* **82**:1126-1135.
- Yang, X., C. M. Kang, M. S. Brody, and C. W. Price. 1996. Opposing pairs of serine protein kinases and phosphatases transmit signals of environmental stress to activate a bacterial transcription factor. *Genes Dev* **10**:2265-2275.
- Yutin, N., and M. Y. Galperin. 2013. A genomic update on clostridial phylogeny: Gram-negative spore formers and other misplaced clostridia. *Environ Microbiol* **15**:2631-2641.
- Zarb, P., B. Coignard, J. Giskeviciene, A. Muller, V. Vankerckhoven, K. Weist, M. Goossens, S. Vaerenberg, S. Hopkins, B. Catry, D. Monnet, H. Goossens, C. Suetens, E. p. p. p. s. National Contact Points for the, and E. p. p. p. s. Hospital Contact Points for the. 2012. The European Centre for Disease Prevention and Control (ECDC) pilot point prevalence survey of healthcare-associated infections and antimicrobial use. *Euro Surveill* **17**.
- Zhang, J., P. C. Fitz-James, and A. I. Aronson. 1993. Cloning and characterization of a cluster of genes encoding polypeptides present in the insoluble fraction of the spore coat of *Bacillus subtilis*. *J Bacteriol* **175**:3757-3766.
- Zhang, L., D. Dong, C. Jiang, Z. Li, X. Wang, and Y. Peng. 2015. Insight into alteration of gut microbiota in *Clostridium difficile* infection and asymptomatic *C. difficile* colonization. *Anaerobe* **34**:1-7.
- Zhang, Q., Y. Feng, L. Deng, F. Feng, L. Wang, Q. Zhou, and Q. Luo. 2011. SigB plays a major role in *Listeria monocytogenes* tolerance to bile stress. *Int J Food Microbiol* **145**:238-243.
- Zhang, S., and W. G. Haldenwang. 2005. Contributions of ATP, GTP, and redox state to nutritional stress activation of the *Bacillus subtilis* sigmaB transcription factor. *J Bacteriol* **187**:7554-7560.
- Zheng, L., R. Halberg, S. Roels, H. Ichikawa, L. Kroos, and R. Losick. 1992. Sporulation regulatory protein GerE from *Bacillus subtilis* binds to and can activate or repress transcription from promoters for mother-cell-specific genes. *J Mol Biol* **226**:1037-1050.

- Zheng, L. B., W. P. Donovan, P. C. Fitz-James, and R. Losick. 1988. Gene encoding a morphogenic protein required in the assembly of the outer coat of the *Bacillus subtilis* endospore. *Genes Dev* **2**:1047-1054.
- Zheng, L. B., and R. Losick. 1990. Cascade regulation of spore coat gene expression in *Bacillus subtilis*. *J Mol Biol* **212**:645-660.
- Zilhao, R., G. Naclerio, A. O. Henriques, L. Baccigalupi, C. P. Moran, Jr., and E. Ricca. 1999. Assembly requirements and role of CotH during spore coat formation in *Bacillus subtilis*. *J Bacteriol* **181**:2631-2633.
- Zilhao, R., M. Serrano, R. Isticato, E. Ricca, C. P. Moran, Jr., and A. O. Henriques. 2004. Interactions among CotB, CotG, and CotH during assembly of the *Bacillus subtilis* spore coat. *J Bacteriol* **186**:1110-1119.

Annexes

Article: The σ^B signalling activation pathway in the enteropathogen *Clostridium difficile*

Nicolas Kint^{1,2}, Carolina Alves Feliciano^{1,2}, Audrey Hamiot^{1,2}, Milica Denic^{1,2}, Bruno Dupuy^{1,2} and Isabelle Martin-Verstraete^{1,2*}

¹ Laboratoire Pathogénèse des Bactéries Anaérobies, Institut Pasteur, Paris, France.

² Université Paris Diderot, Sorbonne Paris Cité, Paris, France.

*Corresponding author : Laboratoire Pathogénèse des Bactéries Anaérobies, Institut Pasteur, and University Paris Diderot, Sorbonne Paris Cité, Paris, France; *Phone*: +33140613561; *email*: isabelle.martin-verstraete@pasteur.fr

Key words: General stress response, phosphatase, partner switching, signalling pathway, nitric oxide, oxygen tolerance

σ^B signalling pathway in *C. difficile*

Summary

Clostridium difficile is the main cause of antibiotic-associated diarrhoea. Inside the gut, *C. difficile* must adapt to the stresses it copes with, by inducing protection, detoxification and repair systems that belong to the general stress response involving σ^B . Following stresses, σ^B activation requires a PP2C phosphatase to dephosphorylate the anti-anti-sigma factor RsbV that allows its interaction with the anti-sigma factor RsbW and the release of σ^B . In this work, we studied the signalling pathway responsible for the activation of σ^B in *C. difficile*. Contrary to other firmicutes, the expression of *sigB* in *C. difficile* is constitutive and not auto-regulated. We confirmed the partner switching mechanism that involved RsbV, RsbW and σ^B and we showed that CD2685, newly renamed RsbZ, and its phosphatase activity are required for RsbV dephosphorylation triggering σ^B activation. While CD0007 and CD0008, whose genes belong to *sigB* operon, are not involved in σ^B activity, depletion of the essential iron-sulphur flavoprotein, CD2684, whose gene forms an operon with *rsbZ*, prevents σ^B activation. Finally, we observed that σ^B is heterogeneously active in a subpopulation of *C. difficile* cells from the exponential phase, likely leading to a “bet-hedging” strategy allowing a better chance for the cells to survive adverse conditions.

Introduction

Clostridium difficile, a gram-positive, anaerobic and spore-forming bacterium, is the main cause of antibiotic-associated diarrhoea and of pseudomembranous colitis, a potentially lethal disease. In the early 2000s, the incidence and severity of *C. difficile* infection (CDI) have increased in North America and Europe owing to the emergence of new isolates of the BI/NAP1/027 lineage (Rupnik et al. 2009, Wiegand et al. 2012). *C. difficile* is acquired from the environment through the ingestion of spores: a form of resistance, transmission and dissemination of this bacterium (Deakin et al. 2012). Disruption of the normal intestinal microbiota, notably by antibiotics, induces substantial changes in metabolite pools (Theriot et al. 2014). These changes include an increased concentration of bile salts that triggers spores germination. Then, *C. difficile* vegetative cells multiply and colonise the intestinal tract. The toxigenic strains of *C. difficile* produce two toxins, TcdA and TcdB, which are the major virulence factors required for the development of symptoms. These toxins cause the alteration of actin cytoskeleton in intestinal epithelial cells that leads to a major neutrophil recruitment favouring an intensive local inflammation process (Peniche et al. 2013, Jose and Madan 2016). Although toxins are regarded as primary virulence factors, the establishment of *C. difficile* in its colonic niche is also dependent on additional virulence factors such as the adhesin Cwp66, the flagellum, the fibronectin-binding protein FbpA, and the surface layer precursor protein SlpA (Janoir 2016).

In the gut, *C. difficile* vegetative cells face different stresses including low physiologic oxygen (O₂) tensions (Espey 2013, Rivera-Chavez et al. 2017), pH variations, antibiotics and hyperosmolarity. Bacteria are also exposed to bile acids and cationic antimicrobial peptides (CAMPs) produced by the host and/or by the microbiota (Abt et al. 2016b). Moreover, the inflammation process triggered by several *C. difficile* factors (toxins, S-layer proteins and flagellin) leads to the production by the host immune system of reactive oxygen species (ROS), nitric oxide (NO) and reactive nitrogen species (RNS) (Abt et al. 2016b, Jose and Madan 2016). Thus, to adapt and colonise this hostile environment, *C. difficile* must induce protection, detoxification and repair systems. We have recently shown that the alternative sigma factor of the general stress response, σ^B (Hecker et al. 2007, Guldimann et al. 2016), plays a crucial role in the regulation of these different processes in *C. difficile* (Kint et al. 2017). Accordingly, *sigB* inactivation leads to a higher sensitivity to several stresses the bacterium copes within the gut such as acidic pH, antimicrobial peptides, ROS, NO, RNS and O₂. In this enteropathogen, σ^B controls the expression of about 25 % of the genes at the onset

of stationary phase (Kint et al. 2017). In addition, the colonisation fitness of the *sigB* mutant is greatly affected in dioxenic mice when compared to wild-type strain (Kint et al. 2017). Despite σ^B involvement in stress protection and in gut colonization, little is known about the mechanisms involved in its activation in *C. difficile*.

Since the expression of σ^B regulon represents a major cost for the bacteria, σ^B activity is tightly controlled. In other firmicutes, σ^B activity is modulated by a well-characterised post-translational mechanism called partner switching, in which the interaction and activation of proteins are mediated by reversible threonine and serine phosphorylation (Hecker et al. 2007, de Been et al. 2011). In unstressed cells and during exponential growth phase, the anti- σ factor RsbW phosphorylates the anti-anti- σ factor RsbV blocking its activity (Alper et al. 1996). This enables RsbW to sequester σ^B thereby preventing its association with RNA polymerase core enzyme. During stationary growth phase or when cells are exposed to a stress, a signal is conveyed to specific PP2C phosphatase(s) that dephosphorylate(s) RsbV. The unphosphorylated form of RsbV interacts with RsbW, leading to the release and activation of σ^B and the transcription of its target genes (Yang et al. 1996, Vijay et al. 2000, van Schaik et al. 2005). The stress signals triggering σ^B activation differ among the firmicutes. They can be divided into two groups i) environmental stresses such as ethanol, elevated temperature, hyperosmolarity and low pH (Boylan et al. 1993, Voelker et al. 1995, van Schaik et al. 2004, Pane-Farre et al. 2006) ii) energetic stresses like carbon or phosphate starvation, O₂ deprivation and ATP depletion (Voelker et al. 1995, Vijay et al. 2000, Zhang and Haldenwang 2005).

In this work, we sought to elucidate how σ^B becomes active in *C. difficile*. We first studied the regulation of *sigB* expression and then focused on the partner switching mechanism controlling σ^B activity. We identified the PP2C phosphatase that acts upstream of this partner switching and turn σ^B active. We sought to identify other actors/sensors and their putative role in the σ^B activation pathway. Finally, *sigB* expression and σ^B activity was studied at a single cell level within a population of *C. difficile* vegetative cells using fluorescent microscopy. Altogether the results obtained bring new insights into σ^B activation signalling pathway in *C. difficile* and highlight the differences compared to other firmicutes.

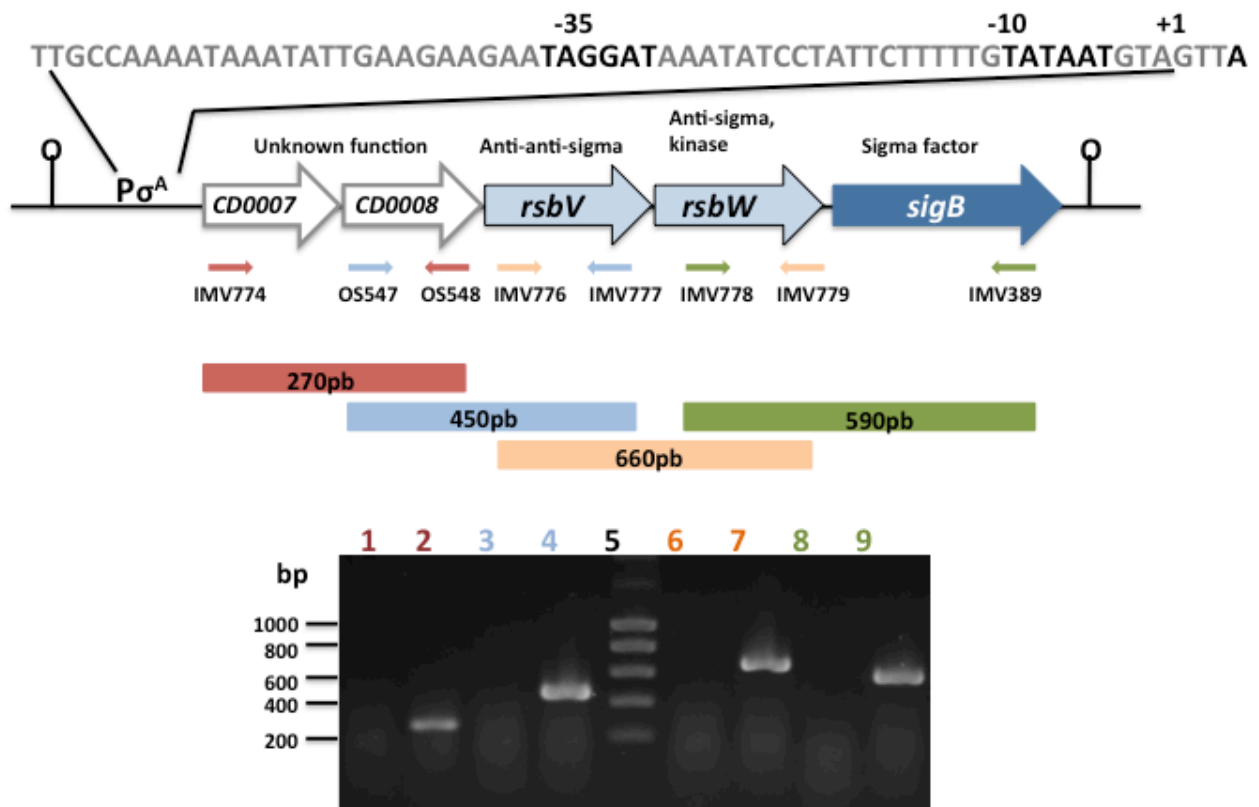


Figure 1: Genetic organisation of the *CD0007-CD0011* locus. Organisation of *sigB* operon. Gene function is indicated below each gene. TSS mapping experiment indicated the presence of a σ^A -dependent promoter upstream of *CD0007* (Soutourina et al, 2013). The -35 and -10 boxes as well as the TSS are indicated in bold. PCR were both realised on RNAs without reverse transcription (lane 1, 3, 6 and 8) and on cDNA synthesised from the same RNAs by reverse transcription using IMV389 primer (lane 2, 4, 7 and 9). PCR was then performed with primers annealing in *CD0007* and *CD0008* (IMV774/OS548, lane 1 and 2), in *CD0008* and *CD0009* (OS547/IMV777, lane 2 and 3), in *CD0009* and *CD0010* (IMV776/IMV779, lane 6 and 7) and in *CD0010* and *CD0011* (IMV778/IMV389, lane 8 and 9). Lane 5: Ladder.

Table 1: Expression of *sigB* operon in the *sigB* mutant and complemented strain.

To study σ^B autoregulation, cells were harvested after 10 h of growth in TY. The results represent the mean of three independent experiments.

Gene ID	Name	Function	qRT-PCR 10 h	
			<i>sigB</i> /630 Δ <i>erm</i>	<i>sigB</i> + pB <i>sigB</i> /630 Δ <i>erm</i>
<i>sigB</i> operon				
<i>CD0007</i>		Unknown	0.91	0.58
<i>CD0008</i>		Unknown	0.71	0.53
<i>CD0009</i>	<i>rsbV</i>	Anti-anti-sigma factor	0.80	0.66
<i>CD0010</i>	<i>rsbW</i>	Anti-sigma factor, kinase	0.44	0.39
<i>CD0011</i>	<i>sigB</i>	Sigma factor	0.16	10.27

Results

Genetic organisation of *sigB* operon

The genetic environment of *sigB* gene is rather conserved among the firmicutes harbouring this σ factor such as *Bacillus subtilis*, *Bacillus cereus*, *Listeria monocytogenes* and *Staphylococcus aureus* (Wise and Price 1995, Wu et al. 1996, Wiedmann et al. 1998, van Schaik et al. 2004). The *sigB* gene forms an operon with the genes encoding the proteins involved in the control of its activation, i.e. the anti-anti-sigma factor and the anti-sigma factor, RsbV and RsbW, respectively. In *C. difficile*, *sigB* (*CD0011*) is the last gene of a locus containing five genes (*CD0007-0011*). *CD0007* and *CD0008* encode a 98 amino acid protein with a functional uncharacterized YtxH conserved domain (pfam12732) and an 86 amino acid protein without identified domain, respectively. Using THMM and Signal-P software, no signal peptides were detected for these small proteins, but one trans-membrane helix was predicted for *CD0007* (amino acids 12 to 29) and for *CD0008* (amino acids 5 to 24). *CD0009* and *CD0010* share 35 % and 39 % of identity with RsbV and RsbW of *B. subtilis*, respectively. To determine whether these five genes form an operon, we performed RT-PCR experiments. PCR products were detected using pairs of primers located in adjacent genes, with RNAs processed by reverse transcriptase but not with untreated RNAs, serving as a negative control (Fig. 1). Since, DNA fragments were amplified only if neighbouring genes were co-transcribed, these results indicate that *sigB* is the last gene of a five-gene operon containing *rsbV* and *rsbW*.

Absence of auto-regulation and constitutive expression of *sigB*

A previous genome-wide transcriptional start site (TSS) experiment mapped a single TSS in *sigB* operon located 34 bp upstream of the first codon of *CD0007* (Soutourina et al. 2013). Upstream of this TSS, we found a -10 (TATAAT) box similar to the consensus sequence of σ^A -dependent promoters while the -35 (TAGGAT) region is less conserved (Fig. 1). This promoter clearly differs from the consensus of σ^B -dependent promoters recently defined in *C. difficile* (Kint et al. 2017). The presence of a single σ^A -dependent promoter suggested that *sigB* expression is not auto-regulated in *C. difficile*, contrary to the positive control of its own transcription observed in other firmicutes. Accordingly, we did not detect any σ^B -dependent change of expression of *CD0007*, *CD0008*, *rsbV* or *rsbW* by qRT-PCR (Table 1). These results are in agreement with our previous transcriptomic study (Kint et al. 2017). To determine whether expression of *sigB* operon varies during *C. difficile* growth, we

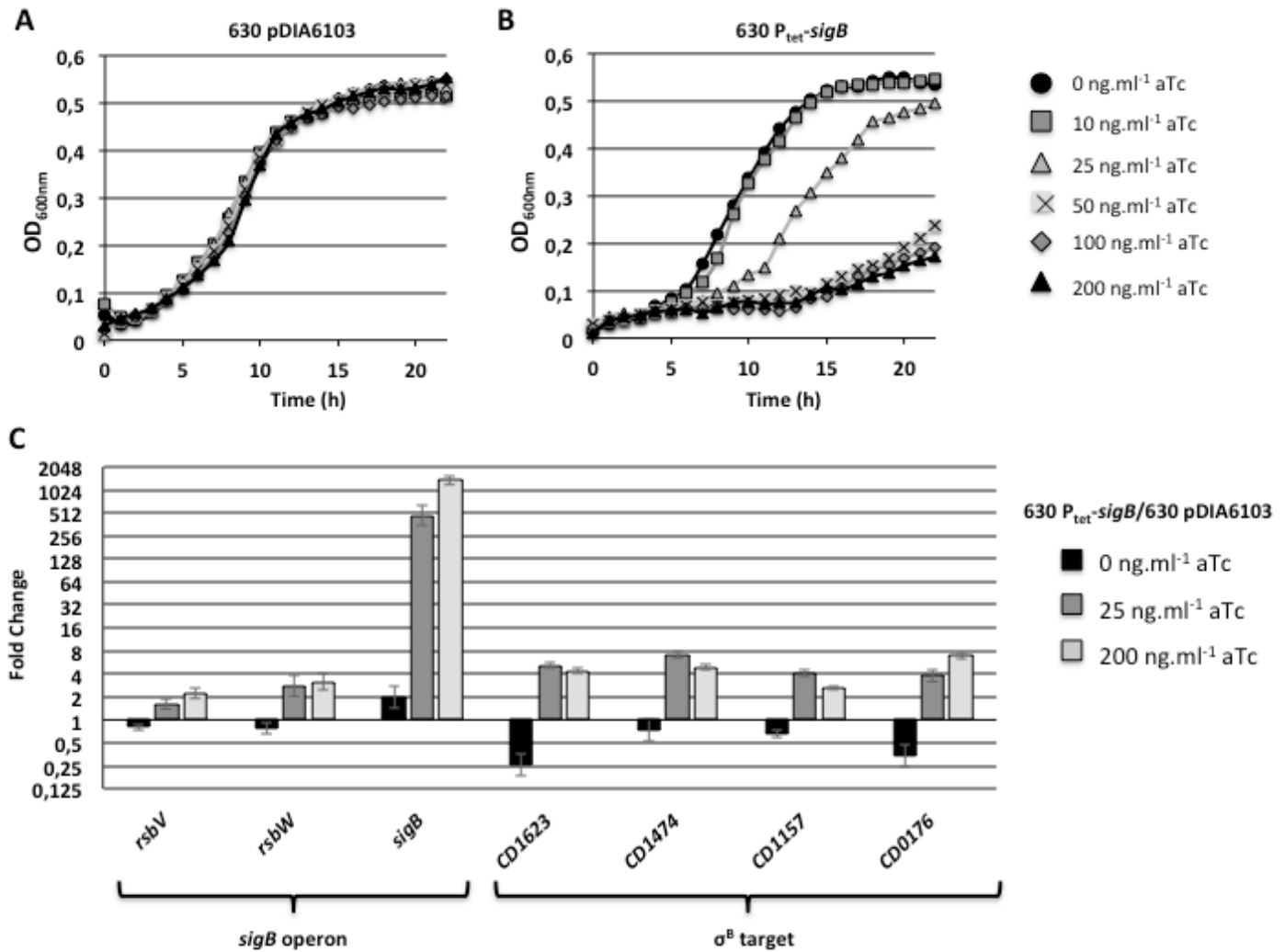


Figure 2: *sigB* overexpression is toxic for *C. difficile*. Growth curves of 630 Δ *erm* strain containing either pDIA6103 (**A**) or P_{tet}-*sigB* (**B**) in TY in presence of different concentrations of aTc. These data are the mean of 4 independent experiments. **C**) Fold change of the expression of *rsbV*, *rsbW* and *sigB* genes and of some σ^B target genes between 630 Δ *erm* + P_{tet}-*sigB* and 630 Δ *erm* + pDIA6103 without aTc (black), with 25 ng.ml⁻¹ (dark gray) or 200 ng.ml⁻¹ of aTc (light gray). These results are the means of 2 independent experiments.

monitored its expression by qRT-PCR during growth in TY. We did not observe significant difference in *sigB* operon expression throughout the growth (data not shown). Altogether, these results highlight an absence of σ^B auto-regulation and a constitutive *sigB* operon expression in *C. difficile*.

Toxicity of *sigB* overexpression

As the expression of σ^B regulon represents a major cost for the bacteria, *sigB* expression and/or σ^B activity must be tightly controlled. To determine the effect of *sigB* overexpression, we cloned this gene into pDIA6103 plasmid allowing its expression under the control of P_{tet} promoter, which is inducible in presence of anhydrotetracycline (aTc) (Fagan and Fairweather 2011, Soutourina et al. 2013). Addition of increasing concentrations of aTc in the culture had no effect on the growth of the wild-type strain harbouring pDIA6103 empty vector (Fig. 2A). By contrast, the growth of the wild-type strain containing P_{tet} -*sigB* was reduced in presence of 25 ng.ml⁻¹ of aTc and almost abolished from 50 ng.ml⁻¹ (Fig. 2B). To monitor the level of *sigB* overexpression, we extracted RNA after a 4 h growth in TY without aTc or containing either 25 ng.ml⁻¹ or 200 ng.ml⁻¹. Without aTc, we did not observe difference in *rsbV*, *rsbW* or *sigB* gene expression between the wild-type strain containing or not P_{tet} -*sigB* (Fig. 2C). By contrast, *sigB* gene was overexpressed 400- and 1,400-fold compared to its expression level detected in strain harbouring pDIA6103 in presence of 25 and 200 ng.ml⁻¹ of aTc, respectively (Fig. 2C). Of note, *sigB* expression increased only 10-fold when *sigB* was expressed under the control of its own promoter and the growth of this strain was not affected (Table 1 and data not shown). These results indicated that a proper expression level of *sigB* is important for the fitness of *C. difficile*. In agreement with the absence of *sigB* operon auto-regulation, we did not observe increased expression of *rsbV* and *rsbW* genes (Fig. 2C). Moreover, while *sigB* is drastically over-expressed, the expression of several *C. difficile* σ^B -target genes transcribed from a σ^B -dependent promoter only moderately increased. Indeed, the expression of *CD1623* and *CD1157* encoding flavodiiron proteins likely involved in the oxidative stress response (Folgosá et al. 2018b) as well as *CD1474* and *CD0176*, encoding a reverse rubrerythrin and an NADH rubredoxin reductase, respectively, was upregulated only up to 5-fold (Fig. 2C). The different expression level between *sigB* and its target genes highlights a post-transcriptional mechanism involved in the control of σ^B activity.

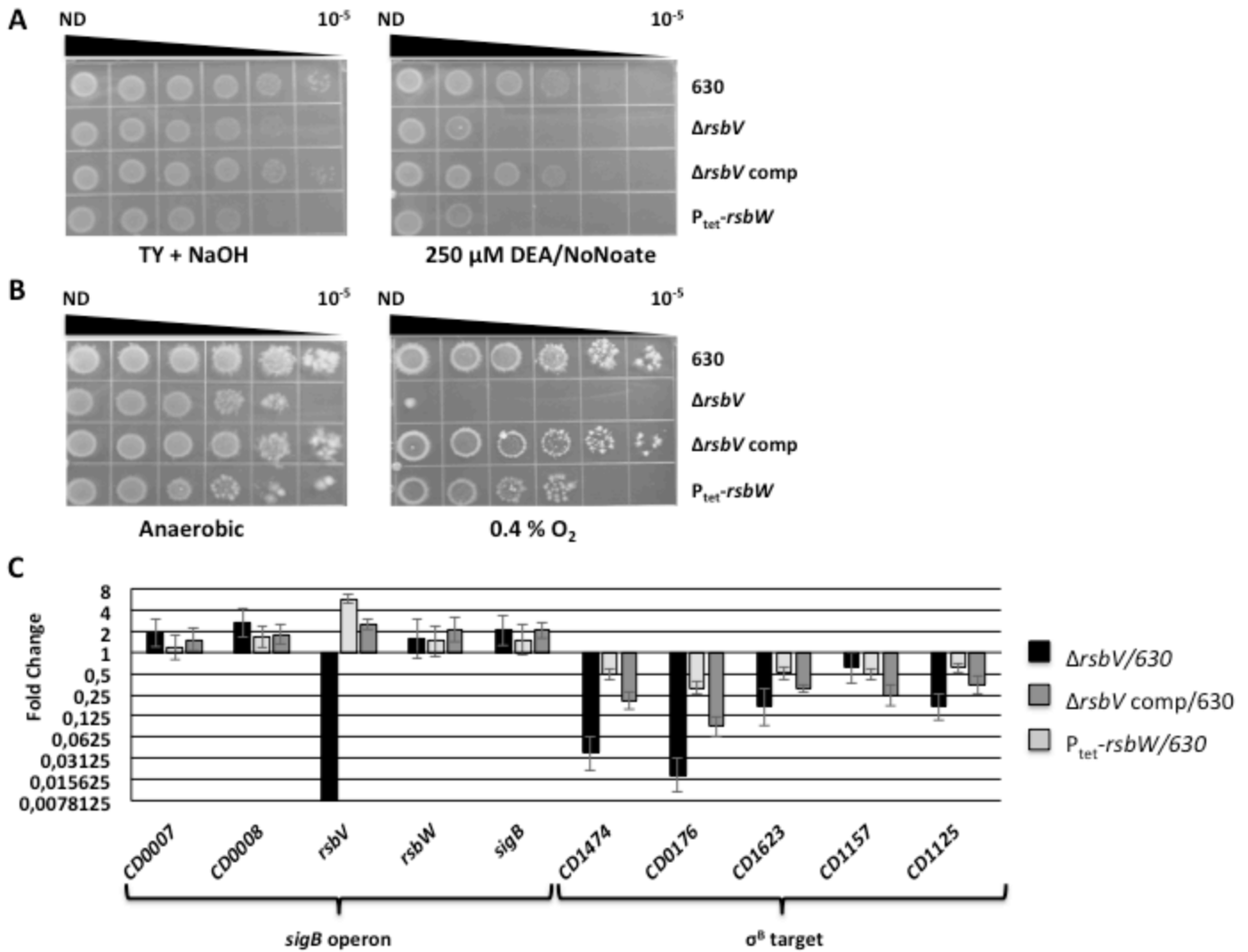


Figure 3: Conservation of the partner switching mechanism in *C. difficile*. Serial dilutions of the different strains were spotted on TY plates containing 25 ng.ml⁻¹ of aTc. Plates were incubated 24 h at 37°C for NO tests (**A**) or 64 h in presence of 0.4 % of O₂ for low O₂ tolerance assay (**B**). Growth controls were performed with plates supplemented with NaOH or plates incubated in anaerobiosis atmosphere for NO tests and low O₂ tolerance assay, respectively. These pictures are representative of 3 independent experiments. **C**) Effect of *rsbV* deletion or *rsbW* over-expression on the expression of *sigB* operon genes and σ^B target genes at the onset of stationary phase. Fold change of the differential expression of the genes belonging to the *sigB* operon and σ^B target genes involved in oxidative and nitrosative stress management in 630 Δerm $\Delta rsbV$ + pDIA6103 (black), 630 Δerm $\Delta rsbV$ + $P_{tet}-rsbV$ (light gray) and 630 Δerm + $P_{tet}-rsbW$ (dark gray) compared to 630 Δerm + pDIA6103. These results are the mean with the standard deviation of 4 independent experiments.

σ^B activation by a partner switching mechanism

According to their role in the release and activation of σ^B in *B. subtilis* and in other firmicutes (Boylan et al. 1992, Benson and Haldenwang 1993b), we speculated that RsbV and RsbW positively and negatively control σ^B activation, respectively. To test this hypothesis, we first deleted *rsbV* gene using allelic exchange (Ng et al. 2013, Ehsaan et al. 2016). As observed for *sigB* mutant (Kint et al. 2017), the growth of $\Delta rsbV$ mutant is not affected in TY (data not shown). However, we observed a higher sensitivity to diethyl-amine NoNoate (DEA/NoNoate), a NO-donor compound, and a lower tolerance to low O₂ tension for $\Delta rsbV$ mutant compared to the wild-type strain and the complemented strain (carrying P_{tet}-*rsbV*) (Fig. 3A and 3B). These results are reminiscent of the phenotypes previously observed in *sigB* mutant supporting the positive role of RsbV on σ^B activity control.

Since RsbW sequesters σ^B and inhibits its activity and because of the growth defect observed in the strain overexpressing *sigB* (Fig. 2), we assumed that *rsbW* deletion might be toxic in *C. difficile* as observed in *B. subtilis* (Benson and Haldenwang 1992, Boylan et al. 1992, Benson and Haldenwang 1993b). Therefore, to conclude on the role of RsbW in σ^B activation, we cloned *rsbW* gene into pDIA6103 to induce its expression upon aTc addition. No growth defect was observed when we overexpressed *rsbW* with aTc concentrations below 200 ng.ml⁻¹ (Fig. S1). However, the strain overexpressing *rsbW* showed a higher sensitivity to DEA/NO compared to the wild-type strain even in presence of low aTc concentration (25 ng.ml⁻¹) (Fig. 3A). Under these conditions, *rsbW* overexpression resulted in a lower O₂ tolerance but to a lesser extent than *rsbV* deletion (Fig. 3B). Altogether, these results suggest a negative role of RsbW on σ^B activity control as observed in other firmicutes.

To confirm the involvement of RsbV and RsbW in σ^B activation, we monitored by qRT-PCR the expression of several σ^B -target genes at the onset of stationary phase, when σ^B is fully active (Kint et al. 2017). The deletion of *rsbV* did not affect significantly the expression of *sigB* operon except for *rsbV* itself (Fig. 3C). However, the expression of *CDI474*, *CD0176* and *CDI623* encoding proteins likely involved in O₂ or ROS detoxification pathways (Kint et al. 2017, Folgosa et al. 2018b) decreased in $\Delta rsbV$ mutant compared to wild-type strain (Fig. 3C). Similarly, we observed a 2-fold overexpression of *rsbW* in presence of 25 ng.ml⁻¹ of aTc, that leads to a lower expression of the different σ^B -target genes but to a lesser extent than *rsbV* inactivation. The low level of *rsbW* overexpression (2-fold) might explain the reduced effect on σ^B regulon expression (Fig. 3C) and the moderate phenotype observed in presence of 0.4 % of O₂ compared to $\Delta rsbV$ mutant (Fig. 3B).

Table 2: Interaction of the different proteins involved in the σ^B activation pathway in bacterial adenylate cyclase two hybrids.

	Fused to pUT18C						Fused to pUT18					
	-	RsbV	RsbW	SigB	RsbZ	CD2684	-	RsbV	RsbW	SigB	RsbZ	CD2684
Fused to pKNT25	-						72±36					
	RsbV		963±498	89±5	532±342			245±58	94±5	100±79		
	RsbW	95±60		1954±869			2078±806	1735±924	3076±818			
	SigB	97±4	738±657		121±30		94±4	118±39		101±26		
	RsbZ		115±13		81±16		160±64		118±39	38±15		115±36
CD2684					99±53					152±70		
Fused to pKNT25	-	84±12					81±16					
	RsbV		4054±1651	101±1	49±36			211±42	98±9	1471±441		
	RsbW		369±169	470±331				1910±490	2176±576	78±22		
	SigB		94±8	1350±516			96±3	2044±605		80±55		
	RsbZ		37±15		100±16			222±153		103±38		142±11
CD2684					127±9					135±10		

Values shown are the average β -galactosidase activities (in Miller unit) of the indicated pair-wise fusions. Each value are the means and the standard deviation of 4 or 5 independent experiments.

As *rsbV* deletion did not modify the expression level of *sigB* (Fig. 3C), we wanted to determine whether it could affect the amount of σ^B protein. For this purpose, we expressed a gene encoding a HA-tagged σ^B protein under the control of its own promoter in 630 Δ *erm*, *sigB* or Δ *rsbV* mutant strains. Cellular extracts were prepared from overnight cultures and σ^B -HA was detected by Western blot using an antibody raised against HA tag. We detected a same amount of σ^B -HA protein in the different genetic backgrounds indicating an absence of effect of *rsbV* deletion on the amount of σ^B -HA (Fig. S2A). This suggests that RsbV acts most likely at the level of σ^B activity through a post-translational mechanism. Thus, these results support that the partner switching mechanism described in other firmicutes (Yang et al. 1996) is conserved in *C. difficile* and enables a proper σ^B activation and σ^B regulon expression.

Conservation of the protein-protein interactions involved in the partner switching mechanism

The partner switching mechanism involves protein-protein interactions between RsbV, RsbW and σ^B and relies on the phosphorylated state of RsbV. The amount of the anti-anti- σ factor RsbV~P is dependent on the kinase activity of the anti- σ factor RsbW as well as on the activity of specific phosphatase(s) (Dufour and Haldenwang 1994, Alper et al. 1996, Yang et al. 1996, Vijay et al. 2000). To determine the existence of interactions between RsbV, RsbW and σ^B of *C. difficile*, we used a Bacterial Adenylate Cyclase Two Hybrid (BACTH) system, which is based on the interaction-mediated reconstruction of a cyclic AMP (cAMP) signalling cascade. Proteins of interest, which are genetically fused to two fragments (T25 and T18) of the catalytic domain of *Bordetella pertussis* adenylate cyclase, are co-expressed in BTH101 *Escherichia coli cya* strain (Karimova et al. 1998). Their interaction results in a functional complementation between T25 and T18 fragments, leading to cAMP synthesis that activates the expression of *lacZ*. DNA fragments encoding RsbV, RsbW and σ^B were cloned into the four BACTH expression vectors to generate recombinant plasmids expressing hybrid proteins in which the examined polypeptides were fused at the N-terminus or the C-terminus of either T25 or T18 fragments (See *Experimental procedures*). To test the efficiency of functional complementation between the different hybrid proteins, β -galactosidase activity was tested. As shown in Table 2, RsbW associates with both RsbV, and σ^B . By contrast, no association between RsbV and σ^B have been observed in our assays (Table 2). These results indicate that proteins interactions involved in the partner switching mechanism and observed in other firmicutes are conserved in *C. difficile*.

Identification of PP2C phosphatase CD2685

In other firmicutes, the dephosphorylation of RsbV by specific PP2C phosphatase(s) enables its interaction with RsbW and triggers the activation of σ^B (Yang et al. 1996, Vijay et al. 2000, van Schaik et al. 2005). To identify such PP2C phosphatases in *C. difficile*, we looked for proteins similar to RsbP and RsbU, the two phosphatases involved in RsbV dephosphorylation in *B. subtilis*. Two PP2C phosphatases are encoded in *C. difficile* genome: SpoIIE (CD3490), involved in the sporulation process (E. Cuenot and I. Martin-Verstraete, unpublished results), and CD2685. The last 200 amino acid residues of CD2685 share 27 % and 25 % identity with RsbP and RsbU, respectively. The C-terminal region of CD2685 also shares similarities with other PP2C phosphatases involved in σ^B activation in pathogenic firmicutes such as *L. monocytogenes*, *B. cereus* and *S. aureus*. No trans-membrane helices or signal peptides are predicted for CD2685. CD2685 protein contains three domains: i) the well characterised serine/threonine PP2C phosphatase domain in the C-terminal part (amino acid 369 to 588), ii) a putative coiled coil domain (amino acid 335 to 360) and iii) a putative sensory GAF domain (amino acid 31 to 183). GAF domains are found in several proteins including cGMP-specific phosphodiesterase, adenylyl-cyclase, guanylyl-cyclase or phytochrome (Aravind and Ponting 1997). Based on these *in silico* analysis, we hypothesised the possible involvement of CD2685 in the activation of σ^B .

CD2685 in σ^B activation

To address the role of CD2685 in the signalling pathway leading to σ^B activation, we deleted *CD2685* gene by allele genetic exchange. We also complemented $\Delta CD2685$ mutant with *CD2685* gene expressed under the control of P_{tet} promoter. The growth of $\Delta CD2685$ mutant was not affected in TY medium (data not shown). However, we observed a growth defect in the complemented strain with 50 ng.ml⁻¹ of aTc, and growth was almost abolished when higher concentrations were added (Fig. S1). These results were also observed in 630 Δerm strain harbouring the same plasmid, suggesting that *CD2685* over-expression is toxic for *C. difficile* (Fig. S1). Since 25 ng.ml⁻¹ of aTc did not affect the growth of $\Delta CD2685$ complemented strain, we decided to perform the following experiments in this condition.

To study whether CD2685 indirectly controls σ^B targets expression, we extracted RNA from the wild-type strain, the $\Delta CD2685$ mutant and the complemented strains harvested at the onset of stationary phase and we performed qRT-PCR experiments. Interestingly, although the expression of genes belonging to *sigB* operon was not affected, the expression of several σ^B target genes including *CDI474*, *CD0176* and *CDI623* decreased 35-, 58- and 8-fold in

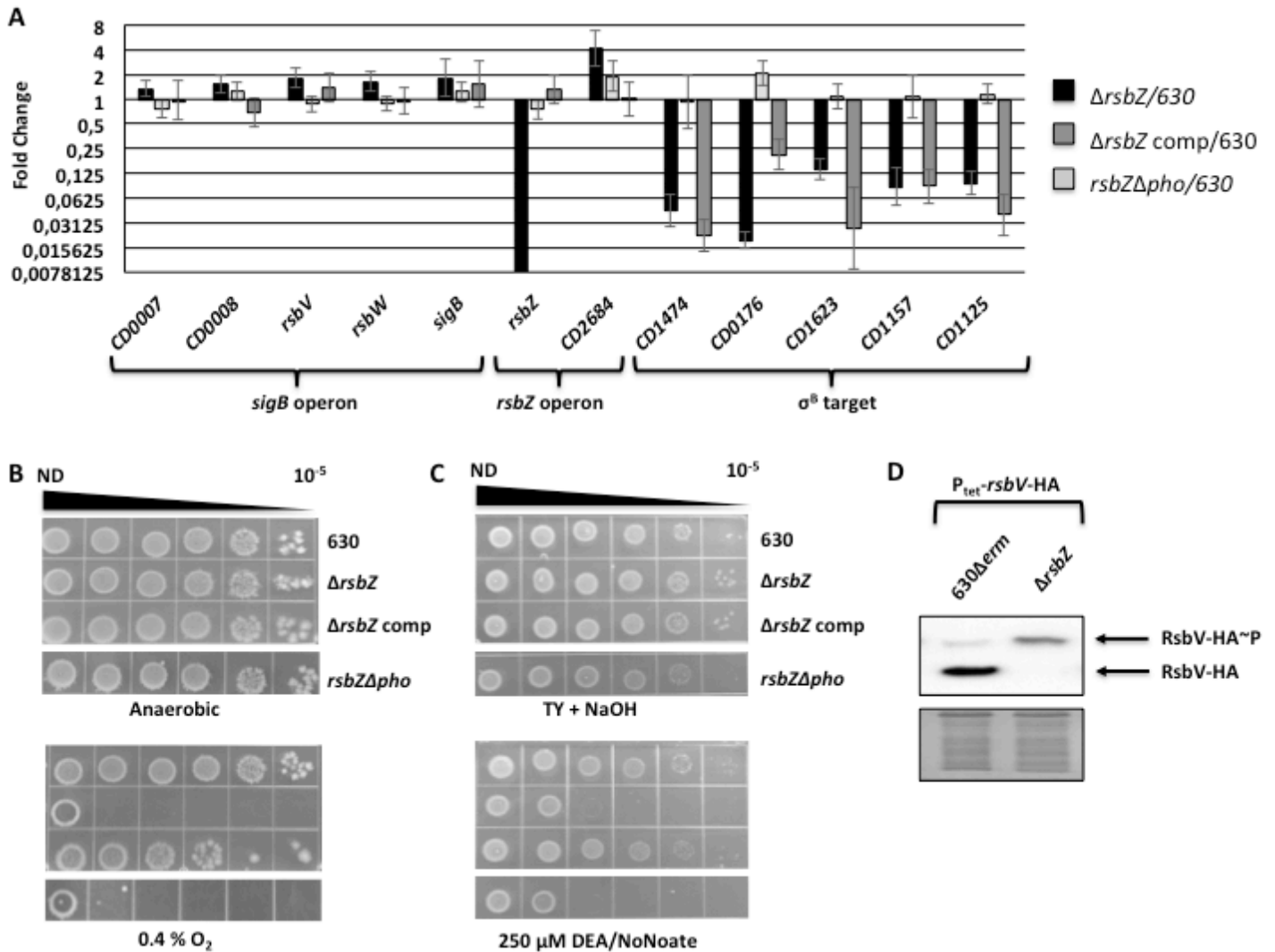


Figure 4: CD2685/RsbZ phosphatase is responsible for σ^B activation in *C. difficile*. **A**) Effect of *rsbZ* deletion of or its phosphatase domain (*rsbZ* Δ *pho*) on the expression of *sigB* operon genes and σ^B target genes at the onset of the stationary phase. Fold change of the differential expression of the genes belonging to *sigB* operon, *rsbZ* operon and of σ^B target genes involved in oxidative and nitrosative stress management in 630 Δerm $\Delta rsbZ$ + pDIA6103 (black), 630 Δerm $\Delta rsbZ$ + P_{tet}-*rsbZ* (light gray) and 630 Δerm $\Delta rsbZ$ + P_{tet}-*rsbZ* Δpho (dark gray) compared to 630 Δerm + pDIA6103. Low O₂ tolerance (**B**) and NO stress assays (**C**). Serial dilutions of the different strains were spotted on TY plates containing 25 ng.ml⁻¹ of aTc. Plates were incubated 64 h in presence of 0.4 % of O₂ (B) or 24 h at 37°C for NO tests (C). Growth controls were performed in anaerobiosis atmosphere or in presence of NaOH for low O₂ tolerance assays and NO tests, respectively. **D**) RsbV phosphorylation state in wild-type and $\Delta rsbZ$ backgrounds. Cellular extracts were run on 12 % acrylamide gel containing 50 μ M of Phos-Tag™ compounds allowing the separation of phosphorylated and non-phosphorylated proteins. Western blot was performed with an antibody raised against the HA tag. Loading control was realized using a 12 % acrylamide gel followed by Coomassie staining. qRT-PCR results are the mean with the standard deviation of 4 independent experiments and pictures are representative of 4 independent experiments.

$\Delta CD2685$ mutant compared to the wild-type strain (Fig. 4A). The expression of genes encoding proteins possibly involved in nitrosative stress protection such as the second flavodiiron protein (CD1157) and the nitro-reductase (CD1125), also decreased when $CD2685$ was deleted (Fig. 4A). These results are in agreement with the lower O_2 tolerance (Fig. 4B) and with the higher sensitivity to DEA/NO (Fig. 4C) of $\Delta CD2685$ mutant compared to the wild-type and the complemented strains.

To test whether $CD2685$ deletion can impact σ^B in a post-transcriptional way, we expressed a gene encoding a σ^B HA-tagged protein in $\Delta CD2685$ mutant. No difference in σ^B -HA production in stationary phase was detected between the wild-type and $\Delta CD2685$ mutant strains (Fig. S2A lane 2 and 5). Altogether, these results show the indirect involvement of $CD2685$ on the control of σ^B regulon expression. Based on these results, we renamed the $CD2685$ phosphatase RsbZ for regulation of σ^B protein Z.

RsbZ controls σ^B activity by dephosphorylating RsbV

According to its PP2C phosphatase domain, we assumed RsbZ is involved in σ^B activation by dephosphorylating the anti-anti sigma factor RsbV. To confirm the interaction between these two proteins, we used the BACTH system described above. No association have been detected between RsbZ and RsbW or RsbZ and σ^B . By contrast, a high β -galactosidase activity was quantified from the hybrids obtained with RsbZ and RsbV supporting RsbZ is able to associate with RsbV (Table 3). This result highlighted the possible role of RsbV~P as a RsbZ substrate. To study the phosphorylation state of RsbV, we expressed a gene encoding a RsbV HA-tagged protein under the control of P_{tet} promoter in both $630\Delta erm$ and $\Delta rsbZ$ genetic backgrounds. Cellular extracts prepared from both strains after 4 h of growth in presence of 100 ng.ml^{-1} of aTc were separated with the Phos-Tag™ compound that allows the discrimination of phosphorylated and unphosphorylated proteins. By Western blot analysis using an antibody raised against the HA tag, we only detected the phosphorylated form of RsbV (RsbV~P) in $\Delta rsbZ$ background while we observed both an intense signal corresponding to the unphosphorylated form of RsbV and a faint signal corresponding to RsbV~P in $630\Delta erm$ background (Fig. 4D). These results suggest that RsbZ is responsible for the dephosphorylation of RsbV~P in *C. difficile*.

To confirm the requirement of the PP2C phosphatase domain for RsbZ activity and for σ^B activation, we expressed $rsbZ$ gene that lacks the 3' part of the gene corresponding to the PP2C phosphatase domain ($rsbZ\Delta pho$) under the control of P_{tet} promoter in mutant. The growth of $\Delta rsbZ$ expressing $rsbZ\Delta pho$ gene was not or slightly affected by the addition of

increasing amounts of aTc (Fig. S1). We confirmed by Western blot that RsbZ Δ pho HA-tagged protein was produced using an antibody raised against the HA tag (Fig. S2B). We then compared the ability of both the truncated RsbZ and the full-length RsbZ proteins to complement Δ *rsbZ* mutant. In presence of 25 ng.ml⁻¹ aTc, *rsbZ* was expressed at a wild-type level in both strains (Fig. 4A). While complementation of Δ *rsbZ* mutant with a gene encoding the full-length protein restored σ^B target gene expression at a wild-type level, complementation of this mutant with a gene encoding the truncated RsbZ Δ pho form did not (Fig. 4A). These results were in agreement with the higher DEA/NO sensitivity and the lower O₂ tolerance observed in Δ *rsbZ* expressing only *rsbZ* Δ pho (Fig. 4B and 4C lane 4). Altogether, these results confirm that RsbZ phosphatase activity is essential for σ^B activation.

Regulation of *rsbZ* expression and identification of the transcriptional start site

In *C. difficile*, a tight control of *sigB* expression and of σ^B activation is needed to allow a proper growth of the cells. Since RsbZ is involved in σ^B activation by RsbV dephosphorylation and because *rsbZ* overexpression leads to a growth defect (Fig. 4D and S2), we hypothesised that *rsbZ* expression could be regulated according to the growth phase. Therefore, we monitored *rsbZ* expression at different time point during *C. difficile* growth. The *rsbZ* expression level did not differ according to the growth phase suggesting a constitutive expression (data not shown) as observed for *rsbP* in *B. subtilis* (Vijay 2000). The *rsbZ* gene belongs to a locus containing also *CD2684* and *CD2686* (Fig. S3). To identify *rsbZ* TSS and to determine if *CD2684* and *rsbZ* form an operon, we performed a 5' RACE experiment (see *Experimental procedures*). When we synthesized a cDNA using a primer annealing in *CD2684* located downstream of *rsbZ* (NK134, Fig. S3), we identified a single TSS located 30 bases upstream of *rsbZ* start codon. Thus, we inferred that these two genes are co-transcribed and form an operon. We deduced -10 (TATGTT) and -35 (TTGTTT) boxes sharing similarities with the consensus sequence recognised by σ^A . Previous studies showed that expression of *rsbZ* and *CD2684* is positively controlled by the first sporulation sigma factor, σ^F (Fimlaid et al. 2013). Indeed, *sigF* inactivation leads to a 3- and 5-fold decreased expression of *rsbZ* and *CD2684*, respectively (Fimlaid et al. 2013). Since *CD2686* located upstream of *rsbZ* is transcribed from a σ^F -dependent promoter (Saujet et al. 2013), the control of *rsbZ* operon expression by σ^F is likely due to a transcription read-through from *CD2686* promoter (Fig. S3). To test whether the control of *rsbZ* operon by σ^F has an impact on O₂ tolerance, we exposed *sigF* mutant to 0.4 % of O₂. We did not observe decrease in O₂ tolerance for *sigF* mutant compared to wild-type strain in our conditions (data not shown)

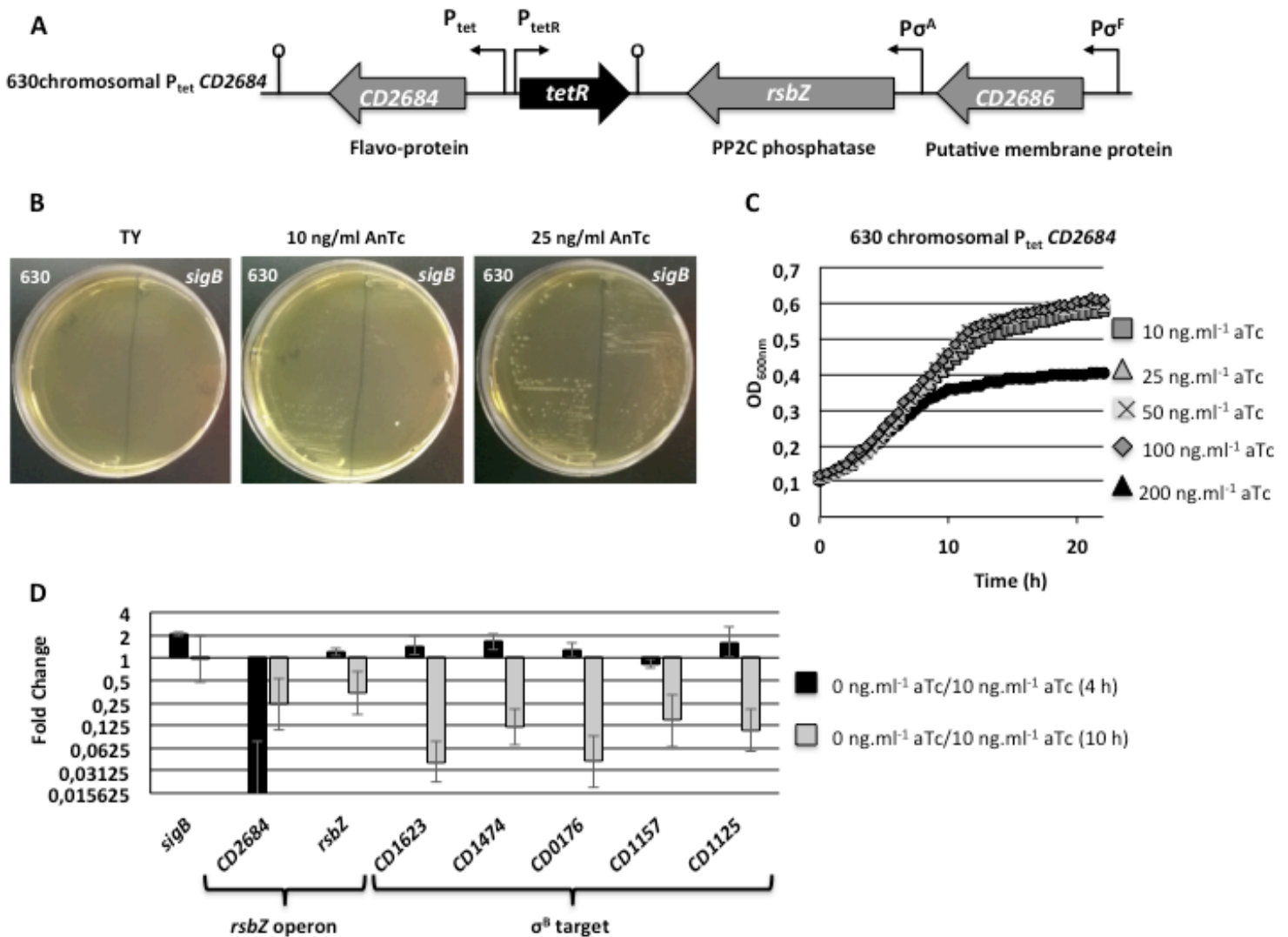


Figure 5: The essential protein CD2684 is involved in σ^B signalling pathway. A) Construction of conditional *CD2684* mutant. The entire P_{tet} element from pRPF185 (Fagan and Fairweather 2011) was inserted into the chromosome between *rsbZ* and *CD2684* allowing *CD2684* expression of under the control of P_{tet} and its induction following aTc addition. **B)** *CD2684* is essential in *C. difficile*. Growth phenotype of 630 Δ *erm* (left part) or *sigB* mutant (right part) carrying a chromosomal P_{tet} *CD2684* copy on TY plates without aTc or with 10 and 25 ng.ml⁻¹ of aTc after 24 h at 37°C. **C)** Growth of 630 Δ *erm* chromosomal P_{tet} *CD2684* in TY with different aTc concentrations. **D)** Effect of *CD2684* expression shut down on the expression of *sigB* operon and σ^B target genes. Fold change of the differential expression of *sigB*, of genes of *rsbZ* operon and of different σ^B target genes encoding proteins involved in oxidative and nitrosative stress management between 630 Δ *erm* chromosomal P_{tet} *CD2684* grown without aTc or with 10 ng.ml⁻¹ of aTc. The graph shows the expression fold change after 4 h (black) or 10 h (light gray) of growth. Pictures are representative of 3 independent experiments and growth results represent the mean of 3 independent experiments. qRT-PCR results are the mean with the standard deviation of 3 independent experiments.

suggesting that the level of *rsbZ* expression from its own promoter is sufficient to trigger σ^B activation.

Study of the role of CD0007 and CD0008

In other firmicutes, genes present in *sigB* operon are often involved in σ^B activation by acting upstream of the PP2C phosphatase (Kang et al. 1996, de Been et al. 2010, Martinez et al. 2010). Since *CD0007* and *CD0008* belong to *sigB* operon (Fig. 1), we studied the possible role of these two proteins in σ^B activation in *C. difficile*. We constructed both $\Delta CD0007$ and $\Delta CD0008$ single mutants as well as $\Delta CD0007$ -*CD0008* double mutant and exposed these strains to low O₂ tension and to NO donor compounds. No difference in growth or in NO or O₂ sensitivity was observed between wild-type strain and the 3 mutants (Figure S4A and B). These results suggest that neither *CD0007* nor *CD0008* plays a positive role in σ^B activation in the tested conditions. In agreement, the expression of the σ^B -target genes was not or only slightly affected by the deletion of *CD0007* and/or *CD0008* at the onset of stationary phase (Fig. S4C). Based on these results, we conclude that *CD0007* and *CD0008* are not involved in σ^B signalling pathway in *C. difficile*.

CD2684 encodes an essential iron-sulphur flavoprotein

Proteins whose genes cluster with the gene(s) encoding the phosphatase(s) involved in RsbV dephosphorylation have also been shown to take part in the control of σ^B activity in other firmicutes (Brody et al. 2001, Chen et al. 2012). Thus, we assumed the iron-sulphur flavoprotein, *CD2684*, could contribute to σ^B activation in *C. difficile*. Despite several attempts, we were unable to inactivate *CD2684* by allele exchange or ClosTron (Heap et al. 2007, Heap et al. 2010) suggesting that *CD2684* could be essential in *C. difficile*. Thus, using the allele exchange strategy, we integrated into the chromosome of both $630\Delta erm$ and *sigB* mutant strains the entire P_{tet} element from pRPF185 upstream of the translational initiation codon of *CD2684* (Fig. 5A). This insertion enabled us to control *CD2684* expression according to the amount of aTc added. Both $630\Delta erm$ and *sigB* mutant strains carrying P_{tet}-*CD2684* were unable to grow on plates in the absence of aTc (Fig. 5B). While 10 ng.ml⁻¹ of aTc enabled growth restoration in the wild-type strain, 25 ng.ml⁻¹ of the inducer was required to observe a full restoration of growth in *sigB* mutant (Fig. 5B). Based on these results, we conclude that *CD2684* is an essential gene in *C. difficile* independently of the presence of σ^B . In liquid culture, $630\Delta erm$ strain harbouring a chromosomal copy of P_{tet} promoter upstream of *CD2684* showed a growth defect in the absence of aTc after 6 h (Fig. 5C). After 10 h, the

final OD_{600nm} value was lower for cultures grown in absence than in presence of the inducer (Fig. 5C). We then monitored by qRT-PCR the level of *CD2684* expression in wild-type strain at two different time points (4 h and 10 h) with or without 10 ng.ml⁻¹ of aTc. As observed in Fig. 5D, the expression level of *CD2684* decreased by a 66-fold factor after 4 h of growth in absence of aTc. These results confirmed a shutdown of *CD2684* expression in absence of aTc even if we failed to detect an impact on growth at 4 h. We assumed that the observed residual growth without aTc resulted from the stability of CD2684 protein produced during the overnight liquid culture done in presence of aTc. In addition, *CD2684* expression decreased only 4-fold after 10 h for cultures grown without aTc (Fig. 5D). This lower ratio for *CD2684* expression after 10 h of growth might be due to aTc degradation. At 10 h, a depletion of the amount of CD2684 protein might be responsible for the growth arrest observed.

CD2684 depletion prevents σ^B activation

To study whether CD2684 is involved in the control of σ^B activity, we compared the expression level of *sigB*, *rsbZ* and some σ^B target genes between the strain harbouring a chromosomal copy of P_{tet} upstream of *CD2684* grown with or without 10 ng.ml⁻¹ of aTc. We extracted RNAs after 4 h and 10 h of growth, *i.e.* when the growth of the strain was not (4 h) or was affected (10 h) by the absence of aTc. At 4 h, apart from *CD2684* expression shutdown, we did not observe any significant difference change in the expression level of the tested genes (Fig. 5D). After 10 h of growth in absence of aTc, *sigB* expression was not affected while *rsbZ* expression slightly decreased with a 3-fold factor. Strikingly, we observed a more pronounced decreased expression of σ^B target genes in absence of aTc (Fig. 5D). Indeed, expression of both *CD1623* and *CD0176* decreased 25-fold while expression of *CD1474*, *CD1157* and *CD1125* decreased 8-, 9- and 7-fold, respectively (Fig. 5D). These results strongly suggest that CD2684 depletion prevents σ^B activation in *C. difficile* at the onset of stationary phase and support the involvement of this protein in σ^B signalling pathway.

Heterogeneity of *sigB* expression and σ^B activity in a population of *C. difficile* cells

To follow *sigB* operon expression at a single cell level within *C. difficile* population during both exponential and stationary phases, we fused the promoter region located upstream of *CD0007* to the SNAP^{Cd} gene (Pereira et al. 2013, Cassona et al. 2016). To monitor σ^B activity, we also fused the promoter region of *CD1474* that harbours a σ^B consensus sequence (Soutourina et al. 2013, Kint et al. 2017) to SNAP^{Cd} gene. Expression of P_{*sigB*}-SNAP^{Cd} and

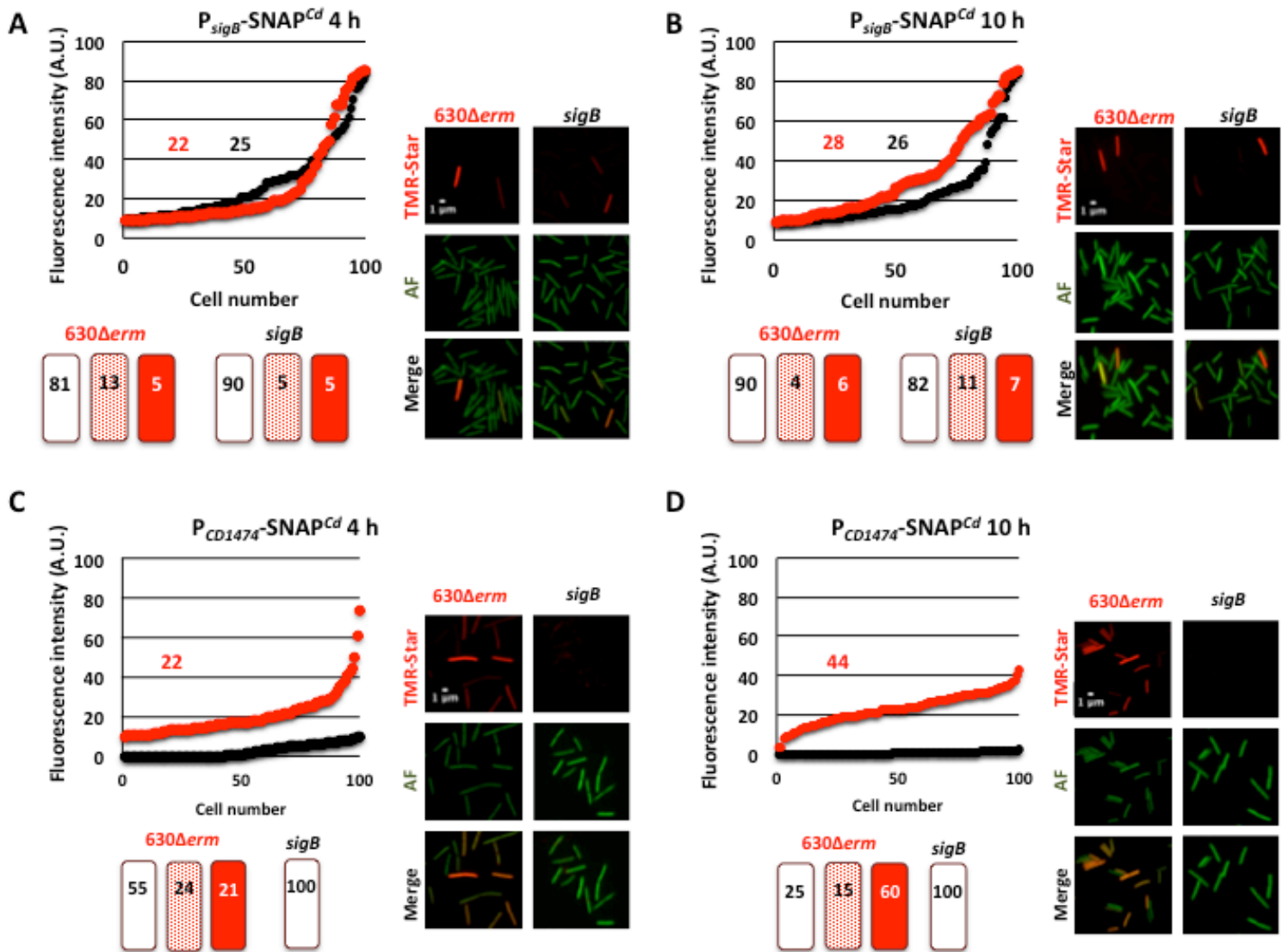


Figure 6: $P_{sigB}\text{-SNAP}^{Cd}$ and $P_{CD1474}\text{-SNAP}^{Cd}$ expression during the growth. Quantitative analysis of fluorescence intensity in arbitrary units (A.U.) in vegetative cells expressing $P_{sigB}\text{-SNAP}^{Cd}$ (**A and B**) or $P_{CD1474}\text{-SNAP}^{Cd}$ (**C and D**) in $630\Delta erm$ strain (red) and $sigB$ mutant (black) after 4 h and 10 h of growth. 100 cells were scored at each time point for each strain and the numbers represent the average of fluorescence intensity. The schemes below the graphs represent the number of cells showing no (pixel values < 9 A.U.), weak (between 9 and 19 A.U.) or strong (>19 A.U.) expression of the reporter fusion. The pictures on the right side represent a field of observed cells from both the $630\Delta erm$ strain and the $sigB$ mutant. AF: auto-fluorescence. These data are representative of 3 independent experiments. Scale bar, 1 μm .

P_{CD1474} -SNAP^{Cd} fusions were monitored in vegetative cells of both $630\Delta erm$ and *sigB* mutant strains by fluorescence microscopy using the SNAP substrate TMR-Star. In agreement with the σ^A promoter found upstream of *CD0007*, P_{sigB} -SNAP^{Cd} expression was detected in both genetic backgrounds without significant difference (Fig. 6A and 6B). Strikingly, P_{CD1474} -SNAP^{Cd} expression was already detected in $630\Delta erm$ background after 4 h of growth (Fig. 6C). Since P_{CD1474} -SNAP^{Cd} expression was completely abolished in *sigB* mutant, these results confirmed that σ^B is strictly required for *CD1474* expression (Kint et al. 2017) and indicated that σ^B is active in *C. difficile* from the exponential growth phase. While P_{sigB} -SNAP^{Cd} expression was rather constant between 4 h and 10 h (Fig. 6A and 6B), P_{CD1474} -SNAP^{Cd} expression was induced at the onset of the stationary phase as observed by the increased average fluorescence intensity (Fig. 6D). This result confirms induction of σ^B activity at the onset of the stationary phase in *C. difficile*, as observed in other firmicutes.

Interestingly, both P_{sigB} -SNAP^{Cd} and P_{CD1474} -SNAP^{Cd} expressions were heterogeneous within *C. difficile*. Indeed, P_{sigB} -SNAP^{Cd} expression was detected in both backgrounds only in a small fraction of vegetative cells at the two tested time points (between 10 and 20 % when weak and strong expression were added) (Fig. 6A and 6B). Similarly, we observed that during the exponential growth phase, 45 % of cells carrying the P_{CD1474} -SNAP^{Cd} fusion in the $630\Delta erm$ background had a weak and strong expression level (Fig. 6C). By contrast, the percentage of cells that displayed P_{CD1474} -SNAP^{Cd} expression increased at the onset of stationary phase to reach 75 % (Fig. 6D). In addition, the cells fraction with a strong signal was 3-fold higher at 10 h compared to 4 h. Altogether, these results indicate that both *sigB* expression and σ^B activity are stochastic within a subpopulation of *C. difficile* vegetative cells, likely leading to a “bet-hedging” mechanism.

Discussion

In this study, we deciphered the σ^B activation signalling pathway in *C. difficile* (Fig. 7). The partner switching mechanism responsible for σ^B activation that involves RsbV and RsbW is functional in *C. difficile*. This post-translational mechanism described in other firmicutes relies on the phosphorylation state of RsbV that is dependent on the activity of PP2C phosphatases. We identified CD2685/RbsZ as the phosphatase of RsbV in *C. difficile*. While the PP2C phosphatase C-terminal domain is highly conserved, the N-terminal sensory domains and the associated signalling pathways vary considerably among species (de Been et al. 2011, Pane-Farre et al. 2017). In *B. subtilis* and *L. monocytogenes*, RsbU phosphatases function with the stressosome, a signal integration and transduction hub multi-protein that is

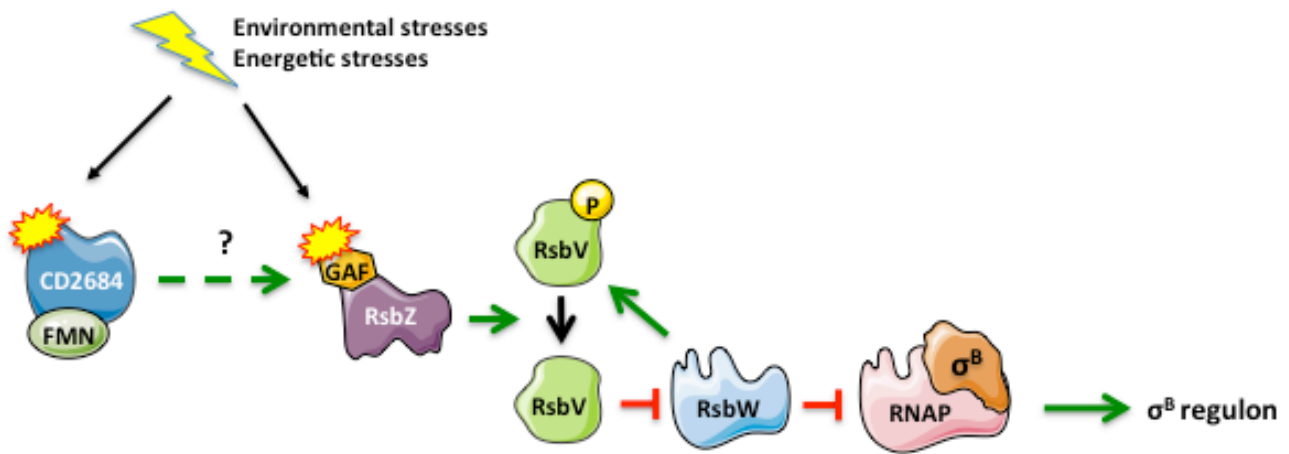


Figure 7: Model of σ^B signalling pathway in *C. difficile*. Established and predictive signalling pathway for the control of σ^B activity in *C. difficile*. Environmental or energetic stresses not yet identified are indicated by the “flash” symbol. Locations of potential stimulus perception are indicated by “explosion” symbols. The CD2684 essential iron-sulphur flavoprotein might be involved in stress detection or be involved in cellular process that results in RsbZ phosphatase activation. This activation leads to RsbV dephosphorylation that enables its interaction with the RsbW anti-sigma factor. This protein-protein interaction results in σ^B release, its association with RNA-polymerase core enzyme and the transcription initiation of its target genes.

absent in *C. difficile*. In *B. subtilis* and *B. cereus*, the input N-terminal domain of the phosphatases, RsbP and RsbY, is a PAS (Per-Arnt-Sim) or a REC (signal receiver domain) domain, respectively (Vijay et al. 2000, de Been et al. 2010). Interestingly, a different GAF domain is associated with the phosphatase domain of CD2685 in *C. difficile* explaining why we choose a specific name for this phosphatase, RsbZ. In *B. cereus*, the RsbK sensor protein that activates RsbY also contains a GAF domain, which is proposed to sense an intracellular unidentified stress (de Been et al. 2010). In addition to RsbZ, we showed that CD2684, encoded by the gene in operon with *rsbZ*, also participates in the control of σ^B activity through an uncharacterised mechanism (Fig. 7). CD2684 is an essential iron-sulphur protein sharing similarities with FMN-dependent oxidoreductases. Since most of the genes positively controlled by σ^B encode proteins involved in oxidative or nitrosative protection (Kint et al. 2017) and because iron-sulphur clusters are among the first targets of oxidizing compounds (Py et al. 2011), we assumed that CD2684 might be a sensor triggering σ^B activation when oxidized. However, we were unable to show any induction of σ^B activity after O₂, H₂O₂ or DEA/NO treatment (N. Kint, unpublished results). In *B. subtilis*, the gene encoding the PP2C phosphatase RsbP belongs to an operon with *rsbQ*, encoding an α/β hydrolase. RsbQ interacts with the PAS domain of RsbP and is required for a proper σ^B activity (Brody et al. 2001). In addition, it has been proposed that an unidentified metabolite produced by RsbQ leads to σ^B activation through the RsbP PAS domain (Nadezhdin et al. 2011). Contrary to RsbP and RsbQ, no interaction was detected between CD2684 and RsbZ using the BACTH system (Table 2). This result suggests that the effect of CD2684 on σ^B activity does not involve a direct interaction with RsbZ but rather acts through either another protein or the synthesis of a metabolite. The essentiality of CD2684 in both the wild-type strain and *sigB* mutant support the idea that this oxidoreductase might be involved in the production of a crucial metabolite for *C. difficile*. As proposed for the PAS domain of RsbP in *B. subtilis* (Nadezhdin et al. 2011), this compound could be detected by the GAF domain located in the N-terminal part of RsbZ modulating its phosphatase activity (Fig. 7). Unfortunately, we did not achieve the production of a stable RsbZ protein lacking the GAF domain preventing us to study the role of this domain in *C. difficile*. Further studies are needed to characterize the function of the essential CD2684 and to elucidate its exact role in σ^B signalling pathway.

While σ^B and its regulatory proteins (RsbV and RsbW) are absent in most of the species of the *Clostridiaceae* family, almost all the species belonging to the Clostridia Cluster XI now reclassified in the *Peptostreptococcaceae* family harbour the 5-gene *sigB* operon organisation found in *C. difficile* (Fig. S5). Strikingly, these species also harbour a genetic

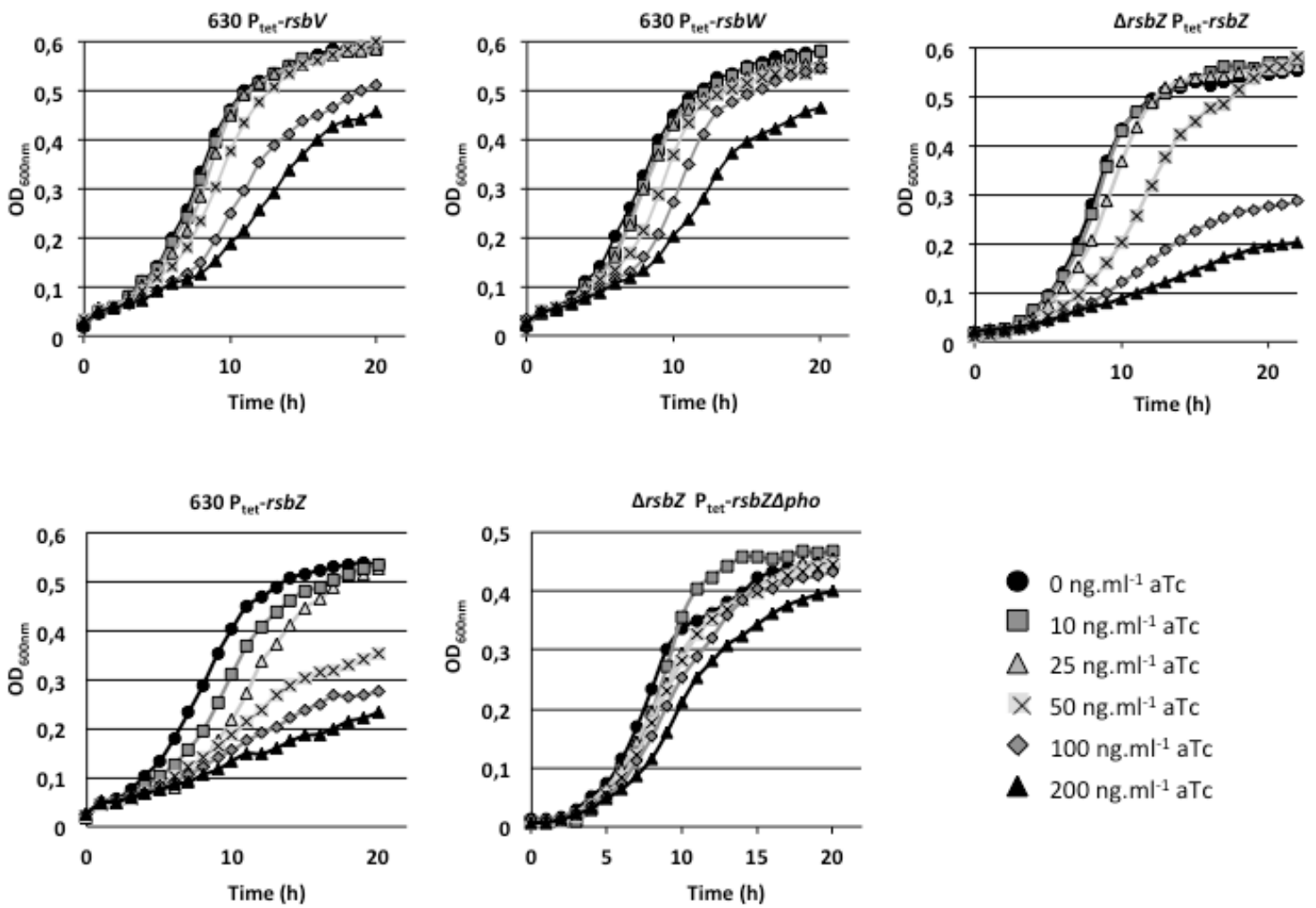


Figure S1: Overexpression of genes involved in the partner switching mechanism. Growth curves of the 630 Δ erm + P_{tet}-rsbV, 630 Δ erm + P_{tet}-rsbW, 630 Δ erm Δ rsbZ + P_{tet}-rsbZ, 630 Δ erm + P_{tet}-rsbZ and 630 Δ erm Δ rsbZ + P_{tet}-rsbZ Δ pho in presence of different concentration of aTc. These data are the mean of 4 independent experiments.

locus encoding both a PP2C phosphatase associated to a GAF domain and an FMN oxidoreductase sharing high level of identity with CD2684 (Fig. S5). Conversely, another class of PP2C phosphatase, which does not contain a GAF domain, is present in species belonging to *Hungateiclostridiaceae*, *Eubacteriaceae* and *Tissierellaceae* families. In addition, the corresponding gene is not genetically associated with a gene encoding a CD2684 homolog (Fig. S5). These differences strongly suggest the existence of two distinct σ^B activation pathways in Clostridiales, one specific to the *Peptrostreptococcaceae* and one specific to other families (Fig. S5). However, the genomic organization as well as the smaller set of proteins involved in the control of σ^B activity could reflect a more ancestral general stress response activation process in Clostridiales than in Bacillales as proposed for the sporulation process (Paredes et al. 2005, Galperin et al. 2012).

A major breakthrough of our study is also the absence of an auto-regulation of *sigB* expression in *C. difficile*. Indeed, in other firmicutes, σ^B activation leads to an increased *sigB* transcription through an internal σ^B -dependent promoter located upstream of *rsbV*, *rsbW* and *sigB* resulting in a positive feedback loop (Kalman et al. 1990, Becker et al. 1998, Senn et al. 2005). Since *sigB* is transcribed only from a σ^A -dependent promoter in *C. difficile*, there is no positive feedback loop increasing *sigB* expression or σ^B activity. In *C. difficile*, strains overexpressing *sigB* or genes such as *rsbV* and *rsbZ* showed a growth defect likely due to an over-activation of σ^B . Interestingly, *B. subtilis* growth is also affected when *sigB* expression or σ^B activity is higher than the physiological level, since $\Delta rsbW$ and $\Delta rsbX$ mutants form pinpoint colonies (Kalman et al. 1990, Benson and Haldenwang 1992, Boylan et al. 1992). In *B. subtilis* and *L. monocytogenes*, *rsbX*, which clusters with *sigB*, encodes a PP2C phosphatase responsible for resetting the stressosome involved in the detection of environmental stresses activating σ^B (Marles-Wright et al. 2008, Marles-Wright and Lewis 2008). This reset restricts the positive feedback loop and enables σ^B signalling pathway to return to its initial state, avoiding toxicity due to an excess of active σ^B (Voelker et al. 1997, Xia et al. 2016). The absence of a positive feedback loop on the transcription of *sigB* operon in *C. difficile* limiting its expression might explain the absence of any RsbX homolog in this bacterium.

Most of the RsbV protein detected in our Phos-Tag experiment was dephosphorylated in wild-type strain after 4 h of growth (Fig. 4D). Even if we cannot rule out the inability of RsbW to phosphorylate all produced RsbV proteins, this result supports the existence of a σ^B activity during the exponential phase. It is worth noting that in *S. aureus*, a significant proportion of RsbV is dephosphorylated during the exponential growth phase, leading to σ^B

activation and to the transcription of some σ^B -targets (Giachino et al. 2001, Senn et al. 2005, Pane-Farre et al. 2009). We provided evidences that σ^B is already active during the exponential phase without external stress exposure in *C. difficile* through the monitoring of P_{CD1474} -SNAP^{Cd} reporter fusion by fluorescence microscopy. However, we observed a difference in the percentage of cells expressing *sigB* and *CD1474* that could result from a weak *sigB* expression level in *C. difficile* that might be under the fluorescence detection threshold. This idea is supported by the high level of *sigB* overexpression observed in the strain harbouring P_{tet} -*sigB* in the presence of only 25 ng.ml⁻¹ of aTc (400-fold, Fig. 2C) while *sigB* was only overexpressed 10-fold when its expression was under the control of its own promoter (Table 1). Heterogeneous σ^B activity has also been observed in *L. monocytogenes* in stressed and non-stressed cells (Utratna et al. 2012, Utratna et al. 2014, Guldimann et al. 2017). This heterogeneity in σ^B activity might lead to a specialised sub-population resulting in “bet-hedging” strategy that would maximize the survival chances in adverse environments (Eldar and Elowitz 2010, Guldimann et al. 2017). Interestingly, the existence of specialised sub-population has been recently reported for toxin expression in *C. difficile*. During stationary phase, *tcdA* expression is indeed governed by σ^{TcdR} through a bistable switch and is also observed in sporulating cells indicating that toxin production and sporulation are not mutually exclusive programs (Ransom et al. 2018a). Conversely, sub-populations triggering stress response and sporulation might be different since σ^B represses sporulation while it does not control toxin production (Kint et al, 2017). We can assume that following spore germination, a rapid σ^B activation in a sub-population of vegetative cells during exponential growth phase might prepare *C. difficile* to face the stressful conditions encountered in the gut. Since the colonization fitness of the *sigB* mutant is highly impaired in dixenic mice (Kint et al. 2017), it is tempting to speculate that this preadapted sub-population might be important for an efficient gut colonisation by *C. difficile*.

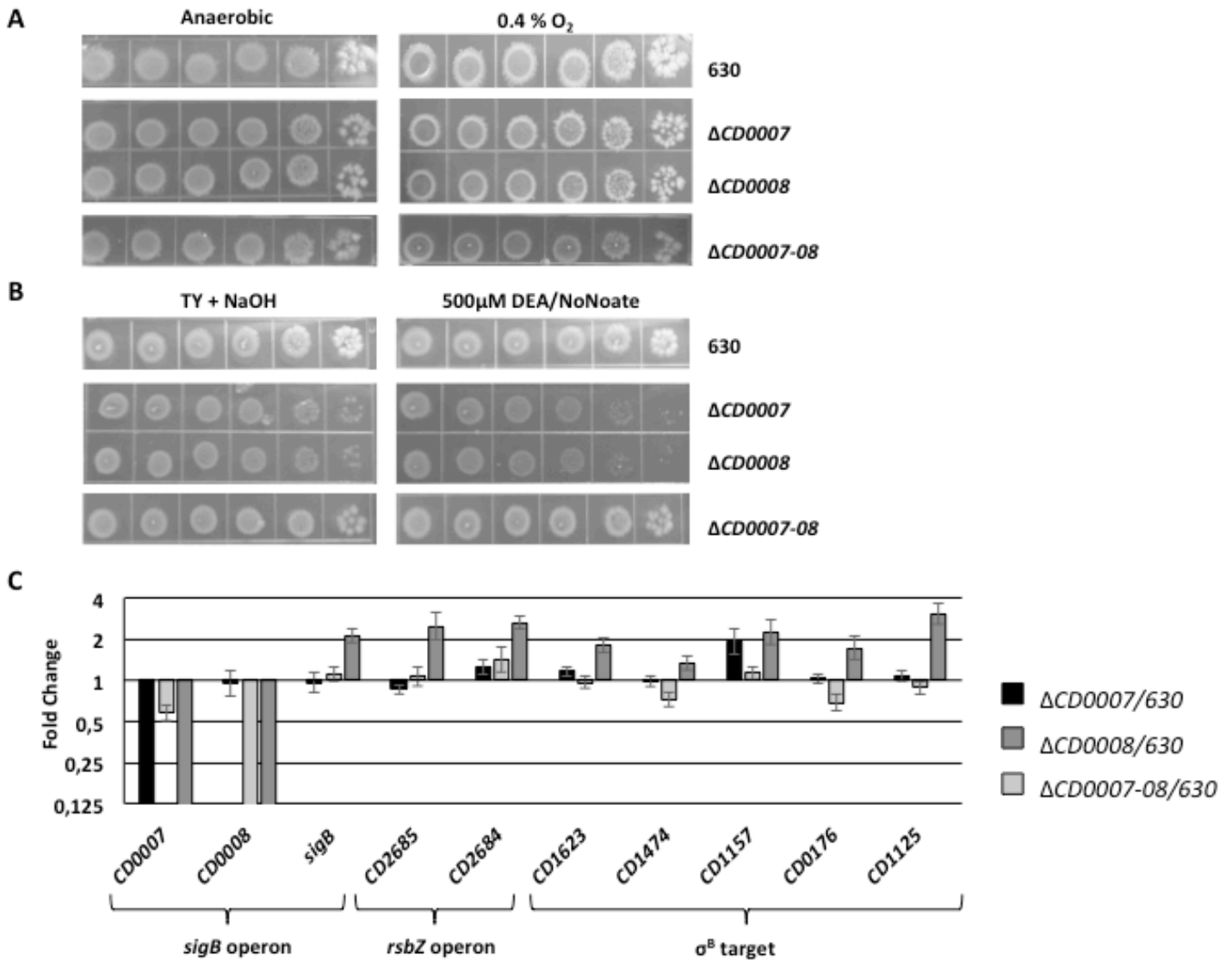


Figure S4: CD0007 and CD0008 are not involved in σ^B signalling pathway. Low O₂ tolerance (**A**) and NO stress assays (**B**). Serial dilutions of the different strains were spotted on TY plates. Plates were incubated 64 h in presence of 0.4 % of O₂ for low O₂ tolerance assay (A) or 24 h at 37°C for NO tests (B). Growth controls were performed with plates incubated in anaerobiosis atmosphere or supplemented with NaOH for low O₂ tolerance assays and NO tests, respectively. **C**) Effect of *CD0007*, *CD0008* or *CD0007-08* deletion on the expression of *sigB* operon genes and σ^B target genes at the onset of the stationary phase. Fold change of the differential expression of genes belonging to *sigB* operon, to *rsbZ* operon and of σ^B target genes involved in oxidative and nitrosative stress management in 630 Δ *erm* Δ *CD0007* (black), 630 Δ *erm* Δ *CD0008* (light gray) and 630 Δ *erm* Δ *CD0007-08* (dark gray) compared to 630 Δ *erm*. Pictures are representative results of 3 independent experiments and qRT-PCR results are the mean with the standard deviation of 3 independent experiments.

Experimental procedures

Bacterial strains and growth conditions

C. difficile strains and plasmids used in this study are presented in Table S1. *C. difficile* strains were grown anaerobically (5% H₂, 5% CO₂, 90% N₂) in TY (Bacto tryptone 30 g.l⁻¹, yeast extract 20 g.l⁻¹, pH 7.4) or in Brain Heart Infusion (BHI; Difco). For solid media, agar was added to a final concentration of 17 g.l⁻¹. When necessary, cefoxitin (Cfx, 25 µg.ml⁻¹), thiamphenicol (Tm, 15 µg.ml⁻¹) or erythromycin (Erm, 2.5 µg.ml⁻¹) were added to *C. difficile* cultures. *E. coli* strains were grown in LB broth. When indicated, ampicillin (100 µg.ml⁻¹), chloramphenicol (15 µg.ml⁻¹) or kanamycin (50 µg.ml⁻¹) was added to the culture medium. The non-antibiotic analogue aTc was used for the induction of expression of the *sigB*, *rsbV*, *rsbW* or *rsbZ* (*CD2685*) genes expressed under the control of the P_{tet} promoter that were cloned into pDIA6103 (Fagan and Fairweather 2011). Growth of *C. difficile* strains in the presence of different concentration of aTc was followed using a GloMax® Explorer plate-reader (Promega). Overnight cultures were diluted at an OD_{600nm} of 0.05 in TY medium supplemented with 0, 10, 25, 50, 100 or 200 ng.ml⁻¹ of aTc in 96 wells plates. The plates were sealed with a gas-impermeable adhesive film (DY992 R&D systems) and OD_{600nm} was monitored every 30 min at 37°C.

Construction of *C. difficile* strains and plasmids

All routine plasmid constructions were carried out using standard procedure. All primers used in this study are listed in Table S2. $\Delta rsbV$, $\Delta rsbZ$, $\Delta CD0007$, $\Delta CD0008$ and $\Delta CD0007-0008$ knock out mutant generated in this study were created using the *codA*-mediated allele exchange method (Cartman et al. 2012, Peltier et al. 2015). Briefly, for all these genes, 1.5 kb fragments located up- and downstream of the gene to be deleted were PCR amplified from 630 Δerm genomic DNA using primers NK46/NK47 and NK48/NK49 for $\Delta rsbV$, NK21/NK22 and NK23/NK24 for $\Delta rsbZ$, NK38/NK39 and NK40/NK41 for $\Delta CD0007$, NK42/NK43 and NK44/NK45 for $\Delta CD0008$ and NK38/39 and NK42/NK43 for $\Delta CD0007-0008$ (Table S2). To construct *CD2684* conditional mutant, two fragments of 1.5 kb corresponding to the end part of *rsbZ* and the entire *CD2684* gene were amplified with NK108/NK229 and N228/NK109, respectively. A P_{tet} and *tetR* gene fragment overlapping both the end of *rsbZ* in 5' extremity and the beginning of *CD2684* in 3' extremity was amplified from pRPF185 plasmid with NK230 and NK231 in order to insert it right after the stop codon of *rsbZ* and before the initiation codon (TTG) of *CD2684*. Purified PCR fragments

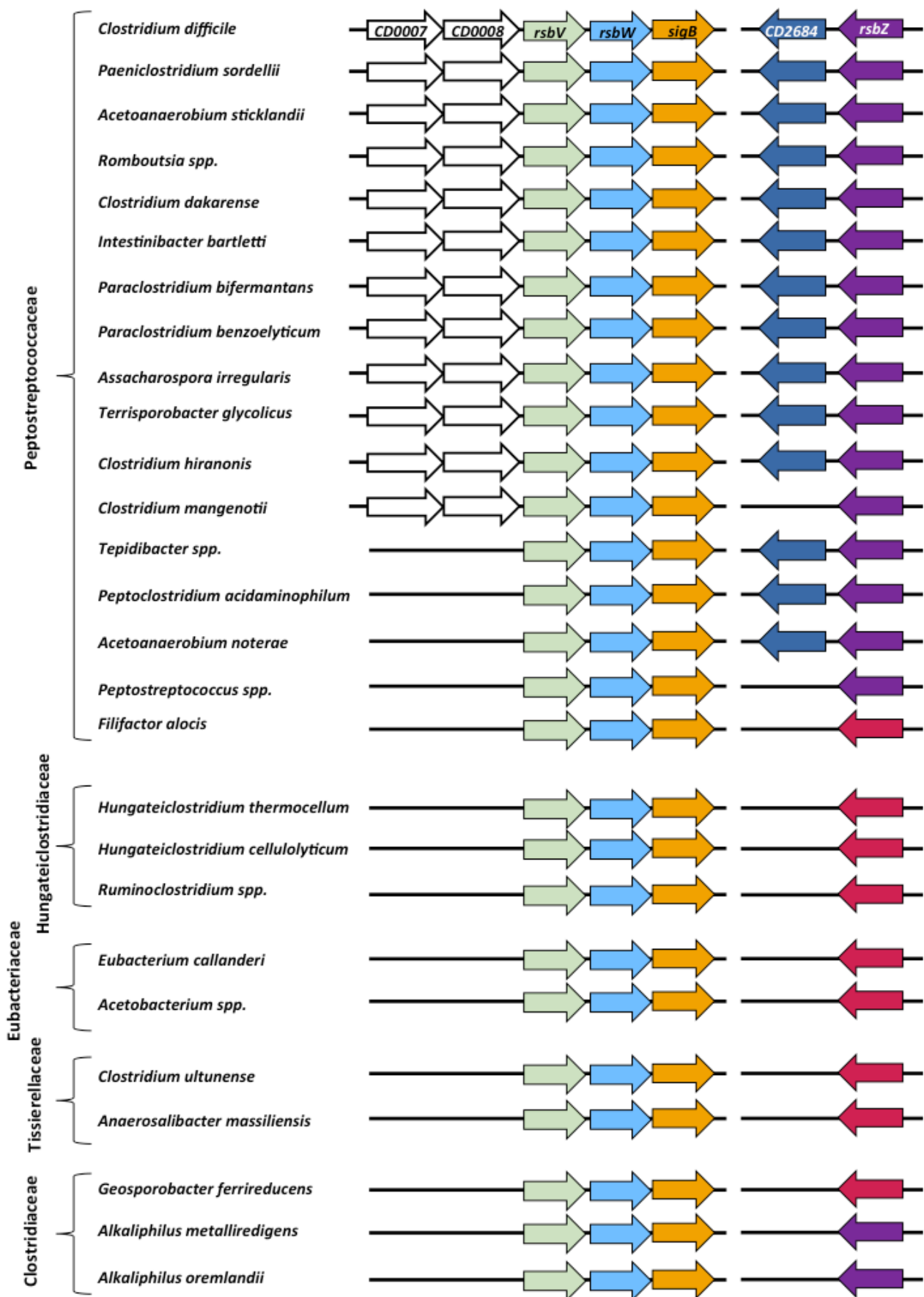


Figure S5: Conservation of the *sigB* and the *CD2684-rsbZ* locus in Clostridiales.

Schematic representation of the *sigB* and *rsbZ* locus organization in Clostridiales. Arrows represent open reading frames whose products have homology to *C. difficile* 630Δ*erm* CD0007, CD0008, RsbV, RsbW, σ^B, CD2684 and RsbZ according to blastP search. Colours represent putative function of the predicted proteins: unknown (white), anti-anti-sigma factor (green), anti-sigma factor (white blue), sigma factor (orange), iron-sulphur flavoprotein (dark blue), PP2C phosphatase with GAF domain (purple) and PP2C phosphatase with PAS domain (red).

were then directly introduced into the pMTLSC7315 plasmid using the Gibson Assembly® Master Mix (Biolabs). The sequences of the resulting plasmids were verified by sequencing. Plasmids introduced in HB101/RP4 *E. coli* strain were transferred by conjugation into *C. difficile* 630 Δ *erm* strain. Transconjugants were selected on BHI plates supplemented with Tm and *C. difficile* selective supplement (SR0096, Oxoid). Isolation of faster growing single-crossover integrants was performed by serially restreaking on BHI plates supplemented with Cfx and Tm and confirmed by PCR. Single-crossover integrants were then restreaked on *C. difficile* minimal medium (CDMM) plates supplemented with fluorocytosine (50 $\mu\text{g}\cdot\text{ml}^{-1}$) allowing the isolation of double crossover events (Cartman et al. 2012). For *CD2684* conditional mutant, aTc (100 $\text{ng}\cdot\text{ml}^{-1}$) was added to the CDMM plates to maintain *CD2684* expression. To confirm the loss of the plasmid, fluorocytosine resistant clones were restreaked on BHI plates supplemented with Cfx and Tm supplemented with aTc for *CD2684* conditional mutant. The Tm sensitive clones were checked by PCR for the presence of the expected deletion or for the insertion of P_{tet} element for *CD2684* conditional mutant.

For construction of plasmids overexpressing the different genes, fragments were PCR amplified using DNA from the 630 Δ *erm* strain. For each construction, a PCR fragment containing the ribosome binding site as well as the gene was cloned into pDIA6103 between the *Stu*I and *Bam*HI sites. For the construction of the strain expressing *rsbZ* Δ *pho*, we PCR amplified *rsbZ* gene lacking the part corresponding to the amino acids 336 to 587 containing the PP2C phosphatase domain. In the resulting plasmids, the genes (*sigB*, *rsbW*, *rsbV*, *rsbZ* or *rsbZ* Δ *pho*) were expressed under the control of P_{tet} promoter. To construct the translational fusions coding for σ^{B} -, *RsbV*- and *RsbZ* Δ *pho*-HA-tagged proteins, plasmids pDIA6325, pDIA6637 and pDIA6579, carrying *sigB*, *rsbZ* or *rsbZ* Δ *pho* were inverted PCR amplified using primers NK188/NK189, NK192/193 and NK194/195, respectively. PCR fragments were then digested by *Dpn*I to remove the plasmid templates, phosphorylated by T4 Polynucleotide Kinase and ligated by T4 Ligase to recircularize the plasmid. The resulting plasmids were verified by sequencing, introduced into HB101/RP4 *E. coli* strain and then transferred into *C. difficile* strains by conjugation. Transconjugants were selected on BHI plates supplemented with Tm and *C. difficile* selective supplement.

Cell lysis, Phos-Tag™ and Western-immunoblot

Whole cell lysates were prepared as previously described (Fagan and Fairweather 2011). Briefly, cultures of *C. difficile* were harvested by centrifugation at 5000 r.p.m for 10 min at 4°C and the pellets were frozen at -20°C. Bacteria were thawed and resuspended to an

OD_{600nm} of 40 in PBS containing 0.12 µg.ml⁻¹ of DNase I. For analysis by SDS-PAGE, an equal volume of 2X SDS sample buffer was added to protein samples (Laemmli 1970). SDS-PAGE and Western immunoblotting were carried out using standard method using anti-HA antibody. Phos-tag™ experiments followed by western-immunoblot were performed according to the manufacturer's instruction. Briefly, after cell lysis, cell extracts were run on a 12 % SDS-PAGE supplemented with 50 µM of Phos-Tag™ acrylamide (AAL-107M, Wako) and 100 µM of MnCl₂. After gel running, the gel was soaked with agitation three times in fresh transfer buffer supplemented with 10 mM of EDTA for 10 min. Gel was then soaked 10 min in fresh transfer buffer without EDTA before gel transfer to the PVDF membrane. Western immunoblotting using anti-HA antibody was then carried out using standard method.

Spotted dilution assays

O₂ tolerance assays and NO stress assays were performed as previously described (Kint et al. 2017). Five microliters of serial dilutions (from 10⁰ to 10⁻⁵) of *C. difficile* strains grown for 8 h in the TY medium were spotted on TY plates supplemented i) with 25 ng.ml⁻¹ of aTc and 0.05% of taurocholate and incubated in the presence of 0.4 % O₂ tension; or ii) with 25 ng.ml⁻¹ aTc containing 250 or 500 µM of DEA/NO. The last dilution allowing growth was recorded after incubation at 37°C for 64 h for the O₂ tests and for 24 h for the NO stress tests.

Transcriptional SNAP^{Cd} fusions

To construct SNAP fusions, we used pFT47, a pMTL84121 plasmid derivative containing a synthetic SNAP^{Cd} sequence (Pereira et al. 2013, Cassona et al. 2016). To construct *CD1474*-SNAP^{Cd} transcriptional fusion, a 200 bp PCR product containing the promoter region of this gene (position -206 to +19 from the TSS) was amplified using genomic DNA and primer pairs CF19/CF20 and inserted between the EcoRI and XhoI sites of pFT47 to obtain PDIA6457. The insert sequence was checked by sequencing. The plasmid was transferred by conjugation into *C. difficile* 630Δ*erm* strain and *sigB*, Δ*rsbV* or Δ*rsbZ* mutant giving CDIP661, CDIP668, CDIP728 and CDIP953 strains, respectively (Table S1). To construct *sigB*-SNAP^{Cd} transcriptional fusion, plasmid pDIA6325 used for complementation containing both the sequence located upstream of *CD0007* (position -120 to +50 from the TSS) and *sigB* gene was digested by XhoI and StuI to remove the *sigB* gene and keep the σ^A dependent promoter located upstream *CD0007*. SNAP^{Cd} gene was PCR amplified using pFT47 DNA and primers pairs NK155/NK156. The DNA fragment was digested by DpnI to remove pFT47 plasmid trace and inserted between the XhoI and StuI sites of pDIA6325 to obtain

pDIA6589. The resulting plasmid was then transferred into 630 Δ *erm* strain and *sigB* mutant, giving CDIP843 and CDIP845 strains, respectively.

Fluorescence microscopy and image analysis

Overnight culture of CDIP843, CDIP845, CDIP661 and CDIP668 strains were diluted at an OD_{600nm} of 0.05 into 5 ml of BHI. For SNAP labelling, 200 μ l of culture were mixed with 250 nM SNAP-Cell TMR-Star (New England Biolabs) and incubated 30 min at 37°C in the dark at each time point (4, 10, 24 and 48 h) (Pereira et al. 2013, Cassona et al. 2016). After labelling, cells were collected by centrifugation (4000 g for 3 min) and washed 3 times with 1 ml of PBS. For fluorescence microscopy, cells were mounted on 1.7 % agarose coated glass slides to keep the immobilized cells, and to obtain sharper images (Glaser et al. 1997). The images were taken with exposure times of 200 ms for autofluorescence and 500 ms for SNAP. Cells were observed on a Nikon Eclipse TI-E microscope 60x Objective and captured with a CoolSNAP HQ2 Camera. For quantification of the SNAP-TMR Star signal resulting from transcriptional fusions, the pixel intensity was measured, and corrected by subtracting the average pixel intensity of the background. Images were analysed using ImajeJ.

Bacterial adenylate cyclase two hybrids system (BACTH) and β -galactosidase assays

Protein-protein interactions were analysed by the BACTH system (Euromedex). All the procedures for plasmids constructions and *E. coli* co-transformations were performed according to the manufacturer's instruction. Briefly, this system exploits the catalytic domain of the adenylate cyclase from *B. pertussis* (CyA) that is composed of two different fragments T25 and T18. When T25 and T18 are separated, CyA is not active. However, when these fragments are fused with interacting proteins, the heterodimerisation of these hybrid proteins allows a functional complementation and so production of cAMP leading to *lacZ* gene expression. The open reading frames of *rsbV*, *rsbW*, *sigB* or *rsbZ* were cloned into plasmids allowing fusions with T18 or T25 either in C-terminal or N-terminal position. After verification by sequencing, the different association of T18 and T25 fusion plasmids were co-transformed in *E. coli* strain BTH101 (Table S1). Co-transformation with the T25 and T18 expressing plasmids served as a control for the basal β -galactosidase activity. The β -galactosidase activity was measured after an overnight culture of co-transformants in LB medium in the presence of 0.5 mM of isopropyl- β -D-thiogalacto-pyranoside. 100 μ l of overnight culture was mixed with 400 μ l of M63 medium and 500 μ l of Z buffer (Na₂HPO₄

0.06 M, NaH₂PO₄ 0.04 M, KCl 0.01M, MgSO₄ 0.001 M, DTT 0.001 M and SDS 0.0037 %). After addition of 20 µl of chloroform, the tubes were mixed exactly 10 s. Tubes were pre-incubated 5 min at 28°C and 200 µl of pre-heated ONPG (4 mg.ml⁻¹) was added. When the yellow coloration appeared, 500 µl of Na₂CO₃ (1 M) was added to the tube to stop the reaction. After elimination of cell fragments, the OD_{420nm} was measured. β-galactosidase activity was quantified as Miller unit [1000*(OD_{420nm}/(time of incubation (min))*volume of extract (ml)*OD_{600nm} of the culture)].

RNA extraction, quantitative RT-PCR analysis and 5' RACE experiment

To test the expression of σ^B target genes, overnight cultures of the different strains were diluted to an OD_{600nm} of 0.05 in 10 ml of TY medium supplemented with 25 ng.ml⁻¹ aTc when needed. Cells were harvested after 10 h of growth. 630Δ*erm* strain cells were harvested after 4, 10, 16, 20 or 24 h of growth. To test the effect of *sigB* overexpression, CDIP219 and CDIP393 (Table S1) grown in 10 ml of TY medium without aTc or with 25 ng.ml⁻¹ or 200 ng.ml⁻¹ of aTc were harvested after 4 h of growth. To study the effect of CD2684 depletion, overnight culture of *CD2684* conditional mutant was made in presence of 10 ng.ml⁻¹ of aTc to allow a growth. After dilution to an OD_{600nm} of 0.05 in 10 ml of TY medium without or with 10 ng.ml⁻¹ of aTc, cells were harvested after 4 or 10 h of growth. RNA extraction, cDNAs synthesis and real-time quantitative PCR were performed as previously described (Saujet et al. 2011, Soutourina et al. 2013). The quantity of cDNAs of a gene was normalised to the quantity of cDNAs of the *pgi* and *ccpA* genes. The relative change in gene expression was recorded as the ratio of normalised target concentrations (the threshold cycle [ΔΔC_T] method) (Livak and Schmittgen 2001). 5' RACE experiment was realised with the 5' RACE system for Rapid Amplification of cDNA Ends kit (Invitrogen) according to the manufacturer's instructions. Briefly, a first strand cDNA was synthesised from total RNA extracted after 10 h of growth in TY using Superscript II and primer NK134 annealing in *CD2684*. A C-tail was then added to the 3' end of the cDNA using TdT and dCTP. The resulting fragment was amplified by the Abridged Anchor Primer and NK31 annealing in *rsbZ*. The resulting fragment was then sequenced by IMV830 annealing in *rsbZ* to define the TSS.

Acknowledgments

We are thankful to Johann Peltier and Gouzel Karimova for helpful discussions, to Jean-Marc Ghigo for his help with oxygen assays, to Julian Garneau for his help with the bioinformatic analysis of *sigB* and *rsbZ* operon and to Claire Morvan for a critical reading of

the manuscript. This work was funded by the Institut Pasteur and the University Paris 7. NK is a Post-doctoral fellow from University Paris 7. Research in this work and CAF fellowship was funded by ITN Marie Curie, Clospore (H2020-MSCA-ITN-2014 64206).

Supplementary tables

Table S1: Strains and plasmids used in this study.

Strains	Genotypes	Origins
<i>E. coli</i>		
10-beta	F ⁻ <i>mcrA</i> D(<i>mrr-hsdRMS-mcrBC</i>) f80 <i>lacZ</i> DM15 <i>DlacX74 deoR</i> , <i>recA1 araD139 D(ara-leu)7697 galK rpsL(StrR) endA1 nupG</i> ,	NEB®
HB101 (RP4)	<i>supE44 aa14 galK2 lacY1 Δ(gpt-proA) 62 rpsL20 (Str^R)xyl-5 mtl-1 recA13 Δ(mcrC-mrr) hsdS_B(r_Bm_B⁻) RP4 (Tra⁺ IncP Ap^R Km^R Tc^R)</i>	Laboratory stock
BTH101	F ⁻ <i>cya-99 araD139 galE15 galK16 rpsL1 (Str^r) hsdR2 mcrA1 mcrB1</i>	Euromedex®
ECO497	BTH101 + pKNT25- <i>rsbV</i> + pUT18- <i>rsbW</i>	
ECO498	BTH101 + pKNT25- <i>rsbV</i> + pUT18- <i>rsbZ</i>	
ECO499	BTH101 + pKNT25- <i>sigB</i> + pUT18- <i>rsbW</i>	
ECO500	BTH101 + pKNT25- <i>sigB</i> + pUT18- <i>rsbZ</i>	
ECO501	BTH101 + pKNT25 + pUT18	
ECO534	BTH101 + pKT25 + pUT18C	
ECO536	BTH101 + pKT25- <i>sigB</i> + pUT18C- <i>rsbZ</i>	
ECO538	BTH101 + pKT25- <i>rsbV</i> + pUT18C- <i>rsbZ</i>	
ECO540	BTH101 + pKT25- <i>sigB</i> + pUT18C- <i>rsbW</i>	
ECO542	BTH101 + pKT25- <i>rsbV</i> + pUT18C- <i>rsbW</i>	
ECO775	BTH101 + pKNT25- <i>rsbZ</i> + pUT18C- <i>rsbV</i>	
ECO776	BTH101 + pKNT25- <i>rsbZ</i> + pUT18C- <i>sigB</i>	
ECO777	BTH101 + pKNT25- <i>rsbZ</i> + pUT18- <i>rsbV</i>	
ECO778	BTH101 + pKNT25- <i>rsbZ</i> + pUT18- <i>sigB</i>	
ECO779	BTH101 + pKT25- <i>rsbZ</i> + pUT18C- <i>rsbV</i>	
ECO780	BTH101 + pKT25- <i>rsbZ</i> + pUT18C- <i>sigB</i>	
ECO781	BTH101 + pKT25- <i>rsbZ</i> + pUT18- <i>rsbV</i>	
ECO782	BTH101 + pKT25- <i>rsbZ</i> + pUT18- <i>sigB</i>	
ECO783	BTH101 + pKNT25- <i>rsbW</i> + pUT18C- <i>rsbV</i>	
ECO784	BTH101 + pKNT25- <i>rsbW</i> + pUT18C- <i>sigB</i>	
ECO785	BTH101 + pKNT25- <i>rsbW</i> + pUT18- <i>rsbV</i>	
ECO786	BTH101 + pKNT25- <i>rsbW</i> + pUT18- <i>sigB</i>	
ECO787	BTH101 + pKT25- <i>rsbW</i> + pUT18C- <i>rsbV</i>	
ECO788	BTH101 + pKT25- <i>rsbW</i> + pUT18C- <i>sigB</i>	
ECO789	BTH101 + pKT25- <i>rsbW</i> + pUT18- <i>rsbV</i>	
ECO790	BTH101 + pKT25- <i>rsbW</i> + pUT18- <i>sigB</i>	
ECO810	BTH101 + pKNT25 + pUT18C	
ECO811	BTH101 + pKT25 + pUT18	
ECO812	BTH101 + pKNT25- <i>rsbW</i> + pUT18- <i>rsbZ</i>	
ECO813	BTH101 + pKNT25- <i>rsbV</i> + pUT18C- <i>rsbW</i>	
ECO814	BTH101 + pKNT25- <i>rsbV</i> + pUT18C- <i>rsbZ</i>	
ECO815	BTH101 + pKNT25- <i>sigB</i> + pUT18C- <i>rsbW</i>	
ECO816	BTH101 + pKNT25- <i>sigB</i> + pUT18C- <i>rsbZ</i>	
ECO817	BTH101 + pKT25- <i>rsbV</i> + pUT18- <i>rsbW</i>	
ECO818	BTH101 + pKT25- <i>rsbV</i> + pUT18- <i>rsbZ</i>	
ECO819	BTH101 + pKT25- <i>sigB</i> + pUT18- <i>rsbW</i>	
ECO820	BTH101 + pKT25- <i>sigB</i> + pUT18- <i>rsbZ</i>	
EC1091	BTH101 + pKT25-CD2684 + pUT18-CD2685	
EC1092	BTH101 + pKT25-CD2684 + pUT18C-CD2685	
EC1093	BTH101 + pKNT25-CD2684 + pUT18-CD2685	
EC1094	BTH101 + pKNT25-CD2684 + pUT18C-CD2685	

EC1095	BTH101 + pUT18-CD2684 + pKT25-CD2685	
EC1096	BTH101 + pUT18-CD2684 + pKNT25-CD2685	
EC1097	BTH101 + pUT18C-CD2684 + pKT25-CD2685	
EC1098	BTH101 + pUT18C-CD2684 + pKNT25-CD2685	
ECO1114	BTH101 + pUT18-RsbV + pKT25-SigB	
ECO1115	BTH101 + pUT18-RsbV + pKNT25-SigB	
ECO1116	BTH101 + pUT18C-RsbV + pKT25-SigB	
ECO1117	BTH101 + pUT18C-RsbV + pKNT25-SigB	
ECO1118	BTH101 + pUT18-SigB + pKT25-RsbV	
ECO1119	BTH101 + pUT18-SigB + pKNT25-RsbV	
ECO1120	BTH101 + pUT18C-SigB + pKT25-RsbV	
ECO1121	BTH101 + pUT18C-SigB + pKNT25-RsbV	
<i>C. difficile</i>		
630 Δ erm		Laboratory stock
CDIP219	630 Δ erm + pDIA6103 Δ gusA	Soutourina et al, 2013
CDIP546	630 Δ erm sigB(CD0011)::erm	Kint et al, 2017
CDIP547	630 Δ erm sigB ::erm + pDIA6103-P _{sigB} -sigB	Kint et al, 2017
CDIP393	630 Δ erm + pDIA6103-P _{tet} -sigB	pDIA6306 \rightarrow 630 Δ erm
CDIP595	630 Δ erm + pDIA6103-P _{tet} -CD0007	pDIA6385 \rightarrow 630 Δ erm
CDIP596	630 Δ erm + pDIA6103-P _{tet} -CD0008	pDIA6386 \rightarrow 630 Δ erm
CDIP597	630 Δ erm + pDIA6103-P _{tet} -CD2684	pDIA6387 \rightarrow 630 Δ erm
CDIP1015	630 Δ erm + pDIA6103-P _{tet} -rsbV	pDIA6637 \rightarrow 630 Δ erm
CDIP613	630 Δ erm Δ rsbZ	pDIA6306 \rightarrow 630 Δ erm
CDIP638	630 Δ erm Δ rsbZ + pDIA6103-P _{tet} -rsbZ	pDIA6400 \rightarrow CDIP613
CDIP642	630 Δ erm Δ rsbZ + pDIA6103 Δ gusA	pDIA6103 \rightarrow CDIP613
CDIP662	630 Δ erm Δ CD0007	pDIA6430 \rightarrow 630 Δ erm
CDIP664	630 Δ erm Δ CD0008	pDIA6431 \rightarrow 630 Δ erm
CDIP687	630 Δ erm Δ CD0007 + pDIA6103	pDIA6103 \rightarrow CDIP662
CDIP688	630 Δ erm Δ CD0007 + pDIA6103-P _{tet} -CD0007	pDIA6385 \rightarrow CDIP662
CDIP689	630 Δ erm Δ CD0008 + pDIA6103	pDIA6103 \rightarrow CDIP664
CDIP690	630 Δ erm Δ CD0008 + pDIA6103-P _{tet} -CD0008	pDIA6386 \rightarrow CDIP664
CDIP698	630 Δ erm Δ rsbZ + pDIA6103-rsbZ Δ pho	pDIA6571 \rightarrow CDIP613
CDIP712	630 Δ erm Δ CD0007-CD0008	pDIA6581 \rightarrow 630 Δ erm
CDIP713	630 Δ erm Δ rsbV (CD0009)	pDIA6580 \rightarrow 630 Δ erm
CDIP843	630 Δ erm + pFT47-P _{sigB} -SNAP ^{Cd}	pDIA6589 \rightarrow 630 Δ erm
CDIP845	630 Δ erm sigB::erm + pFT47-P _{sigB} -SNAP ^{Cd}	pDIA6589 \rightarrow CDIP546
CDIP918	630 Δ erm + P _{sigB} -sigB HA C-ter	pDIA6591 \rightarrow 630 Δ erm
CDIP922	630 Δ erm sigB ::erm + pDIA6103-P _{sigB} -sigB HA C-ter	pDIA6591 \rightarrow CDIP546
CDIP942	630 Δ erm Δ rsbZ + pDIA6103-P _{tet} -rsbZ Δ pho HA C-ter	pDIA6594 \rightarrow CDIP613
CDIP978	630 Δ erm + pDIA6103-P _{tet} -rsbZ	pDIA6410 \rightarrow 630 Δ erm
CDIP982	630 Δ erm + pDIA6103-P _{tet} -rsbZ Δ pho	pDIA6579 \rightarrow 630 Δ erm
CDIP1004	630 Δ erm + pDIA6103-P _{tet} -rsbW (CD0010)	pDIA6638 \rightarrow 630 Δ erm
CDIP1005	630 Δ erm Δ rsbV + pDIA6103-P _{tet} -rsbV	pDIA6306 \rightarrow CDIP713
CDIP1006	630 Δ erm Δ rsbV + pDIA6103	pDIA6103 \rightarrow CDIP713
CDIP1008	630 Δ erm sigB ::erm + pDIA6103-P _{tet} -CD0007	pDIA6385 \rightarrow CDIP546
CDIP1012	630 Δ erm Δ rsbZ + pDIA6103-P _{tet} -sigB	pDIA6306 \rightarrow CDIP613
CDIP1140	630 Δ erm Δ rsbV + pDIA6103-P _{sigB} -sigB HA C-ter	pDIA6591 \rightarrow CDIP713
CDIP1141	630 Δ erm Δ rsbZ + pDIA6103-P _{sigB} -sigB HA C-ter	pDIA6591 \rightarrow CDIP613
CDIP1116	630 Δ erm + pDIA6103-P _{tet} -rsbV HA C-ter	pDIA6639 \rightarrow 630 Δ erm

CDIP1117	630 Δ erm <i>sigB::erm</i> + pDIA6103-P _{tet} - <i>rsbV</i> HA C-ter	pDIA6639 → CDIP546
CDIP1118	630 Δ erm Δ <i>rsbV</i> + pDIA6103-P _{tet} - <i>rsbV</i> HA C-ter	pDIA6639 → CDIP713
CDIP1119	630 Δ erm Δ <i>rsbZ</i> + pDIA6103-P _{tet} - <i>rsbV</i> HA C-ter	pDIA6639 → CDIP613
CDIP661	630 Δ erm + pFT47- <i>CDI474</i>	pDIA6457 → 630 Δ erm
CDIP668	630 Δ erm <i>sigB::erm</i> + pFT47- P _{CD1474} -SNAP ^{Cd}	pDIA6457 → CDIP546
CDIP1235	630 Δ erm P _{tet} - <i>CD2684</i> chromosomic	pDIA6813 → 630 Δ erm
CDIP1248	630 Δ erm <i>sigB::erm</i> P _{tet} - <i>CD2684</i> chromosomic	pDIA6813 → CDIP546
Plasmids		Origins
pDIA6103	pRPF185 Δ <i>gusA</i> , Cm ^R -Tm ^R	Soutourina et al, 2013
pFT47	Cm ^R -Tm ^R	Pereira et al, 2013
pMTL-SC7315	Cm ^R -Tm ^R	Cartman et al, 2012
pDIA6306	pDIA6103-P _{tet} - <i>sigB</i> , Cm ^R -Tm ^R	Kint et al, 2017
pDIA6325	pDIA6103-P _{sigB} - <i>sigB</i> , Cm ^R -Tm ^R	Kint et al, 2017
pDIA6457	pFT47-P _{CD1474} -SNAP ^{Cd} Cm ^R -Tm ^R	This work
pDIA6400	pMTL-SC7315- Δ <i>rsbZ</i> (<i>CD2685</i>) Cm ^R -Tm ^R	This work
pDIA6410	pDIA6103-P _{tet} - <i>rsbZ</i> (<i>CD2685</i>), Cm ^R -Tm ^R	This work
pDIA6579	pDIA6103-P _{tet} - <i>rsbZ</i> Δ <i>pho</i>	This work
pDIA6430	pMTL-SC7315- Δ <i>CD0007</i> , Cm ^R -Tm ^R	This work
pDIA6431	pMTL-SC7315- Δ <i>CD0008</i> , Cm ^R -Tm ^R	This work
pDIA6580	pMTL-SC7315- Δ <i>rsbV</i> , Cm ^R -Tm ^R	This work
pDIA6581	pMTL-SC7315- Δ <i>CD0007-08</i> , Cm ^R -Tm ^R	This work
pDIA6589	pFT47-P _{sigB} -SNAP ^{Cd} , Cm ^R -Tm ^R	This work, from pDIA6325
pDIA6591	pFT47-P _{sigB} - <i>sigB</i> HA C-ter, Cm ^R -Tm ^R	This work, from pDIA6325
pDIA6594	pDIA6103-P _{tet} - <i>rsbZ</i> Δ <i>pho</i> HA C-ter, Cm ^R -Tm ^R	This work
pDIA6385	pDIA6103-P _{tet} - <i>CD0007</i> , Cm ^R -Tm ^R	This work
pDIA6386	pDIA6103-P _{tet} - <i>CD0008</i> , Cm ^R -Tm ^R	This work
pDIA6387	pDIA6103-P _{tet} - <i>CD2684</i> , Cm ^R -Tm ^R	This work
pDIA6637	pDIA6103-P _{tet} - <i>rsbV</i> , Cm ^R -Tm ^R	This work
pDIA6638	pDIA6103-P _{tet} - <i>rsbW</i> , Cm ^R -Tm ^R	This work
pDIA6639	pDIA6103-P _{tet} - <i>rsbV</i> HA C-ter	This work, from pDIA6637
pDIA6813	pMTL-SC7315-P _{tet} - <i>CD2684</i> , Cm ^R -Tm ^R	This work
pKT25	Kan ^R	BACTH kit, Euromedex®
pKNT25	Kan ^R	BACTH kit, Euromedex®
pUT18	Amp ^R	BACTH kit, Euromedex®
pUT18C	Amp ^R	BACTH kit, Euromedex®
pDIA6644	pKT25- <i>sigB</i> , Kan ^R	This work
pDIA6645	pKT25- <i>rsbW</i> , Kan ^R	This work
pDIA6646	pKT25- <i>rsbV</i> , Kan ^R	This work
pDIA6647	pKT25- <i>rsbZ</i> , Kan ^R	This work
pDIA6648	pKNT25- <i>sigB</i> , Kan ^R	This work

pDIA6649	pKNT25- <i>rsbW</i> , Kan ^R	This work
pDIA6650	pKNT25- <i>rsbV</i> , Kan ^R	This work
pDIA6651	pKNT25- <i>rsbZ</i> , Kan ^R	This work
pDIA6652	pUT18- <i>sigB</i> , Amp ^R	This work
pDIA6653	pUT18- <i>rsbW</i> , Amp ^R	This work
pDIA6654	pUT18- <i>rsbV</i> , Amp ^R	This work
pDIA6655	pUT18- <i>rsbZ</i> , Amp ^R	This work
pDIA6656	pUT18C- <i>sigB</i> , Amp ^R	This work
pDIA6657	pUT18C- <i>rsbW</i> , Amp ^R	This work
pDIA6658	pUT18C- <i>rsbV</i> , Amp ^R	This work
pDIA6659	pUT18C- <i>rsbZ</i> , Amp ^R	This work
pDIA6868	pKT25- <i>CD2684</i> , Kan ^R	This work
pDIA6869	pKNT25- <i>CD2684</i> , Kan ^R	This work
pDIA6870	pUT18- <i>CD2684</i> , Amp ^R	This work
pDIA6871	pUT18C- <i>CD2684</i> , Amp ^R	This work

Table S2: Oligonucleotides

Name	Sequence	
NK13	GATCAGGCCTGTAAATACTAATAAATAGTT	5' CD2685 StuI
NK14	GGGATCCTAAGTCCTTTTTTATCG	3' CD2685 BamHI
NK15	AGGCCTAAAGATAATTATGATGATG	5' CD2684 StuI
NK16	GGGATCCCGAATACAATTATACATAAT	3' CD2684 BamHI
NK17	AGGCCTTTTGTATAATGTAGTTAGATA	5' CD0007 StuI
NK18	GGGATCCAGCTTCCTACTAAC	3' CD0007 BamHI
NK19	AGGCCTGTAATAAGTAAAAGCTTTG	5' CD0008 StuI
NK20	GGGATCCTCTAAATTTGAATCAATA	3' CD0008 BamHI
NK21	CTCGAGTTATTTGAGAGATATTGAAAC	5' CD2685 DCO XhoI PCR1
NK22	TCATACTCAATTTCTCCCCCTA	3' CD2685 DCO PCR1
NK23	TAGGGGGAGAAATTGAGTATGAGGTATAAACCGATTAG AAAACTTT	5' CD2685 DCO PCR2-rev-comp NK22
NK24	GGGATCCAACCTTGAGTATGAGCTCTA	3' CD2685 DCO BamHI PCR2
NK104	TGGTCATGAGATTATCAAAAGGACTGAAATCCAAGCAC AAGC	DCO CD0007 5'PCR1
NK39	CCACCTTTTTTACAACCTCTTTTATTGC	DCO CD0007 3'PCR1
NK40	GCAATAAAAGAAGTTGTAATAAAAGGTGGGCTTTGATGA TGAGGGAGATGTAAAC	DCO CD0007 3'PCR2 rev comp NK39
NK105	ATCGTAGAAATACGGTGTTTTTTTTCAACATCATATCTAT CAATAGC	DCO CD0007 5'PCR2
NK106	TGGTCATGAGATTATCAAAAGGAAGAAGATTTTGTAAG GCACTTG	DCO CD0008 5'PCR1
NK43	AATTTGCCACCCCATGCATTCA	DCO CD0008 3'PCR1
NK44	TGAATGCATGGGGGTGGCAAATTGGAAATAGGAGGTTT TTACATGTCTA	DCO CD0008 3'PCR2 rev comp NK43
NK107	ATCGTAGAAATACGGTGTTTTTTTTTCGCATCACTTATCTT TTTGC	DCO CD0008 5'PCR2
NK110	TGGTCATGAGATTATCAAAAGGACTAAGAGAGAAGAG TTCAA	DCO <i>rsbV</i> 5'PCR1

NK47	TAGACATGTA AAAACCTCCTATTTCTTTT	DCO <i>rsbV</i> 3'PCR1
NK48	AAAAGGAAATAGGAGGTTTTTACATGTCTAAAGAAAGA TTTTTACTATAACAGGTCTAG	DCO <i>rsbV</i> 3'PCR2 rev comp NK47
NK49	ATCGTAGAAATACGGTGT TTTTTCTTGTTCCTTTTTTCAA GGAG	DCO <i>rsbV</i> 5'PCR2
NK129	GATCGGATCCCTACCTATCTTGCATACCAACAGAAACTT G	3' <i>rsbZ</i> Δphosphatase domain BamHI
NK130	GCAATAAAAAGAAGTTGTA AAAAAGGGGAAATAGGAGG TTTTTACATGTCTA	DCO <i>CD0007-08</i> PCR2 5'rev comp NK39
NK108	TGGTCATGAGATTATCAAAAAGGGATAAACTAAGAGGT TCAATAAG	DCO <i>ptet CD2684</i> 5' PCR1
NK109	ATCGTAGAAATACGGTGT TTTTTTAGTCGCGCAAATACT CTATC	DCO <i>ptet CD2684</i> 3' PCR2
NK228	CGTTAACAGATCTGAGCTCCTTGATTATGGATTCAAACG ATAAAA	DCO <i>ptet CD2684</i> 5' PCR2
NK229	CTAGCTTGATGCAGAATTCGTCTACCTATCCTTTAACAT AAC	DCO <i>ptet CD2684</i> 3'PCR1
NK230	TTTTATCGTTTGAATCCATAATCAAGGAGCTCAGATCTG TTAACG	DCO <i>ptet CD2684</i> , <i>ptet</i> element 3'
NK231	GTTATGTTAAAGGATAGGTAGACGAATTCTGCATCAAG CTAG	DCO <i>ptet CD2684</i> , <i>ptet</i> element 5'
NK148	GATCAGGCCTGGAAATAGGAGGTTTTTACATGTCTA	5' <i>StuI rsbV</i>
NK149	GATCCTCGAGCTTTATAGTCTCACAAGCCAAAG	3' <i>XhoI rsbV</i>
NK155	GATCAGGCCTATGGATAAAGATTGTGAAATGA	<i>StuI</i> 5' SNAP ^{cd} (ORF)
NK156	GATCCTCGAGTTATTCCTTACCCAAGTCCT	<i>XhoI</i> 3' SNAP ^{cd} (ORF)
NK181	GATCGGATCCTTATTCCTTACCCAAGTCCT	<i>BamHI</i> 3' SNAP ^{cd} (ORF)
NK210	GATCGGATCCCTTTATAGTCTCACAAGCCAAAG	3' <i>RsbV BamHI</i>
NK211	GATCAGGCCTAAGAAAGATTTTTACTATAACAGG	5' <i>RsbW StuI</i>
NK212	GATCGGATCCGCTCTTTTGTATCCATATTTAGG	3' <i>RsbW BamHI</i>
NK194	GTTCCAGATTACGCTTAGGGATCCTATAAGTTTTAAT	<i>RsbZ Δpho HA C-ter</i> inverse PCR 1
NK195	ATCGTATGGGTACCTATCTTGCATACCAACAGA	<i>RsbZ Δpho HA C-ter</i> inverse PCR 2
NK192	GTTCCAGATTACGCTTAAACTTTGGCTTGTGAGAC	<i>RsbV HA C-ter</i> inverse PCR 1
NK193	ATCGTATGGGTATCCCTCCACTTTAAATATTTTAT	<i>RsbV HA C-ter</i> inverse PCR 2
NK188	GTTCCAGATTACGCTTAAAAAATATAAAAAAAGTATT GACC	<i>SigB HA C-ter</i> inverse PCR 1
NK189	ATCGTATGGGTATAAATTTTTTCATATTCTTTTTTCAGC	<i>SigB HA C-ter</i> inverse PCR 2
NK112	GATAGGATCCAATGAAAAATGTAGCTAATGC	BACTH <i>BamHI sigB</i> 5' pKNT25/pKT25 and PUT18/pUT18C
NK113	GATAGAATCCCTAAATTTTTTTCATATTCTTTT	BACTH <i>EcoRI sigB</i> 3' pKNT25/pUT18
NK114	GATAGAATTCCTTTATAAATTTTTTTCATATTC	BACTH <i>EcoRI sigB</i> 3' pKNT25/pUT18C
NK115	GATAGGATCCATTGAGTATGACTAATGGCAG	BACTH 5' <i>BamHI CD2685</i> pKNT25/pKT25 and pUT18C/pUT18
NK116	GATAGAATCCCCCTATCCTTTAACATAACTATT	BACTH 3' <i>EcoRI CD2685</i> pKNT25/pUT18
NK117	GATAGAATTCATCTACCTATCCTTTAACATAAC	BACTH 3' <i>EcoRI CD2685</i> pKNT25/pUT18
NK118	GATAGGATCCTTTGGCTTGTGAGACTATAAA	BACTH 5' <i>BamHI RsbW</i> pUT18/pUT18C and pKNT25/pKT25
NK119	GATAGAATCCCAATATCAACTCCTAAATATTTAG	BACTH 3' <i>EcoRI RsbW</i>

NK120	GATAGAATTCATTAAATATCAACTCCTAAATAT	pUT18/pKNT25 BACTH 3' EcoRI RsbW pUT18C/pKT25
NK121	GATAGGATCCGTCTATGAATATTGATTCAAATTTAG	BACTH 5' BamHI RsbV pUT18/pUT18C and pKNT25/pKT25
NK122	GATAGAATTCCTCCCTCCACTTTAAATATTT	BACTH 3' EcoRI RsbV pUT18/pKNT25
NK123	GATAGAATTCGTTTATCCCTCCACTTTAA	BACTH 3' EcoRI RsbV pUT18C/pKT25
NK183	GATAGGATCCATT GATTATGGATTCAAACGATA	BACTH 5' BamHI CD2684 pUT18/pUT18C and pKNT25/pKT25
NK184	GATAGAATTCAATTATATTGAATCAATATATATC	BACTH 3' EcoRI CD2684 pUT18C/pKT25
NK185	GATAGAATTCCTATTGAATCAATATATATCTTTAA	BACTH 3' EcoRI RsbV pUT18/pKNT25
NK124	CAATTTACACAGGAAACAGC	BACTH 5' pUT18/pUT18C
NK125	GAGCAGATTGTACTGAGAG	BACTH 3' pUT18/pUT18C
NK126	CGGATAACAATTTACACAGG	BACTH 5' pKT25/pKNT25
NK127	GAGAGTGCACCATATTACTTAG	BACTH 3' pKNT25
NK128	GTTGTAACGACGGCCG	BACTH 3' pKT25
IMV388	GAGTCCAAGAAGAATACAGGA	qRT-PCR <i>sigB</i>
IMV389	AAGCCTCCATAGCCTCTAAAAC	qRT-PCR <i>sigB</i>
IMV774	CCAAAAGAAGTTCTACATGAAACA	qRT-PCR <i>CD0007</i>
IMV775	AACATCTCCCTCATCATCAA	qRT-PCR <i>CD0007</i>
IMV776	TGGAATGTTTGTCTTGATGGA	qRT-PCR <i>rbsV (CD0009)</i>
IMV777	AGCTCCTAAGCCTGTTGAGTCT	qRT-PCR <i>rbsV (CD0009)</i>
IMV778	TCCAAAAGAGAGTGGTCTTGG	qRT-PCR <i>rbsW (CD0010)</i>
IMV779	AGTCATTTTTATTTTGTCCCTTG	qRT-PCR <i>rbsW (CD0010)</i>
OS547	GGCAAATTGGAGCAGTGTTA	qRT-PCR <i>CD0008</i>
OS548	TCTTATATGCCTTTTCAACAACCTT	qRT-PCR <i>CD0008</i>
NK30	AGAGCAGAAGGTGAACGAGA	qRT-PCR <i>CD2685 (rsbZ)</i>
NK31	TCAAGAGTGATGCAACAGATGA	qRT-PCR <i>CD2685 (rsbZ)</i>
IMV846	TTGCACAGCATGTGGATTTT	qRT-PCR <i>CD2684</i>
IMV847	CCATCACAATCTGTCCACCTT	qRT-PCR <i>CD2684</i>
IMV668	TGCCCTGTATGTGGAGCTAA	qRT-PCR <i>CD1623</i>
IMV669	CCAGCTGCTCCATTTCCTAC	qRT-PCR <i>CD1623</i>
IMV670	ACATGAAGGAGATGCTGCAC	qRT-PCR <i>CD1474/CD1524</i>
IMV671	GCTGAACATGCTGCTAAATTT	qRT-PCR <i>CD1474/CD1524</i>
IMV575	CCAAGGCAAGATAGCAGGAG	qRT PCR <i>CD1157-norV</i>
IMV576	CTGCACCAATGCCATACAC	qRT PCR <i>CD1157-norV</i>
IMV747	GGGGTTAAACCAAAATGCTGA	qRT-PCR <i>CD0176</i>
IMV748	CCTTGCTTTACTGCCAGAGG	qRT-PCR <i>CD0176</i>
IMV790	GCTACAAAAACTGGGCAAAA	qRT-PCR <i>CD1125</i>
IMV791	ACATTTCCCATTCGTTTCAT	qRT-PCR <i>CD1125</i>

References

- Abt, M. C., P. T. McKenney, and E. G. Pamer. 2016. *Clostridium difficile* colitis: pathogenesis and host defence. *Nat Rev Microbiol* **14**:609-620.
- Alper, S., A. Dufour, D. A. Garsin, L. Duncan, and R. Losick. 1996. Role of adenosine nucleotides in the regulation of a stress-response transcription factor in *Bacillus subtilis*. *J Mol Biol* **260**:165-177.
- Aravind, L., and C. P. Ponting. 1997. The GAF domain: an evolutionary link between diverse phototransducing proteins. *Trends Biochem Sci* **22**:458-459.
- Becker, L. A., M. S. Cetin, R. W. Hutkins, and A. K. Benson. 1998. Identification of the gene encoding the alternative sigma factor sigmaB from *Listeria monocytogenes* and its role in osmotolerance. *J Bacteriol* **180**:4547-4554.
- Benson, A. K., and W. G. Haldenwang. 1992. Characterization of a regulatory network that controls sigma B expression in *Bacillus subtilis*. *J Bacteriol* **174**:749-757.
- Benson, A. K., and W. G. Haldenwang. 1993. Regulation of sigma B levels and activity in *Bacillus subtilis*. *J Bacteriol* **175**:2347-2356.
- Boylan, S. A., A. R. Redfield, M. S. Brody, and C. W. Price. 1993. Stress-induced activation of the sigma B transcription factor of *Bacillus subtilis*. *J Bacteriol* **175**:7931-7937.
- Boylan, S. A., A. Rutherford, S. M. Thomas, and C. W. Price. 1992. Activation of *Bacillus subtilis* transcription factor sigma B by a regulatory pathway responsive to stationary-phase signals. *J Bacteriol* **174**:3695-3706.
- Brody, M. S., K. Vijay, and C. W. Price. 2001. Catalytic function of an alpha/beta hydrolase is required for energy stress activation of the sigma(B) transcription factor in *Bacillus subtilis*. *J Bacteriol* **183**:6422-6428.
- Cartman, S. T., M. L. Kelly, D. Heeg, J. T. Heap, and N. P. Minton. 2012. Precise manipulation of the *Clostridium difficile* chromosome reveals a lack of association between the *tcdC* genotype and toxin production. *Appl Environ Microbiol* **78**:4683-4690.
- Cassona, C. P., F. Pereira, M. Serrano, and A. O. Henriques. 2016. A Fluorescent Reporter for Single Cell Analysis of Gene Expression in *Clostridium difficile*. *Methods Mol Biol* **1476**:69-90.
- Chen, L. C., J. C. Chen, J. C. Shu, C. Y. Chen, S. C. Chen, S. H. Chen, C. Y. Lin, C. Y. Lu, and C. C. Chen. 2012. Interplay of RsbM and RsbK controls the sigma(B) activity of *Bacillus cereus*. *Environ Microbiol* **14**:2788-2799.
- de Been, M., C. Francke, R. J. Siezen, and T. Abee. 2011. Novel sigmaB regulation modules of Gram-positive bacteria involve the use of complex hybrid histidine kinases. *Microbiology* **157**:3-12.
- de Been, M., M. H. Tempelaars, W. van Schaik, R. Moezelaar, R. J. Siezen, and T. Abee. 2010. A novel hybrid kinase is essential for regulating the sigma(B)-mediated stress response of *Bacillus cereus*. *Environ Microbiol* **12**:730-745.
- Deakin, L. J., S. Clare, R. P. Fagan, L. F. Dawson, D. J. Pickard, M. R. West, B. W. Wren, N. F. Fairweather, G. Dougan, and T. D. Lawley. 2012. The *Clostridium difficile* *spo0A* gene is a persistence and transmission factor. *Infect Immun* **80**:2704-2711.
- Dufour, A., and W. G. Haldenwang. 1994. Interactions between a *Bacillus subtilis* anti-sigma factor (RsbW) and its antagonist (RsbV). *J Bacteriol* **176**:1813-1820.
- Ehsaan, M., S. A. Kuehne, and N. P. Minton. 2016. *Clostridium difficile* Genome Editing Using *pyrE* Alleles. *Methods Mol Biol* **1476**:35-52.
- Eldar, A., and M. B. Elowitz. 2010. Functional roles for noise in genetic circuits. *Nature* **467**:167-173.
- Espey, M. G. 2013. Role of oxygen gradients in shaping redox relationships between the human intestine and its microbiota. *Free Radic Biol Med* **55**:130-140.
- Fagan, R. P., and N. F. Fairweather. 2011. *Clostridium difficile* has two parallel and essential Sec secretion systems. *J Biol Chem* **286**:27483-27493.
- Fimlaid, K. A., J. P. Bond, K. C. Schutz, E. E. Putnam, J. M. Leung, T. D. Lawley, and A. Shen. 2013. Global analysis of the sporulation pathway of *Clostridium difficile*. *PLoS Genet* **9**:e1003660.
- Folgosa, F., M. C. Martins, and M. Teixeira. 2018. The multidomain flavodiiron protein from *Clostridium difficile* 630 is an NADH: oxygen oxidoreductase. *Sci Rep* **8**:10164.

- Galperin, M. Y., S. L. Mekhedov, P. Puigbo, S. Smirnov, Y. I. Wolf, and D. J. Rigden. 2012. Genomic determinants of sporulation in Bacilli and Clostridia: towards the minimal set of sporulation-specific genes. *Environ Microbiol* **14**:2870-2890.
- Giachino, P., S. Engelmann, and M. Bischoff. 2001. Sigma(B) activity depends on RsbU in *Staphylococcus aureus*. *J Bacteriol* **183**:1843-1852.
- Glaser, P., M. E. Sharpe, B. Raether, M. Perego, K. Ohlsen, and J. Errington. 1997. Dynamic, mitotic-like behavior of a bacterial protein required for accurate chromosome partitioning. *Genes Dev* **11**:1160-1168.
- Guldimann, C., K. J. Boor, M. Wiedmann, and V. Guariglia-Oropeza. 2016. Resilience in the Face of Uncertainty: Sigma Factor B Fine-Tunes Gene Expression To Support Homeostasis in Gram-Positive Bacteria. *Appl Environ Microbiol* **82**:4456-4469.
- Guldimann, C., V. Guariglia-Oropeza, S. Harrand, D. Kent, K. J. Boor, and M. Wiedmann. 2017. Stochastic and Differential Activation of sigmaB and PrfA in *Listeria monocytogenes* at the Single Cell Level under Different Environmental Stress Conditions. *Front Microbiol* **8**:348.
- Heap, J. T., S. A. Kuehne, M. Ehsaan, S. T. Cartman, C. M. Cooksley, J. C. Scott, and N. P. Minton. 2010. The ClosTron: Mutagenesis in *Clostridium* refined and streamlined. *J Microbiol Methods* **80**:49-55.
- Heap, J. T., O. J. Pennington, S. T. Cartman, G. P. Carter, and N. P. Minton. 2007. The ClosTron: a universal gene knock-out system for the genus *Clostridium*. *J Microbiol Methods* **70**:452-464.
- Hecker, M., J. Pane-Farre, and U. Volker. 2007. SigB-dependent general stress response in *Bacillus subtilis* and related gram-positive bacteria. *Annu Rev Microbiol* **61**:215-236.
- Janoir, C. 2016. Virulence factors of *Clostridium difficile* and their role during infection. *Anaerobe* **37**:13-24.
- Jose, S., and R. Madan. 2016. Neutrophil-mediated inflammation in the pathogenesis of *Clostridium difficile* infections. *Anaerobe* **41**:85-90.
- Kalman, S., M. L. Duncan, S. M. Thomas, and C. W. Price. 1990. Similar organization of the sigB and spoIIA operons encoding alternate sigma factors of *Bacillus subtilis* RNA polymerase. *J Bacteriol* **172**:5575-5585.
- Kang, C. M., M. S. Brody, S. Akbar, X. Yang, and C. W. Price. 1996. Homologous pairs of regulatory proteins control activity of *Bacillus subtilis* transcription factor sigma(b) in response to environmental stress. *J Bacteriol* **178**:3846-3853.
- Karimova, G., J. Pidoux, A. Ullmann, and D. Ladant. 1998. A bacterial two-hybrid system based on a reconstituted signal transduction pathway. *Proc Natl Acad Sci U S A* **95**:5752-5756.
- Kint, N., C. Janoir, M. Monot, S. Hoys, O. Soutourina, B. Dupuy, and I. Martin-Verstraete. 2017. The alternative sigma factor sigmaB plays a crucial role in adaptive strategies of *Clostridium difficile* during gut infection. *Environ Microbiol* **19**:1933-1958.
- Laemmli, U. K. 1970. Cleavage of structural proteins during the assembly of the head of bacteriophage T4. *Nature* **227**:680-685.
- Livak, K. J., and T. D. Schmittgen. 2001. Analysis of relative gene expression data using real-time quantitative PCR and the 2(-Delta Delta C(T)) Method. *Methods* **25**:402-408.
- Abt, M. C., P. T. McKenney, and E. G. Pamer. 2016. *Clostridium difficile* colitis: pathogenesis and host defence. *Nat Rev Microbiol* **14**:609-620.
- Alper, S., A. Dufour, D. A. Garsin, L. Duncan, and R. Losick. 1996. Role of adenosine nucleotides in the regulation of a stress-response transcription factor in *Bacillus subtilis*. *J Mol Biol* **260**:165-177.
- Aravind, L., and C. P. Ponting. 1997. The GAF domain: an evolutionary link between diverse phototransducing proteins. *Trends Biochem Sci* **22**:458-459.
- Becker, L. A., M. S. Cetin, R. W. Hutkins, and A. K. Benson. 1998. Identification of the gene encoding the alternative sigma factor sigmaB from *Listeria monocytogenes* and its role in osmotolerance. *J Bacteriol* **180**:4547-4554.
- Benson, A. K., and W. G. Haldenwang. 1992. Characterization of a regulatory network that controls sigma B expression in *Bacillus subtilis*. *J Bacteriol* **174**:749-757.
- Benson, A. K., and W. G. Haldenwang. 1993. Regulation of sigma B levels and activity in *Bacillus subtilis*. *J Bacteriol* **175**:2347-2356.

- Boylan, S. A., A. R. Redfield, M. S. Brody, and C. W. Price. 1993. Stress-induced activation of the sigma B transcription factor of *Bacillus subtilis*. *J Bacteriol* **175**:7931-7937.
- Boylan, S. A., A. Rutherford, S. M. Thomas, and C. W. Price. 1992. Activation of *Bacillus subtilis* transcription factor sigma B by a regulatory pathway responsive to stationary-phase signals. *J Bacteriol* **174**:3695-3706.
- Brody, M. S., K. Vijay, and C. W. Price. 2001. Catalytic function of an alpha/beta hydrolase is required for energy stress activation of the sigma(B) transcription factor in *Bacillus subtilis*. *J Bacteriol* **183**:6422-6428.
- Cartman, S. T., M. L. Kelly, D. Heeg, J. T. Heap, and N. P. Minton. 2012. Precise manipulation of the *Clostridium difficile* chromosome reveals a lack of association between the *tcdC* genotype and toxin production. *Appl Environ Microbiol* **78**:4683-4690.
- Cassona, C. P., F. Pereira, M. Serrano, and A. O. Henriques. 2016. A Fluorescent Reporter for Single Cell Analysis of Gene Expression in *Clostridium difficile*. *Methods Mol Biol* **1476**:69-90.
- Chen, L. C., J. C. Chen, J. C. Shu, C. Y. Chen, S. C. Chen, S. H. Chen, C. Y. Lin, C. Y. Lu, and C. C. Chen. 2012. Interplay of RsbM and RsbK controls the sigma(B) activity of *Bacillus cereus*. *Environ Microbiol* **14**:2788-2799.
- de Been, M., C. Francke, R. J. Siezen, and T. Abee. 2011. Novel sigmaB regulation modules of Gram-positive bacteria involve the use of complex hybrid histidine kinases. *Microbiology* **157**:3-12.
- de Been, M., M. H. Tempelaars, W. van Schaik, R. Moezelaar, R. J. Siezen, and T. Abee. 2010. A novel hybrid kinase is essential for regulating the sigma(B)-mediated stress response of *Bacillus cereus*. *Environ Microbiol* **12**:730-745.
- Deakin, L. J., S. Clare, R. P. Fagan, L. F. Dawson, D. J. Pickard, M. R. West, B. W. Wren, N. F. Fairweather, G. Dougan, and T. D. Lawley. 2012. The *Clostridium difficile* *spo0A* gene is a persistence and transmission factor. *Infect Immun* **80**:2704-2711.
- Dufour, A., and W. G. Haldenwang. 1994. Interactions between a *Bacillus subtilis* anti-sigma factor (RsbW) and its antagonist (RsbV). *J Bacteriol* **176**:1813-1820.
- Ehsaan, M., S. A. Kuehne, and N. P. Minton. 2016. *Clostridium difficile* Genome Editing Using *pyrE* Alleles. *Methods Mol Biol* **1476**:35-52.
- Eldar, A., and M. B. Elowitz. 2010. Functional roles for noise in genetic circuits. *Nature* **467**:167-173.
- Espey, M. G. 2013. Role of oxygen gradients in shaping redox relationships between the human intestine and its microbiota. *Free Radic Biol Med* **55**:130-140.
- Fagan, R. P., and N. F. Fairweather. 2011. *Clostridium difficile* has two parallel and essential Sec secretion systems. *J Biol Chem* **286**:27483-27493.
- Fimlaid, K. A., J. P. Bond, K. C. Schutz, E. E. Putnam, J. M. Leung, T. D. Lawley, and A. Shen. 2013. Global analysis of the sporulation pathway of *Clostridium difficile*. *PLoS Genet* **9**:e1003660.
- Folgosa, F., M. C. Martins, and M. Teixeira. 2018. The multidomain flavodiiron protein from *Clostridium difficile* 630 is an NADH: oxygen oxidoreductase. *Sci Rep* **8**:10164.
- Galperin, M. Y., S. L. Mekhedov, P. Puigbo, S. Smirnov, Y. I. Wolf, and D. J. Rigden. 2012. Genomic determinants of sporulation in Bacilli and Clostridia: towards the minimal set of sporulation-specific genes. *Environ Microbiol* **14**:2870-2890.
- Giachino, P., S. Engelmann, and M. Bischoff. 2001. Sigma(B) activity depends on RsbU in *Staphylococcus aureus*. *J Bacteriol* **183**:1843-1852.
- Glaser, P., M. E. Sharpe, B. Raether, M. Perego, K. Ohlsen, and J. Errington. 1997. Dynamic, mitotic-like behavior of a bacterial protein required for accurate chromosome partitioning. *Genes Dev* **11**:1160-1168.
- Guldimann, C., K. J. Boor, M. Wiedmann, and V. Guariglia-Oropeza. 2016. Resilience in the Face of Uncertainty: Sigma Factor B Fine-Tunes Gene Expression To Support Homeostasis in Gram-Positive Bacteria. *Appl Environ Microbiol* **82**:4456-4469.
- Guldimann, C., V. Guariglia-Oropeza, S. Harrand, D. Kent, K. J. Boor, and M. Wiedmann. 2017. Stochastic and Differential Activation of sigmaB and PrfA in *Listeria monocytogenes* at the Single Cell Level under Different Environmental Stress Conditions. *Front Microbiol* **8**:348.
- Heap, J. T., S. A. Kuehne, M. Ehsaan, S. T. Cartman, C. M. Cooksley, J. C. Scott, and N. P. Minton. 2010. The Clostron: Mutagenesis in *Clostridium* refined and streamlined. *J Microbiol Methods* **80**:49-55.

- Heap, J. T., O. J. Pennington, S. T. Cartman, G. P. Carter, and N. P. Minton. 2007. The Clostron: a universal gene knock-out system for the genus *Clostridium*. *J Microbiol Methods* **70**:452-464.
- Hecker, M., J. Pane-Farre, and U. Volker. 2007. SigB-dependent general stress response in *Bacillus subtilis* and related gram-positive bacteria. *Annu Rev Microbiol* **61**:215-236.
- Janoir, C. 2016. Virulence factors of *Clostridium difficile* and their role during infection. *Anaerobe* **37**:13-24.
- Jose, S., and R. Madan. 2016. Neutrophil-mediated inflammation in the pathogenesis of *Clostridium difficile* infections. *Anaerobe* **41**:85-90.
- Kalman, S., M. L. Duncan, S. M. Thomas, and C. W. Price. 1990. Similar organization of the sigB and spoIIA operons encoding alternate sigma factors of *Bacillus subtilis* RNA polymerase. *J Bacteriol* **172**:5575-5585.
- Kang, C. M., M. S. Brody, S. Akbar, X. Yang, and C. W. Price. 1996. Homologous pairs of regulatory proteins control activity of *Bacillus subtilis* transcription factor sigma(b) in response to environmental stress. *J Bacteriol* **178**:3846-3853.
- Karimova, G., J. Pidoux, A. Ullmann, and D. Ladant. 1998. A bacterial two-hybrid system based on a reconstituted signal transduction pathway. *Proc Natl Acad Sci U S A* **95**:5752-5756.
- Kint, N., C. Janoir, M. Monot, S. Hoys, O. Soutourina, B. Dupuy, and I. Martin-Verstraete. 2017. The alternative sigma factor sigmaB plays a crucial role in adaptive strategies of *Clostridium difficile* during gut infection. *Environ Microbiol* **19**:1933-1958.
- Laemmli, U. K. 1970. Cleavage of structural proteins during the assembly of the head of bacteriophage T4. *Nature* **227**:680-685.
- Livak, K. J., and T. D. Schmittgen. 2001. Analysis of relative gene expression data using real-time quantitative PCR and the 2(-Delta Delta C(T)) Method. *Methods* **25**:402-408.
- Marles-Wright, J., T. Grant, O. Delumeau, G. van Duinen, S. J. Firbank, P. J. Lewis, J. W. Murray, J. A. Newman, M. B. Quin, P. R. Race, A. Rohou, W. Tichelaar, M. van Heel, and R. J. Lewis. 2008. Molecular architecture of the "stressosome," a signal integration and transduction hub. *Science* **322**:92-96.
- Marles-Wright, J., and R. J. Lewis. 2008. The *Bacillus subtilis* stressosome: A signal integration and transduction hub. *Commun Integr Biol* **1**:182-184.
- Martinez, L., A. Reeves, and W. Haldenwang. 2010. Stressosomes formed in *Bacillus subtilis* from the RsbR protein of *Listeria monocytogenes* allow sigma(B) activation following exposure to either physical or nutritional stress. *J Bacteriol* **192**:6279-6286.
- Nadezhdin, E. V., M. S. Brody, and C. W. Price. 2011. An alpha/beta hydrolase and associated Per-ARNT-Sim domain comprise a bipartite sensing module coupled with diverse output domains. *PLoS One* **6**:e25418.
- Ng, Y. K., M. Ehsaan, S. Philip, M. M. Collery, C. Janoir, A. Collignon, S. T. Cartman, and N. P. Minton. 2013. Expanding the repertoire of gene tools for precise manipulation of the *Clostridium difficile* genome: allelic exchange using pyrE alleles. *PLoS One* **8**:e56051.
- Pane-Farre, J., B. Jonas, K. Forstner, S. Engelmann, and M. Hecker. 2006. The sigmaB regulon in *Staphylococcus aureus* and its regulation. *Int J Med Microbiol* **296**:237-258.
- Pane-Farre, J., B. Jonas, S. W. Hardwick, K. Gronau, R. J. Lewis, M. Hecker, and S. Engelmann. 2009. Role of RsbU in controlling SigB activity in *Staphylococcus aureus* following alkaline stress. *J Bacteriol* **191**:2561-2573.
- Pane-Farre, J., M. B. Quin, R. J. Lewis, and J. Marles-Wright. 2017. Structure and Function of the Stressosome Signalling Hub. *Subcell Biochem* **83**:1-41.
- Paredes, C. J., K. V. Alsaker, and E. T. Papoutsakis. 2005. A comparative genomic view of clostridial sporulation and physiology. *Nat Rev Microbiol* **3**:969-978.
- Peltier, J., H. A. Shaw, E. C. Couchman, L. F. Dawson, L. Yu, J. S. Choudhary, V. Kaeffer, B. W. Wren, and N. F. Fairweather. 2015. Cyclic diGMP regulates production of sortase substrates of *Clostridium difficile* and their surface exposure through ZmpI protease-mediated cleavage. *J Biol Chem* **290**:24453-24469.
- Peniche, A. G., T. C. Savidge, and S. M. Dann. 2013. Recent insights into *Clostridium difficile* pathogenesis. *Curr Opin Infect Dis* **26**:447-453.

- Pereira, F. C., L. Saujet, A. R. Tome, M. Serrano, M. Monot, E. Couture-Tosi, I. Martin-Verstraete, B. Dupuy, and A. O. Henriques. 2013. The spore differentiation pathway in the enteric pathogen *Clostridium difficile*. *PLoS Genet* **9**:e1003782.
- Py, B., P. L. Moreau, and F. Barras. 2011. Fe-S clusters, fragile sentinels of the cell. *Curr Opin Microbiol* **14**:218-223.
- Ransom, E. M., G. M. Kaus, P. M. Tran, C. D. Ellermeier, and D. S. Weiss. 2018. Multiple factors contribute to bimodal toxin gene expression in *Clostridioides (Clostridium) difficile*. *Mol Microbiol*.
- Rivera-Chavez, F., C. A. Lopez, and A. J. Baumler. 2017. Oxygen as a driver of gut dysbiosis. *Free Radic Biol Med* **105**:93-101.
- Rupnik, M., M. H. Wilcox, and D. N. Gerding. 2009. *Clostridium difficile* infection: new developments in epidemiology and pathogenesis. *Nat Rev Microbiol* **7**:526-536.
- Saujet, L., M. Monot, B. Dupuy, O. Soutourina, and I. Martin-Verstraete. 2011. The key sigma factor of transition phase, SigH, controls sporulation, metabolism, and virulence factor expression in *Clostridium difficile*. *J Bacteriol* **193**:3186-3196.
- Saujet, L., F. C. Pereira, M. Serrano, O. Soutourina, M. Monot, P. V. Shelyakin, M. S. Gelfand, B. Dupuy, A. O. Henriques, and I. Martin-Verstraete. 2013. Genome-wide analysis of cell type-specific gene transcription during spore formation in *Clostridium difficile*. *PLoS Genet* **9**:e1003756.
- Senn, M. M., P. Giachino, D. Homerova, A. Steinhuber, J. Strassner, J. Kormanec, U. Fluckiger, B. Berger-Bachi, and M. Bischoff. 2005. Molecular analysis and organization of the sigmaB operon in *Staphylococcus aureus*. *J Bacteriol* **187**:8006-8019.
- Soutourina, O. A., M. Monot, P. Boudry, L. Saujet, C. Pichon, O. Sismeiro, E. Semenova, K. Severinov, C. Le Bouguenec, J. Y. Coppee, B. Dupuy, and I. Martin-Verstraete. 2013. Genome-wide identification of regulatory RNAs in the human pathogen *Clostridium difficile*. *PLoS Genet* **9**:e1003493.
- Theriot, C. M., M. J. Koenigskecht, P. E. Carlson, Jr., G. E. Hatton, A. M. Nelson, B. Li, G. B. Huffnagle, Z. L. J, and V. B. Young. 2014. Antibiotic-induced shifts in the mouse gut microbiome and metabolome increase susceptibility to *Clostridium difficile* infection. *Nat Commun* **5**:3114.
- Utratna, M., E. Cosgrave, C. Baustian, R. Ceredig, and C. O'Byrne. 2012. Development and optimization of an EGFP-based reporter for measuring the general stress response in *Listeria monocytogenes*. *Bioeng Bugs* **3**:93-103.
- Utratna, M., E. Cosgrave, C. Baustian, R. H. Ceredig, and C. P. O'Byrne. 2014. Effects of growth phase and temperature on sigmaB activity within a *Listeria monocytogenes* population: evidence for RsbV-independent activation of sigmaB at refrigeration temperatures. *Biomed Res Int* **2014**:641647.
- van Schaik, W., M. H. Tempelaars, J. A. Wouters, W. M. de Vos, and T. Abee. 2004. The alternative sigma factor sigmaB of *Bacillus cereus*: response to stress and role in heat adaptation. *J Bacteriol* **186**:316-325.
- van Schaik, W., M. H. Tempelaars, M. H. Zwietering, W. M. de Vos, and T. Abee. 2005. Analysis of the role of RsbV, RsbW, and RsbY in regulating (Abram et al.)B activity in *Bacillus cereus*. *J Bacteriol* **187**:5846-5851.
- Vijay, K., M. S. Brody, E. Fredlund, and C. W. Price. 2000. A PP2C phosphatase containing a PAS domain is required to convey signals of energy stress to the sigmaB transcription factor of *Bacillus subtilis*. *Mol Microbiol* **35**:180-188.
- Voelker, U., T. Luo, N. Smirnova, and W. Haldenwang. 1997. Stress activation of *Bacillus subtilis* sigma B can occur in the absence of the sigma B negative regulator RsbX. *J Bacteriol* **179**:1980-1984.
- Voelker, U., A. Voelker, B. Maul, M. Hecker, A. Dufour, and W. G. Haldenwang. 1995. Separate mechanisms activate sigma B of *Bacillus subtilis* in response to environmental and metabolic stresses. *J Bacteriol* **177**:3771-3780.

- Wiedmann, M., T. J. Arvik, R. J. Hurley, and K. J. Boor. 1998. General stress transcription factor sigmaB and its role in acid tolerance and virulence of *Listeria monocytogenes*. *J Bacteriol* **180**:3650-3656.
- Wiegand, P. N., D. Nathwani, M. H. Wilcox, J. Stephens, A. Shelbaya, and S. Haider. 2012. Clinical and economic burden of *Clostridium difficile* infection in Europe: a systematic review of healthcare-facility-acquired infection. *J Hosp Infect* **81**:1-14.
- Wise, A. A., and C. W. Price. 1995. Four additional genes in the sigB operon of *Bacillus subtilis* that control activity of the general stress factor sigma B in response to environmental signals. *J Bacteriol* **177**:123-133.
- Wu, S., H. de Lencastre, and A. Tomasz. 1996. Sigma-B, a putative operon encoding alternate sigma factor of *Staphylococcus aureus* RNA polymerase: molecular cloning and DNA sequencing. *J Bacteriol* **178**:6036-6042.
- Xia, Y., Y. Xin, X. Li, and W. Fang. 2016. To Modulate Survival under Secondary Stress Conditions, *Listeria monocytogenes* 10403S Employs RsbX To Downregulate sigmaB Activity in the Poststress Recovery Stage or Stationary Phase. *Appl Environ Microbiol* **82**:1126-1135.
- Yang, X., C. M. Kang, M. S. Brody, and C. W. Price. 1996. Opposing pairs of serine protein kinases and phosphatases transmit signals of environmental stress to activate a bacterial transcription factor. *Genes Dev* **10**:2265-2275.
- Zhang, S., and W. G. Haldenwang. 2005. Contributions of ATP, GTP, and redox state to nutritional stress activation of the *Bacillus subtilis* sigmaB transcription factor. *J Bacteriol* **187**:7554-7560.

Supplementary tables of the Article: CotL, a new morphogenetic spore coat protein of *Clostridium difficile*

Table S1. Bacterial strains and plasmids used in this study.

Strains	Genotypes	Origin
<i>E. coli</i>		
10-beta	F ⁻ <i>mcrA</i> D(<i>mrr-hsdRMS-mcrBC</i>) f80 <i>lacZ</i> D _{M15} D <i>lacX74</i> <i>deoR</i> , <i>recA1</i> <i>araD139</i> D(<i>ara-leu</i>)7697 <i>galK</i> <i>rpsL</i> (Str ^R) <i>endA1</i> <i>nupG</i>	NEB
HB101 (RP4)	<i>supE44</i> <i>aa14</i> <i>galK2</i> <i>lacY1</i> D(<i>gpt-proA</i>) 62 <i>rpsL20</i> (Str ^R) <i>xyl-5</i> <i>mtl-1</i> <i>recA13</i> D(<i>mcrC-mrr</i>) <i>hsdS_B</i> (Γ _B m _B) RP4 (Tra ⁺ IncP Ap ^R Km ^R Tc ^R)	Laboratory stock
BL21 (DE3)	<i>fhuA2</i> (<i>lon</i>) <i>ompT</i> <i>gal</i> (λ <i>DE3</i>) (<i>dcm</i>) Δ <i>hsdS</i> λ <i>DE3</i> = λ <i>sBamHI</i> Δ <i>EcoRI-B</i> <i>int::(lacI::PlacUV5::T7</i> <i>genI</i>) <i>i21</i> Δ <i>nin5</i> / <i>E.coli</i> strain for T7 expression, protease deficient B strain	NEB
ECO832	BL21 (DE3) pET20- <i>CD1065</i>	This work
<i>C. difficile</i>		
630Δ <i>erm</i>		Laboratory stock
AHCD532	630Δ <i>erm</i> <i>sigE::erm</i>	Pereira <i>et al.</i> , 2013
AHCD535	630Δ <i>erm</i> <i>sigK::erm</i>	Pereira <i>et al.</i> , 2013
CDIP734	630Δ <i>erm</i> pFT47	This work
CDIP782	630Δ <i>erm</i> <i>CD1065::erm</i>	This work
CDIP753	630Δ <i>erm</i> pFT58	This work
CDIP851	630Δ <i>erm</i> pDIA6617	This work
CDIP871	630Δ <i>erm</i> pMTL84121	This work
CDIP873	630Δ <i>erm</i> <i>CD1065::erm</i> pMTL84121	This work
CDIP881	630Δ <i>erm</i> pDIA6561	This work
CDIP882	630Δ <i>erm</i> <i>sigE::erm</i> pDIA6561	This work
CDIP883	630Δ <i>erm</i> <i>sigK::erm</i> pDIA6561	This work
CDIP948	630Δ <i>erm</i> <i>sigE::erm</i> pDIA6617	This work
CDIP950	630Δ <i>erm</i> <i>sigK::erm</i> pDIA6617	This work
CDIP952	630Δ <i>erm</i> <i>CD1065::erm</i> pDIA6626	This work
CDIP986	630Δ <i>erm</i> pDIA6613	This work
CDIP987	630Δ <i>erm</i> <i>sigE::erm</i> pDIA6613	This work
CDIP989	630Δ <i>erm</i> <i>sigK::erm</i> pDIA6613	This work
CDIP1070	630Δ <i>erm</i> pDIA6664	This work
CDIP1072	630Δ <i>erm</i> <i>sigE::erm</i> pDIA6664	This work
CDIP1071	630Δ <i>erm</i> <i>sigK::erm</i> pDIA6664	This work
CDIP1035	630Δ <i>erm</i> pDIA6634	This work
CDIP1039	630Δ <i>erm</i> <i>CD1065::erm</i> pDIA6634	This work
CDIP1036	630Δ <i>erm</i> pDIA6632	This work
CDIP1040	630Δ <i>erm</i> <i>CD1065::erm</i> pDIA6632	This work
CDIP1037	630Δ <i>erm</i> pDIA6633	This work
CDIP1041	630Δ <i>erm</i> <i>CD1065::erm</i> pDIA6633	This work
CDIP1038	630Δ <i>erm</i> pDIA6631	This work
CDIP1042	630Δ <i>erm</i> <i>CD1065::erm</i> pDIA6631	This work
CDIP1057	630Δ <i>erm</i> pDIA6661	This work
CDIP1058	630Δ <i>erm</i> <i>CD1065::erm</i> pDIA6661	This work
CDIP1066	630Δ <i>erm</i> pDIA6663	This work

CDIP1067	630 Δ <i>erm sigE::erm</i> pDIA6663	This work
CDIP1068	630 Δ <i>erm sigK::erm</i> pDIA6663	This work
Plasmids	Relevant properties	Origin
pET20	<i>E. coli</i> expressing vector (Amp ^R)	
pDIA6636	pET20-CD1065-His ₆	This work
pMTL007	group II intron, ErmBtdRAM2 and <i>ltrA</i> of pMTL20 <i>lacZ</i> -TTErm ;BtdRAM2, Cm ^R /Tm ^R	Heap <i>et al.</i> , 2007
pDIA6563	pMTL007-CE5-CD1065-123s (Cm ^R /Tm ^R)	This work
pMTL84121	<i>Clostridium</i> modular plasmid containing <i>catP</i> (Cm ^R /Tm ^R)	Heap <i>et al.</i> , 2009
pFT47	pMTL84121-SNAP ^{Cd} (for transcriptional fusions) (Cm ^R /Tm ^R)	Pereira <i>et al.</i> , 2013
pFT58	pMTL84121-linker-SNAP ^{Cd} (for translational fusions) (Cm ^R /Tm ^R)	Pereira <i>et al.</i> , 2013
pDIA6626	pMTL84121- P _{$\sigma_{E/\sigma K(CD1065)}$} -CD1065	This work
pDIA6561	pFT47 P _{$\sigma_{E/\sigma K(CD1065)}$} -SNAP ^{Cd}	This work
pDIA6613	pFT47 P _{$\sigma K(CD1065)$} -SNAP ^{Cd}	This work
pDIA6617	pFT58 P _{$\sigma_{E/\sigma K(CD1065)}$} -CD1065-SNAP ^{Cd}	This work
pDIA6631	pFT58 P _{<i>spoIVA</i>} - <i>spoIVA</i> -SNAP ^{Cd}	This work
pDIA6633	pFT58 P _{<i>cotB</i>} - <i>cotB</i> -SNAP ^{Cd}	This work
pDIA6634	pFT58 P _{<i>cotE</i>} - <i>cotE</i> -SNAP ^{Cd}	This work
pDIA6632	pFT58 P _{<i>cdeC</i>} - <i>cdeC</i> -SNAP ^{Cd}	This work
pDIA6661	pFT58 P _{<i>cotD</i>} - <i>cotD</i> -SNAP ^{Cd}	This work
pDIA6663	pFT58 P _{$\sigma K(CD1065)$} -CD1065-SNAP ^{Cd}	This work
pDIA6664	pFT47 P _{$\sigma E(CD1065)$} -SNAP ^{Cd}	This work

The *erm* gene encodes the erythromycin resistance cassette. The *cat* gene encodes the chloramphenicol resistance cassette leading to resistance to chloramphenicol, Cm^R and to thiamphenicol, Tm^R. Amp^R means that the plasmid harbors a resistance cassette responsible for ampicillin resistance.

Table S3. Oligonucleotides used in this study.

^aRestriction sites and tails used for Gibson assembly cloning are underlined.

Primer	Sequence (5' to 3') ^a	Description
M13R	CAGGAAACAGCTATGAC	Sequencing pMTL84121
M13F	GTTTTCCCAGTCACGAC	Sequencing pMTL84121
EBS	CGAAATTAGAACTTGCGTTTCAGTAAAC	PCR Clostron
ErmRAM-F	ACGCGTTATATTGATAAAAATAATAATAGTGG G	PCR <i>erm</i> intron fw
ErmRAM-R	ACGCGTGC GACTCATAGAATTATTCCTCCCG	PCR <i>erm</i> intron rev
CF58	TTTATGAAAAAATTAGATACAGAG	CD1065 5'- intron
CF59	CTAAAAATAATTATCTAATTACTT	CD1065 3'- intron
CF184	GGAATTCCATATGAAAAAATTAGATACAGAGT CA	5' CD1065 NdeI
CF185	CCGCTCGAGTTCATGAGGGTTAGACTTTTT	3' CD1065 XhoI
CF120	GGAATTCTTTTTATCATCAAATATAGAGAT	5' promoter CD1065 fw EcoRI
CF121	CCGCTCGAGTATATTGAATTATATTCATACTAT T	3' promoter CD1065 rev XhoI
CF124	TATCCATATGACCATGATTACGTTTACAAAA	5' promoter <i>cotD</i> fw

	AGTCTACCTTCATC	
CF126	TATCCATATGACCATGATTACGTTTTTATCATC A AATATAGAGAT	5' promoter <i>CD1065</i> fw
CF127	TCTTTATCAGCAGCTGCGGATCCTTCATGAGGG TTAGACTTTTT	3' <i>CD1065</i> rev
CF130	ATAAGAATGCGGCCGCTATTCATGAGGGTTAG ACTTTTT	3' <i>CD1065</i> rev NotI
CF133	GGAATTCTAAGAATTTTTATTTATATTATATAT C	5' P2 Promoter <i>CD1065</i> fw
CF148	TATCCATATGACCATGATTACGAAAGTGCTAC TATTTCAAATAGTA	5' promoter <i>cdeC</i> fw
CF149	TCTTTATCAGCAGCTGCGGATCCTCTGTGGCAA CTTGGCTTCC	3' <i>cdeC</i> rev
CF154	TATCCATATGACCATGATTACGCCTTATCCATT ACTATACCAAATT	5' promoter <i>cotE</i> fw
CF155	TCTTTATCAGCAGCTGCGGATCCGAATTGCCCA TAAATACCTTCA	3' <i>cotE</i> rev
CF158	TATCCATATGACCATGATTACGAATAGCCAAC AAGTACCTTAAA	5' promoter <i>cotB</i> fw
CF159	TCTTTATCAGCAGCTGCGGATCCCATGTTTTTA TAACTCTCCAATATT	3' <i>cotB</i> rev
CF162	TATCCATATGACCATGATTACGTTACTTAGCAT A GTCTATGTATATA	5' promoter <i>spoIVA</i> fw
CF163	TCTTTATCAGCAGCTGCGGATCCTAACAAAAT AGTTATAATATTAGAACT	3' <i>spoIVA</i> rev
CF184	GGAATTCATATGAAAAAATTAGATACAGAGT CA	5' <i>CD1065</i> NdeI for pET20 cloning
CF185	CCGCTCGAGTTCATGAGGGTTAGACTTTTT	3' <i>CD1065</i> XhoI for pET20 cloning
CF189	TATCCATATGACCATGATTACGTAAGAATTTTT A TTTATATTATATATC	5' P2 <i>CD1065</i> fw
CF202	GATGAAAACCTCCTTGTTGT	3' promoter <i>cotD</i> rev
CF203	ACAACAAGGAGGTTTTTCATCATGTGGATATAT CAGAAAACCTATAC	5' promoter <i>cotD</i> fw
CF204	TCTTTATCAGCAGCTGCGGATCCGAACATTTTT TGAGATTCTTCTAA	3' <i>cotD</i> rev
CF206	TATGAATATAATTCAATATACTCGAG	5' <i>CD1065</i> fw
CF207	GAATTGTGAGTGATATATAATATAAAT	3' P1 <i>CD1065</i> rev
CF134	TGA AAA AAT TAG ATA CAG AGT CAT TA	qRT-PCR <i>CD1065</i>
CF131	TGC CAT CTA GAT TCT TAC CTA	qRT-PCR <i>CD1065</i>
LS17	CAGCTAAATGGTTCCAAAATGA	qRT-PCR <i>CD1581</i>
LS18	TCCTGAATCTGAACATCCACA	qRT-PCR <i>CD1581</i>
LS100	CACCACCTCAATGTGGAAAA	qRT-PCR <i>CD1192</i>
LS101	GCTCCTGCTATCTCATTACGC	qRT-PCR <i>CD1192</i>
LS102	GGCCATAGTGGTAGCAAAA	qRT-PCR <i>CD0126</i>
LS103	TGGCAAGGGATGGATTTATT	qRT-PCR <i>CD0126</i>
LS106	CCCCAAAGTGGTTCAGGTAA	qRT-PCR <i>CD2629</i>
LS107	TGCCCTAAAGCTCCTTCAAC	qRT-PCR <i>CD2629</i>
LS114	TGCATTGGCTTCAAGAAAAA	qRT-PCR <i>CD2470</i>
LS115	GCAATAACATCCACGCCTAAA	qRT-PCR <i>CD2470</i>
LS141	TTGCTATGGAAGCTGACCACT	qRT-PCR <i>CD1511</i>
LS142	TTGTTCTGCAACTGATGTGAGA	qRT-PCR <i>CD1511</i>
LS143	CAGGCCCAAATGGTAGAAAA	qRT-PCR <i>CD1433</i>
LS144	GAAGGCATTCCAGCATTCTC	qRT-PCR <i>CD1433</i>
LS145	GCTGCATCTACTCCATTAGCAA	qRT-PCR <i>CD1613</i>

LS146	GCAATCATCACAATCGCAGT	qRT-PCR <i>CD1613</i>
LS147	CCAATGTCCTGACCAAATGA	qRT-PCR <i>CD0551</i>
LS148	CTGCCCAGAAGAACCAACTT	qRT-PCR <i>CD0551</i>
LS149	CTATGCAAGTTCGCCTGGA	qRT-PCR <i>CD3569</i>
LS150	CCACCAATTCCCTTAACACC	qRT-PCR <i>CD3569</i>
LS151	AGCATCACCAAATCCAATCC	qRT-PCR <i>CD1067</i>
LS152	AACTTGGCTTTCCACTTCCA	qRT-PCR <i>CD1067</i>
LS155	GAAAAACCCTTAACCCCTGA	qRT-PCR <i>CD1230</i>
LS156	TCATCCTGATCTTCCGTTGA	qRT-PCR <i>CD1230</i>
LS158	TTAAGGCTGCTGGACTTGGT	qRT-PCR <i>CD0598</i>
LS159	AGTTACCGAATCGCCAAAGA	qRT-PCR <i>CD0598</i>
LS160	AAAGCTGCAGGTCTTGGTTC	qRT-PCR <i>CD2401</i>
LS161	AAATCGGTTACGGGATTTGA	qRT-PCR <i>CD2401</i>
LS198	CATCATTGCTGTCCACCATC	qRT-PCR <i>CD3349</i>
LS199	CCCTACTCCTGGACCTGTTG	qRT-PCR <i>CD3349</i>
LS206	GCGGAGGAGTACTTTCTGGA	qRT-PCR <i>CD0332</i>
LS207	GCTGATTGCCCATTTTCGTAT	qRT-PCR <i>CD0332</i>
LS208	AGCAGCAAACAATGCACAAT	qRT-PCR <i>CD3230</i>
LS209	TCCCTCCAAGTCAAGATTT	qRT-PCR <i>CD3230</i>
LS338	GCAGGGCTTGAAATGTAAA	qRT-PCR <i>CD2247</i>
LS339	GATGCAGCAAACAACATTGC	qRT-PCR <i>CD2247</i>
IMV552	CCAGGAGCAAAAGAGGCTTTA	qRT-PCR <i>CD2688</i>
IMV553	TCCAGCCATTTGTTGTTTCAG	qRT-PCR <i>CD2688</i>

Table S4: Effect of *CD1065* inactivation on the expression of sporulation-specific genes.

Total RNAs were extracted from the wild-type and *CD1065* mutant strains after 14 h (for σ^E - or σ^F - target genes) or 24 h (for σ^G - or σ^K - target genes) of growth in SM medium. The results presented correspond to the mean of at least 3 independent experiments.

Gene ID	Name	Expression ratio wt/ <i>CD1065</i> mutant	Know/predicted Sigma factor needed for expression
CD1065	<i>cotL</i>	332,34 ± 239,83	σ^E / σ^K
CD2470	<i>gpr</i>	1,29 ± 0,12	σ^F
CD1192	<i>spoIIIA</i>	0,95 ± 0,21	σ^E
CD0126	<i>spoIIID</i>	1,21 ± 0,34	σ^E
CD2629	<i>spoIVA</i>	0,96 ± 0,17	σ^E
CD1511	<i>cotB</i>	0,98 ± 0,32	σ^E
CD2247	<i>cspBA</i>	0,93 ± 0,27	σ^E
CD1230	<i>sigK</i>	0,86 ± 0,30	σ^E / σ^K
CD2688	<i>sspA</i>	1,06 ± 0,79	σ^G
CD0551	<i>SleC</i>	1,76 ± 1,17	σ^K
CD2968	<i>dpaA</i>	1,08 ± 0,44	σ^K
CD3569	<i>yabG</i>	0,86 ± 0,40	σ^K
CD1613	<i>cotA</i>	1,01 ± 0,45	σ^K
CD0598	<i>cotCB</i>	0,69 ± 0,30	σ^K
CD2401	<i>cotD</i>	1,88 ± 1,53	σ^K
CD1433	<i>cotE</i>	1,55 ± 1,09	σ^K
CD1581	<i>cdeM</i>	0,82 ± 0,68	σ^K
CD1067	<i>cdeC</i>	0,70 ± 0,45	σ^K
CD0332	<i>bclA1</i>	1,28 ± 1,04	σ^K
CD3230	<i>bclA2</i>	0,75 ± 0,37	σ^K
CD3349	<i>bclA3</i>	1,14 ± 0,78	σ^K

Abstract

The strict anaerobe and sporogenic *Clostridium difficile* is the most common cause of antibiotic-associated diarrhoea. Spores have a central role in the *C. difficile* infectious cycle: resistance outside the host, persistence of bacteria during infection and transmission of the disease. When ingested by the host, in the presence of certain bile salts, *C. difficile* spores germinate in the colon to form vegetative cells that secrete toxins and cause the symptoms of infection.

Vegetative cells are exposed to several stresses, among them, reactive oxygen/nitrogen species (ROS/RNS) produced by the host immune system during inflammation. Furthermore, although the intestinal tract is regarded as mainly anoxic, low oxygen (O₂) tensions are present in the large intestine and tend to increase after antibiotic treatments. To survive to this hostile oxidative environment, *C. difficile* had to develop mechanisms of protection, detoxification pathways and repair systems. The alternative sigma factor of the general stress response, σ^B , plays an important role in the protection of *C. difficile* against the different stresses the bacterium is facing inside the host including O₂ and ROS. Among the genes positively controlled by σ^B , we identified genes encoding proteins likely involved in O₂ tolerance and ROS detoxification, such as the two reverse rubrerythrins (revRbrs), CD1524 and CD1474, and the flavodiiron proteins (FDPs), CD1157 and CD1623. We showed that the two revRbrs and the FDP CD1623 are expressed in a σ^B -dependent manner and heterogeneously in a cell population. A dual genetic control was demonstrated for the FDP encoding gene *CD1157*, through σ^A - and σ^B -dependent promoters. We demonstrated that *CD1157* displays O₂-reductase activity while the two revRbrs have both H₂O₂- and O₂-reductase activity, being H₂O₂ the preferred substrate. Moreover, we showed that a double $\Delta CD1474\text{-}\Delta CD1524$ mutant and a *CD1157* mutant are less tolerant to low O₂ tension and that the *CD1623* mutant is more sensitive to air exposure. These findings demonstrate a key role for these proteins in O₂ tolerance and oxidative stress response in *C. difficile*.

During the infection cycle, in the colon some vegetative cells are transformed into spores. The spore surface layers, the coat and exosporium, enable the spores to resist physical and chemical stress. However, little is known about the mechanisms of their assembly. In this work, we characterized a new spore protein, CotL, which is required for the assembly of the spore coat. We showed that the *cotL* gene is expressed in the mother cell compartment under the dual control of the sporulation sigma factors, σ^E and σ^K . CotL was localized in the spore coat, and the spores of the *cotL* mutant had a major morphologic defect at the level of the coat/exosporium layers. Therefore, the mutant spores contained a reduced amount of several coat/exosporium proteins and a defect in their localization in sporulating cells. Finally, *cotL* mutant spores were more sensitive to lysozyme and were impaired in germination, a phenotype likely associated with the structurally altered coat. Collectively, these results strongly suggest that CotL is a morphogenetic protein essential for the assembly of the spore coat in *C. difficile*.

Keywords: *Clostridium difficile*, Spore, Coat, Morphogenesis, CotL, Oxygen, ROS, detoxification, Rubrerythrins, Flavodiiron proteins